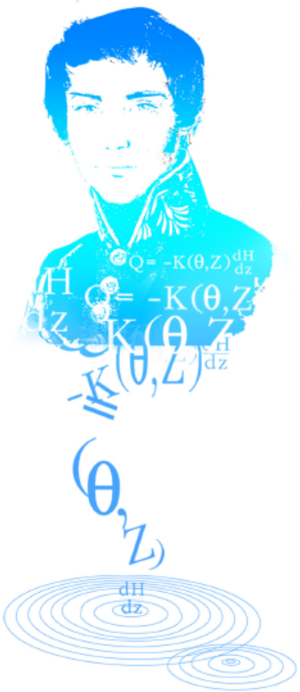

# THÈME 1 / *TOPIC 1*

## Connaissance des réservoirs
## Reservoirs knowledge

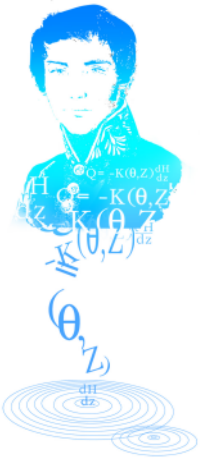

# SOMMAIRE

## Reservoirs knowledge • Connaissance des réservoirs

| References | Abstract | Authors | Organization |
|---|---|---|---|
| **ORAL COMMUNICATIONS** | | | |
| DARCY-01 | Alluvial Aquifers in North China Plain | Han Zaisheng | Department of Hydrogeology and Environmental Geology, China Geological Survey China |
| DARCY-09 | Geochemical Modeling through Groundwater Mineralization Appraisal: Sines Coastal Aquifer, SW Portugal | P. Galego Fernandes, P.M. Carreira, M.O. Silva | Instituto Tecnológico e Nuclear Sacavém Portugal |
| DARCY-11 | Modeling of chlorinated solvents transport and natural attenuation in groundwater | F. Quiot, C.Rollin, O.Bour, et al | INERIS, Verneuil-en-Halatte – France |
| DARCY-12 | Practical Applications of Quasi-Static Ground Water In Low Permeability Phreatic Aquifers | Shrikant Daji Limaye | Ground Water Institute, Pune, India. |
| DARCY-13 | Les très grands systèmes aquifères du monde | Jean Margat | président honoraire de l'AIH comité français |
| DARCY-18 | Can we identify vertical exchanges in multi-layered aquifer from groundwater chemistry ?<br>a theoretical background applied to the Aquitaine Basin. | O. Atteia, L. André, M. Franceschi, A. Dupuy | Institut EGID, Pessac Cedex, BRGM, service EAU, France |
| DARCY-29 | Groundwater influence on river nitrate concentration in crystalline rock aquifers | V.Ayraud, L.Aquilina, T.Labasque, A.C.Pierson-Wickmann, J.Molénat, H.Pauwels, E.Fourré, C.Tarits, O.Bour, V.Durand, P.Le Corre, P.Mérot et P. Davy | Géociences Rennes, 35000 Rennes, France |
| DARCY-32 | Reconstructing natural groundwater flow in a perturbed multi-layer aquifer system. | D.Baird, C.Le Gal La Salle, A.Love, C.Simmons | Flinders University, Adelaide, South Australia |
| DARCY-44 | Geochemical modelling in a regional deep aquifer and relations with groundwater flows.<br>Aquitaine Basin, south-west of France | L. André, M. Franceschi, O. Atteia | BRGM - Water Division, Orléans, France ; Institut EGID Bordeaux 3, University Michel de Montaigne, Pessac France |
| DARCY-56 | Spatial variability of the geochemistry of a chalk aquifer at a regional scale: Role of the structural context (Haute-Normandie, France) | D.Valdes , J.P. Dupont, B.Laignel, N. Massei, S. Ogierand Th. Leboulanger | UMR CNRS 6143, Université de Rouen, Mont-Saint-Aignan, France |
| DARCY-57 | Using stable isotope analysis to characterise the regional hydrology of the Souss-Massa basin, south-west of Marocco. | L. Bouchaou, Y. Hsissou, M. Qurtobi, Kh. Dindane, S. Boutaleb, & S. Krimissa | Laboratoire de Géologie Appliquée et Géo-Environnement (LAGAGE), Faculté des Sciences, Université Ibn Zohr, Agadir, Maroc ; Centre National des Etudes Scientifiques et Techniques Nucléaires (CNESTEN), Rabat, Maroc ; Faculté polydisciplinaire de Taza. Université Sidi Mohamed Ben Abdallah Fès, Maroc. |
| DARCY-58 | The Guaraní Aquifer System: advances in the knowledge. | O. Tujchneider, M. Paris, M. Perez and M. D´Elía | Facultad de Ingeniería y Ciencias Hídricas. Universidad Nacional del Litoral, Santa Fe, Argentina. |
| DARCY-61 | Advective versus diffusive flux in a low permeability clay sequence | W.A. Timms and R.I. Acworth | Water Research Laboratory, School of Civil and Environmental Engineering,<br>University of New South Wales, Manly Vale, NSW 2093, AUSTRALIA |
| DARCY-64 | Reflections on the impact of the Messinian Salinity Crisis on the hydrogeology of the Rhodanian basin | R. de La Vaissière, F. Lalbat and B. Blavoux | Laboratoire d'Hydrogéologie, Université d'Avignon, Avignon, France |
| DARCY-77 | Environmental tracer methods (3H, 3He, 85Kr, 39Ar, 14C and 4He) to resolve the age structure of groundwater: example of two study cases | J.A. Corcho Alvarado F. Barbecot, R. Purtschert, T. Paces, W. Aeschbach-Hertig, R.Kipfer | IDES Laboratory, UMR 8148 IDES, Bâtiment 504, Université Paris-Sud, 91405 Orsay Cedex, France. corcho@geol.u-psud.fr<br>2 Climate and Environmental Physics Division, Phys. Institute, Univ. Bern, Sidlerstrasse 5, CH-3012 Bern, Switzerland |
| DARCY-87 | Isotopic study (B, Li, Fe, U, Th) of two confined aquifers in the eastern part of the Paris basin: implication for hydrological and WRI processes | J. Casanova, J.P. Girard, C., C. Innocent, R. Millot, M. Motelica, S. Buschaert | BRGM, Orléans France ; ANDRA, Châtenay-Malabry, France |
| DARCY-101 | Estimation of permeability from groundwater dating by chlorine-36: the case of the "Continental Intercalaire" aquifer (Northern Sahara) | Jean-Luc Michelot, Abdelhamid Guendouz | UMR CNRS-UPS "IDES", Bat. 504, Orsay, France ; University of Blida, Science Engineering Faculty, Soummaâ-Blida, Algeria |
| **POSTERS** | | | |
| DARCY-02 | Recharging conditions and ages of the groundwater of the Bekaa's valley (Lebanon), hydrogeologic, hydrochemical and isotopic studies | Sadek Awak | Université de Paris-Sud (Paris 11) – Orsay Département des sciences de la Terre, France |

| | | | |
|---|---|---|---|
| DARCY-04 | Tectonics and groundwater in French Southern Alps | Pierre De Bretizel | Association des Amis des Sources France |
| DARCY-07 | Geochemical signatures in groundwater in crystalline rock (Massif Central, France) | Jean Barbier | retraité/in retirement, France |
| DARCY-08 | Tracing high pH mineral waters ascribed to ultramafic rocks (Central Portugal): Conceptual vs numerical modelling | José Manuel Marques and al. | Instituto Superior Técnico, Lisboa, Portugal |
| DARCY-09 | Geochemical Modeling through Groundwater Mineralization Appraisal: Sines Coastal Aquifer, SW Portugal | P. Galego Fernandes, P.M. Carreira, M.O. Silva | Instituto Tecnológico e Nuclear Sacavém Portugal |
| DARCY-14 | Compaction of water/gas bearing formations: Experiences in Northern Italy | P. Macini, E. Mesini | University of Bologna - Italy |
| DARCY-16 | Existence of deep flux on an active faults line extended through Arax basin, Armenia | K. Kharatian, Y. Travi | Department of Geology, Yerevan State University, Yerevan, Armenia |
| DARCY-17 | From local investigation to global management: multiscale integration of data for groundwater assessment in regional aquifers | F. Larroque, B. de Grissac, A. Dupuy, M. Franceschi, T. Condom | Institut EGID Bordeaux 3, Pessac France, SMEGREG, Bordeaux, France |
| DARCY-20 | Natural depletion of a large aquifer explained by isotopic, geochimical and hydrodynamic data | O. Douez, Dupuy A., Franceschi M. and Atteia O. | Institut EGID Bordeaux 3, Pessac France, SMEGREG, Bordeaux, France |
| DARCY-23 | Vadose zone characterisation in a mountainous hydrogeologic system: Serra da Estrela mountain (Central Portugal) case study | Espinha Marques, J.; Marques, J.M.; Afonso Martins, A.; Samper, J.; Rocha, F.T.; Inácio, M.; Duarte, J.M.; Constantino, A.T.; Teixeira, J.; Borges, F.S.; Carvalho, J.M. & Chaminé, H.I. | Dep. Geologia (CGUP), Universidade do Porto, Porto, Portugal. Dep. Engª de Minas e Georrecursos, IST, Lisboa, Portugal Dep. Edafologia, UTAD, Vila Real, Portugal. ETSI Caminos, Canales y Puertos, Univ. Coruña, Spain. Centro de Minerais Industriais e Argilas, Univ. Aveiro, Portugal. Agroconsultores, Engª Recursos Agrários, Lisboa, Portugal. Dep. Engª Geotécnica, ISEP, Porto, Portugal |
| DARCY-34 | 66.7 km tracer test in Fontaine de Vaucluse karst | Ducluzaux B | EKS Hydrogéologie, Lacenas, France |
| DARCY-35 | Hydrochemistry of water percolation in the Trebiciano Abyss (Karst of Trieste) | Enrico Merlak, Clarissa Brun, Fabio Gemiti & Rino Semeraro | Geokarst Engineering srl, Trieste, Italy |
| DARCY-40 | Hydrogeological caracterization of the Oxfordian limestones at the Bure URL | Cruchaudet M. , Delay J. | ANDRA – Laboratoire de Recherche Souterrain de Meuse / Haute-Marne, BURE France |
| DARCY-46 | News arguments for karst presence in Northern France chalk.<br>Implication for Boulonnais area hydrogeology. | Aude A., Brunin A.S., Fayeulle M., Bracq P. | Université du Littoral Côte Opale, Wimereux, France. |
| DARCY-48 | Contribution of the structural geology to the knowing of water and gas transfers in the carbonate aquifer of Quézac (Lozère, France) | Durand V., Deffontaines B., Léonardi V. and Macquar J.-C. | UMR Sisyphe, UPMC, PARIS, France |
| DARCY-49 | Evaluation of the accuracy of the specific yield estimation obtained from Magnetic Resonance Soundings | Boucher M., Baltassat J-M., Girard J-F., Lachassagne P., Legchenko A. | BRGM, Orléans, France ; ISTO, UMR6113, Orléans; BRGM, EAU/RMD, Montpellier ; IRD, LTHE, Grenoble, France |
| DARCY-51 | Isotopic measurement of ng quantities of Th, in natural waters. Coupling 234U/238U and 230Th/232Th ratios to provide time-constraints on the evolution of aquifer groundwaters. | Innocent C., Casanova J., Buschaert S. | BRGM, Orléans, France ; ANDRA, Châtenay-Malabry cedex, France |
| DARCY-60 | Hydrogeological problems and groundwater modelling of the Gavorrano mine area (Italy) | Barsuglia F., Garzonio C. A., | Università di Firenze Laboratorio Materiali Lapidei e Geologia dell'Ambiente e del Paesaggio, Italy |
| DARCY-62 | Groundwater system compartmentalized by a tectonic zone in Kanto plain, central Japan | Masaya Yasuhara, Akihiko Inamura, Masaaki Takahashi, Takeshi Hayashi, Hiroshi Takahashi, and Masahiko Makino | Geological Survey of Japan, 1-1-1 Higashi, Tsukuba, Ibaraki 305-8567, Japan |
| DARCY-73 | Measurements of the chemico-osmotic efficiency coefficient in the Callovo-Oxfordian shale of the Paris Basin. | Gueutin, P., de Greef, V., Cruchaudet, M., Gonçalvès, J., Cosenza, P. et Violette, S. | UMR SISYPHE, Université Pierre et Marie Curie, PARIS, LMS, Laboratoire de Mécanique des Solides, Ecole Polytechnique, PALAISEAU ANDRA, Laboratoire de recherche souterrain de Meuse/Haute-Marne, BURE, France |
| DARCY-75 | Input of chemical and isotopic studies in the elaboration of the new conceptual flow model of the Maastrichtien aquifer system in Senegal | Aranyossy J.F., Faye A., Møller K.N., Sarr M., Emsellem Y. | ANDRA, France. University Cheich Antia Diop, Dakar, Senegal. COWI A/S, Denmark. SGPRE / MHHE, Senegal. ItalPros, |
| DARCY-82 | Les grands transferts hydrodynamiques dans le bassin sédimentaire du Nord Ouest Saharien de l'Algérie (Monts des Ksour - Plate forme Saharienne)". | Mansour. H, Merzoughi. T, Nadji. A, Foukrache. M, Zeroual. I | FSTGAT, Département des Sciences de la Terre – Université d'Oran ; GTZ/AHT, groupe : projet gestion intégrée de l'eau. Béni Abbes, Béchar, Algérie |
| DARCY-83 | Multi isotopic and geochemical characterisation of water bodies in the Adour-Garonne district: clues for interconnection et heterogeneities – The CARISMEAU research project | Négrel Ph., Petelet-Giraud E., Roy S. , Dutartre Ph. a, Fournier I. | BRGM, Orléans France ; Agence de l'Eau Adour-Garonne, Toulouse, France |
| DARCY-88 | An assessment of the groundwater resources in the western margin of the Taoudenni basin, Mauritania | Bertone F., Renard P., Kerrou J., Moix P. and Perrochet P | BCEOM, Montpellier, France<br>Centre d'Hydrogéologie, Université de Neuchâtel, Suisse |
| DARCY-89 | Fissured hydrogeosystems of the basement : state of knowledge and consequence on their management | Faillat J.P. | Centre Universitaire de Nîmes, Nîmes |
| DARCY-90 | Interaction between different groundwaters: characterizing multiple sources through strontium isotope tracing, sedimentary versus fractured bedrock aquifers | Négrel Ph., Petelet-Giraud E. , Pauwels H. | BRGM, Orléans, France |
| DARCY-100 | Acquisition of isotopic composition in carbon of groundwater in the recharge area | Gillon M., Barbecot F., Marlin C., Gibert E. | Laboratoire IDES UMR 8148, CNRS-Université Paris Sud-11, bâtiment 504, 91 405 Orsay cedex. |
| DARCY-118 | Hydrogeologic invetsigation and water suplly systems in north alentejo region (Portugal) | Chambel A., Duque J., Benedova, K. | University of Evora, Geophysic Center of Évora, Department of Geociences, Apartado 94, 7002-554 Évora, Portugal ; Politechnical Institute of Beja, Agriculture High School of Beja, Apartado 158, 7801-902 Beja ; Charles University, Faculty of Science, Albertov 6, 128 43 Prague 2, Czech Republic |

# Communications orales

# *Oral Communications*

# DARCY 01

# Alluvial Aquifers in North China Plain

Han Zaisheng
China Geological Survey, Beijing 100011, China, hzaisheng@mail.cgs.gov.cn

## Abstract

The alluvial plain located in North China is one of the most important aquifers in East Asia which area is 140000km². The recharges of shallow groundwater system are mainly rainfall. There are also recharges from surface water in riverside and irrigated area. Groundwater flow is from the front of mountains to coastal plain. The Isotopic data of deep aquifers show that the water flow from the front of mountains to the middle and coastal plain need about several thousands to more than 10 thousands years. Long term groundwater overexploited especially in deep aquifers not only cause many bore to go dry but also cause many eco-environmental problems. The detail investigation on the aquifers has been taken. Sustainable of Groundwater Usage for the social – economical develompent are advanced.

## Geography and Hydrology

North China Plain is one of the focus regions of China. Beijing, the capital of China, Tianjin city, most part of Hebei province and part of Shandong and Henan province are situated in this plain. The alluvial plain located in North China is one of the most important aquifers in East Asia. From Taihang Mountains in the west to Bohai Sea in the east, from Yan Mountain in the north to the Yellow river in the south, the area of north China plain is 140000 km². The altitude is lower than 100m. According the formation and physiognomy, it could be divided to alluvial plain in front of mountain, the middle plain, and the coastal plain. There are some lakes and billabongs, especially in the middle and east part. The plain belong to semi-arid and semi-humid climate regions. The average annual precipitation is 500-600mm. The rainfall and evaporation are asymmetrical. 80% of the precipitation are fasten on Jun to September. The plain is a part of Yellow river, Hai River and Luan river catchments. Because of the upper reservoirs holding back, these rivers are almost dry up in most periods.

## Quaternary Aquifers

The plain is large sediment basin of Cenozoic. It is the most significant; consist of alluvial sediments of up to 1000-3000m. In which, the Quaternary thickness is more than 600m in depression area and 200m in apophasis area. Groundwater exists in the Quaternary and tertiary pore aquifers. The aquifers system is 350-500m in thickness. The quaternary aquifers could be divided into four groups in the middle plain, and the coastal plain. The upper two groups are shallow aquifers. The lower two groups are deep confined aquifers. The bottoms of shallow aquifers are generally in depth of 40-60m. In alluvial plain in front of mountain, for mixed extractive, the shallow groundwater systems extend to 120-150 m depth. The bottoms of deep confined aquifers are 350-550 m depth. In the middle and coastal plain, there are the salt aquifers between shallow and deep fresh aquifers.

According to water circular and system character, there are three Groundwater systems in North China plain: Luanhe River system, Hai River system and ancient Yellow River system. They could be subdivided into 7 second grade subsystems, 17 third grade subsystems and

28 forth grade subsystems. They are the basis for groundwater system analysis and assessment. See Fig.1 and Table 2. The quaternary aquifers of Luan river system are composing with coarse sands. They are rechargeable with rain water and surface water. Those aquifers of Hai river system are complex. They are various from foreland to coastal area. The section of Fig. 2 shows the structure for the quaternary stratum. The shallow aquifers of ancient Yellow river system are recharged sufficiency. But the deep one is interbedded with clay.

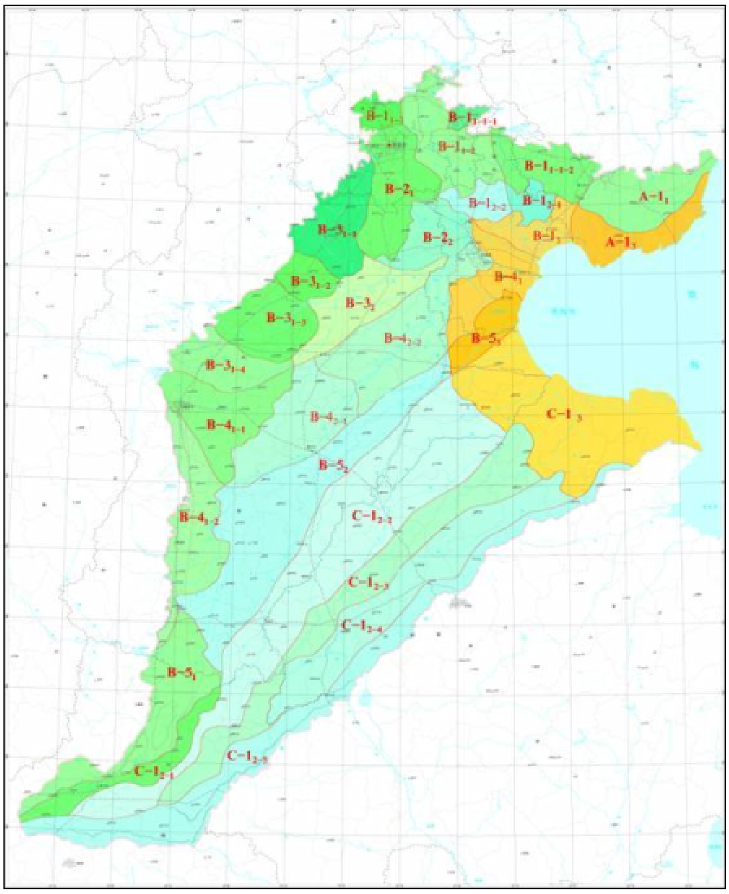

Figure 1: Groundwater systems of North China plain

## Water Circular and Characters

The recharges of shallow groundwater system are mainly rainfall. There are also recharges from surface water in riverside and irrigated area. Groundwater flow is from the front of mountains to coastal plain. The coefficients of Transmissivity are 500-1000 $m^2$/d in the front of mountains, 100-500 $m^2$/d in the middle plain, and generally less than 50$m^2$/d in coastal plain. The discharges of shallow groundwater system are exploitation and evaporation. A mass of shallow groundwater exploitation decreased the evaporation and increased the recharge in recent years. The TDS of shallow groundwater are in orderliness. The fresh water is distributed in the front of mountains. There is the salt water in coastal area where the TDS of water is more than 5g/l. between them is the transition area. Fig.2.

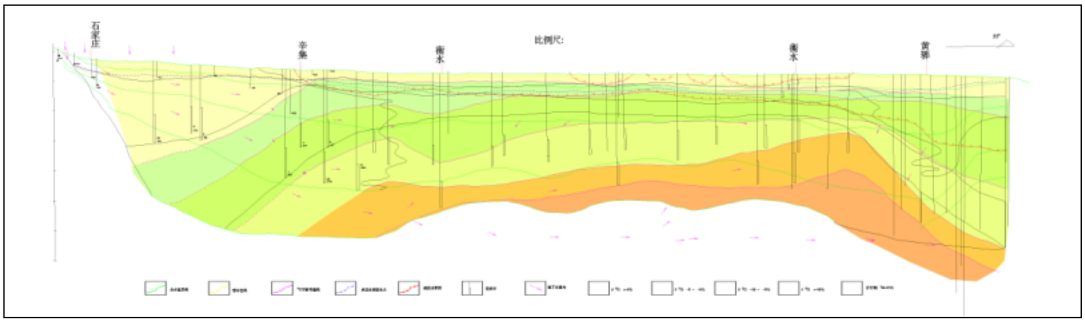

Figure 2: Hydrogeololical cross section

The deep confined aquifers could not be recharge by rainfall directly. The flank groundwater flow would recharge these aquifers. The Isotopic data of water in deep aquifers show that the water flow from the front of mountains to the middle and coastal plain need about several thousands to more than 10 thousands years. In the condition of extensive exploitation, those aquifers are recharge by border shallow aquifers and aquitard. Exploitation is the mainly discharge of deep groundwater system. The main consist of pumping water are the storage in deep confined aquifers and neighbor aquitard. That is the causes of land subsidence. The chemical types of this groundwater are mainly $Na\text{-}HCO_3.SO_4$ and $Na.Mg\text{-}HCO_3$.

| **Situation** | **Plain in front Of Mountains** | **Middle plain** | **Costal plain** |
|---|---|---|---|
| C (pmc) | 24.50 ~ 111.07 | 6.29 ~ 18.40 | 2.44 ~ 18.52 |
| $\delta^{18}O$(‰) | -10.5 ~ -8.7 | -12.5 ~ -10.2 | -10.7 ~ -9.5 |
| $\delta D$ (‰) | -72 ~ -65 | -87 ~ -74 | -81 ~ -75 |
| Cl (mg/l) | 5.57 ~ 62.30 | 1.64 ~ 329.6 | 242.70 ~ 524.7 |
| $\delta^{18}O$ temperature | 9.4 ~ 15.06 | 4.06 ~ 8.43 | 7.97 ~10.31 |
| $^{3}H$(TU) | 6 ~ 47 | 1~ 3 | 1 ~ 6 |
| $\delta^{13}C$ (PDP) | -10.39 ~ -9.28 | -10.23 ~ -7.75 | -11.46 ~ -7.92 |
| TDS(mg/l) | 342 | 908 | 1786 |
| pH | 7.7 | 7.95 | 7.9 |
| Chemical type | HCO3-Na.Ca | Cl.HCO3-Na | Cl-Na |
| Vogel (ka B.P.) | 10 ~ Modern | 21 ~ 12 | 30 ~ 12 |

Table 1: Geochemical and Isotopic parameters of Groundwater in Deep confined aquifers

## Groundwater Resources

The assesment of groundwater resources is base upon an understanding of the recharge over a region and considering the environmental factors. The achievement of groundwater resources evaluation is as Table 2, the average annual fresh groundwater recharge in North China plain is 19 -$10^9 m^3$ per year. Thereinto the recharge for shallow aquifers is16.8 -$10^9 m^3$ per year, Recahrge to deep confinded aquifers is 2.4 - $10^9 m^3$ per year. This typcal results in the exploitable yield being less than the recharge volum. They are restricted by the technical, economic and eco-environmental conditions. The rechrge to the deep confined aquifers is by the flow from the basin margin in the west, and by leakage from overlying aquifers. However the rate of horizontal flow is very slow and vertical leakage is little. Much of the groundwater in the deep confined aquifers can be considered to represent fossil water with limited recharge.

| **Sub systems** | | **Area (Km$^2$)** | **Annual preci.(mm)** | **Recharge (Mm$^3$/yr)** | **Exploitable (Mm$^3$/yr)** |
|---|---|---|---|---|---|
| A | Luan river system | 7000 | 552 | 1440 | 1238 |
| B | Hai river system | 75340 | 500 | 14400 | 13018 |
| C | Ancient Yellow River system. system | 56900 | 584 | 3280 | 3036 |
| | **Total (or average)** | **139240** | **548** | **19120** | **17292** |

*Table 2: Groundwater resources in North China Plain*

Groundwater resources of the alluvial plain constitute the primary water supply for urban, industry as well as irrigation. In last 30 years, the exploitation and utilization of groundwater has been carried out extensively in this plain. The annual groundwater extractions is 21-$10^9 m^3$ in 2000. Thereinto, those from shallow aquifer is 17.8 -$10^9 m^3$ , those from deep aquifer is 3.3 -$10^9 m^3$ . The groudwater usage is as Table.3. Groundwater is about 2/3 of total water supplied of the area. Groundwater over-exploitation is befallen in some area of the plain.

| **Province** | **Total** | **Industry** | **Agriculture** | **Civil** | **Other** |
|---|---|---|---|---|---|
| Beijing | 2487 | 436 | 1532 | 528 | |
| Tianjin | 555 | 15 | 316 | 105 | 119 |
| Hebei | 12862 | 1476 | 10136 | 125 | |
| Shandong | 2756 | 571 | 1827 | 358 | |
| Henan | 2538 | 294 | 1999 | 245 | |
| **Total** | **21198** | **2792** | **15801** | **2486** | **119** |

*Table 3: Groundwater Usage in North China Plain (Mm$^3$/yr)*

## Groundwater related Ecological Issues

Groundwater has played a key role in the history and development in the plain. The huge extent of over-explloitation of groundwater in the alluavial plain has created a boroad range of largely environmental problems. Long term groundwater overexploited especially in deep aquifers not only cause many bore to go dry but also cause many eco-environmental problems. Groundwater level both of shallow and deep aquifers in most part of the plain have declined more than 15 m during last 30 years. In some urban and irrigated area, the declined extent of groundwater level are ever large. Several ecological issues were occurred cause by groundwater overexploitation. The situations of land subsidence, sea water intrusion, water quality degradation are investigated and verify. The grounwater overexplited ocuured in the area of Beijing city and Hebei Province. Continuance decline of grounwater level present to these region. Figur3 shows the setuation in Beijing dowtown. The North China plain has witnessed the most excessive pumping of groundwater in the world and covers the largest subsidence area with the most funnels. The groundwater level in coastal region falls below sea level.

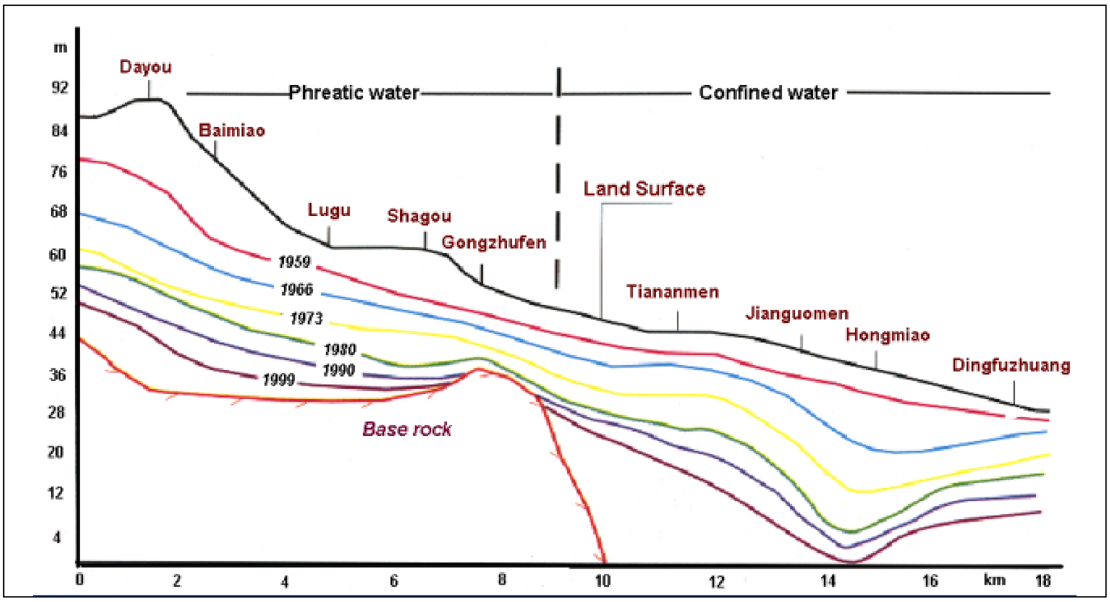

Figure 3: Groundwater level in Beijing Downtown

The deep confined aquifers could not be recharge by rainfall directly. The flank groundwater flow would recharge these aquifers. In the condition of extensive exploitation, those aquifers are recharge by border shallow aquifers and aquitard. The main consist of pumping water are the storage in deep confined aquifers and neighbor aquitard. That is the causes of land subsidence. In 2005, the areas of land subsidence more than 1000mm reach 8635 km$^2$. The areas of land subsidence more than 500 mm reach 30080 km$^2$. The most land subsidence in Beijing city is 0.79 m. The most land subsidence in Tianjin city is 3.18 m. The most land subsidence in Hebei Province is 2.45 m. The most land subsidence in Shandong Province is 0.94 m. The several areas of land are continuing developing. They are tending to gear into joint area in the plain.

Land subsidence due to groundwater withdrawal induces very serious economic and social problems. Subsidence in urban area, such as Tianjin and Cangzhou, effects are widespread and affect not only the nature structures but also the man-made ones. Damages could be

record but it is nearly impossible to establish their actual coast. Hazards are mainly structural damage, damage to well casing, lessened efficiency of storm-drainage facility, submergence of coastal lowland, etc. The disastrous of land subsidence are tide and waterlog due to less of land surface elevation. Relationship between Land subsidence and the groundwater level of deep aquifers has been root out as fig.4. We could find 50m and 70m of the depth of groundwater level is the key point of land subsidence. The aquifers dynamic pressure condition changed in evidence at those water levels.
For controlling subsidence, a monitoring networks focusing in North China plain is under establishing. It will monitor the rate of land subsidence as well as groundwater levels which covering 70000 km$^2$.

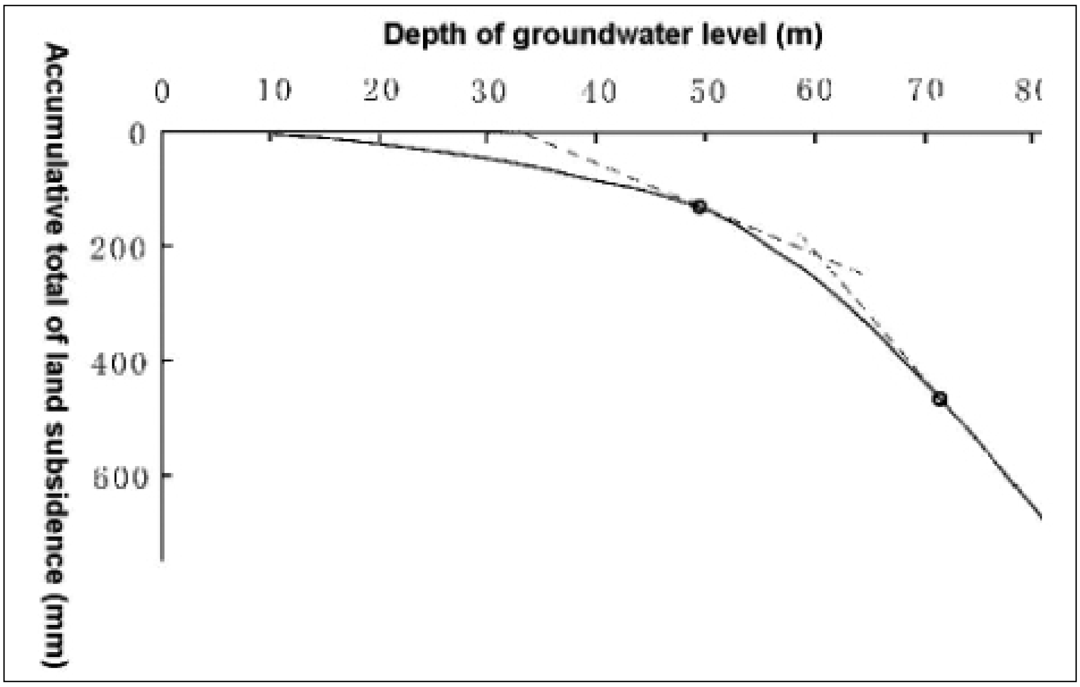

Figure 4: Relationship of Land subsidence and the groundwater level of deep aquifers

The shallow aquifers were polluted by the urban and industry waste water. The contaminated area is about half of the plain. The salted water have move down to the fresh water aquifers due to the excessive exploitation.

## Sustainable of Groundwater Usage

For the social – economical develompent in North China plain, one of the Chinese most important regions, sustainable of groundwater resources usage is integrant. The detail investigation on the aquifers has been taken. A numeric model with FEFLOW of WASY software for the plain is established. **All the groundwater models are basis on Darcy Law which was presented in 1856.** The 3-D model is used to simulate and forecast the situation both shallow and deep aquifers Fig.5. The data base of the aquifers were established. They are consistes of basic geograph information, geological information, hydrogeologival condition information, groundwater quantity and quality information and dynamic monitoring informatin,etc. The data of year 2000-2003 were used to establish and calibrate the model. The hydrogeological

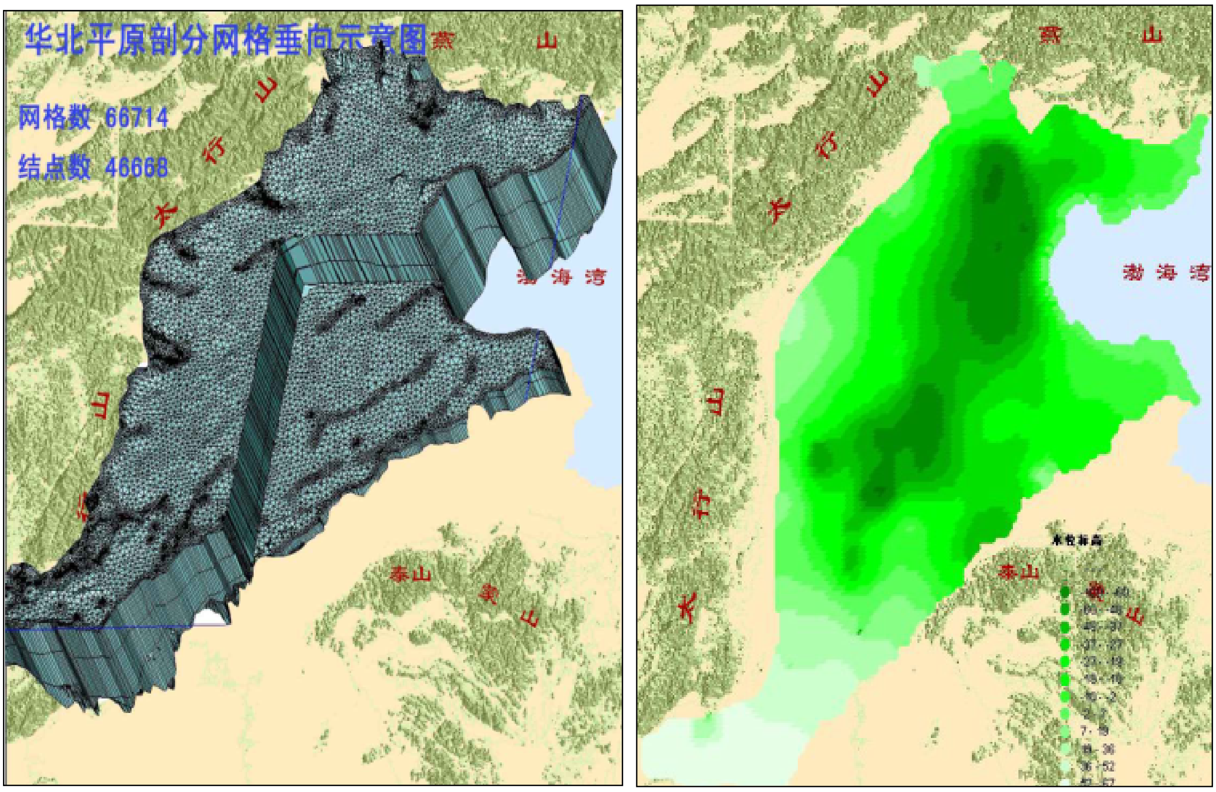

Figure 5: Numerical Model of North China plain

concept model are the whole plain with the area of 140000 km$^2$ and the aquifers depth to 550 m. Several measures for groundwater conservation are evaluated by the model.

The nature water circular have been breakaged by the surface reserviors in the rivers upstream. Only in the flood seasons the alluvial aquifers could be recharged. The extractived groundwater are large than the recharge for the aquifers. Fig 6 shows the groundwater level in the plain front of Taihang Mountains could come back after recharged. Artificial recharge is the most important way for groundwater protection and aquifers recovery. Aquifer recharge enhanscement with excess surface runoff and urban wastwater are water resources safeguard measures. There are large area in front og mountains in the plain where coarse sands and gravel outcrop. The surface artificial recharge system would be efficient.

Reducing groundwater extractions, by a variety of means, will generally be the most cost – effetive method of solving groundwater relative eco-enviromental problems. The long-distance

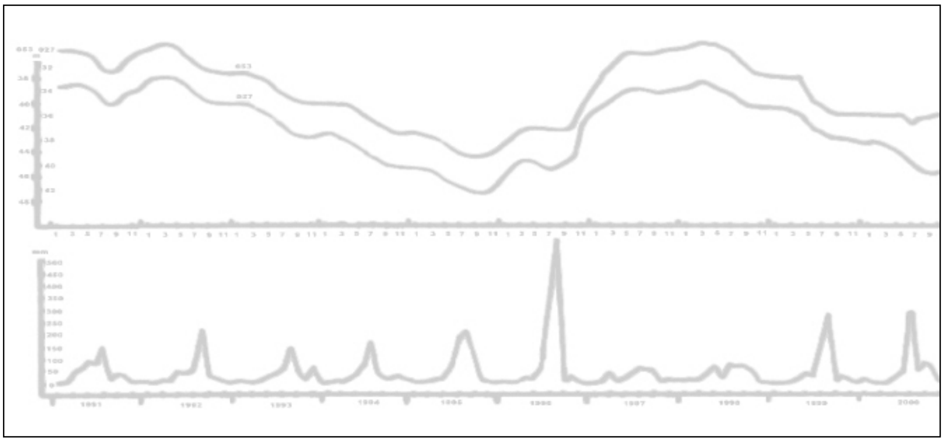

Figure 6: Groundwater level at the riverside and monthly precipitation

water transfer project from Yangtze river to North China plain will implement in 2010. Conjunect use of surface water and groundwater, the explitation of groundwater in deep confined aquifers will decrease. Some surface run flow would be resume. And the enviroment of water could improve.

Agricultural sustainability in the North China Plain, is highly dependent on water resource availability. Over twanty percent of the area in the Plain is irrigated using groundwater. It is imperative that these practices tested in small plots now be demonstrated in commercial applications to conserve groundwater resources and maintain agricultural sustainability needed to feed China's increasing population. Reducing groundwater abstraction for iirigation is considered with water saving.

To make more sufficiency usage for local waste water and salted groundwater is a way for save fresh water. Treat with and Reused urban and industry waste water which amount is $7*10^9m^3$ per year in this area have potential. There are some new groundwater well field could be for water supply meet an emergency. They must be regulating used with other water resources, such as surface reservoir and water transferred from other catchments.

Sustainable groundwater usage in North China plain could achieve in an integrated manner of all available management options.

## Conclusion

The alluvial aquifers in North China plain are an important source for water supply of the intensive development area. The detail hydrgeological investigation on the aquifers has been taken. Several eco-environmental isuus have occured due to groundwater over exploitation. Mesures for ssustainable of Groundwater usage have been evaluated and bring into effect. Those are Aquifer recharge enhanscement, irigate water saving, more for local waste water and salted groundwater sufficiency usage, etc.

## References

- Han Zaisheng (2004) Groundwater Investigation in China. Research Basin and Hydrological Planning, A.A. Balkema Publishers, Page : 165 - 169
- He Qingcheng(2005) Land subsidence in the North China Plain, Proceeding of the 7th International symposium on land Subsidence, Shanghai Scientific & Technical Publisher, Page 18-29
- Liu Changming and Yu Jingjie(2001), Groundwater Exploitation and its Impact on the Environment in the North China Plain, Water International, 2(26), 261-272
- Stephen Foster, Hector Garduno and et al, (2004) Quaternary Aquifer of the North China Plain—assessing and achieving groundwater resource sustainability, Hydrogeology Journal, Springer-Verlag GmbH, Vol.12, No. 1, Pages: 81 - 93
- Zhang Guanghui, Fei Yuhong (2003) Groundwater evolvement and countermeasure in Hai river plain, Academic Publishing House [in Chinese]
- Zhang Zonghu, Shen Zhaoli, Xue Yuqun et al. 2000, Evolution of Groundwater Environment in the North China Plain, Beijing Geological Publishing House [in Chinese]

# DARCY 9

# Geochemical Modeling Through Groundwater Mineralization Appraisal: Sines Coastal Aquifer, SW Portugal

GALEGO FERNANDES Paula[1], CARREIRA Paula M.1 and SILVA Manuel Oliveira[2]

[1] Instituto Tecnológico e Nuclear, Departamento de Química,
Estrada Nacional nº10, 2-686-953 Sacavém, Portugal.
[2] Departamento de Geologia da Universidade de Lisboa, Campo Grande,
Edifício C6, Piso 3, 1749-016 Lisboa Portugal

## Abstract

The Sines coastal sedimentary basin corresponds to a tecthonical ditch with a NE-SW orientation filled with Mesozoic and Cenozoic deposits. Two hydrogeological systems were identified: the Mio-Pliocene and the Jurassic. The aquifers recharge is made directly on the outcrop areas, although the Jurassic terrains receive also some contribution from the overlain Miocene layers. The main flow direction of Jurassic aquifer is E to W towards the Atlantic Ocean.

The groundwaters are mainly of the calcium-bicarbonate type related to the lithological composition of the reservoirs (calcareous and dolomitic units). Using mass balance model and statistics analysis it was proven that the water-rock interaction process is the major mechanism responsible for the groundwater salinity. If we assume the evolution from the Mio-Pliocene waters to Jurassic waters, it is expected that waters progressively increase the concentrations of chemical constituents. To evaluate this, using a simple mass balance model through the PHREEQC program were tested different scenarios in order to justify the groundwater mineralisation of both aquifers.

## 1. Introduction

The growing request of good quality water for public, industrial and agricultural use is in nowadays a major concern for groundwater management and protection. The groundwater geochemical evolution have been recognized as being important tools in the resolution of problems such as identification of pollution sources, interrelationships between surface and groundwater, identification of salinity sources and in the appraisal of conceptual models of the systems.

The region studied corresponds to the Sines coastal sedimentary basin where two hydrogeological systems were recognized: the Mio-Pliocene and the Jurassic. Both systems supply water to the entire region, which contains highly populated and industrialized areas, although in the remaining region agriculture represents an important activity. Some local losses in the water quality were identified which could be associated to human activities or due to the aquifer matrix lithology.

Water resources assessment and management require a multidisciplinary approach involving chemical, physical and geological data. In this context geochemical inverse modeling has been used in regional groundwater studies in order to identify the predominant reactions in the aquifer. However, this simple mass balance approach cannot be successfully applied to areas where groundwater mixing occurs. In order to address this problem multivariate mixing had been developed and applied in situations where different water types exist.

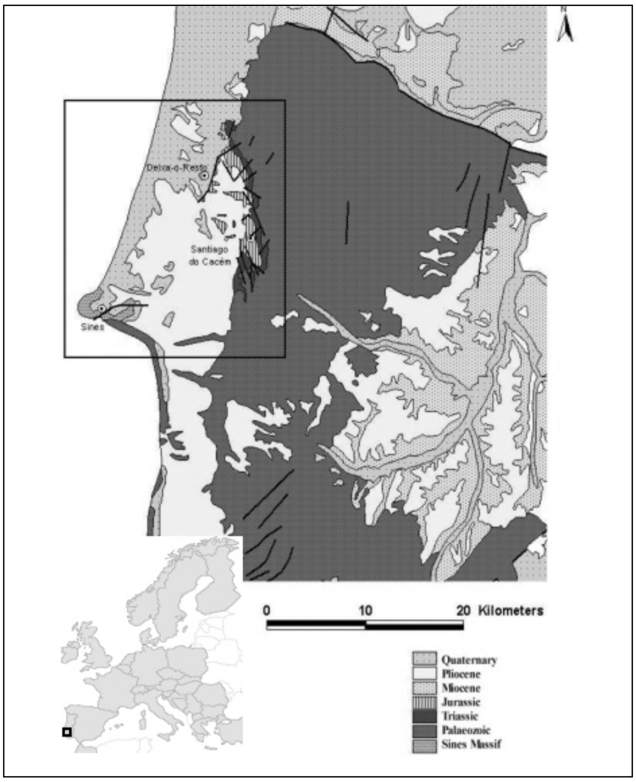

*Figure 1: Location of Sines basin.*

## 2. Geological and Hydrogeological Setting

The Sines sedimentary basin is situated in the Portuguese Atlantic coast and corresponds to a tectonic ditch with a NE-SW orientation filled with Mesozoic and Cenozoic deposits (Inverno, 1993) (Figure 1). The basin deposits have an angular contact with Paleozoic basement rocks in the E and S, with the Sines Subvolcanic Massif at the SW and with Quaternary and Tertiary deposits through the Deixa-o-Resto fault in the west. The local Mesozoic sequence begins with Triassic deposits consisting of sandstone, evaporite and carbonate series (Grés de Silves Formation) overlaid by tuff of the Volcanic-Sedimentary complex.

Carbonate layers with clastic rocks at the top compose the Jurassic sequence. The Liassic is represented by dolomite, dolomitic marl and oolitic limestone with an average thickness of 100 m. Oolitic limestone, microcristaline limestone and rare dolomite and marl compose the Dogger, presenting a maximum thickness of 400 meters. The Malm with about 600 m is constituted by a sequence of conglomerates, limestone, clay and marl (Manuppela and Moreira, 1989).

Miocene deposits (clayey sandstone, marl and marly limestone), Plio-Plistocene detrital (sand and clay) and recent alluvial and dune deposits partially covered by the Mesozoic formations.

Two hydrogeological systems were identified in the Sines basin: the Mio-Pliocene and the Jurassic areas (Figure 2). These hydrogeological systems supply the entire region, in which some areas are highly populated and industrialized. In the Mio-Pliocene system the recharge of the aquifer comes directly from the outcrop areas, while in the Jurassic areas the recharge occurs directly in outcrops of carbonate formations and furthermore receives some contribution from the overlain Miocene layers. The main discharge of the systems should be in the continental platform, although some small natural springs spout inland. These two aquifers seem to have a hydrological connection through recharge of the Jurassic aquifer through the Miocene layers.

In the Sines Basin the precipitation varies from 600 mm to 765 mm at Santiago do Cacém and the potential evapotranspiration is about 750 mm/year (Lavaredas and Silva, 1999a). Analyzing the precipitation records shows the influence of the topography in the amount of precipitation over Sines Basin. The values of mean annual precipitation increase to the interior where the altitude is higher (Grândola and Cercal Ridges of mountains).

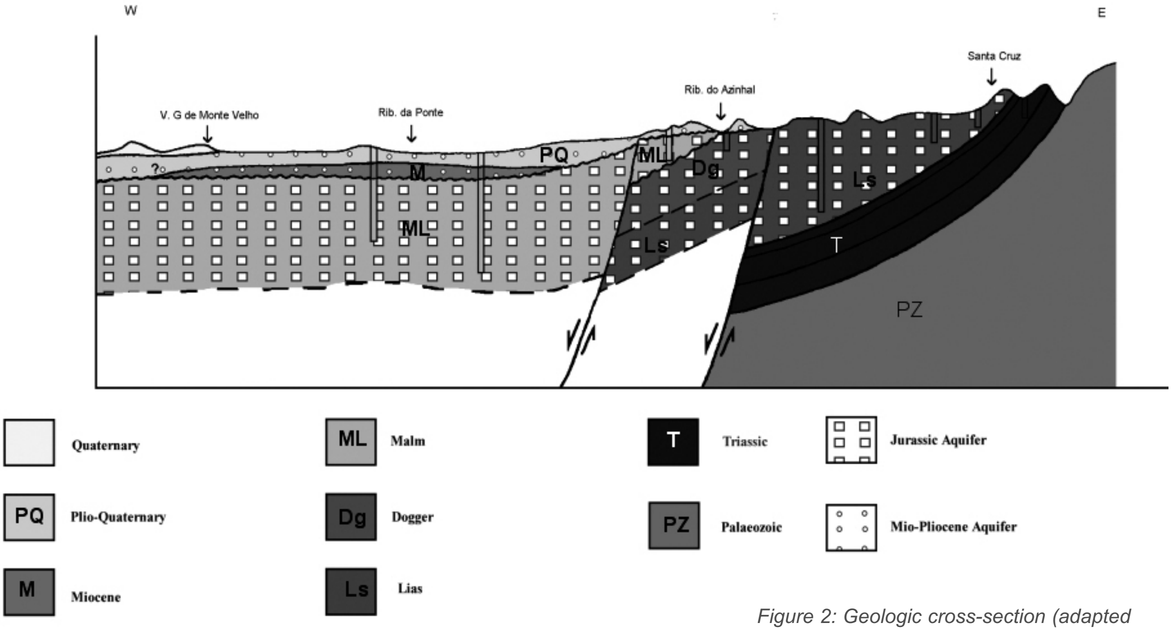

Figure 2: Geologic cross-section (adapted from Inverno et al, 1993).

The main groundwater flow direction of the Jurassic aquifer is E to W towards the Atlantic Ocean. In the central part of the area, near Santo André Lagoon, a concentration of wells supplying water to Santiago do Cacém city, yields a piezometric depression (Figure 3), although the system is not in stress and does not present “important” variations in time from one season to another. This could be a result of a recharge contribution from the Tertiary formations to the Jurassic system (Galego Fernandes, 2004a).

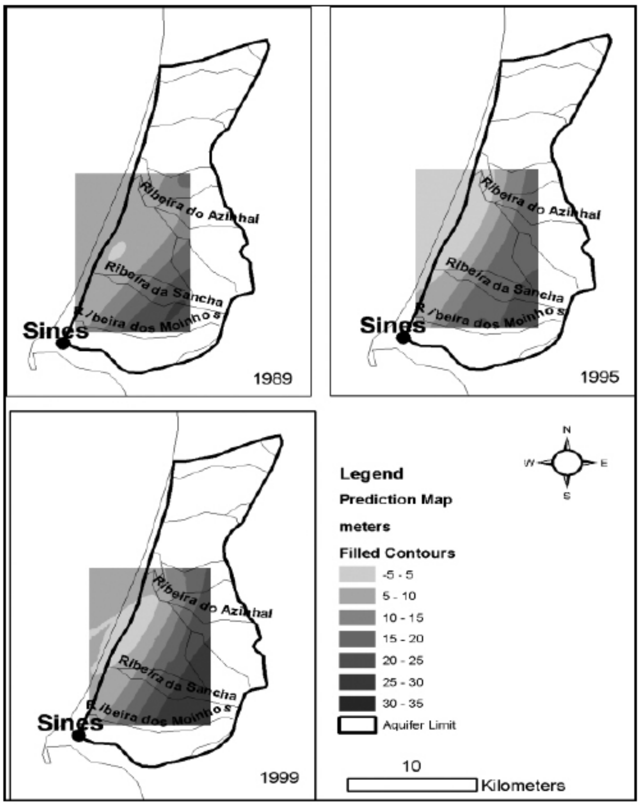

Figure 3: Sines basin piezometric map

## 2. Field and laboratory methods

Five field campaigns were performed between 1997 and 2001 in the Sines area where a total of 40 points were sampled (dug wells, drill wells and springs). Groundwater samples were collected for physical-chemical analysis. A piezometric characterisation was also established. The physical and chemical analyses were performed in all water samples; major cations and anions and for some of the campaigns the content in Fe, Cu, Al and Mn were determined.
Temperature (ºC), pH and electrical conductivity (□S/cm) were determined in situ at the time of the sampling. Total alkalinity was measured a few hours after the sampling by $H^2SO_4$ titullation at 0.1 N until the pH value of 4.45
The following methods were used in chemical analyses performed at the Waters Laboratory of Centro de Geologia from the Universidade de Lisboa (FCUL) and at the Laboratório da Direcção Regional do Ambiente do Alentejo (DRAA): EDTA complexometry for Ca and Total Hardness; Mass spectrometry for Cl, $NO_3$, $SO_4$, F, Br; atomic absorption for Na and K.

## 4. Hydrochemical features

Several hydrogeological and hydrochemical studies of the Sines basin, in order to evaluate its groundwater resources and to allow the chemical characterization and evolution along the flow paths have been performed (Lavaredas and Silva 1999a, 1999b, Galego Fernandes and Silva, 1999, Galego Fernandes et al., 2001a, 2001b, 2004b ).
We use physical and chemical data from the Sines basin groundwater system, which resulted in the most recent and more complete campaigns performed in the region between 1999 and 2001. The average, standard deviation, maximum and minimum values of the data from this period are given in Table 1.

| 1999 | | | 2001 | | | | | |
|---|---|---|---|---|---|---|---|---|
| | Average | Standard Deviation | Max | Min | Average | Standard Deviation | Max | Min |
| EC (µS/cm) | 729.2 | 258.3 | 1420 | 175 | 708.3 | 224.9 | 1179 | 235 |
| pH | 6.9 | 0.4 | 7.6 | 5.7 | 7.7 | 0.2 | 7.9 | 7.6 |
| Na (mg/l) | 37.9 | 16.1 | 82.3 | 0.04 | n.a. | n.a. | n.a. | n.a. |
| Mg (mg/l) | 30.8 | 13.9 | 57.3 | 5 | n.a. | n.a. | n.a. | n.a. |
| K (mg/l) | 2.8 | 1.4 | 7.9 | 0.8 | n.a. | n.a. | n.a. | n.a. |
| Ca (mg/l) | 65.9 | 28.2 | 120 | 5.75 | 67.0 | 27.3 | 101.6 | 4.8 |
| $HCO_3$ (mg/l) | 298.6 | 128.0 | 566 | 41 | 277.6 | 132.5 | 518 | 32 |
| $SO_4$ (mg/l) | 47.8 | 44.4 | 200.0 | 3.0 | 47.2 | 40.6 | 166.0 | 11.2 |
| Cl (mg/l) | 84.5 | 44.1 | 258.0 | 26.0 | 73.4 | 46.0 | 243.0 | 26.3 |
| $NO_3$ (mg/l) | 19.8 | 15.0 | 93.4 | 4.7 | 26.3 | 32.8 | 147.0 | 0.2 |
| Fe (mg/l) | 0.067 | 0.077 | 0.400 | 0.002 | n.a. | n.a. | n.a. | n.a. |
| $CO_2$ (mg/l) | 22.6 | 11.6 | 45.8 | 4.4 | n.a. | n.a. | n.a. | n.a. |
| Cu (mg/l) | 0.008 | 0.024 | 0.144 | 0.001 | n.a. | n.a. | n.a. | n.a. |
| Al (mg/l) | 0.083 | 0.098 | 0.597 | 0.007 | n.a. | n.a. | n.a. | n.a. |
| $PO_4$ (mg/l) | 0.033 | 0.031 | 0.130 | 0.002 | n.a. | n.a. | n.a. | n.a. |
| Mn (mg/l) | 0.010 | 0.020 | 0.119 | 0.002 | n.a. | n.a. | n.a. | n.a. |

*Table 1: Comparison between1999 and 2001 campaigns in Sines basin. To 1999 campaing n=38 and to 2001 campaign n=20. n.a. – not analysed*

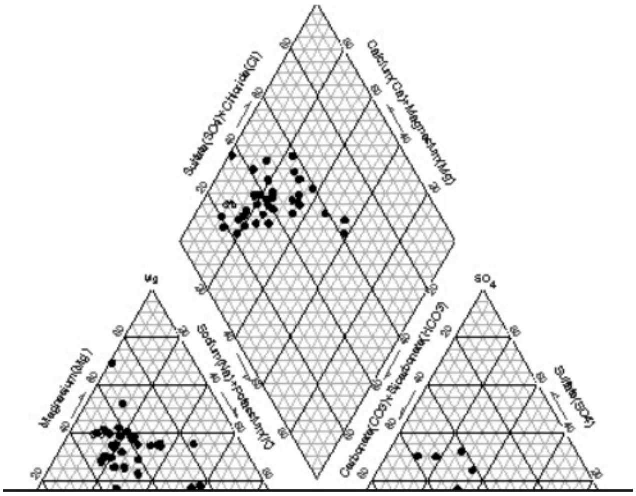

The lithological composition of the aquifer's matrix is dominated by calcareous and dolomitic layers, recognized in the groundwater chemical evolution where the water-rock interaction processes are considered important in the definition of their calcium-bicarbonate type visible in a Piper diagram (Figure 4), in which dispersion in the cation (calcium and magnesium) content of the groundwater samples is shown.

*Figure 4: Piper diagram showing the ionic composition of groundwater in Sines Basin from 1999 campaign.*

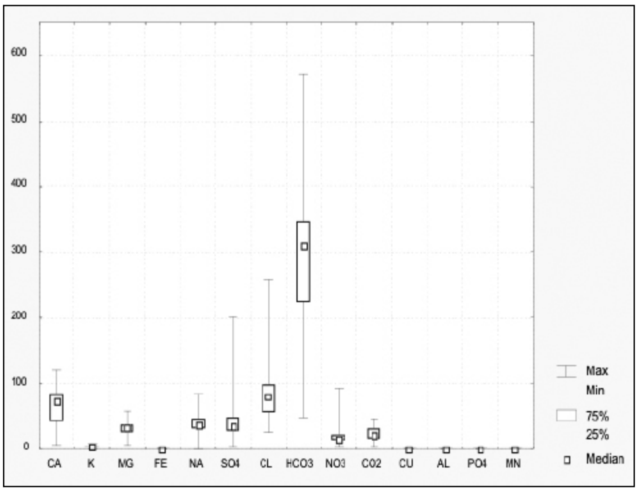

*Figure 5: Box Plot of chemical analysis from 1999 campaign in Sines basin*

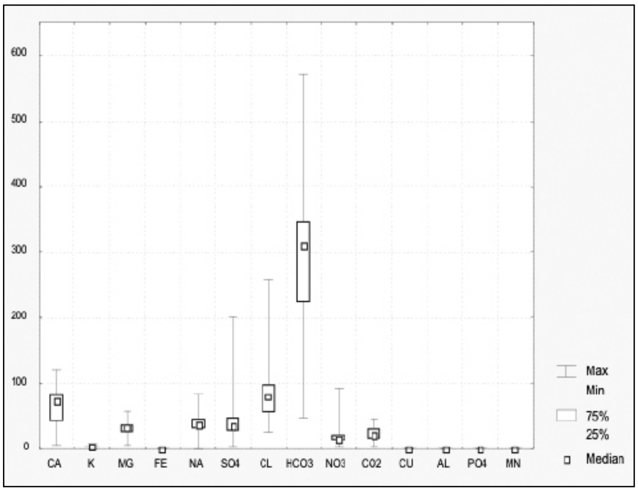

*Figure 6: Box Plot of standardised parameters in Sines basin from 1999.*

This groundwater evolution could be associated either to lithological heterogeneities within the sedimentary basin or whichever with human activities by the use of fertilizers/pesticides.

Boxplot of the chemical concentrations show that bicarbonate, calcium, sulphate, chloride and nitrate have the largest dispersions (Figure 5). The enrichment in chloride and sodium from values of 70 to 200 mg/l and 25 to 70 mg/l, respectively, is present in the waters located near the Moinhos River (in the S of the area). The increase in the salt concentration could be associated to different mechanisms: water-rock interaction processes, dissolution of Hetangian evaporites, mixture with actual seawater through the river substratum and/or mixture with ancient seawater trapped The chloride, nitrate and sulphate content also show a significant difference between the medium and maximum values, mean values are near a quarter of the maximum values, suggesting local contamination inputs to the groundwater system. The wide range of values in the bicarbonate content, from 50 to 600 mg/l, is the result of the lateral geological variations of the layers conferring to the groundwater different concentrations of bicarbonate.

After the standardizing of the results (Figure 6), all the physical and chemical parameters from the statistical point of view have the same weight in the groundwater evolution and characterization. For some parameters, such as $PO_4$, Al, Cu, Mn, $SO_4$, $NO_3$ and Fe, the median is close to the minimum which suggests the presence of an anthropogenic source to the aquifer system, probably indicating pollution input to the groundwater by agricultural or cattle breeding activities.

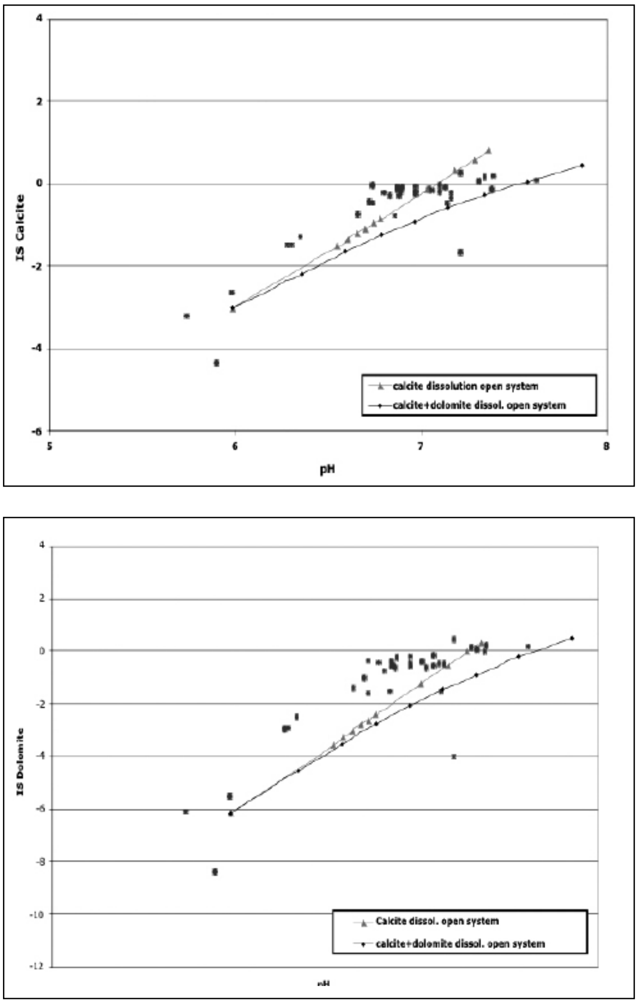

Figure 7: Calcite and Dolomite Saturation Index versus pH.

### 4.1. Hydrogeochemical evolution of groundwater

If we assume the evolution from the Miocene waters to Jurassic waters, it is expected that waters progressively increase the concentrations of chemical constituents. The higher Ca and $HCO_3$ concentration could be explained by the calcite and dolomite dissolution. Calculated saturation index (S.I.) indicated that the majority of groundwaters are in equilibrium with respect to calcite and dolomite (Figure 7). The progressively increasing pH values, Ca, Na, $SO_4$ and $HCO_3$ concentrations due to increased water rock interaction would ultimately result in saturation with respect to calcite and dolomite, materialised by the Jurassic waters that are in equilibrium or saturated in those minerals.

#### 4.1.1. Possible scenarios: calcite dissolution at open system or calcite and dolomite dissolution at open system

Using a simple mass balance model through the PHREEQC program, these two scenarios were tested. The reaction path was assumed to be such that Miocene waters observed at shallow depths evolved to more mineralised waters. We considered a path that initiated in sample F5 and that was calculated the behaviour of groundwater mineralisation with different percentages of calcite dissolution.

Figure 8 shows the results of modelling, with calcite dissolution in open and calcite and dolomite dissolution at open system. Were also projected all the samples analysed to evaluate the behaviour of groundwater from the both aquifers. It is possible to notice the presence of a group of Jurassic waters that are projected along the line that represent the waters evolution in open system, indicated that probably Jurassic waters have an important contribution from the Miocene water-rock interaction.

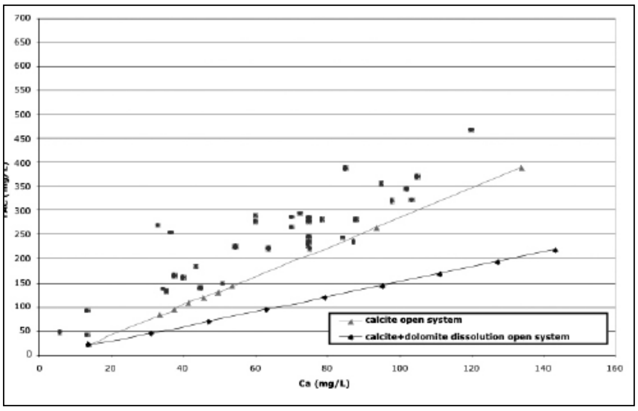

*Figure 8: Results of the simple mass balance modeling, showing the relationship between TAC and Ca concentration.*

### *4.1.2. Mixing between Miocene and Jurassic waters*

The samples F5 and F3 were considered as representative Miocene and Jurassic aquifers, respectively (Table 2). An ideal mixing solution with a given chemistry is calculated in accordance with the mixing ratio by using the program PHREEQC (Parkhust and Appelo, 1999). The purpose of the modelling was to delineate the hydrogeochemical status of some Jurassic waters which are probably influenced by mixing. The results projected in a Piper diagram when compared with groundwaters samples from the both aquifers indicated that chemical mixing is also likely to be taking place in Jurassic aquifer (Figure 9).

| | pH | T | EC | Ca | K | Mg | Fe | Na | SO$_4$ | Cl | HCO$_3$ | NO$_3$ | CO$_2$ | Cu | Al | Mn |
|---|---|---|---|---|---|---|---|---|---|---|---|---|---|---|---|---|
| F3 | 6,74 | 19,2 | 1093 | 120 | 3,28 | 42,75 | 0,01 | 53,5 | 42 | 88 | 570,96 | 37,9 | 45,76 | 0,00231 | 0,07632 | 0,0021 |
| F5 | 5,98 | 19,8 | 246 | 13,25 | 3,43 | 5 | 0,13 | 29 | 3 | 49 | 48,8 | 20,6 | 18,92 | 0,00476 | 0,07856 | 0,00761 |

*Table 2: Composition of F3 (Jurassic) and F5 (Miocene) groundwater. (EC - µS/cm, T- ºC and remain parameters mg/L).*

Under such conditions, mixing occurs simultaneous with geochemical reactions thereby influencing mass transfer; therefore, application of simple mass balance models only considering chemical reactions is not satisfactory. Therefore, is important consider the hydraulic mixing in the studied aquifers where is suggested that the geochemical reactions were less important than mixing in influencing the chemical composition of Jurassic groundwater.

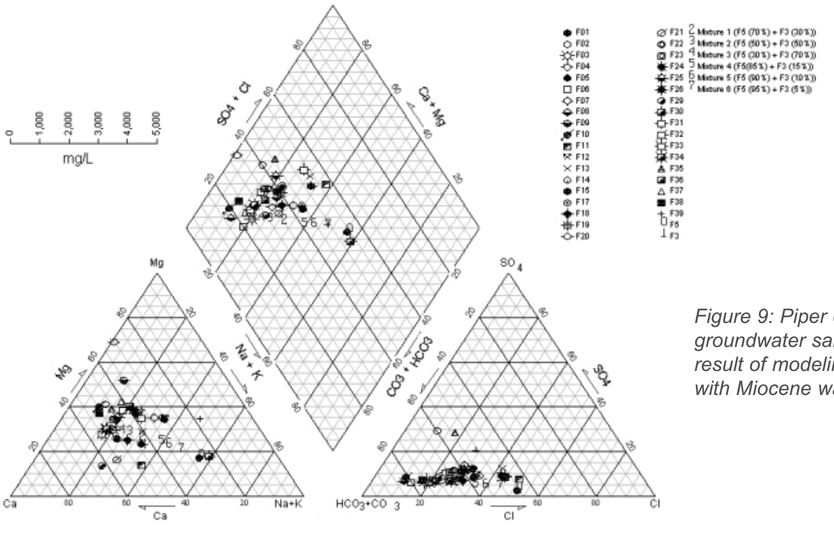

*Figure 9: Piper diagram with groundwater samples and the result of modeling (mixing Jurassic with Miocene waters*

## 5. Conclusions

The hydrogeological system in the Sines basin supplies a highly populated region having industrial and agricultural activities. The amount of precipitation stores a consistent recharge, leading to an aquifer system that is not in hydraulic stress and does not present major temporal variations both in quantity and quality.

Simple mass balance modelling using hydrochemical data showed that Jurassic waters evolved from shallow groundwaters (Miocene aquifer) mainly by calcite and dolomite dissolution. Furthermore, mixing modelling suggested that the chemical composition of Jurassic groundwater is influenced by hydraulic mixing between a more mineralised Jurassic groundwater and a shallow Miocene groundwater with lower content in the major elements.

In Sines in nowadays the protection limits for the groundwater quality are respected. However, through the use of qualitative and quantitative evaluations, some nitrate contamination problems are still identified as a result of some agricultural and cattle breeding activities, which lead us to suggests a rigorous control of possible contamination sources, such as effluent management and others.

## Acknowledges

P. Galego Fernandes acknowledges to FCT (Portugal) the Ph grant SFRH/BD/932/2000. The study was supported by FCT research project POCTI/35258/CTA/2000.

## References

- Galego Fernandes P, Silva M (1999) Contribution to the Hydrogeological Characterization of the aquifer system of Sado's Basin. International Association of Hydrogeologists, Bratislava, publ. CD-ROM.
- Galego Fernandes P, Carreira P, Silva M O (2001a) A Hidrogeoquímica na definição do modelo hidrodinâmico do sistema aquífero da Bacia do Sado (Hydrogeochemistry in the hydrodinamic model definition in the Sado basin aquifer). VI Congresso de Geoquímica dos países de Língua Portuguesa – XII Semana de Geoquímica, Faro, p. 435-439.
- Galego Fernandes P, Carreira P, Silva M O (2001b) Use of hydrochemistry and isotopes as tracers in the Sado-Sines sedimentary basin (S Portugal). New Approaches to Characterising Groundwater Flow, XXXI IAH Congress, Munich, v. I, p, 65-70.
- Galego Fernandes P. (2004a) Estudo Hidrogeológico dos sistemas aquíferos Sado-Sines - Evolução Hidrogeoquímica e Isotópica: Dissertação para obtenção do grau de Doutor em Geologia, especialidade Hidrogeologia, FCUL, Departamento de Geologia, 213 p.
- Galego Fernandes P, Carreira P, Silva M O (2004b) Identification of anthropogenic inputs through PCA into Sines Coastal Aquifer (SW Portugal). 32nd International Geological Congress, Florence, Abstract volume, publ. Cd-ROM
- Inverno C (1993) Estratigrafia (Substrato hercínico) (Stratigraphy Hercinic substratum)). Notícia explicativa da folha 42C Santiago do Cacém, Carta geológica 1/50 000, serviços geológicos de Portugal.
- Lavaredas J, Silva M O (1999a) Hydrogeochemistry of Sines aquifer system. European Union of Geosciences 10, Strasbourg. v. 4, no. 1, p. 749.
- Lavaredas J, Silva M O (1999b) Sines's aquifer system - Some contribution for its knowledge. International Association of Hydrogeologists, Bratislava, publ. CD-ROM.
- Manuppella G, Moreira J (1989) Calcários e dolomitos das áreas de Melides – Santiago do Cacém (Limistones and dolomites in Melides area – Santiago do Cacém). Estudos, Notas e Trabalhos, D.G.G.M., Lisboa, v. 31, p. 79-94.
- Parkhust D L, Appello C A J (1999) User's Guide to Phreeqc (version 2) – A Computer Program for Speciation, Batch-Reaction. One Dimensional Transport and Inverse Geochemical Calculation. USGS Water-Resour. Invest. Rep. 99-4259, 312.

# DARCY 11

# Modeling of chlorinated solvents transport and natural attenuation in groundwater

QUIOT Fabrice1; ROLLIN Claire[1]; BOUR Olivier[1]; JORDANA Salvador[2]; RUIZ Eduardo[2];
GUIMERÀ Jordi[2]; SCHWARTZ Jean[3]; GOBLET Patrick[4].

[1] INERIS, Parc Technologique ALATA - BP 2, 60550 Verneuil-en-Halatte
France, fabrice.quiot@ineris.fr
[2] ENVIROS, Spain S.L., Passeig de Rubí 29-31, 08197 Valldoreix
Spain, sjordana@enviros.biz
[3] ANTEA, Direction Technique, 3 avenue Claude Guillemin
BP 6119, 45061 Orléans Cedex 2 – France, j.schwartz@antea-ingenierie.fr
[4.] Ecole des Mines de Paris (ENSMP), Centre d'Informatique Geologique,
35 Rue Saint Honore, 77305 Fontainebleau – France, Patrick.Goblet@ensmp.fr

## Abstract

The objective of this study is to test differents modeling approaches and the reliability of the codes used in water risk assessment for a site contaminated with chlorinated solvents. The final goal is to elaborate, within the framework of the TRANSPOL research program, a guideline that could be used as a scientist support for contaminated aquifers management. The models performed by 4 teams (ANTEA, ENSMP, ENVIROS and INERIS) to simulate a contamination of groundwater by perchloroethene were compared. The total amount of perchloroethene discharged into the aquifer was unknown and a simplified conceptual model was considered. A first synthesis of the results obtained shows two principal difficulties : evaluate source concentration and simulate natural attenuation phenomenon (sorption/degradation). More accurate diagnosis is needed in order to reduce the uncertainties of model parameters.

## 1. Context and Object

When applying a risk assessment approach to contamined sites, of primary importance is the evaluation of the fate of pollutants in groundwaters and soils. This knowledge is based on the result of extensive investigations, available data from monitoring of pollutants in time and space and numerical modeling of the pollutants transport in the environment. In practice, results may vary greatly among users, according to the available data and the requested aims of the risk assessment.

The lack of a reliable methodology may impair high quality expertise. In this context, INERIS (the French National Institute for Industrial Environment and Risks, www.ineris.fr) has developed a research program, TRANSPOL, to bring a better and common practice of the use of transport models for different groups of pollutants. The chosen way to reach this objective is based on the comparison of the methodologies used by private consultancies, universities and research centers.
This article presents results of a real case study, named Real Case 3, concerning chlorinated solvents fate, transport and natural attenuation in groundwater. The aim of this study is to develop a natural attenuation model to predict the fate and transport of chlorinated solvents and their degradation products in saturated groundwater systems.

## 2. Site description

A contaminated alluvial aquifer in northern Spain (cf. Figure 1), has been studied by ENVIROS since 2000. Figure 2 presents a conceptual cross section model of the site.

The site has a length of 1 000 meters along the direction of groundwater flow (S-N) and is 600 meters wide. A river crosses this site (Ter river).

The aquifer thickness is 16 meters including a 6 meters thick vadose zone. The sedimentary materials are unconsolidated and very heterometric (from clay to rolling cobbles), with an heterogeneous composition (from limestone and sandstone to metamorphic and igneous rocks).

perchloroethene (PCE) is the primary solvent contaminant that was originally disposed at this industrial site. However, concentrations of chlorinated solvent degradation products such as trichloroethene (TCE), cis-dichloroethene and trans-dichloroethene (cis-DCE, trans-DCE) were measured in the monitoring wells located downstream from the source location.

The observation well network is made up of 19 piezometers. 6 of these boreholes are pumping well (with pumping rate ranging between 1 100 to 70 000 m$^3$/year – in PL2 pumping rate is unknown).

There are three potential recharge zones (Cf. Figure 1, irrigation zones are in green). The regional average natural net infiltration value is approximately 150 mm/y.

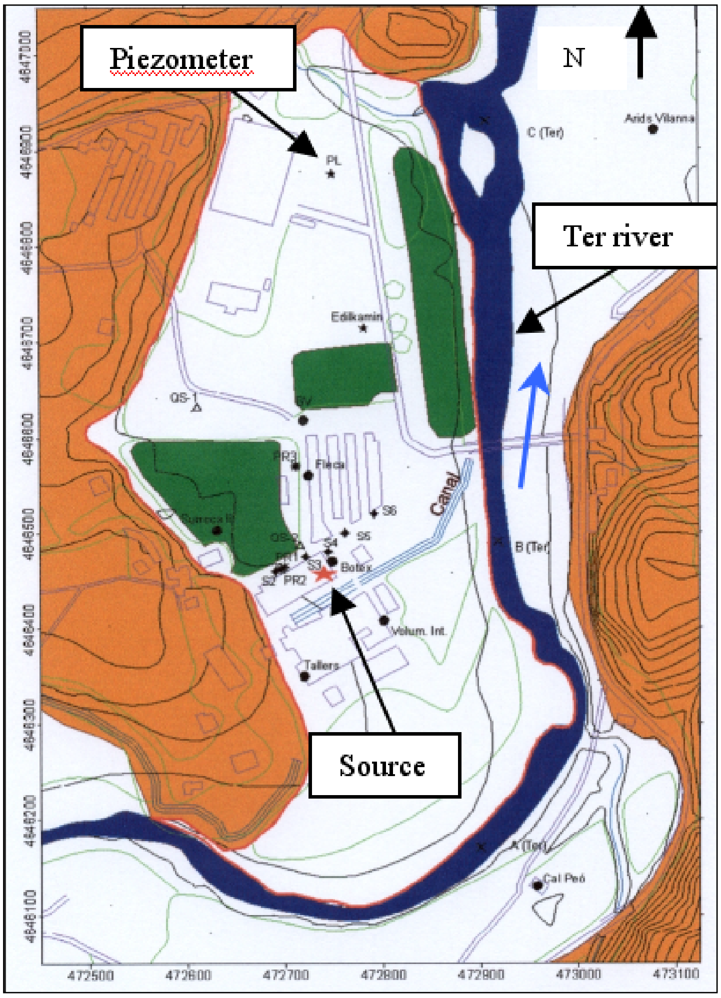

Figure 1: Site details and well locations (UTM coordinates)

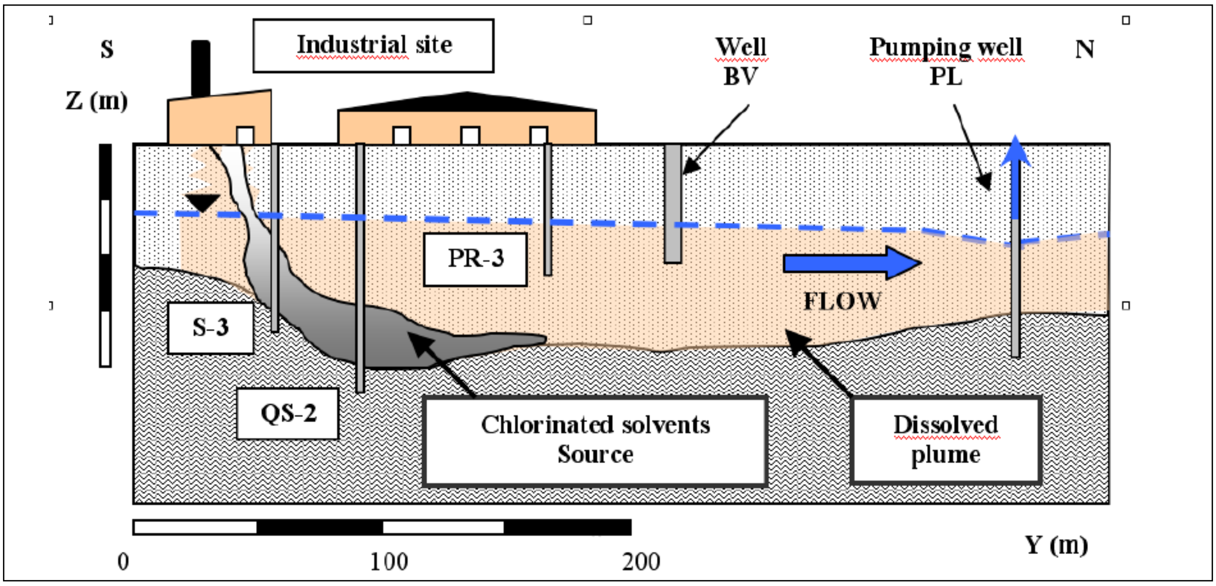

Figure 2: South – North section of the site

## 3. Conceptual model

At a first step, a workshop was held with all modellers to introduce the context (Cahier des charges n°1, Rollin & Bour, 2002), to identify the processes contributing to the behaviour of the pollutant, to select the hydrodynamic and transport parameters, the sources appearing to be the most appropriate…, as they would do in a proper risk assessment.
Conclusions of its workshop were given in a second "Cahier des Charges" (Rollin, 2003). It presents the conceptual model, initial conditions, calibration data (heads and concentrations values)…, these specifications are presented below. Some values and a range of variation were given as an indication. These values resulted from site investigation or from literature.

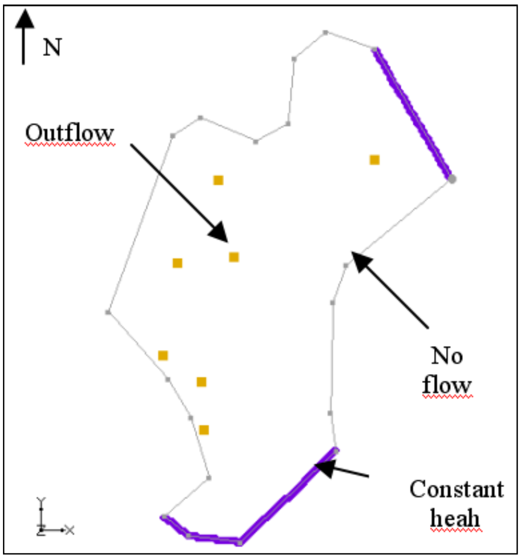

Figure 3: Modelled domain and boundary conditions

### *Conceptual model for groundwater flow*

The boundary conditions are summarised on Figure 3. Flow conditions are assumed to be at steady state. The groundwater hydraulic head values at the model boundaries were based on measured data (december 2003).
The aquifer is modelled as a single, continuous, unconfined unit with spatially variable transmissivity values. The different transmissivity zones implemented in the model were based on pumping tests results and calibration of heads values.

### *Conceptual model for contaminant transport*

The source of PCE is a modelled injection of mass straight to the saturated zone. The injection is located inside a 30 m diameter circle centred in the middle of the industrial building.

The total amount of PCE discharged into the aquifer is an unknown quantity, as it is often occuring on contaminated sites.
The time simulation is 10 years :

- initial time $t_0$ (12 december 1995) : PCE concentration is zero ;
- $t_1$ (15 november 2000) : the plume is stabilised (measured concentrations -16 november 2000- were used to calibrate transport parameters) ;
- $t_0$ to $t_1$ : the injection rate is constant during the first 5 years (R1 in kg/d) ;
- $t_1$ to $t_2$ : the injection rate starts decreasing slightly from the beginning of the 6th year until the end of the 10th year.

High concentrations of PCE and chlorinated solvent degradation products such as trichloroethene, cis-dichloroethene and trans-dichloroethene were observed in the monitoring wells. Reductive dechlorination of chlorinated solvents is therefore suspected.
The kinetics of all the degradation reactions (cf. Figure 4) are assumed to be first order kinetics.

$$\text{PCE} \longrightarrow \text{TCE} \longrightarrow \text{DCE} \longrightarrow \text{VC (Vinyl Chloride)}$$

*Figure 4: Anaerobic degradation pathway of chlorinated solvents*

### Groundwater flow simulations

The relationship between the aquifer and the river was not taken into account by all the teams. The groundwater flow codes were used to simulate the groundwater head distribution. The calibration results were assessed using the differences between calculated and observed heads in 16 piezometers. Errors in computed head values are listed in Table 2.
Table 3 presents the hydraulic conductivity values calibrated in the models.

Sorption processes could be taken into account. It was suggested to use the Kd approach.
Values of transport parameters range are between different literature values and/or estimated values obtained by the concentrations calibration process:

- porosity ;
- dispersivity ;
- molecular diffusion ;
- sorption constants (Kd) ;
- kinetic reaction rates of dechlorination.

| | **ANTEA** | **École des Mines de Paris** | **ENVIROS** | **INERIS** |
|---|---|---|---|---|
| 3D Flow Modeling | MARTHE - DF<br>V. 6.3<br>(déc. 2002) | METIS - EF<br>V1 (mars 2004)<br>and<br>MODFLOW 2000- DF<br>V. GMS 4.0 | TRANSIN- EF<br>V. IV | MODFLOW 2000 - DF<br>V. GMS 5.0<br>(mai 2004) |
| 3D Transport Modeling | MARTHE - DF<br>V. 6.3<br>(déc. 2002) | Metamodel - kriging<br>and<br>RT3D - TVD<br>V. GMS 4.0 | TRANSIN - EF<br>V. IV | RT3D - TVD<br>V. GMS 5.0<br>(mai 2004) |

*EF: finite elements ; DF : finite differences ; TVD : total variation diminuting*

*Table 1: Teams and codes used in the intercomparison bench*

## Groundwater flow simulations

The relationship between the aquifer and the river was not taken into account by all the teams. The groundwater flow codes were used to simulate the groundwater head distribution. The calibration results were assessed using the differences between calculated and observed heads in 16 piezometers. Errors in computed head values are listed in Table 2.
Table 3 presents the hydraulic conductivity values calibrated in the models.

| | **ANTEA** | **ENSMP** | **ENVIROS** | **INERIS** |
|---|---|---|---|---|
| Mean error | 0.04 | 0.14 | 0.09 | 0.04 |
| Mean Abs. Error | 0.05 | 0,06 | 0.04 | 0.03 |
| Root mean Sq. error | 0.002 | 0.004 | 0.002 | 0.001 |

*Table 2: Hydrodynamic calibration – Error summary*

Hydraulic conductivity range from 70 to 350 m/d. The final calibrated values are included in the range of values suggested in the specifications (results of investigations: 60 to 600 m/d).
An anisotropy factor was tested by ENSMP and calibration results were better for piezometers near the source.

| | **ANTEA** | **ENSMP** | **ENVIROS** | **INERIS** |
|---|---|---|---|---|
| Hydraulic conductivity (m/d) | 109<br>and 150 | 150 | 73 | 350, 200<br>and 70 |
| Recharge (mm/y) | 146<br>irrigation zones | 150<br>uniform | Not defined | 150<br>irrigation zones |
| Pumping rate well PL2 (m$^3$/d) | 5 | 0,1 | 0 | 10 |

*Table 3: Hydrodynamic calibration - Hydraulic conductivity*

## Contaminant transport simulations

The models reproduced successfully the general trends of the contamination plumes but the time of peak arrival and the concentration at the observation points may vary more or less according to the use and the different features of the numerical codes. Results show that with such a simple conceptual model (homogeneous, isotropic and with a steady flow with steady boundary conditions), it is impossible to reproduce the oscillating concentrations observed. Thus the concentrations calibration objective was to fit the order of magnitude.
The transport parameters used in the models are summarised in Table 4. Transport properties were estimated based on literature values (for similar types of geologic materials) and calibration (using measured concentrations).

| | | **ANTEA** | **ENSMP** | **ENVIROS** | **INERIS** |
|---|---|---|---|---|---|
| PCE Injection rate R1(kg/d) | | 0,650 | 0,170 | 0,170 | 0,030 |
| Source surface m$^2$ | | 707 | 100 | 91 | 25 |
| Effective porosity $n_e$ (%) | | 10 | 30 | 10 | 20 and 30 |
| Dynamic dispersivity | aL | 30 | 22 | 10 | 20 |
| (m) | aT | 3 | 8,5 | 8 | 4 |
| Molecular diffusion (m$^2$/d) | | Not definited | PCE, TCE DCE and CV $1x10^{-4}$ | PCE, TCE DCE and CV $1x10^{-6}$ | Not definited |
| Bulk density of aquifer (kg/m$^3$) | | 1700 | 1600 | Not definited | Not definited |
| Sorption coefficient Kd (m$^3$/kg) | PCE | $1,4x10^{-4}$ | $9,4x10^{-5}$ | Not definited | Not definited |
| | TCE | $5,8x10^{-5}$ | $9,4x10^{-5}$ | | |
| | DCE | $5,2x10^{-5}$ | $9,4x10^{-5}$ | | |
| | CV | Not definited | $9,4x10^{-5}$ | | |
| First order degradation constant $\lambda$ (d$^{-1}$) | PCE | 0,0004 | 0,0026 | 0,0030 | 0,0030 |
| | TCE | 0,0140 | 0,0001 | 0,0594 | 0,0020 |
| | DCE | 0,0007 | 0,0005 | 0,0174 | 0,0005 |
| | CV | Not definited | 0,0003 | 0,0300 | 0,0030 |

*Table 4: Parameters selected for transport calibration*

The differences in source volume are linked by the choice of its surface and by the injection rate considered (30 to 650 g/d). The variation of the extension of the source and the injection rate are different and influence the range of variation of PCE (TCE, DCE and VC) concentration in models.

Figure 5, Figure 6 and Figure 7 present PCE, TCE and DCE results for six piezometers distributed from source to downstream at 1800 days of simulation (calibration date).

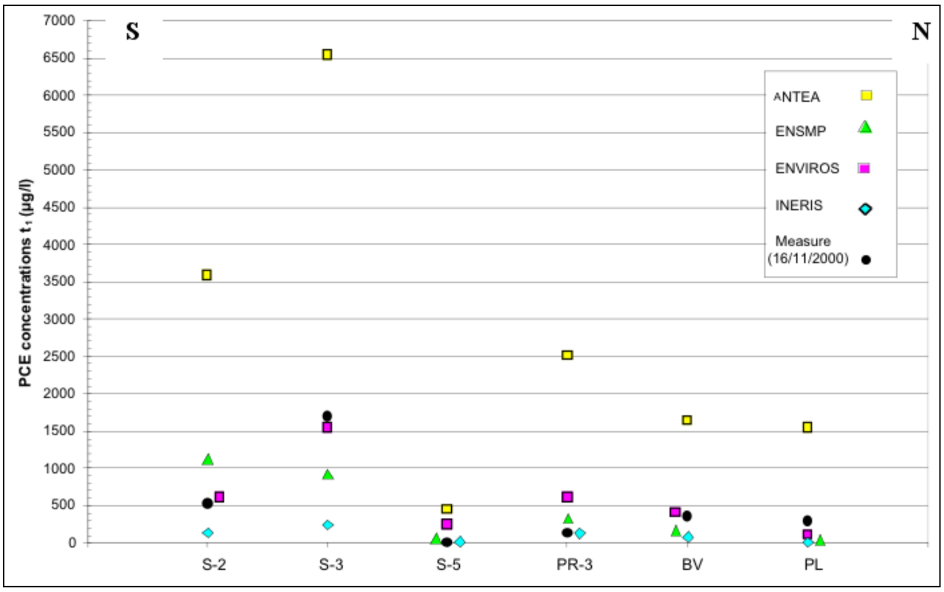

*Figure 5: PCE concentrations (µg/l) at $t_1$*

The higher PCE concentrations are calculated by ANTEA. They consider higher PCE injection rate and source concentration, equal to the solubility (150 mg/l). This hypothesis may be justified by the fact that PCE concentrations are very high in the aquifer near the source (but solubility value is not reached in observation wells, maximum is 29 mg/l in S-2). ANTEA made the choice to calibrate, at a first time, concentrations with piezometers near the source.

Three others models give similar results for PCE except near the source.

Indeed PCE concentrations in S-2 and S-3 are less important for INERIS than ENSMP and ENVIROS. INERIS considers a smaller source concentration and calibrates concentrations principally on piezometers downstream the source. This assumption may be justified by the fact that piezometers downstream the source integrate multiple source information.

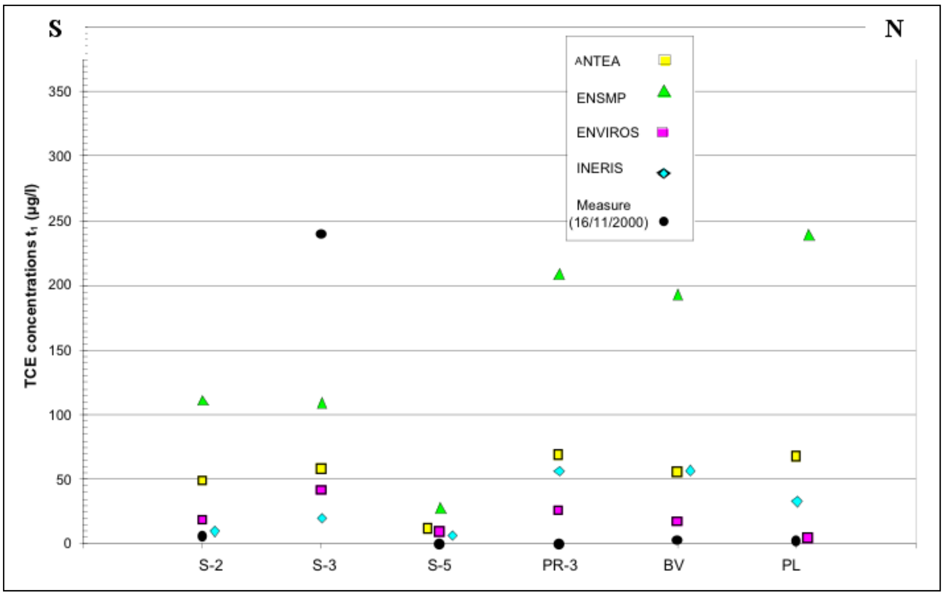

*Figure 6: TCE concentrations (µg/l) at $t_1$*

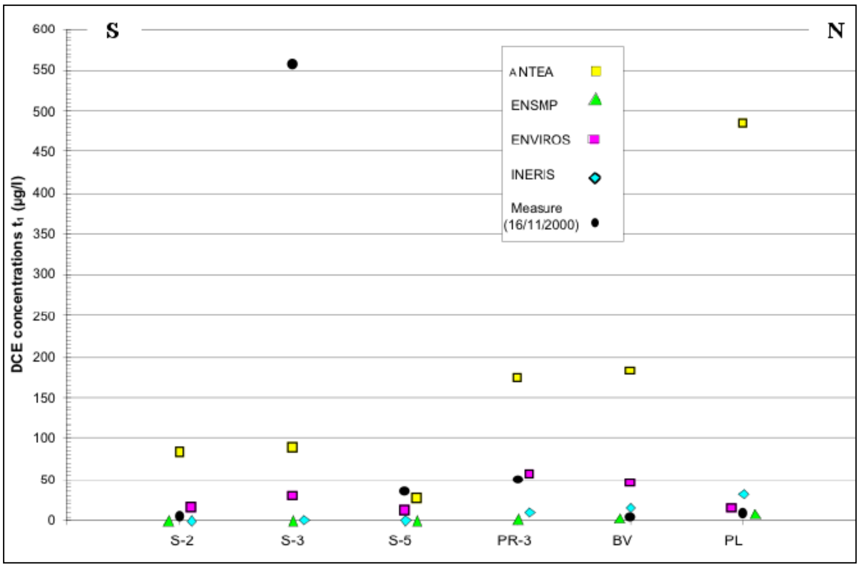

Figure 7: DCE concentrations (µg/l) at $t_1$

Variations of TCE and DCE concentrations results compared to the measured values are mainly due to sorption and degradation conditions. Table 4 summarises the assumed values of sorption and degradation coefficients. Each team gave a different calibrated value.

The four teams considered degradation of chlorinated solvents but values of first order degradation constant are very different. For example in ENVIROS and INERIS models, the first order PCE degradation constant is about 0.003 $d^{-1}$ (constant half life degradation : 230 d), it is about 0.0026 $d^{-1}$ for ENSMP (267 d) but only 0.0004 d-1 for ANTEA (1733 d).

Close to the source area, concentrations observed of DCE is higher than the one of TCE. Thus in the developed models (expect for ENSMP) the degradation factor of TCE is faster than the one of DCE.

Only two teams (ANTEA and ENSMP) considered sorption of chlorinated solvents. The retardation factor considered are 3.4 (PCE); 2 (TCE) and 1,9 (DCE) for ANTEA and 1.5 (PCE, TCE and DCE) for ENSMP

As shown in Figure 8, ANTEA privileges PCE sorption (with high PCE injection) and ENVIROS PCE degradation (with no sorption).

For ENVIROS, no retardation due to sorption processes has been considered. Then values of PCE mass out (by well or limits) and remaining in the model were lower than ANTEA values. The high degradation allows to calibrate concentrations despite a high injection rate.

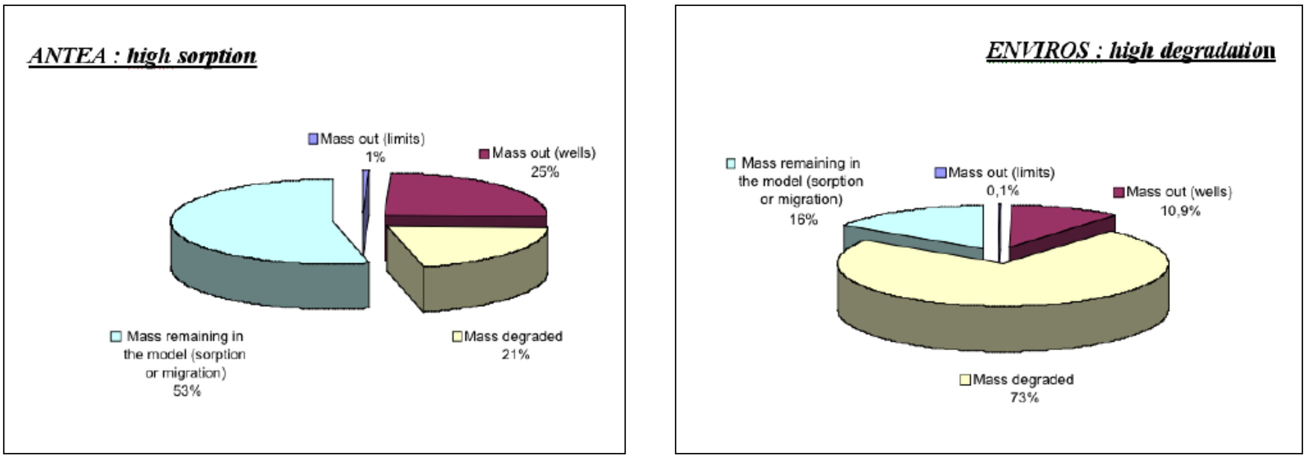

Figure 8: Comparison between ANTEA and ENVIROS PCE mass balance (kg) (0 to 1800 days)

## 5. Conclusion

Multi-species (PCE, TCE and DCE) models were used for modeling transport (homogeneous and isotropic) and natural attenuation processes occurring at a chlorinated solvents release site. Different codes have been used by four modeling teams (ANTEA, ENSMP, ENVIROS and INERIS). The models intercomparison methodology was based on comparison between flow and transport calibration results, calibration parameters values, hypothesis respected and natural attenuation phenomenon considered (particularly sorption and degradation).

Results show difficulty to evaluate :
- source concentration ;
- sorption and degradation.

A more accurate diagnosis is needed in order to reduce the uncertainty of model parameters and to try to improve the conceptual model. Thus, more accurate data were studying for the second semester 2005, concerning :
- the hydraulic conductivity ;
- the presents distribution of pollutants ;
- the location and rate of source term ;
- the degradation and sorption rate of each substance.

These new data will lead to realise a second phase of intercomparison to evaluate these parameters contribution to the new calibration results.
TRANSPOL results are presented on website : http://transpol.ineris.fr/

## Acknowledgements

We thank the participants of the TRANSPOL program for their contributions to the research program (ANTEA, ENSMP and ENVIROS) as well as the French Ministry of the Environment and of the Sustainable Development for the financial support.

## References

- Dan, A. ; Goblet, P. (2004) – Programme TRANSPOL II (INERIS 2003). ENSMP-CIG-LHM/RD/04/18.
- Poirot, N. ; Schwartz, J. (2004) – Impact d'un déversement de composés chlorés sur la qualité des eaux souterraines – TRANSPOL II - Cas Réel n°3. ANTEA- A33548/A.
- Quiot, F. (2004) – Modélisation hydrogéologique d'une nappe alluviale polluée par des solvants chlorés TRANSPOL - Cas Réel n°3. INERIS-DRC-04-55503/DESP-R01.
- Rollin, C. ; Bour, O. (2002) – TRANSPOL II Cahier des charges pour la réalisation d'un modèle numérique (CdC n°1). Cas réel n°3 : impact d'un déversement de composés chlorés sur la qualité des eaux souterraines – INERIS-DRC-02-25294/DESP-R18.
- Rollin, C. (2003) – TRANSPOL II Cahier des charges pour la réalisation d'un modèle numérique (CdC n°2). Cas réel n°3 : impact d'un déversement de composés chlorés sur la qualité des eaux souterraines - INERIS-DRC-03-46524/DESP-R01.
- Ruiz, E. ; Jordana, S. ; Guimerà, J. (2004) – Simulations of the impact of a spill of chlorinated compounds on groundwater quality – TRANSPOL II - CR-3. ENVIROS R-2225-r1.

# DARCY 12

## Practical Application of Quasi-Static Stage of Ground Water in Low Permeability, Phreatic Aquifers in Hard Rock Terrain.

Dr. LIMAYE, Shrikant Daji.
Director, Ground Water Institute, 2050 Sadashiv Peth, Pune 411 030, India.
limaye@vsnl.com

### Abstract

In many developing countries, whatever small quantity of water available from hand-dug wells in phreatic aquifers of low hydraulic conductivity is the lifeline for drinking water supply and small-scale irrigation for millions of the rural people. However, phreatic aquifers of low and very low hydraulic conductivity (K) have received much less attention in hydrogeological studies than the highly productive confined aquifers. These aquifers include sparsely fractured basalt and granite underlying a few meters thick cover of clayey weathered zone; alluvium with predominance of clay and silt; and marley limestone. Frictional forces play an important role in the regime of ground water flow and 'reservoir knowledge' is essential for managing exploitation and recharge augmentation in these aquifers. For the phreatic flow in small watersheds, the total head available for the flow as well as the gradient is often very small, especially in summer season. Under these conditions, the Darcy's Law could be written as:
$Q = K\,A\,(g - g')$
Where g is the gradient causing the flow and g' is the threshold gradient necessary to cause motion against the friction between the pellicular water and the water in slow motion, in the aquifer with low-permeability (K). When g becomes equal to g' the gravitational flow would stop but forces of transpiration by phreatophytic trees and evaporative forces at the wet patches at the exposed faces of the aquifer, would still cause some movement of water. This is the quasi-static stage of phreatic ground water in low permeability, water-table aquifers. During the summer season the natural springs at the exposed face of the aquifer may be reduced to only wet patches, but a little distance away from the exposure, the aquifer carries some water which may be used by digging a well for providing drinking water supply to a small hamlet. This paper discusses the practical applications of quasi-static stage under conditions of low values of K and horizontal variations in K.

### Introduction

If all the strata were of very high porosity and of uniformly high hydraulic conductivity (permeability), any precipitation would have immediately infiltrated and the ground water resources would have drained into the sea within a very short time. The earth would have become a dry place indeed. Luckily, we have vertical variations in the permeability of strata giving rise to confined aquifers and horizontal variations in permeability controlling the movement of water from recharge area to discharge area. In a phreatic aquifer in a hard-rock terrain, comprising soft, weathered & fractured strata overlying an impermeable basement, the recharge area is spread all over the watershed. The recharge collected over the basin is guided towards lower elevations by the profile of underlying hard basement. Ground water discharge from a watershed occurs at the springs oozing out at the intersection of water table with ground surface, on the stream-bank or streambed, or as underflow below the streambed. Any horizontal variations in the permeability result in deflecting, bisecting or exposing the flow. This divides a watershed into smaller segments with smaller values of the hydraulic head operating the flow. Movement of phreatic ground water is under gravitational force and all loss of head along the

flow-path is due to frictional forces. A wooden block kept on an inclined plane would start sliding down, only when the angle of inclination of the plane becomes more than the angle of repose. During ground water movement, the frictional forces act between the moving water and the pellicular water adhering to the matrix. In the low-permeability strata the surface area on which these frictional forces act is much larger than that in the high permeability rocks. In phreatic flow in small watersheds, the total head available for the flow as well as the gradient is often very small, especially in summer season. Under these conditions, the Darcy's Law could be written as:
$Q = K A (g – g')$

Where Q is the volume of water flowing in cu. m per day, A is the area in sq. m, K is the hydraulic conductivity in m/day, g is the gradient causing the flow and g' is the minimum or the 'threshold' gradient required for overcoming the frictional forces in the low-permeability aquifer.

## Earlier Work

Mr. Daji G. Limaye, the author's father, being one of the pioneering hydrogeologists in India, observed during his field work in low permeability fractured basaltic rocks of western India (Deccan traps) that the dug-wells on a basaltic plateau could yield a small quantity of water in summer, even though the springs issuing out from the exposed face of the phreatic aquifer at the edge of a plateau were dry. This means that a dry, exposed face of a low-permeability phreatic aquifer does not necessarily mean a totally dry condition of the aquifer away from the exposure. This led him to think about the role of frictional force in low permeability phreatic aquifers (D.G.Limaye, 1949), which could stop the movement of ground water.

In the region of Monsoon rains like India, the rainfall occurs in four months (June to September) of rainy season, followed by four months of mostly dry winter and four months of hot, dry summer. In small watersheds or sub-basins, the value of gradient g causing the flow of ground water is high at the end of Monsoon rains but it gradually reduces towards summer, due to depletion of water table caused by natural outflow. Several dug wells pumping water during winter season also expand their area of influence and accelerate the depletion. In view of this, each dug well has a limit of expansion of its area of influence till the gradient of flow reaches the 'threshold gradient'. This sets up a limit for recoverable ground water in low-permeability basalt rocks of western India. (Limaye D G & Limaye S D, 1979)

However, when g becomes equal to g', only the gravitational force is balanced by the friction. Evaporation and transpiration forces are more powerful. The phreatic flow does not completely stop but attains a stage in which the flow is controlled by the evaporation and transpiration from the exposed portions of the phreatic aquifer. The phreatic ground water body thus reaches a 'quasi-static' stage.

## Practical Cases

Fig 1 shows a cross section along the gently sloping bed of a stream rising on a plateau and falling over its steeply sloping edge. The phreatic aquifer, comprising laterite, lateritic clay and fractured rock forms a cover over an impervious basement. The aquifer gets fully recharged during the Monsoon rains and water table at the end of the rainy season assumes position indicated by line (a). The spring (indicated by the arrow) issuing at the junction of the low permeability cover with the underlying hard rock drains ground water in the watershed during the

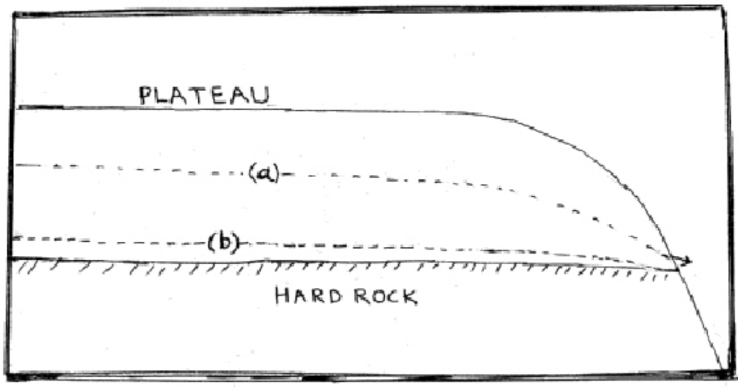

Figure 1: Spring draining ground water from a plateau

dry winter season. The water table recedes towards the base of phreatic aquifer, which often has a lower permeability. The discharge gradually reduces to a mere trickle by the beginning of dry & hot summer season. Line (b) indicates the depleted position of the water table by mid-summer, when the spring is just a wet patch, supporting some vegetation. A quasi-static stage is now reached as the gradient driving the ground water flow is at 'threshold value'.

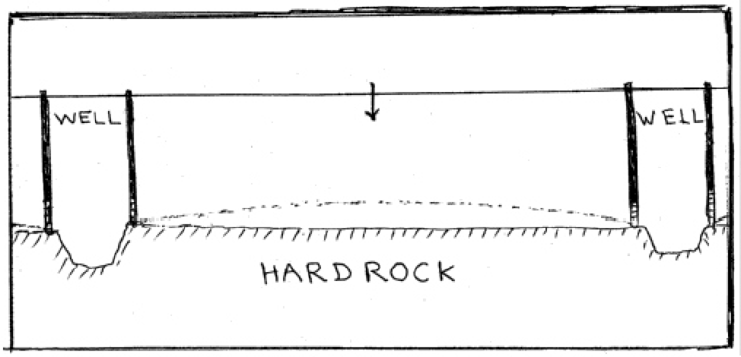

Figure 2: Arrow indicating a possible location for a new dug well between almost dry wells.

Sometimes, the strata exposed at the face of the spring are weathered into very low-permeability clayey formation, having a high capillary suction. If the total head driving the flow is less than the value of this capillary rise, then also a 'quasi-static' stage is reached. The tension-saturated capillaries support vegetation but prevent the delivery of water from the spring, at atmospheric pressure. However, away from the exposed face at this spring, the aquifer has some saturated thickness. If an open well is dug into this small thickness of saturated aquifer it could yield about a few hundred litres per day. This negligible supply of water often proves to be a lifeline for a tribal village of ten to fifteen huts, perched on the plateau.

Another case in point is from a flat terrain with a saturated phreatic aquifer overlying an impervious basement (Fig. 2). Here, the ground water movement is slow due to flatness of the terrain. But ground water pumpage in winter season for domestic and irrigational use from a large number of dug wells causes depletion of the water table from its post-monsoon position. These dug wells penetrate through the phreatic aquifer and go a few metres deep into the hard basement rock. The masonry wall supporting the excavation in the upper soft strata has adequate number of holes to allow inflow of water from the phreatic aquifer. The incoming water gets stored in the bottom portion of the well and is conveniently pumped. Water level in the well is usually kept below the base of the phreatic aquifer so that the pressure of water accumulated in the well does not obstruct the delivery of water into the well. Wells, which have been over-pumped during the rainy season and in winter, reach their 'threshold gradient' quickly and become practically dry at the beginning of the summer, as shown in Fig.2. Between two such dry wells, the aquifer has still some saturated thickness and could support a small yield in a newly dug well, at the location indicated by an arrow in Fig. 2. Instead of digging a new well, villagers often follow the wise practice of keeping some wells 'unused' during monsoon and winter season and bring them into use exclusively during summer season.

## Conclusions

Quasi-static stage of ground water is reached in low permeability phreatic aquifers when the gravitational force, acting through the slope of water table, is balanced by frictional force between the pellicular water & water free to move.

Evaporation and transpiration at the exposed faces of the phreatic aquifer are more powerful than gravitational force and cause some movement of water.

If clayey strata occur at the exposed face, strong capillary forces come into play. Discharge at atmospheric pressure from the spring, is not possible if the head in the phreatic aquifer behind the clayey strata is less than the height of capillary rise.

Quantity of water available in summer from these aquifers may be very small but it could the lifeline for many rural people, especially in semi-arid, hard rock regions in India, as it saves for the village women the trouble of walking a few kilometers every day in hot summer to some distant source of polluted surface water to fetch drinking water supply for the family.

The area of influence of each dug well is limited. If recharge augmentation of phreatic aquifer is to be done during Monsoon rains, a large number of wells in the watershed are to be used as recharge points. Additionally, percolation tanks are also constructed by putting bunds across small streams so that a large area of the tank-bed is available for vertical infiltration of water being recharged.

## References

- Limaye D.G, 1949- "On ground water statics in Deccan trap country with practical suggestions for well digging". Institution of Engineers of India, Bombay Centre, 29th Annual Report, pp 154-180.
- Limaye D G & Limaye S D, 1979- A study on recoverable ground water in Basalts (Deccan traps) of India." IAH Congress on methods of evaluation of ground water resources, Vilnius, USSR, IAH Memoirs Volume 15, pp 185-188.

# Les très grands systèmes aquifères du Monde

Jean MARGAT, membre honoraire de l'AIH
BRGM, Orléans, France
jeanmargat@wanadoo.fr

L'avancement des connaissances hydrogéologiques dans la plupart des pays, exprimé par de nombreuses monographies et cartographies de synthèse nationales et continentales, rend possible et opportune au seuil du XXIème siècle une vision mondiale, comme en d'autres secteurs des Géosciences. Tout d'abord en se référant à une typologie des conditions hydrogéologiques primordiales, basée sur les principes de la légende internationale des cartes hydrogéologiques (AIH/UNESCO 1995), ce qui est le propos de la synthèse cartographique du projet «WHYMAP» initié par l'AIH, l'UNESCO et la Commission de la Carte Géologique du Monde (CCGM). Une vision des conditions hydrogéologiques mondiales peut aussi être structurale et mettre en évidence les systèmes aquifères de premier ordre dont la géographie est moins perçue et diffusée que celle des grands bassins hydrographiques.

De même que les écoulements d'eaux de surface sont organisés en bassins hydrographiques de toutes tailles et que quelques bassins fluviaux géants monopolisent une part importante de tout l'écoulement des terres émergées, les systèmes aquifères indentifiables sont eux aussi d'étendues très variées et quelques grands systèmes rassemblent des parts notables des stocks et des écoulements d'eau souterraine mondiaux. Mais leur géographie est moins évidente et doit davantage être révélée par les étutes hydrogéologiques structurales.

Ces grands systèmes aquifères sont tous constitués par des roches sédimentaires et compris dans la classe «bleue» de la carte «WHYMAP» mentionnée plus haut.

37 systèmes aquifères de première grandeur, dont les étendues s'échelonnent de 100 000 à 2 000 000 km$^2$ ou plus, sont répartis sur tous les continents et en toutes zones climatiques. Leur situation est représentée en figure 1 et leurs principales caractéristiques sont résumées dans le tableau .

## Ces grands systèmes aquifères sont de trois types structuraux

I • Bassins sédimentaires généralement multicouches plus ou moins complexes, en fonction de leur structure inégalement accidentée et de leur constitution stratigraphique, qui peut s'étendre de l'Antécambrien au Quaternaire, et atteindre des puissances de plusieurs milliers de mètres (jusqu'à 20 000 m dans la plate-forme russe).
Ils sont composés par une alternance de couches très perméables et transmissives (formations détritiques – sables, grès...) n'interdisant pas des communications verticales («drainance») ou imperméables (roches salines), compliquée par des passages latéraux de faciès. Ils comportent une ou plusieurs couches aquifères à nappe libre et un nombre variable de couches aquifères à nappes captives en partie interconnectées, à eau souvent saumâtre ou salée en profondeur où le renouvellement est beaucoup plus faible et les temps de séjour sont les plus longs. C'est le type le plus répandu.

Les exemples sont nombreux : Grand Bassin Artésien d'Australie, Bassins Sahariens (SASS, Aquifère Nubien), Northern Great Plains Aquifer System d'Amérique du Nord (Canada, Etats-Unis), Bassin de Sibérie occidentale… Ces bassins peuvent se répartir suivant deux variantes structurales :

- Dans le modèle « parisien » dont le Bassin de Paris est un prototype classique, « les petits plats sont mis dans les grands… » : des auréoles sédimentaires aquifères affleurantes en périphérie, à nappes libres et sources de débordement, sont en continuité avec les aquifères profonds à nappes captives, parfois artésiennes ;
- Dans le modèle « pannonique », dont le Bassin de Hongrie est un exemple moins étendu, les couches supérieures recouvrent entièrement les aquifères profonds reconnus seulement par forage et moins facilement identifiables, et les échanges par drainance ou favorisés par des failles sont prédominants. Ces bassins sont souvent en même temps « artésiens » lorsqu'ils comportent des aires de jaillissement potentiel initial sur de grandes étendues par suite de conditions d'altitude et de pression de l'eau favorables qui en font des accumulateurs d'énergie appréciables.

II • Fosses d'effondrement subsidentes, à comblement principalement alluvial, à nappe libre mais pouvant être aussi multicouches et comporter plusieurs nappes captives, avec également des aires d'artésianisme.
Exemples : Central Valley de Californie, plaines du nord de Chine, Bassin Indo-Ganga – Brahmaputra en Inde.

III • Accumulations détritiques de piedmont de grandes chaînes montagneuses ; aquifères principalement à nappe libre.
Exemple : aquifère des High Plains (Ogallala) aux Etats-Unis.

Toutefois certains de ces grands aquifères présentés comme des systèmes uniques sont en fait des agrégats de systèmes aquifères contigus et similaires mais indépendants, comme l'Ogallala Aquifer des High Plains des Etats-Unis ou les Bassins de la plateforme de Russie.

Ces grands systèmes aquifères couvrent ensemble près de 35 millions de km$^2$, près du quart des terres émergées. Ils doivent contenir la majeure partie des réserves d'eau douce souterraine continentales bien que tous n'aient pas fait l'objet d'estimation de réserve (cf. tableau 1). Aussi recèlent-ils l'essentiel des ressources en eau souterraine non renouvelables (réserves extractibles dans des conditions économiques et environnementales acceptables) reconnues et en partie en exploitation dans plusieurs pays en zone aride (Arabie Saoudite, Libye, Algérie principalement). Ils ont aussi été sujets à la plus grande partie des déstockages opérés au cours du XX$^{ème}$ siècle, soit du fait de surexploitation, soit par suite d'exploitation « minière » de ressources non renouvelables, qui doivent être globalement de l'ordre de 1 000 km$^2$ au minimum et qui ont entraîné d'amples dépressions, souvent supérieures à 100 m. Ces grands aquifères participent sans doute dans une moindre mesure à l'écoulement souterrain mondial (de l'ordre de 12 000 à 13 000 km$^2$/an) car celui-ci est engendré essentiellement par les aquifères libres, dont beaucoup d'aquifères locaux à nappe phréatique des zones humides.

Les fonctions de ces grands systèmes aquifères dans le cycle des eaux continentales mondial et leur place dans l'économie de l'eau sont étroitement liées à leur position climatique.

En zones humides, ils participent à la régulation des écoulements de surface et ils sont largement exploités, voir surexploités, notamment en Chine, en Inde, aux Etats-Unis.

En zones aride et semi-aride, ils participent peu aux rares écoulements et leur exploitation mobilise surtout leurs ressources non renouvelables, notamment en Afrique saharienne, au Moyen-Orient et en Australie (où elle est maintenue très réduite).
En zone sub-arctique d'Europe et d'Asie septentrionales (Russie, Sibérie), les conditions de permafrost régnantes jusqu'à de grandes profondeurs (plusieurs centaines de m) «gèlent» leur fonction hydrologique et restreint beaucoup leur exploitabilité.

L'état inégal des recensements des prélèvements actuels d'eau souterraine, suivant les pays,

ne permet pas de chiffrer complètement la part de l'exploitation de ces grands systèmes aquifères dans l'exploitation d'eau souterraine mondiale estimée à environ 800 km2/an au moins. Quelques exemples peuvent seulement être cités (Tableau 2) : ils totalisent déjà quelques 130 km$^2$/an, dont une vingtaine aux dépens de ressources non renouvelables (bassins du Sahara et d'Arabie) mais les intensités relevées sont très variées.
Enfin ces systèmes aquifères sont souvent - un sur deux - transfrontaliers ; leur étude comme la gestion de leurs ressources, renouvelables ou non renouvelables, posent des problèmes de coopération et de partage en partie similaires à celles des bassins hydrographiques plurinationaux, mais aussi plus spécifiques (transferts d'influence des exploitations).

| **Système aquifère** | **Indice du tableau 1** | **Pays** | **Date en km$^2$/an** | **Prélèvements** | **Référence** |
|---|---|---|---|---|---|
| Nubian sandstone aquifer system (NSAS) avec Post-nubian | 1 | Egypte,<br>Libye,<br>Soudan | 2000 | 2,2 | CEDARE/IFAD, FAO 2003 |
| Système aquifère du Sahara septentrional (SASS) | 2 | Algérie,<br>Libye,<br>Tunisie | 2000 | 2,5 | OSS 2003 |
| Murzuk Basin | 3 | Libye | 2000 | 1,75 | A. M. EL GHERIANI 2002<br>UNESCO/Projet ISARM 2004 |
| Bassin Sénégalo-Mauritanien | 5 | Mauritanie, Sénégal, Guinée, Bissau, Gambie | 2000 | 0,26 | UNESCO/projet ISARM 2004 |
| Système aquifère Iullemeden –Irhazer | 6 | Algérie, Mali, Niger, Nigeria | 2000 | 0,22 | UNESCO/projet ISARM 2004 |
| Bassin du lac Tchad | 7 | Niger, Nigeria, Tchad | 2000 | 0,25 | UNESCO/projet ISARM 2004 |
| Central Valley California | 16 | USA | 1990 | 20 | USGS |
| Ogallala Aquifer | 17 | USA | 2000 | 21,5 | USGS |
| Arabian Aquifer System | 22 | Arabie Saoudite, Emirats Arabes Unis, Bahrein, Qatar | 1995 | 15,2 | FAO 1997<br>A.A. Ghum Alghamdi 2002 |
| Indus Basin | 23 | Pakistan | 2000 | 46,7 | IGRAC/M.A. Kahlown 2004 |
| Huang-Huai-Hai | 29 | Chine | 1997 | 20 | China Water Vision 2000 |
| Bassin de Paris | 32 | France | 2000 | 2 | BRGM IFEN 2004 |
| Great artesian Basin | 3 | Australie | 2000 | 0,55 | M.A. Habermehl, UNESCO, 2002 |

*Tableau 2 – Prélèvements d'eau souterraine actuels dans quelques grands systèmes aquifères du Monde*

Tableau 1: les très grands systèmes aquifères du >Monde

| N° cf carte | Dénomination | Pays | Superficie 1 000 $km^2$ | Structure Hydrologique (P : puissance maximale en m) | Volume d'eau en réserve théorique 1000 $m^2$ | Flux moyen d'alimentation en $km^2$/an | Références |
|---|---|---|---|---|---|---|---|
| 1 | Système aquifère nubien (NAS) :<br>Système aquifère des Grès de Nubie (NSAS)<br>Aquifère post-nubian (PNAS) | Egypte, Libye, Soudan, Tchad | 2 199 dont 1 800 à eau douce | Multicouche<br>Cambro-Ordovicien à Oligocène<br>Grès continentaux prédominants<br>P = 3 500 m | 542<br>eau douce | ~ 1 | M. Bakhabakhi 2002<br>CEDARE/IFAD (FAO 2003)<br>UNESCO / OSS 2005 |
| 2 | Système aquifère du Sahara septentrional (SASS) | Algérie, Libye Tunisie | 1 019 | Multicouche<br>Cambro-Ordovicien au Miocène<br>Continental intercalaire<br>et Complexe terminal<br>P = 1 600 m | 60 | ~ 1 | OSS 2003, 2004<br>UNESCO/OSS 2005 |
| 3 | Bassin de Murzuk-Djado | Libye, Algérie Niger | 450 | Multicouche<br>Cambro-Ordovicien à Crétacé<br>P = 2 500 m | 4,8<br>en Libye | ~ 0,15 | UNESCO/OSS 2005 |
| 4 | Bassin de Taoudenit Tanezrouf | Algérie, Mauritanie, Mali | 2 000 | Multicouche<br>Infracambrien à Tertiaire (CT)<br>P = 4 000 | 0,018 exploitable au Mali et en Mauritanie | ~ 0,3<br>au Mali | UNESCO/OSS 2005 |
| 5 | Bassin Sénégalo-Mauritanien | Mauritanie, Sénégal, Gambie, Guinée Bisseau | 300 | Multicouche<br>Aquifère principal : Maestrichtien<br>P = 600 M | 1,5 | ~ 9 | B. Diagana 1997<br>UNESCO/OSS 2005 |
| 6 | Système aquifère d'Iullemeden-Irhazer | Niger, Algérie, Mali, Nigéria | 635 | Multicouche<br>Cambro-Ordovicien à Eocène<br>3 sous-bassins<br>P = 1 500 m | 10 à 15 | | A. DODO 1992<br>UNESCO/OSS 2005 |
| 7 | Bassin du Lac Tchad | Niger, Nigéria, Tchad, Cameroun, RCA | 1 917 | Multicouche<br>Continental intercalaire, Continental terminal et Plio-Quaternaire<br>P = 7 000 m | 0,6 au Niger (0,05 exploitable)<br>~ 0,4 exploitable au Tchad | 3,6 au Niger | CBLT 1977<br>J.L. Schneider 2001<br>UNESCO/OSS 2005 |
| 8 | Sudd-Basin Umm Ruwaba Aquifer | Soudan, Ethiopie | 365 | Multicouche<br>Néogène-Quaternaire<br>P = 3 000 m | 0,11 | 0,34 | ICID 1983<br>UN 1987<br>OACT 1993 |
| 9 | Bassin d'Ogaden-Juba | Ethiopie, Somalie, Kenya | ~ 1 000 | Multicouche<br>Nappes libres et captives<br>P = 12 000 m | | ~ 10 | UN 1987 |
| 10 | Bassin du Congo | Congo RD, Congo, Angola, RC Afrique Gabon | 750 | Multicouche<br>Mésozoïque ("Karoo")<br>Quaternaire alluvial<br>P = 3 500 m | | ~ 100 | I. Zektser 2004<br>AAC 1993 |
| 11 | Upper Kalahari Basin | Angola, Botswana, Zambie, Zimbabwe | ~ 700 | Multicouche<br>Carbonifère, Crétacé (« Karoo ») à Néogène | | ~ 30 à 60 | |

| N° cf carte | Dénomination | Pays | Superficie 1 000 $km^2$ | Structure Hydrologique (P : puissance maximale en m) | Volume d'eau en réserve théorique 1000 $m^2$ | Flux moyen d'alimentation en $km^2$/an | Références |
|---|---|---|---|---|---|---|---|
| 12 | Lower Kalahari Basin | Afrique du Sud, Botswana, Namibie | ~ 350 | Multicouche<br>« Karoo » à Néogène | | ~ 1 à 2 | |
| 13 | Karoo Basin | Afrique du Sud | 600 | Multicouche<br>Cambrien à Jurassique<br>P = 7 000 m | 3 à 5 (dolomites) | 16 à 37 | AAC 1993<br>I. Zektser 2004 |
| 14 | Northern Great Plains Aquifer System (USA) / Interior Plains (Canada) | Canada, USA | ~ 2 000 | Multicouche<br>Paléozoïque à Eocène | | | UN 1976<br>USGS 2003 |
| 15 | Cambrian-Ordovicien Aquifer System (Central Region) | USA | 250 | Multicouche<br>Cambro-Ordovicien | | | USGS 2003 |
| 16 | Central Valley California | USA | 80 | Aquifère alluvial Quaternaire multicouche, à nappes libres et captives<br>P = 600 m | 1,73 | ~ 71 | USGS |
| 17 | Orgallala Aquifer High Plains | USA | 450 | Alluvions tertiaires<br>P = 150 m | ~ 15 | 6 à 8 | USGS |
| 18 | Atlantic and Gulf Coastal Plain Aquifers | USA, Mexique | 1 150 | Multicouche<br>Paléozoïque à Tertiaire<br>Ensemble d'aquifères contigus<br>P = 12 000 m | | | USGS |
| 19 | Amazon Basin | Brésil, Colombie, Pérou, Bolivie Brésil | 1 500 | Multicouche<br>Paléozoïque à Tertiaire<br>P = 2 000 m | 32,5 | | A. Rebouças 1988 |
| 20 | Maranhao Basin | Brésil | 700 | Multicouche<br>Ordovicien à Crétacé<br>P = 3 000 m | 17,5 | 4 | A. Rebouças<br>AIH 1976-1988 |
| 21 | Guarani Aquifer (Parana & Chaco) ou Mercosul Aquifer System | Brésil, Argentine, Paraguay Uruguay | 1 195 | Multicouche<br>Silurien à Crétacé<br>P = 800 m<br>Total basin : 5 000 m | 57 | 234 | A. Rebouças 1988-1976<br>L.M. Araújo & al. 1979 |
| 22 | Arabian Aquifer System | Arabie Saoudite, Jordanie, Koweit, Bahrein, Qatar Pakistan | 1 485 en Arabie Saoudite | Multicouche<br>Cambrien à Néogène<br>P = 6 500 m | 2,185 en Arabie Saoudite | 1,2 | W. Abderrhaman<br>UNESCO 2002<br>UN 1982 |
| 23 | Indus Basin | Pakistan | ~ 320 | Aquifère alluvial à nappe libre<br>P = 300 m | | 66(usable potentiel) | ICID 2000 |
| 24 | Indo-Ganga-Brahmaputra Basin<br>Bhabhar et Tarai Aquifers | Inde, Népal Bangladesh | ~ 600 | Aquifère alluvial à nappes libres et captives<br>P = 6 000 m | | | |

| N° cf carte | Dénomination | Pays | Superficie 1 000 $km^2$ | Structure Hydrologique (P : puissance maximale en m) | Volume d'eau en réserve théorique 1000 $m^2$ | Flux moyen d'alimentation en $km^2$/an | Références |
|---|---|---|---|---|---|---|---|
| 25 | West Siberia | Russie | 3 200 | Multicouche<br>Paléozoïque à Crétacé<br>p.p. sub-permafrost<br>P = 6 000 m<br>Eaux douces +<br>eaux salées | 1 000 | 82 sur 2,5 M $km^2$ ("predictive fresh grouwdwater field") | UN 1986<br>I. Zektser 2004 |
| 26 | Tunguss Basin | Russie | 1 000 | Multicouche<br>Cambrien à Trias.<br>Sub-permafrost<br>Eaux douces et<br>eaux salées<br>P > 4 000 m | | | UN 1986<br>I. Zektser 2004 |
| 27 | Angara Lena Basin | Russie | 600 | Multicouche<br>Cambrien à Jurassique<br>Eaux douces et<br>eaux salées<br>P = 3 000 m | | 12,6 | UN 1986<br>I. Zektser 2004 |
| 28 | Yakut Basin | Russie | 720 | Multicouche<br>Sub-permafrost<br>Eaux douces et<br>eaux salées<br>Infra-Cambrien à Crétacé<br>P = 12 000 m | | 18 | UN 1986<br>I. Zektser 2004 |
| 29 | North China Aquifer system (Huang-Huai-Hai Plain) | Chine | 320 | Aquifère alluvial<br>Quaternaire multicouche<br>Nappes libres et captives<br>P = 1 000 m<br>Artésianisme | 0,018 | 49,2 (48,1 exploitable) | China Water Vision 2000<br>I. Zektser 2004 |
| 30 | Song-Liao Plain | Chine | 311 | Aquifère alluvial<br>quaternaire multicouche<br>libres et captives<br>P = 300 m | | 33,4 (23,8 exploitable) | I. Zektser 2004 |
| 31 | Tarim Basin | Chine | 520 | Aquifère alluvial<br>multicouche nappes<br>libres et captives<br>Artésiancisme<br>P = 1 200 m | | | |
| 32 | Bassin de Paris | France | 190 | Multicouche<br>Trias à Néogène<br>P = 3 200 m | 0,5 à 1 | 20 à 30 | NU 1990 |
| 33 | Russian Platform Basins | Russie | ~ 3 100 | Ensemble de<br>multicouches contigus<br>Infra-cambrien<br>à Quaternaire<br>Sub-permafrost au N<br>P = 20 000 m | | | NU 1990 |
| 34 | North Caucasus Basin | Russie | 230 | Multicouche<br>Carbonifère à Néogène<br>P = 10 000 m | | | NU 1990 |
| 35 | Pechora Basin | Russie | 350 | Multicouche<br>Ordovicien à Tertiaire<br>P = 3 000 m<br>En partie<br>sub-permafrost | | | NU 1990 |

| N° cf carte | Dénomination | Pays | Superficie 1 000 km² | Structure Hydrologique (P : puissance maximale en m) | Volume d'eau en réserve théorique 1000 m² | Flux moyen d'alimentation en km²/an | Références |
|---|---|---|---|---|---|---|---|
| 36 | Great Artesian Basin | Australie | 1 700 | Multicouche Trias à Crétacé<br>P = 3 000 m | 20<br>8,7 | 1,1 | M.A. Habermehl<br>UNESCO 2002<br>Water Resources and Use, Australia, 2003 |
| 37 | Canning Basin | Australie | 430 | Multicouche Dévonien à Crétacé<br>P = 1 000 m | | | Lau & al. 1987<br>J.E. I. Zektser 2004 |

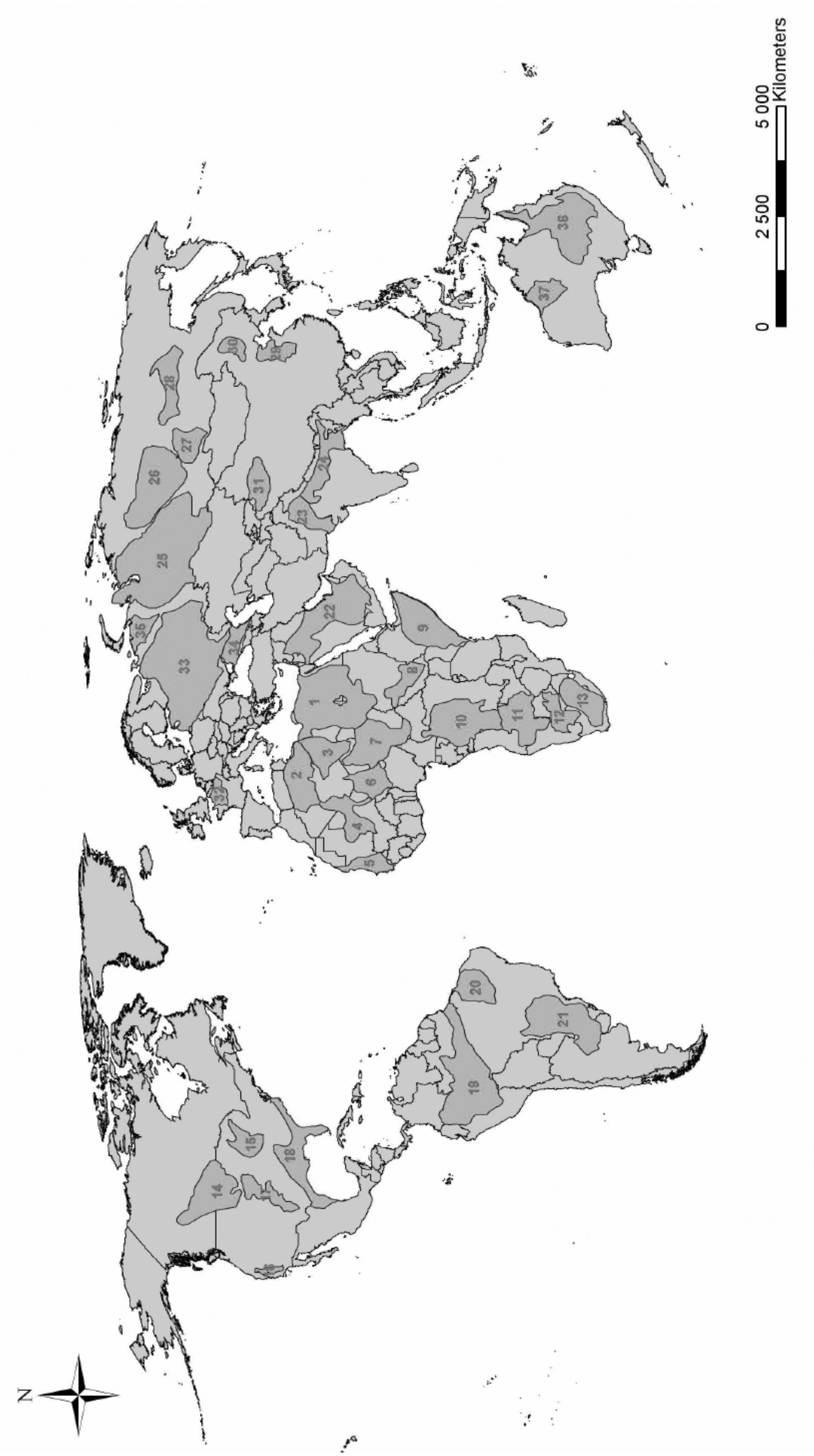

figure1: les très grands systèmes aquifères dans le monde

# DARCY 18

# Can we identify vertical exchanges in multi-layered aquifer from groundwater chemistry ? A theoretical background with an application to the Aquitaine Basin.

Atteia O.[1], André L.[2], Franceschi M. (1), Dupuy A.[1]

[1] Institut EGID Bordeaux 3, University Michel de Montaigne, 33607 Pessac France,
atteia@egid.u-bordeaux.fr.
[2] BRGM - Water Division, 3 avenue C. Guillemin, BP 6009, F-45060 Orléans Cedex 2, France ;
l.andre@brgm.fr

## Abstract

The interactions between aquifer and aquitards becomes more and more important for the management of large sedimentary multi-layer aquifer systems. In fact recent hydrodynamic modeling tend to outline the role of vertical leakage between superimposed aquifers. This led us to analyze in detail what could be the effects of exchange of matter between aquifers and aquitards. To explain the gradients several phenomena are studied : leakage, dissolution of minerals or ion exchange within an aquifer, and dissolution of minerals or ion exchange from an overlying aquitard. Each process are studied and compared. It is shown that, given the assumptions made, the influence of each process can be differentiated where the aquifer-aquitard system is well enough characterized. Our work suggests that the composition of major aquitards may have a significant effect on the chemistry of the aquifer water.

## Introduction

In regional sedimentary basins, several aquifers, isolated by aquitards of variable thickness are often found (Raoult et al., 1998 ; Taigbenu and Onyejekwe, 2000 ; Mehta et al., 2000). Several studies, using for instance noble gas concentration (Castro et al., 2000), $^{36}$Cl (Love et al., 2000), or $CO_2$ fluxes (Chiodini et al., 1999) have shown that vertical fluxes exist within these aquitards. In order to understand better the exchange of matter between aquifer and aquitard we suggest a method based on the chemical composition of the groundwater.

The chemical composition of groundwater in such systems results mainly from water-rock interactions and transport of elements. Interactions include congruent or non-congruent dissolution of minerals, precipitation, adsorption or ion exchange whereas the transport of species may result from advection, dispersion and/or diffusion. Water facies are based on the concentration of major elements in solution. Na, Cl and $SO_4$ can reach high concentrations in groundwater as the minerals containing these ions are highly soluble. Ca and Mg concentrations often lie between these two endpoints as they are often controlled by equilibrium with carbonate minerals. Our approach will be centered on the elements showing high concentrations and the corresponding minerals.

Several geochemical studies suggest a smooth evolution of the groundwater chemical composition along the flow direction (Hiscock et al., 1996). Concentration variations are often justified by mixing of two aquifers or dissolution of minerals within the aquifer (Appelo and Postma, 1993). Such a mixing can significantly modify the groundwater composition only where important fluxes from two aquifers of very different composition converge, which is fairly rare. Besides, in an ideally homogeneous aquifer the dissolution of minerals should lead to concentrations close to the solubility value. However, for ions like Cl , Na or $SO_4$ , the groundwater solutions are undersaturated with respect to Cl, Na or $SO_4$ bearing minerals, in most aquifers. Moreover the highly soluble minerals delivering these ions by dissolution are often not found in most of the considered aquifers (Plummer et Sprinkle 2001). Therefore, the dissolution process cannot easily justify the smooth spatial variations of concentration in a homogeneous aquifer and needs clarification.

## Modeling strategy and assumptions

We use an idealized aquifer system that includes two types layers : an aquifer of high or intermediate permeability and an aquitard of low to very low permeability. The aquifer is assumed to consist mostly of sand. The aquitard might be pure clay or clay including layers of evaporites or other minerals. The physical characteristics of each medium (porosity, permeability) are considered to be homogeneous and isotropic. The flow conditions are also considered constant : a known velocity in a regular flow field is assumed in the aquifer ; the flow in the aquitard is assumed to be zero and with no density effect. To develop the steady state equations, we consider that the mass of selected elements is almost infinite by setting boundary conditions at infinite distance. The mass balance limits are then analyzed in the discussion section.

Both aquifer and aquitard may include minerals that can dissolve as well as a portion of 'inert' minerals (e.g quartz). As we consider easily soluble minerals, the thermodynamic equilibrium between water and sediment is considered to be reached everywhere (i.e. local equilibrium assumption). Moreover, the minerals are assumed to be evenly distributed in space.

So the differents processes are :

- Dissolution in a homogeneous aquifer
- Influence of leakage
- Simple diffusion from aquitard
- Dissolution in the aquitard and diffusion
- Ion exchange and diffusion

We try to describe how the various interactions between aquifers and aquitards systems influence groundwater chemistry. The ions released by diffusion from the aquitard may arise from three different sources : brine as pore water in the aquitard, dissolution of salts and ion exchange. These sources, combined with diffusion, are analyzed separately.

We have considered simplified conditions with homogeneous aquifer or aquitard layers and regular boundary conditions. These hypothetical conditions may not exist in any real aquifer system but they make the basis for any further analysis. In order to get closer to real conditions, we investigate in this section two directions.

Is the longitudinal gradient of concentration resulting from one process can be so different from others ? and be recognized directly ?

What is the duration of the presented processes and their respective boundary conditions, that may separate the processes along the geological time scales ?

## Longitudinal gradients of concentration

Several processes delivering ions to solution were investigated. In a completely homogeneous aquifer, and assuming local equilibrium, dissolution from minerals present in the aquifer may lead to abrupt spatial variation of concentration close to the location of the dissolution front (Lasaga, 1998). This implies that salts of S and Cl will not remain in an aquifer over geological time scales. Diffusion from an aquitard containing brine in its pore volume will lead to a slow accumulation of ions in the aquifer along the flow direction. Dissolution of mineral phases existing in the aquitard will generate the same type of concentration gradient except that it may remain over a longer timescale due to the larger amounts of matter available in the solid phase. Exchange between aquifer water and the CEC of clays embedded in the aquitard will result in a diffusion process from the clays but with higher amounts of ions in the solution and a depletion of bivalent cations in the aquifer. Leakage may lead to a non negligible flux of water from the aquitard and thus, if this water is saturated with one mineral, it will generate large concentration variations over short distances.

Under the boundary conditions of interest, the four investigated processes : diffusion, dissolution and diffusion, leakage, and ion exchange + diffusion, all lead to a linear increase in groundwater concentration distribution with distance. The only criterion to determine the presence, or predominance, of one process will thus be to assess the average increase in the $C/C_{eq}$ ratio in the aquifer with distance down flow. The importance of the parameters values will thus be investigated in order to determine if the $C/C_{eq}$ ratio can be used to distinguish processes. This is done in the following section.

## Varying parameters

Any one of the processes described above will be detected only where the concentration of an element in the aquitard pore water is significantly higher than the concentration prevailing in the aquifer.

The case of leakage is original as concentrations depend, among other parameters, on the area and permeability of the zone where the aquitard head is higher than that in the aquifer. It is difficult to give any general value for the extent and properties of the leakage zone. The resulting concentrations increase with the length of the leaking zone. The major parameter in this approach is the vertical permeability of the aquitard, which may vary over more than three orders of magnitude. This value is very difficult to estimate at the regional scale. However the problem has to be considered from the point of view of aquifer management. Keeping this approach in mind, leakage is of interest only where it can affect significantly the fluxes within the aquifer. For the average properties that we considered, values of leakage greater than 0.5 $mm.y^{-1}$ will significantly modify the aquifer flow (Fig. 1). By considering this limit we obtain the range of concentrations shown in Fig. 2.

In the case of diffusion, only a few parameters influence the computed concentrations. The major role is played by the diffusion coefficient which is often unknown, mostly because of unknown tortuosity. However, even if the coefficient is varied between $5.10^{-4}$ to $10^{-2}$ $m^2.y^{-1}$ the diffusion by itself still gives the lowest concentrations among all the processes investigated. Increase in D is in fact partly compensated for by a decrease in the concentration gradient in the aquitard ; if D increases by a factor of 20, the resulting concentration increases only by a factor of 3. The diffusion flux is also sensitive to the aquitard porosity, a change in porosity by a factor 2 leading to a change in concentration by a factor of 1.6. However the total porosity of a clayey aquitard is unlikely to vary outside the range of 0.2 to 0.4 and this parameter plays a secondary role compared to the variation of the diffusion coefficient.(a) Boundary conditions

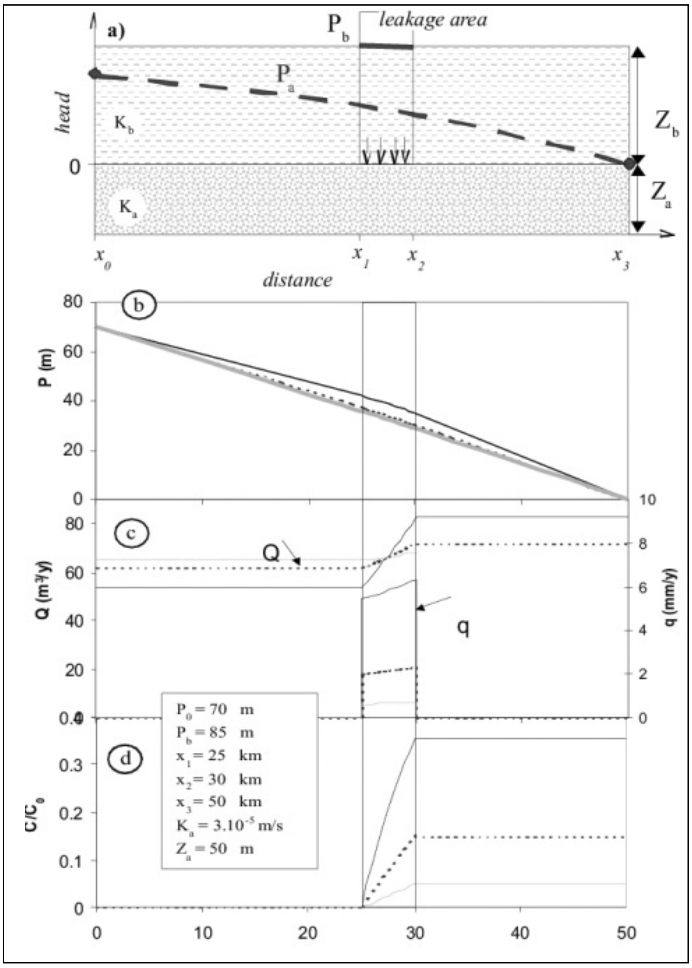

Figure 1: Influence of leakage.

for the analysis of leakage. Pa is the head in aquifer, Pb is the head in the aquitard at the ground surface, with leakage occurring only between x1 and x2 , Ka and Kb are the permeabilities, and Za and Zb are the thickness of the aquifer and aquitard respectively.

(b) Distribution of head values with distance. (c) Distribution of the flux along the aquifer.

(d) Evolution of the C /Co ratio, where C is concentration in the aquifer and Co is concentration in the aquitard. Thick line, Zb = 250 m, Kb = $10^{-9}$ m $s^{-1}$ ; dashed line, Zb = 750 m, Kb = $10^{-9}$ m $s^{-1}$ ; thick shaded line, Zb = 250 m, Kb = $10^{-10}$ m $s^{-1}$.

More parameters affect the situation where mineral dissolution exists; the major ones being diffusion coefficient again, aquifer thickness and the percentage of mineral in the aquitard solid phase. Due to the dissolving minerals, the diffusion flux remains higher than for the case considered in the previous paragraph . It can be seen in Fig. 3 that after 1 My the $C/C_{eq}$ ratio (where $C_{eq}$ is the concentration in the aquitard) is equal to 0.28 for x/v = 10 ky ; while after the same duration and distance, the $C/C_0$ ratio (where $C_0$ is the concentration in the aquifer) wher only diffusion is active is 10 times lower The influence of the diffusion coefficient is more important. An increase in a factor of 20 in the diffusion coefficient value leads, in the presence of dissolution, to an increase of the concentration by a factor of 4.5. The major unknown will often be the amount of highly soluble minerals in the aquitard at the regional

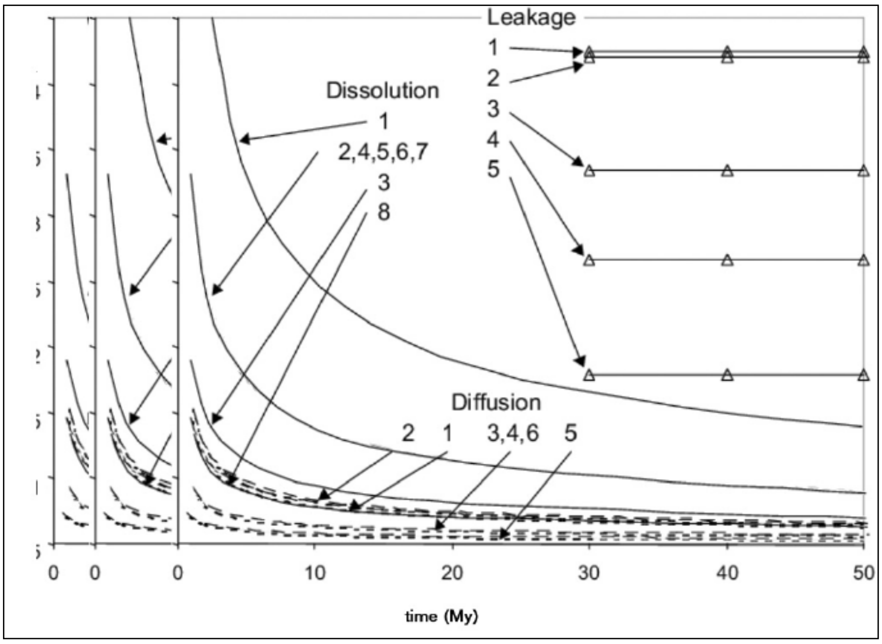

Figure 2: Variation of concentration with time in millions of years, for each of the modeled processes.

scale. The presented approach apply only where the diffusive properties are close to the clay's ones, i.e. where the evaporite fraction is lower than 10 to 20%. A different approach should be considered in case of pure layers of evaporites identified within the aquitard. A change in a factor 10 for the mineral fraction (1 to 10%) leads to a change in a factor of 3 for the resulting concentration. Assuming complete mixing, the aquifer thickness does not influence the resulting concentration because the diffusive flux decreases for an increasing concentration in the aquifer.

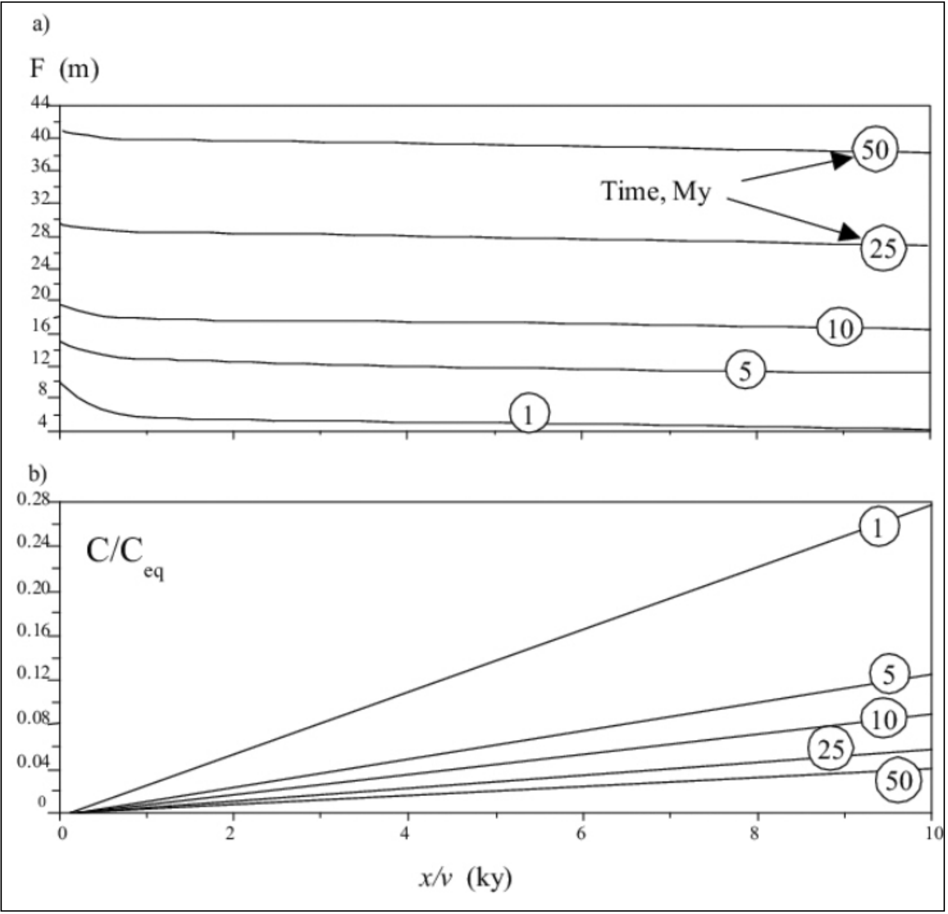

*Figure 3: Dissolution and diffusion from the aquitard, vertical position of dissolution front and concentration in the aquifer.*
*(a) Vertical position of the dissolution front (F in m)*
*(b) average normalized concentration ($C/C_{eq}$) and along normalized time ($x/v$) for several time periods of dissolution: 1, 5, 10, 25, and 50 Myr.*

Ion exchange in an aquifer of the type considered here will be completed typically in 5 to 15 pore volumes. However, ion exchange and diffusional transport from an adjacent aquitard may well have an important effect of aquifer groundwater chemistry over geological time scales. This process can be identified by considering ion ratios, and in this sense absolute concentrations do not have to be compared with those developed by the other mechanisms. In the systems considered, Na concentrations in the aquifer ground waters are strongly affected by Ca availability. This availability will vary considerably with the amount of calcite present. In addition, the presence of thick interbedded clay layers can lead to a dramatic decrease of flow rate locally within the aquifer. In this case, a specific analysis must be conducted by using the real local pore velocities in the aquifer. This may lead to a much longer time scale of influence of such exchanging layers on the composition of the aquifer water.
It appears that concentrations delivered by a significant leakage are always higher than that observed for any other processes.

## Temporal evolution

When varying parameters, we considered that an infinite amount of matter was available in the aquitard. However the amount of matter available to maintain the aquitard-to-aquifer fluxes is not infinite. We calculated for leakage, diffusion and diffusion+dissolution the duration that the minerals or solutes may remain within the aquitard ('flushing time'). The estimated duration is obtained by the ratio of the amount of matter present in the aquitard to the flux leaving to the aquifer. For diffusion alone, the time is obtained when 95% of the amount is depleted. The parameters were varied as above, and the resulting variation in the results is shown by an error bar in the estimated time.
Fig. 4 shows that the 'flushing time' is determined largely by the considered process. Where a 1000 m thick aquitard is present, the ion concentrations in groundwater may remain stable for at least 150 My for all processes. For a 100 m thick aquitard, some of the processes studied can lead to a depletion of salts within the aquitard. If soluble minerals such as gypsum or halite are present in the aquitard, their effect may influence ion concentration in the aquifer over a long time, i.e. from 100 to 750 My. On the contrary, if concentrated solutions are present in the aquitard without soluble minerals, the effect of diffusion will remain in the aquifer only for 7 to 26 My. Leakage may deplete the soluble minerals in the entire aquitard after a duration of 8 to 45 My. The prediction for the leakage duration must be considered with a lot of care. In fact, the leakage intensity is largely dependent on the difference between the ground level and the piezometric surface. Because of climate change, this gradient may vary drastically across time scales of tens of thousands years. It might thus be difficult to make reliable predictions on the duration of the leakage effect. For ion exchange, the flushing time might be longer than for diffusion alone, but it will also depend on the amount of calcium transported to the exchange area, which may vary according to local conditions in the considered aquifer. This may lead to an ion exchange effect active for long duration (10's My) only at places where the aquifer flow is slow.

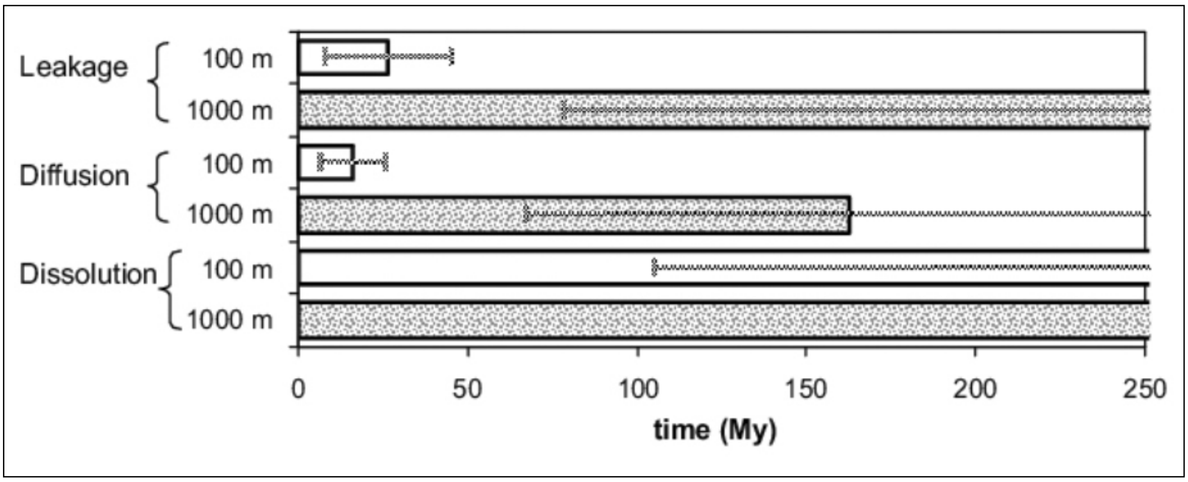

*Figure 4: Estimates of the time to deplete an aquitard layer of its soluble components (minerals and pore water), using two thickness: 100 and 1000 m.*

## Heterogeneity

Up to now we have considered the simple case of a homogeneous aquifer having 10's of m thickness bounded by 100's m thick aquitards. In most aquifers, deposits are complex (Koltermann and Gorelick, 1995) and layers of low permeability are interbedded within sand. Thus we will now consider applying to 'real' world, i.e. more complex deposits. In fact the equations remain the same but now apply to thin zones with a change in the boundary conditions. The highly soluble mineral content in these thin clay layers are assumed to be the same as in previous sections and will, sooner or later, be exhausted. Our interest will thus be focussed on the lifetime of minerals in the clay zones.

Where minerals are present in the clay layers, the lifetime of this source of salts can be approximated as the time when the dissolution front reaches the mid-thickness of the clay layer. For sand and clay layers of 2 m thickness, the clay layer will be depleted over a 2 km length, after a duration of 0.1 My. Therefore, interbedded clay sources may not remain active more than 1 My in most situations.

For diffusion alone, the case is more complex because there is a change in boundary conditions : when diffusion in a clay layer occurs in both directions, there is a zero flux across the central plane at the middle of it. This gives a more complex solution than eq.10. To solve it, we used the solution of Sudicky and Frind. (1982). Several calculations show that the lifetime of solutes within the clay layers is small. For instance, with a zero flux boundary condition at 1 m in both sand and clay layers, depletion over 25 km will last only approximately 12 ky with $v = 5$ m.y$^{-1}$ , $_{wb} = 0.4$ and $_{wa} = 0.2$. Therefore, thin clay layers do not seem to be significant diffusion sources over geological time scales.

Although interbedded clay layers might be rapidly depleted of their ion content, they may isolate several parts of the aquifer. These barriers can lead to different ion concentrations for each layer of the aquifer, that are often observed in the field (McMahon, 2001). Despite the vertical heterogeneity of concentrations, a detailed analysis of the formulae developed for thick aquitards shows that the average concentration in the aquifer is the same in a homogeneous aquifer and in an aquifer including interbedded clay layers.

For ion exchange, simple mass balance calculations show that the flux of Ca can be an important limiting factor and that clay layers embedded within the aquifer can remain active exchangers for several My. However, this behavior largely depends on the amount of calcite present in sediments that is difficult to estimate.

## Conclusion

Throughout this paper we tried to estimate the effects of aquifer/aquitard interactions on the resulting concentration gradients in the aquifer. This theoretical approach indicates that quite complex boundary conditions can be simplified in many instances and lead to analytical solutions. Whilst these solutions must be calculated numerically, these formulae help to understand the roles of the different variables and make sensitivity analysis easier than would be the case with numerical models. This approach shows the very different patterns resulting from leakage, dissolution, diffusion and ion exchange. The results may help to understand better the evolution of chemistry in deep ground waters.

Calculations on leakage showed that at places where leakage is significant for the global flow in the aquifer system, it may lead to important changes in concentration in the aquifer, provided that mineralized solutions exist in the aquitard. Therefore where hydrodynamic modeling of an aquifer system suggests the existence of leakage, this can be verified by analyzing the concentration gradients of several ions. Diffusion itself seems to play a secondary role, except in a young aquifer or aquitards deposited under brine conditions. However diffusion limits the flux of matter through the aquitard and thus slows the dissolution or ion exchange fluxes from the aquitard. That is why these processes can be identified even tens of My after burial, even though aquifer groundwater might have been renewed a thousand times. Ion exchange should now be viewed with an emphasis on aquitard CEC. The role of ion exchange from the aquitard should be considered where ion exchange is recognized in ground waters from an aquifer of substantial age.

## References

- Appelo, C.A. and Postma, D. (1993) Geochemistry, Groundwater & Pollution, Balkema, A. A.
- Castro, M.C., Stute, M. and Schlosser, P. (2000) Comparison of 4He ages and 14C ages in simple aquifer systems: implications for groundwater flow and chronologies, Applied Geochem., 15(8): 1137-1167.
- Chiodini, G., Frondini, F., Kerrick, D.M., Rogie, J., Parel (1999) Quantification of deep CO2 fluxes from Central Italy. Examples of carbon balance for regional aquifers and of soil diffuse degassing, Chem. Geol., 159(1-4): 205-222.
- Hiscock, K.M., Dennis, P.F., Saynor, P.R. and Thomas, M.O. (1996) Hydrochemical and stable isotope evidence for the extent and nature of the effective Chalk aquifer of north Norfolk, UK, J. Hydrol., 180(1-4): 79-107.
- Koltermann, C.E. and Gorelick, S.M. (1995) Heterogeneity in sedimentary deposits: A review of structure-imitating, process-imitating, and descriptive approaches , Water Resources Res., 32(9): 2617.
- Lasaga, A. (1998) Kinetic Theory in the Earth Sciences, University Press (Princeton).
- Love, A.J., Herczeg, A.L., Sampson, L., Cresswell, R.G. and (2000) Sources of chloride and implications for 36Cl dating of old groundwater, southwestern Great Artesian Basin, Australia, Water Resources Res., 36( 6): 1561.
- Mehta, S., Fryar, A.E. and Banner, J.L., (2000) Controls on the regional-scale salinization of the Ogallala aquifer, Southern High Plains, Texas, USA, Applied Geochem., 15(6): 849-864.
- Plummer LN, Sprinkle CL (2001) Radiocarbon dating of dissolved inorganic carbon in groundwater from confined parts of the Upper Floridan aquifer, Florida, USA, Hydrogeol. J., 9: 127-150.
- Raoult, Y., Lauverjat, J., Boulegue, J., Olive, P. and Bari (1998) Etude hydrogéologique d'une ligne d'écoulement de l'aquifère de l'Albien dans le Bassin de Paris entre Gien-Auxerre et Paris, Bull. Soc. Géol. France, 169 (3): 453-457.
- Sudicky, E.A. and Frind., E.O. (1982) Contaminant transport in fractured porous media: Analytic solutions for a system of parallel fractures., Water Resources Res., 18(6): 1634-1642.
- Taigbenu, E.A. and Onyejekwe, O.O. (2000) A flux-correct Green element model of quasi three-dimensional multiaquifer flow, Water Resources Res., 36 , No.: 3631.

## DARCY 29

# Groundwater influence on river nitrate concentration in crystalline rock aquifers

Ayraud V.*, Aquilina L., Labasque T., Pierson-Wickmann A.-C., Molénat J., Pauwels H., Fourré E.,
Tarits C., Bour O., Durand V., Le Corre P., Mérot P. et P. Davy
*Géociences Rennes, 35000 Rennes, France
virginie.ayraud@univ-rennes1.fr

Although, crystalline rock cover more than 20% of continental areas, groundwater residence time and its relation with river chemistry is very poorly constrained. Groundwater residence times were determined by CFC analysis at 7 site study within a context of crystalline aquifer in Brittany. Results indicate a strong control of the physical rock heterogeneity which leads to homogeneous groundwater residence times at the regional scale. In the weathered rocks (altered or highly fissured) which develop on the first 20-30 meters groundwater circulates for 18±3 years whatever the studied site. This long residence time implies slow vertical velocities which must be balanced by a high anisotropy.

Knowledge of both residence times and NO3 concentrations of groundwater allows to predict evolution of nitrate concentration within river. Intensification of agricultural practices lead to a drastic increase of groundwater nitrate concentration during the mid-80's whereas maximum in annual mean river nitrate concentration appeared only during the mid-90's. In temperate areas river flow can be divided in two major periods: high discharge (winter) and low discharge (summer). Comparison of groundwater nitrate concentration with evolution of concentration in river between high or low discharge periods indicates that the supplying hydrogeological compartment and transfer process differs. Maximum nitrate concentration in river occurs during high discharge period and is related to subsurface horizontal transfer whereas during low-discharge period the slow transfer from the weathered part of the aquifer is the main water supply and implies a NO3 concentrations increase as long as water residence time. This transfer mechanism indicates that a limitation of nitrate fertilization in catchments would lead to an annual maximum nitrate concentration decrease within 2 to 5 years but during low discharge periods nitrate concentration should remain high for a least 2 decades.

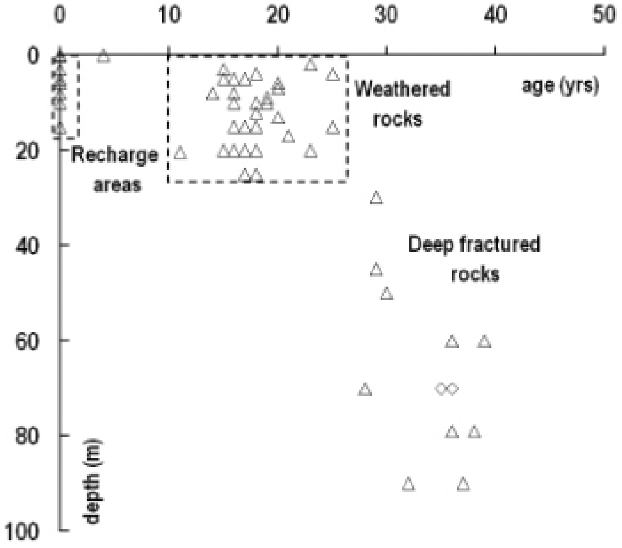

Figure1: Groundwater age as function of depth

# DARCY 32

# Reconstructing Natural Groundwater Flow and Geochemical Processes in a Perturbed Multi-Layer Aquifer System.

BAIRD Dallas[1,2,*], LE GAL LA SALLE Corinne[2,3], LOVE Andrew[2,4], SIMMONS Craig[1,2]

[1] Flinders University, SoCPES, GPO Box 2100, Adelaide, SA, 5001 Australia.
[2] Centre for Groundwater Studies, c/- SoCPES, GPO Box 2100, Adelaide, SA, 5001 Australia.
[3] Centre Universitaire de Formation et de Recherche de Nîmes, LaboGIS, 30035 Nîmes, France
[4] Dept. of Land, Water and Biodiversity Conservation, GPO Box 2834, Adelaide, SA, 5001 Australia.
[*] Corresponding author: dallas.baird@flinders.edu.au

## Abstract

A combined hydraulic and hydrogeochemical approach is helping to improve our understanding of a perturbed multi-layer aquifer system in the Northern Adelaide Plains, South Australia. Excessive groundwater pumping from a confined Tertiary carbonate aquifer has reversed the historical upward hydraulic gradient. Although significant contamination has occurred by leakage through leaky wells, large scale leakage through a confining layer does not appear to be significant. Carbon-14 activities verify the original groundwater flow direction. Stable isotopes of water reveal that although subsurface flow from the adjacent mountain ranges is the dominant recharge mechanism, areas missing an important confining layer also receive a significant amount of evaporated water. The stable isotopes of water, together with Cl concentrations, reveal climatic changes over the past tens of thousands of years. Groundwater chemistry is predominantly affected by evapotranspiration. Carbon-13 and strontium isotopes indicate that carbonate mineral dissolution is also an important geochemical process.

## 1. Introduction

Developing accurate conceptual models of natural groundwater systems is crucial when determining the groundwater residence time and recharge rate, modelling the system, and assessing the sustainable yield of the resource. Disturbances to the natural groundwater system, by excessive groundwater extraction, for example, can hinder our understanding of the natural groundwater flow. In situations where the present day potentiometric surface no longer represents the natural system, historical data and geochemical studies can provide the necessary information to “reconstruct” natural, undisturbed conditions and develop accurate conceptual models (Schlehuber et al, 1989; Edmunds et al, 2002). However, contamination of aquifers by leakage through confining layers or leaky wells can limit the usefulness of geochemical tracers. It is essential when using tracers such as carbon-14 to determine groundwater recharge rates that these natural conditions are understood by identifying the geochemical processes that affect the concentration of geochemical tracers, and that the effects of any contamination by leakage through confining layers or leaky wells are accounted for.

One area greatly affected by excessive groundwater extraction is the multi-layered aquifer system of the Northern Adelaide Plains (NAP), South Australia. The region relies heavily on groundwater for an important horticulture industry. The multi-layer aquifer system consists of a sequence of Quaternary age clays, silts, sands and gravels containing relatively saline groundwater, overlying confined Tertiary age limestone and calcareous sandstone deposits which provide good quality groundwater for irrigation. Prior to significant groundwater extraction, the confined carbonate aquifers were artesian (Smith, 1979; Gerges, 2001). Several decades of excessive groundwater extraction has seen a significant cone of depression develop in the centre of the region. This has resulted in radial groundwater flow towards the cone of depression and reversing the vertical hydraulic gradient so that saline groundwaters in overlying aquifers may flow downwards into the fresh carbonate aquifers. This problem is exacerbated by numerous leaky boreholes in the region.

This paper first builds on the present understanding of the groundwater hydrology using an environmental tracer approach. The potential for leakage is then examined, and the groundwater chemistry is assessed for contamination. A hydrogeochemical model is then discussed for a 30km long fresh groundwater corridor in the most heavily exploited aquifer. By determining the location and extent of anthropogenic effects, the undisturbed groundwater chemistry can be better understood, allowing us to "reconstruct" the pre-irrigation conditions.

## 2. Hydrogeological Setting

Centred approximately 40km north of Adelaide, South Australia, the NAP is a gently sloping to flat alluvial plain, bordered by the southern Mount Lofty Ranges (MLR) to the east, and Gulf St Vincent to the west (Fig. 1). The area has a low relief, sloping gently from the foothills in the east towards the coast. An escarpment in the east is formed by the Para Fault, above which the MLR rise to more than 600m. A number of watercourses occur on the escarpment, however, only two water courses, the Gawler River and the Little Para River, reach the coastline. Even these are seasonal, only flowing to the sea during wetter months or after heavy rainfall events.

The region enjoys a Mediterranean climate, with hot, dry summers and cool, wet winters. Rainfall across the plains is less than 500 mm/yr, but increases to more than 800mm/yr in the more elevated areas of the adjacent hills. Potential evaporation greatly exceeds rainfall for most of the year.

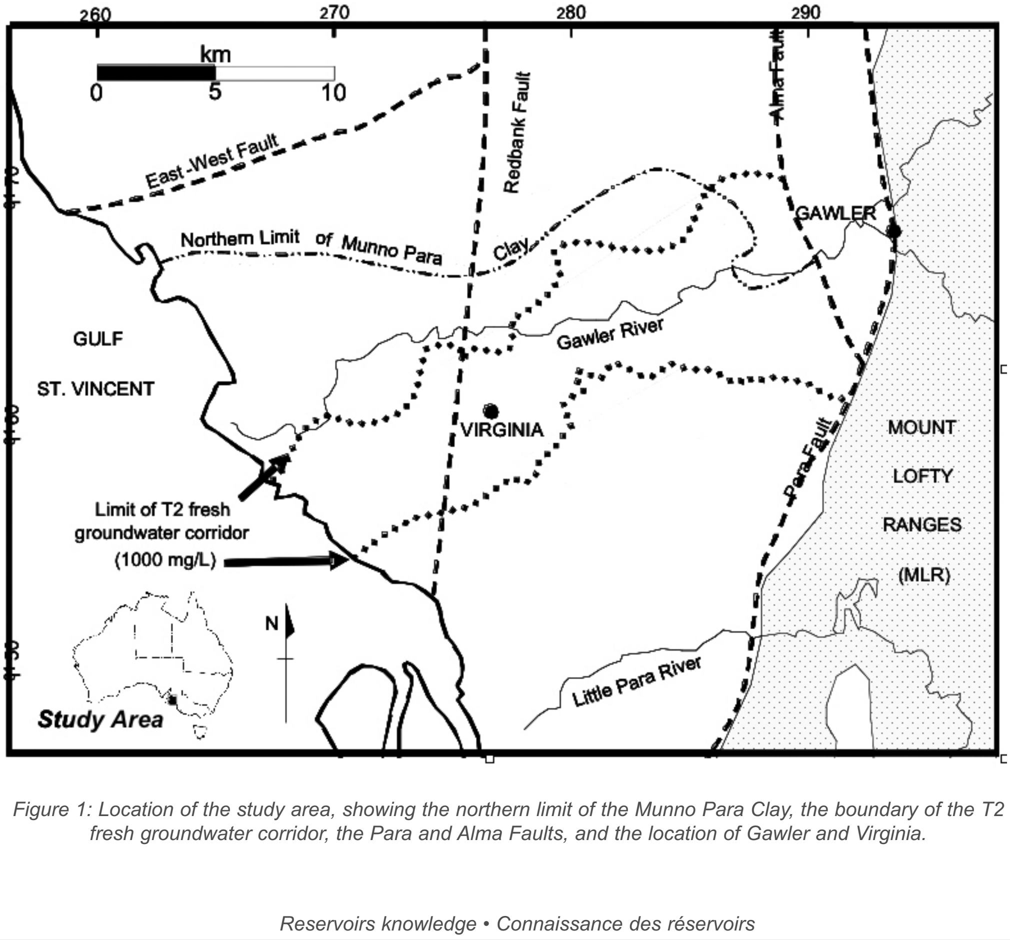

*Figure 1: Location of the study area, showing the northern limit of the Munno Para Clay, the boundary of the T2 fresh groundwater corridor, the Para and Alma Faults, and the location of Gawler and Virginia.*

The Adelaide Plains sub-basin is a graben formed by one in a series of block faults in Precambrian rocks of the Adelaide Geosyncline. These rocks consist primarily of siltstones, quartzites, dolomites and finer grained sedimentary rocks deposited in largely marine environments. On the plains, Quaternary clays, sands and gravels deposited in alluvial environments overlie Tertiary limestones and calcareous sandstones (Fig.2). In the Gawler area in the northeast of the study area, the Alma Fault Block (AFB) is formed by the Alma and Para Faults. Here, the Tertiary aquifer is comprised of undifferentiated siliceous sediments. The sediments in the basin form a wedge shape which thins to the north; the thickness of the sediments increases from approximately 100m in the north to approximately 400m in the south.

The aquifers are numbered in order of increasing depth. The Quaternary aquifers (Q1 to Q4) have salinities ranging from 1,000 to 15,000mg/L, with freshest groundwaters occurring near the major watercourses. The upper Tertiary aquifers (T1 and T2) are also generally freshest beneath the rivers, with salinities ranging from about 700 to 3,000mg/L. Two lower Tertiary aquifers (T3 and T4) are highly saline, however, they are separated from the fresher aquifers by thick clays and silts. The most important aquifer in the region is the T2 aquifer, a well-cemented limestone generally 80 to 120m thick. The aquifers in the Quaternary sediments are separated from each other and the Tertiary sediments by varying thicknesses of clay. In some areas, these confining layers can be thin or absent. The main confining unit in the region is the Munno Para Clay, a 6-8m thick layer separating the T1 and T2 aquifer. This confining layer is missing to the north of the Gawler River and in the Gawler area in the north-east of the NAP.

Recharge to the sedimentary aquifers occurs predominantly as subsurface flow (referred to as mountain block recharge; Wilson and Guan, 2004; Manning and Solomon, 2005). Groundwater in fractured rock aquifers in the MLR flows into confined aquifers that abut onto the fractured rock under the ground surface (Gerges, 1986; 2001). Hydraulic connection across these faults was demonstrated by Gerges (1999) in an area to the south of the NAP.

The T2 aquifer provides the majority of groundwater for irrigation, particularly around the Virginia area. Approximately 18,000 ML/yr is extracted from the Tertiary aquifers in the NAP region, about 14,000 ML/yr from the T2 aquifer alone (Gerges, 2001). This greatly exceeds natural recharge. A cone of depression up to 70m below natural groundwater levels has developed, resulting in radial groundwater flow. Leakage through leaky boreholes has resulted in significant rapid local increases of salinity. Within the 750km$^2$ NAP area, there are approximately 4400 licensed, disused or abandoned wells, as many as 5-6% of which may be leaking (Schuster, 2000). Leaky wells are therefore a significant threat to the long-term sustainability of the fresh groundwater resource. They are also a potential source of contamination for detailed groundwater chemistry investigations which must be identified and corrected for.

## 3. Methodology

Data used in this investigation include historical data and samples collected specifically for this study. The historical data provided major ions and general parameters, and enabled a more complete coverage of the NAP and the fresh groundwater corridor. Well data and chemical analyses are available from the Department of Water, Land and Biodiversity (DWLBC) Drillhole Enquiry System (online database; https://info.pir.sa.gov.au/des/desHome.html). Data from as early as the 1930's is available, when the Tertiary aquifers were still artesian. Samples displaying anomalous chemical data such as poor ion balance or unrealistic values, or with unsuitable well construction, were not included.

In addition to the historical data, 47 samples across the NAP were also collected from monitoring wells and private wells to examine other tracers in addition to major ion chemistry. Samples were analysed for major ions, stable isotopes δ2H, δ18O and δ13C, radioactive tracers $^{14}$C and tritium, and radiogenic $^{87/86}$Sr. All stable isotopes were analysed using stable isotope mass spectrometer. Approximately half of the carbon-14 samples were analysed by Liquid Scintillation Counting (LSC) at CSIRO in Adelaide, while the remainder were analysed by Accelerated Mass Spectrometry (AMS) at ANSTO in Lucas Heights. Tritium was analysed after electrolytic enrichment by LSC at ANSTO Environment. Strontium isotopes were analysed at Adelaide University's School of Earth and Environment Sciences.

Samples collected for this study had pH determined by a calibrated pH meter connected to a flow cell at the well head, and display pH values consistently 0.2-0.4 pH units lower than the historical data in similar areas. This has significant implications for the calculation of saturation indices for carbonate minerals, and is discussed further below. While the data was collected for the entire NAP region, most of the geochemical evolution discussed here refers to the fresh T2 corridor extending from Gawler through Angle Vale and Virginia to the coast.

## 4. Conceptual Model

The present potentiometric surface is greatly disturbed, so while the current direction for potential groundwater flow is known, this does not reflect the natural (undisturbed) conditions of the NAP. Two conceptual models are presented for the NAP: the hydrogeological reconstruction of pre-1940's natural system (Fig. 2a), and the present day system in response to several decades of groundwater extraction (Fig. 2b). Although the precise hydraulic heads of the various aquifers is unknown before significant extraction began, the Tertiary aquifers were flowing prior to the mid-1940's (Smith, 1979). The key features of the pre-1940's conceptual model are that groundwater flowed from the Mount Lofty Ranges towards Gulf St Vincent and groundwater had potential for upward flow. Although regular monitoring of water levels did not begin until after significant disturbances to the system, Shepherd (1971) presented a potentiometric surface for the Tertiary aquifers for September, 1959. This indicated groundwater flowing across the NAP in a west-south-westerly direction, perpendicular to the coastline. The natural groundwater flow also had an upward hydraulic gradient Gerges (1999; 2001), with the potentiometric surface of the Tertiary aquifers being higher than the Quaternary aquifers. In some areas, the Q2 aquifer had a higher potentiometric surface than the Q1 aquifer. These historical hydraulic gradients, combined with salinity profiles, led Gerges (1986) to suggest that groundwater recharge to the NAP aquifers occurred as subsurface flow from the adjacent mountain ranges. The present day conceptual model shows that radial flow towards the main pumping centre at Virginia, and potential for downward flow, now dominates.

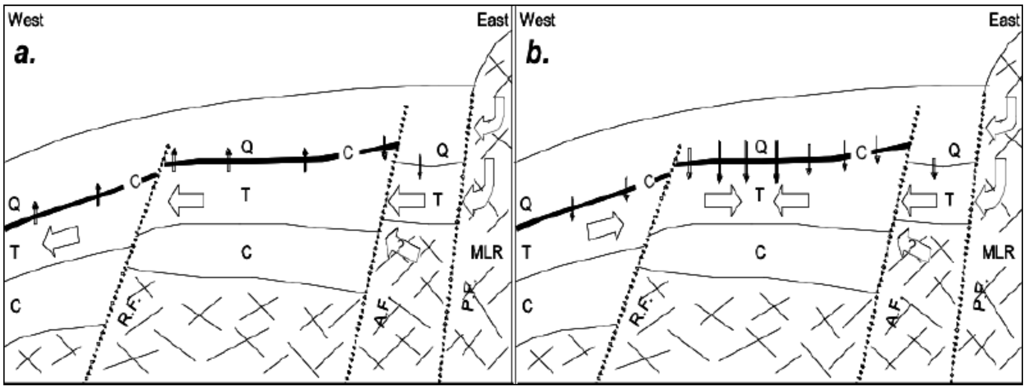

*Figure 2: Simplified conceptual models for pre-1940's (a) and present (b) systems along the T2 fresh groundwater channel. Block arrows indicate lateral groundwater flow, small arrows indicate potential vertical flow between the Quaternary and Tertiary aquifers. Q = Quaternary aquifers. T = Tertiary aquifers. C = confining layers. MLR = Mount Lofty Ranges (fractured rock). RB = Redbank Fault. AF = Alma Fault. PF = Para Fault.*

### *4.1. Recharge and groundwater flow*

Using environmental tracers, it has been possible to refine the conceptual model for groundwater flow and recharge. Carbon-14 can provide information on the geochemical processes groundwater has undergone during recharge and flow, as well as provide an indication as to the age of the water due to radioactive decay. Carbon-14 activities across the NAP range from 1.4 to 90.3pmC. Highest activities occur in the Gawler region and decrease along the flowpath towards the coast. The uncorrected activities suggest residence times up to tens of thousands of years. The distribution of $^{14}$C activities confirms the direction of groundwater flow indicated by the 1959 potentiometric surface, with "modern" activities decreasing with increasing distance from the MLR The Quaternary aquifers have generally higher $^{14}$C activities, suggesting that they must receive some component of modern recharge. If upward leakage from the Tertiary aquifers were the only mechanism of recharging the deeper Quaternary aquifers, the $^{14}$C activities would be similar.

The stable isotopes of water, $\delta^{18}$O and $\delta^{2}$H, were examined to provide information regarding the source of water, the processes it has undergone prior to recharge, and of mixing between waters with differing signatures. In addition to the samples collected from the NAP, existing data from samples in the MLR are also utilised for this interpretation. Data for the MLR is from two sources, both approximately 35km south-east of Virginia. Ivkovic et al (1998) investigated groundwaters in the Piccadilly Valley, while Radke et al (2000) examined the much larger Upper Onkaparinga region. Although these groundwaters are located on the eastern side of the topographic divide, $\delta^{2}$H values for MLR groundwaters just south of the NAP (Dighton et al, 1994) have a similar range and values ($\delta^{2}$H between -30.0 and -24.8‰), justifying the use of the Ivkovic and Radke data ($\delta^{2}$H between -31.5 and -23.2‰). The Ivkovic data were sampled at a higher average elevation than the Radke data, and are slightly more depleted due to altitude and rainfall amount effects.

The $\delta^{2}$H and $\delta^{18}$O values for all groundwaters range from -31.5 to -18.6‰ and -6.22 to -3.50‰, respectively. Most groundwaters plot along or near the Local Meteoric Water Line (LMWL; Fig. 3), indicating that groundwaters are of a meteoric origin, and no connate or trapped seawater remains in the aquifers. Plotting along the LMWL also suggests that minimal fractionation due to evaporation occurred prior to recharge due to rapid infiltration of water to the water table.

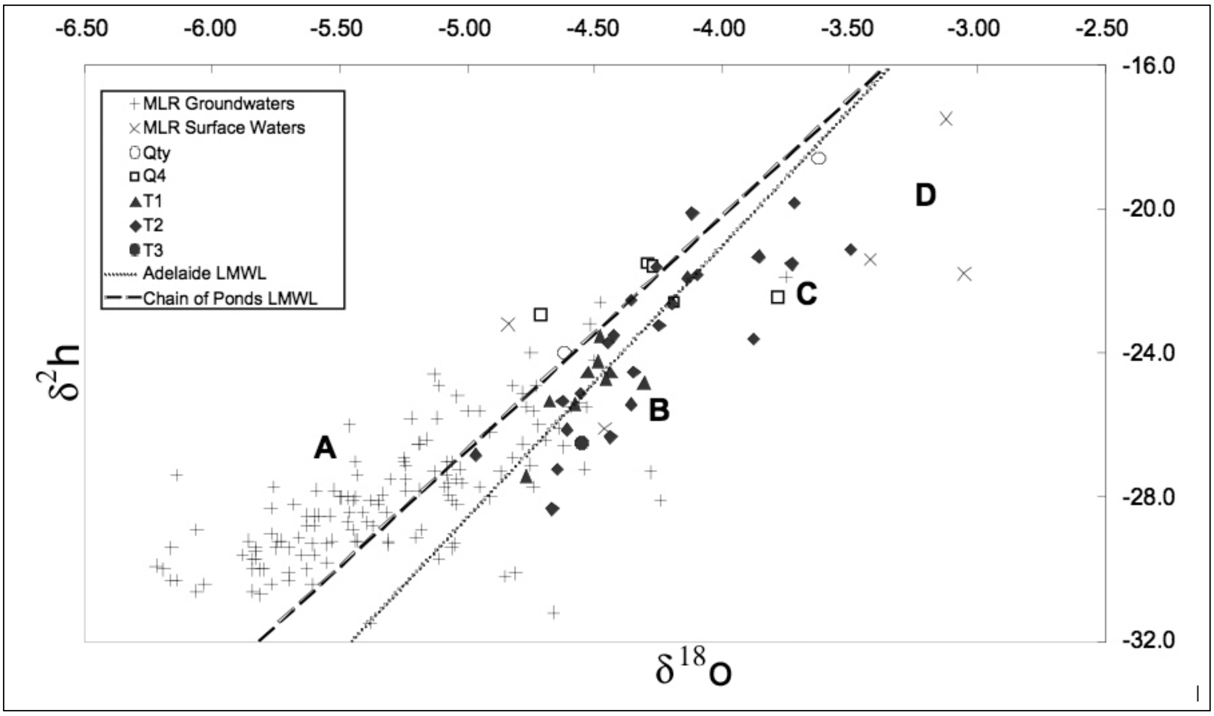

Figure 3: $\delta^{18}$O and $\delta^{2}$H values for groundwaters and surface waters in the MLR and NAP.

Four broad, overlapping yet distinct groups of waters are observed in Figure 3. Group A ($\delta^{18}$O -6.22 to -3.75‰; $\delta^{2}$H -31.5 to -21.9‰) represents the MLR groundwaters, which is the most depleted group of groundwaters. These groundwaters plot along a relatively low slope when compared with the Adelaide LMWL. However, a LMWL determined for Chain of Ponds in the MLR (Ivkovic et al, 1998) also has a lower slope than the Adelaide LMWL. The lower slope of the Chain of Ponds LMWL and the MLR groundwaters may be due to the site being more inland than the Adelaide LMWL site (Ivkovic et al, 1998; Radke et al, 2000). Evaporation of falling rain, particularly in arid environments, can lead to lower slopes (Clark and Fritz, 1997).

Group B ($\delta^{18}$O -4.97 to -4.10‰; $\delta^{2}$H -28.3 to -20.1‰) contains the bulk of the NAP groundwaters (except for groundwaters in the Gawler region). They are more enriched than the MLR groundwaters although the two groups overlap, and they also plot along the LMWL. NAP groundwaters are more depleted further along the groundwater flowpath (Fig. 4a). A similar trend was observed by Love et al (1994) for a coastal aquifer system in the Otway Basin, also located in SE Australia. Possible causes for the variation included lower temperatures resulting from climatic changes and continental effects caused by sea level fluctuations, which resulted in a coastline 200-300km further west during the last glacial maximum. Similar processes would also have influenced rainfall in the NAP region.

Group C ($\delta^{18}$O -3.88 to -3.50‰; $\delta^{2}$H -23.6 to -18.6‰) comprises of groundwaters in the Gawler area of the NAP where the Munno Para Clay is absent. They are enriched, and appear to have been subjected to slight evaporation, or have mixed with evaporated water. Group D ($\delta^{18}$O -3.42 to -3.05‰; $\delta^{2}$H -21.8 to -17.5‰) includes all but two of the MLR surface waters and show considerable evaporation effects relative to the groundwaters. The two other MLR surface waters are depleted and plot with the MLR groundwaters, possibly reflecting baseflow contributions or sample collection shortly after rainfall.

With the exception of groundwaters in the Gawler area, the bulk of NAP samples (Group B) overlap the MLR groundwaters, but are notably more enriched. This enrichment does not appear to be due to evaporation, as they plot along the LMWL. This suggests that recharge to the NAP aquifers is predominantly by subsurface flow from the MLR, however, this recharge must come from the lower slopes of the MLR where the groundwater isotope signature is not too depleted. Groundwater in the more elevated parts of the MLR have more depleted values, and must discharge elsewhere.

Groundwaters in the Gawler area (Group C) plot between NAP groundwaters and surface waters, suggesting either mixing between surface waters and MLR groundwaters, or contribution from direct recharge across the plains. Heavy groundwater extractions in this area combined with thin confining layers means that downward leakage is possible. It is difficult to confirm this, however, as the stable isotope values for the Quaternary aquifer groundwaters do not all display such enriched signatures. It may also be possible that infiltration of stream and river water runoff from the Para Fault scarp face, either at the fault or in the foothills above the fault, provides this enriched signature. This suggests that an evaporated source of water is important to the water balance of this area.

### *4.2. Potential for leakage*

The present day conceptual model (Fig.2a) shows that there is potential for downward leakage to the T2 aquifer across the entire NAP. It is essential to determine whether leakage is occurring in order to use $^{14}$C ages to establish groundwater recharge rates. If recent $^{14}$C has been introduced, recharge rates estimated will be greater than the actual rate. Leakage to the confined aquifers is known to occur through leaky wells, where sudden increases in TDS or Cl concentration are the first indicators of such leakage. The presence of tritium or nitrate can also indicate contamination, and may occur where subtle changes in TDS or Cl concentration are not detected. Conversely, the absence of nitrate or tritium does not necessarily mean contamination has not occurred, as they may be removed over time by denitrification and tritium radioactive decay. As such, the absence of nitrate or tritium does not necessarily mean that contamination has not occurred.

Measured tritium values in the NAP range from 0.4 to 1.4 TU. Although tritium was recorded in wells across the NAP, indicating contamination, the groundwaters in the Gawler area also showing enriched stable isotope signatures all contained measurable tritium. This may indicate contamination by leakage or it could be due to natural recharge. Tritium concentrations in the MLR indicate relatively rapid movement to considerable depth. Ivkovic et al (1998) report tritium values greater than 1.4 TU at 200m depth. Therefore, high tritium concentrations in the Tertiary aquifers near to the subsurface recharge boundary may result from subsurface flow. Measurable nitrate levels in the NAP ranged from 0.01 to 114 mg/L, although most contained less than 6 mg/L. While 39% of all Tertiary groundwater samples contained $NO_3$ (50% of T1, 33% of T2), nearly 71% of all Quaternary aquifer groundwater samples contained measurable $NO_3$. Approximately 20% of T2 wells specifically sampled for this study contained measurable nitrate. These values reveal the extent of leakage that is occurring in the NAP. A combination of Cl concentration increases, the presence of $NO_3$ or anomalously high $^3$H or $^{14}$C could be used to indicate potential contamination.

Gerges (2001) used salt balances to determine that lateral through-flow has replenished groundwater removed from storage, and not downward leakage from the relatively saline Quaternary aquifers. Leakage from the Quaternary aquifers to the Tertiary aquifers through leaky wells was estimated at between 600 and 1600 ML/yr. It is also possible to calculate how long downward leakage may take from the overlying saline aquifers to the T2 aquifer through the main confining layer using Darcy's Law:

$$V_z = K_v i_v / n_e$$

where $V_z$ is the vertical average linear velocity, $K_v$ is the vertical hydraulic conductivity of the confining layer, iv is the vertical hydraulic gradient across the layer and ne is the effective porosity of the confining layer. Along the T2 fresh groundwater corridor in the most heavily pumped area, the T2 aquifer is separated from the more saline T1 aquifer by 6m of Munno Para Clay. The average $K_v$ for this unit is $2.1 \times 10^{-6}$ m/day, and the minimum recorded porosity is 0.37 (Gerges, 1999). Using the peak head difference of approximately 40m between the T1 and T2 aquifers in the centre of the cone of depression, it is estimated that it would take more than 400 years for relatively saline T1 groundwater to enter the T2 aquifer. This estimate is valid for the centre of the cone of depression, and does not reflect average values across the NAP. Smaller head differences and higher porosities observed elsewhere would mean that more time is required for leakage to occur. Given that the potential for downward flow has only been possible for a maximum of 50 years, and that the Munno Para Clay is an effective confining layer where present (Gerges, 2001), contamination of the confined T2 aquifer is a result of leakage through wells. Where the Munno Para Clay is absent (e.g. in the Gawler area), less effective confining layers may allow some downward leakage to occur. The relatively low transmissivity of the T2 aquifer (Shepherd, 1971; Gerges, 2001) means that contamination would initially be relatively localised.

Chloride concentrations along the T2 flowpath are shown in Fig.4b. The Cl concentration initially decreases slightly across the Alma Fault from around 225 to 180 mg/L. This could be due to fresher groundwater recharge from fractured rock aquifers on the AFB or palaeoclimate changes. The Cl concentration then increases to around 300mg/L near Virginia before decreasing to around 250mg/L further along the flowpath. There are no low Cl concentration sources available for mixing which could be responsible for this decrease. The highest Cl concentrations along the fresh groundwater channel occur beneath the area of greatest groundwater extraction and bore density, and might appear to be the result of large scale downward leakage in the area. However, historical records from prior to 1950 (1935 to 1949) indicate that the same concentrations and trends existed at this time. As the pre-1950's records were taken prior to significant groundwater extraction, when the number of leaky wells was negligible and the T2 aquifer still had artesian pressures, it appears that leakage has not significantly altered the groundwater chemistry over a large scale in the region. Contamination is likely to be localised to wells at this point in time, and vertical leakage through the aquitards is unlikely over such a large area.

Love et al (1994) also observed decreasing Cl concentrations (from around 1600 to 210mg/L) along a groundwater flowpath in a confined aquifer in the Otway Basin. Minimum Cl concentrations occurred between 18ka and 10ka, during a cooler and more arid period. Higher evapotranspiration rates since this period have resulted in increasing Cl concentrations. Similar trends in stable isotope and Cl concentrations have been observed in both the Otway Basin and the NAP. The changes in Cl concentration along the T2 fresh groundwater flowpath are therefore not due to leakage, and most likely reflect changes in palaeoclimate over the past tens of thousands of years.

## 5. Geochemical Evolution

### 5.1. Origin of solutes

Most groundwaters in the NAP are dominated by Na and Cl. Relatively fresh groundwaters are generally Na-Ca-Cl-$HCO_3$ type groundwaters, and tend towards a Na-Cl type as salinity increases. Evapotranspiration is the dominant process controlling groundwater chemistry in the MLR and the NAP. Accession of sea salts, dry deposition and ET of rainfall during summer months allow salts with a largely marine signature to accumulate in the soil zone. During winter when groundwater recharge occurs, infiltrating waters dissolve some of these salts and transport them to the water table.

The ratio of conservative ions Br/Cl follows a seawater dilution line (SWDL) when plotted against Cl (Fig. 4c), suggesting that the source of solutes is marine. Dissolution of halite within the formation is not a source of Cl, which would be indicated by considerably lower Br/Cl ratios. Combined with the stable isotope data which show that all groundwaters are of a meteoric origin, it is apparent that the solutes in the NAP groundwaters reflect the recharge history, not the depositional history, of the aquifer.

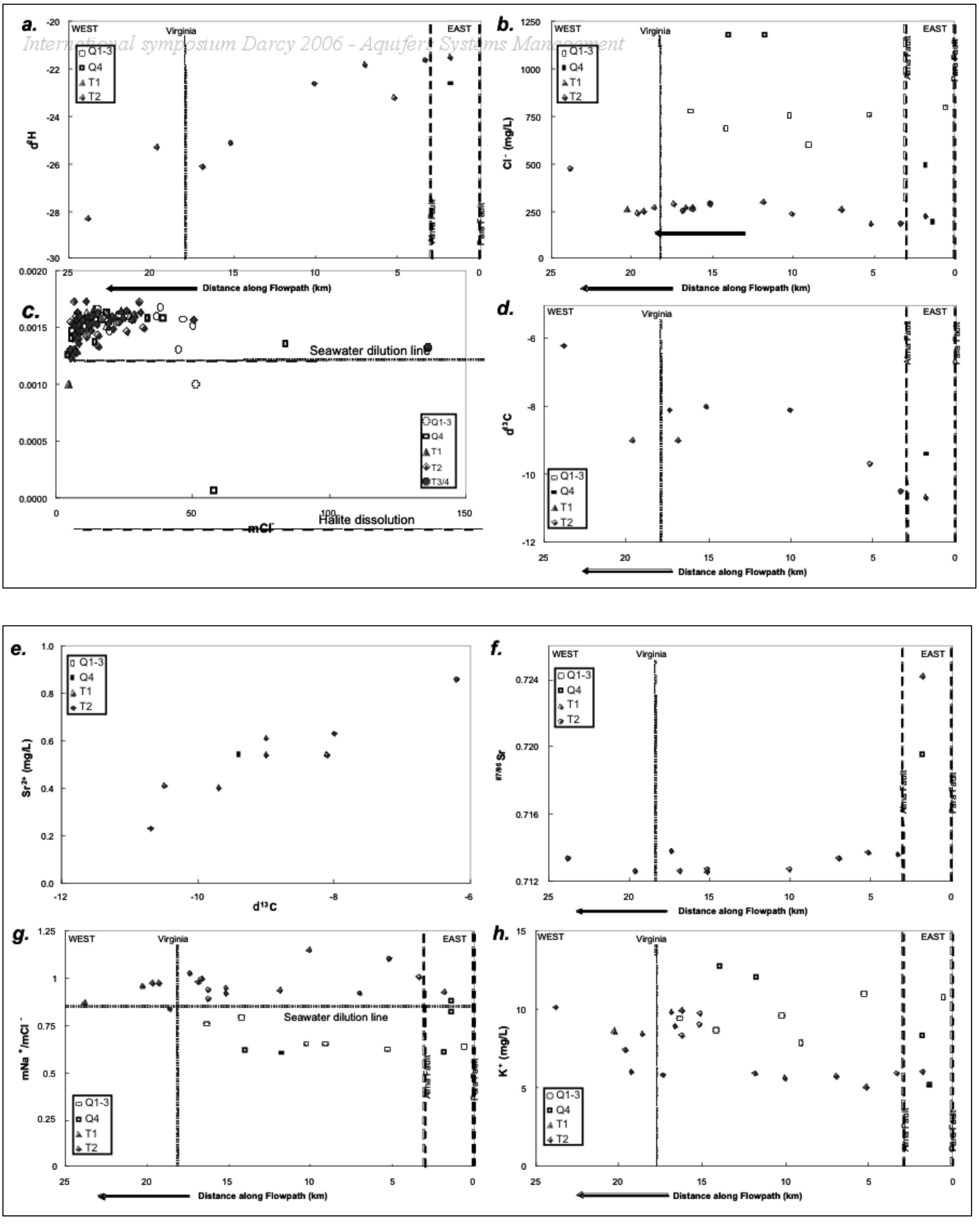

Figure 4: Geochemical trends for the NAP groundwaters.

### *5.2. Geochemical processes*

Ca and $HCO_3$ concentrations indicate that carbonate mineral dissolution is an important water-rock interaction occurring in the aquifer. $HCO_3$ concentrations increase from 150mg/L on the AFB to approximately 270 mg/L in the carbonate aquifer. $HCO_3$ concentrations then vary between 225 and 300 mg/L along the rest of the flowpath. Ca concentrations increase from 25 mg/L on the AFB to around 75 mg/L and remain relatively constant.

The saturation indices for carbonate minerals were determined using PHREEQC (Parkhurst and Appelo, 1999). Most groundwaters tend to be considerably supersaturated with respect to calcite and dolomite. $CO_2$ degassing during sampling would result in carbonate mineral supersaturation and precipitation, along with a pH increase (e.g. Langmuir, 1971; Mahlknecht et al, In Press). NAP groundwaters are nearer to saturation when pH is reduced by 0.5 pH units (e.g. Edmunds et al, 2003). The pH of historical data used in this study was presumably not measured in field. This is suggested by the pH levels of historical data being consistently 0.2-0.4 pH units higher than samples measured in the field. Samples collected in the field have probably also been subjected to some degassing, but not to the same extent as the historical data. The result is that calculated saturation indices for NAP groundwaters differ from the true in-situ values, and provide only an approximate guide as to whether a mineral will dissolve or precipitate. It is likely that NAP groundwaters are at saturation.

Calcite saturation indices for groundwaters along the T2 fresh groundwater corridor range from -1.42 to oversaturated. Lowest values are in the undifferentiated sediments on the AFB indicating that carbonate dissolution can occur near the recharge zone. Saturation indices rapidly approach equilibrium along the flowpath, and exceed saturation approximately 5km along the flowpath. It is more likely that equilibrium is obtained at some point further along the flowpath than indicated, and is maintained rather than exceeded greatly saturation. Carbonate mineral saturation indices for the Quaternary aquifers are generally lower than the Tertiary aquifers due to a relatively lower concentration of carbonate minerals in the Quaternary sediments.

Carbon-13 can provide information regarding the processes affecting dissolved carbonate species in groundwater. The $\delta^{13}C$ values across the NAP region range from -15.1 to -6.0‰, and generally become more enriched along the flowpath ($\delta^{13}C$ from -10.7 to -6.2‰; Fig. 4d). The $\delta^{13}C$ of soil zone $CO_2$ in SE Australia is approximately -23‰. In open system conditions, dissolved $CO_2$ will have a similar value. A fractionation factor of +8‰ between soil $CO_2$ and dissolved $HCO_3$ results in DIC with $d^{13}C$ of approximately -15‰ (Clark and Fritz, 1997). During congruent dissolution of carbonate minerals, 1 mol of $HCO_{3^-}$ is added from carbonate dissolution for every 1 mol derived from soil $CO_2$, according to the reaction:

$$CaCO_3 + CO_2 + H_2O \longrightarrow Ca^{2+} + 2HCO_3^-$$

Carbonate minerals have a δ13C of approximately 0‰, so congruent dissolution of carbonate minerals by a groundwater with $\delta^{13}CDIC$ of -15‰ will result in groundwater with $\delta^{13}CDIC$ of -7.5‰. Incongruent dissolution of dolomite or high Mg-calcite will lead to further enrichment of $\delta^{13}C$ of carbonate species. The range of values in the NAP indicates reaction between soil zone $CO_2$ and marine carbonate matrix by congruent and incongruent carbonate dissolution.

Carbonate mineral dissolution is also evidenced by $Sr^{2+}$ concentrations and $^{87}Sr/^{86}Sr$ ratios. Unpublished data for siltstone, regolith and soil at Scott Creek in the MLR indicate high $^{87}Sr/^{86}Sr$ ratios between 0.728464 and 0.815905 (R. Cranswick, pers.comm.). As a result of these high host rock ratios, groundwaters from the same area also have high values compared with the seawater ratio, ranging from 0.726173 to 0.753041. Although measurements of $^{87/86}Sr$ were not performed on the NAP aquifer matrix, these units were deposited during the same period as the Murray Group sediments in the Murray Basin (Drexel and Preiss, 1995). Dogramaci and Herczeg (2002) found that the overall $^{87/86}Sr$ ratio (carbonate and silicate) for these deposits were between 0.70869 and 0.70934, with values in carbonate minerals ranging between 0.7084 and 0.7087. This is equivalent to seawater ratios for Tertiary age marine sediments of between 0.7077 to 0.7089 (Burke et al, 1982; Palmer and Elderfield, 1985). Carbonate minerals in the Tertiary aquifers of the NAP can be expected to have similar values. Dogramaci and Herczeg (2002) found that $^{87/86}$Sr ratios for groundwaters from the Murray Group Aquifer to range between 0.7084 and 0.7112. These values resulted from carbonate mineral dissolution, however, higher values down-gradient resulted from upward leakage from a silicate aquifer.

The $^{87/86}$Sr ratio for groundwaters in the NAP range from 0.709951 to 0.724204, although most samples are between 0.7125 and 0.716. These values are intermediate between the values for the MLR and expected values for the Tertiary limestone. Sr concentrations along the fresh T2 channel increase from 0.23 to 0.86 mg/L, and increase with increasing $\delta^{13}$C (Fig. 4e). This suggests that carbonate mineral dissolution is the likely source of Sr in NAP groundwaters. It may be possible to quantify carbonate mineral reactions using Sr isotopes, which may be beneficial in correcting $^{14}$C ages (e.g. Bishop et al, 1994). $^{87/86}$Sr ratios initially decrease along the groundwater flowpath, however, they then increase beyond Virginia (Fig. 4f). This trend is the opposite of Cl concentrations, such that the peak of the Cl concentration corresponds with the lowest $^{87/86}$Sr ratios. The relatively radiogenic $^{87/86}$Sr value at the start of the flowpath indicates recharge from the MLR. Dissolution of the carbonate matrix along the flowpath leads to progressively lower values. The cause of the increase in $^{87/86}$Sr beyond Virginia remains unresolved at this time, although aquifer heterogeneity or changes in weathering rates over time are possible explanations. Mixing is unlikely, as an increase in Cl concentration would be expected with an increase in $^{87/86}$Sr values.

While carbon and strontium isotopes indicate that carbonate mineral dissolution occurs along the groundwater flowpath, there needs to be a mechanism which drives the reaction at saturation, otherwise no dissolution will occur. Possible mechanisms include mixing between two different waters, ion exchange, or gypsum dissolution encouraging dedolomitisation. Calcite dissolution at saturation may be driven by $Ca^{2+}$ removal by ion exchange (e.g. Plummer et al, 1990; Mahlknect et al, In Press). The molar Na/Cl ratio for the T2 aquifer groundwaters along the fresh groundwater corridor (Fig. 4g) show an excess of Na over the seawater ratio. This may be partly explained by Na-silicate dissolution, however, exchange for Ca in solution may also be responsible. In the Quaternary aquifers, the Na/Cl ratio is less than the seawater ratio, suggesting reverse ion exchange. The trend of K along the flowpath (Fig. 4h) suggest that its concentration is affected by ion exchange. In the T2 aquifer, K concentrations decrease slightly between Gawler and Virginia from 6 to 5.6 mg/L, while all other major cations increase, suggesting ion exchange where K is removed from solution in exchange for Ca. Near Virginia, K concentrations increase dramatically to approximately 10 mg/L. This may be an ion-exchange front associated with the increasing salinity of palaeowaters.

Increasing sulphate concentrations along the groundwater flowpath indicate water-rock interactions are contributing sulphate. This may be due to gypsum dissolution or pyrite oxidation. XRD and lithological logs in the NAP do not reveal the presence of gypsum or anhydrite (Rattray, 1999; Vanderzalm, 2004), while pyrite has been observed in some layers. Saturation indices for gypsum suggest that gypsum is not present in the system. Preliminary modelling with NETPATH (Plummer et al, 1994) is inconclusive as to the source of $SO_4$.

## 6.Conclusions

The historical groundwater flow direction across the NAP, from the MLR to the coast, has been verified using $^{14}$C activities. Stable isotopes of water have been used to establish end-members for MLR groundwater, NAP groundwaters, Gawler area groundwaters and surface waters. The majority of NAP groundwaters show little indication of evaporation, suggesting that subsurface recharge is the dominant source of recharge to the confined Tertiary aquifers. However, groundwaters in the Gawler area show some evaporation effects, indicating that an evaporated water source is an important part of the groundwater balance in the area. In terms of contamination, groundwaters displaying significant increases in Cl concentration, the presence of nitrate or tritium, or anomalously high $^{14}C$ activities can be considered as contaminated. Due to effective confining layers, leakage through wells is the dominant source of contamination across most of the NAP, which is localised to near the well. Downward leakage may be occurring where the Munno Para Clay is absent in the Gawler area, as indicated by enriched stable isotopes of water and the presence of tritium. The Cl concentration peak under the most heavily exploited area appears to be a relict of the natural system, and not regional contamination. Together with the stable isotopes of water becoming more depleted along the flowpath, they reveal climatic variations from the previous tens of thousands of years.

Groundwaters are dominated by Na and Cl, resulting from evapotranspiration of rainfall and dry deposition of marine salts in the MLR. Carbonate mineral dissolution is the dominant geochemical process, resulting in increasing $\delta^{13}C$ and Sr concentrations, and decreasing 87/86Sr ratios. An increase in $^{87/86}Sr$ further beyond Virginia requires further investigation. Increasing SO4 concentrations indicate contribution from water-rock interactions, although whether this is due to gypsum dissolution or pyrite oxidation is yet to be resolved.

Future work will involve modelling of the reactions occurring in the system and corrections to carbon-14 ages. Possible contamination means that the $^{14}C$ activities for some samples may not be reliable. It may be possible to correct the $^{14}C$ activities based on the tritium content (e.g., Mazor et al, 1986). However, the non-conservative behaviour of these tracers may limit their usefulness. It may also be possible to better constrain carbonate reactions using Sr isotopes, in order to obtain more accurate corrected ages. However, it should be considered that gypsum dissolution may also provide an additional source of Sr to the groundwaters. There is the potential with the stable isotopes of water to establish a relationship between elevation and $\delta^2H$ and $\delta^{18}O$. From this, it may be possible to determine the elevation in the MLR which predominantly contributes to NAP recharge, and possibly determine the depth of circulation of the MLR groundwaters. This would be an important tool in understanding groundwater flow in similar fractured rock environments, and will be investigated more thoroughly. Further work is also required to complete the geochemical model provided here.

## Acknowledgements

The authors thank J. Safta, H. Zulfic and other staff at the South Australian Department of Water, Land and Biodiversity (DWLBC) for assistance with sampling and analyses and advice regarding the NAP. Staff at CSIRO Land and Water and ANSTO provided stable isotope and radiocarbon analyses. J. Foden and D. Bruce at Adelaide University School of Earth and Environmental Sciences provided Sr isotope analyses. J. Pritchard is thanked for review of this manuscript. This study was supported with the aid of AINSE grants 03/072 and 04/097 for tritium and radiocarbon analyses. DB was supported by an APA Scholarship and CGS stipend.

## References

- Bishop, P.K., Smalley, P.C., Emery, D. and Dickson, J.A.D., 1994. Strontium isotopes as indicators of the dissolving phase in a carbonate aquifer: implications for 14C dating of groundwater. Journal of Hydrology, 154: 301-321.
- Burke, W.H., Denison, R.E., Hetherington, E.A., Koepnick, R.B., Nelson, H.F. and Otto, J.B. 1982. Variation of seawater 87Sr/86Sr throughout Phanerozoic time. Geology, 10: 516-519.
- Clark, I.D. and Fritz, P., 1997. Environmental Isotopes in Hydrogeology. Lewis Publishers, Boca Raton, Florida, 328 pp.

- Dighton, J.C., Herczeg, A.L., Leaney, F.W., Lennard, R.P., Love, A.J. and Gerges, N.Z. 1994. Stable isotope and radiocarbon data for groundwaters from the Adelaide Metropolitan Area, Centre for Groundwater Studies Report No.56.
- Dogramaci, S.S. and Herczeg, A.L., 2002. Strontium and carbon isotope constraints on carbonate-solution interactions and inter-aquifer mixing in groundwaters of the semi-arid Murray Basin, Australia. Journal of Hydrology., 262: 50-67.
- Drexel, J.F. and Preiss, W.V., 1995. The Geology of South Australia. Vol. 2, The Phanerozoic. South Australia. Geological Survey. Bulletin, 54.
- Edmunds, W.M., Carrillo-Rivera, J.J. and Cardona, A., 2002. Geochemical evolution of groundwater beneath Mexico City. Journal of Hydrology, 258(1-4): 1-24.
- Edmunds, W.M., Guendouz, A.H., Mamou, A., Moulla, A., Shand, P. and Zouari, K. 2003. Groundwater evolution in the Continental Intercalaire aquifer of southern Algeria and Tunisia: trace element and isotopic indicators. Applied Geochemistry, 18(6): 805-822.
- Gerges, N.Z., 1986. Underground Water Resources of the Adelaide Metropolitan Area with the Latest Understanding of Recharge Mechanism, Proceedings of the International Conference of Groundwater Systems Under Stress, Brisbane. Australian Government Publishing Service, Canberra., pp. 165-175.
- Gerges, N.Z., 1999. The Geology and Hydrogeology of the Adelaide Metropolitan Area, PhD Thesis, Flinders University, Adelaide, 243 pp.
- Gerges, N.Z., 2001. Northern Adelaide Plains groundwater review. DWR Report 2001/013, Department for Water Resources, Adelaide.
- Ivkovic, K.M., Watkins, K.L., Cresswell, R.G. and Bauld, J., 1998. A Groundwater Quality Assessment of the Fractured Rock Aquifers of the Piccadilly Valley, South Australia. AGSO Record 1998/16, Australian Geological Survey Organisation, Canberra.
- Langmuir, D., 1971. The geochemistry of some carbonate ground waters in central Pennsylvania. Geochimica et Cosmochimica Acta., 35: 1023-1045.
- Love, A.J., Herczeg, A.L., Leaney, F.W., Stadter, M.F., Dighton, J.C. and Armstrong, D. 1994. Groundwater residence time and palaeohydrology in the Otway Basin, South Australia: 2H, 18O and 14C data. Journal of Hydrology, 153(1-4): 157-187.
- Mahlknecht, J., Gárfias-Solis, J., Aravena, R. and Tesch, R., In Press. Geochemical and isotopic investigations on groundwater residence time and flow in the Independence Basin, Mexico. Journal of Hydrology.
- Manning, A.H. and Solomon, D.K., 2005. An integrated environmental tracer approach to characterizing groundwater circulation in a mountain block. Water Resources Research, 41(12): 18pp. DOI:10.1029/2005WR004178
- Mazor, E., Jaffé, F.C., Fluck, J. and Dubois, J.D., 1986. Tritium corrected 14C and atmospheric noble gas corrected 4He applied to deduce ages of mixed groundwaters: Examples from the Baden region, Switzerland. Geochimica et Cosmochimica Acta., 50(8): 1611-1618.
- Palmer, M.R. and Elderfield, H., 1985. Sr isotope composition of sea water over the past 75 Myr. Nature, 314: 526-528.
- Parkhurst, D.L. and Appelo, C.A.J., 1999. User's Guide to PHREEQC (Version 2) - A Computer Program for Speciation, Batch-Reaction, One-Dimensional Transport and Inverse Geochemical Calculations, Water-Resources Investigations Report 99-4259. US Geological Survey, Denver, Colorado, 312 pp.
- Plummer, L.N., Busby, J.F., Lee, R.W. and Hanshaw, B.B., 1990. Geochemical Modeling of the Madison Aquifer in Parts of Montana, Wyoming, and South Dakota. Water Resources Research, 26(9): 1981-2014.
- Plummer, L.N., Prestemon, E.C. and Parkhurst, D.L., 1994. An Interactive Code (NETPATH) for Modeling NET Geochemical Reactions Along a Flow PATH. Version 2.0. Water-Resources Investigations Report 94-4169, U.S. Geological Survey, Reston, Virginia.
- Radke, B.M., Ivkovic, K.M., Watkins, K.L., Cresswell, R.G. and Bauld, J., 2000. A Groundwater Quality Assessment of the Upper Onkaparinga Region, Southern Mt Lofty Ranges, South Australia. Australian Groundwater Quality Assessment Project Report No. 9, Bureau of Rural Sciences, Kingston, ACT.
- Rattray, K.J., 1999. Geochemical Reactions Induced in Carbonate Bearing Aquifers Through Artificial Recharge. MSc Thesis, Flinders University of South Australia, Adelaide, 304 pp.
- Schlehuber, M.J., Lee, T.-C. and Hall, B.S., 1989. Groundwater level and hydrochemistry in the San Jacinto basin, Riverside County, California. Journal of Hydrology, 106(1-2): 79-98.

- Schuster, C.D., 2000. A preliminary report on the geophysical testing of wells that have abnormally high salinity, NAP Corroded Casing Survey 1999/2000. PIRSA RB 2000/00014, Primary Industries and Resources South Australia, Adelaide.
- Shepherd, R.G., 1971. The Hydrogeology of the Northern Adelaide Plains Basin. Mineral Resources Review, South Australia, 134: 52-61.
- Smith, D.L., 1979. Land use and groundwater history of the Northern Adelaide Plains. Engineering and Water Supply Department, South Australia, Adelaide, 70 pp.
- Vanderzalm, J.L., 2004. Hydrogeochemical Processes during Aquifer Storage and Recovery (ASR) with Reclaimed Water in a Carbonate Aquifer. PhD Thesis, Flinders University of South Australia, Adelaide, 317 pp.
- Wilson, J.L. and Guan, H., 2004. Mountain-block hydrology and mountain-front recharge. In: J.F. Hogan, F.W. Phillips and B.R. Scanlon (Eds.), Groundwater Recharge in a Desert Environment: The Southwestern United States. American Geophysical Union, Water Science and Applications Series, v. 9, Washington, D.C., pp. 113-137.

# DARCY 44

# Geochemical modelling in a regional deep aquifer and relations with groundwater flows. Aquitaine Basin, south-west of France

André L. (1), Franceschi M. (2), Atteia O. (2)

[1] BRGM - Water Division, 3 avenue C. Guillemin, BP 6009, F-45060 Orléans Cedex 2, France ;
l.andre@brgm.fr
[2] Institut EGID Bordeaux 3, University Michel de Montaigne, 33607 Pessac France,
franceschi@egid.u-bordeaux.fr;
atteia@egid.u-bordeaux.fr.

## Abstract

We propose here a modelling approach of the Eocene sand aquifer in the Aquitaine Basin showing that geochemical data can be used to identify flow directions. Four main geochemical processes - dissolution, redox, acid–base reaction, and ion exchange - of varying intensity could explain most of the observed spatial variability in groundwater composition. The developed model was used to select the most probable water pathways at the aquifer scale. In this context, geochemistry clearly demonstrates the role played by subsurface structures on water flow velocities and residence time (estimated with $^{14}C$ data) in their vicinity. In addition, the concentrations of several ions could only be justified by the aquitard –aquifer interactions.

## Introduction

The Eocene sands aquifer,a deep regional aquifer is located in the south Aquitaine Basin. It constitutes an important water resource used for various purposes (drinking water, agriculture, thermal spa and gas storage and). Recently, the conflicts for water use have led to detailed studies of the hydrogeology of the aquifer (Labat, 1998). The hydrodynamic characterisation allowed identification of some main flow lines and the approximate behaviour of the aquifer near geologic structures.

The water chemistry has been first approached by a description of the spatial variation of ions and by the calculation of the residence time (Blavoux et al., 1993). The approach presented here uses geochemical indicators and modelling, both linked to the structural or deep sedimentologic features in order to locate potential mass transfers. After an analysis of the regional geology and the sampling locations used for observations, the physicochemical, chemical and isotopic data are presented.

Geochemical modelling is used to deal with the interactions of several elements and dissolution processes. An initial step is devoted to a detailed inspection of the reactions that can occur, or not, in the studied aquifer. The modelling results are then validated using independent variables. Particular attention is paid to the points having an original behaviour or water composition that could not be predicted using the first group of assumptions.

The results of the geochemical modelling step are interpreted in terms of potential flow at the aquifer scale. Similar regional approaches were used by several authors to interpret the geochemical evolution in regional aquifers (e.g. Hendry and Schwartz, 1990; Weaver and Bahr, 1991; Gerla, 1992; Sracek and Hirata, 2002). The quantitative approach of the reaction linked with the information on the aquifer solid and isotope data allowed to enhance the confidence in geochemical models.

The modelling results were able to locate flow barriers at the regional scale and to elucidate the circulations in complex geological structure. The developed approach, involving the analysis of geochemical reactions, validation variables and aquitard–aquifer interactions, seems to be applicable to other deep aquifer.

## Hydrogeologic and geologic settings

The Aquitaine Basin is limited in the east by the foothills of Montagne Noire, in the south by the North Pyrenean Piedmont, in the west by the Atlantic Ocean and in the north by the Poitou Plateau. We will be interested here in the southern sector of the basin located to the south of the Garonne river. The Eocene sands aquifer, located in this part of the Aquitaine Basin, extends over 150 km from east to west and 200 km from south to north and constitutes a part of a multi-layer system. To manage this resource, the interactions with the under- and overlying aquifers are fairly important because the Eocene sands aquifer has very restricted outcrops. The average thickness of the quartz sand deposit is estimated as 50 m, with a high porosity of 20–35%, and average permeability, estimated from aquifer testing and modelling results to approximately 3.10$^{-5}$ m/s (Labat, 1998). The average interstitial velocity, using a gradient of 0.001 and an effective porosity of 20%, is close to 5 m/y.

Groundwater flow is mainly oriented from SE towards NW but outflow from the aquifer is not completely identified (Fig. 1). In the centre of the basin, the estimated age of the groundwater (using $^{14}$C data) is close to 20–25 ky. This is consistent with the effective advection calculated above.

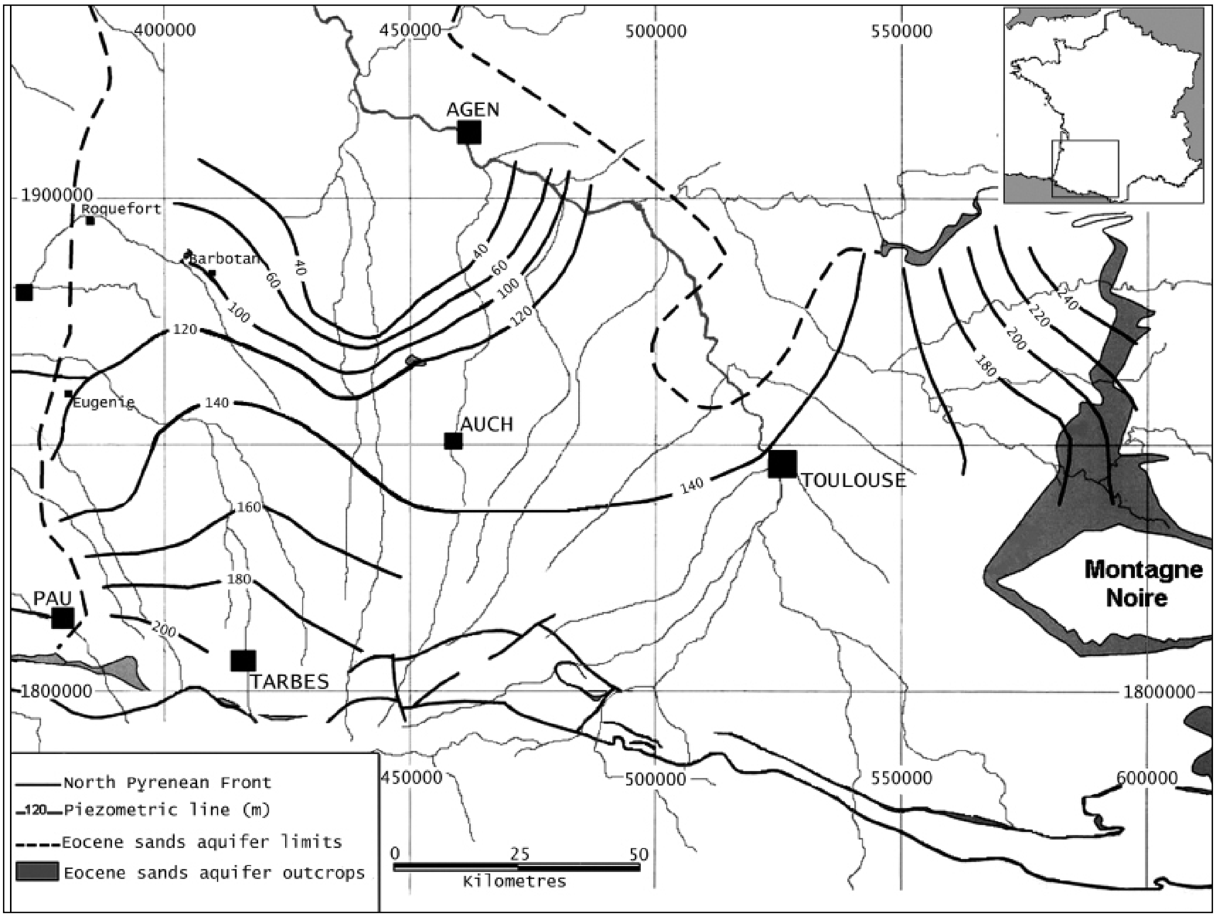

*Figure 1: The study region and the piezometric map of the Eocene sands aquifer*

Sands deposits mineralogy is very poor, containing mainly quartz, augmented with calcite, and, at places, dolomite and K-feldspars (Andre et al., 2002). Detrital sediments were eroded from the Massif Central, the Montagne Noire, and the emerging Pyrenees mountains. These eroded sediments were deposited in vast marshy plains. Geological structures, identified by the exploration, have affected this surface. They include local structures (e.g. the domes of Garlin or Saint-Medard) as well as larger structures (e.g. the Audignon anticline, located at the western border of the aquifer, and the Celt–Aquitaine flexure which seems to divide the aquifer in two quite distinct zones). It seems that most of the structures are related to the deformation of deep Triassic sands (Rey, 1995; Serrano, 2001).

The Dano–Paleocene calcareous and dolomitic aquifer, lying beneath the Eocene sands, is separated from them by clay deposits of variable thickness, from 10 to 100 m. The Eocene sands aquifer is covered by several hundreds of meters of Tertiary molasses. Aquitard mineralogy, although less well investigated, is richer, with quartz, feldspars, mica and several clay types (detrital limestone levels with sandy-clay deposits). At the bottom of the molasse deposits, crystallised gypsum has been observed in cuttings at many places.

## Groundwater chemistry

Waters from the Eocene sands aquifer mostly show a calcium bicarbonate facies. Sodium bicarbonate waters remain exceptional and sodium sulphate waters occur at a few wells. Most of the waters have a total dissolved solid concentration lower than 1000 mg/L. The chemical composition interpretation clearly evidences three main geochemical facies, a calcium bicarbonate facies, a sodium bicarbonate facies with low total dissolved solids (e.g. sample from well 13) or average mineralised (e.g. sample from well 17) and a sodium sulphate facies (e.g. sample from well 4).

The distribution of the sulphate and chloride concentrations shows a regional zonation as the one observed for chloride. In the south, weakly mineralised waters have concentrations lower than 0.50 meq/L, with, contrasting with chloride, an increase from south to north, the concentration going from 0.20 meq/L near the outcrops to 1.50 meq/L at well 11. In the north, the concentrations lie between 2 and 23 meq/L.

Sulphur is present under various forms, the most common being dissolved sulphate. Sulphide can also be present but the concentrations of this species are always relatively low (lower than 1 mg/L), and represent at most only 10% of the quantity of total sulphur. Sulphide arises, mostly, from local phenomena of bioreduction.

The spatial distribution of the $\delta^{34}S$ values observed in sulphates from waters indicates four distinct zones (Fig. 2 ) :

- Zone A, along the edge of the Pyrenees, in the zone of outcrop of the aquifer, where the $\delta^{34}S$ values are close to values found for sulphates from precipitation (+ 3.2‰ < $\delta^{34}S$ < + 8.2‰ CDT) (Pearson and Rightmire, 1980).
- Zone B, the largest zone, which extends from the Montagne Noire, in the East, towards the centre of the basin. Values of $\delta^{34}S$ and $^{18}O(SO4\ )$ are close to those measured in the gypsum crystals sampled in the molasse cover, at the top of the aquifer. The mean values of $\delta^{34}S$ and $\delta^{18}O$ measured on solid gypsum are respectively 12.72 ± 1.20‰ CDT and 14.9‰ SMOW. These values agree with those quoted in the literature for sulphate evaporates (Claypool et al., 1980).
- Zone C, a stretched shape oriented SW–NE, shows negative to very negative values (from - 0.4 to - 20.1‰ CDT), with a decrease from the south northward. The values of $\delta^{18}O(SO_4)$ follow the same trend with a decrease along the same axis. These values seem to reflect a different origin of dissolved sulphates than in zone B, a plausible explanation being the oxidation of sulphide minerals (Dazy et al., 1980).

- One particular point in the west (e.g. Well 13—Zone D), close to the aquifer boundary, shows significant enrichments in sulphur 34 ($\delta^{34}SO4 > 33‰$ CDT). A proposed explanation for this is the action of bioreduction processes.

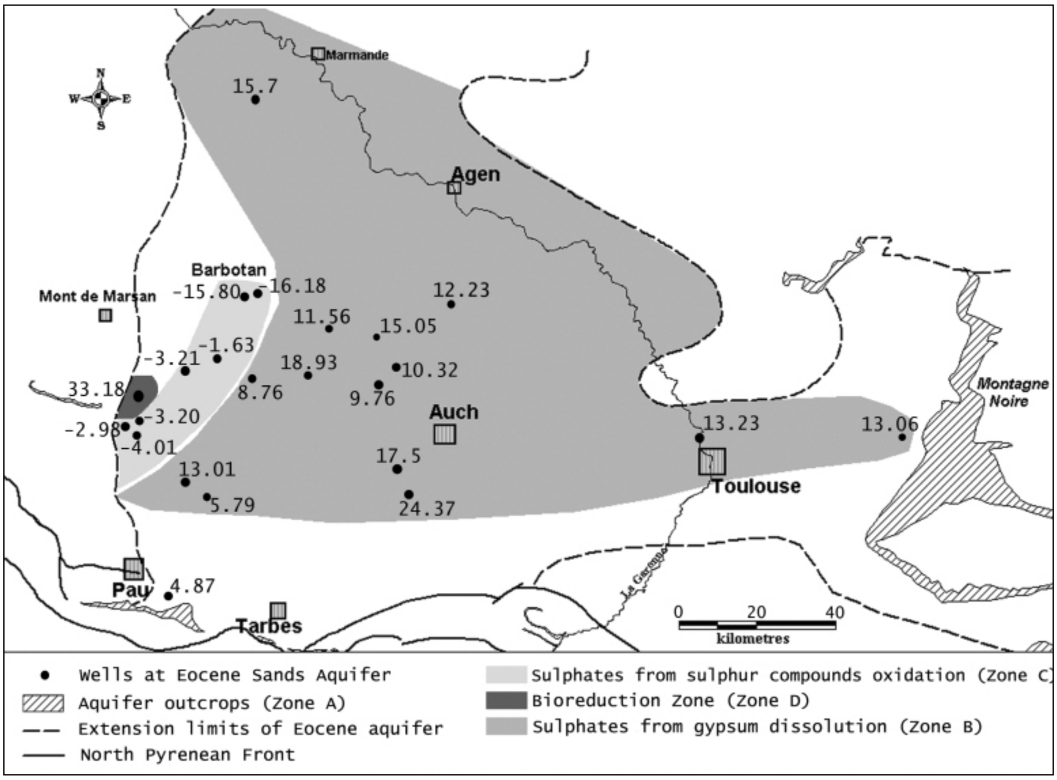

*Figure 2: Map of sulphur-34 values in dissolved sulphates*

Three distinct hydrochemical processes have been identified to be responsible of these evolutions :

1. Waters equilibrium with calcite from recharge areas to discharge places ;

As described in part 4, Ca-$HCO_3$ water is the predominant type in the Eocene sands aquifer, produced by dissolution of carbonate minerals such as calcite. The $CO_2$ produced by the oxidation of organic matter and root respiration in the unsaturated zone and dissolved by the recharge water is at the origin of such dissolution. On figure 6, plotting pH measured in the field, versus $pCO_2$, we can note a good correlation with the calcite saturation line. So, equilibrium with calcite and potential dissolution of dolomite will be used in the geochemical modelling to set the Ca-Mg-$CO_3$ system.

2. Cation exchange between waters and the aquifer material ;

This process explains the observed increase in $Na^+$ concentration without an associated increase in $Cl^-$ concentration. Many studies have shown this kind of process (Back, 1966; Freeze and Cherry, 1979; Thorstenton et al., 1979; Chapelle and Knobel, 1983; Appelo and Postma, 1999). In an aquifer where carbonates minerals are present, cation exchange may be accompanied by calcite dissolution (and dolomite), as $Ca^{2+}$ ($Mg^{2+}$) is removed from solution and replaced by $Na^+$. The carbonate mineral dissolves and provides more $Ca^{2+}$ (and $Mg^{2+}$) in solution to exchange with $Na^+$ and causing $HCO_3^-$ concentration to increase. In the Eocene sands, the series sometimes include argillaceous or argillaceous-sandstones interbeds, able to play a role as ion exchangers. Depending on location, these layers show variable thickness. Under these conditions, ion exchangers will be considered in the modelling approach and will be used to explain Na-$HCO_3$ type of some waters.

3. Pyrite oxidation and gypsum dissolution that can explain the regular increase of sulphur concentration along pathways :

- gypsum or anhydrite dissolution. Where it occurs, this process has been applied in a closed system consisting of a confined aquifer with calcite remaining at saturation. During the gypsum (or anhydrite) dissolution, delivering sulphate and calcium to the water, calcite becomes saturated and, as it precipitates, the $HCO_3^-$ concentration decreases and the pH increases.
- pyrite oxidation. This process must be detailed in order to model it. Waters from the Eocene sands aquifer revealed small quantities of oxygen (0 to 0.15 mg/L) and redox potentials ranging between -50 mV and 0 mV, signifying slightly reduced media, and suggesting that pyrite oxidation is not associated with oxygen reduction. Among several other possibilities, the following reactions involving iron oxides and pyrite (Holmes and Crundwell, 2000) were the only combination able to reproduce the concentrations of Fe, $H_2S$, $SO_4$ in solution

$$Fe(OH)_3 + 3\,H^+ \rightleftarrows Fe^{3}_{+} + 3\,H_2O$$

$$FeS^2 + 14\,Fe^{3}+ + 8\,H_2O \rightleftarrows 15\,Fe^{2}_{+} + 2\,SO_4^{2}- + 16\,H^+$$

$$Fe^{2+} + HCO_3^- \rightleftarrows H^+ + FeCO_3$$

The overall reaction is written as

$$FeS_2 + 14\,Fe(OH)_3 + 11\,H^+ + 15\,HCO_3^- \rightleftarrows 2\,SO_4^{2}- + 34\,H_2O + 15\,FeCO_3$$

Geochemical modelling and distinction in groundwater flows

These processes identified, a modelling approach allowed us to quantify those. This step by step modelling used a limited number of mineral phases that were identified in the solid and successfully reproduces the concentration of major ions at each sampling points. Numerous constraints that were imposed on the model and its validation by pH or $^{13}C$ allowed us to justify and quantify the geochemical processes occurring in solution.

The geochemical processes governing the chemical composition of waters from Eocene sands aquifer are summarized by the figure 3.

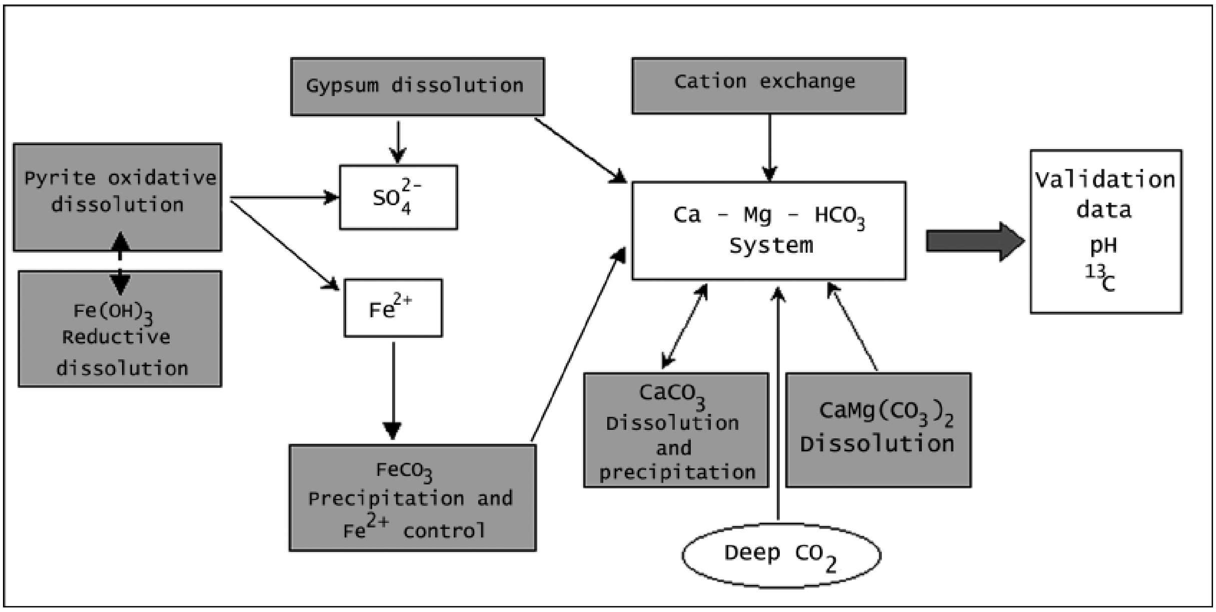

*Figure 3: Geochemical processes governing the chemical composition of waters from Eocene sands aquifer*

Afterwards, based on the local reconstitution of chemical composition of waters, geochemical modelling was used to delineate geochemical pathways. The origin of local chemical composition variations has been identified and the role played by deep geological structure has been outlined (Fig. 4). It appears that a concept of “open” and “closed” structures seems to be applicable in this region. This concept would enlarge the classical discussion of faults as barriers or conducts for flow.

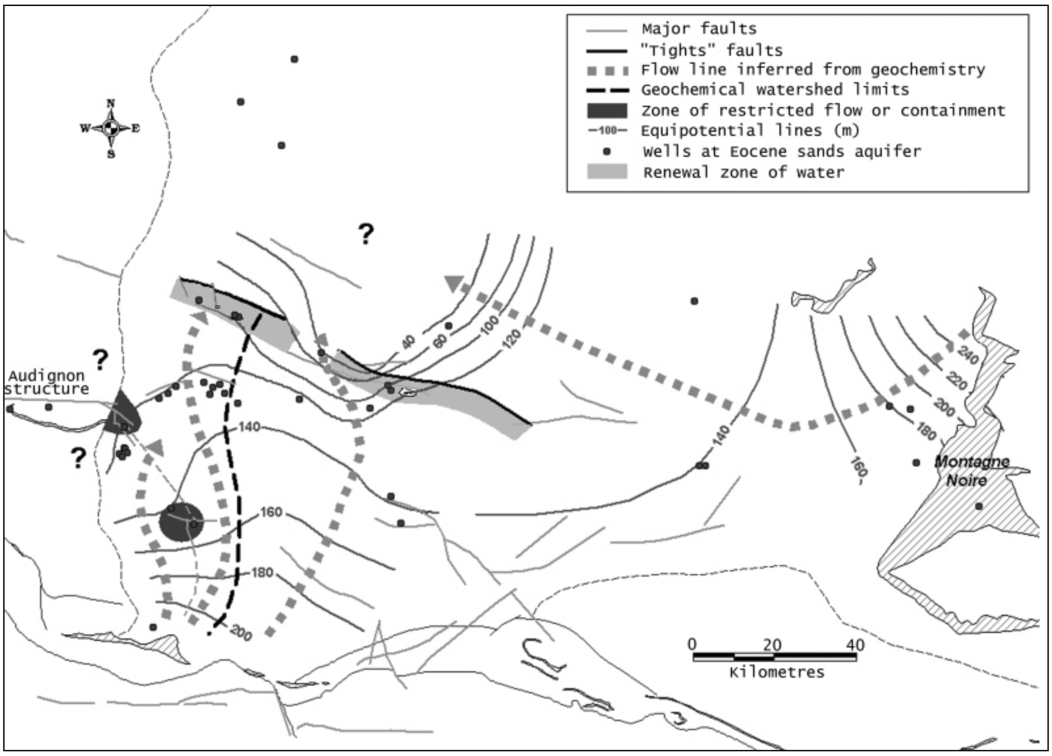

Figure 4: Major flow direction derived from modeling results

The study also shows that the chemical composition of waters cannot be explain without evoking the influence of aquitards. Considering the poor mineralogy of the sands, the increase of total dissolved solids along pathways seems to be associated to mass transfers from the gypseous molasses, present at the top of the aquifer. This transfer of ions occurs according two processes: leakage, principally in the northern part of the aquifer, and diffusion, mainly in the south of the study area.

## Conclusions

The results of this study show that detailed hydrochemical data coupled with geochemical modelling can help to elucidate the hydrologic and geologic factors controlling water chemistry on a regional basin.

In the context of the Aquitaine Basin, the geochemical modelling has proven its ability to constrain efficiently the groundwater flow in an aquifer were few data are available. However, the developed approach shows that a detailed analysis of each reaction, the use of validation variables and information on mineral phases present in the solid are required. At contrary, the concentration increase for one dissolved species can be attributed to the wrong reaction. Along the paper, we also showed that a geochemical model was able to provide four types of hydrodynamic information: estimates of regional flow directions, existing flow barriers, mixing between aquifer waters and interactions between aquifer and aquitard. However, this information remains qualitative, the only solution to reach more quantitative flow patterns is the use of 3D multilayer models including hydrodynamics, transport and chemistry. The chemistry may constrain flow but the opposite is also true: the flow pattern governs mixing and residence time.

## References

- André L., Franceschi M., Pouchan P., Atteia O. (2002) Origines et évolution du soufre au sein de l'aquifère des Sables Infra-Molassiques du Bassin Aquitain. C.R. Géosciences 334 :749-756.
- Blavoux B., Dray M., Fehri A., Olive P., Groning M. et al, (1993) Paleoclimatic and hydrodynamic approach to the Aquitaine Basin deep aquifer (France) by means of environmental isotopes and noble gases, 1993, Intern. Symp. on App. of Isotope Techn., 293-305.
- Claypool G.E., Holser W.T., Kaplan I.R., Zak I. (1980) The age curves of sulphur and oxygen isotopes in marine sulphate and their mutual interpretation, Chem. Geol., 28: 199-260.
- Dazy J., Rochat J., Olive Ph. (1980) Nouvelles données géochimiques et isotopiques sur les eaux thermales d'Uriage-les-Bains (Isère), 105ème Congrès National des Sociétés Savantes, Caen, 1980, Sciences, II: 111-122.
- Gerla P.J., (1992) Pathline and geochemical evolution of groundwater in a regional discharge area, Red River Valley, North Dakota. Ground Water, 30:743-754.
- Hendry M.J., Schwartz F.W. (1990) The chemical evolution of groundwater in the Milk River Aquifer, Canada. Ground Water, 28:253-261.
- Labat N. (1998) Rôle de particularités sédimentaires et structurales sur le comportement des sables sous-molassiques soumis aux fluctuations induites par les stockages souterrains de gaz. Application à l'étude de leur influence sur l'hydrodynamisme des émergences locales, Thèse : Bordeaux 3 : 1998, 228 p.
- Pearson F.J., Rightmire C.T. (1980) Sulphur and oxygen isotopes in aqueous sulphur compounds In Handbook of Environmental Isotopes. Geochemistry. P. Fritz and J. Ch. Fontes, Elsevier, 1980, Chapter 6, 227-258.
- Rey J. (1995) Le Bassin d'Aquitaine : composition, évolution et structure In Du Lias Nord aquitain aux molasses miocènes – Généralités Livret Guide d'excursion, STRATA, Actes du laboratoire de Géologie Sédimentaire et Paléontologie de l'Université Paul Sabatier – Toulouse, 1995, Série 2, Mémoire, 7-140.
- Serrano O. (2001) Le Crétacé Supérieur/Paléogène du bassin d'avant-pays Nord-Pyrénéen (Bassin d'Aquitaine) : sédimentologie, stratigraphie et évolution géodynamique, Thèse : Rennes : 2001.
- Sracek O., Hirata R. (2002. Geochemical and stable isotopic evolution of the Guarani Aquifer System in the state of Sao Paulo, Brazil. Hydrogeol. J., 10(6): 643-655.
- Weaver T.R., Bahr J.M. (1991) Geochemical evolution in the Cambrian-Ordovician Sandstome aquifer, Eastern Wisconsin. 2. Correlation between flow paths and groundwater chemistry. Ground Water, 29:510-515.

# DARCY 56

## Spatial variability of the geochemistry of a chalk aquifer at a regional scale: role of the structural context (Haute-Normandie, France)

Valdes D, Dupont J-P, Laignel B, Massei N, Ogier S and Leboulanger T

UMR CNRS 6143 Morphodynamique Continentale et Côtière, Université de Rouen,
76821 Mont-Saint-Aignan Cedex, France

### Abstract

Major ions concentrations ($Ca^{2+}$, $HCO_3^-$, $Mg^{2+}$, $Cl^-$, $Na^+$, $NO_3^-$, $SO_4^{2-}$) in the Chalk aquifer in the Eure department (France) were collected and mapped by means of GIS tools. The PCA analysis of the geochemical maps allowed separation into two types of spatial distribution: the autochthonous ions ($Ca^{2+}$, $HCO_3^-$) and the allochthonous ions ($Cl^-$, $Na^+$, $NO_3^-$, $SO_4^{2-}$). The map of the aquifer thickness reflects the geometry of the aquifer and so reflects the structural context and the piezometric level reflects the aquifer flow. Spatial autocorrelations and crosscorrelations reveal relationships between the allochthonous concentrations and the structural context. The mineralization increases along the flow. The most important mineralization gradients are related to an increase in the Mg/Ca ratio with a decrease of the flow section (anticlines or faults). These results give evidence of the predominance of an internal control on aquifer geochemistry by the geometry and the structural context of the aquifer.

### 1. Introduction

Heterogeneities of atmospheric inputs and natural water-rock reactions give rise to significant diversity of the geochemical properties of an aquifer. The geochemistry of groundwater in the Chalk has been widely studied in the Paris Basin (Kloppmann et al., 1998; Negrel and Petelet-Giraud, 2005) and in England (Hiscock et al., 1996; Edmunds et al., 2003).

The dominant components of chalk groundwaters are $Ca^{2+}$ and $HCO_3^-$. These ions and $Mg^{2+}$ have an autochthonous origin resulting from the dissolution of chalk. The ratio Mg/Ca is commonly used as an indicator of the residence time of the water (Hiscock et al., 1996; Kloppmann et al., 1998; Edmunds and Smedley, 2000), the calcite solubility being superior to the dolomite dissolution (Bakalowicz, 1979). $Mg^{2+}$ may also result from percolation through tertiary deposits. $Cl^-$, $Na^+$, $SO_4^{2-}$ and $NO_3^-$ principally have an allochthonous origin. $Cl^-$ ions in groundwater may originate from rainfall recharge (sea salts, industrial atmospheric emission of HCl, Meybeck, 1983, 1986; Négrel, 1999) and human activity over the catchment (domestic sewage, landfill leachate, fertilisers, de-icing salts, …, Sherwood, 1989). The highest Cl- values in groundwater are usually attributed to human influence. [$Na^+$] can be attributed to atmospheric inputs. [$SO_4^{2-}$] are principally related to a man-made origin, as the positive relationship between [$Cl^-$] and [$SO_4^{2-}$] found by Négrel and Petelet Giraud (2005) suggest. $NO_3^-$ is found naturally at low concentrations, but the high levels result principally from anthropogenic activities as agriculture (Widory et al., 2004).To summarize, bedrock geology, climate, soil type and vegetation are known to be the major factors regulating geochemistry, as are anthropogenic influences such as land use, population density and pollution.

In this study we investigate the major ions geochemistry of a Cretaceous Chalk aquifer at a regional scale of 6000 km$^2$ and with high resolution, using 150 sampling sites. The high resolution of the data allows to finely investigate the spatial variability of the aquifer geochemistry, that gives insight about the underlying factors controlling hydrogeological processes. The value of coupling these analysis with statistical analysis as PCA analysis has been demonstrated by Wang (2001) or Reis (2004). Spatial analyses, such as spatial correlations, are rarely used, but they may give new insights about the directional structure of the data or the spatial dependence between two regionalized variables.

The originality of this work is to study the impact of hydrological and structural settings on the aquifer geochemistry.The objectives of this study are to propose a new approach for investigating spatial variability of groundwater geochemistry, which aims to understand the influence of the groundwater flow and of the structural. The present study proposes: (i) to map the spatial distribution of each geochemical species, of the groundwater flow and of the structural context at high spatial resolution; (ii) to perform PCA with the whole of the maps with the aim to group the ionic species by functioning type; (iii) to study the directional features of the data and the spatial dependences between the geochemical properties and the context by means of spatial correlations.

## 2. Hydrogeological settings, data and methods

### *2.1. Hydrologeological settings*

The Eure department (corresponding to the Eure district) is located in a catchment of about 11000 km$^2$. This study focuses on the Eure department (about 6000 km$^2$) rather than the catchment in full because a part of the data are available only in this department. This department is rural, with little urbanization, and most of the area is used for farming and livestock.

The Chalk plateaus are covered with impervious, clay-with-flints, some 5-40m thick and aligned on N-S axis, resulting from weathering of the Chalk during different periods of the Cenozoic (Laignel et al., 2002); Quaternary loess (Lautridou, 1985) and Tertiary deposits forming infills to weathered surfaces (pockets) or in a continuous cover form. The typical regional geology is presented in figure 1.

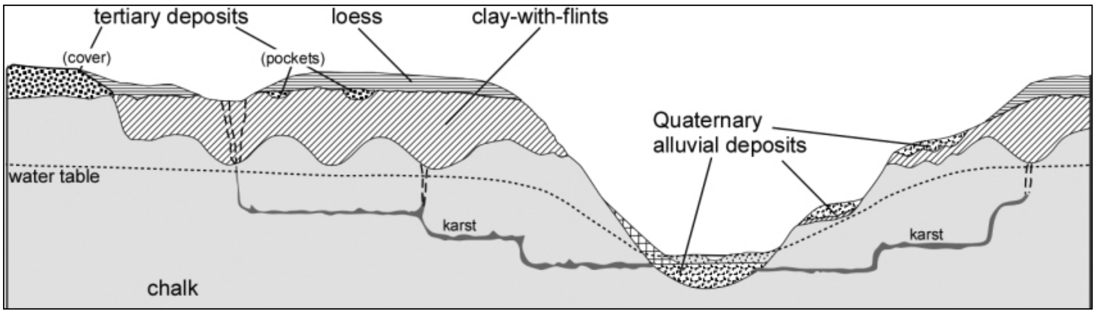

*Figure 1: Typical regional geology (by Laignel, 2003)*

The plateaus are constituted by Cretaceous formations. Most of the formations come from the Upper Cretaceous, except Jurassic formations at the west of the Eure department. The spatial distribution of the outcropping formations shows the oldest levels (Cenomanian) in the south and the most recent in north east (Campanian). All the Upper Cretaceous formations are chalk except the Cenomanian which has a sand facies ("Perche Sands") in the south of the Eure department. Tertiary deposits cover the Chalk in the north east of the region between the Eure and the Seine rivers. They are composed of clayey sands and clays with smectite content up to 90 %, this smectite often containing $Mg^{2+}$ (Laignel, 2003) which may be brought to the Chalk aquifer by percolation. The structural map (fig.2c) shows (i) the predominance of N140-150 orientation for the fault of the Seine (Fc) and the anticlines and synclines in the south and east of the Eure department and (ii) two faults in the north-west: Fa with the north compartment uplifted and Fb with the south compartment uplifted (Wazi, 1988).

The Chalk aquifer in Haute-Normandy has been demonstrated to have karst characteristics (Rodet, 1997; Massei et al., 2003). The flow velocity in the karst aquifer is very heterogeneous. The structure drainage is composed of fissures and conduits which act as underground drainage routes for the highly localized transport of water with velocity estimated at from 50 to 300 m/hr (Calba et al, 1979).The aquifer discharges eventually to the Seine river (fig. 2a). Three major rivers: the Iton, the Risle and the Eure discharge into the Seine, divide the aquifer to the south of the Seine into three important groundwater basins which flow from south to north. The climate is temperate and maritime, with average temperatures of 10 to 12°C and average annual rainfall varying spatially from 600 to 800 mm, the highest annual rainfall is located in the west and in the north-east of the department (fig. 2b).The saturated aquifer thickness (fig. 2c) varies spatially from a few meters to more than 300 m. Significant variations in aquifer thickness could be related to the variations of the chalk base and then to the geological structure. The greatest thicknesses are located on the synclinal axis (in the south and in the north-east of the department) and the lowest aquifer thicknesses correspond to anticlinal axis (south of the department) excepted the north west of the department which correspond to the outlet of the aquifer. Around the faults, the aquifer thickness varies suddenly, decreasing on the uplifted compartment.

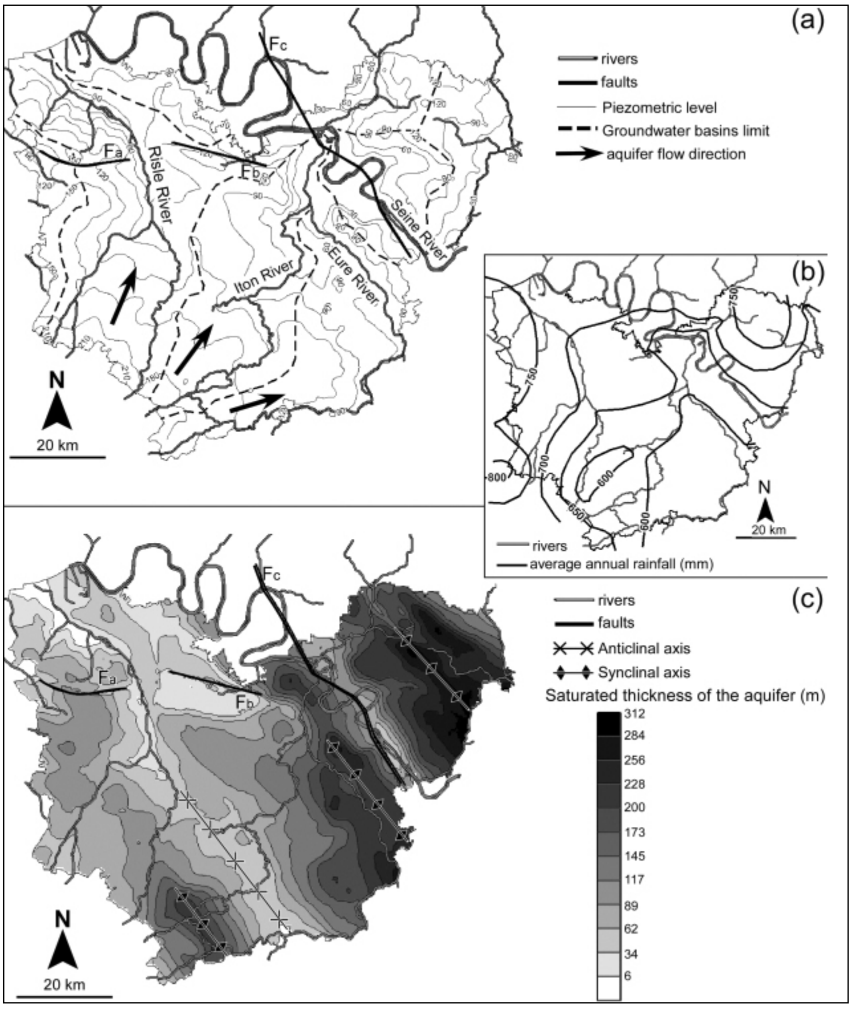

Figure 2: Hydrological and structural settings

### *2.2. Data sets and methods*

The ADES database (Accès aux Données des Eaux Souterraines: the french national groundwater database, BRGM) provided the mean geochemical properties of 157 springs or wells of the Chalk aquifer in and around the Eure department. The study focuses on the following geochemical parameters: $Ca^{2+}$, $HCO_3^-$, $Mg^{2+}$, $Cl^-$, $Na^+$, $NO_3^-$, $SO_4^{2-}$, $CO_2$ and pH. Sampling was conducted during dry periods, without any contribution of surface waters. The main statistics for each variable are given in the Table1.
A detailed study of the ADES data led us to cancel less than 5% of the data : for each sampling site, the number of measures vary between 2 to 20 with a mean of 5 data per site; when the standard deviation is too important respect to the mean, the data was cancelled. Data on the piezometric head and the aquifer thickness were provided by the BRGM with an high resolution (500 m lag). The data were interpolated by ordinary kriging with IDRISI software using an omnidirectional variogram which represents the variance between two samples for increasing lag space without taking the direction between the samples into account, and then it does not influence the directional structure of the data which will later be studied. The geochemical and hydrological variables were mapped with a 2000 m lag.

|  | $Ca^{2+}$ (mg.l-1) | $HCO_3^-$ (mg.l-1) | $Mg^{2+}$ (mg.l-1) | $Cl^-$ (mg.l-1) | $Na^+$ (mg.l-1) | $NO_3^-$ (mg.l-1) | $SO_4^2$ (mg.l-1) | pH | $CO_2$ (mg.l-1) | Thick. (m) | Piezo (m) |
|---|---|---|---|---|---|---|---|---|---|---|---|
| Samples number | 150 | 146 | 150 | 155 | 151 | 153 | 149 | 154 | 117 | - | - |
| min | 68.0 | 174.4 | 3.3 | 12.2 | 7.2 | 14.3 | 13.0 | 7.20 | 34.9 | - | - |
| max | 126.2 | 370.5 | 18.0 | 28.0 | 12.9 | 43.9 | 15.7 | 7.46 | 53.1 | 303.0 | 220.9 |
| mean | 102.4 | 299.4 | 7.3 | 20.9 | 10.7 | 26.0 | 14.1 | 7.30 | 44.1 | 114.9 | 93.6 |
| Standard deviation | 9.7 | 37.4 | 2.8 | 3.2 | 1.3 | 7.1 | 0.5 | 0.05 | 4.2 | 73.1 | 49.6 |

*Table 1*

PCA were performed on the regionalized geochemical variables ($Ca^{2+}$, $HCO_3^-$, $Mg^{2+}$, $Cl^-$, $Na^+$, $NO_3^-$ and $SO_4^{2-}$; and $CO_2$, pH), the aquifer thickness and the piezometric level were added as supplementary variables and do not contribute to the factorial space of the PCA
The correlations analyses in hydrology are usually used for time-series (Mangin, 1984; Box et al., 1994). These analyses may be used for spatial data using spatial autocorrelations or cross correlations.
The spatial autocorrelations give information about the spatial structure of a regionalized variable (Zhang and Selinus, 1998). This function quantify the linear dependence of successive values over the space. Each variable is correlated to itself for increasing lag space and for all the directions, in order to characterize the spatial variability of the regionalized variable. The correlogram. C(k) estimates the spatial variability of the regionalized variable for all the directions , resulting in a 2D autocorrelation function. r(k) is the spatial autocorrelation function.

$$C(k,\theta) = \frac{1}{n}\sum_{d=1}^{n-k}(x_d - \overline{x})(x_{d+k} - \overline{x}) \tag{1}$$

$$r(k,\theta) = \frac{C(k,\theta)}{\sigma_x{}^2} \qquad \text{where} \qquad \sigma_x{}^2 = \frac{1}{N}\sum_{d=0}^{N}(x_d - \overline{x})^2 \tag{2}$$

where k is the lag (k=0 to m), is the direction (the autocorrelation function being symmetric, θ= 0 to 180°), n is the length of the space series, x is a single regionalized value, $\overline{x}$ is the mean of the regionalized value, m is the truncation point, adjusted experimentally by (Mangin, 1984) to n/3 and $\sigma_x^2$ is the variance of the variable. An example is presented in figure 3a.

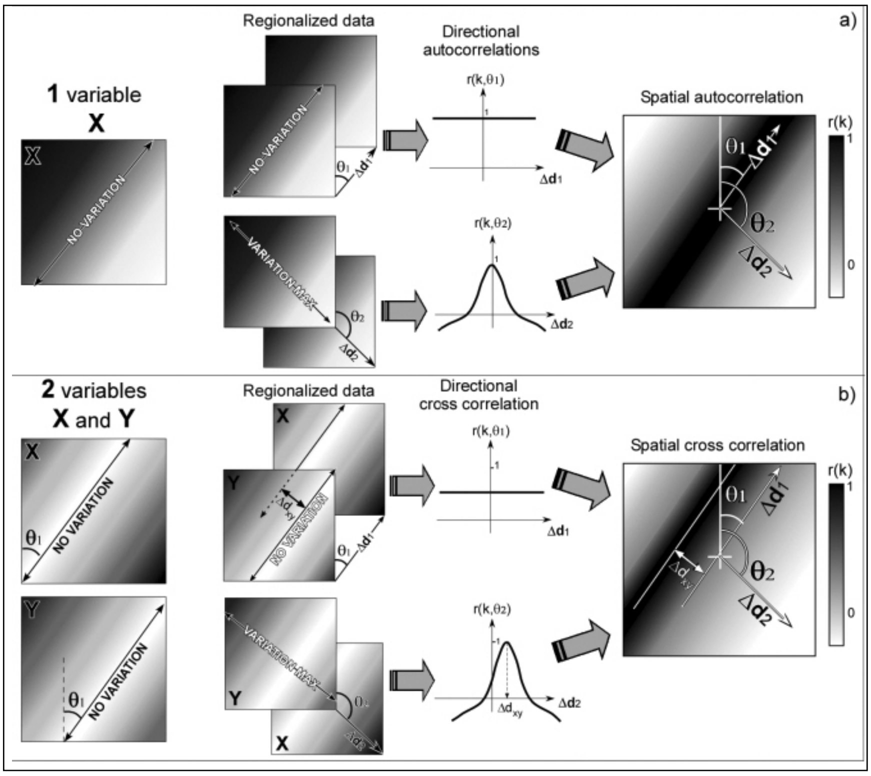

*Figure 3: Principles of a) spatial cross correlations and b) spatial cross-correlations*

The spatial cross correlations give information about the spatial dependence between two regionalized variables (Zhang and Selinus, 1998). Each variable is correlated to the other variable for increasing lag space and for all the directions, in order to characterize the spatial dependence between the two regionalized variables (x and y) over the space for all the directions θ.

$$C(k,\theta)=\frac{1}{n}\sum_{d=1}^{n-k}(x_d-\overline{x})(x_{d+k}-\overline{y}) \qquad (1)$$

$$r(k,\theta)=\frac{C(k,\theta)}{\sigma_x\sigma_y} \quad \text{where} \quad \sigma_x=\sqrt{\sigma_x^{\,2}}\ ,\ \sigma_y=\sqrt{\sigma_y^{\,2}} \qquad (2)$$

where _ is the standard deviation of the variable. The cross correlation function is not symmetric, varies between 0° to 360°. An example is presented in figure 3b.

## 3. Results

The Chalk aquifer groundwaters are globally Ca/$HCO_3$ type, but the ions concentrations are not homogeneous throughout the Eure department on looking at important standard deviations for each ionic species (Table 1).

### *3.1. PCA of the geochemical spatial distributions*

PCA were performed from the raster (with a 2000 m lag) of the geochemical data and of the aquifer properties. [$Ca^{2+}$] and [$HCO_3^-$] are well correlated to [$CO_2$] and anti-correlated to pH. The spatial distributions of [$Cl^-$], [$Na^+$], [$NO_3^-$] and [$SO_4^{2-}$] are well correlated between each other. [$Mg^{2+}$] plots between ($Ca^{2+}$, $HCO_3^-$) and ($Cl^-$, $Na^+$, $NO_3^-$, $SO_4^{2-}$). The correlation between the piezometric level and the whole of the ionic species is negative. The correlation between the saturated thickness and the other variables is below 0.5. The structure of the factorial space is strong, two factors explain 77% of the total variance (fig. 4).

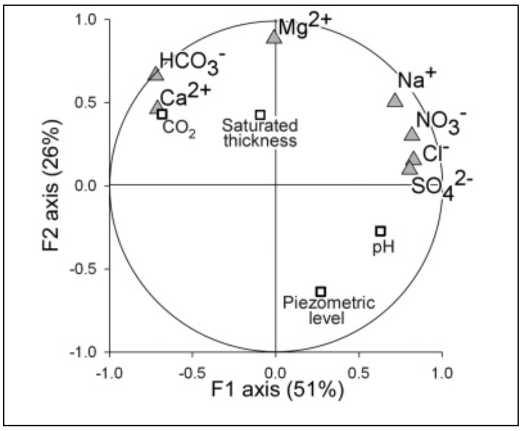

*Figure 4: Factorial space of the PCA. □ = contributive variables, **□** = supplementary variables*

F1 (51%) may be interpreted as the origin of the ions. It is related to the “autochthonous ions” (i.e. the ions originating from the aquifer: $Ca^{2+}$ and $HCO_3^-$) in the positive part opposed to the “allochthonous ions” ( i.e. originating from the surface: $Na^+$, $Cl^-$, $NO_3^-$, $SO_4^{2-}$) in the negative part. The central $Mg^{2+}$ position is explained by its mixed origin: autochthonous when it is a product of the chalk dissolution or allochthonous when it is brought by the Tertiary deposits. The high scores of F1 factor, corresponding to the highest concentrations of allochthonous ions, are found to the south of the Eure department; and the lowest scores in the north-east of the Eure department, on the anticlinal axis (fig. 5a). $Cl^-$ is a good example of allochthonous ion which is also a conservative element. The spatial distribution of [$Cl^-$] (fig. 6a) is used to represent the allochthonous ions without disturbance by an internal contribution or reaction. [$Cl^-$] seems to be structured according to the structural directions.

F2 (26%) may be interpreted as the groundwater mineralization. All the variables are located in the positive part of F2 axis (fig.4). $CO_2$ is well correlated to $Ca^{2+}$ and $HCO_3^-$ and the piezometric level is opposed to all the geochemical variables, so opposed to the mineralization. The low scores of the F2 factor, corresponding to a low mineralised water, are located to the south. The F2 factor increases from the south to the Seine river but stops in the east and north of the study area, with the presence of the faults Fa and Fb. The highest mineralization is then located on the left bank of the Seine River and to the south of the faults Fa and Fb (fig. 5b).The map of the ratio Mg/Ca (fig. 6b) shows that the highest ratios are found between the Eure river and the Seine River under the tertiary deposits which bring $Mg^{2+}$ to the Chalk aquifer. Excepted this zone, the highest scores, are found in the south on the syncline S1 , and in the south of the faults Fa and Fb revealing more important residence time.

The spatial distributions of the F1 and F2 factors values are well structured, the first observations seem to show relationships between the spatial distribution of the geochemistry data and the morphostructural context: flow, faults, etc.

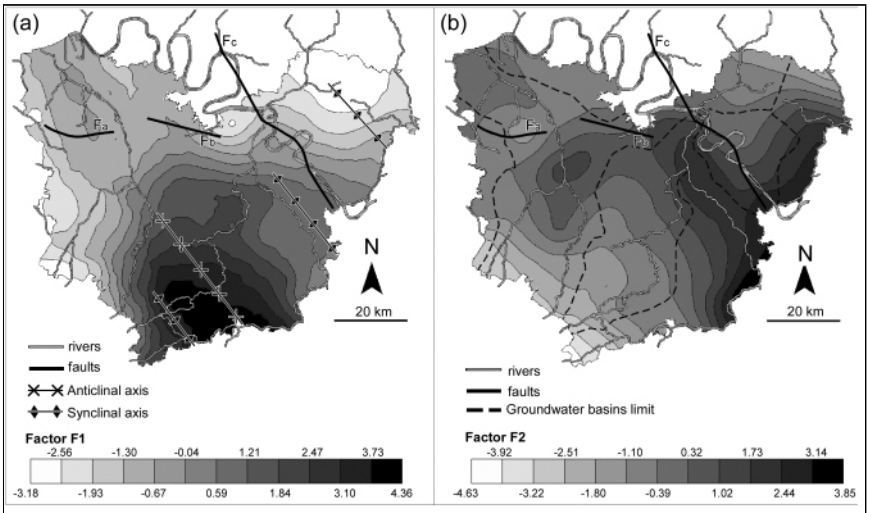

*Figure 5: (a) Spatial distribution of the F1 factor (b) spatial distribution of the F2 factor*

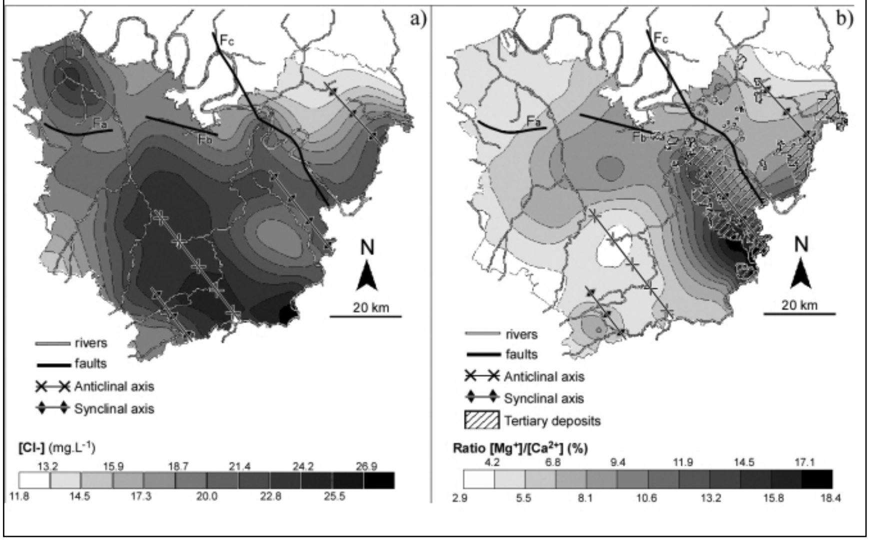

*Figure 6: (a)Spatial distributions of (a) $[Cl^-]$ (b) Ratio $[Mg^{2+}]/[Ca^{2+}]$*

## *3.2 Spatial Analyses*

Spatial autocorrelations were performed for three variables: the piezometric level, the saturated thickness and [Cl-] (fig. 7). The two first variables describe the hydrological and structural context and the third is used to represent the allochthonous ion.

For the piezometric head, good autocorrelations lie in the direction 127 ± 5 °N perpendicularly to the aquifer which flows globally in the 37 °N direction. For the aquifer thickness, good autocorrelations lie in the direction 145 ± 5 °N corresponding to the structural directions of the anticlines, synclines and Seine fault (Fc). [Cl-] shows two principal directions corresponding to the two directions of the hydrological and structural context: at a small lag: 145 ± 5°N direction (structural context) and at a little bit more important lag the 127 ± 5 °N a direction (hydrological direction).

The spatial autocorrelations allow to give evidence of well defined structures and significant directional features of the hydrologic and structural context.

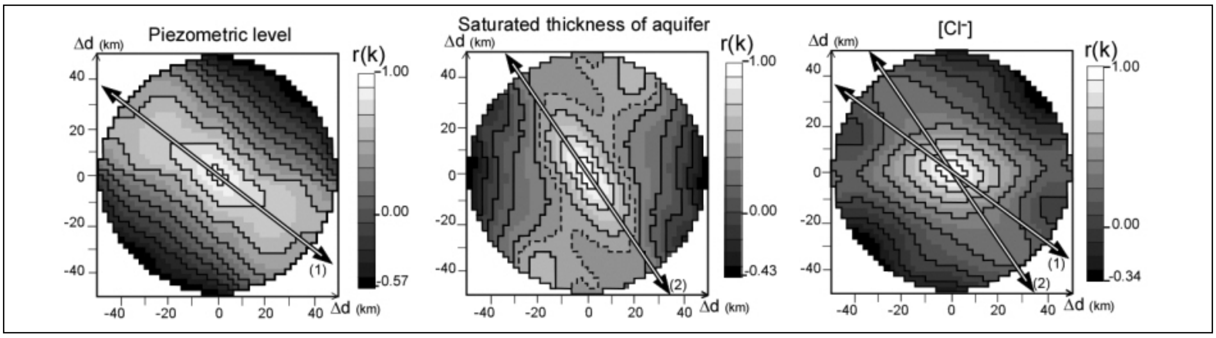

Figure 7: Spatial Autocorrelations (1) 127°N, (2) 145°N

Spatial cross-correlations were performed between (1) the piezometric head and [Cl-] and (2) the aquifer thickness and [Cl-] (fig.8). The cross correlation with the aquifer thickness is relatively symmetric about the axis 145°N with negative scores around this axis (fig. 8a), meaning a negative correlation between the aquifer thickness and [Cl-] along the structural (in the geological meaning) direction 145°N. The cross correlation between the piezometric level and [Cl-] is not symmetric (fig. 8b). The scores of the cross correlation are negative under the line 127°N and are positive above this line. The results of the spatial autocorrelations seem to indicate a relationship between the concentrations of allochthonous ions and the hydrological and structural context.

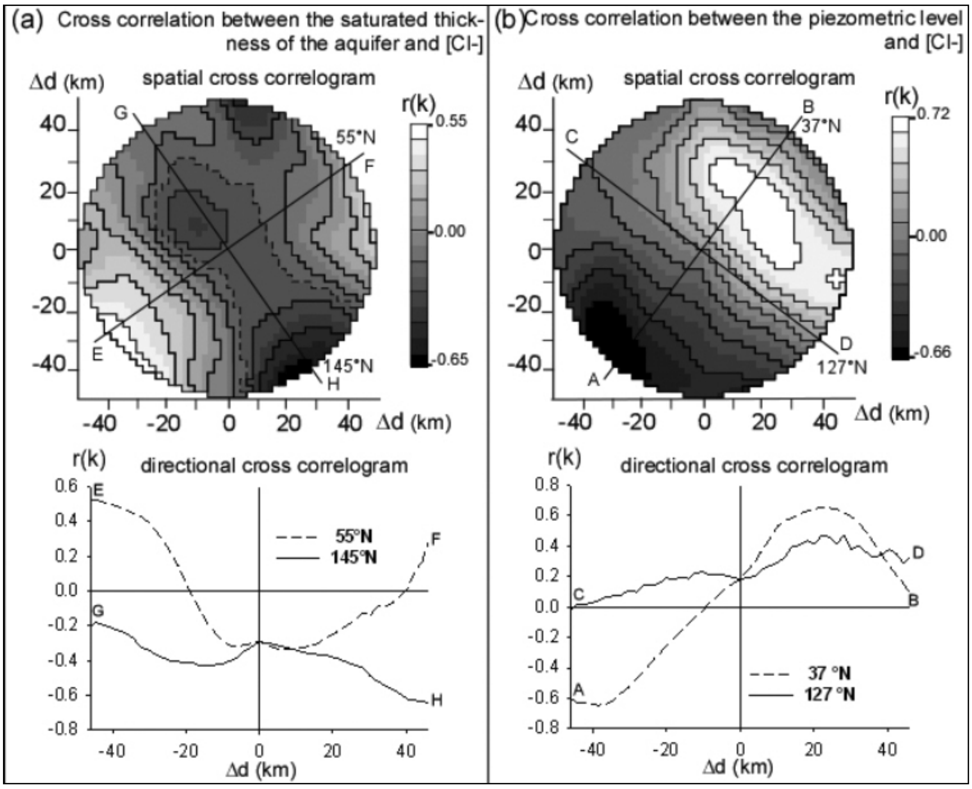

Figure 8: Spatial cross correlation (a) between the saturated thickness of the aquifer and the [Cl-] concentration; (b) between the piezometric level and the [Cl-] concentration

## 4. Discussion

Geochemical properties of the Chalk aquifer are controlled by factors of different scales from microscale (e.g. chemical reaction) to macroscale (e.g. regional flow and structural settings). The results reveal a strong organization of the geochemical properties of the Chalk aquifer of the Eure department. The PCA shows that 77% of the total variance of the geochemical maps is well represented by two processes: the contribution of the allochthonous ions to the aquifer and the aquifer mineralization. The aim of this study is to explain the observed spatial distributions of the geochemistry, to determine the control factors and particularly to understand the role of the aquifer flow and of structural context on the aquifer geochemistry.
To visualize the role of these two supposed factors, a physical profile of the aquifer and geochemical profiles were performed along the flow from the south to the Seine river in the 37°N direction (fig. 9). The physical profile of the aquifer consists in the profiles of the DEM, the chalk top, the piezometric level and the chalk bottom; these data allow to see easily the variations of the saturated thickness of the aquifer.

### *4.1. Spatial distribution of the allochthonous ions and control factors*

The origin and the spatial distribution of the allochthonous ions is usually attributed to the atmospheric inputs or/and to the anthropogenic factors as the land use or the domestic sewage (Meybeck, 1983; Sherwood, 1989; Negrel and Petelet-Giraud, 2005)
In France, Meybeck (1986) defined the variation in elemental chemistry of rainwater in an eastward direction away from the Atlantic Ocean. According to him, in Haute-Normandy, the approximate $Cl^-$ concentration in rain would vary from 7 to 5 $mg.l^{-1}$ from west to east. This gradient of concentration in the rainwater is not observed on the allochthonous ions: the highest chlorine concentrations (fig.6a) are observed with the lowest values of annual rainfall (fig. 2b). The anthropogenic pollutions have a well known influence on the concentration of the $Cl^-$, $Na^+$, $NO_3^-$ or $SO_4^{2-}$ ions in the groundwaters (Kloppmann et al., 1998; Edmunds and Smedley, 2000; Edmunds et al., 2003; Negrel and Petelet-Giraud, 2005). Nevertheless, the anthropogenic factors bringing each allochthonous ion are different and so have a different spatial distribution. For example, $SO_4^{2-}$ is principally brought by the industrial pollutions, $NO_3^-$ is principally brought by the agriculture pollution; these two anthropogenic factors have not the same spatial distribution, nevertheless the spatial distribution between $SO_4^{2-}$ and $NO_3^-$ are well correlated. The anthropogenic factor contributes then to the allochthonous ions concentrations in the aquifer but can not be the only explanatory factor.The “external” factors: rainwater quality or anthropogenic factor can not explain the similar spatial distributions of these different allochthonous ions; these results lead us to suppose the existence of an “internal” control of these concentrations.
In the PCA, two variables were chosen to describe the context, but neither the piezometric level nor the aquifer thickness are well correlated with the concentration of allochthonous ions. Nevertheless, the spatial autocorrelations and cross correlations give evidence of relationships between them. The negative correlation between the aquifer thickness and $[Cl^-]$ along the structural direction 145 °N means that the highest values of $[Cl^-]$, and more generally for the allochthonous ions concentrations, correspond to the lowest aquifer thickness (fig. 9). In fact, the lowest contributions of allochthonous ions correspond to the synclines where the aquifer thickness is the most important and the highest concentrations to the anticlines. Then the allochthonous ions seem to be more or less diluted according to the thickness of water. The structural context influences the water thickness and so is indirectly a major factor influencing the contribution of the allochthonous ions.

The increase in correlation between the piezometric level and $Cl^-$ along the direction 37°N (global direction of the aquifer flow) seems to indicate the allochthonous ions are transported along the flow.
This study shows that the anthropogenic factors are not the only factor explaining the spatial distribution of the allochthonous ions. The example of [Cl-] demonstrates the major control of the structural context and of the flow on the spatial distribution of the allochthonous ions.

### *4.2. Mineralization of the aquifer: spatial distribution and control factor*

The mineralization of the Chalk aquifer in the Eure department is well represented by the F2 factor of the PCA. The facies change (sands / chalk) of the cenomanian formation in the south of the department induces a change of the water geochemistry, the water is low mineralized in the Perche Sands (conductivity <250 $mS.cm^{-1}$, data provided by the ADES databank) and will rapidly mineralise when the water begins to flow in the chalk, in which the exchange with the rock allows the increase in $Ca^{2+}$, $HCO_3^-$ and $Mg^{2+}$ concentrations.

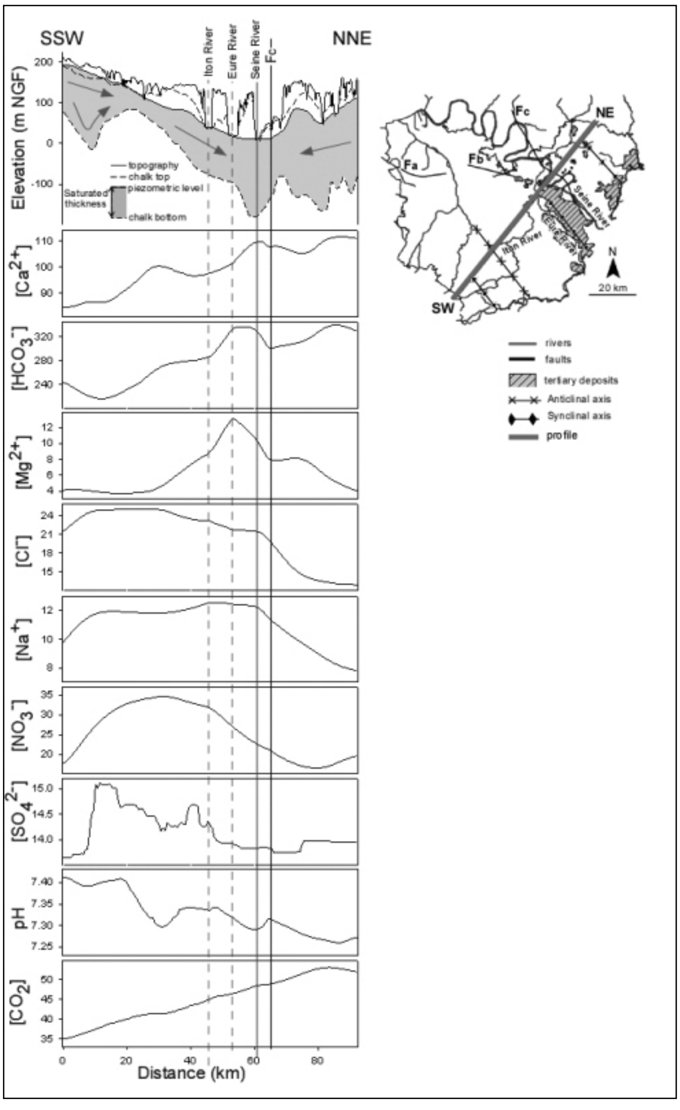

*Figure 9: Geometric-geochemical profile ($mg.l^{-1}$)*

The value of the projection of the piezometric level on the F2 axis in the PCA variable space is very negative and opposed to the mineralization (opposed to the projection of all the ions). This negative correlation between the piezometric level and the mineralization give evidence that the Chalk aquifer water globally mineralises along the flow , from the south to the downstream of the aquifer: the Seine River. The increase in the concentration of $Ca^{2+}$, $HCO_3^-$ and $Mg^{2+}$ (excepted under the Tertiary deposits) results from the chalk dissolution. The chalk groundwaters are or close to saturation with calcite so that a change of one variable in the carbonate system ($Ca^{2+}$, $HCO_3^-$, $Mg^{2+}$, pH and $CO_2$) is balanced by a change in the concentration of one or more of the other ionic species (Bakalowicz, 1979). The pH of the waters decreases from upstream to downstream (increase in acidity) opposed to the increase in $CO_2$ (fig. 9). The increase in $Ca^{2+}$, $HCO_3^-$ and $Mg^{2+}$ concentration along the flow is well correlated to the increase in $CO_2$ concentration (correlation with $Ca^{2+}$ or $HCO_3^- > 0.8$) and well negative correlated with the pH (negative correlation between the pH and $Ca^{2+}$ or $HCO_3^-$). The change of the geochemical conditions allow the increase in the saturation with calcite and then allows the chalk dissolution inducing an increase in $Ca^{2+}$, $HCO_3^-$ and $Mg^{2+}$ concentrations.

The well organized structure of the autochthonous ions is related to the geomorphology of the department : three main groundwater basins allowing the visible evolution of the autochthonous ions from the upstream to the downstream of the aquifer.
The spatial distribution of the ratio Mg/Ca give evidence of the heterogeneity of the flow capacity of the aquifer, resulting in zones with residence time more or less important. Three zones present an high ratio Mg/Ca (fig 8), these high ratios seems to be related the geometry of the aquifer and so to the structural context, (fig.10). The first is located in the syncline in the south of the department, the morphology of the aquifer (raising of the bottom between the syncline and the anticline, fig 9) act as a barrier for the flow (the aquifer thickness decreases from about 300 m to about 50 m) implying an increase in the residence time and then the increase in the ratio Mg/Ca. The two others zones are located in the south of the faults Fa and Fb (schematic profile fig. 10). For the fault Fa, the northern compartment is uplifted, the bottom of the aquifer raises then suddenly , the flow section decreases and limits the flow which is evacuated laterally compared to the obstacle of the fault.. For the fault Fb, the southern compartment is uplifted implying a decrease of the flow section and then difficulties for the aquifer flow which mainly diffuse laterally (fig. 10).

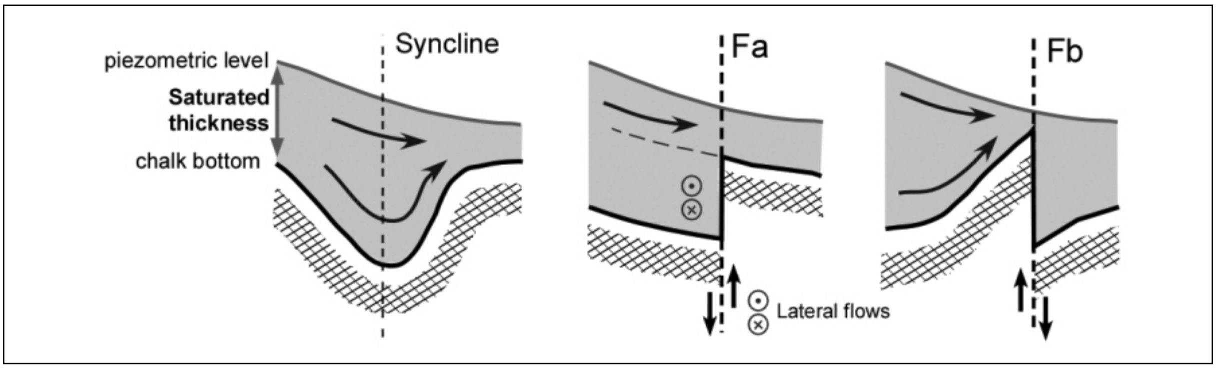

*Figure 10: Impact of the structural settings on the aquifer flow and then on the geochemistry*

The structural context (geometry of the aquifer) has an important influence on the aquifer flow inducing residence time more or less important and influencing the dissolution and then the geochemistry of the aquifer.

## Conclusion

The Chalk aquifer waters of the Eure department are globally $Ca/HCO_3$ type but the high resolution of the data shows spatial heterogeneities of the major ions: the contribution of surface water (allochthonous ions) or the global mineralization of the Chalk aquifer.
The spatial variability of the geochemistry of an aquifer has usually been explained by the spatial variability of the recharge water quality influenced in his turn by anthropogenic factors or by the spatial variability of the rainwater quality. But these factors are not able to explain entirely the spatial distributions observed.
The originality of this study is to compare the spatial distributions of the geochemistry and the spatial distributions of the physical properties of the Chalk aquifer (the piezometric level and the aquifer thickness). This coupled approach of the geochemical properties and of the geological and hydrological contexts allowed to show that:
(i) The most important allochthonous ions concentrations are found for the lowest aquifer thickness corresponding to the anticlines. The allochthonous ions are more or less diluted according to the thickness of the Chalk aquifer.

(ii) The global mineralization increases along the flow, corresponding to an increase in the chalk dissolution rate. The most important mineralization rates are related to important residence times, and correspond to zones where the aquifer flow capacity is limited because of decrease of the flow section (anticlines or faults).

These results give evidence of the predominance of an internal control of the geochemistry of the groundwaters: the geometry of the aquifer and so the structural context. This factor plays an important role on the contribution of the allochthonous ions. That controls too the potential of $CaCO_3$ dissolution along the aquifer flow. More, the influence of external factors as Tertiary deposits has been demonstrated ($Mg^{2+}$ supply).

The “classical” factors previously studied by others authors as the rainwater quality, the land use, the industrial pollutions, etc have not been investigated here. For example the differences between the spatial distributions of $Cl^-$ and $NO_3^-$ concentrations may probably be explained by the land use. That will be the subject of another paper which will use the similar space approaches (spatial autocorrelations and cross-correlations) coupled with the analysis of time-series. The results included in this paper show that the use of the spatial autocorrelations and the cross-correlations makes it possible to illustrate the continuous character of the distribution of the geochemical characteristics of the aquifer studied (in spite of its kartified properties). Within this framework, the confrontation of the spatial organization of the geochemical data with the data of the structural context and hydrogeologic data allows to propose a hierarchy of the contribution of all the factors if one envisages to include other sets of data such as the land use.

Thus the methodology used in this study (spatial analysis between geochemistry and physical properties) show a wide interest since it can be applied to the entire Chalk aquifer of the Paris Basin or to others aquifers (chalk or an other rock) and even to others spatial problems in environment or with others data types in another research field.

## References

- Bakalowicz M. (1979) Contribution de la géochimie des eaux à la connaissance de l'aquifère karstique et de la karstification. Ph. D thesis, Université Paris VI.
- Box GEP., Jenkins GM and Reinsel G. C. (1994) Time series analysis: forecasting and control. 3rd ed. Prentice-Hall International, Inc.
- Calba F, Charrière G, Conrad G, Lefebvre D and Rodet J (1979) Relations entre le développement du karst de la craie, la dynamique et la qualité des eaux souterraines du Pays de Caux. Bulletin Trimestriel de la Société Géologique de Normandie et des Amis du Museum du Havre 66(4), 45-68.
- Edmunds WM, Shand P, Hart P and Ward RS (2003) The natural (baseline) quality of groundwater: a UK pilot study. The Science of The Total Environment 310(1-3), 25-35.
- Edmunds WM and Smedley PL (2000) Residence time indicators in groundwater: the East Midlands Triassic sandstone aquifer. Applied Geochemistry 15(6), 737-752.
- Eisenlohr L, Bouzelboudjen M, Kiraly L and Rossier Y (1997) Numerical versus statistical modelling of natural response of a karst hydrogeological system. Journal of Hydrology 202(1-4), 244-262.
- Goovaerts P, Sonnet P and Navarre A (1993) Factorial kriging analysis of springwater contents in the Dyle River basin, Belgium. Water Resources Research 29(7), 2115-2125.
- Hiscock KM, Dennis PF, Saynor PR and Thomas MO (1996) Hydrochemical and stable isotope evidence for the extent and nature of the effective Chalk aquifer of north Norfolk, UK. Journal of Hydrology 180(1-4), 79-107.
- Kloppmann W, Dever L and Edmunds WM (1998) Residence time of Chalk groundwaters in the Paris Basin and the North German Basin: a geochemical approach. Applied Geochemistry 13(5), 593-606.
- Laignel B (2003) Caractérisation et dynamique érosive de systèmes géomorphologiques continentaux sur substrat crayeux. Exemple de l'Ouest du Bassin de Paris dans le contexte nord-ouest européen. Livret I: Axes et Développement de la Recherche. H.D.R., Université de Rouen.
- Laignel B, Quesnel F and Meyer R (2002) Classification and origin of the clay-with-flints of the western Paris basin (France). Z.F. Geomorphologie 46(1), 69-91.

- Langmuir D (1971) The geochemistry of some carbonate ground waters in central Pennsylvania. Geochimica et Cosmochimica Acta 35(10), 1023-1045.
- Lautridou JP (1985) Le cycle périglaciaire pléistocène en Europe du Nord-Ouest et plus particulièrement en Normandie, Université de Caen.
- Mangin A (1984) Pour une meilleure connaissance des systèmes hydrologiques à partir des analyses corrélatoire et spectrale. Journal of Hydrology 67, 25-43.
- Massei N, Wang HQ, Dupont JP, Rodet J and Laignel B (2003) Assessment of direct transfer and resuspension of particles during turbid floods at a karstic spring. Journal of Hydrology 275(1-2), 109-121.
- Meybeck M (1983) Atmospheric inputs and river transport of dissolved substances., Dissolved loads of rivers and surface water quantity/quality relationships. Proc. Hamburg symposium, 1983, Published by International Association of Hydrological Sciences; IAHS Publication 141, Editors Webb B.W., 173-192.
- Meybeck M (1986) Chemical composition of headwater streams in France. Sciences Geologiques - Bulletin 39(1), 3-77.
- Morell I, Gimenez E and Esteller MV (1996). Application of principal components analysis to the study of salinization on the Castellon Plain (Spain). Science of The Total Environment 177(1-3), 161-171.
- Négrel P (1999). Geochemical Study of a Granitic Area -- The Margeride Mountains, France: Chemical Element Behavior and 87Sr/86Sr Constraints. Aquatic Geochemistry 5(2), 125 - 165.
- Negrel P and Petelet-Giraud E (2005) Strontium isotopes as tracers of groundwater-induced floods: the Somme case study (France). Journal of Hydrology 305(1-4), 99-119.
- Quesnel F (1997) Cartographie numérique en géologie de surface - Application aux altérites à silex de l'ouest du Bassin de Paris. Ph. D., Université de Rouen.
- Reis AP, Sousa AJ, Ferreira da Silva E, Patinha C and Fonseca EC (2004) Combining multiple correspondence analysis with factorial kriging analysis for geochemical mapping of the gold-silver deposit at Marrancos (Portugal). Applied Geochemistry, 19(4): 623-631.
- Rodet J (1997) Typologie des karsts dans la craie du bassin de Paris. Annales de la Société Géologique du Nord 5, 351-359.
- Sherwood WC (1989) Chloride loading in the South Fork of the Shenandoah River, Virginia, U.S.A.,. Environmental Geology (Historical Archive) 14(2), Page 99.
- Wang Y, Ma T and Luo Z (2001) Geostatistical and geochemical analysis of surface water leakage into groundwater on a regional scale: a case study in the Liulin karst system, northwestern China. Journal of Hydrology 246(1-4), 223-234.
- Wazi N (1988) Le Crétacé du Roumois (Vallée de l'Oison) et le tertiaire-quaternaire des régions voisines de la basse vallée de la Seine (Haute-Normandie). Statigraphie et tectonique, Université de Rouen.
- Widory D, Kloppmann W, Chery L, Bonnin J, Rochdi H and Guinamant JL (2004) Nitrate in groundwater: an isotopic multi-tracer approach. Journal of Contaminant Hydrology 72(1-4), 165-188.
- Zhang C and Selinus O (1998) Statistics and GIS in environmental geochemistry -- some problems and solutions. Journal of Geochemical Exploration 64(1-3), 339-354.

# DARCY 57

# Using stable isotope analysis to characterise the regional hydrology of the Souss-Massa basin, south-west of Marocco.

*L. Bouchaou (1), Y. Hsissou (1), M. Qurtobi (2), Kh. Dindane (1), S. Boutaleb (3), & S. Krimissa (1)

(1) Laboratoire de Géologie Appliquée et Géo-Environnement (LAGAGE), Faculté des Sciences,
Université Ibn Zohr, B.P 8106, Cité Dakhla, 80000 Agadir, Maroc.
(2) Centre National des Etudes Scientifiques et Techniques Nucléaires (CNESTEN), Rabat, Maroc
(3) Faculté polydisciplinaire de Taza. Université Sidi Mohamed Ben Abdallah Fès, Maroc.
* lbouchaou@yahoo.fr

## Abstract

The Souss river flow situated between the high Atlas Mountain in the north and Anti-Atlas in the south, is closely related to the rain fluctuations and shows inter annual variation, seasonal regime from year to year. The climate is semi-arid to arid, the rainy season extending from November to March and the dry season from April to October. The rainfall and the average runoff vary in time and space, ranging from 200 mm/y in the plains (mean altitude: 460 m a.s.l.) to 600 mm/y in the mountains (altitude >700 m a.s.l.). The long-term mean annual precipitation decreased in 20 years from 343 mm in Aoulouz (700 m a.s.l.) to 232 mm in Taroudant (232 m a.s.l.). The temporary Souss River is the main collector of superficial waters in the basin. The location near mountains (with high rainfall) allows an important inflow by its tributaries especially those coming from the High Atlas Mountain. This flow coming from a high altitude is infiltrated in the piedmont area and in the beds of rivers which present high permeable conglomerates.

The shallow aquifer of the plain is the main resource for drinking, irrigation and industrial water in the region. In order to improve the management of these precious resources, several studies, to better understand the hydrological functioning of the aquifer system and define the relationship between surface runoff (rivers and dams) and groundwater, have been carried out during the last years.

This study summarizes the application of isotope hydrological tools to infer water sources in this part of the Souss region. The isotopic contents of waters are ranged from - 8‰ & to -5.2‰ for $\delta^{18}O$, from -52‰ to -34‰ for $\delta^{2}H$, and from 0 to 5.5 TU for tritium.

Hydrogen and oxygen isotope signatures reveal a significant infiltration before evaporation, indicating a recent recharge through fractures in Atlas Mountain crystalline and limestone rocks and infiltration of surface water in the alluvial cones at the margin of the Atlas basins. $^{18}O$, _H and tritium values indicate a mixing between recent and old groundwaters; the latter were recharged under more humid climatic conditions than that at present. The old groundwaters encountered in deep wells are not connected to modern recharge, indicating that water followed a long flow path. The slight evaporation recorded by stable isotopes in water from the southern margin close to the Anti-Atlas mountains indicates that there groundwaters are subject to a drier climate, marking the Anti-Atlas Mountains, which form a barrier against the influence of the Sahara.

The upstream watershed, which is the place of condensation and the beginning of the Atlas Mountain, shows more characteristic $^{2}H$ and $^{18}O$-depleted waters. This finding can be explained by the altitude and the continental effects. On the other hand, $^{2}H$ and $^{18}O$-enriched waters values towards the ocean, show an evaporation effect near the condensation source or the irrigation returns, specially in the irrigated perimeters. The rain isotope values indicate a main recharge from the Atlasic Mountain (figure 1), whereas the contribution of the local rains is negligible in downstream. The $^{2}H$-$^{18}O$ relationship displays straight lines with variable slopes on an upstream-downstream movement. The slopes, which are below 8 in certain areas, represent the evaporation during the infiltration either by runoff or by irrigation returns. Besides, the different values of slopes correspond to the variables isotopic values observed at a regional scale within the basin.

# DARCY 58

# The Guaraní Aquifer System: State-of-the-art in Argentina

TUJCHNEIDER, Ofelia[1,2], PEREZ, Marcela[1], PARIS, Marta[1], D´ELIA, Mónica[1]

[1] Universidad Nacional del Litoral, CC 217, (3000) Santa Fe, Argentina. e- mail: gig@fich.unl.edu.ar
[2] CONICET, CC 217, (3000) Santa Fe, Argentina. pichy@fich.unl.edu.ar

## Abstract

The Guaraní Aquifer System (SAG) is one of the world's most important fresh groundwater reservoirs. It underlies four South American countries: Argentina, Brazil, Paraguay and Uruguay, which use this resource for several purposes with very different exploitation levels. This mega transboundary aquifer is lodged in aeolian and fluvial sandstone from the Triassic-Jurassic, usually covered by basalt formations from the Cretaceous which provide a high confinement degree. Due to the vast SAG´s extension, this paper is focalized in a bordering area between Argentina and Uruguay. An analysis of the geological and hydrochemical data available in this area allowed delineating zones with different characteristics, especially regarding to the high salinity groundwater contents and the lying conditions of the water-bearing formations. The interpretation of these results highlights the occurrence of deep thermal groundwater towards the southwest portion of the SAG in Argentina, in which the border has not been defined yet.

## Introduction

The Guaraní Aquifer System (SAG) constitutes one of the world's most important fresh groundwater reservoirs due to its estimated area (1,200,000 km$^2$) and volume (40,000 km3). Underlying a region of approximately 24,000,000 inhabitants, the SAG is shared by four South American countries: Argentina, Brazil, Paraguay and Uruguay, which use the resource for very different purposes and exploitation levels (Figure 1).

In Brazil, the SAG underlies the eight most developed states of this country. In São Paulo State, the most industrialized, the aquifer is more and more exploited. Nowadays, it is mainly used for domestic and industrial water supply, irrigation, therapeutic bath and mineral water.

In Argentina and Uruguay, the main use is the balneotherapy and recreational clubs; although in the later country the SAG is also used for water supply and irrigation. Besides, in Uruguay, seven deep pumping wells were drilled in the ´90s. In 1994, the first Argentinean infrabasaltic well was constructed in Federación city (Entre Ríos province). On the other hand, in Paraguay, the main use is the water supply to rural villages located in the eastern sector of the country.

This papers presents the results of the analysis and interpretation of the geological and hydrochemical information (existing and generated) corresponding to those wells currently functioning in an area of approximately 78,000km$^2$, (Figure 1). This area involved part of the Argentinean-Uruguayan boundary as well as the north-centre of the Entre Ríos province (Argentina). The purpose of this paper is to corroborate the zones in which the deep wells have been pumping water with high saline contents. The water samples obtained from these wells have been first related with the type of sediments that stored the water. Then, these samples have been also compared with those low salinity water samples typically characterising the SAG´s water in most of its vast extension.

From the analysis of these results and the new data obtained it is possible to consider the occurrence of deep hot groundwater at the right bank of the Paraná River in its medium reach

(Santa Fe province). This allows advancing in the knowledge of the Guaraní Aquifer System west border in Argentina, where the limit has not been define yet.

## Geological and hydrogeological settings

The sedimentary sequence comprising and related to the Guaraní Aquifer System is described below (Table 1). The geological formations are known in each country under different names.

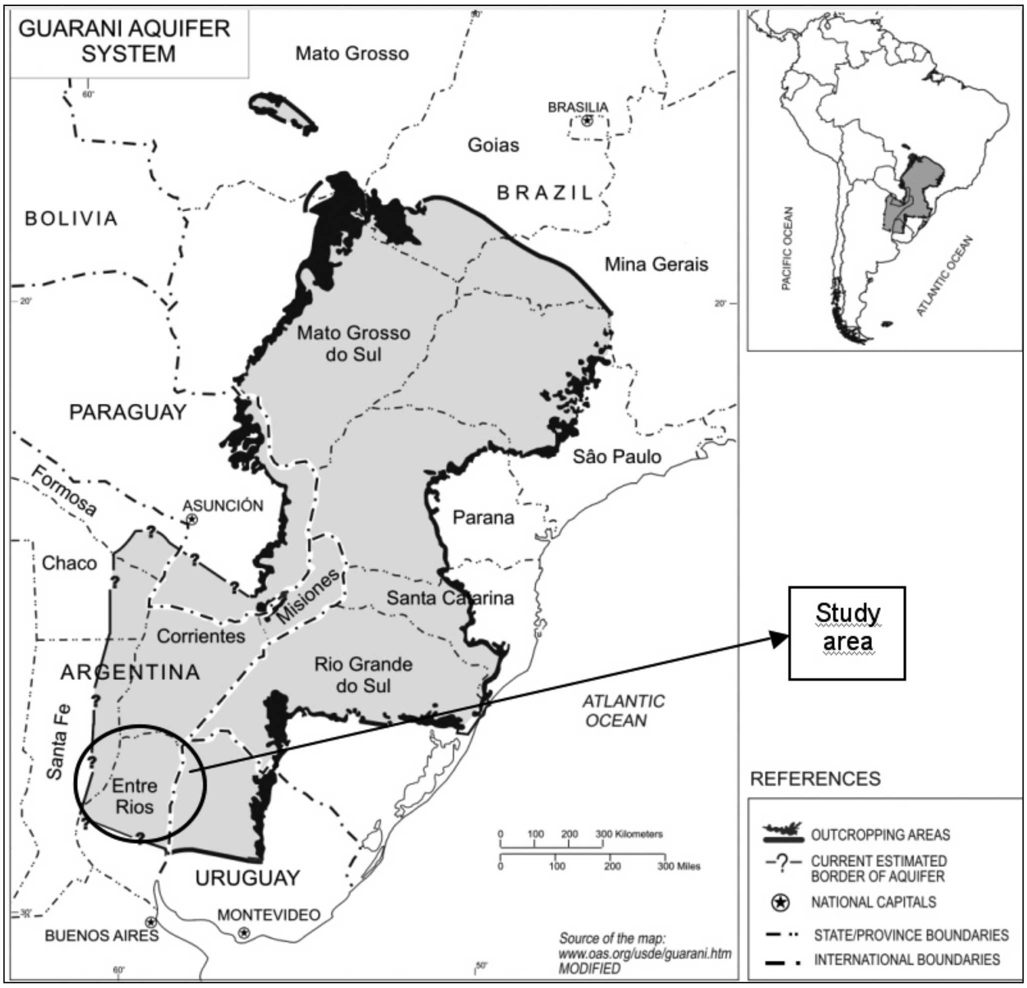

Source of the map: www.oas.org/usde/guarani.htm MODIFIED

*Figure 1: Guarani Aquifer System occurrence and location of the study area*

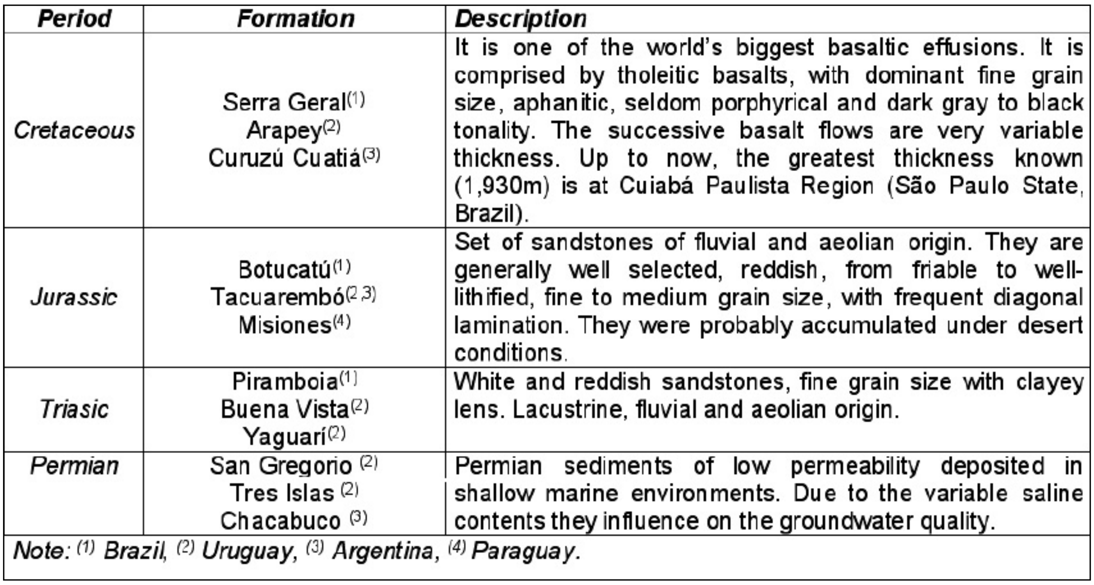

| Period | Formation | Description |
|---|---|---|
| *Cretaceous* | Serra Geral(1)<br>Arapey(2)<br>Curuzú Cuatiá(3) | It is one of the world's biggest basaltic effusions. It is comprised by tholeitic basalts, with dominant fine grain size, aphanitic, seldom porphyrical and dark gray to black tonality. The successive basalt flows are very variable thickness. Up to now, the greatest thickness known (1,930m) is at Cuiabá Paulista Region (São Paulo State, Brazil). |
| *Jurassic* | Botucatú(1)<br>Tacuarembó(2,3)<br>Misiones(4) | Set of sandstones of fluvial and aeolian origin. They are generally well selected, reddish, from friable to well-lithified, fine to medium grain size, with frequent diagonal lamination. They were probably accumulated under desert conditions. |
| *Triasic* | Piramboia(1)<br>Buena Vista(2)<br>Yaguarí(2) | White and reddish sandstones, fine grain size with clayey lens. Lacustrine, fluvial and aeolian origin. |
| *Permian* | San Gregorio (2)<br>Tres Islas (2)<br>Chacabuco (3) | Permian sediments of low permeability deposited in shallow marine environments. Due to the variable saline contents they influence on the groundwater quality. |
| ***Note:*** *(1)* ***Brazil,*** *(2)* ***Uruguay,*** *(3)* ***Argentina,*** *(4)* ***Paraguay.*** | | |

Table 1: Sedimentary sequence comprising and related to the SAG

This mega-aquifer is lodged in aeolian and fluvial sandstones of continental origin deposited in the Triassic and Jurassic. These sandstones are generally covered by Cretaceous basaltic formations which provide different confining degrees. Covering approximately 60-65% of its extension, the basalt thickness ranges from 200 to more than 1,000m. Therefore, regarding to this characteristic the aquifer system can be considered as either confined or outcropped (Montaño et al. 2004).

Particularly, in Argentina the basaltic package outcrops in the northeastern sector of the country, where it is very fissured. The basalt formation becomes deeper westwards and its thickness decreases both westwards and southwards.

The pattern of the sandy sediments is due to: the Paraná Sedimentary Basin boundaries, the structural configuration of the geologic basin and the basaltic deposits that cover the sandstones.

The thickness of the aquifer system ranges from few meters up to 800m in Brazil and 600m in Uruguay. The depth varies throughout its area and it can reach up to 1,800m. Not surprisingly in view of the large area this groundwater-bearing formation has, the hydraulic parameters present a great spatial variability. In some parts, the hydraulic conductivity ranges from 0.3 to 5.0 m/day. Generally, in the sandstone outcrop areas the effective porosity is of about 15% and in the confining areas the storage coefficient is $10^{-4}$.

Other distinctive characteristics of the SAG are: artesian pressures and high yields at many locations ($500m^3/h$ where the aquifer thickness is greater), good quality groundwater and temperature varying between 38°C to 60°C by geothermic gradient.

Generally, the water stored in this aquifer system is of very good quality, with an average salinity of 300mg/l. The outcropping areas are characterized by water of a calcium-bicarbonate composition. The confining areas, otherwise, are characterized by water of a sodium-bicarbonate composition.

In accordance with Fili and Tujchneider in Montaño et al. (1998), in Argentina it is possible to identify within the aquifer system two subsystems: one of them with low salinity water and higher temperatures, located in the north-centre of Entre Ríos province. The other one, with salt water and lower temperatures, located at what it could be the southern border of the aquifer system in the Argentinean territory.

In a similar way, Montaño et al. (2004) defined two subsystems for the aquifer in Uruguay. The areas where these authors focused on the investigations correspond to the boundary between Argentina-Uruguay and Brazil-Uruguay. They called Typical SAG to the aquifer system lodge in the sediments of the Tacuarembó, Yaguarí and Buena Vista geological formations. The water stored in this subsystem has no restrictions for drinking water. The other subsystem is called Permian SAG. It underlies the Typical SAG and comprises Permian sedimentite deposited in marine environments, conditioning the water quality.

Due to the large extension of the SAG the piezometric surface is hard to define. Gilboa et al., (in Araujo et al. 1999) outlined the first piezometric map. Since this time, several water-level contour maps were draft by different authors, many of them showing only a sector of the aquifer system and its particular behaviour. For instance, Sracek and Hirata (2002) drew preferential flow lines for São Paulo State (Brazil). They made important considerations about the validity of the piezometric and hydraulic information because many of the values reported did not consider the water density and viscosity-temperature correction.

Nevertheless, in a general way, it can be indicated that the direction of the groundwater flow in the SAG's north sector (Brazil) goes from the outcropping areas of the Botucatú formation to the axis of the basin. Therefore, the general direction of the ground water flow is from north east to south west. At some areas, however, there are local directions toward the south west. The groundwater elevation varies from 300 to 700 m. It can be also indicated that the area located between the Paraná and Uruguay rivers, would probably be the SAG´s discharge area.

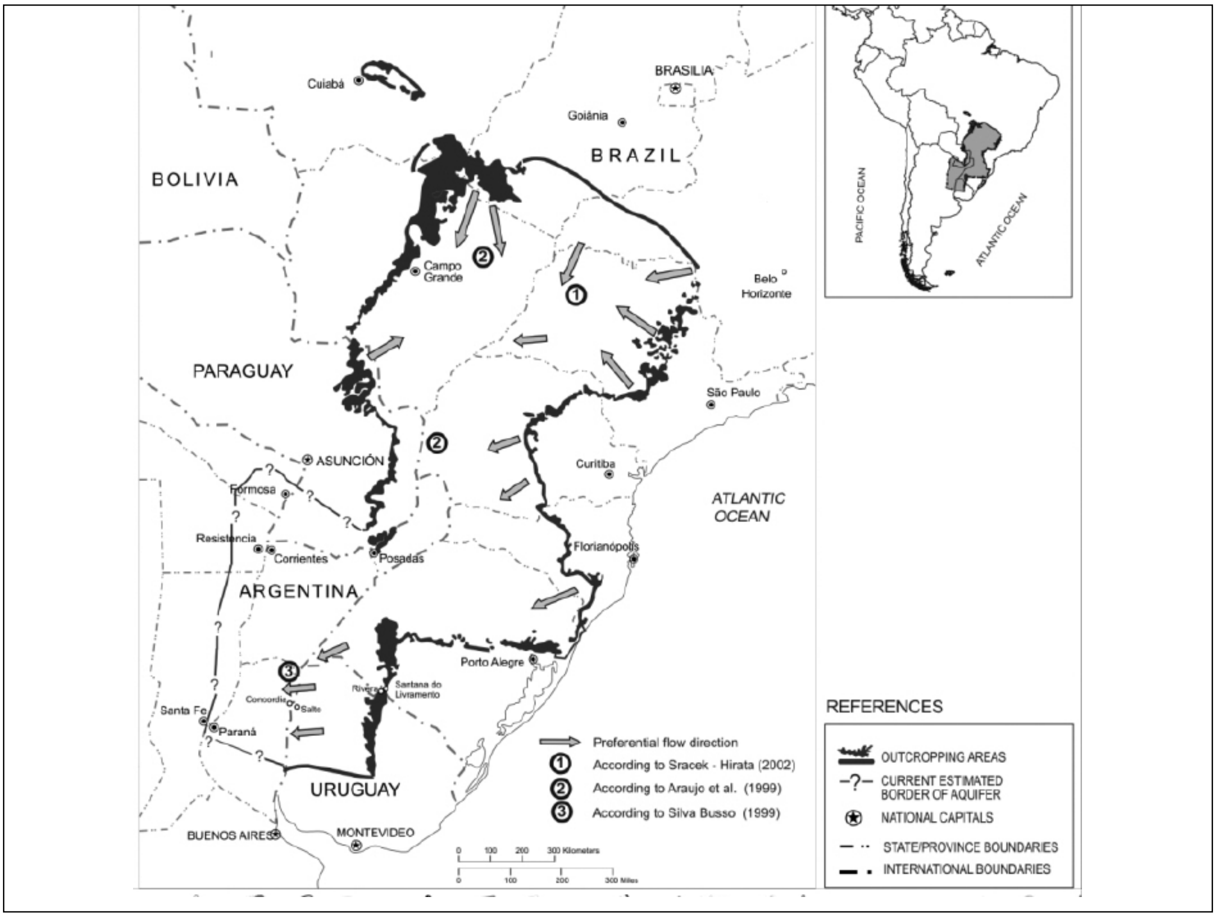

*Figure 2: General groundwater flow directions (Source: Tujchneider et al. 2003).*

Silva Busso (1999) performed an analysis of the confinement pressures related to the depth of the aquifer formation in Entre Ríos province (Argentina) and North West of Uruguay. For this author, Uruguay's recharge areas are located between 110 to 120m above sea level. The hydraulic potentials decrease from north east towards south west.

Therefore, among the specialists, there is not a single criterion about the SAG´s flow pattern up to now. This is a subject of current investigations. Figure 2 shows a simplify scheme of the main flow direction according to the authors mentioned above (Tujchneider et al. 2003).

## Materials and methods

The regional and local background information about geology, hydrogeology and hydrochemist (Montaño et al. 1998; Fili 2001; Tujchneider et al. 2003; Tujchneider and Tineo 2005) was revised and reinterpreted.

In the order to evaluate the possibility of occurrence of the Guaraní Aquifer System in the right margin of the Paraná River alluvial valley, a geophysical exploration by the electrical resistivity method was carried out. Therefore, four vertical electrical soundings (VESs) were conducted at Garay Department (Santa Fe province, Argentina).

The hydrochemical data set was composed by 48 analyses of calcium, magnesium, sodium, potassium, bicarbonate, chloride, sulphate (all of them expressed in meq/l), Total Dissolved Solids (expressed in mg/l) and pH. These records correspond to water samples collected at different times and places, distributed in the study area.

After evaluating the analytical error using the ionic balance, the data were categorized according to Piper-Hill classification.

To obtain the statistics and frequency distributions of these ionic series, an univariate statistical analysis was done. Then, to identify homogeneities in the data set, R-mode and Q-mode Cluster Analysis were applied. R-Pearson and euclidian distance coefficients were used respectively. The linkage criterion was unweighted average pairs. Natural logarithm and standard transformations were applied to the series.

## Results and Discussion

The geological formations comprising the SAG are known in Argentina, Brazil, Paraguay and Uruguay under different names, but well-known in the region as Botucatú, Tacuarembó or Misiones sandstones. They are confined by the Serra Geral or Arapey basalt formation.

In Argentina, the sandstones occupy part of the Chaco Paranense Sedimentary Basin, underlying the provinces of Misiones, Corrientes, Entre Ríos, north centre of Santa Fe, eastern of Córdoba, south of Chaco and east centre sector of Santiago del Estero. In Corrientes province, the sandstones outcrop in some limited areas located in the centre and south sectors of the province, but prevailing in the subsurface (Figure 1).

For the medium reach of Paraná River alluvial valley, Table 2 shows the regional stratigraphycal sequence from the rocks that compose the crystalline basement to the more recent sediments according to Fili (2001), Tujchneider and Tineo (2005). Figure 3 presents a regional stratigraphycal cross-section summarizing all this integrated information.

Applying the ionic balance and adopting the admissible limit for the error, the chemical data set was constituted by 32 analyses. According to the Piper-Hill classification all the water samples in the cations triangle are sodium. However, in the anionic triangle 44% are bicarbonate and the remaining 56% are chloride. Figure 4 shows the spatial locations of these samples.

Regarding to the coefficient of variation, skewness and kurtosis as well as the mean and median values of the chemical data series, bicarbonate and pH are normal distributed.

Water samples collected from María Grande, La Paz and Villaguay (Entre Ríos province, Argentina) deep confined pumping wells presents high TDS values, which are located outside the 75 percentile. Sulphate, chloride, calcium and sodium contents show a similar behaviour as the TDS values, and also for the same wells.

According to Seoane and Silva Busso (2005), different authors have been mentioned the presence of fluoride in groundwater samples collected in the SAG´s Brazilian aquifer areas. About the origin of the fluoride they consider three causes. The first cause related to rocks originated by basaltic and alkaline magma intrusion, sometimes rich in fluoride. Secondly, hydrothermal deposits rich in fluoride derived from igneous rocks. Finally, remobilization of fluoride spread in percolated rocks. In the bordering area between Argentina and Uruguay, the fluoride contents range from 0.01 to 3.8mg/dm$^3$. The possible geochemical origin could be the basalt deposits of the Serra Geral formation.

Figure 5 shows the dendrogram for the R-mode cluster analysis. It should be noticed not only the considerable influence of sulphate, sodium, chloride and calcium in TDS composition and variability but also the marked relation between bicarbonate concentrations and pH as a water sample acid-alkalinity indicator.

Figure 6 shows the dendrogram for the Q-mode cluster analysis. This plot allows individualizing two main water samples groups which are coincident with those identified by the Piper-Hill classification. Group 1 is defined by bicarbonate waters. Group 2 is defined by chloride sulphate waters. With a higher similarity level it is possible to identify four subgroups which are shown spatially distributed in Figure 7. This figure shows that the data collected from María Grande, Villaguay and La Paz wells (Entre Ríos province, Argentina) constitute a set with internal homogeneity but with a clear heterogeneity regarding to the all remaining observations. It is also important to notice how the data collected in a same place show changes in the water chemical composition through the time.

| ***Age*** | ***Fomation*** | ***Lithology*** | |
|---|---|---|---|
| Holocene | Undistinguishable recent and current alluvial deposits | Sands and clayey silts | |
| Upper Pleistocene<br>Médium Pleistocene | "Pampa Group" | Clays, silts and loess | |
| Lower Pleistocene<br>Upper Pliocene | Ituzaingó ("Puelches" sands) | ochre, quartzose, fluvial sands | |
| Upper Miocene | Paraná | Green clays and Grey marine sands | |
| Coger Miocene<br>Eocene | Olivos / Fray Bentos | Reddish, calcareous and gypsiferous clays | |
| Paleocene<br>Upper Cretaceous | Mariano Boedo / Yeruá | Calcareous sandstones<br>Claystones | |
| Lower Cretaceous<br>Upper Jurassic | Serra Geral<br>Tacuarembó | Basalt and<br>Quartzose sandstones | GUARANI AQUIFER |
| Upper Triassic | Buena Vista | Quartzose sandstones | SYSTEM |
| Lower Permian | Chacabuco | Claystone and tuffite | |
| Upper Carboniferous | Charata<br>Sachayoj | Siltstones and sandstones<br>Lutaceous claystone and sandstones | |
| Precambrian | Basement rocks | Granite-gabbro and metamorphic rocks | |

*Table 2: Regional stratigraphical sequence*

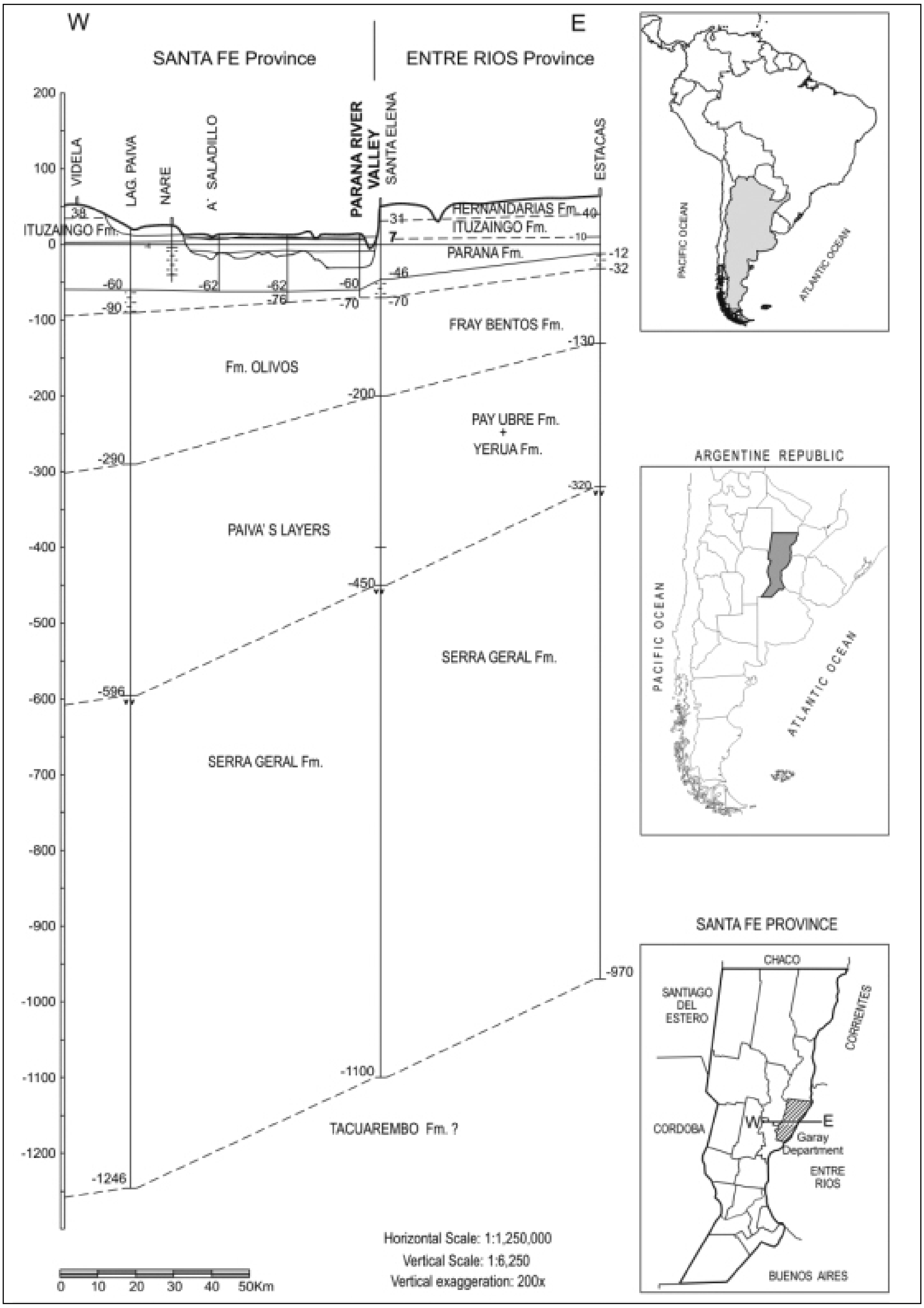

*Figure 3: Regional stratigraphical cross section (Source: Tujchneider et al. 2005*

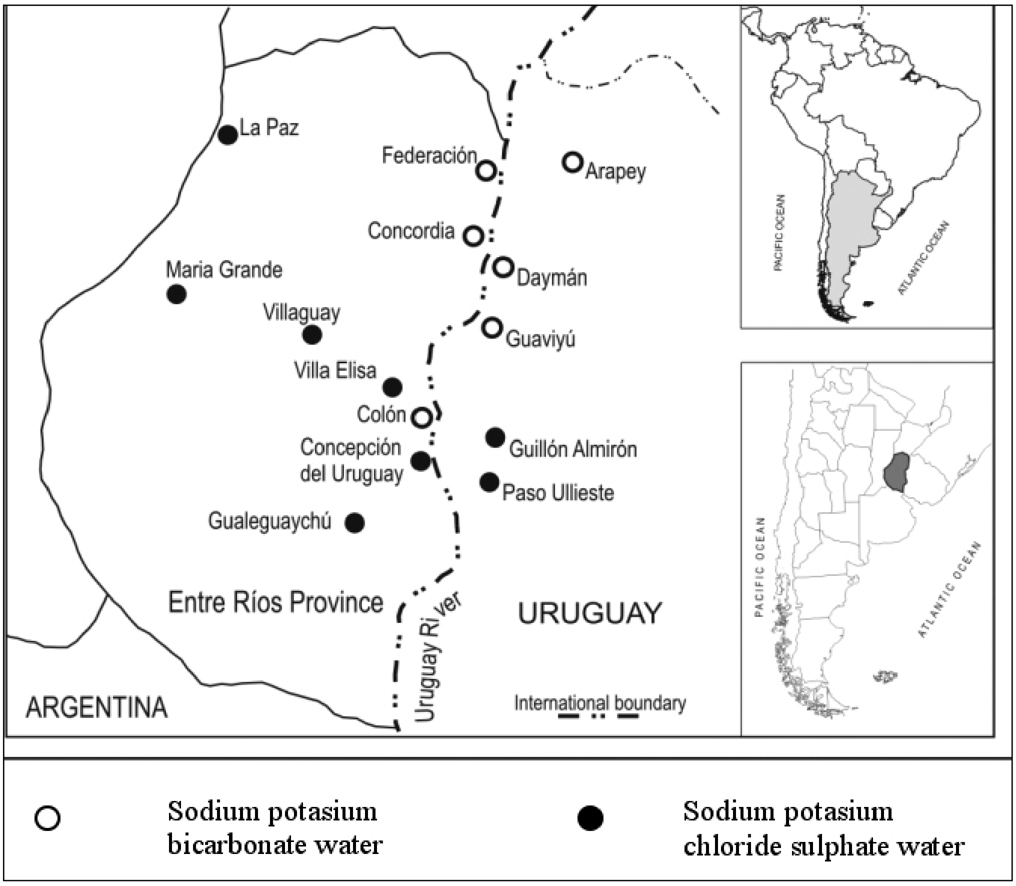

*Figure 4: Spatial locations of data set according to Piper-Hill classification*

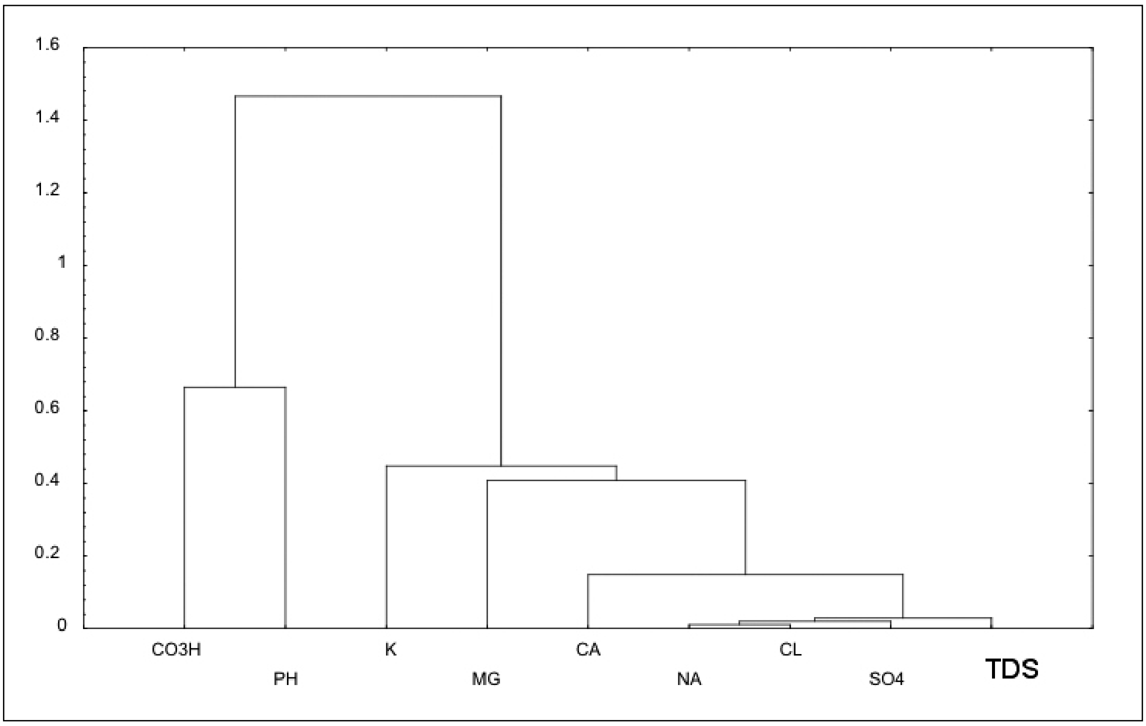

*Figure 5: R-mode dendrogram*

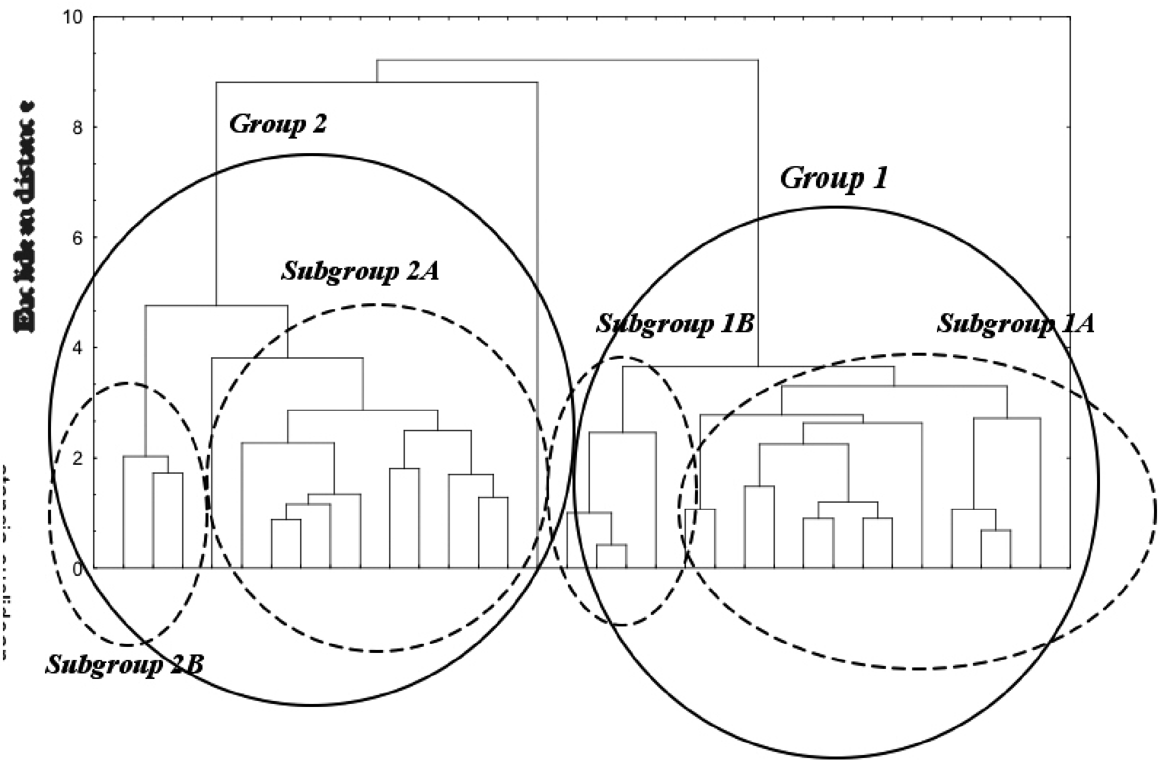

| | | | | | |
|---|---|---|---|---|---|
| C_1 | Federación 12/94 | C_12 | Dayman | C_23 | Villa Elisa 12/04 |
| C_2 | Federación 04/95 | C_13 | G. Almirón 10/88 | C_24 | Colón 03/97 |
| C_3 | Federación 12/97 | C_14 | G. Almirón 03/97 | C_25 | Concordia 11/97 |
| C_4 | Federación 03/99 | C_15 | G. Almirón | C_26 | Concordia 03/99 |
| C_5 | Arapey 08/95 | C_16 | Guaviyú 06/96 | C_27 | La Paz 12/04 |
| C_6 | Arapey 11/97 | C_17 | Guaviyú 03/97 | C_28 | María Gde 12/04 |
| C_7 | Arapey | C_18 | Villa Elisa 03/97 | C_29 | Paso Ulliestie |
| C_8 | Dayman 07/85 | C_19 | Villa Elisa 03/97 | C_30 | Villaguay 03/04 |
| C_9 | Dayman 01/92 | C_20 | Villa Elisa 04/97 | C_31 | Gualeguaychú 03/99 |
| C_10 | Dayman 07/92 | C_21 | Villa Elisa 07/97 | C_32 | C. del Urug. 04/99 |
| C_11 | Dayman 08/97 | C_22 | Villa Elisa 08/98 | | |

*Figura 6: Q-mode dendrogam*

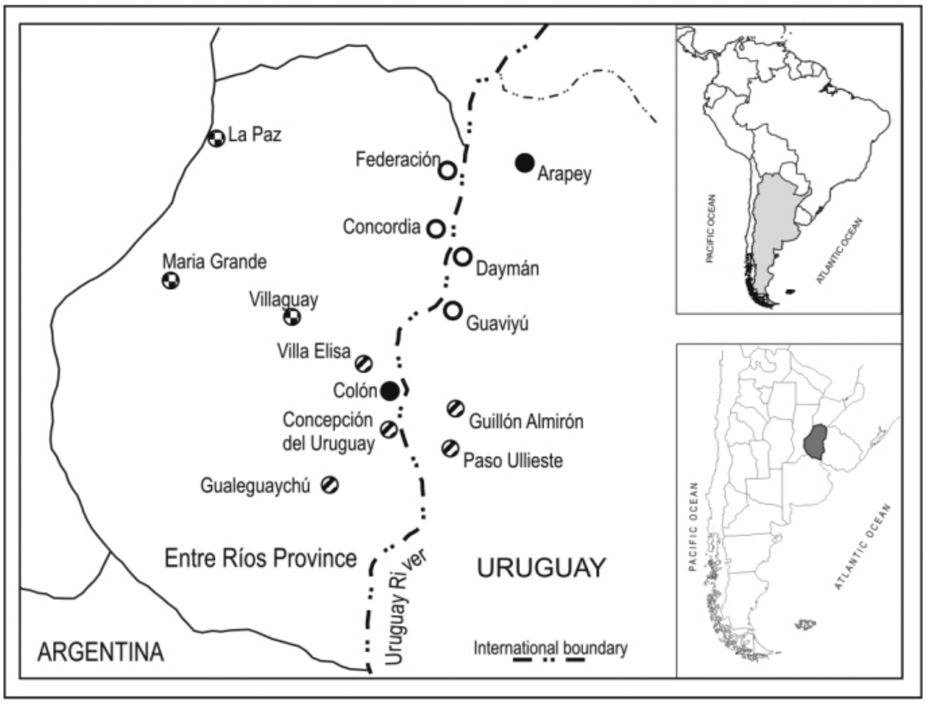

*Figure 7: Locations of groups and subgroups identified in the Q-mode cluster analysis*

## Final remarks

From the analysis of both the available information and the new advances generated by the field studies, the depths and thickness of the geological formation identified in the study area could be corroborated. For the right bank of the Paraná River in Garay Department (east-centre of Santa Fe province, Argentina), the top of the basalt elevation is clearly identified at a depth between 683 to 693m, with an average thickness of 692m. In this area, underlying the basalt formation, sediments that could be saturated were identified at approximately 1,360m deep. These sediments would belong to Tacuarembó Formation (sandstone of Tacuarembó). Depending on the comparisons between the lithological well log descriptions of the several deep pumping wells drilled in Entre Ríos province, permeable sediments intercalated in the basalt formation could be found also in Santa Fe province. These layered materials would behave hydraulically as aquifers and could store very salty water.

From the analysis of the chemical data, the differences between those wells pumping fresh groundwater (Group 1) and those which pump salty groundwater (Group 2) clearly arise. Group 1 involves water samples from: Federación, Colón, Concordia (Argentina), Arapey, Daymán and Guaviyú (Uruguay). In this group the samples belonging to Federación, Concordia, Daymán and Guaviyú are of very good quality. It is considered that these wells really pump the SAG´s groundwater. On the other hand, Colón and Arapey groundwater samples have more saline contents.

The water samples of Villa Elisa, Gualeguaychú, Concepción del Uruguay (Argentina), Guichón, Almirón, and Paso Ulliestie (Uruguay) belong to Subgroup 2A. They are brackish water. Water samples from María Grande, La Paz and Villaguay (Argentina) are in Subgroup 2B and they are very brackish water. It is clear that brackish groundwater would belong to the layered permeable levels intercalated in the basalt formation overlying the SAG´s water-bearing sandstone, which stores fresh groundwater.

Likewise, changes in the water sample chemical characteristics at some exploitation locations have been possible to identify.

It is considered that the SAG is one of the most complex aquifer systems of the world. Due to its great spatial variability, more and better hydrogeological information is required, both at regional and local scale. The "homogeneity" many authors mention is because the lack of data or detailed studies.

Taking into account what has previously been stated, it should be emphasized the need of controlling in a more effective way not only the well design features and construction practices but also the well performance and operation. Lithological logs, sediment samples for mechanical analyses, water samples for chemical analyses, information about groundwater levels, types of aquifers crossed and reached are recommended aspects that should received more attention for the design of such wells. Some environmental problems have just been detected due to both the inadequate well construction procedures and the bad management of the saline effluents at surface.

In Santa Fe province, detailed studies are required in order to advance in the purpose of establishing the west side border of the SAG and reducing the uncertainties associated to those developments that could be carried out for producing deep hot groundwater.

## References

- Araujo LM, França AB, Potter PE (1999). "Hydrogeology of the Mercosul aquifer system in the Paraná and Chaco-Paraná Basisns, South America and comparison with the Navajo-Nugget aquifer system, USA. Hydrogeology Journal 7(3): 317-339.
- Filí M (2001). Síntesis Geológica e Hidrogeológica del noroeste de la Provincia de Entre Ríos, República Argentina (Geologic and hydrogeologic synthesis in the north-east of Entre Rios province, Argentine Republic). Boletín Geológico y Minero 112: 25-36.
- Montaño J, Tujchneider O, Auge M, Filí M, Paris M, D'Elía M, Perez M, Nagy MI, Collazo P, Decoud P (1998). Acuíferos Regionales en América Latina. Sistema Acuífero Guaraní. Capítulo Argentino-Uruguayo (Regional Aquifer in Latin America. Guarani Aquifer System. Argentinean Uruguayan Chapter). Centro Internacional de Investigaciones para el Desarrollo de Canadá (C.I.I.D.) y Centro de Publicaciones de la Universidad Nacional del Litoral. Santa Fe, Argentina.
- Montaño J, Da Rosa Filho E, Hernandez M (2004). Características hidrogeológicas del Sistema Acuífero Guaraní (Hydrogeological characteristics of the Guaraní Aquifer System). In: http://www.alhsud.com/castellano/articulos_listado.asp. Cited 01 Abr 2004.
- Seoane Borracer N, Silva Busso A (2005). Aspectos sobre la distribución de fluoruros en el Sistema Acuífero Guaraní en Argentina y Uruguay (Some aspects about the fluoride distribution in the Guarani Aquifer System at Argentina and Uruguay). Paper presented at IV Argentine Hydrogeology Congress, Nacional University of Río Cuarto, Río Cuarto, Córdoba, Argentina, 25-28 October 2005. Proceedings. Volume 1:171-180.
- Silva Busso A (1999). Contribución al conocimiento de la geología e hidrogeología del Sistema Acuífero Termal de la Cuenca Chacoparanense Oriental Argentina (Contribution to the geological and hydrogeological knowledge of the Thermal Aquifer System in the East Chacoparanense Basin). Thesis, University of Buenos Aires, Argentina. [in Spanish].
- Sracek O, Hirata R (2002). Geochemical and stable isotopic evolution of the Guaraní Aquifer System in the state of Sao Paulo, Brazil. Hydrogeology Journal 10(6):643-655.
- Tujchneider O, Perez M, Paris M, D´Elía M (2003). Sistema Acuífero Guaraní: un recurso compartido por cuatro países (The Guaraní Aquifer System: A resource shared by four countries). In: Basile, Mancinelli, Pouey, Riccardi, Zimmermann (Eds) III Argentine Hydrogeology Congress. National University of Rosario. Rosario, Argentina, 23-26 September 2003. Proceedings. Volume 2: 71-91.
- Tujchneider O, Tineo A (2005). Geohydrology in plain areas. A conceptual model of a complex system Los Saladillos, Santa Fe Province, Argentina. In: Bocanegra, Hernández, Usunoff (Eds) Groundwater and Human Development. Balkema. 12:145-158.

# DARCY 61

# Advective versus diffusive flux in a low permeability clay sequence

W.A. Timms and R.I. Acworth
i.acworth@unsw.edu.au

Water Research Laboratory, School of Civil and Environmental Engineering,
University of New South Wales, Manly Vale, NSW 2093, AUSTRALIA

Low permeability clay sequences in the Murray-Darling Basin of Australia often contain high salinity water and overlie major groundwater resources. Knowledge of salt flux mechanisms through these aquitards is of critical importance because fresh water resources could over time become contaminated. The possibility of combined advective and diffusive chloride transport mechanisms were examined within a 40 m deep succession of laterally extensive and homogeneous smectite dominated clay at the Yarramanbah site, located about 380 km north-west of Sydney. Early work in the area suggested that salinization was due to discharge of deep alluvial groundwater within a constricted outlet of the Yarramanbah catchment area of 360 $km^2$. However, ongoing investigations of shallow groundwater level dynamics and pore pressure propagation accounted for groundwater level variability without advection up through the sequence. The objective of this work was to verify a conceptual model for fluxes through the clay sequence based on independent hydrogeochemical evidence.

Clay samples were obtained at 1 m intervals to 30 m depth for physical and chemical analysis during installation of five nested piezometers to compliment existing monitoring bores. Groundwater levels were logged at hourly intervals in piezometers at 15, 28, 50, 80 and 102 m depth. Based on density corrected hydraulic heads, calculated vertical flux between deep and shallow groundwater over a 5 year period was close to zero. Vertical hydraulic conductivity of the clay sequence, derived from observed amplitude and phase changes of pore pressure propagation, resulted in an average value of $2.8 \times 10^{-9}$ m/s. Chloride concentrations between 3.2 and 27.1 meq/100g (n=30) for 1:5 extracts, indicating a very high salt storage per hectare within the upper 15 meters of the ground surface.

Major ion analysis of pore water samples obtained on 8 occasions over a 5 year period showed little variation over time. Groundwater salinity of Na-Cl type waters decreased in a linear manner with increasing depth (chloride 8,300 and 390 mg/L at 5.5 m and 55 m depth respectively). The variation in groundwater chemistry over time and with depth, provided an opportunity to identify fluxes due to advective mixing and diffusion of chloride due to the significant concentration gradient. The flux of chloride attributed to diffusion only through the clay sequence was in the order of ~1 $g/m^2$/year downwards, based on estimated porosity, tortuosity and diffusion coefficients. The possibility of both advective and diffusive chloride transport through the clay sequence was assessed by 1D PHREEQC transport models. Knowledge of flux and transport mechanisms through the clay sequence is critical to effective management of salinity. If proven incorrect, early conceptual models of regional groundwater discharge mean that investment in water balance management in the upper catchment may be misdirected.

# DARCY 64

# Reflections on the impact of the Messinian Salinity Crisis on the hydrogeology of the Rhodanian basin

de La VAISSIERE Rémi[1], LALBAT Frédéric[1] and BLAVOUX Bernard[1]

[1] Laboratoire d'Hydrogéologie Université d'Avignon, France,
remi.delavaissiere@univ-avignon.fr

## Abstract

The Messinian Salinity Crisis in the Mediterranean area is an exceptional event in the geological history. This crisis had a geomorphological impact on the entire Mediterranean basin because of the Messinian entrenchment and the filling of the Pliocene rias according to a Gilbert delta type organization. In the Rhone valley, the cretaceous limestone karstification is the most spectacular hydrogeologic phenomenon. But the consequences of this crisis must be also considered for all the aquifers which are in contact with Messinian karsts or Pliocene rias. This present paper aims at giving three examples in molassic foreland basins along the Rhone valley (the basins of Valence, Valréas and Carpentras). It shows that aquifer potentialities exist at the base of the Pliocene filling and it emphasize on groundwater leakage between karstic, molassic and Pliocene aquifers. This approach should be taken into account for each perimediterranean river basins.

## Introduction

The Messinian Salinity Crisis in the Mediterranean area is an exceptional event in the geological history. This crisis had a geomorphological impact on the entire Mediterranean basin because of the Messinian entrenchment and the filling of the Pliocene rias according to a Gilbert-delta type organization. In the Rhone River valley, the cretaceous limestone karstification is the most spectacular hydrogeologic phenomenon. Fontaine-de-Vaucluse spring near Avignon is the most famous example. But the consequences of this crisis must be also considered for all the aquifers which are in contact with Messinian karsts or Pliocene rias. This present paper aims at giving three examples in molassic foreland basins along the Rhone River valley (Valence, Valréas and Carpentras basins).

## Geological history

The studied area is located in the South-East of France in the Rhone River valley between the Alpine chain to the east and the European craton (Massif Central) to the West (fig. 1). This area comprises a succession of molassic foreland basins due to the orogenesis of the Alps during the Miocene (Carpentras, Valréas, Valence). These foreland basins are filled with multilayered sands, sandstones, clays and marls with a maximum thickness of 600 m. At the end of Miocene, before the Messinian salinity crisis, the Rhone River and its tributaries flowed into the Mediterranean Sea. During the Messinian crisis the rivers cut down the rock to reach the Rhone base level following the huge lowering of the Mediterranean Sea (Clauzon 1982; Gargani 2004).

The end of the crisis was defined by the immediate flooding of the Mediterranean Sea due to the opening of the Gibraltar straits (about -5.32 My BP) (Blanc 2002). The paleo-canyons were subsequently rapidly flooded by the Mediterranean Sea. The sea had progressed in the Rhone valley to the south of Lyon, at approximately 250 km inland from the current shoreline (fig. 1).

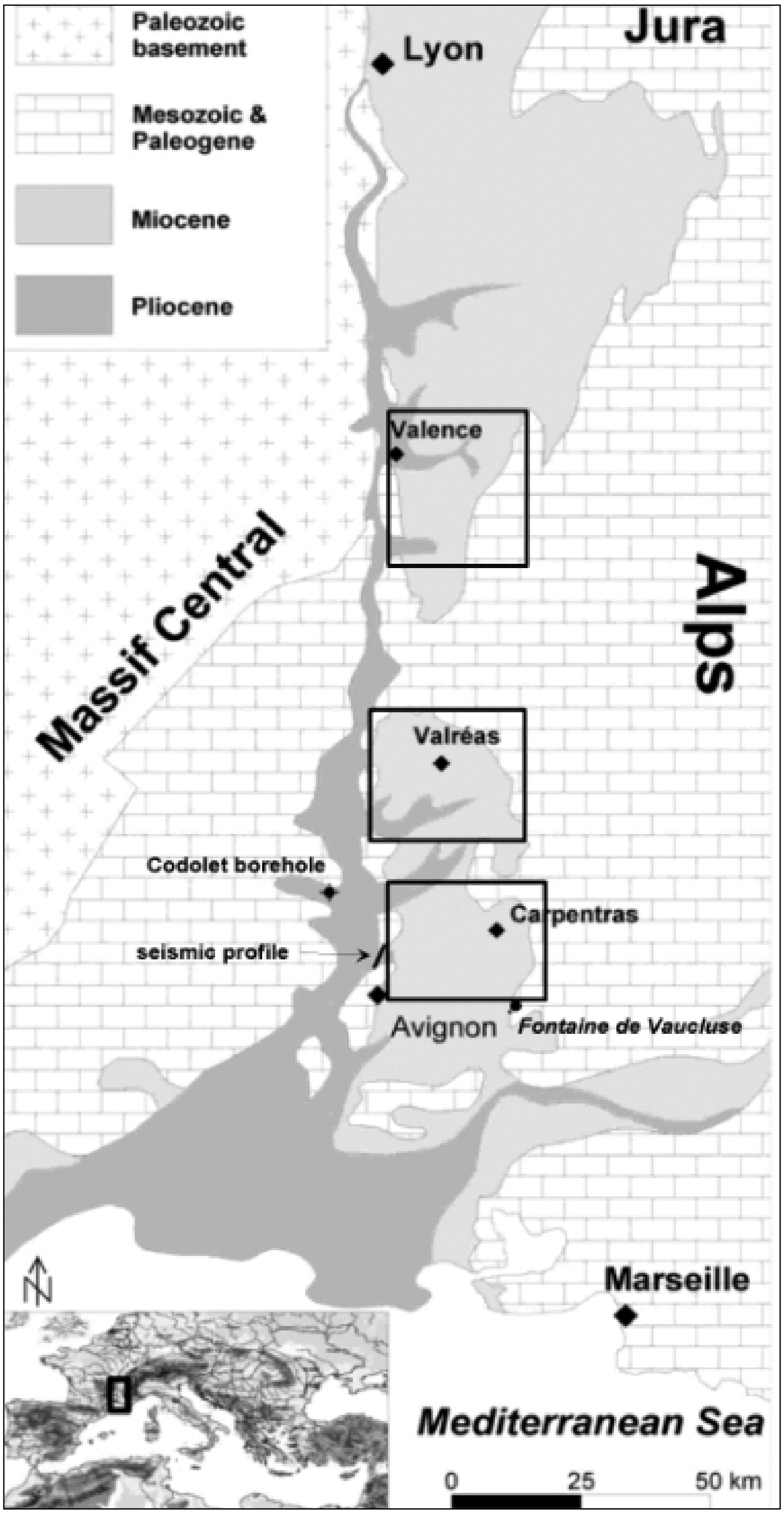

*Figure 1: The Pliocene Rhone ria. Localisation of the three molassic foreland basins, Codolet borehole and the seismic profile*

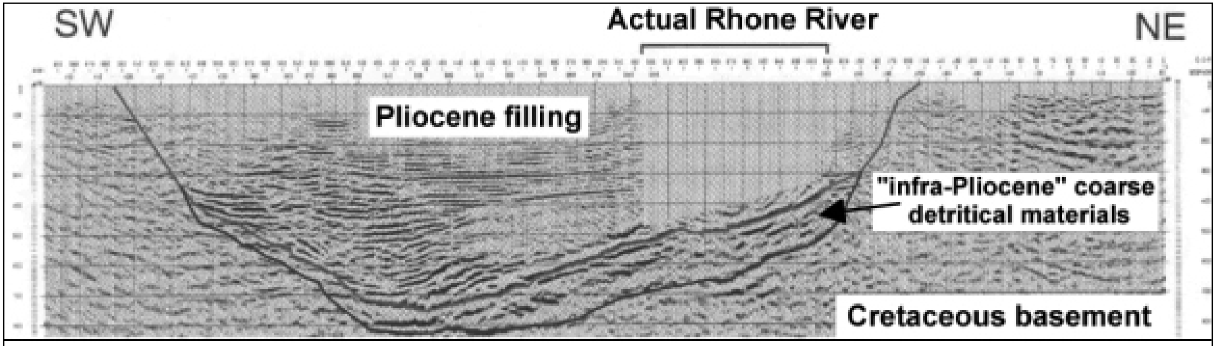

Figure 2 Seismic cross-section profile of the Pliocene Rhone ria (modified from Schlupp et al. 2001)

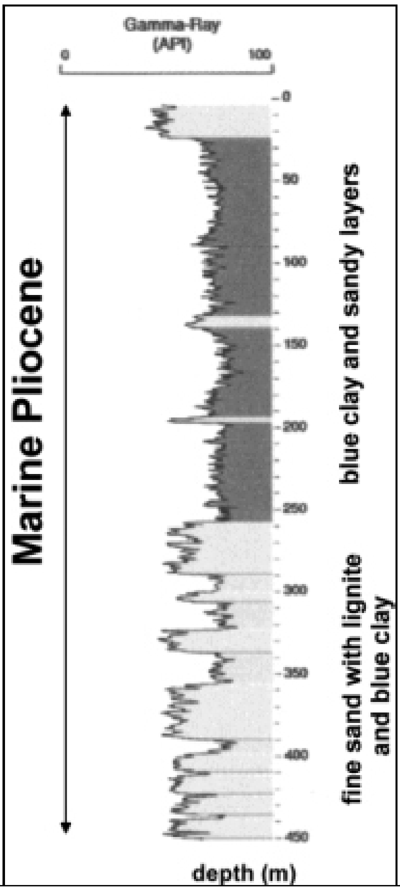

Figure 3: Diagraphy of the Codolet borehole (modified from Ferry et al. 1997).

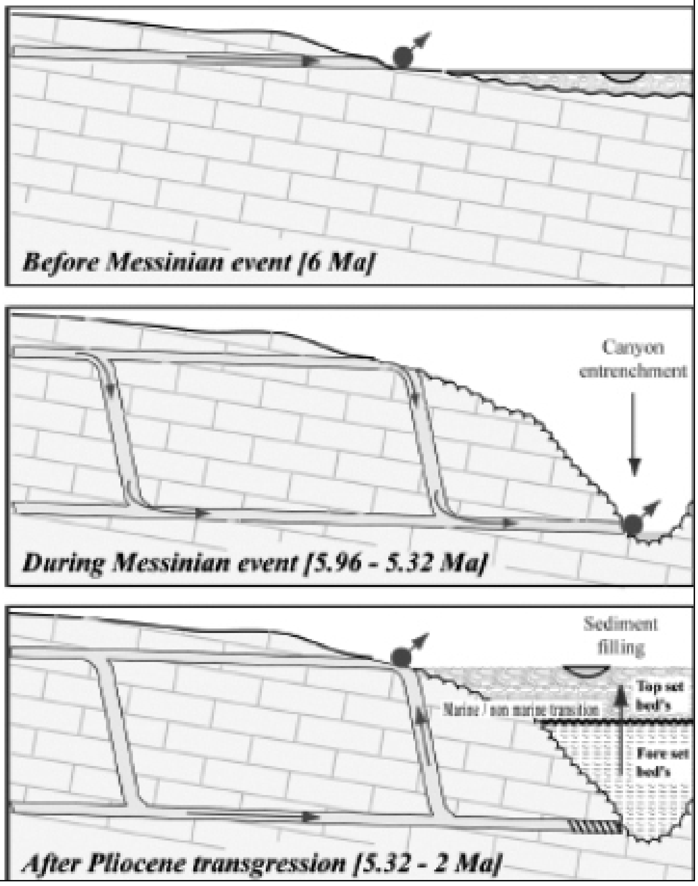

Figure 4: Diagrammatic model of karst drainage evolution corresponding to the Messino-Pliocene eustatic impulse (Audra et al. 2004).

## Morphogeological impact of the Crisis

Following the powerful dismantling, the canyons were initially filled with coarse detritical materials called «infra-Pliocene» by Ballesio (1972). In the region of Avignon, 70 km inland from the Mediterranean coast, high-resolution seismic reflection investigations have shown this layer (fig. 2).

When the canyons have been changed into ria, they have gradually been filled in with sediments according to a Gilbert-delta type sedimentary organization. The Codolet borehole is located in the Ceze ria near Avignon and gives an example of this sedimentation. Indeed it presents a first sandy and a second clayey horizon above the «infra-Pliocene» coarse horizon (fig. 3).

This drastic drop in base level affected the karst development of the Cretaceaous carbonate in the Rhone valley (fig. 4). The deep karst drainage was blocked by the filling of the ria, forcing the water to rise through vauclusian systems like Fontaine-de-Vaucluse spring.

## Hydrogeological setting

### Valence basin

The first basin is located in the middle of the Rhone River valley, 180 km inland from the Mediterranean coast. The area covers approximately 720 km$^2$ and the aquifer consists of sands, sandstones and marls with a maximum thickness of 500 m. It borders on the Alpine front in the east (Vercors plateau). The map in figure 5 shows that three paleo-tributaries joined the Messinian Rhone River. The Rhone canyon have been filled by marine Pliocene clays and sea sands over 300 m thick.

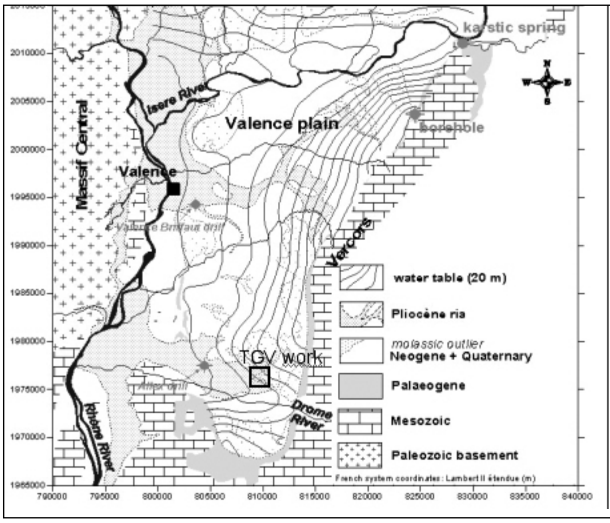

Figure 5: Situation of the Valence plain
(geomorphological and piezometric maps)

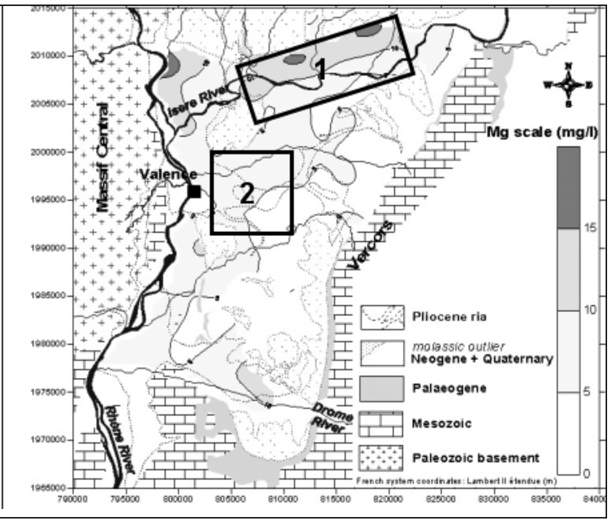

Figure 6: Distribution of the magnesium content
of the surface-water table

Figure 5 depicts the positions of the marine sedimentary prism and shows that three tributaries of the Rhone River flowed from the plain. Surprisingly, no marine sandy clay is in contact with the Vercors plateau. However, Urgonian limestones of Vercors plateau present a large karst development. In the eastern part of the plain a borehole cuts an active karst feature beneath 407 m of tertiary recovering at an altitude of +61 m asl. In addition, at the northern end of the Vercors plateau, a Vaucluse type karst spring (Thais cave) was explored along a flooded 715 m distance, reaching the depth -91 m compared with the spring level, i.e. + 79 m asl (Billaud, 2004). Karstification related to the entrenchment of a Messinian canyon by tributaries of the Rhone River is a plausible hypothesis for the karstic phenomena on the western side of the Vercors. If the Messinian hydrographic network really entrenched Vercors the western side of the Vercors, the base level of the hypothetical canyons can be estimated between -81 to -27 m asl (de La Vaissière et al. 2006). Those levels are compatible with the levels of karstification seen in the spring and borehole. While Thais cave presently functions as an output of the karst system, it should have functioned like Fontaine-de-Vaucluse, i.e. as an input or swallow point of the karst aquifer, while it presently functions as an output of the system (Audra et al., 2004).

The piezometric map of the molassic aquifer shows an overall flow from the East to the West of the plain and follows the relief (fig. 5). Two major discharges of the Miocene aquifer are located below the city of Valence and the Drome River valley in the vertical location of the Pliocene rias. The Briffaut (near Valence city) and Allex (in the valley of the Drome river) drills cross-cut the Pliocene horizon. They present high values of specific capacity (Q/s), respectively 2.6 and 5 $m^3$/h/m. In addition, the southeastern TGV railway work (high speed train) (see fig. 5) has put in evidence that a horizon of "infra-Pliocene" breccias lays between the Pliocene clays and the Miocene molasses. This layer, which is 100 times more permeable than the molasse itself (breccias $10^{-5}$ versus molasse $10^{-7}$ m/s), corresponds to the Messinian dismantling.

Radiocarbon dating was carried out in the molassic aquifer and showed an increase of the time residence from East side to the West related to an increase of the magnesium content. The groundwater age increase from modern to 4000 years along a flow path of 10 km. The magnesium can be used as an easy tool to estimate the residence time of groundwater. Downstream in the molassic aquifer, the magnesium content is in the range 20-30 mg/l under the Isere valley and in the east of Valence city (respectively rectangles 1 and 2 fig. 6). However, the magnesium content of the shallow groundwater table (fig. 6) shows a great difference between the rectangle 1 with an average content of 13 mg/l and the rectangle 2 with an average content of 6 mg/l.

This difference means that, in the Isere River valley, long residence time groundwater highly discharges from the underlying molassic aquifer. Comparatively, groundwater from the underlying molassic aquifer poorly discharges into the shallow aquifer in the Valence plain. A part of the discharge system of the molassic Valence aquifer is thus formed by the Pliocene and the «infra-Pliocene» permeable layers.

## Valréas basin

The second studied area is located in the south of the Rhone River valley, 100 km inland the coast. The area covers approximately 500 $km^2$ and the aquifer is constituted by multilayered sands, sandstones, clays and marls, with a maximum thickness of 600 m. A Pliocene ria is located in the southern part of the basin (the paleo-Aigues). It reaches a thickness of 250 m and it is infilled with marine Pliocene clays and sea sands

Groundwater flows from the northeast to the southeast of Valréas basin (Huneau 2000). The piezometric map shows that the main discharge area is located vertically on the ria of the paleo-Aigues axis (fig. 7). The molassic aquifer turns confined under the Pliocene clays. In each case the boreholes reach the Miocene under the Pliocene cover, they are artesian but the wells in the Pliocene sediments are never really productive. The Pliocene clayey-sandy deposits in Aigues ria have been assimilated to an hydraulic barrier.

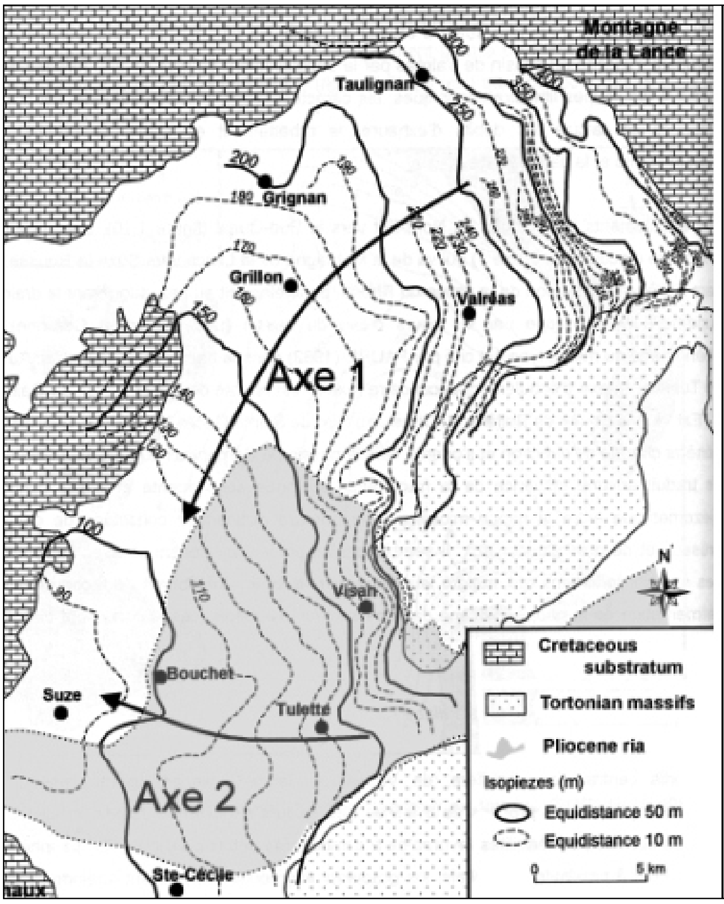

Figure 7: Situation of the Valreas basin: geomorphological and piezometric maps (from Huneau 2000)

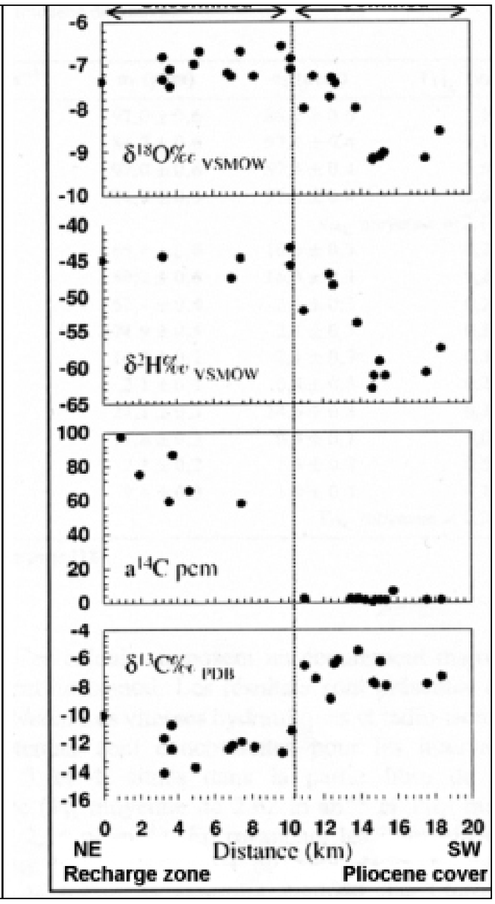

Figure 8: Isotopic variation along the flow line direction (axe 1) (from Huneau 2000)

An isotopic study of the molassic aquifer was carried out in 1997 (Huneau 2000). Radiocarbon dating along a twenty kilometres flow path reveals a strong increase of the time residence (from modern to more than 30000 years) in the confined part of the aquifer. Stable isotopes show a strong depletion and it may therefore be assumed that they have infiltrated during the Würm glacial stage (fig. 8). Abrupt changes in the isotopic composition of groundwater may reflect discontinuities and indicate a lack of flow from the unconfined to the confined aquifer. The confined part of the system may have only a restricted or a non-existent drainage through the Pliocene ria. So the main discharge way is the unconfined shallow aquifers in the alluvium.

## Carpentras basin

Carpentras basin is our third example. This basin is located 70 km inland from the coast. Its area and its Miocene filling are almost the same as in the Valréas basin. Both (Valréas and Carpentras basins) are very close by their location and their geology but they are not similar by their hydrogeology.

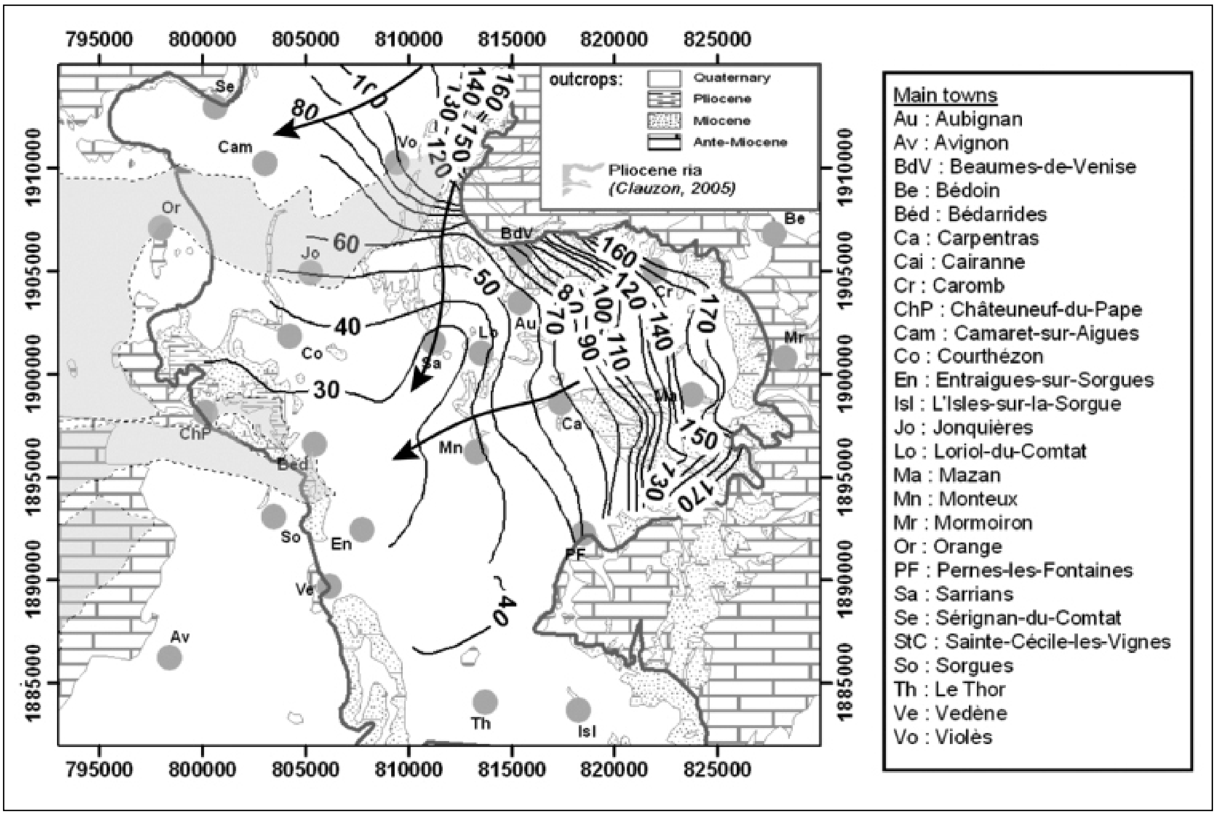

*Figure 9: Piezometric map of Carpentras basin. The plain curves indicate hydraulic heads in meters above sea level (Faure 1982). The bold grey line is the basin limit. Projection: French Lambert II coordinates system*

The Pliocene ria of paleo-Ouvèze crosses over the northern part of Carpentras basin (fig. 9). Pliocene deposits are very clayey in it. The sandy levels are thin and rare. So there are very few boreholes in the ria area and they have a very low transmissivity. Thus piezometry in the ria is not known very well but the piezometric map (fig. 9) seems to show a groundwater divide along the ria. The hydraulic gradients are low around Camaret and Jonquières because there is almost no flow through the ria.

In the north of the ria, groundwater flows westwards and goes out the molassic basin to the Late-Cretaceous sandy sediments near Orange and Serignan. In the south, the flow lines converge to a drainage axis in the middle of the basin. The direction of this axis (NNE-SSW) is the same as the one of the main faults which mark the Cretaceous substratum (Nîmes fault).

In Carpentras basin an Early-Cretaceous karstic aquifer is in contact with the molassic aquifer. It is the western extension of Fontaine-de-Vaucluse system. Very few boreholes reach the karst under the Miocene cover and a piezometric map cannot be drawn. Nevertheless water levels are known in the karst by places and they are always greater than the Miocene aquifer level. So groundwater could flows from the karst to the molassic aquifer. The flow rate is necessarily lower than 1 $m^3.s^{-1}$ because the hydraulic budget of Fontaine-de-Vaucluse system is balanced (Puig 1987; Couturaud 1993).

The karst under Carpentras basin is probably a karstic network reused during the Messinian crisis (Audra et al. 2004). Its outlet was at the level of the Messinian hydrographical network and it was sealed by the Pliocene clayey and sandy filling. Actually waters of the covered karst have chemical characteristics of high residence time waters compared with the active karst waters (Couturaud 1993). Their conductivity is around 700 µS.cm-1 (around 400 µS.cm-1 in the active karst of Fontaine-de-Vaucluse), Mg/Ca ratio is around 0.8 (around 0.1 in the active karst).

## Discussion

The Messinian Salinity Crisis has an impact on the Rhone River aquifer systems and leads to flows between karstic, Miocene and Pliocene reservoirs.

Marine Pliocene is especially known as a substratum of the non-marine Pliocene and Quaternary aquifers. This paper shows that the marine Pliocene filling can influence the molassic aquifers functioning. Up to now, the first assumption was to regard the marine Pliocene filling as a hydraulic barrier with the groundwater flows because of their primarily argillaceous filling. The recognized facies of the rias of paleo-Aigues and paleo-Ouvèzes of the basins of Valreas and Carpentras would confirm this idea. On contrary, the data of drillings in the rias of Valence basin and the Cèze ria show aquifer potentialities for freshwater supply and small irrigation on the Pliocene sandy levels. Moreover, the conglomeratic layer located at the base of the rias would also be used as a discharge for the connected aquifers. These results seem to bring a new assumption on the role of the Pliocene ria to groundwater discharge systems.

This new assumption leads us to reinterpret the hydrogeological data in the basin of Valréas. The small hydraulic gradients indicate a drainage of the Pliocene ria. Futhermore, on the assumption of a hydraulic barrier, groundwater of the Valréas basin should be as old as the Pliocene filling. Even if the noted ages are very significant for such a small basin, they imply a renewal of groundwater. This renewal is attributed to circulation necessarily existing through the conglomeratic layer at the base of the paleo-Aigues ria.

The role of the Messinian crisis on the karstic development in the South-East of France is the most spectacular phenomenon. Many examples exist where active circulations are under the low marine level reached during the Quaternary Period: Fontaine de Vaucluse (Puig 1987; Couturaud 1993; Gilli et al. 2004), the underwater spring of Port-Miou (Gilli et al. 2000; Blavoux et al. 2004) or the spring of Font Estramar (Aunay et al. 2003). Such developments must be then attributable to the significant lowering of the Mediterranean base level during the Messinian event.

At the time of the crisis, the karstic network of Fontaine de Vaucluse had a discharge system into the Rhone Messinian canyon. This network was recognized under the basin of Carpentras (Couturaud, 1993). Besides, the hydraulic gradients between the karst and the Miocene aquifer let consider such exchanges which would use the fracturing (Nîmes fault) or re-use of an ante-Miocene karstic network. In this way, another discharge system would be existing between the karstic system and the Pliocene ria.

The groundwater flow patterns in karstic systems and porous aquifers are much contrasted. Such exchanges between those systems are limited only by the permeability of the Miocene and Pliocene filling. The involved volumes might be weak in comparison with the groundwater balance in karstic systems.

## Conclusion

These new considerations presented in this paper might to be take into account to evaluate the aquifer potentialities of the Pliocene filling. The clayey filling above the sandy and coarse horizons is a very interesting barrier from the pollution of the surface. Then the bottom aquifer of the Pliocene ria could be used for freshwater resource and should be investigated by a rigorous approach.

This approach could be described in five stages. The first step is to situate the Pliocene ria by using the existing data (boreholes, electric loggings). The second step might to precise the Messinian canyon shape with high resolution seismic profiles. The result brings the localisation of the base of the Messinian canyon. Vertically to the maximum depth, an exploration borehole has to cross the Pliocene filling and reach the substratum (3rd steps). Concurrently, sedimentology and sequence stratigraphy studies can be done by using diagraphies. The fourth step has to evaluate the productivity of the filling by pumping test. If the productivity is good, then the last step is to analyse the groundwater quality.

Nowadays, there are strong constraints on groundwater (quantitative and qualitative) for the majority of the perimediterranean countries. In the future, these constraints will be more and more important with the increase in the water needs. These needs are related to the population growth and the global change (tendency to aridity in the Mediterranean area). New resources must be sought and exploited to meet these needs. Within this context, the aquifers of the Pliocene fillings of the Messinian canyons must be prospected. The Rhone and the Nil valleys are the sectors where the Messinian canyons are known. However, water resources remain to be evaluated. Moreover, all the other Messinian paleo-affluents of the Mediterranean Sea can also be prospected for new water supply.

## References

- Audra P, Mocochain L, Camus H, Gilli E, Clauzon G, Bigot J-Y (2004) The effect of the Messinian Deep Stage on karst development around the Mediterranean Sea. Examples from Southern France. Geodinamica Acta 17(6): 27-38
- Aunay B, Dörfliger N, Le Strat P, Ladouche B, Bakalowicz M (2003) Evolution géologique, mise en place de la karstification et thermalisme des aquifères karstiques péri-méditerranéens. Exemple du karst des Corbières d’Opoul. In: 10ème journée technique du Comité Français de l’AIH. Circulations hydrothermales en terrains calcaires, Carcassone: 15-22
- Ballesio R., (1972). Étude stratigraphique du Pliocène rhodanien. PhD, University of Lyon I, France [in French]
- Billaud Y (2004) Rapport d’exploration de la grotte de Thaïs. Spelunca, 96: 5-7
- Blanc P-L (2002) The opening of the Plio-Quaternary Gibraltar Strait: assessing the size of a cataclysm. Geodinamica Acta 15: 303-317
- Blavoux B, Gilli E, Rousset C (2004) Alimentation et origine de la salinité de la source sous-marine de Port-Miou (Marseille-Cassis). Principale émergence d’un réseau karstique hérité du Messinien. C.R. Geoscience 336: 523-533
- Bobillon G (2005) Passage de la cotière d’Eurre par la ligne TGV. In: Journées Association des Hydrogéologues du Service Public, Valence
- Clauzon G (1982) Le canyon messinien du Rhône: une preuve décisive du «desicated deep-basin model» [Hsü, Cita et Ryan, 1973]. Bull. Soc. géol. France 24(7): 597-610
- Clauzon G, Fleury J, Schlupp A, Mocochain L (2005) Réunion de l’Association des Hydrogéologues du Service Public (AHSP) à Valence, Évolution géodynamique du Bas-Rhône (section Orange-Baucaire) depuis 6 Ma. inédit, Valence (France)

- Couturaud A (1993). Hydrogéologie de la partie occidentale du système karstique de Vaucluse. PhD, University of Avignon, France [in French]
- de la Vaissière R, Faure G, Clauzon G, Blavoux B (2006) Impact of the Messinian Salinity crisis on the hydrogeology of the Valence plain (South-East France). In: Duran, Andreo, Carrasco (Eds) Karst, climate change and groundwater. Hidrogeologia y Aguas Subterraneas 18: 385-393, Spain, Madrid
- Faure G (1982). Étude hydrogéologique du bassin Miocène de Carpentras - Relation entre l'aquifère molassique et le substratum - exploitabilité. PhD, University of Lyon I, France [in French]
- Ferry S, Ballesio R, Monier Ph (1997) Modalités du remplissage sédimentaire de la ria pliocène du Rhône. Problèmes en suspens après les premiers travaux de l'ANDRA. In: Journées scientifiques ANDRA, Bagnoles sur Cèzes
- Gargani J (2004) Modelling of the erosion in the Rhone valley during the Messinian crisis (France). Quaternary International 121: 13-22
- Huneau F (2000) Fonctionnement hydrogéologique et archives paléoclimatiques d'un aquifère profond méditerranéen. Etude géochimique et isotopique du bassin miocène de Valréas (Sud-Est de la France). PhD, University of Avignon, France [in French]
- Huneau F (2000) Isotopic hydrogeology within the Miocene basin of Carpentras-Valréas (southeastern France). In: Dassargues A (ed) Proc. of TraM'2000 Tracers and Modelling in Hydrogeology, Liège, Belgium, 433-438
- Puig J.M (1987). Le système karstique de la Fontaine de Vaucluse. PhD, University of Avignon, France [in French]
- Schlupp A, Clauzon G, Avouac J-P (2001) Mouvement post-messinien sur la faille de Nîmes: implications pour la sismotectonique de la Provence. Bull. Soc. géol. France 172(6): 697-711

# DARCY 77

# Environmental tracer methods ($^3$H, $^3$He, $^{85}$Kr, $^{39}$Ar, $^{14}$C and $^4$He) to resolve the age structure of groundwater: Example of two study cases

J.A. Corcho Alvarado[1,2], F. Barbecot[1], R. Purtschert[2], T. Paces[3], W. Aeschbach-Hertig[4], R.Kipfer[5]
1 IDES Laboratory, UMR 8148 IDES, Bâtiment 504, Université Paris-Sud, 91405 Orsay Cedex, France. corcho@geol.u-psud.fr
2 Climate and Environmental Physics Division, Phys. Institute, Univ. Bern, Sidlerstrasse 5, CH-3012 Bern, Switzerland

Environmental tracer methods (e.g. $^3$H, $^3$He, $^{85}$Kr, $^{39}$Ar, $^{14}$C and $^4$He) were used to resolve the age structure of groundwater in two aquifers of which very scarce or vague information was available before this work. The investigated systems are: a) the semiconfined Fontainebleau sands aquifer located in the shallower part of the Paris Basin (France); and b) the deep and confined Cenomanian sands aquifer of the Bohemian Cretaceous Basin (Czech Republic). The combination of several environmental tracers enabled other processes or parameters of the aquifer systems than the groundwater mean residence time (e.g. mixing processes, dispersion within the aquifer, etc.) to be investigated, and also refining the interpretation of groundwater age. The limited number of sampling sites in the aquifers suggested the use of lumped parameter approaches for the assessment of groundwater dynamics (Zuber and Maloszewski, 2001).

In the Fontainebleau sands aquifer, the commonly used young groundwater tracers ($^3$H, $^3$He and $^{85}$Kr) could not resolve the whole age structure of groundwater, as large fractions of the sampled groundwater has ages older than 50 years (Corcho Alvarado, 2005; Corcho Alvarado et al., in preparation). The radioisotope $^{39}$Ar (half-life: 269 years) was used to further constrain the groundwater age distribution. Mean residence times for the abstracted groundwater ranging between 120 and 450 years were estimated. $^{14}$C measurements confirmed that leakage of very old groundwater from underlying aquifers is not occurring in the area.

In the Cenomanian sands aquifer, groundwaters with ages ranging from a few hundreds of years to more than 20 000 years were dated (Corcho Alvarado et al., 2004; Corcho Alvarado, 2005). The calculated tracer ages showed a good linear correlation with the distance from recharge, suggesting that piston flow is a good approximation for the flow type in the aquifer. A vertical flux of helium from deeper layers (crust and mantle) into the aquifer was detected, with a value approximately one order of magnitude lower than that predicted for the degassing of the whole continental crust. Using typical crustal and mantle helium ratios, different sources of helium were distinguished and quantified. It was concluded that the main external source of helium are crustal rocks, although a large contribution of mantle helium was found in one well. The noble gas temperatures and the stable isotope signature showed that groundwater recharged under different climatic conditions.

## References

- Corcho Alvarado J.A., Purtschert R., Barbecot F., Chabault C., Rueedi J., Schneider V., Aeschbach-Hertig W., Kipfer R., Loosli H.H. Constraining the age distribution of highly mixed groundwater using $^{39}$Ar: a multiple environmental tracer ($^3$H/$^3$He, $^{85}$Kr, $^{39}$Ar and $^{14}$C) study in the semi-confined Fontainebleau Sands aquifer (France). *In preparation*
- Corcho Alvarado J.A., Purtschert R. and Pa_es T. (2004). Establishing timescales of groundwater residence times based on environmental tracer data: a study of the Turonian and Cenomanian aquifers of the Bohemian Cretaceous Basin, Czech Republic. In: *32nd International Geological Congress,* Florence, Italy.
- Corcho Alvarado J.A. (2005). Multiple environmental tracer approaches to resolve the age structure of groundwater in European aquifers. Ph.D. Thesis, University of Bern, Switzerland.
- Zuber A. and Maloszewski P. (2001). Lumped-parameter models. *In Environmental isotopes in the hydrological cycle*, V.6. Modelling. UNESCO/IAEA, Tech. Doc. Hydrol. 39, 5–35.

# DARCY 87

# Isotopic study (B, Li, Fe, U, Th) of two confined aquifers in the eastern part of the Paris basin: implication for hydrological and WRI processes

Casanova J.(1), Girard J.-P.(1), Guerrot C.(1), Innocent C.(1), Millot R.(1), Motelica M.(1), Buschaert S.(2)
(1) BRGM, 3 avenue Claude Guillemin BP 6009, 45060 Orléans cedex 2 – France
j.casanova@brgm.fr; jp.girard@brgm.fr ; c.guerrot@brgm.fr ;
c.innocent@brgm.fr; r.millot@brgm.fr; m.motelica@brgm.fr
(2) ANDRA, 1/7, rue Jean Monnet, Parc de la Croix-Blanche, 92298 Châtenay-Malabry cedex – France
stephane.buschaert@andra.fr

In the scientific programme on high-level radioactive waste. conducted by Andra, particular emphasis is placed on the characterisation of Callovo-Oxfordian argillites occurring at about 500 m depth in the eastern part of the Paris basin at Bure. In situ specific scientific experiments and measurements are to be conducted in the coming years to confirm confinement properties. Formation waters from the Oxfordian and Dogger limestone aquifers, bracketing the Callovo-Oxfordian argillites, have been analyzed for their chemical (B, Li, Fe, U, Th) and isotopic ($\delta^{11}$B, $\delta^{7}$Li, $\delta^{56}$Fe, U-series) composition. The samples studied represent groundwater collected from 9 different wells over an area of about 20x30 km around the Bure site. The results show that Oxfordian and Dogger aquifer waters have distinct chemical and isotopic compositions as follows:

**Oxfordian water :**
Conductivity (25°C) = 426-2240 µS/cm
[Li] = 20-200 ppb ; $\delta^{7}$Li = 14-19 ‰
[B] = 35-800 ppb ; $\delta^{11}$B = 1-12 ‰
[Fe] = 36-1145 ppb ; $\delta\ ^{56}$Fe = -2.3 - 0 ‰
[U] = 49-984 ppt ; $^{234}$U/$^{238}$U = 0.54-1.18
[Th] = 0.22-3.69 ppt ; $^{230}$Th/$^{234}$U = 0.001-14.02

**Dogger water :**
Conductivity (25°C) = 4580-13200 µS/cm
[Li] = 400-900 ppb ; $\delta^{7}$Li = 16-18 ‰
[B] = 850-2300 ppb ; $\delta^{11}$B = 19-28 ‰
[Fe] = 14-498 ppb ; $^{56}$Fe = -4 - +1.2 ‰
[U] = 1-738 ppt ; $^{234}$U/$^{238}$U = 0.77-1.55,
[Th] = 0.15-111 ppt ; $^{230}$Th/$^{234}$U = 0.001-3.94

This significant difference in composition indicates, in agreement with prior bulk chemical and stable isotope data (Andra, 2005), that Oxfordian and Dogger formation waters are not in hydrological continuity, and confirms that Callovo-Oxfordian argillites do constitute a barrier to advective flow. Water of Oxfordian and Dogger aquifers show B and Li isotopic compositions significantly depleted relative to sea water, likely generated through water-rock interaction processes. The chemical and isotopic compositions of these two aquifers cannot be explained by a simple mixture of meteoric water and sea water, and is indicative of a possible contribution of secondary brines, more particularly expressed in the Dogger. Iron data (contents and isotopic ratios) are extremely variable and show no correlation to depth, borehole location or hydrogeologic nature of the aquifer. According to U-series, the dominating WRI process corresponds to isotopically congruent dissolution of the grain-surface coating. It leads to a marked $^{234}$U deficit in groundwater. This U isotopic signature is observed for most water inflow in the Oxfordian and some in the Dogger. The evolution of groundwater with depth is linked to a decrease of U content related to precipitation, followed - in stationary regime - by a decrease of the $^{238}$U excess until reaching secular equilibrium. Moreover, a significant proportion of groundwaters are characterized by a deficit in $^{230}$Th indicating that isotopic balance $^{230}$Th - $^{234}$U, obtained in stationary regime after about 300 ky, is not reached. This is an indication that interactions with limestones, involving $^{234}$U fluxes (leaching, dissolution, precipitation), have occurred during the transfer of groundwaters, according to the observations of Deschamps et al. (2004).

## References

- Andra, 2005 - Dossier 2005 argile - Référentiel du site de Meuse/Haute-Marne. Rapport Andra n° C RP ADS 04-0022.
- Deschamps P., Hillaire-Marcel C., Michelot, J.L., Doucelance, R., Ghaleb, B. et Buschaert S. (2004) $^{234}$U/$^{238}$U Disequilibrium along stylolitic discontinuities in deep Mesozoic limestone formations of the Eastern Paris basin: evidence for discrete uranium mobility over the last 1-2 million years. Hydrology and Earth System Sciences, 8(1): 35-46.

# DARCY 101

## Estimation of permeability from groundwater dating by chlorine-36: the case of the "Continental Intercalaire" aquifer (Northern Sahara)

Jean-Luc Michelot* and Abdelhamid Guendouz**
* UMR CNRS-UPS ‘‘IDES’’, Bat. 504, Université Paris-Sud, 91405 Orsay, France
michelot@geol.u-psud.fr
** University of Blida, Science Engineering Faculty, BP. 270, Soummaâ-Blida, Algeria
ah_guendouz@yahoo.fr

In the northern part of Sahara desert, is located a very large aquifer system, the deep "Continental Intercalaire" (C.I.), extending over an area of approximately 600,000 km$^2$. This resource, vital in an arid region, is considered as being "fossil", i.e. mainly inherited from previous climatic conditions, more humid than at present. However, it is important to estimate, even approximately, the "age" of such fossil groundwater: it may provide an independent check on flow velocities that are calculated using Darcy's law, or on the validity at regional scale of punctual measurements of hydraulic conductivity (pumping tests). The radiocarbon method cannot be used for dating of C.I. groundwater, $^{14}$C contents being too low, but chlorine-36, with its long half-life (301,000 a), is a good candidate to obtain information about residence time of C.I. groundwater.

In the northern part of the basin, where the depth of the aquifer ranges between 400 and 1800 m, the main flow direction is from west to east. Chlorine-36 analyses were performed on groundwater samples mainly collected along this flowpath (Figure 1), showing a wide range of $^{36}$Cl contents.

For most of the samples, a significant decay effect was observed (Figure 2). An attempt of dating was made by using an equation that takes into account radioactive decay of the meteoric-epigene input, deep production and chloride dissolution within the aquifer.

The calculated $^{36}$Cl residence time varies from 16 to 500 ka for the minimum ages, and from 25 to 1200 ka for the maximum ages. An increase of residence time is observed up to about 500 km from the recharge zone, corresponding to mean flow velocities of 0.2-0.5 m.a$^{-1}$ and to an average permeability of $1.1 \pm 0.6 \cdot 10^{-5}$ m s$^{-1}$. On the other hand, pumping tests give values of $5 \pm 2\ 10^{-5}$ m.s$^{-1}$.

These two estimates are in the same order of magnitude. The difference between them could be explained by two reasons. First, all the pumping tests were performed in the same area, over some tenths of kilometres, in the exploited central part of the basin, whilst the value estimated from $^{36}$Cl decay corresponds to an average value at the scale of several hundreds of kilometres. Thus, the difference could partly reflect the lithological heterogeneity of the C.I. aquifer at the scale of the whole basin. Secondly, the computation of permeability from $^{36}$Cl data is based on a deliberately over-simple model, with a continuous recharge over several hundreds of thousands years, which is obviously not entirely true.

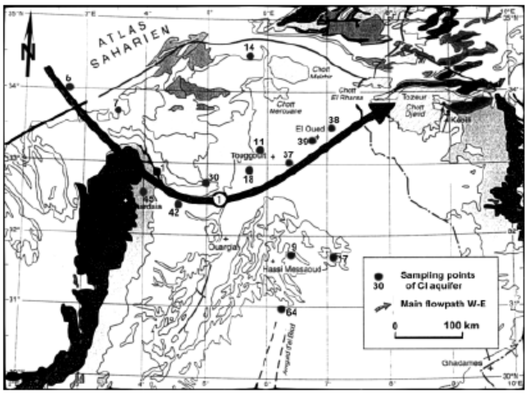

*Figure 1: Map of the sampling sites for $^{36}$Cl analyses of groundwaters from the C.I. aquifer.*

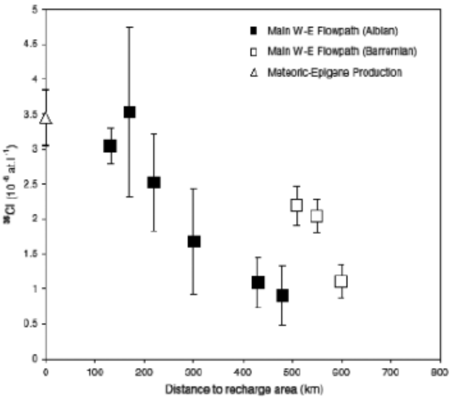

*Figure 2: $^{36}$Cl concentrations of groundwaters from the C.I. aquifer versus distance to the recharge area (Saharan Atlas).*

the case of the "Continental Intercalaire" aquifer (Northern Sahara)

# Posters

# DARCY 02

## Recharging conditions and ages of the groundwater of the Bekaa's valley (Lebanon), hydrogeologic, hydrochemical and isotopic studies.

AWAD S.
Université de Paris-Sud, Laboratoire IDES, Bât : 504, 91405 Orsay Cedex, France
sadekawad@yahoo.fr

### Abstract :

The plain of Bekaa is located in the East part of Lebanon, between 35°37 ', 36°37 ' E and 33°32 ', 34°32 ' N. It is dominated by a semi-arid continental climate in the North and a wetter and a less hot one in the center and the South (the temperature varies between -5 and + 30°C, the pluviometric average is about 600 mm/an, and the evapotranspiration about 50 %). The plain has a morphology with a form of a graben. This plain which is parallel to the lebanese coast, is limited on the two sides East and West by two high mountains directed NE-SW (Anti-Lebanon and Mount-Lebanon respectively), is caused by the existence of several faults.

### Text :

The two mountains are dominated by cenomanian outcrops in the North and Jurassic ones in the South; in the Bekaa's plain these formations are overcome by more recent layers which appear with the form of Eocen in the South and of Neogen in the center and the North. The 4 existent aquifers are: Jurassic, Cenomanian (the two ones are confined, with a deep advanced karst), Eocen (not deep karst) and Neogen (shallow aquifer not karstified). An interconnection between the aquifers exists by ascending drainage and downward one near the faults. The geochemical facies of the aquifers is calco-magnesian, bicarbonated; the water is saturated and can also be supersaturated on calcite and on dolomite. The mineralization which is carried out in an open system is due to the intervention of biogenic $CO_2$ for the recent water, and to the dissolution of the carbonated matrix for the relatively old water. The study of the isotopic contents of $\delta^{18}O$ and $\delta^{2}H$ (% vs VSMOW) confirm the absence of recharging water evaporation during their fast infiltration; the altitude of the aquifers' recharge is from low (Eocen and Neogen) to high altitude (Cenomanian and Jurassic). The dissolution of the sulphates (Gypsum of Cenomanian) is at the origin of the dissolved $SO_4^{2-}$ in the water, these dissolved sulphates will undergo later a reduction process in this aquifer; the existing marcasite's oxidation of in the superior Jurassic is also at the origin of the dissolved sulphates. The Water age goes from 50 years (water of the shallow aquifers (Eocen and Neogen) and those of the springs) to 15000 years (water of the deep aquifers (Jurassic and Cenomanian)). An overexploitation of the groundwater is at the origin of a real danger for the groundwater supply in this area.

### References :

- AOUAD Angele, TRAVI Yves, BLAVOUX Bernard, JOB Jean-Olivier, NAJEM Wajdi; Etude isotopique de la pluie et de la neige sur le Mont Liban : premiers résultats ; Hydrological Sciences-Journal-des Sciences Hydrologiques, 49 (3) 429-441, juin 2004.
- AYALON Avner, BAR-MATTHEWS Miryam, SASS Eytan; Rainfall-recharge relationships within a karstic terrain in the Eastern Mediterranean semi-arid region, Israel: $\delta^{18}O$ and $\delta D$ characteristics; Journal of Hydrology 207 (1998) 18-31.
- ELIYAHU Wakshal & HEIMO Nielsen, Variations of $\delta^{34}S$ ($SO_4$), $\delta^{18}O$ ($H_2O$) and $Cl/SO_4$ ratio in rainwater over northern Israel, from the Mediterranean Coast to Jordan Rift Valley and Golan Heights; Earth and Planetary Science Letters, 61 (1982) 272-282.

- HAKIM Bahzad ; Recherches hydrologiques et hydrochimiques sur quelques karsts méditerranéens Liban, Syrie et Maroc ; Publications de l'Université Libanaise, section des études géographiques II, Beyrouth 1985.
- KHAWLIE Mohamad, DARWISH Talal, MASRI Talih, FAOUR Ghaleb, AWAD Mohamad, HADDAD Theodora, SHA'ABAN Amin ; Integrated environmental management of fragile natural resources on karstic terrain-Coastal Mediterranean, Lebanon ; KARST 2000.

# DARCY 04

# Tectonics and groundwater in French Southern Alps

De Bretizel P.
Malitourne - F41270 - Villebout - amisourc@wanadoo.fr

This is the first display of results on a 10 year research and mapping program performed by the geologists group « les Amis des Sources »in the southern French Alps. (book publishing in progress)

The aim was to bring exhaustive datas about groundwater control by tectonics in this mountainous region. Geomorphological analysis and interpretation by means of digital satellit and air photo processing was the basic tool for geological mapping and field work. It was completed by an inventory of spring occurrences, considered as groundwater showings.

The main new feature highlighted during this campaign is a dense fracturing and faulting network within an area considered until now as mostly folded, according to local geological maps.

Over a 1000 km$^2$ surface, 560 new tectonic structures are outlined , controlling 22 deep aquiferous systems including 8 karstic ones. 228 springs occurrences are described and mapped.

Structurally, the Alpes de Nice are the south western termination of the Alpine Range Outer Zone. They are bounded by two parallel major lineaments : the Vesubie (northwest) and the Roya (southeast) framing a highly dislocated block in which the most frequent deformations are strike slip faults, pull apart diapiric structures, gravity faults, collapses and locally thrust faults.

Mapping such a dense faulting network was necessary to follow up groundwaters flowings and springs occurences distribution.

In the prealpine zone ( Arc de Nice ), the most important groundwater resource is in the Paillon basin : the aquifer is the upper Jurassic limestones, partly karstified and dolomitized. It is partly sealed from surface by the Cenomanian black shales. The groundwater flow, running southward, is controlled by two major faults : the Férion fault collecting surface waters from the eastern slopes of Mt Férion Range and the Sainte Thècle fault collecting surface waters from the northwest foothills of Mt Agel Range. An important outlet of this karst system is offshore, close to the coast line, at Pissarelles springs (east of Nice) : his flow rate reaches 100 l/s. Another important outlet occur inshore : The Sainte Thècle springs with a 120 l/s flow rate.

Two other jurassic karst systems occur along the coast with offshore outlets : The Larvotto springs (Monaco) controlled by the jurassic collapses of Mt Agel southern slopes (flow rate : 49 l/s) and the Cabbé springs controlled by the La Rocca thrust fault on eastern foothills of Mt Agel (flow rate : 200 l/s).

Karst systems occur as well inside the Jurassic-Trias carbonate beds surrounding the Mercantour paleozoïc nucleus at the northern part of the Alpes de Nice. Here, the sedimentary formations are strongly dislocated by slabbing from the basement, thus inducing karstic dissolutions. The main outlets emerging out of these karsts are the Fournes spring ( flow rate : 30 l/s) in the Vésubie valley and, in the upper Roya valley, the SteCatherine borehole (flow rate : 24 l/s), the Tornou springs (flow rate : 10 l/s), the Viévola spring (flow rate : 50 l/s). East of the Col de Tende, groundwaters of the Marguareis Karst highlands spring out northward and eastward in the italian valleys of the Pesio and the Tanaro.

Along the Mercantour main ridge, numerous outlets spring out from cristalline rocks, paleozoïc conglomerates and siltstones where groundwaters flowing is controlled by distensive fracturing. Most of them are cold waters such as the Lac Vert de Fontanalbe group (flow rate : 15 l/s), the Causega spring (flow rate : 30 l/s), the Pilon spring (flow rate : 70 l/s), the Gaisses spring (30 l/s).

In the Berthemont valley, near Roquebillère, occur the only hot springs known in the Alpes de Nice. Here, where two deep faults cross, water temperature reaches 27° with a 47l/s flow rate in boreholes.

## References :

Collectif CFH . 2006 – Aquifères et eaux souterraines en France.

# DARCY 07

# Geochemical signatures in groundwater in crystalline rock (Massif Central, France)

Jean BARBIER
12 rue Guy de Maupassant, 45100 Orléans, France
jean.barbier@noos.fr

The shallow groundwater in crystalline formations in France (30 % of the surface area) carries several geochemical signatures. Those of non-geological origin are seen for the most part on anions (atmospheric chloride, chloride and nitrate of organic origin). Those of geological origin concern for the most part cations (alkali and alcaline earths). Neutral species are distributed between these two categories—exogenous biological ($CO_2$) or endogenous geological ($SiO_2$) influences.

This distinction, made based on the difference in the electrical charge of solutes, is a result of water-solid phase interaction phenomena. The elements, whether exogenous or endogenous, are almost immediately subject to ion exchange (cations forming outer-sphere complexes), specific sorption (inner-sphere complexes), or reprecipitation (incongruent silicate dissolution).

- Ion exchange controls the relationships between Na, Mg, Ca, Sr, etc. It imposes approximately linear concentration ratios on divalent elements. Between divalent and monovalent elements like Na, the relationship follows that predicted by the Gaines-Thomas ion exchange model.
- Specific sorption (on 2:1 phyllite, for example) results from relatively low concentrations of cations with a strong ionic radius (K, Rb, Ba, etc.). Likewise, specific sorption on ferric hydroxide explains weakly sorbing anion concentrations (phosphates, arsenates, etc.) in groundwater.
- pH, which is related to the degree of confinement of groundwater, controls incongruent silicate dissolution and therefore $SiO_2$ concentrations. Three main families are observed: liberation of silica alone, of equal concentrations of silica and cations ($pH < 6.4$), or of less silica than cations ($pH > 6.4$).
- The geochemical signature of the host rock is only a secondary or even less important aspect because it is, for the most part, obscured by the phenomena listed above.

The consequences of these observations are:

- Exogenous geochemical signatures are easier to identify on elements forming weakly sorbing ions (N, C, Cl) or neutral complexes (B). They are harder to sort out for exchangeable or sorbing ions (Sr, K, P). This is true for both concentrations and isotopic ratios.
- The naturally occurring concentrations of dissolved elements ("geochemical background" or "natural chemical state") can be predicted for a given place provided that we set a criterion with reference to the intensity of the incongruent dissolutions.

Some of these characteristics of groundwater in crystalline formations are also found in groundwater in sedimentary formations. They are probably valid for all countries with similar climates having a marine influence—Spain, Portugal, possibly Ireland and Great Britain—and therefore might well be applicable to a large part of Europe.

## Les signatures géochimiques dans les eaux de sources de terrains cristallins (Massif Central, France)

En France les eaux souterraines peu profondes des terrains cristallins (30 % de la superficie) portent la trace de plusieurs signatures géochimiques. Les signatures d'origine non géologique (exogènes) s'observent essentiellement sur les anions (chlorures atmosphériques, chlorures et nitrates d'origine organique) ; celles qui sont d'origine géologique (endogènes) concernent surtout les cations (alcalins et alcalino-terreux). Les espèces neutres se répartissent entre les deux catégories, influences biologiques exogènes ($CO_2$), ou géologiques ($SiO_2$).

Une telle distinction, fondée sur la charge électrique des solutés, résulte des phénomènes d'interaction entre eaux et phases solides. Les éléments, qu'ils soient d'origine exogène ou endogène, font presqu'immédiatement l'objet d'échanges d'ions (cations formant des complexes de sphère externe), de sorption spécifique (complexes de sphère interne), ou de reprécipitations (dissolution incongruente des silicates) :

- Les échanges d'ions contrôlent les relations entre Na, Mg, Ca, Sr… ; ils imposent aux éléments divalents des rapports de concentration qui sont linéaires en première approximation. Entre éléments divalents et éléments monovalents comme Na, la relation est semblable à celle prévue par le modèle d'échange d'ions de Gaines-Thomas,
- Une sorption spécifique (par exemple sur les phyllites 2/1) rend compte des concentrations relativement faibles en cations à fort rayon ionique (K, Rb, Ba…). Le même phénomène de sorption, sur les hydroxydes ferriques cette fois, explique par ailleurs la faiblesse des concentrations en anions sorbants (phosphates, arséniates…) dans les eaux souterraines,
- Le pH, lié au caractère plus ou moins confiné des eaux, contrôle les dissolutions incongruentes des silicates, et donc les concentrations en $SiO_2$. Trois familles principales sont mises en évidence : libération de silice seule, de silice à égalité avec les cations ($pH < 6,4$ environ), et enfin de silice en quantité inférieure aux cations ($pH > 6,4$),
- La signature géochimique propre des roches-hôtes elles-mêmes s'avère être de second ou troisième ordre en importance, car en grande partie occultée par les trois phénomènes énumérés ci-dessus.

Les conséquences de ces observations sont de plusieurs ordres :

- Les signatures géochimiques exogènes sont plus faciles à identifier sur les éléments formant des ions peu sorbants (N, C, Cl) ou des complexes neutres (B) ; elles sont plus difficilement déchiffrables pour les ions échangeables ou sorbants (Sr, K, P). Ceci vaut pour les concentrations, comme pour les ratios isotopiques,
- Les concentrations naturelles en éléments dissous (« fond géochimique », « état chimique naturel ») peuvent être prédites en un endroit donné, pourvu que l'on se fixe un critère relatif à l'intensité des dissolutions incongruentes.

Ces caractères, propres aux eaux des terrains cristalins, se retrouvent en partie dans les eaux de terrains sédimentaires. Ils concernent par ailleurs selon toute probabilité, tous les pays de climat analogue à influence océanique, Espagne, Portugal, peut-être Irlande et Grande-Bretagne, et sont donc susceptibles d'avoir une portée assez générale en Europe.

## Introduction

The EU Water Framework Directive (Directive 2000/60/EC) implicitly raises the issue of how to determine the natural or background values of elements in both ground- and surface waters. Toxic or undesirable elements are, of course, of primary concern, even if they are only present as traces. The directive refers to the rather subjective notion of "good status". By comparison, the notion of "natural" chemical state is certainly much more precise and can be scientifically measured. Several European programmes have consequently been devoted to this. The natural state can be determined by geochemical signatures identifiable in groundwater bodies. Signatures related to anthropogenic contamination should obviously be disregarded and the natural state determined solely as a function of the signatures not associated with human activities. This paper discusses the case of French bedrock aquifers. Indeed, with a total surface area of 550,000 $km^2$, France is one of the largest countries in the European Union, and has about 170,000 $km^2$ of crystalline bedrock groundwater aquifers. The zone studied is located in the Massif Central, the region, with Brittany, having in France the largest surface area of Hercynian outcrops. The presence of a large number of wells facilitates statistical studies and we know that the chemical composition of the groundwater is highly varied.
This article is the third in a series on the natural chemical state of groundwater and integrates the conclusions of the previous two (Barbier 2005, 2006), extending them to include data from two groundwater databases—ADES (Accès aux Données sur les Eaux Souterraines), a natio-

nal groundwater databank developed by several French ministries and public institutions, and INFOTERRE (BRGM, French Geological Survey) dedicated to wells and their geological environments.

## Laws governing groundwater geochemistry

In addition to the classic laws governing mineral solubility (silica, calcite, barite, etc.) and ion equilibrium, we have discerned at least seven laws governing the geochemistry of groundwater in the French Massif Central, not to mention secondary laws that can be derived from them. The first five concern unpolluted water and the last two water affected by anthropogenic input.

### *Law 1: Chloride concentrations decrease as we move inland*

This observation was first made by Meybeck (1984) at the national scale for surface water in creeks. It applies to spring water, and consequently groundwater, in all of the south-western quarter of France (Fig. 1). For unpolluted water the relationship between chloride concentration [Cl] and distance to the ocean, D, is hyperbolic, $[Cl] = a.D^{(-x)}$. It is harder to demonstrate for the rest of France because we must then decide whether to take into account the geographic distance to the ocean or this distance but in the direction of prevailing winds, or the presence not only of the Atlantic Ocean, but also of the Channel, the North Sea and the Mediterranean. This law, the physical significance of which is discussed below, is a prerequisite for the second law.

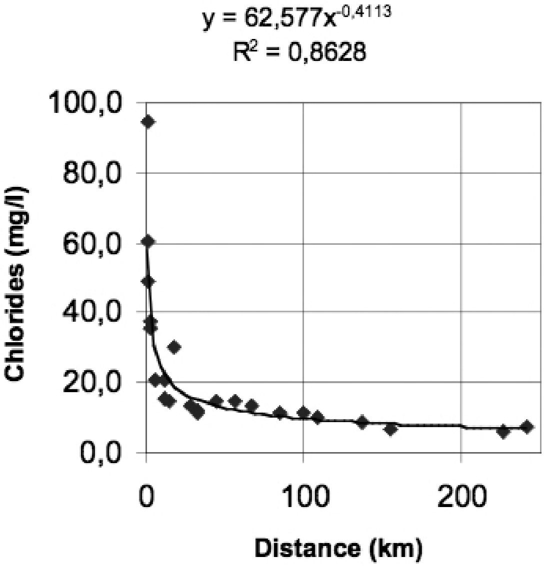

*Figure 1: Relationship between chloride concentration and distance to the ocean, for groundwater between the France Massif Central and the Atlantic Ocean (from the ADES databank)*

### *Law 2: Chloride concentrations decrease with increasing altitude*

In the French Massif Central, we observe, for groundwater, a law similar to Law 1 (fig. 2). At a given distance from the ocean, for nitrate-poor unpolluted water, there is a correlation between chloride concentration [Cl] and altitude E of the type $[Cl] = b.E^{(-y)}$. These two equations can be combined to give the general law:

$[Cl] = c.D^{(-x)}.E^{(-y)}$

This equation enables us to identify most water bodies affected by (1) chloride-bearing anthropogenic input, which can come from water treatment plants, fertilizers, sludge spreading, etc. Indeed, water that satisfies this law is generally located in forests and thus shows their protected quality.

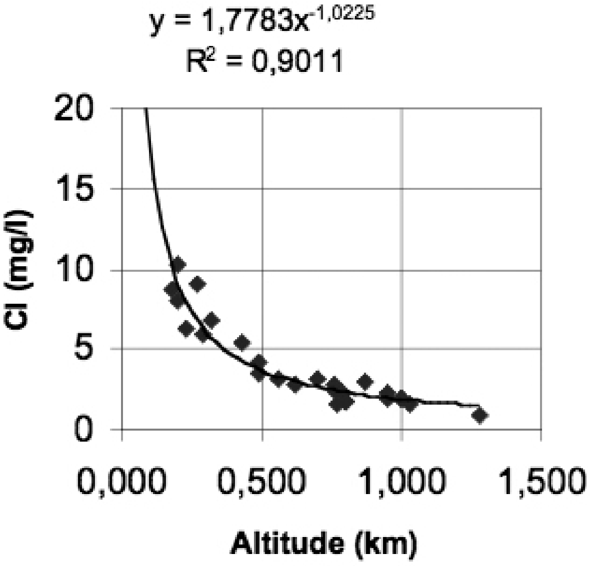

*Figure 2: Relationship between chloride concentration and altitude, in the French Massif Central (from Barbier, 2005, and the ADES databank)*

An exponential law was initially suggested (Barbier, 2005) to take into account the fact that if D or E are nil (sea coast), concentrations would theoretically be infinite if the law were hyperbolic as in eq. 1. The argument might not be pertinent, as laws expressed as D-x are known in the field of physics, i. e. heat transfer.

Two possible explanations for the distribution of chloride concentrations are evapotranspiration and the composition of precipitation (Barbier, 2005). Figure 1 enables us to eliminate the first because, in order to take into account the difference between the sea coast and altitude, that is to say a factor of around 100 (Figs. 1 and 2), we would have to assume an evaporation of more than 99 % of precipitation, which is absurd. The distribution of chloride shown in figures 1 and 2 can be more easily explained by atmospheric fallout, either dry or wet (with rain).

### *Law 3: Silicate hydrolysis is measured by $SiO_2$ concentrations up to a pH of around 6.3 and by alkalinity over the entire pH range*

Silicate hydrolysis frees cations, the electroneutrality is provided by the anion bicarbonate supplied from $CO_2$ in the water, due to carbonic equilibrium. The $CO_2$ in the soil or in the unsaturated zone (USZ) comes from the decomposition of organic matter from plants and plant-eating animals. The organic matter comes from photosynthesis, the transformation of atmos-

pheric $CO_2$ into chlorophyll, under the effect of solar radiation. So $CO_2$, and therefore also bicarbonate, are essentially of atmospheric origin.
Figure 4 shows the relationship between bicarbonate, or, in a first estimation, the alkalinity of the water (taking into account the pH range), and silica concentration. This relationship is linear up to a pH of around 6.3-6.5 (beyond which it has not been determined; Barbier, 2006). This is probably evidence of the influence of neoformations resulting from the incongruent dissolution of silicates. At high pH (6.3 to 8), the formation of 2:1 phyllite rich in $SiO_2$ is plausible, whereas 1:1 silicates (kaolinite, halloysite) would be formed at lower pH. It is therefore clear that, in general, the degree of silicate hydrolysis can be estimated more satisfactorily using bicarbonate than silica concentrations.

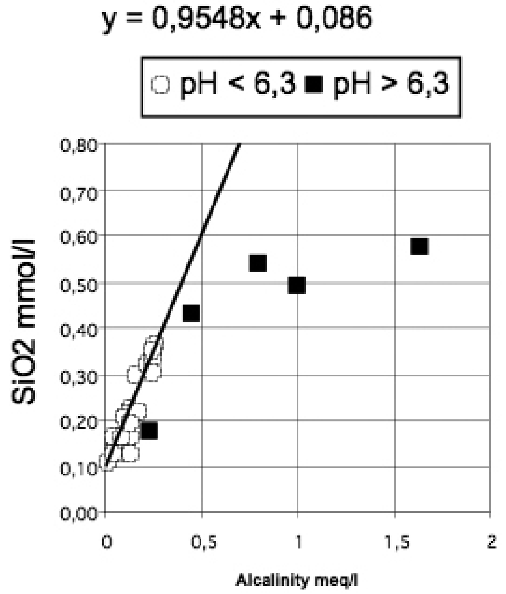

*Figure 3. Relationship between dissolved silica concentration and alkalinity in the French Massif Central (from Barbier, 2006 and ADES database)*

Dissolved $CO_2$ partial pressures (and free $CO_2$ concentrations) are much lower in groundwater with a pH higher than around 6.3, than in water with a lower pH: 0,05 mmol/l vs. 0,5 mmol/l. The water evidently followed different hydrogeological pathways, as illustrated by figure 4. The chemical characteristics, high pH, low dissolved $CO_2$ and, in some cases, low Eh (300 mV compared to 450 mV in general), suggest those of aquifers that are, if not captive, at least isolated from the atmosphere. The groundwater probably flowed laterally under a covering layer of low permeability rock. The schema in figure 4 is only partially conceptual and is based on measurements taken on a line of cored wells, with electric well logs and geochemical analyses of the rock (Barbier, 1972). These measurements revealed a porous and permeable layer (low resistivity) underlying a layer of massive rock, which is in agreement with the more recent model of horizontal fissuring in crystalline bedrock (Wyns, 2003).

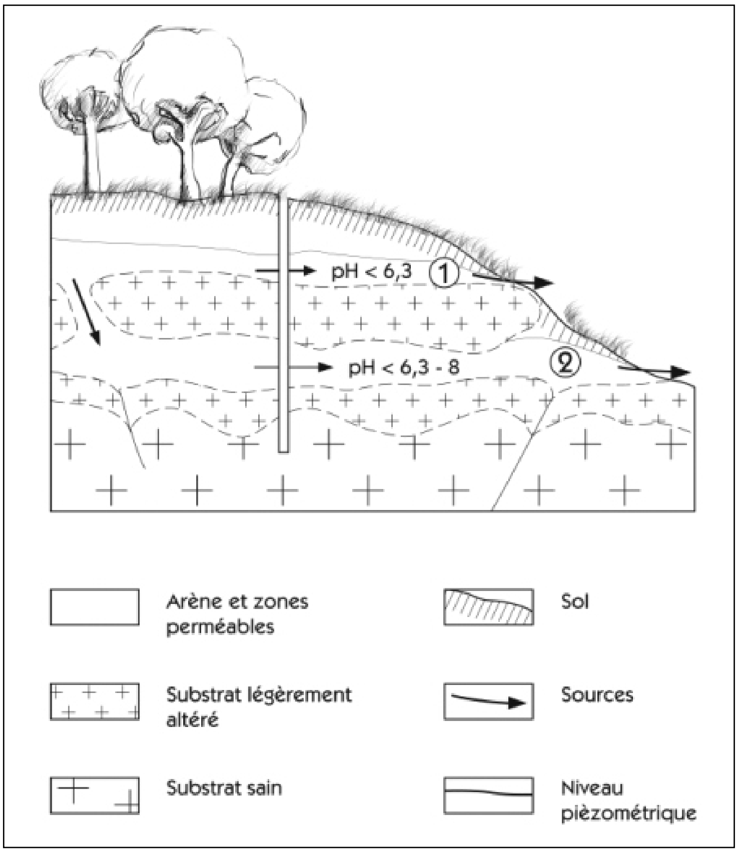

*Figure 4: Conceptual schema illustrating groundwaters having different geochemical characteristics (1 and 2) and their evolution as a function of their flowpaths. White: saprolite and permeable ground; small crosses: slightly weathered bedrock.*

## Consequences

These three laws have several consequences on the estimation of the groundwater geochemistry, geochemical signatures transmitted by anions and the question of the natural state of water:

- In the French Massif Central, chloride and especially bicarbonate account for most of the anionic charge in spring water unaffected by anthropogenic input. The total concentration of other major anions ($SO_4$, $NO_3$) is usually around 0.1 meq/l, and therefore negligible compared to that of bicarbonate (alkalinity 0.05 – 2 meq/l, Fig. 3), and even to that of chloride in the lower plains at an altitude of less than 200 m (chloride > 7 mg/l or 0.2 meq/l, Figs. 1 and 2). Since the sum of $SO_4$ and $NO_3$ is around 0.1 meq/l, if we measure the two field parameters, altitude and alkalinity, we can make a first approximation of the total anion charge in groundwater that is not affected by anthropogenic input. This charge is theoretically also that of the cations, due to electrical equilibrium, leading the way to an estimation of major groundwater parameters using only field measurements (including altitude, alkalinity).

- The geochemical signatures of the major anions are all of meteoric origin, "exogenous" in relation to the aquifers: chloride is of marine origin, bicarbonate comes indirectly from photosynthesis via dissolved $CO_2$, nitrate and sulphate come from the atmosphere. Anions (or neutral complexes such as those of B) such as Cl, N, C can then be used to determine the origin of contamination.

- Bicarbonate (or alkalinity, depending on the pH range) characterizes the geochemical signature of the stage of advancement of a reaction, essentially that of water/silicate interactions. The schema in figure 3 shows that a chemical composition ("natural state") cannot be assigned, a priori, to a groundwater body as a function of its geological environment. The composition depends on the degree or stage of silicate hydrolysis and whether the hydrolysis occurs in an open or confined aquifer. At a given location (Fig. 4), therefore, the composition of groundwater can vary significantly in space, as a function of the hydrogeological pathways.

### *Law 4: Cation exchange controls the concentration of cations forming outer-sphere complexes: Na, Mg, Ca, Sr*

In Massif Central groundwater, Na, Mg and Ca cations represent about 95 % of the cation charge. These ions form outer-sphere complexes and are therefore exchangeable. There is a very clear correlation between their concentration, as well as of that of Sr, which belongs to the same family of exchangeable cations, and the total anion charge (Fig. 5). This can be attributed to cation exchange phenomena and the presence in aquifer formations of minerals such as smectite or vermiculite. Indeed, the relationship between $(Na+)^2$ and $(Ca^{2+})$ is linear (Barbier, 2006), which is in agreement with the Gaines-Thomas model

$$K_{Ca,Na} = \frac{\left[Ca_{éch}\right]}{\left[Na_{éch}\right]^2} * \frac{\left(Na^+\right)^2}{\left(Ca^{2+}\right)}$$

Accordingly, the (Ca)/(Mg) ratio of around 1.3 corresponds rather well to published data for the selectivity coefficient $K_{Ca,Mg}$ (Bruggenwert et Kamphorst, 1979). Consequently, the ion exchangers must all have approximately the same composition. Although this appears, at first, to be surprising due to the heterogeneity of the Massif Central bedrock (granite, gneiss, micashist, etc.), it can, however, be explained. Geologically, the bedrock is made up, for the most part, of acidic rock, basic or ultrabasic complexes being nearly nonexistent. Chemically, we have here a result of Schofield's (1947) ratio law. In very diluted water, which is the case here, cation exchangers preferentially bind divalent cations (Mg, Ca, Sr) and release monovalent cations (Na). This is the principle used in water softeners. However, here the "water softeners" hardly work at all any more because, after thousands of years of water circulation, they have become saturated with divalent cations. Hence the 97 % charge of Ca + Mg as exchangeable cations (Salvador-Blanes, 2001). The relative chemical homogeneity of ion exchangers can be explained, in part, by geological factors—acid rocks, but is mainly due to a climate factor—interaction with groundwater over several thousands of years, the end of permafrost dating back 15,000 years at low altitudes (Kaiser, 1960).

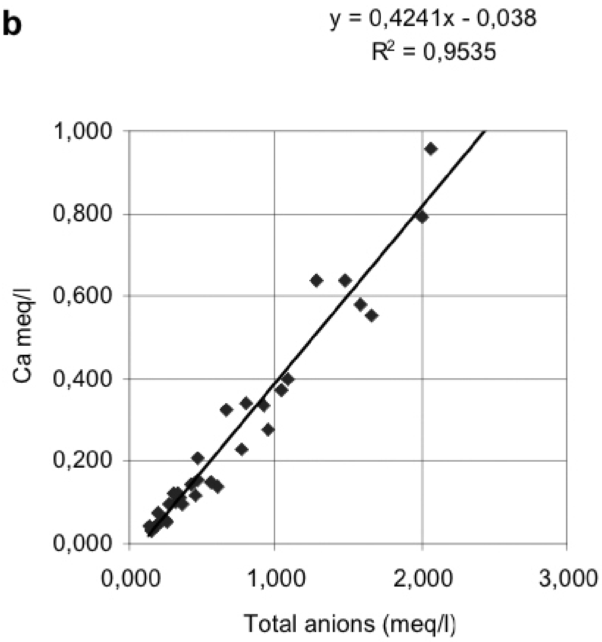

*Fig. 5: Relationship between calcium and total anion concentration*

The geochemical signature of the cations forming outer-sphere complexes is therefore endogenous (related to the aquifers themselves) and mineralogical. It corresponds to the presence of ion exchangers (2:1 phyllite, vermiculite or smectite). Indeed, if the total cation charge depends on several factors including chloride geochemistry (distance to the ocean and altitude, laws 1 and 2) and the degree of silicate hydrolysis (law 3), the cation ratio depends on their selectivity coefficients, for example, $K_{Ca,\ Sr}$ for Sr.

The geochemical characteristics of the host rock (therefore of the aquifers) rank only third. This is represented by scattered points around linear trends that link cation concentrations and total anion charge (e.g. Fig. 5). The signature of aquifers (richness in a given element) is therefore decipherable, but its importance is only secondary, or even tertiary, after the silicate reactions (among others) and ion exchange laws.

### ***Law 5: Cations forming inner-sphere complexes (K, Ba, Rb, etc.) behave in a similar manner***

As opposed to cations forming outer-sphere complexes, larger cations (K, Ba, Rb, etc.) are not correlated to the total anion charge (Fig. 6; Barbier, 2006). Their concentrations would also be controlled by sorption on solids rather than by more or less intensive weathering of the host rock.

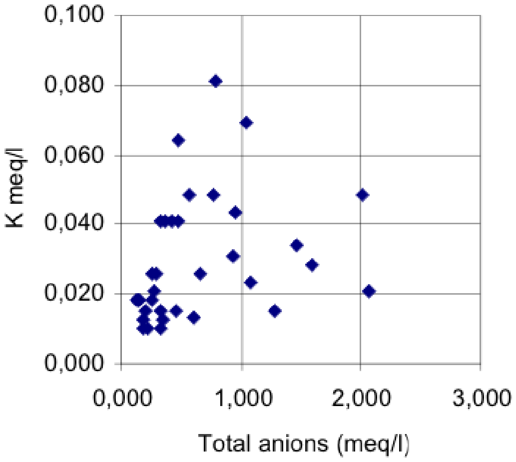

*Fig. 6. Relationship between potassium and total anion concentration*

Indeed, toxic elements like Pb or Ni, probably behave in a similar way to K, that is to say, to cations forming inner-sphere complexes. Although they are negligible in terms of the global budget of elements, polluting metals are not. In rock like the Massif Central leucogranite, the K/Pb ratio is about 1,000 (Ranchin, 1971) and both elements are classically hosted by the same minerals. In Massif Central groundwater, K can slightly exceed concentrations of 1 mg/l, whereas Pb does not exceed the analytical threshold of 1 µg/l (Barbier and Chery, 1997). The K/Pb ratio in groundwater is therefore identical to, or higher than, that of the rock and therefore Pb has a behaviour identical to that of K.

The same reasoning was used for the Mg/Ni ratio, which is around 100 in the same leucogranite. In groundwater, the Mg and Ni concentrations are, respectively, around 1 mg/l and below the analytical threshold of 1 µg/l. The Mg/Ni ratio is therefore at least 1,000. This shows that Ni does not have a behaviour in groundwater similar to that of Mg. It is not controlled by ion exchange laws, unless we assume a very high selectivity coefficient $K_{Ni,\ Mg}$.

We can therefore deduce that metals forming inner-sphere complexes will behave in a similar manner to K, that is to say, in particular, that they will depend little on the degree of silicate hydrolysis. In the absence of precise metal concentration measurements for trace metals (Pb, Ni and Cu, Zn, Cd, etc.), it is not possible to say more at the present time.

Other solutes are affected by specific sorption phenomena but they are anions such as phosphate or arsenate. We have been able to show a positive correlation between arsenate concentration and pH (Barbier, 2001), in agreement with the theory, but have not yet been able to show an inverse correlation between cations and pH.

## The influence of organic input

Many groundwaters have nitrate concentrations of several tens of mg/l and therefore also have excessive chloride contents according to laws 1 and 2 (Meybeck, 1984 ; Barbier, 2005). They, therefore, contain large amounts of dissolved $CO_2$, between 1 and 3 mmol/l. The absence of any boron anomalies (concentrations # 3 µg/l) rules out domestic pollution. These groundwaters practically never correspond to forested watersheds—which reinforces the idea of an anthropogenic influence. The simultaneous presence of high free $CO_2$ concentrations would seem to indicate an influence of the organic matter type. It would be reasonable to suspect, taking into account land use in the Massif Central, an agricultural influence, and more specifically, livestock production. Animal urine alone, the principal chloride elimination vector, can explain the increase in the Cl, N and C concentrations, the oxidation of urea $CO(NH_2)_2$ being a plausible source of N and C.

### *Law 6: Organic input does not modify the $SiO_2$/alkalinity relationship for acid pH (<6.3)*

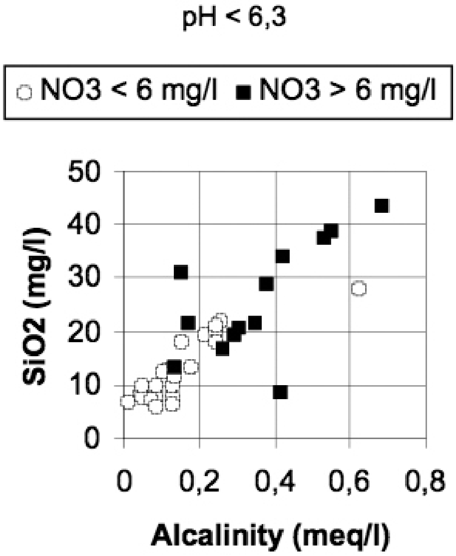

*Fig. 7: Relationship between dissolved silica and alkalinity, nitrate-poor (< 6 mg/l) or –rich (> 6 mg/l) water.*

For pH < 6.3, the correlation between dissolved silica ($SiO_2$) and alkalinity is the same whether the water is rich (> 6 mg/l) or poor (< 6 mg/l) in nitrate, and therefore rich or poor in dissolved $CO_2$ (fig. 7). Consequently, organic matter has no influence on the correlation between bicarbonate (alkalinity) and dissolved silica, as long as the pH remains acidic. Two explanations are possible:

- The input of organic matter, which would entail an increase in $CO_2$ in solution, might keep the waters at an acid pH, therefore blocking their evolution towards a geochemistry with a low $SiO_2$/alkalinity ratio characteristic of waters with a neutral or slightly alkaline pH (> 6.3, Fig. 3).

- The presence of organic matter, discernible by the chloride, nitrate and dissolved $CO_2$ concentrations, might accelerate silicate hydrolysis.

We favour the second interpretation. Indeed, figure 7 shows that almost no waters containing nitrate have low silica concentrations. Short of imagining a possible biased examination of the data (Barbier and Chery, 1997 ; ADES database) that might have inadvertently favoured those having both high nitrate and low silica concentrations, an acceleration of silicate hydrolysis is the only feasible explanation.

From a chemical point of view, this explanation can be validated by kinetics. Indeed, the rate of silicate hydrolysis, if it has not been determined (its order, in particular), is certainly a positive function of the $H^+$ ion concentration.Due to carbonic equilibrium, the latter depends on the dissolved $CO_2$ concentration, and therefore on the influence of organic matter (OM). Consequently, any increase in the OM concentration could accelerate silicate hydrolysis and therefore increase the silica/alkalinity (or silica/cation) pair in solution.

If this is the case, it is not necessarily the primary silicates (mica, feldspar) that are involved. In this pH range (< 6.3), the hydrolysis of poorly crystallized and/or small secondary silicates (vermiculite, smectite) is also possible as both poor crystallization and small size facilitate mineral solubility.

### *Law 7: Organic input with Cl, N and C does not modify the relationship between exchangeable cations*

From a chemical point of view, the presence of nitrate and chloride anions implies increased concentrations of cations. Figure 8 shows the correlation between Ca and total anions, in the case of waters rich or poor in nitrate (respectively, > 6 mg/l and < 6 mg/l). The relationship is clearly the same in both cases. The same is true for the other exchangeable cations—Na, Mg and Sr (not shown).

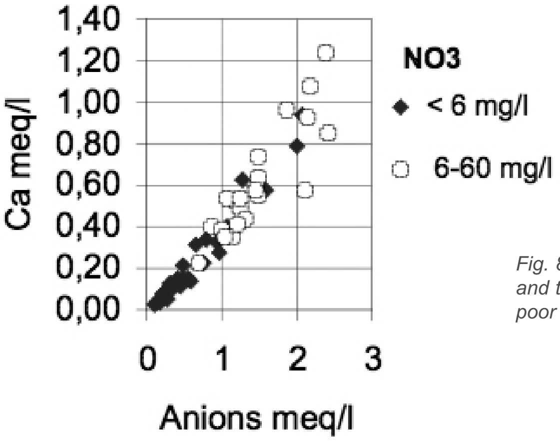

*Fig. 8: Relationship between calcium and total anion concentration, nitrate-poor (< 6 mg/l) or –rich (> 6 mg/l) water.*

This is not surprising. The total charge of exchangeable cations (only slightly lower than that of total cations or anions) reaches a maximum of 2 meq/l in the groundwater (Fig. 5). However, the cation exchange capacity (CEC) of saprolite is around 20 meq/100 g, or about 400 meq/l (Salvador-Blanes, 2001). Even if we disregard the rock/water ratio, the CEC of the saprolite, and undoubtedly also that of the aquifers, is evidently several hundreds of times greater than the cationic charge of groundwater. Consequently, except in cases of massive pollution, the quantity of cations from anthropogenic input is too low to modify the action of natural ion exchangers or influence the exchangeable cation concentrations of Na, Mg, Ca, Sr, etc.
Consequently, as concerns geochemical signatures, it is futile to seek to identify a source of pollution by means of exchangeable cations for example, Sr and its isotopes.

### Consequences for the evaluation of the natural state of groundwater

Based on the laws discussed here, it is, therefore, possible to estimate the geochemical composition of a groundwater using only a few parameters. For example, field parameters measurable at springs can be used in the following cases:

- For water unaffected by organic input, altitude and alkalinity data (laws 1 to 3) enable us to make a good estimation of chloride and bicarbonate concentrations and, therefore, most of the anion charge. About 95 % of cations are exchangeable, and the respective proportions are controlled by ion exchange (law 4). Taking into account the Gaines-Thomas model and the presence of monovalent (Na) or divalent (Mg, Ca, Sr) cations, their relationship with the total anion charge is determined using a second degree equation. This is a consequence of the correlation between monovalent and divalent ions: $(Na^+)^2 = k\ (Ca^{2+})$ (Barbier, 2006). It is, therefore, possible to calculate the concentrations of Ca, Mg, etc. using the total anion charge determined in the laboratory (Fig. 9). The calculation can also be done using field measurements (altitude for chloride and alkalinity for bicarbonate).

- Water affected by organic input is easily identifiable by conductivity. In principle (and in a first approximation), the conductivity of uncontaminated water depends solely on alkalinity and altitude because the atmospheric charge in ($SO_4$ + $NO_3$) varies little and is of the second order. Moreover, the conductivity associated with the cation charge is known because it is, theoretically, equal to the anion charge, and the proportion of metals that make it up is also known (laws 4, 5 and 7). Therefore, in the field, a surprisingly high conductivity easily identifies water with an organic component.

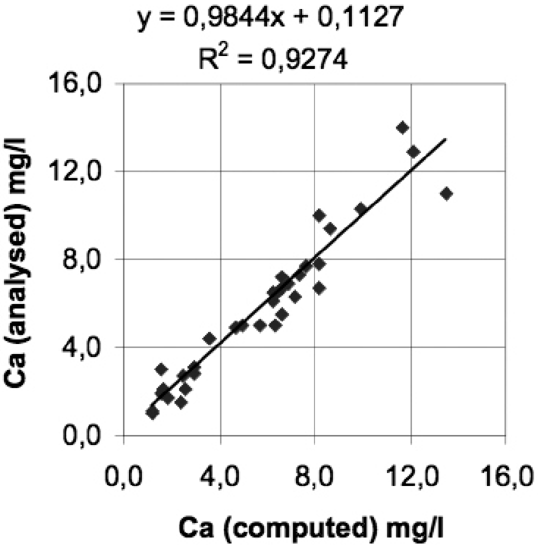

*Fig. 9: Computed vs. analyzed Ca concentrations, Haute-Vienne department (from ADES database).*

It is therefore possible to determine the natural geochemical state of a water body. However, we must first solve two problems:

- For waters with no organic input, the correlation between silica and alkalinity (Fig. 4), which was used to establish law 3, shows that alkalinity depends on what might be called groundwater "aging". It cannot be estimated a priori, and only field or laboratory measurements enable its determination. On the other hand, if the alkalinity is known, we can determine most of the geochemistry of a groundwater (concentrations in Cl, $HCO_3$, Na, Ca, Mg, Sr, as well as that of $SiO_2$ for pH < 6.3).

- For waters with organic input (nitrate, high chloride concentration), the natural state can be calculated once we have assigned a value for alkalinity (law 6), which enables us to correct the increased alkalinity caused by the organic input. It is easy to correct the excess in cations input along with the nitrate and chloride.

Determining the natural state of a water is, therefore, not problematic for a certain number of elements once we know the alkalinity, that is to say the stage of advancement of silicate hydrolysis reactions. In other words, the concentrations of these elements should be normalized to alkalinity. The main question remaining concerns the behavior of elements forming inner-sphere complexes in solution, which are probably controlled by specific sorption phenomena: K, Ba, and probably Pb and Ni.

## Conclusion

The geochemistry of groundwater in the French Massif Central obeys at least seven laws independent of classic relationships such as carbonic equilibrium, mineral solubility, etc. These laws are:

- 1 and 2: Chloride concentrations are controlled by the distance to the ocean and altitude.
- 3: There is a linear correlation between dissolved silica and alkalinity up to a pH of around 6.3. Globally, therefore, alkalinity represents a better estimation of the water/rock interaction than silica.
- 4: The principal cations in solution are those that form outer-sphere complexes. They are exchangeable, and their mutual relationships are governed by ion exchange laws.
- 5: There is no correlation between large cations (K, Ba, etc.) forming inner-sphere complexes and the degree of water/rock interaction (alkalinity).
- 6: Organic input does not modify the silica/alkalinity ratio and seems to accelerate water/silicate interactions.
- 7: Organic input does not modify the exchangeable cation ratios.

There is at least one additional law that would account for the behaviour of large cations forming inner-sphere complexes: K, Ba but also toxic metals Pb, Ni, etc.

The signatures of non-geological origin (exogenous) are seen for the most part on anions (atmospheric chloride, chloride, nitrate of organic origin). Those of geological origin (endogenous) concern mainly cations (alkali and alkaline earths). Neutral species are distributed between these two categories—exogenous biological ($CO_2$) or endogenous geological ($SiO_2$) influences. The actual geochemical signature of the aquifer host rocks is, in fact, only of secondary or tertiary importance because it is for the most part obscured by the phenomena listed above.

The consequences of these observations are:

- Exogenous geochemical signatures are easier to identify on elements forming weakly sorbing ions (N, C, Cl) or neutral complexes (B). They are harder to sort out for exchangeable or sorbing ions (Sr, K, P). This is true for both concentrations and isotopic ratios.

- The naturally occurring concentrations of dissolved elements ("geochemical background" or "natural chemical state") can be predicted for a given location provided that we set a criterion with reference to the intensity of the incongruent dissolutions.

It is therefore possible to determine the natural background of groundwaters at a given stage in their evolution (water/silicate interaction, estimated by alkalinity) using the results of chemical analyses done in the laboratory, even if they reveal the presence of organic input. The effects of contamination can be corrected. In the absence of any pollution, the following parameters, measurable in the field, enable us to determine, for the most part, the natural composition of the groundwater: altitude (chloride), alkalinity (bicarbonate), silica (silica/alkalinity relationship if the pH < 6.3), total cations (determined approximately from the chloride and bicarbonate data), cations ratios (ion exchange laws).

Some of these characteristics of groundwater in crystalline formations are also found in groundwater in sedimentary formations. They are probably valid for all countries with similar climates having a marine influence—Spain, Portugal, possibly Ireland and Great Britain—and therefore might well be applicable to a large part of Europe.

## References

- Barbier J (1972) Altération superficielle et mobilisation du sodium dans certains granites à deux micas. Bull. BRGM, 2e série, sect. IV, pp. 33-48.
- Barbier L.,Chery L. (1997) Relation entre fond géochimique naturel et teneurs élevées en métaux lourds dans les eaux (antimoine, argent, baryum, chrome, nickel, plomb, zinc). Application (Auvergne) et validation. Rapport BRGM R 39544, 51 p.
- Barbier J (2001) Occurrences naturelles d'arsenic en France : roches, sols et milieux associés. Les Techniques de l'Industrie minérale, 11, 51-65.
- Barbier J. (2005) Altitude et géochimie des eaux de source, Nord-ouest du Massif central, France. C. R. Geosciences 33, 763-768.
- Barbier J (2006) Echanges d'ions et sorption dans les eaux de nappes aquifères en socle cristallin, Massif central, France. La Houille Blanche, 3, 1-5.
- Bruggenwert MGM, Kamphorst A. (1979) Survey of experimental information on cation exchange in soils, in: GH Bolt ed., Soil Chemistry, Elsevier, 5B, chap. 5.
- Kaiser K (1960) Klimatzeugen des periglacialen Dauerfrostbodens in Mittel- und West-europa. Eiszeitalter Ggw, 11, 121-141.
- Meybeck M (1984) Les fleuves et le cycle géochimique des éléments. Thèse Univ. Paris 6, pag. mult.
- Ranchin G (1970) La géochimie de l'uranium et la différentiation granitique dans la province du Nord-Limousin. Thèse Univ. Nancy, 483 p.
- Salvador-Blanes S (2002) Déterminisme de la répartition spatiale des éléments majeurs et traces dans les sols en contexte métamorphique.Thèse Univ. Tours, 298 p.
- Schofiel RK (1947) A ratio law governing the equilibrium of cations in the soil solution. International Congress of Applied Chemistry, Proc. 11th Mg [London], 3, 257-261.
- Wyns R. (2003) fissuration profonde induite par l'altération : processus d'acquisition et répartition 3D des propriétés physiques des profiles d'altération. ASF 2003, 9e Congrès Français de Sédimentologie, Bordeaux, France.

# DARCY 08

# Tracing high pH mineral waters ascribed to ultramafic rocks (Central Portugal): Conceptual vs numerical modelling

MARQUES José M.1, MATIAS Maria J.[1], CARREIRA Paula M.[2], CARVALHO
M. Rosário[2], GOFF Fraser[3], BASTO Maria J.[1], GRAÇA Rui C.[1],
ANDRADE Mário[1,2], ROCHA Luís[4], AIRES-BARROS Luís[1]

[1] Instituto Superior Técnico, Av. Rovisco Pais, 1049-001, Lisboa, Portugal,
jmmarques@mail.ist.utl.pt
[2] Instituto Tecnológico e Nuclear, Estrada Nacional Nº 10, Sacavém, Portugal,
carreira@itn.pt
[3] Earth and Planetary Sciences Depart., Univ. of New Mexico, Albuquerque, USA, candf@swcp.com
[4] Junta de Freguesia, Av. da Libertação, Cabeço de Vide, Portugal,
jfreg.cabecodevide@mail.telepac.pt

## Abstract

Cabeço de Vide mineral waters have attracted our attention due to their chemical composition (high pH; Na-Cl/Ca-OH type waters) and their association with mafic/ultramafic rocks. Geochemical, isotopic and numerical approaches have contributed to increased knowledge on the nature of those mineral waters. The Mg-$HCO_3$ waters constitute most of the local surface and shallow groundwaters. Since both Mg-$HCO_3$ and the mineral waters have similar $\delta^2H$ and $\delta^{18}O$ signatures we hypothesize an evolution from the $HCO_3$-Mg waters towards the mineral waters. The reaction path simulations show that the progressive evolution of the Ca-$HCO_3$ to Mg-$HCO_3$ waters can be attributed to the interaction of meteoric waters with serpentinites. The sequential dissolution at $CO_2$(g) closed system conditions at depth leads to the precipitation of chrysotile, brucite and calcite, indicating that the waters would be responsible for the serpentinization of fresh ultramafic rocks (dunites) present in depth.

## 1. Introduction

At Cabeço de Vide region (Figure 1), Spas should be considered as one of the main sources of local development. So, increasing knowledge on the local geohydrology is extremely important to achieve the sustainable use of this “invisible” georesource, which could foster a multiplicity of new attractions to develop additional tourism.

The mineral springs of Cabeço de Vide are well known since Roman times. In fact, the Romans built a bath (dated 119 b.c.) for their legions in the study area. Cabeço de Vide mineral waters, due to their uncommon chemical composition and their ocurrence under complex geologic and hydrogeologic conditions have attracted the attention of several scientists for a long time (e.g. Portugal Ferreira and Mendonça 1990; Costa et al. 1993). Especially, their origin has been a challenge for both geologists and hydrogeologists, although most studies have been mainly based on results of detailed geological investigations.

Recently, under the scope of the TERMAVIDE R&D Project (funded by the local Municipality)

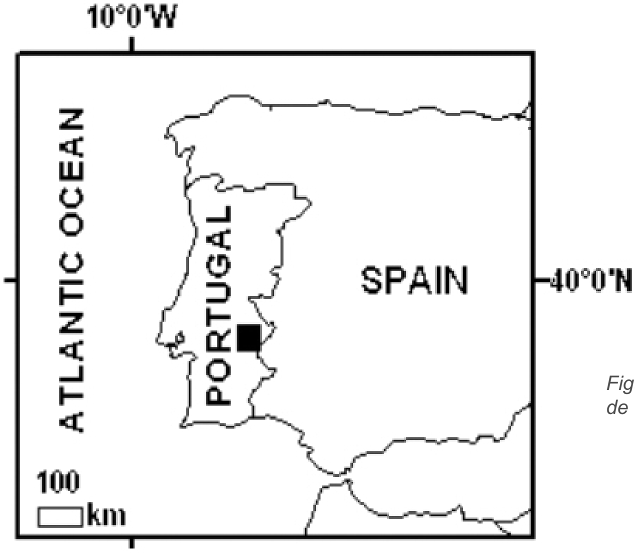

Figure 1: Location map of Cabeço de Vide region.

coupled geochemical, isotopic and hydrogeochemical modeling approaches were designed to increase knowledge on the circulation paths of the waters and their correlation between local surface, shallow and ground waters. The main objective of this paper is to summarise the findings obtained during this project, with a special enphasis on hydrogeochemical and isotopic investigations, comparing the results obtained with recently hydrogeochemical modelling using previous geochemical data.

## 2. Geological and Geomorphological Setting

The study region (Figure 1) is situated at the Ossa Morena Zone of the Iberian Hercynian belt. The Lower Cambrian carbonate sequence was intruded and metamorphosed by mafic and ultramafic rocks forming a NW-SE cumulate-type structure of Ordovician age, which has been subjected to serpentinization - rodingitization processes (Costa et al. 1993). Cabeço de Vide mineral waters issue at the intrusive contact between the mafic/ultramafic rocks and the carbonate sequence, associated with the main regional NNE-SSW trending fault (Figure 2). The ultramafic rocks range from partially serpentinized dunites to serpentinites. The mafic rocks adjacent to the ultramafics are mostly coarse- to fine-grained gabbros. In addition, several other distinct geological formations can be observed in the surroundings of Cabeço de Vide Spas. The most representative are: Precambrian metamorphised rocks (schists and graywakes), Cambrian cloritized schists, quartzites and graywakes and ortogneisses dated at 466 ± 10 Ma and some hyperalkaline syenites.

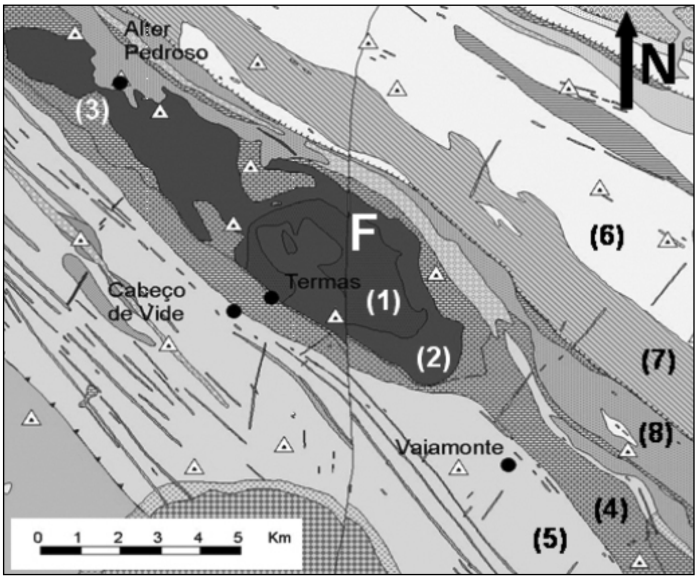

*Figure 2: Geologic map of Cabeço de Vide region. Adapted from ERHSA - Estudo dos Recursos Hídricos Subterrâneos do Alentejo [Study of Alentejo's Groundwater Resourses] - courtesy Fernandes, J. (2002), personal communication. (1) serpentinized ultramafic rocks; (2) mafic and ultramafic rocks; (3) hornfels; (4) carbonate rocks, displaying contact metamorphism; (5) Cambrian rocks: schists, quartzites and greywakes; (6) Pre-Cambrian rocks: metamorphic schists and greywakes; (7) ortogneisses and (8) ortogneisses and hyperalkaline syenites. Termas stands for Cabeço de Vide Spa. F stands for the main regional NNE-SSW trending fault.*

The studied region extends from the Cabeço de Vide Spa (≈ 20 km SW of Portalegre city) towards the S. Mamede Mountain ridge (≈ 5 km NE of Portalegre city). This mountain ridge (ca. 1027 m a.s.l.) is the main geomorphologic feature of the Cabeço de Vide region. The relief of Cabeço de Vide area (≈ 260 - 300 m a.s.l.) tends to be rather flat (typical of Alentejo Province of Portugal). The topography rises gradually from the Cabeço de Vide Spa at a distance of 20 km from Portalegre city (620 m a.s.l.), after which the gradient becomes steeper, with a maximum elevation at the crest of the S. Mamede Mountain.

## 3. Sampling procedures and analytical methods

Water samples have been collected from streams, springs, dug wells and boreholes, for chemical and isotopic analysis. Temperature (ºC), pH, electrical conductivity (µS/cm) and redox potential (mV) were determined in the field at the time of collection. Total alkalinity was measured a few hours after collection. Major and minor elements in waters were determined at Laboratório de Mineralogia e Petrologia of Instituto Superior Técnico (LAMPIST) / Portugal, using the following methods: atomic absorption spectrometry for Ca and Mg; emission spectrometry for Na, K, Li, Rb and Cs; colorimetric methods for $SiO_2$, $Fe_{total}$, F and Al; ion chromatography for $SO_4$, $NO_3$ and Cl; potentiometry for alkalinity. Trace elements concentrations in waters were determined at Los Alamos National Laboratory (LANL) / USA, using the ICP-MS methodology. The $\delta\,^2H$ and $\delta\,^{18}O$ measurements (vs V-SMOW, Vienna - Standard Mean Ocean Water) were performed by mass spectrometry (SIRA 10–VG ISOGAS) at the Instituto Tecnológico e Nuclear (ITN - Portugal) following the analytical methods of Epstein and Mayeda (1953) and Friedman (1953), with an accuracy of ± 1 ‰ for $\delta^2H$ and ± 0.1 ‰ for $\delta\,^{18}O$. The $^3H$ water content (reported in Tritium Units, TU) was also determined at ITN, using electrolytic enrichment followed by liquid scintillation counting method (standard deviation varies between ± 0.9 and ± 1.3 TU, depending on tritium activity of the water samples). The $\delta^{13}C$ and $^{14}C$ determinations in waters were performed at the Geochron Labs/USA by accelerator mass spectrometry (AMS). The $\delta^{13}C$ values are reported in o/oo vs V-PDB (Vienna - Peedee Belemnite) standard, with an accuracy of ± 0.1 o/oo. $^{14}C$ is given in pmC (per cent with respect to the so-called "modern carbon").

## 4. Hydrogeological setting

### *4.1 Water chemistry vs water-rock interaction*

At Cabeço de Vide region, the different geologic formations led to the development of surface, shallow and ground waters displaying different facies. Groundwaters issuing within the Cambrian limestones are Ca-$HCO_3$-type waters. Waters sampled in the Precambrian/Cambrian slates and in the granitic rocks belong to the Na/Ca-$HCO_3$ and Na-$HCO_3$-type, respectively. The Mg-$HCO_3$-type waters constitute most of the surface (stream) and shallow groundwaters discharging from the serpentinites, suggesting that water chemistry is strongly host rock dependent. In particular, serpentine dissolution may explain the high Mg (Figure 3) and $SiO_2$ concentrations found in Mg-$HCO_3$- type waters (e.g. Barnes et al. 1967; Barnes and O'Neil 1969):

$$Mg_3Si_2O_5(OH)_4 \text{ (serpentine)} + 6H^+ \rightleftharpoons 3Mg^{2+} + 2H_4SiO_4 + H_2O$$

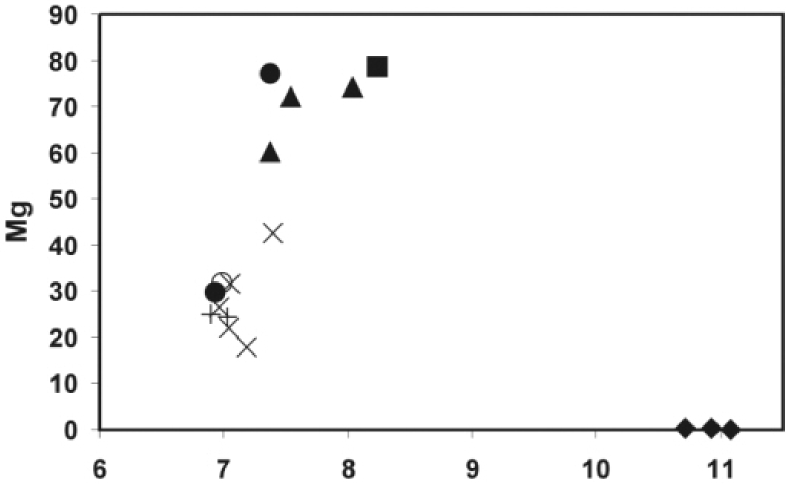

*Figure 3 Mg (mg/L) vs pH plot of waters from different geological formations: (**X**) limestones; (●) gabbros; (▲) serpentinites; (**O**) contact gabbros/serpentinites; (+) contact gabbros/limestones. (■) Cabeço de Vide stream. (♦) Cabeço de Vide mineral waters. Adapted from Marques et al. (2004).*

The main characteristics of Cabeço de Vide mineral waters can be summarized as follows: i) Na-Cl/Ca-OH type, ii) very alkaline pH values (between 10.5 and 11.5), iii) low Mg and $SiO_2$ concentrations (see Table 1), iv) rather low mineralization (dry residium values up to 220 mg/L) and v) the presence of reduced species of sulphur (HS- ≈ 0.7 mg/L). This type of waters has been well documented in the literature (e.g. Barnes and O'Neil 1969; Barnes et al. 1967, Bruni et al. 2001). Some of these authors suggest that serpentinization of the ultramafic rocks may be an important process contributing to the mineral water chemistry through the reaction:

$$2Mg_2SiO_4 + 3H_2O \rightleftharpoons Mg(OH)_2 + Mg_3Si_2O_5(OH)_4$$

which may explain the low Mg (Figure 3) and $SiO_2$ concentrations found in the Cabeço de Vide mineral waters. Usually, as stated by Hostetler et al. (1966), serpentinization is not a single episode in the history of ultramafic bodies, but probably has occurred at various times and places for the same body of rock. The high Ca/Mg ratio of these waters may indicate that rodingite reactions are occurring (Coleman, 1977, p. 107).

| | (L) | (G) | (Sp) | (CV) |
|---|---|---|---|---|
| **T(ºC)** | 19.4 | 18.2 | 19.2 | 19.6 |
| **Cond** | 724 | 785 | 740 | 646 |
| **pH** | 6.96 | 7.37 | 7.54 | 10.93 |
| **Na** | 14.3 | 9.53 | 9.56 | 49.0 |
| **K** | 0.96 | 0.35 | 0.44 | 5.04 |
| **Ca** | 100.0 | 41.9 | 38.7 | 22.5 |
| **Mg** | 26.5 | 77.3 | 72.2 | 0.16 |
| **$HCO_3$** | 469.2 | 540.3 | 542.9 | n.d. |
| **$CO_3$** | 0.24 | 0.70 | 1.06 | 6.9 |
| **$SO_4$** | 20.56 | 14.72 | 14.42 | 5.18 |
| **$NO_3$** | 19.48 | 12.33 | 9.07 | 6.22 |
| **Cl** | 16.68 | 14.44 | 9.08 | 32.14 |
| **$SiO_2$** | 24.6 | 74.3 | 72.8 | 5.50 |
| **OH** | n.d. | n.d. | n.d. | 33.02 |

*Table 1: Physico-chemical characteristics of representative waters from Cabeço de Vide region, issuing from distinct geological formations.*

**Notes:** Groundwaters issuing from (L) limestones (G) gabbros, (Sp) serpentinites. (CV) stands for Cabeço de Vide mineral waters.

### *4.2 Isotope geochemistry*

Environmental isotopes ($^{18}O$ and $^2H$) were used to estimate the relative importance of locally infiltrated meteoric waters to the recharge of the mineral aquifer system. The long term weighted mean value ($\delta^{18}O$ and $\delta\ ^2H$) of precipitation collected in Portalegre meteorological station (597 m a.s.l. / approximately 15 km NE of Cabeço de Vide) was used to help the interpretations. The relation between the concentrations of the environmental stable isotopes deuterium and oxygen-18 in all the water samples is similar to the relationship in global meteoric water line (GMWL: $\delta\ ^2H = 8\ \delta\ ^{18}O + 10$) defined by Craig (1961), indicating i) that they are meteoric waters, which have not been subjected to surface evaporation (being directly infiltrated into the ground) and ii) that there is no evidence of water/rock interaction at high temperatures (Figure 4), consistent with the low issue temperature (≈ 19.5 ºC) of the Cabeço de Vide mineral waters.

Cabeço de Vide mineral waters and the local Mg-$HCO_3$ waters (issuing from the serpininized dunites) have similar $\delta^2$H and $\delta^{18}$O values (around -27 ‰ and -4.5 ‰, respectively), indicating a common meteoric origin for these waters (Figure 4). Even the $\delta^2$H and $\delta^{18}$O content of the Cabeço de Vide stream waters (running along serpentinized dunites) is very similar to isotopic content of the Cabeço de Vide mineral waters. Considering the long-term mean isotopic composition of precipitation at Portalegre meteorological station ($\delta^2$H = -32.2 ‰; $\delta^{18}$O = -5.44 ‰; ITN 2002) we can admit that the the major source of recharge of the Cabeço de Vide mineral waters would appear to be ascribed to lower elevation sites located at the local mafic/ultramafic outcrop.

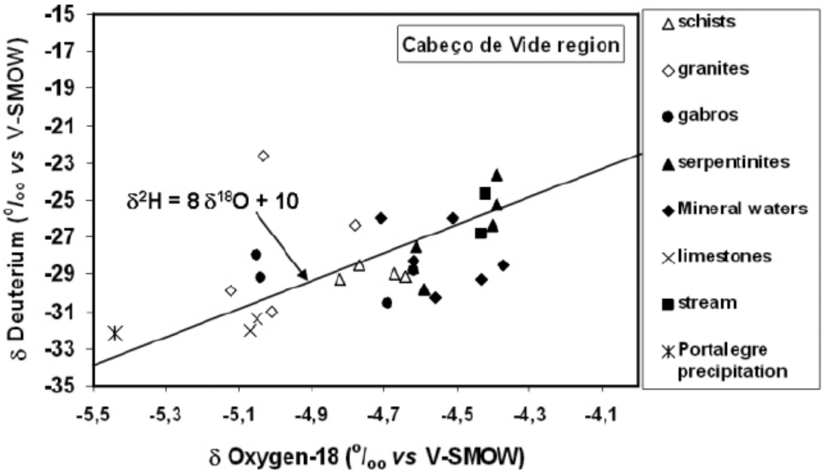

Figure 4: $\delta^2$H vs $\delta^{18}$O relations in water samples from Cabeço de Vide area.
Adapted from Marques et al. (2003).

## *4.3 Conceptual model*

Since both Mg-$HCO_3$ waters and Cabeço de Vide mineral waters have similar isotopic ($\delta^2$H and $\delta^{18}$O) signatures, we believe that the Mg-$HCO_3$ waters could evolve towards the Cabeço de Vide mineral waters through interactions with the country rocks. With this water-rock interaction model, the local Mg-$HCO_3$-type waters seem to be generated in an initial step, under open $CO_2$ conditions, due to meteoric water-serpentinite interactions in a shallow environment, whereas the Cabeço de Vide mineral waters will be produced in a subsequent step, under closed $CO_2$ conditions. In this second step, the increased pH values (due to water-dunite interaction at depth) will favor calcite precipitation (Figure 5).

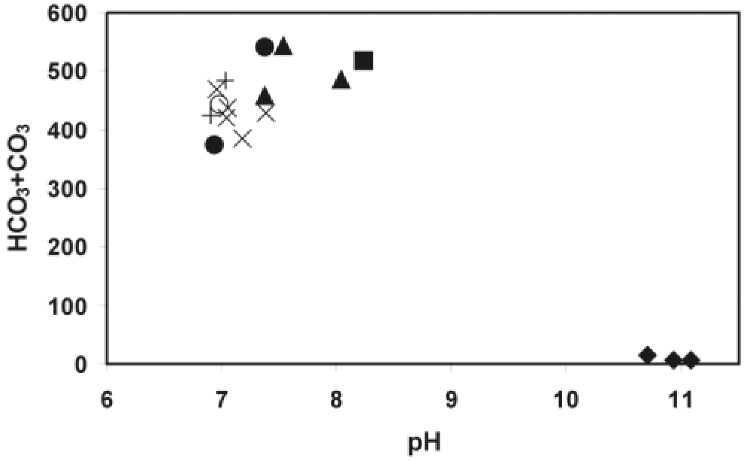

Figure 5: Plot of $HCO_3$ + $CO_3$ (mg/L) vs pH. Symbols as in Figure 3. Adapted from Marques et al. (2004).

In fact, the carbonate deposits occurring along veins of drill cores from Cabeço de Vide area are mainly calcite (Photo 1). Because most of the magnesium will be retained in serpentines and vein brucite (Photo 2), Ca concentrations should increase proportionately in waters during the evolution of the $HCO_3$-Mg-type waters towards the Cabeço de Vide mineral water end member.

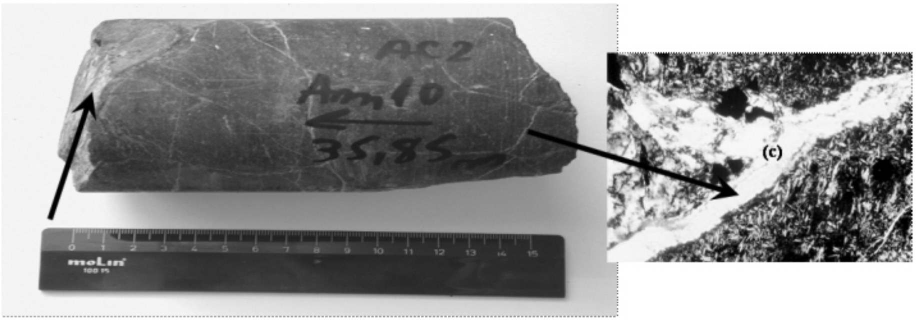

Photo 1: Drillcore from borehole AC2 (Cabeço de Vide Spas) showing typical serpentinized dunite. The arrows indicate the presence of veins filled with calcite.

Photo 2: Drillcore from borehole AC2 (Cabeço de Vide Spas) showing another example of serpentinized dunite. The arrows indicate fiberous serpentine and brucite along fractured zones.

Assuming a common origin for the Mg-$HCO_3$-type and the Cabeço de Vide mineral waters, the high Cl concentrations (accompanied by low $^3H$ values) found in the mineral waters could be attributed to the increased water-rock interaction, as the result of a large flow path and/or long residence time in the subsurface rocks (Figure 6).

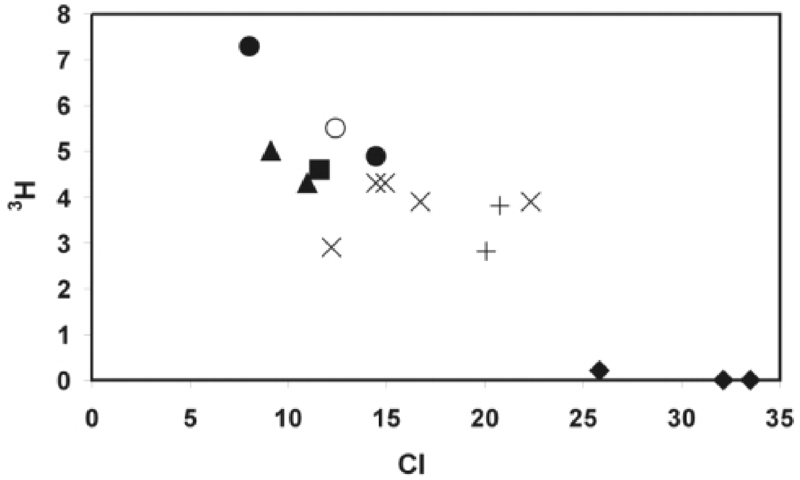

*Figure 6: Plot of $^3H$ (TU) vs Cl (mg/L). Symbols as in Figure 3. Adapted from Marques et al. (2004).*

The absence of $^3H$ determined in the Cabeço de Vide mineral waters (Figure 6) suggest that recharge of Cabeço de Vide mineral system corresponds to an age older than 60 years. Two samples of Cabeço de Vide mineral waters were collected for $^{14}C$-age determinations (AMS determinations; Geochron Laboratories, USA). The values obtained range between 69.12 ± 0.28 pmc and 65.24 ± 0.35 pmc ($AC_5$ and $AC_3$ boreholes), indicating an apparent groundwater age between 2970 ± 40 and 3430 ± 50 years BP, respectively.

The study of carbon isotopes is more complex than that of O or H, due to the existence of a number of different sources of carbon. In most groundwaters, only part of bicarbonate carbon is recent and derived from biogenic $CO_2$. The rest could be derived from aquifer carbonate, which will normally be far older than the half-life of 5730 years and will therefore have dead carbon (negligible $^{14}C$ content). Thus, the interpretation of $^{14}C$ data has limitations but probably provides a limit on maximum age. Keep in mind that the $\delta^{13}C$ values of -22.9 ‰ and -18.0 ‰ of Cabeço de Vide mineral waters (boreholes $AC_3$ and $AC_5$, respectively) suggest i) an organic origin for the carbon in the Cabeço de Vide mineral waters, and ii) a negligible contribution from the local carbonate rocks ($\delta^{13}C$ values ≈ 1.48 ‰), suggesting that $^{14}C$-dating of mineral waters seems to provide rather reliable results.

### *4.4 Geochemical modelling*

High-pH waters are well known as waters associated with ultramafic rocks, namely serpentinized rocks (e.g. Barnes et al., 1978, Drever, 1982, Bruni et al. 2002, among others). To better understand the geochemical processes that most likely have caused the changes in water composition, the irreversible water-rock mass transfer was simulated using chemical speciation, mineral-solution equilibrium, and reaction path modelling. The calculations were carried out by means of the PHREEQC software code (Parkhurst and Appelo, 1999), referring to the WATEQF thermodynamic data base of 2005. As the water pH is the main parameter affected during simulated aqueous changes, it is of interest to evaluate the saturation state of minerals in the weathering environment, and elucidate the effect of pH on the saturation state because early water-rock interaction is dominated by uptake of protons from the water with a corresponding increase in pH (Gíslason and Eugster, 1987a,b). The groundwaters from limestones (L, x) are in equilibrium with calcite (Figure 7) and oversaturated in quartz and chalcedony but undersaturated with respect to amorphous silica (Figure 8) and magnesium carbonates. Groundwaters issuing from gabbros (G,o) are undersaturated with respect to the typical minerals of mafic and ultramafic rocks (e.g. pyroxenes and olivine, Figure 9) and serpentinites (e.g. crhysotile, Figure 10). On the other hand, they are in equilibrium with silica minerals and oversaturated in calcite as result of Ca-aluminosilicate dissolution.

The neutral Mg-$HCO_3$ waters issuing from gabbros (G,o) and serpentinites (Sp, ▲) aquifers are generally undersaturated with respect to the typical minerals of the ultramafic rocks (Figure 9) and serpentinites (Figure 10), as well as with some solid phases usually produced through interaction between these rocks and waters at relatively low temperatures and pressures (brucite, sepiolite, and a variety of Mg-carbonates). These waters are relatively close to saturation with Mg-montmorillonite, Mg-saponite, amorphous silica (Figure 8), and oversaturated in calcite as a result of Ca-aluminosilicate dissolution and solution pH rising. In contrast, the Cabeço de Vide mineral waters (CV, ▲), which are high-pH, Na-Cl/Ca-OH type waters, are generally strongly oversaturated with chrysotile (Figure 10) and diopside, slightly undersaturated with respect to enstatite and forsterite (Figure 9), and undersaturated in calcite, brucite and amorphous silica.

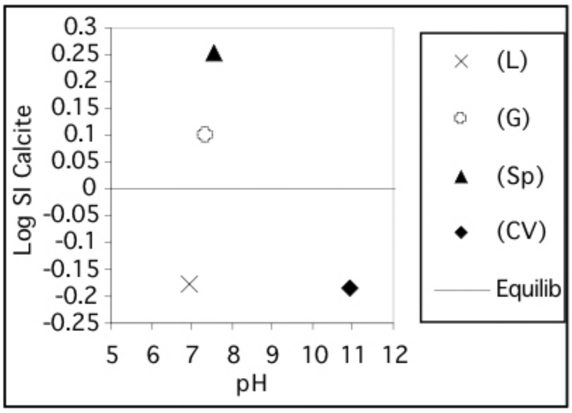

Figure 7: Calcite water saturation index (SI) versus the water pH.

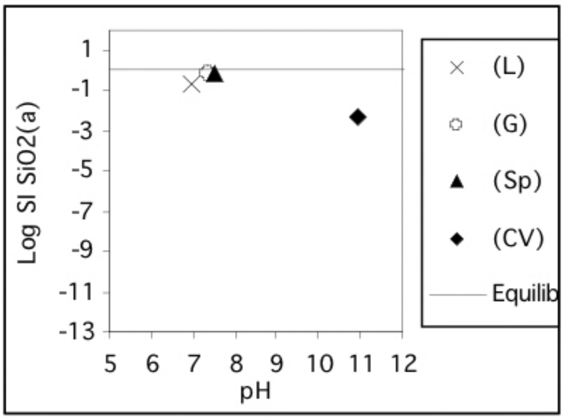

Figure 8: Amorphous (a) silica water saturation index (SI) versus the water pH.

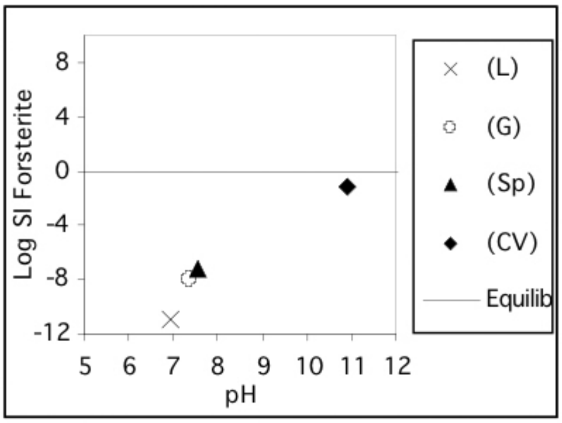

Figure 9: Forsterite water saturation index (SI) versus the water pH.

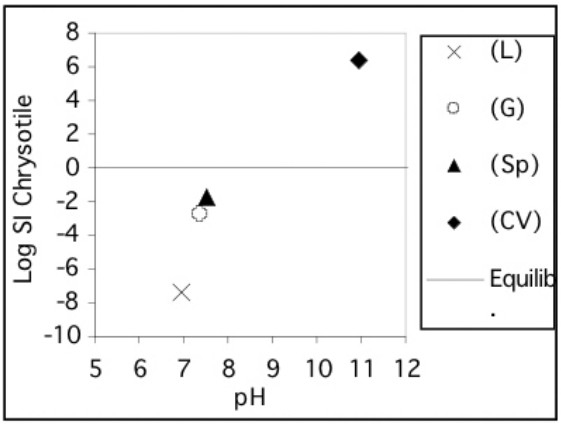

Figure 10: Chrysotile water saturation index (SI) versus the water pH

The progressive evolution from Ca-$HCO_3$-type to Mg-$HCO_3$-type waters can be attributed to low temperature interaction of meteoric waters with serpentinites, at open and/or closed conditions with respect to $CO_2$(g). To prove this hypothesis, the irreversible water-rock mass transfer leading to these chemical changes in the aqueous phase was simulated through progressive reaction of water from the limestones (L, as typically regional groundwater) with serpentinites. The Cambrian limestones represent an important aquifer in the region (the Monforte - Alter do Chão carbonate aquifer) where the fractured carbonate rocks allow the development of Ca-$HCO_3$ waters. Since serpentinites are almost monomineralic rocks, stoichiometric serpentine ($Mg_3Si_2O_5(OH)_4$) was considered to be the only solid phase under dissolution at open system with respect to $CO_2$(g). Calculations were performed in titration mode, which means adding at each step of the reaction progress variable a corresponding amount of chrysotile, and only the chemical composition of the solid reaction was considered (i.e., both reaction kinetics and reactive surfaces of solid phases were left out of consideration).

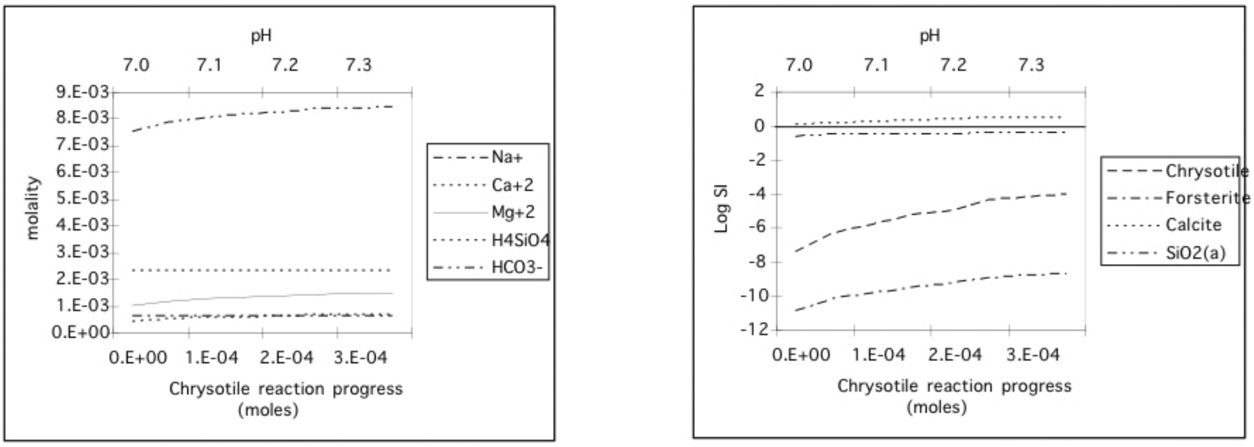

(a) (b)

*Figure 11: The saturation index (SI) variations of Ca-$HCO_3$ water with respect to chrysotile, forsterite, calcite and amorphous silica (a), and the major aqueous species increment (b), during the chrysotile reaction dissolution at open system with respect to $CO_2$(g).*

The saturation state variation of the water with respect to chrysotile, forsterite, calcite and amorphous silica, during the reaction path, are represented in Figure 11 (a), as well the major aqueous species increment (b), versus the pH of the water. During the serpentine dissolution reaction some changes are observed: i) water pH ascent; ii) increase of aqueous Mg and silica concentrations; iii) the water becomes oversaturated in calcite as a result of pH rising; iv) the water becomes close to the saturation with respect to amorphous silica; v) decreasing of the water undersaturation related to forsterite and chrysotile. The very-high pH and Na-OH water composition can only be achieved through the dissolution of ultramafic and serpentinized rock minerals under closed system conditions with respect with $CO_2$(g). The irreversible water-rock mass transfer leading to these chemical changes in the aqueous phase was simulated through reaction path modelling of water from serpentinites aquifer (Sp) reacting with this kind of magnesium minerals. The simulation was carried out in titration mode and in two steps, at reducing conditions ($PO_2=10^{-53}$) and initial $P_{CO2}$ of $10^{-1.74}$: 1) dissolution of dunite rock; 2) dissolution of sepentinite rock.

The dunite dissolution simulation was performed assuming that the olivine end-member forsterite ($Mg_2SiO_4$) is the main dissolved mineral. We also assumed that olivine dissolves stoichiometrically over a wide range of solution pH (Gíslason and Arnórsson, 1993) and that chrysotile, calcite, brucite and amorphous silica can be formed at thermodynamic equilibrium. Figure 12 shows aqueous concentrations variation of $Na^+$, $Ca^{2+}$, $Mg^{2+}$, $HCO_3^-$, $OH^-$ and $H_4SiO_4$ (a) during the reactive process of forsterite dissolution and the saturation state of the water with respect to those minerals (b). Because the serpentinite dissolution simulation assumed that the rock is almost monomineralic, and that stoichiometric serpentine ($Mg_3Si_2O_5(OH)_4$) was the only solid phase under dissolution. Figure 13a shows the aqueous concentrations variations of $Na^+$, $Ca^{2+}$, $Mg^{2+}$, $HCO_3^-$, $OH^-$ and $H_4SiO_4$ during serpentine-water mass transfer.

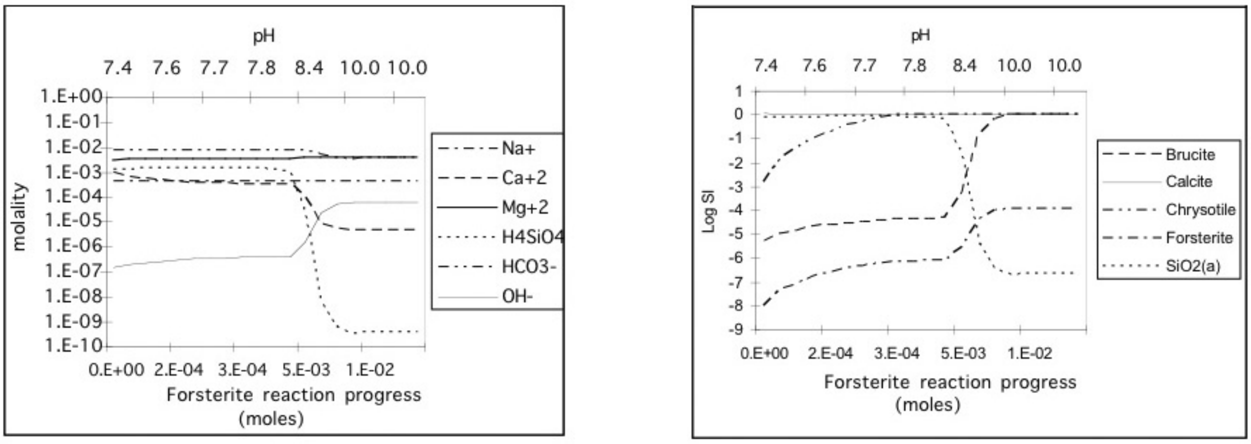

(a) (b)

*Figure 12: (a) Ionic composition and pH of a water from sepentinite aquifer (Sp) as a function of the amount of forsterite reacted; (b) mineral saturation index (SI) for some minerals and pH of a water from sepentinite aquifer (Sp) as a function of the amount of forsterite reacted; minerals are considered to form at thermodynamic equilibrium.*

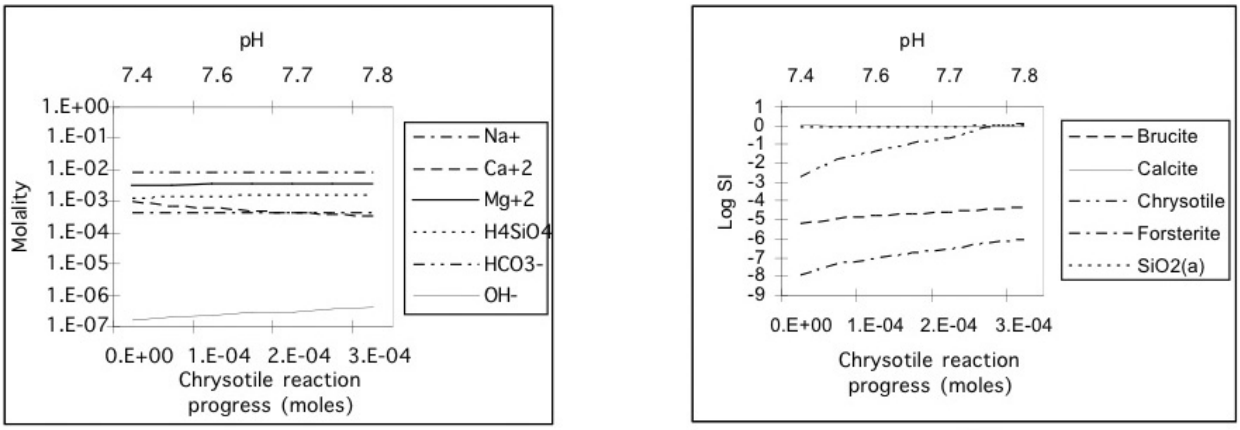

(a) (b)

*Figure 13: (a) Ionic composition and pH of a water from sepentinite aquifer (Sp) as a function of the amount of chrysotile reacted; (b) mineral saturation index (SI) for some minerals and pH of a water from sepentinite aquifer (Sp) as a function of the amount of chrysotile reacted; minerals are considered to form at thermodynamic equilibrium.*

The serpentinite dissolution does not determine a great increase in the pH and activity of aqueous $SiO_2$, since the water becomes saturated in chrysotile after dissolution of $3x10^{-4}$ moles (Figure 13b). During the mineral reaction the precipitation of calcite, brucite and amorphous silica was assumed to be in thermodynamic equilibrium. The general agreement between theoretical paths and analytical data indicates that progressive interaction of surface- and groundwaters with serpentinites leads to the formation of the Mg-$HCO_3$ type waters, under open-system conditions with respect to $CO_2$. The numerical modelling points out the role of calcite precipitation during the closed-system dissolution in depleting the aqueous solution in C and Ca species, allowing the acquisition of a Na-OH composition. The low amounts of aqueous silica are the result of the formation of amorphous silica and chrysoltile solid phases. At their natural conditions, the Cabeço de Vide mineral water system is oversaturated in chrysotile. Nevertheless, we have assumed thermodynamic equilibrium of the waters relative to this mineral. There are limitations in thermochemical calculations of natural geological processes, especially at low temperatures. Kinetics of mineral dissolution and mineral precipitation at low temperature often is too slow for attaining water-rock equilibrium within a reasonable time scale. The low rate of chrysotile precipitation can explain the water oversatutarion and the higher $SiO_2$ values in the natural water system than those obtained during the simulations. The Cabeço de Vide mineral waters (high-pH, Na-Cl/Ca-OH type waters) are depleted in $Ca^{2+}$, $Mg^{2+}$ and $SiO_2$. These geochemical signatures can only be obtained with sequential and progressive interaction of meteoric waters with serpentinites and dunites, in a closed system with respect to $CO_2$. These signatures indicate that the Cabeço de Vide mineral waters would be responsible for the serpentinization at low temperature conditions of the ultramafic rocks present at depth. It should be stated that there is a general agreement between these theoretical paths and the mineral assemblages observed in the cores from mineral water boreholes.

## 5. Concluding remarks

The results obtained in this study increased our knowledge regarding the hydrogeologic conceptual model of the Cabeço de Vide mineral waters, which seem to be dominated by interactions between locally recharged meteoric waters and ultramafic rocks. The local Mg-$HCO_3$-type waters (surface and shallow groundwaters) seem to evolve to the Cabeço de Vide mineral waters (high pH; Na-Cl/Ca-OH-type waters). Mg-$HCO_3$-type waters are generated under open $CO_2$ conditions, whereas the Na-Cl/Ca-OH-type waters are the result of water-rock interactions under closed-system conditions. Mineropetrografic observations from drillcores provide strong evidence that considerable magnesium precipitation occurs when surface waters seep into the ground and react progressively with the ultramafic rocks. Cabeço de Vide mineral waters are unsaturated with respect to Mg-Olivine [forsterite – $Mg_2SiO_4$] but supersaturated with serpentine [chrysolite – $Mg_3Si_2O_5(OH)_4$] indicating that the precipitation of Mg-rich minerals controls aqueous magnesium concentrations. Serpentinization does not represent a single episode in the history of Cabeço de Vide ultramafic body, but probably indicates many episodes at various times and places for the same body of rock. Cabeço de Vide mineral waters should be considered the fluid responsible for present-day serpentinization of the local ultramafic body at depth. These hydrogeological signatures are being used by the concessionaire of Cabeço de Vide Spas for the redefinition of well-head and aquifer protection areas, drilling strategies, and future development plans.

## Acknowledgements

This work has been supported by Cabeço de Vide Municipality, under the Research Contract TERMA-VIDE / No. 693, and by the Centre of Petrology and Geochemistry of Instituto Superior Técnico, Technical University of Lisbon. F. Goff was supported by the $CO_2$-Sequestration Project of Los Alamos National Laboratory.

## References

- Barnes I, LaMarche VC Jr, Himmelberg GR (1967) Geochemical evidence of present-day serpentinization. Science 56: 830-832.
- Barnes I, O'Neil JR (1969) The relationship between fluids in some fresh alpine-type ultramafics and possible modern serpentinization, Western United States. Geol. Soc. America Bull. 80: 1947-1960.
- Barnes I, O’Neil JR, Trescases JJ (1978) Present-day serpentinization in New Caledonia, Oman and Yugoslavia. Geochim. et Cosmochim. Acta 42: 144-145.
- Bruni J, Canepa M, Cipolli F, Marini L, Ottonello G, Vetuschi Zuccolini M, Chiodini G, Cioni R, Longinelli, A (2001) Reactions governing the chemistry of waters interacting with serpentinites. Water-Rock Interaction, Cidu (ed.):145-148.
- Bruni J, Canepa M, Chiodini G, Cioni R, Cipolli F, Longinelli A, Marini L, Ottonello G, Vetuschi Zuccolini M, , (2002). Irreversible water-rock mass transger accompanying the generation of the neutral, Mg-$HCO_3$ and high-pH, Ca-OH spring waters of the Génova province, Italy. Applied Geochem., 17: 455-474.
- Coleman, RG (1977) Ophiolites. Springer-Verlag, Berlin, 229 pp.
- Costa IR, Barriga F, Mata J, Munhá JM (1993) Rodingitization and serpentinization processes in Alter-do-Chão Massif (NE Alentejo). Proceedings of the IX Semana de Geoquímica (Noronha F, Marques M and Nogueira P., eds.). Universidade do Porto. Faculdade de Ciências. Museu e Laboratório Mineralógico e Geológico: 27-31.
- Craig H (1961) Isotopic variations in meteoric waters. Science 133: 1703-1703.
- Drever JI (1982) The geochemistry of natural waters. Prentice Hall, Englewood Cliffs.
- Epstein S, Mayeda T (1953) Variation of $^{18}O$ content of waters from natural sources. Geochimica et Cosmochimica Acta 4: 213-24.
- Friedman I (1953) Deuterium content of natural waters and other substances. Geochimica et Cosmochimica Acta 4: 89-103.
- Gíslason SR, Arnórsson S (1993) Dissolution of primary basaltic minerals in natural waters: saturation state and kinetics. Chemical Geology 105: 117-135.
- Gíslason SR, Eugster HP (1987a) Meteoric water-basalt interactions, I. A laboratory study. Geochim. Cosmochim. Acta 51: 2827-2840.
- Gíslason SR, Eugster HP (1987b) Meteoric water-basalt interactions, II. A field study in N.E. Iceland. Geochim. Cosmochim. Acta 51: 2841-2855.
- Hostetler PB, Coleman RG, Mumpton FA (1966) Brucite in alpine serpentinites. Americam Mineralogist 51: 75-98.
- ITN [Instituto Tecnológico e Nuclear] (2002) Precipitation data base. Portalegre meteorological station (1988 – 2002).
- Marques JM, Andrade M, Goff F, Basto MJ, Matias MJ, Graça RC, Carreira PM, Aires-Barros L, Rocha L (2003) Origin and evolution of high pH mineral waters traced by isotope geochemistry (S-Portugal). Book of Extended Synopses of the International Symposium on Isotope Hydrology and Integrated Water Resources Mamagement. IAEA-Vienna: 180-181.
- Marques JM, Matias MJ, Basto MJ, Graça RC, Aires-Barros L, Andrade M, Carreira PM, Goff F, Rocha L (2004) Water-Rock interaction responsible for the origin of high pH mineral waters (S. Portugal). Water-Rock Interaction (Wanty RB and Seal II RR, eds) 1: 293-297.
- Parkhurst DL, Appelo CAJ (1999) User´s guide to PHREEQC (version 2)-A computer program for speciation, batch-reaction, one-dimensional transport, and inverse geochemical calculations. Water-Resources Investigations Report 99-4259. US. Geological Survey, Denver, Colorado.
- Portugal Ferreira M, Mendonça JL (1990) Enquadramento geológico e hidrogeológico das nascentes de água minero-medicinal de Cabeço de Vide [Geological and hydrogeological background of Cabeço de Vide mineral waters]. Livro de Homenagem a Carlos Romariz: 151-173

# DARCY 14

# Compaction of water/gas bearing formations: experiences in Northern Italy

MACINI Paolo[1], MESINI Ezio[2]

[1] University of Bologna, DICMA, Viale del Risorgimento, 2, 40136 Bologna, Italy, paolo.macini@unibo.it
[2] University of Bologna, DICMA, Viale del Risorgimento, 2, 40136 Bologna, Italy, ezio.mesini@unibo.it

## Abstract

Subsidence problems due to underground fluid withdrawal have been long recorded all over the world, causing heavy effect on the environment. In Italy, numerous cases have been recognized, in the areas of Po Delta and the cities of Venice, Ravenna and Bologna. Many studies are under development to further investigate the influence of gas production on subsidence, coastal regression and upsetting of the hydraulic system. Attention is paid to the studies on the application of new tools and modeling techniques to measure and predict reservoir compaction. The purpose of this research is at first to report the very well known subsidence case histories of the towns of Ravenna and Bologna. Finally, the research discusses the measurement of mechanical properties of Northern Italy clastic formations. In particular the research reports both the laboratory measurements and the in-situ investigations of formation compaction by means of extensometers and radioactive markers. In addition, it has also been attempted an approach to estimate the precision and accuracy of the above techniques, and the perturbation effects induced by in-situ monitoring systems.

## Introduction

The optimal management of a fluid supply system generally emphasizes a balance between supply and demand, and a minimization of physical, economic, and environmental consequences. Fluid removal from subsurface reservoirs, in the form of gas, oil, groundwater, geothermal water, and brine, produces a compaction of the depleted formations which migrates totally or partially to the ground surface thus inducing land subsidence. Land subsidence is the loss of surface elevation as a result of the removal of underground support. The mechanisms by which this can occur may be natural in origin or induced by human activities (natural or anthropogenic land subsidence, respectively). Common causes of anthropogenic land subsidence include the removal of oil, gas, and water from underground reservoirs; dissolution of limestone aquifers (sinkholes); underground mining activities; drainage of organic soils. Overdraft of aquifers is the major cause of areally extensive land subsidence, and as groundwater pumping increases, land subsidence also will increase. This phenomenon is often characterized by large surfaces and slow gradients; in this case, the problem is not particularly evident in regions situated above the mean sea level, at least until a precision leveling campaign takes place or buildings become fissured, underground pipelines crack, well casings fail or stand above ground level, surface drainage patterns change, canals no longer carry original design flows (due to change or reversal of gradient) and differential compaction takes place.

Engineers and scientists involved in studying, planning and designing industrial complexes, urban developments, water supply systems and natural resources exploitation, need to know about the potential hazards, costs, and socio-environmental impacts that can result from land subsidence. The effects of subsidence on the environment are strictly related to the peculiarity of ground movements and to ground elevation. Differential land subsidence can affect the geomorphology of large territories, inducing damages on buildings, more evident in urban areas. Subsidence-related alterations in drainage patterns and local topography can cause severe flooding. Associated problems include increased rates of erosion on farmland, requiring more frequent grading. Uniform subsidence, combined to eustatic sea level rise, can seriously endanger the hydraulic safety of territories which lie completely below the sea level.

Quite often, especially at the onset of the occurrence, land settlement goes unnoticed, to be later discovered when severe damages have already been experienced. At this stage, undertaking effective remedial measures to mitigate the associated environmental and socio-economical impact may prove tremendously expensive. However, in recent times, the awareness about the damages caused by potential anthropogenic land subsidence has significantly grown at both the political and the general public level, thus contributing to lower the alarm threshold. As a major result, the newest plans for subsurface resource development are usually complemented by a study of the related environmental impact which may include, wherever appropriate, numerical predictions of the expected land settlement above (and close to) the exploited system. (Gambolati et al. 2005; Holzer and Galloway 2005, Brighenti et al. 2001)

In Northern Italy, cases of subsidence of more than 2 m took place in the early ‘50s in the Po Delta, due to the exploitation of relatively shallow aquifers containing dissolved gas. Subsidence is recorded in Venice (in the last century, subsidence and eustatism exceeded 20 cm), Ravenna (over 1 m), Bologna and its surroundings (over 2.5 m), and other areas of the Po Plain (Brighenti et al. 1995). Most of the above cases are largely due to groundwater withdrawal, even though recent studies have pointed out that subsidence in Ravenna area was also caused by gas production from onshore and offshore reservoirs (Bertoni et al. 1995). Nowadays, the most critical area is the Northern Adriatic Sea, where Eni (the former Italian State-owned company for oil and gas) discovered numerous gas field with over $30 \cdot 10^9$ Standard $m^3$ of total reserves. The reservoirs are located a few miles offshore, facing the shoreline from the Po Delta North to the Lagoon of Venice (Figure 1). The proposed project for the development of these gas fields is facing considerable problems and doubts among the population and local administration. In fact, many parts of this region are at present located below the sea level, and there are concerns that sea-bottom subsidence might propagate to the shoreline and beyond. Venice Lagoon brings even more delicate problem. In fact, there is a possible risk that gas production would cause irreparable damages to the historic city of Venice, the town of Chioggia and the alteration of the lagoon area ecosystem. These risks have strongly moved the public opinion, causing the Italian government to issue a decree stopping all the project of offshore reservoir development in this area until further studies are completed. As a matter of fact, this action blocked industrial investments of almost $10^9$ U.S. dollars (1996 value), with severe drawbacks for the local economy: in Ravenna area only, the oil industry provides jobs to over 3.000 people.

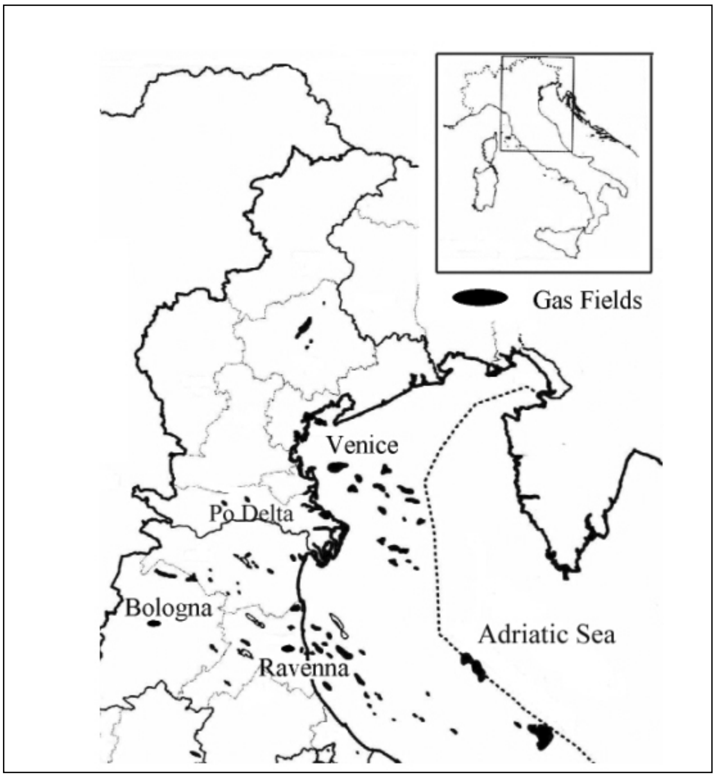

*Figure 1: Simplified map of Northern Italy gas reservoirs. In particular, here are indicated the gas field discovered in front of Venice lagoon, Po Delta and the city of Ravenna.*

In this paper are reported two very well known subsidence studies, in order to highlight possible suggestions for the development of offshore reservoirs in the Northern Adriatic Sea. Here, the case histories of the towns of Ravenna and Bologna are studied, showing that anthropogenic subsidence can produce dissimilar surface sinking. In fact, in both cases different impairments on the industrial and urban town infrastructures were induced: in Bologna by differential foundation sinking, and in Ravenna, in consideration of its vicinity to the coastline, by general sinking that impaired harbor facilities and upset the coastal equilibrium. In-depth studies are currently under way, in order to clarify the problem by developing both a system to monitor coastline subsidence, and models able to predict the effects of gas production, possibly identifying adequate exploitation techniques. To this regard, one can remind that there is a considerable gap between the quality level achieved by the more and more sophisticated mathematical models and the much lower quality of geomechanical measurements used as input data (Brighenti et al. 1998; Cassiani and Zoccatelli 2000). It is evident that models are as good as the data they are built upon. Thus, in order to improve subsidence studies, it is essential to improve measurements of the mechanical properties of the formations under investigation. At last, the paper reports the laboratory measurements of geomechanical parameters performed on clastic formations from Northern Italy and Northern Adriatic offshore, and the in-situ investigations of formation compaction by radioactive markers in the same area. The causes of the discrepancies between lab and *in-situ* measurements, and the possibility of their combined utilization, are also analyzed.

## Subsidence in Ravenna and Bologna area

### *Ravenna*

The Ravenna plain is a subsiding sedimentary basin located in the eastern part of the Po River Plain. It is formed by a succession of marine, deltaic, lagoon, marsh, and alluvial deposits of the Quaternary and upper Pliocene. The pre-Quaternary strata form a complex structure characterized by folds entrapping rich gas reservoirs. The Quaternary sediments are variable in thickness: up to 3000 m in depressions and thinner in the positive buried structures, having about 1500 m minimum depth. From a geotechnical and geological standpoint, the Plio-quaternary complex of this area is characterized by fine sediments with homogeneous mechanical properties. In Ravenna, over the last sixty years the ground has been progressively sinking due to underground fluid production. The subsidence rate reached a maximum at the beginning of the ‘70s, and now is still in progress, though at slower rate. The main reason for subsidence is a massive groundwater withdrawal, initiated after the development, in the second half of the past century, of large industrial settlements, and of intensive irrigation farming, together with the urbanization in proximity of the coastline. Another cause of subsidence, although considered of minor importance, is the exploitation of onshore and offshore gas fields (started around the mid ‘50s and ‘60s, respectively). This subsidence is further aggravated by natural subsidence (1.5 ÷ 3 mm per year) and the eustatic rise of the sea level. The territory of Ravenna, located a few decimeters above the sea level, experienced a ground sinking that was proportional to the decline of the hydraulic head, with constant gradients, so that buildings and industrial constructions were seldom impaired. Here, subsidence totaled more than 1 m. Damages to the territory consist mainly in the overall land surface sinking (with flooding of large coastal areas), in the impairment of the industrial harbor infrastructures and in the upsetting of most of the land reclamation systems. As a consequence, subsidence has been carefully monitored and studied by the local authorities in collaboration with universities and public research centres. In addition, after the involvement of the Italian Government, at the beginning of the ‘80s the Ravenna Municipality established a Joint Study Committee (Municipality, University of Bologna, Eni), which organized topographic, hydrogeologic, geotechnical, and mining surveys in order to study by mathematical modeling the effects of gas and groundwater production from the system of multi-aquifer layers.

The study identified both the water consumption and the geometry of these aquifers, which were intensely exploited since 1950. Consumption data and piezometric variations vs. time, along with the geometry and petrophysical properties of the multi-aquifer system, were used for a modeling study by using a three-dimensional finite element model that reproduced subsidence trends and covered the whole water system of the Ravenna plain. The water production caused a reduction of the hydraulic head, leading to the gradual ground subsidence at an average rate of 3 ÷ 4 cm/year from 1949 to 1972. The rate progressively increased during the following years, attaining 6 ÷ 7 cm/year in 1977. This alarming development persuaded the local Authorities to reduce groundwater withdrawal by closing many water wells, and replacing more and more underground water with surface water. After this decision, aquifers underwent a re-pressurization process. From 1977 to 1982 subsidence rate decreased to an average of 1 cm/year, with a maximum rate of 1.5 cm/year in the Ravenna industrial area. Measurements made in 1986 showed a further decrease: an average rate of 0.5 cm/year to a maximum of 1 ÷ 1.5 cm/year in the coastal area was recorded.

The investigations of the Joint Study Committee were subsequently addressed to assess the influence of gas production on ground subsidence and to compare it to the influence of water withdrawal from the multi-aquifer system. To this purpose, a modeling study of the “Ravenna-Terra” reservoir was carried out. The study has shown that subsidence is maximum in the vicinity of the reservoir axis (60 ÷ 65 cm in an area of about 2 $km^2$), and decreases quickly outside the reservoir limits. Further studies were carried out to assess the influence on subsidence due to gas production from onshore fields. In particular, the “Porto Corsini Terra” and “Dosso degli Angeli” fields were investigated (Figure 2). Maximum subsidence values over these fields were estimated in about 30 cm for Porto Corsini Terra (depth of about 1800 m), whereas for Dosso degli Angeli (depth about 3100 m), being the presence of an active aquifer uncertain, it was estimated to about 100 cm and 60 cm, considering or not the presence of an active aquifer, respectively (Bertoni et al. 1995).

The global results of the Study Committee showed that the severe water withdrawals from the fresh water artesian aquifers was the most important cause for subsidence phenomena in the area. However, in order to associate the assessment for the possible subsidence to its real cause, it was decided to monitor the set of piezometric heads and to extend the study also to the effects of gas production from offshore reservoirs. In particular, considering the vulnerability of coastal area, particular attention was addressed to the Angela-Angelina field, straddled between the sea and the shoreline, with productive layers spanning from 2850 and 3970 m.

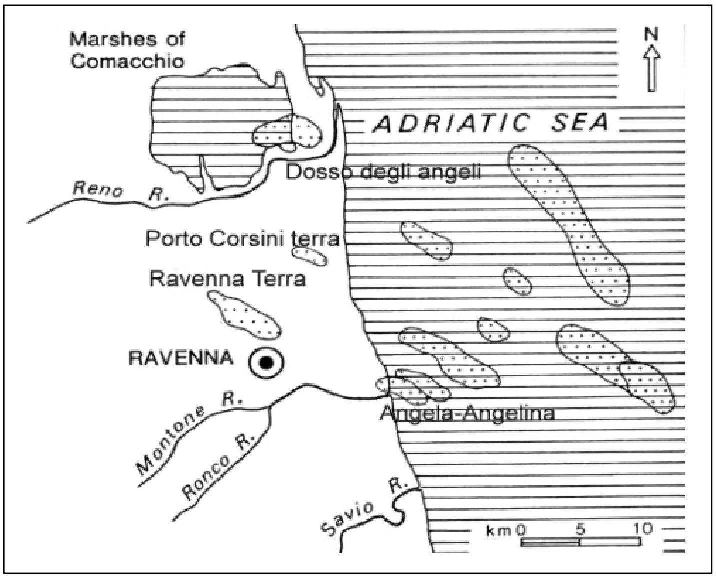

*Figure 2: Ravenna area gas reservoirs location: "Ravenna Terra", "Porto Corsini terra", "Angela-Angelina" and "Dosso degli Angeli".*

In this area, the intensive water withdrawal and an intensive urbanization determined a decrease of the piezometric head, causing an accelerated subsidence and flooding of coastal areas.

As far as surface and deep compaction measurements are concerned, two wells were drilled (385 and 363 m deep) and wireline logs were recorded in order to know a detailed subsoil lithology. In the first, two bar extensometers have been installed at 372 and 224 m respectively. In the second, three "Casagrande" piezometers have been set up in correspondence of the principal aquifer at depths of 360 m, 243 m, and 148 m (Agip-Comune di Ravenna 1997). Radioactive Markers were also suggested to monitor compaction of deep formations directly inside the productive wells of Angela-Angelina. The predictive model of subsidence calculated a maximum ground sinking of about 15 cm, in correspondence of the shoreline in front of the reservoir (Teatini et al. 1998). However, this result is strictly dependent upon a correct choice of the compaction coefficient of the formations under investigation, discussed later in this paper. At present, subsidence in the Ravenna area (both on- and off-shore) is continuously monitored by means of precision leveling and GPS satellite measurements. Figure 3 reports subsidence rates measured during the last decades in the municipality of Ravenna.

The analysis of the effects of land subsidence in Ravenna area can be extended also to the coastal territories of Romagna, between Reno River estuary and Cattolica (Teatini et al. 1998, 2005). As a first conclusion, it can be derived that the reduction of groundwater withdrawal and the increased utilization of surface water supply lead to a substantial reduction of subsidence phenomena. In Ravenna area, the above mentioned groundwater control policies, adopted since the end of the '70s, resulted in a sensible subsidence rate reduction already in the middle '80s. Notwithstanding these results, considering that the pro-capita water consumption is expected to increase by about 10% in the next 20 years, it is worth noting that without important economic investments for new infrastructures for the exploitation and distribution of surface water, subsidence rate will persist, or even increase.

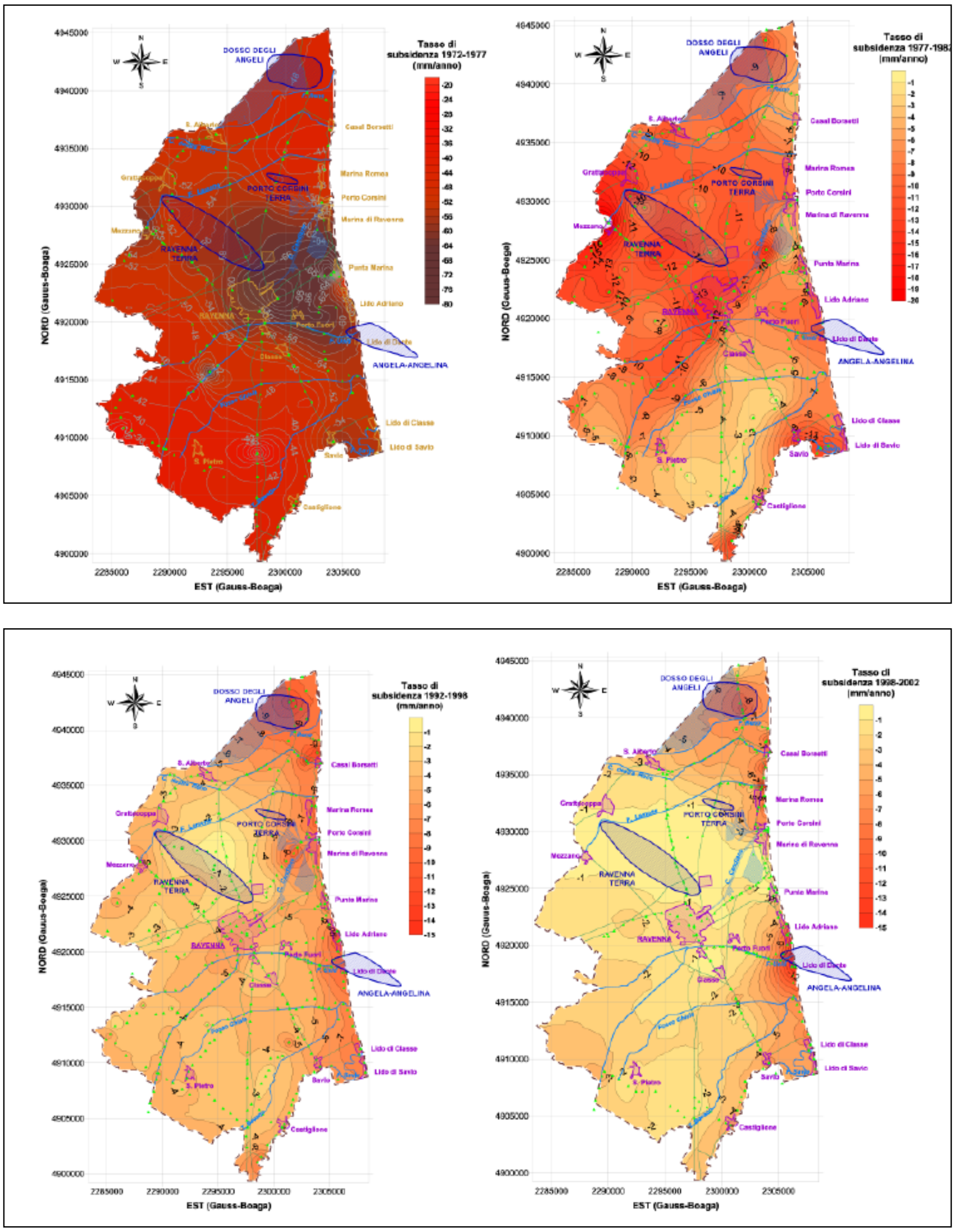

Figure 3: Ravenna area: contour lines of subsidence rate, 1972 – 1977 (top left), 1977 – 1982 (top right), 1992 – 1998 (bottom left) and 1998 – 2002 (bottom right) (from Bertoni 2004).

### Bologna

The town of Bologna lies in the central area of the piede-Apennine section of the Po Plain about 50 m above the mean sea level, and extends to the edge of the hills. In this area two main geological settings are found: the edge of the Apennines and the alluvial plain, with large structural and geotectonic differences. The former is subject to earth upheavals and erosion, whereas the latter undergoes land subsidence with accumulation of sediments. Besides this moderate subsidence on a regional scale, a local subsidence of a considerably higher magnitude occurs in the plain. At present, Bologna is one of the most remarkable cases of urban land subsidence in Italy with regard to the extent of the subsiding area and to the velocity of the vertical displacement. Land subsidence is induced by ground-water exploitation. The subsidence rate varies in space, with maximum values of 6 ÷ 8 cm/year. Also, subsidence gradient shows variations in absolute value and direction in some spots, where gradients up to

1 cm per 100 m per year were measured. One of these sharp gradients is found in the historical center of the city, where damages produced by differential foundations sinking have been detected in several buildings.

Since the 1950, the urban area of Bologna and its surroundings experienced a marked land subsidence: in its North/Western part, it exceeded 2 m. The high sinking rates, along with differential subsidence, have been responsible for severe damages to some buildings in the town centre and to the sewage system. The subsidence of Bologna presents rather different features by respect to the ones of Ravenna area. Firstly, the sediments under compaction have different thickness, from the foot of the hills to the plain, and are characterized by different mechanical properties. Secondly, the largest piezometric sinking is recorded in the gravel-sand alluvial fans, but the largest land subsidence develops in the adjacent compressible shaly layers. The presence of different formations causes high differential ground sinking, which in turn induce serious building fissuring (Brighenti et al. 1995).

Although the effect of subsidence in Bologna is not as sensational as the one of Ravenna, its rate is considerable, with maximum rates over 15 cm/year recorded from 1970 to 1983. Indeed, Bologna seems to exhibit the highest subsidence rate in the whole Po Plain. In the period from 1983 to 1993 less severe subsidence rates were recorded, with a maximum of about 8 cm/year in the urban area, city centre and outskirts, to rates close to zero at the edge of the hills (Folloni et al. 1996; Vicari 1998). Also in Bologna area the main reason for subsidence is water withdrawal: the growing demand for water supply has been accomplished by drilling a large number of wells. In the early ‘80s the piezometric head sank by over 45 m (attaining 70 m below the ground level) with depressurization rates up to 5 m/year. While the phenomenon of land subsidence in Bologna was known since the ‘50s, it became evident only 20 years later. The Northern area of the city was found to be particularly affected by subsidence. One of the most alarming finding was the high ground sinking gradient recorded when moving from the land strip at the foothills towards the plain.

In 1985, the Bologna Municipality, in agreement with the Regional Authorities, sponsored a study devoted to show the interrelations between piezometric head sinking and land subsidence, in the light of planning groundwater management. The study evidenced that subsidence is primarily caused by groundwater withdrawals. The high subsidence rates recorded in the early ‘80s imposed to shut down many water wells, and surface water replaced the supply of underground waters. Land subsidence monitoring and control was performed by leveling and, recently, by differential SAR interferometry (from May 1992 to July 1993, and from June 1997 to August 1998, Figure 4). The comparison of the two subsidence maps shows a decrease of the subsidence velocity from 1992 – 93 to 1997 – 98. The result of SAR interferometry shows subsidence rates from 10 mm/year the city centre up to 60 mm/year in the North-East outskirt (Figure 5). According with Stramondo et al. (2006) it can be affirmed that the combined analysis of remote sensing results, together with the geological and hydrogeological study of the area allowed to advance an interpretation of the detected movements as partially due to natural causes (tectonic subsidence) and to anthropogenic ones (water production).

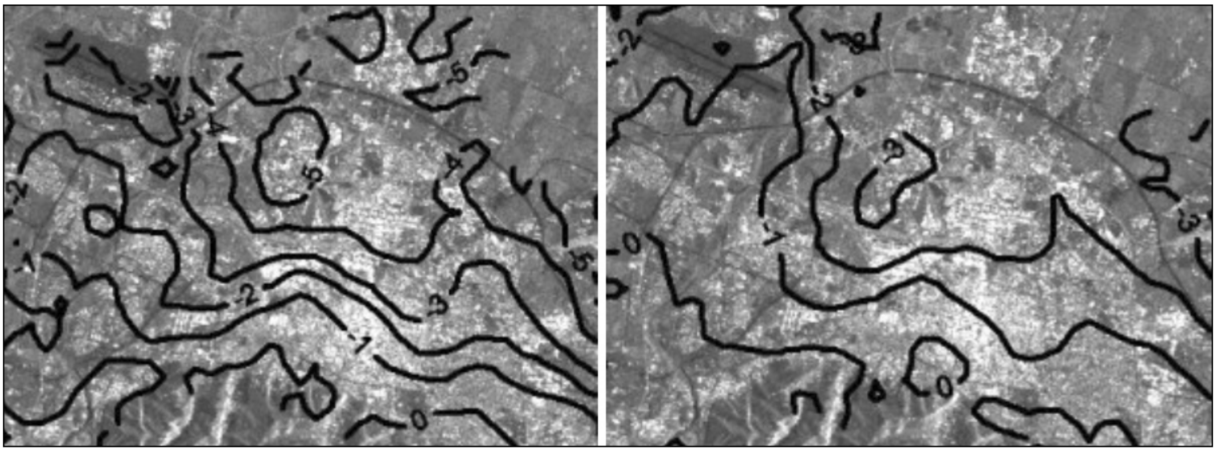

Figure 4: Subsidence rate (cm/year) in Bologna city centre from 1992–93 (left) and 1997–98 (right) http://www.gamma-rs.ch/termov.php?subp=11.

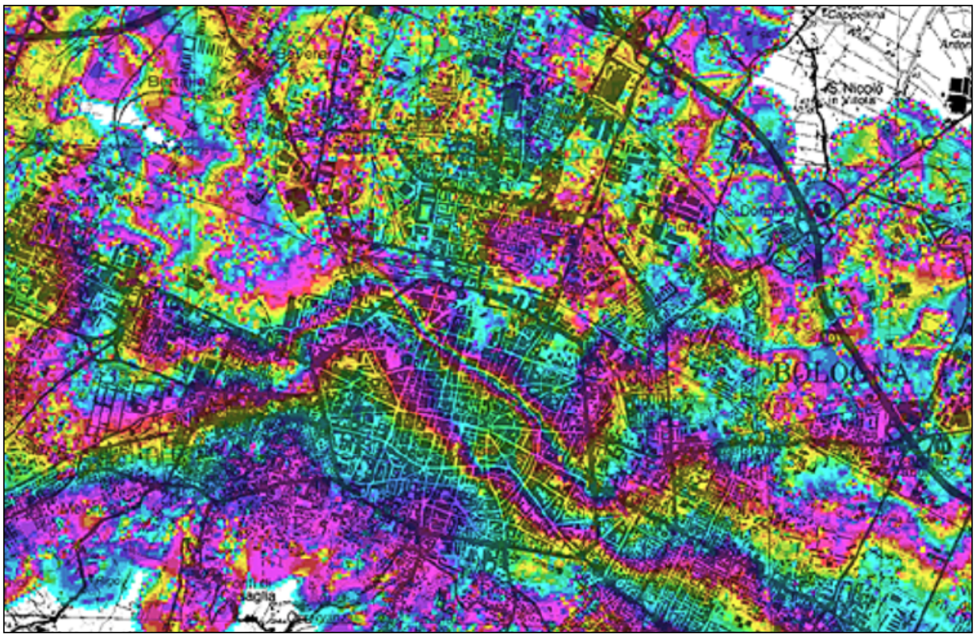

Figure 5: Areas of subsidence in the town of Bologna by satellite imaging. By comparing interferometry mages taken at different times by the ASAR on board ENVISAT, the tiniest movement of the earth surface can be observed. This technique is extremely sensitive, and displacements in the order of millimeters can be measured from space. The maximum displacements are identified by the purple/red colored spots. © ESA http://envisat.esa.int:80/applications/la/_2.html.

## Laboratory measurements and on-site compaction investigation

A laboratory measurement of formation compaction involves the estimation of compressibility coefficients. These are normally investigated with stress/strain tests performed in oedometric or triaxial conditions, in order to obtain the uniaxial compressibility coefficient, the most utilized in subsidence numerical analyses. Normally, all laboratory measurements are carried out on small samples (in the range of a few cm) cored from underground formations with disturbed and undisturbed techniques. Due to the reduced dimension of the samples, it is difficult to provide information on the presence of macro-discontinuities and their effects. Notwithstanding these limitations, lab measurements are valuable in providing direct information on the mechanical behavior of the formations. Other possible disturbances induced on lab samples are due to: a) coring operations, b) transportation and c) laboratory preparation. Obviously, the disturbance increases from consolidated to loose and unconsolidated formations. During coring operations, the material is subjected to vibrations, torsion and to the action of the drilling fluid. Once cut, the cores are also subjected both to tension release and fluid expansion. Moreover, while being prepared for transportation to the lab, the cores may be damaged, especially if protected by a rubber sheath only, as occurs with rubber-sleeve core barrels. Finally, the test plugs are taken from the cores using devices which often require that the sample be frozen first, (especially in friable or loosely cemented rocks), inducing further disturbance. The above disturbance can modify the layout of the grains (grain sliding along the edges, especially in loose or weakly cemented rocks), eventually opening micro-fractures. Moreover, some grains may have plastic deformations, pores may collapse, and fractures may even open up in well-cemented rocks during tensions release. All the above can cause severe changes to the mechanical properties of the material, that are usually irreversible, even if samples are restored to the original stress conditions.

Other causes for error may be the differences between the stress and strain state that exists on-site and the one applied to the cores during lab measurements. Firstly, the overburden pressure may not necessarily be instantly released onto the bottom layers, due to the visco-elastic behavior of many materials, a behavior that is difficult to investigate within a laboratory time frame. In addition, the mechanical characteristics of surrounding formations may be different from those of the reservoir under depletion. In this case, the so-called arch effect can develop, making part of the overlying load to be supported by the stiffer nearby formations (Brighenti et al. 1998).

As far as the on-site compaction investigations are concerned, these are carried out by measuring the changes in distance between two or more points. At present, two main techniques are available and described in the following: a) extensometers, which measure the change in distance between the surface and one or more points at different depths; b) logging, which measures the changes in distance between two or more points in the subsoil by running into a measurement well a specially equipped wireline tool.

### *Extensometers*

In 1955 the United States Geological Survey (USGS) conceived a cable extensometer to make measurements in the San Joaquin Valley. The equipment, a steel cable anchored at the bottom of the well, is held under constant tension by means of a weight at the well bottom, and a counter-weight at the surface. Every variation in the length of the well, resulting from changes in the thickness of the subsoil strata, is revealed by a shifting of the counterweight connected to a recording system. The basic principle of the equipment is to drop the tensor weight down to the well bottom and measure the length of the wire against a benchmark at the surface. One of the most sophisticated version of cable extensometer has been set up in the Groningen gas field (The Netherlands), in which a balance bar provides the cable counterweight connection and the external parts were installed in a shed in which an adequate heating equipment ensured a constant temperature (De Loos 1973). In 1966, the USGS introduced the free pipe (or bar) extensometer, consisting of a protective column (often the casing of an old well) containing a steel bar attached to the formation a few meters below the casing shoe, with a clearance between the two pipes of about 5 cm, to reduce friction. This instrument was used to depths around 1000 m.

In Italy, the first cable extensometer was used in the 1960s to investigate subsidence in the Po Delta. The public debate about such causes had been going on for years, and was eventually solved when conclusive evidence was provided by the combined use of topographic surveys and on-site compaction measurements. The extensometers discussed so far are used to measure the total compaction of layer comprised within the depth of the well. In order to measure the compaction of each single stratum, it is necessary to use several wells of different depths or adopt a multiple completions, which imply fewer costs, but a lower degree of accuracy. In recent years, modern extensometers have been installed in Bologna and Ravenna. Specifically, the Municipality of Bologna installed three bar extensometers in the period from 1987 o 1989 (Brighenti et al. 1998). Two of them were installed in a well, 300 m deep, with the bars anchored at 147 m and 246 m, respectively. The third one was installed in another well, 75 m deep, with the bar anchored at 50 m. More recently, in the neighboring of Ravenna, two extensometric stations have been set up. In the first one, two extensometer bars were installed (1994) at depths around 370 m and 220 m, while in the second one, two extensometers were installed (1997-98) at approximately 20 m and 340 m (Figure 6). These instruments are equipped with electronic data gathering and remote control systems (Agip-Comune di Ravenna 1997).

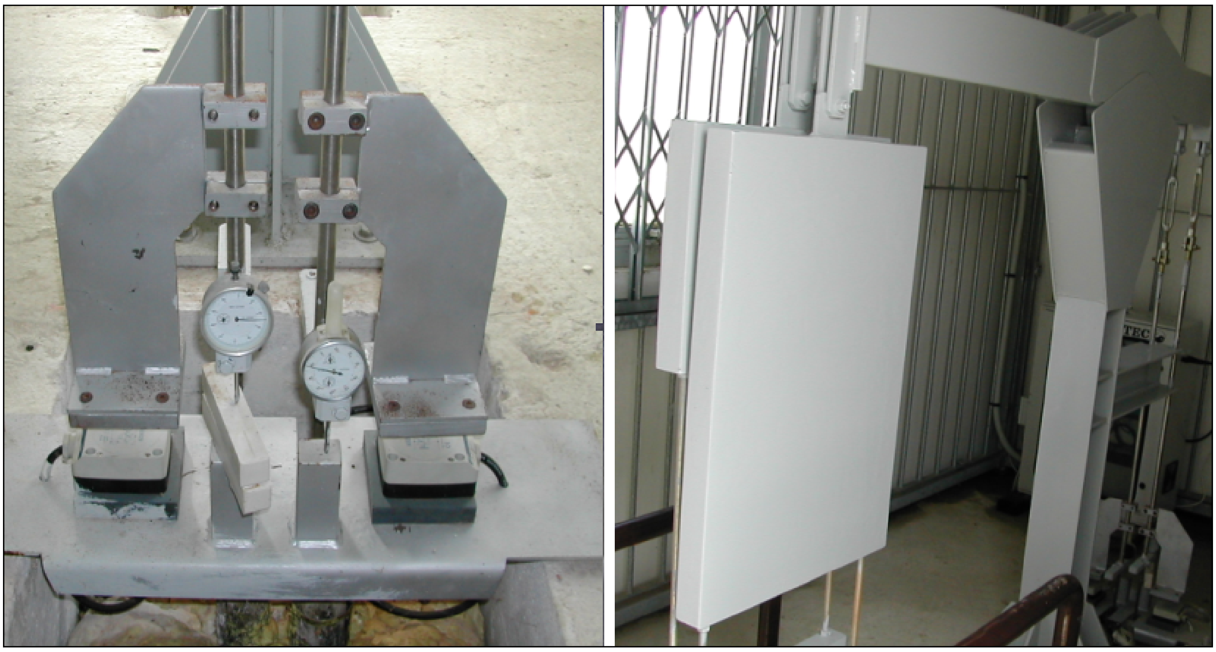

Figure 6: Surface equipment of the bar extensometer installed in the neighboring of Ravenna.

Extensometer equipments (cable or bar) provide sufficiently precise measurements of layers compaction between the land surface and the anchoring point, if the following conditions are satisfied: 1) the surface platform, with respect to which the extensometer movement is measured, must be firmly anchored to the land surface and not allowed to settle; 2) the extensometer must be firmly anchored to the selected underground formations; 3) the measuring system, especially the casing, must not alter the stress and strain state around the borehole. In particular, the casing is much less subjected to compression than the formations to which it is attached by friction (in the case of a cemented pipe, one must consider the pipe-cement and cement-rock friction). In the absence of the appropriate slip joints and/or a soft grouting, in the immediate vicinity of the borehole, the column will tend to reduce compaction of the formation, shifting down the anchoring point of the extensometer (pile effect). 4) the cable or the bar must not change in length. It is therefore essential to avoid the use of materials sensitive to creeping and temperature variations. In any case, it is recommended to use sensors to measure the temperatures at different depths. It is important to minimize the friction forces between the cable, bar or pipe and the casing in the contact points; 5) there must be no instrumental drift. Following the above suggestions, it is possible to measure length variations with very good accuracy, of the order of one part over one million.

### *Logging*

Compaction monitoring by means of well logging techniques (both open hole and cased hole) can be achieved by several methods, the most accurate of which involves the use of Radioactive Markers, or bullet Technique (RMT). The method employs time lapse monitoring of the spacing changes between bullets placed into the formations, and is based on the placement of low-emission radioactive markers in the formation under depletion (Macini and Mesini 2000). In order to evaluate the possible compaction in the very early stage of production, the markers should be implemented before casing operations. The positions of each marker can be determined by specialized wireline Gamma Ray (GR) logging tools, which are run at regular time intervals to estimate the possible temporal changes in the distance between the markers.

RMT adopts marker spacing of the order of 10m, a distance dictated by the geometry of the logging tool. The markers are characterized by a radioactive source ($Cs^{137}$ or $Co^{60}$, with half-times of about 5 years) contained inside a bullet-shaped steel case. Source strength ranges between 150 and 300 _Curie. The radioactive source is sealed inside a leak-proof steel container, inserted into the hardened steel body of the bullet to avoid problems of environmental contamination. The bullets, similar to the ones used for casing perforation, are shot by means of a bullet gun perforator, using a small explosive charge (usually, 5 to 20 g), variable according to the formation properties and borehole conditions. The selection of the correct amount of explosive is very important for the effectiveness of the measurements. In fact, the marker must be implemented not too deep inside the formation (to avoid difficulties for its detection, being the GR response too weak to measure), and not too shallow, to avoid a possible dislodging by centralizers when casing is set. The critical stage of RMT can be split into two major points: a) the detection of markers positions, and b) the measurement of relative distance between each pair of adjacent markers. The location of each marker can be calculated by using several methods, either based on numerical techniques, or on the physical principles of GR measurements.

In 1992, a campaign to control formation compaction due to gas production was started in the North-Central Adriatic Sea, and today several offshore fields are instrumented with radioactive markers. Marker spacing is periodically surveyed every one or two years, depending on the reservoir depressurization. During the measurements the static reservoir pressure is recorded for each interval, which is necessary for the estimation of formation compressibility. It is known that compressibility values obtained by RMT are smaller than the ones obtained with laboratory oedometric tests. The difference is about one order of magnitude, by comparing with the second loading cycle, and even more, by comparing with the first loading cycle. Many studies have been performed recently in the attempt to study the above phenomena, as well as to establish the reliability of RMT measurements and their applicability in subsidence modeling. Analyses have been made in various operative scenarios, taking into account possible uncertainties of the major factor governing subsidence (Macini and Mesini 2002; Baù et al. 2002; Ferronato et al. 2004).

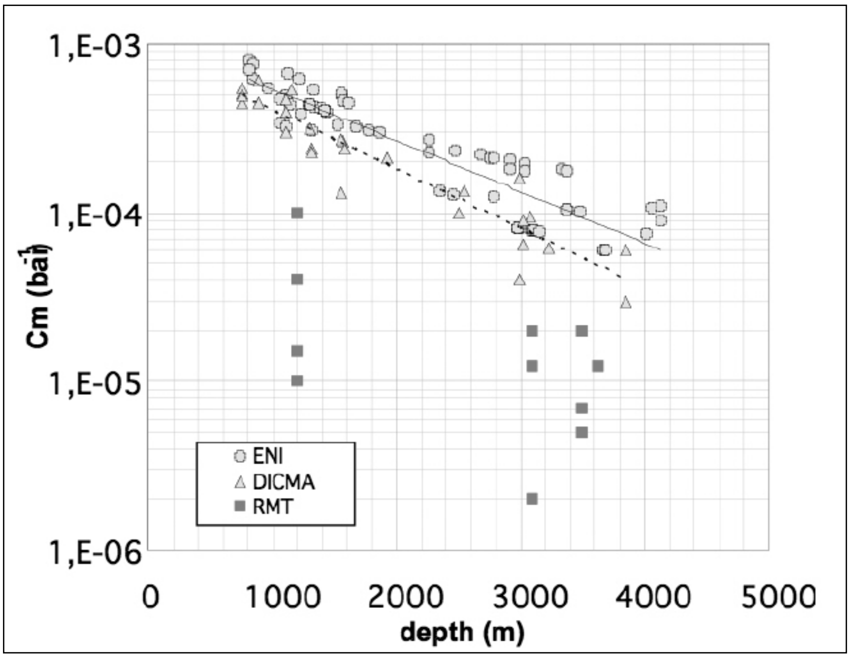

*Figure 7: Differences between lab and in situ uniaxial compressibility (Cm) measurements. Data provided by ENI, University of Bologna (DICMA) and measurements derived from RMT (rearranged from: Brighenti et Al. 1998; Cassiani and Zoccatelli 2000).*

However, it seems that a possible source of error in the interpretation of RMT measurement has been neglected. In fact, a constraint of on-site measurement techniques is that they are necessarily performed in the vicinity of the well bore. Here, due to perturbations of the strain state of the formations induced by drilling and by the presence of a relatively rigid cemented steel casing, the compaction around a cased hole seems lesser than the one of the virgin formation (Macini and Mesini 2006). Moreover, these perturbations are more evident in the close vicinity of the borehole, and in the case of loose or unconsolidated formations (clay, silt and sand), characterized by a rigidity smaller than the one of steel casing. As a result, measuring reservoir compaction inside cased holes, by means of on-site techniques, might not be representative of the compaction in the undisturbed zone, especially when the formation is loose or unconsolidated.

Today, it is common practice in subsidence modeling to utilize compressibility values derived from laboratory measurements, being on-site measurements not yet so much widespread, developed and, in some cases, consistent. The comparison between lab and on-site measured compressibility shows that there are appreciable discrepancies. Also, different compressibility values derived from studies on several Northern Italy and Adriatic gas fields have been found. Figure 7 reports the uniaxial compressibility derived from laboratory measurements in oedometric conditions, performed at our Department (DICMA), regarding Po-Veneto Plains and Ravenna offshore area, and those supplied by ENI (Brighenti et al. 1998). Moreover, the figure reports also RMT-derived compressibility measured in several Adriatic offshore reservoirs. All of these values refer to loose or poorly cemented formations from reservoirs or surrounding rocks, at depths ranging from 500 to 5000 m.

In particular, Figure 7 shows the compressibility vs. depth. One can notice that each of the two groups of values that derive from lab investigation (not necessarily measured by the same technique) is well correlated, and these values do not seem to depend on the sampling site, despite of deriving from formations sampled over a vast geographic area. Also, it can be noticed that ENI values are more conservative with respect to DICMA ones. Moreover, lab measured compressibility are higher (even of one order of magnitude) than the ones estimated on-site.

## Conclusions

After a review of compaction of water/gas bearing formations in Northern Italy (and in particular Bologna and Ravenna areas), the paper focused the probable causes of error in lab measurements of compressibility of samples cored from underground formations. A review of the various techniques for on-site investigations is presented, along with their causes of error due both to imprecise equipment and the different behavior of formation in the vicinity of the borehole.

The comparisons between lab and on-site results, for hydrocarbon reservoirs and aquifers, seem to indicate that on-site investigations are more reliable. However, it should be noted that such an investigation provide only the estimation of the compaction at the time of the measurement, but cannot predict changes in the mechanical behavior of the rock layers as effective vertical stress increase, especially, in normal-consolidated formations. This behavior can be predicted by using laboratory measurements. It is therefore advisable to carry out on-site investigations, as well as laboratory measurements, and to compare these results with those obtained from high-precision leveling.

At present, in Italy the most critical area is the Northern Adriatic offshore, where numerous gas reservoirs with large reserves have been discovered. As a consequence of the environmental and artistic importance of the Venice lagoon, the Italian Authorities are requesting in-depth studies in order to correctly identify the various mechanisms governing subsidence phenomena. In particular, investigations are currently under way by developing both sophisticated systems to monitor coastline subsidence, and mathematical models able to predict the effects of gas production, possibly identifying the adequate tools and exploitation techniques. Numerous tools and techniques are available, such as those that allow for an appropriate choice of the compaction coefficients, by comparing the results of laboratory and on-site measurements. The development of advanced mathematical modeling, the possibility to provide reliable and consistent input data, together with the accurate high precision leveling, GPS or SAR, is transforming the subsidence management into a proven and adequate technique, that in the future will not be enforced without important economic investments.

## References

- Agip-Comune di Ravenna (1997) Installazione di due stazioni assestimetriche per il controllo della compattazione superficiale nei pozzi Smarlacca 1 e PCTA 1. Ravenna Municipality Report.
- Baù D, Ferronato M, Gambolati G & Teatini P (2002) Basin-scale compressibility of the northern Adriatic by the radioactive marker technique. Géotechnique 52(8):605-616.
- Bertoni W, Brighenti G, Gambolati G, Ricceri G & Vuillermin F (1995) Land subsidence due to gas production in the on- and off-shore natural gas fields of the Ravenna area, Italy. Proc. 5th International Symposium on Land Subsidence, The Hague:13-20.
- Bertoni W (2004) La subsidenza di Ravenna: lo stato attuale in relazione alla coltivazione dei giacimenti a gas. Servizio geologico e protezione civile, Ravenna Municipality Report.
- Brighenti G, Borgia GC & Mesini E (1995) Subsidence studies in Italy. In Chilingarian GV, Donaldson EC, Yen TF Eds, Subsidence due to fluid withdrawal, Elsevier, Amsterdam:215-283.
- Brighenti G, Macini P & Mesini E (1998) Subsidence in Northern Italy: compaction measurements of water-gas bearing formations. Proc. 8th IAEG Congress, Vancouver:207-214.
- Brighenti G, Macini P & Mesini E (2001) Underground Fluid Withdrawals and Subsidence in Coastal and Urban areas of Northern Italy. Proc. International Symposium “EngGeolCity-2001, Engineering Geological Problems of Urban Areas”, Ekaterinburg.
- Cassiani G & Zoccatelli C (2000) Towards a reconciliation between laboratory and in-situ measurements of soil and rock compressibility. Proc. 6th International Symposium on Land Subsidence, Ravenna, Vol. II:3-15.
- De Loos JM (1973) In situ compaction measurements in Groningen observation wells. Verhandelingen Kon. Ned. Geol. Mijnbourwk., 28:80-102.
- ESA European Space Agengy (1998) Processing by GAMMA http://www.gamma-rs.ch/findit.php?search_term=&content=bologna.
- Ferronato M, Gambolati G, Teatini P & Baù D (2004) Radioactive marker measurements in heterogeneous reservoirs: numerical studies. International Journal of Geomechanics 4(2):79-92.
- Folloni G, Radicioni F, Russo P (1996) La subsidenza del territorio bolognese dal 1983 al 1993. Inarcos, 6:400-413.
- Gambolati G, Teatini P & Ferronato M (2005) Anthropogenic land subsidence. Encyclopedia of Hydrological Sciences, Anderson MG Ed. Wiley & Sons, New York.
- Holzer TL, Galloway DL (2005) Impact on land subsidence caused by withdrawal of underground fluids in the United States. Geol. Society of America, Reviews in Engineering Geology, 16:87-99.
- Macini P & Mesini E (2000) Compaction monitoring from radioactive marker technique. Proc. 6th International Symposium on Land Subsidence, Ravenna, Vol. II:43-55.
- Macini P & Mesini E (2002) Measuring reservoir compaction through radioactive marker technique. Journal of Energy Resources Technology 124:269-275.
- Macini P, Mesini E, Salomoni V & Schrefler B (2006) Casing influence while measuring in situ reservoir compaction. Journal of Petroleum Science and Engineering 50:40-54.
- Stramondo S, Saroli M, Tolomei C, Moro M, Doumaz F, Pesci A, Loddo F, Baldi P & Boschi E (2006) The subsidence in Bologna city (Italy) and in the Po Plain detected by InSAR SBAS technique. Geophysical Research Abstracts 8:71-92.
- Teatini P, Gambolati G, Tomasi L & Putti M (1998) Simulation of land subsidence due to gas production at Ravenna coastline. In CENAS, Kluwer Water sciences and tech. lib., n. 28:133-150.
- Teatini P, Ferronato M, Gambolati G, Bertoni W, Gonella M, Morelli M & Severi P (200) Land subsidence due to groundwater withdrawal in the Emilia-Romagna coastland. Proc. 7th International Symposium on Land Subsidence, Shangai:55-64.
- Vicari L (1998) Il controllo e la sostenibilità della subsidenza in Emilia-Romagna. Proc. Geofluid 98, Piacenza:7-18.

# DARCY 16

## Evidence of deep flux assending into Arax basin aquifers through active fault extension

Kharatian K.[1], Travi Y.[2]
[1] Department of Geology, Yerevan State University, 1 Alex Manukyan, 375025 Yerevan, Armenia
[2] Laboratory of Hydrogeology, University of Avignon, 33 Louis Pasteur, 84000 Avignon, France
kharatiankaren@yahoo.com

This study concerns the isotope behavior of confined aquifer of Arax basin, the West part of central Armenia. The stable isotopes ($^{18}O$, $^{2}H$, $^{13}C$) analyses have been conducted during 2 years study. The samples of water were taken as from aquifer boreholes so out of natural outlets. The hydrogeological and hydrochemical context of Arax basin have been specified, especially the existence of deep water (with positive $\delta^{18}O$ and $\delta^{13}C$).

At the time of any regional (M>6) and local (3<M<6) seismic activity ,,anomalous,, variations in $\delta^{18}O$, He and piezometric heads were observed.

The relationsheep between $\delta^{18}O$ and $\delta^{2}H$ indicated that the Arax basins groundwater isotopicaly re-equilibrated with deep $CO_2$. This re-equilibration induces the ,, permanent aporevishment, of $\delta^{18}O$ (Fontes, 1976). An evidence of positive $\delta^{13}C$ CMTD values is also the result of deep $CO_2$ existence (Clark et Fritz, 1997). The source of the deep $CO_2$ could be the carbonate-metamorphic matrix (Morse et Mackenzie, 1990) of Arax basin in depth of about 2000m.

The existence of positive $\delta^{18}O$ and $\delta^{13}C$ values and high mineralisation (10-15 g/l.) of water samples taken out of water outlets could be explained by the thermo-metamorphic exchange reaction between groundwater and adjacent strate.

The presence of the thick Quaternary stratum of travertins in the area of investigation, the formation of travertins up to now, as well as the results of these investigations confirm the idea of the existence of active fault extended through basin in Arax-Vedi direction.

### References

Clark I., Fritz P. 1997 – Environmental isotopes in Hydrogeology. Lewis Pulishers, New York, 328p.
Fontes J.-C. 1976 – Isotopes du milieu et cycles des eaux naturelles. Quelques aspects. These de doctorat d` Etat , Paris, 208p.
Morse J., Mackenzie F. 1990 – Geochemistry of sedimentary carbonates. Elsevier, Amsterdam, 707p.

# DARCY 17

# From local investigations to large management: multiscale integration of data for groundwater assessment in regional aquifers

LARROQUE François[1], de GRISSAC Bruno[2], DUPUY Alain[1],
FRANCESCHI Michel[1], CONDOM Thomas[1]

[1] EGID University of Bordeaux 3, [1] allée Daguin, 33607 Pessac, France, larroque@egid.u-bordeaux.fr
[2] SMEGREG, 74 Rue Georges Bonnac, 33000 Bordeaux, France

## Abstract

Although a lot of aquifer management applications exist, few methodologies seem to be adapted to the resolution of regional scale problems. The applications for multilayered aquifers are also limited. A methodology is applied to a real management case concerning the regional Aquitaine multilayered aquifer (France). A representative hydrodynamic model is built using MODFLOW 2000 code in association with a local semi analytical 2D model for transient wells simulations. To reduce some potential environmental risks induced by overexploitation of Eocene resources, a substituting pumping field is planned. Several different scenarii of local management are tested and integrated into the global model. Global simulations are used to specify the implantation of the planned pumping field. The local impact of the planned pumping field is also simulated. The management of the pumping plan is made by coupling the different models with optimization techniques. The obtained optimal solutions allow proposing viable exploitation alternatives integrating shifted environmental constraints.

## Introduction

Regional aquifers are specific hydrogeologic systems because of their large horizontal extension. This huge geographical area is generally associated to an important vertical extension especially for regional sedimentary multilayered aquifers. To proceed to a quantitative management of such aquifers it is necessary to study several temporal and spatial scales to fully characterize the system and to take into account all phenomena, using different data types and complementary tools. The objective of the work presented in this paper is to introduce a common framework for the study of large aquifers for an applied research of groundwater resources. A specific strategy of integration of data, from field investigation to numerical models and optimization procedures, is here presented to take into account all characteristics of multilayered aquifers.

To reduce some potential environmental risks induced by overexploitation of Eocene resources, a substituting pumping field is planned. Oligocene resources are aimed and the annual exploitation planned is about $4\ 10^6\ m^3$. To fully characterize the impact of this future exploitation on the whole system and to find the best pumping configuration, the following study framework is applied:

- construction of a quasi 3D transient regional model of groundwater flow describing the whole hydrogeologic system. Simulations are used to specify the implantation of the planned pumping field ;
- geological and structural characterization of the local selected site (high resolution seismic reflexion prospection and exploration wells) ;
- hydrogeological characterization of local aquifer units (pumping tests, long time pumping tests, study of natural piezometric head) ;

- modelling of local impact of the exploitation of the planned pumping field on the nearest existing pumping field of the target aquifer (both 2D analytical and semi-analytical models) ;
- local update of the regional numerical model, simulation of the planned pumping fields for different configurations obtained from the local model and estimation of the impact for the whole aquifer system ;
- management of the pumping plan respect to major environmental and economics constraints (optimization model linked to the regional flow model).

## Prior information and hydrogeological settings

Near Bordeaux (Gironde, France), groundwater is the main supply for drinking water. For this reason, the confined Eocene aquifer has been intensely exploited since the beginning of the century. However, in response to a new management policy, new potential resources have to be studied to protect the Eocene resource in term of quantity and quality. The Oligocene aquifer, shallower than the Eocene, appeared as an interesting target able to produce enough water for a good quality supply. The Medoc area appeared as a potential exploitation area. However, former studies of the geological formations in this region were not sufficient to give an accurate image of the hydrogeological circulation. The estimation of the impact of large withdrawals by the potential new exploitation requires a good knowledge of the reservoir geometry and an estimation of the relations between the different aquifers of the complex multi-layered tertiary system.

The study area is a part of the large Aquitaine Tertiary Basin, in the northern part of the Aquitaine (S-W of France) (Figure 1). This large sedimentary basin is composed by several sedimentary formations from Cretaceous layers to plio-quaternary deposits. Groundwater occurs under confined and unconfined conditions in geological formations mainly composed by limestone and sandy materials. The aquifer layers, covering a total area of 31000 km$^2$ are from the deepest to the shallower: deep Cretaceous, Eocene, Oligocene, Miocene and Plio-quaternary shallow formations. Confinement between aquifer layers is to aquitards of highly varying permeability. The multilayered aquifer is bounded westwards by the Atlantic shoreline. Eastwards, the aquifers layers present pinching out features at various distances, depending of the width of corresponding deposits area (Larroque, 2004).

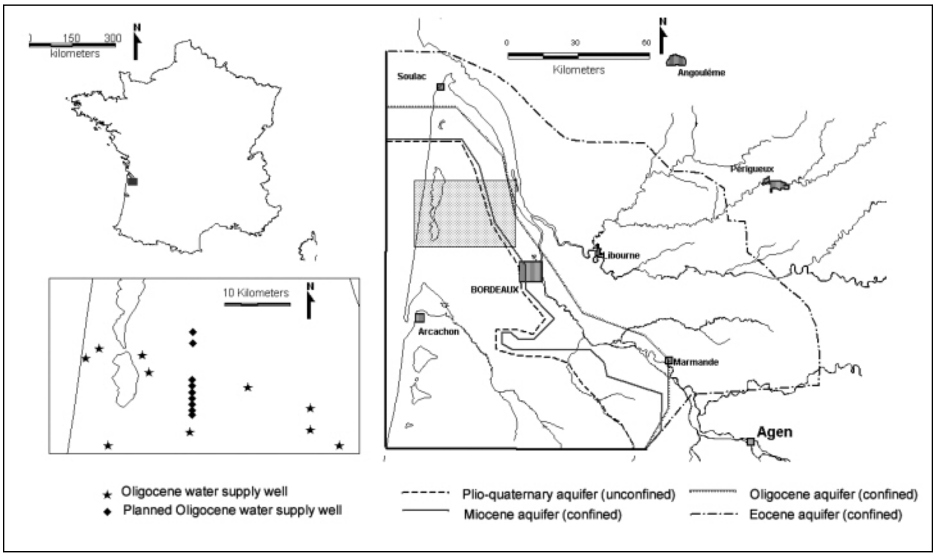

*Figure 1: Extension of hydrogeological formations and planned Oligocene pumping field*

## Improving geological and hydrogeological models

The tertiary aquifer succession in the area is composed, from the deepest to the shallowest part, by

1. the Eocene, formed by sandy limestone and nummulitic sands, overlaid by a marly layer,
2. the oligocene limestone, here called “calcaire à Astéries” formation,
3. the Miocene sandy limestone formations
4. Plio-quaternary formations made of gravels, sands and clays coming from Pliocene fluvial sediments.

From the tectonic point of view, the layers present a small regional dip, on the order of 0,1°. However, the studied area is located in the NW-SE extension of the “Bordeaux fault”. This well-known structure in the vicinity of the City of Bordeaux influenced the sedimentation during the Mesozoic. Pyrenean deformations induced reactivation of this fault from the Eocene to the end of the Oligocene. On the seashore, this fault was also identified in the Jurassic formations, but the deformations during Tertiary times appear to be mainly soft. Between Bordeaux and the seashore, on the study area, the influence of this structure is not well known, but the comprehension of its impact on Tertiary deposits is fundamental to understand the hydrogeological setting.

The study of the seismic lines made it possible to build the hydrogeological log of the area. We can identify : the Plio-quaternary formation (R1), the Miocene aquifer (R2), the Miocene aquiclude (E2), the Oligocene aquifer (R3), the Oligocene aquiclude (E3) and finally the Eocene calcareous aquifer (R4a) sometimes separated from another sandy aquifer (R4b) by a thin marly formation (Figure 2).

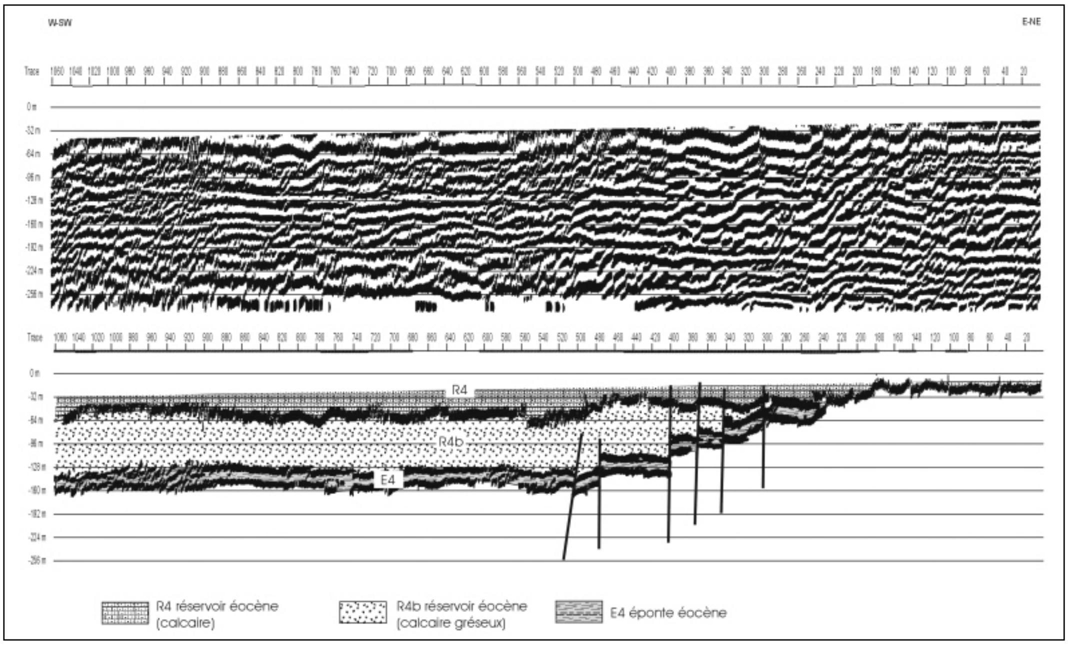

*Figure 2: Example of local seismic profiles and associate interpretation (Larroque and Dupuy, 2004)*

The combination of the seismic profiles and exploration wells display the structure of the Tertiary deposits in the central Medoc area (Figure 3). Previous work pointed out the influence of the western extension of the "Bordeaux fault" on the Oligocene and Miocene deposits. However it appears today that this influence only generates soft deformations in Oligocene deposits, without discontinuities in the formations

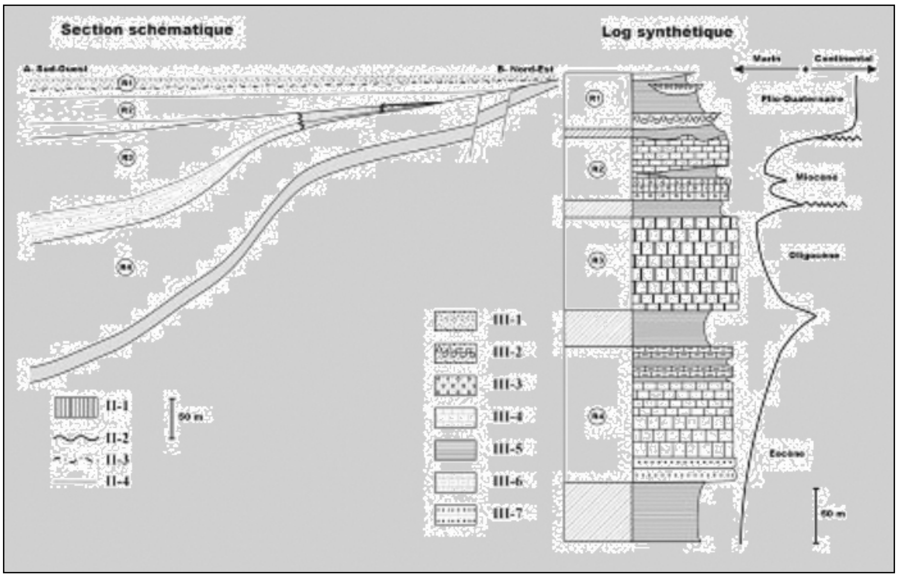

*Figure 3: Geological and hydrogeological structure of the Tertiary in the Medoc area (Larroque and Dupuy, 2004)*

## Local scale modelling: the semi-analytical approach

A 2D semi-analytical approach is here employed to provide an accurate description of the impact of planned groundwater extraction on the vicinity of the pumping field. A two dimensional model is built using a Voronoi grid (figure 4).

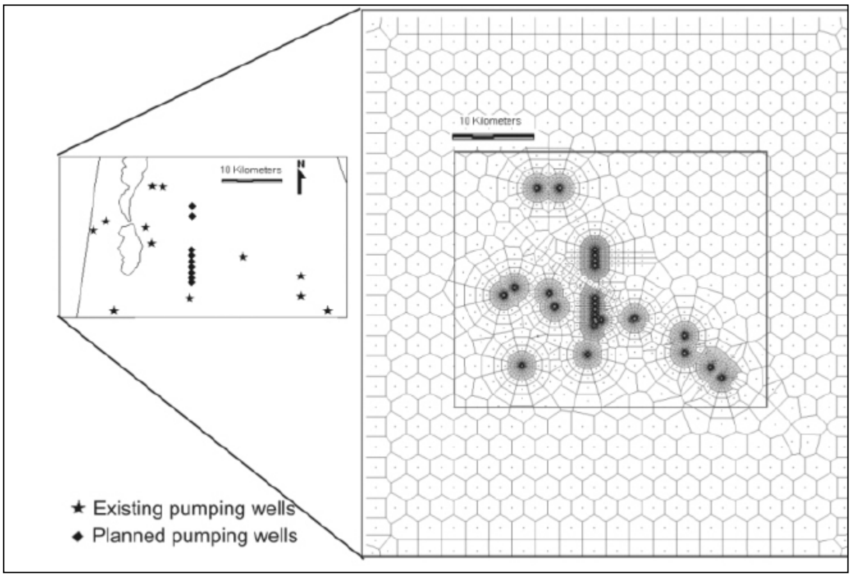

*Figure 4: 2D local model of medoc an oligocene aquifer (Larroque and Dupuy, 2005)*

Transient simulation is realised including the 9 planned wells exploited with the predicted pumping rate of 150 m$^3$/h, 12 hours per day. The total time duration of the simulation is 12 months. The pressure distribution computed for the pumping field shows maximum values of drawdowns reaching 32 meters after 12 months. The drawdowns decrease quickly while moving away from the exploitation field. Thus the impact on others existing wells is limited. On the other hand, the drawdowns computed for the exploitation field are not compatible with the local geometry of the aquifer, inducing probably a local dewatering. It appears clearly that a new configuration and/or a new site has to be considered for the pumping field to satisfy the increase of water demand in the area.

## Large scale modelling: toward management models

A regional model is used to estimate the impact of the exploitation on the whole system. The finite-difference computer code MODFLOW (Harbaugh et al., 2000), which numerically approximates the equations of groundwater flow is retained. The model covers a total area of 31000 km$^2$, including 8 layers matching 4 main confined aquifers and the 4 aquitards. The subsurface unconfined aquifer is taken into account just like the relations between aquifers and surface hydrographic network (Figure 5). The study area is discretised into 30,895 cells by layers with 185 columns and 167 rows, using square cells of 1 km. Initial values of transmissivity and storativity, known from pumping test, are integrated. Calibration was done under steady-state and transient-state. Transient-state simulations were carried out for a period of 20 years. The final computed heads show a good agreement with the observation. The relative mean error is in order of 5%.

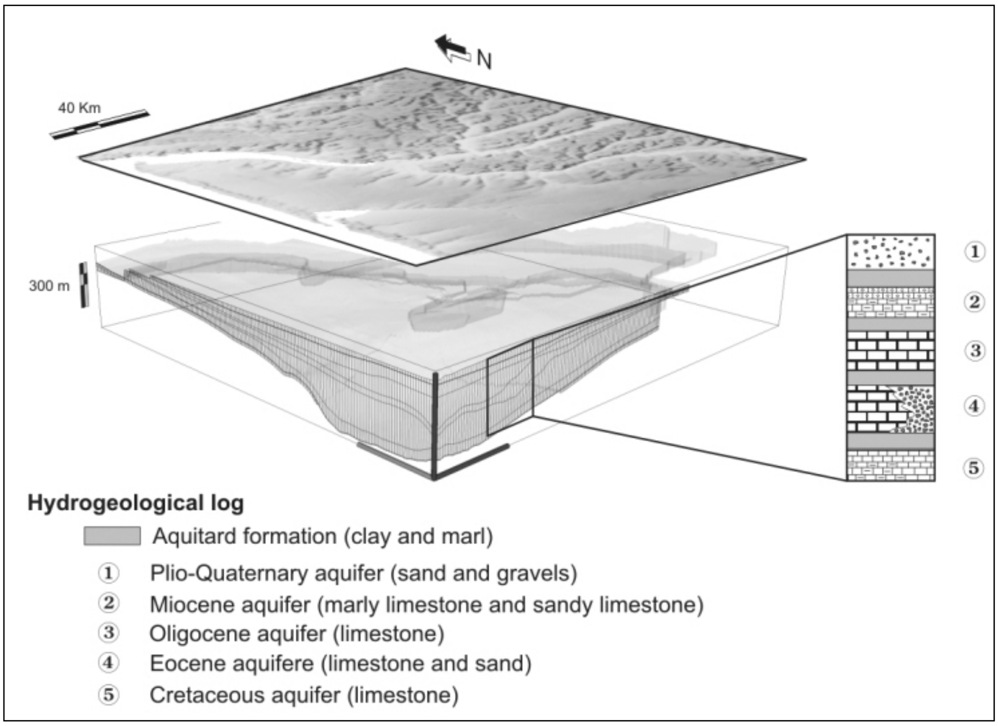

*Figure 5: Quasi 3D groundwater model of regional multilayered system (Larroque and Dupuy, 2005)*

## Conclusion

A multiscale approach was conducted to fully characterize the impact of a large pumping field on a complex multilayered aquifer. The use of two kinds of models each one representative of a particular phenomena scale lead us to a better understanding of the impact of the planned exploitation.

A regional multilayered FD model indicates that the groundwater pumping increase can be supported by the aquifer system, without particular problems. The regional impact on the exploited aquifer is quite moderate and the disturbances induced by leaking exchanges with others aquifers are minimal.

A local 2D semi-analytical model characterizes the impact of the exploitation at a local scale. It is shown that the drawdowns generated at the periphery of the pumping field after 1 year of exploitation are not compatible with the geometry of the oligocene aquifer. Local dewatering of the aquifer seems to be inevitable.

Thanks to this general framework some technical solutions planned have been dismissed and an optimal pumping plan was given. In addition, other tracks underlined during this procedure allowed us to suggest new propositions for water substitution resources. To conclude, this work highlights the interests to use several scale to fully characterize complex regional multi-layered aquifers in order to resolve applied problems.

## References

- Harbaugh A W, Banta E R, Hill M C, McDonald M C (2000) MODFLOW-2000, the U.S. Geological Survey Modular Ground-Water Model-User guide to modularization concepts and the ground-water flow process, Open-File report 00-92, 121 p.
- Larroque F (2004) Global management of complex aquifer system : application to the medocan multilayered aquifer system , Ph. D Thesis, Bordeaux 3 University, 254 p.
- Larroque F and Dupuy A (2004) Apports de la méthode sismique réflexion haute résolution à l'identification des structures profondes des formations tertiaires en Médoc (Gironde, France) : implications hydrogéologiques, C.R. Geoscience 336, 1111–1120
- Larroque F and Dupuy A (2005) Multi-scale modelling of large pumping field: the case study of the Oligocene aquifer (Gironde, France), In: Proc Fifth International Conference on Calibration and Reliability in Groundwater Modelling, From Uncertainty to Decision Making (ModelCARE 2005), pp. 112-117.

# DARCY 20

# Natural depletion of a large aquifer explained by isotopic, geochimical and hydrodynamic data

Douez O., Dupuy A., Franceschi M. and Atteia O.
Institut EGID - University of Michel de Montaigne – Bordeaux 3
1, allée Daguin, 33607 , Pessac, France
olivier.douez@egid.u-bordeaux.fr

Isotopic, geochemical and hydrodynamic parameters can bring significant information to apprehend the behaviour of deep aquifers such as the main upper Infra-Molassic Sands (IMS) aquifer of the Aquitain Basin (Southwest of France), located in a multilayered aquifer system.

The activity of the $^{14}C$ of the water of the IMS gives an apparent age varying from – 5,000 and – 35,000 years BP. The majority of the samples ranges from – 15,000 to – 29,000 years. The data of the subjacent aquifers also show similar ages. The spatial distribution of these data cannot show directions of flow and recent water age near the outcrops are not observed.
The mineralisation of the groundwater of the IMS in the eastern part can be explained only by the contribution of solutions coming from the upper molassic formation.
So, we can infer a recharge of the main aquifer by vertical downwards leakage. Moreover, the small surface of the outcrops could not give a significant recharge. The functioning of the IMS aquifer by a simple piston effect is not possible but seems to follow a pattern by vertical leakage.

The noble gases contents of the IMS water indicate paleo-temperatures several degrees lower than the current average temperature. The $\delta^{18}O$ and $\delta\ ^{2}H$ values confirm that the climate was colder than today.
Chronics of piezometric data show a decrease of the water level of the IMS. This decrease of pressure seems to be due to a natural depletion of the aquifer and not to the exclusive fact of pumping.
These last data prove that the current infiltration cannot maintain a permanent level of the groundwater. The aquifer has been in transitory state of draining since the last major phase of recharge which took place during the Pleistocene around the Last Glacial Maximum.

We can think that there is a relation of order between the dimension of the recharge and the dimension of the aquifer; the recharge cycle must be proportional to the size of the aquifer system. Major climatic events are at the origin of the recharge of the IMS groundwater, and more generally of some other aquifers of the multilayered system.

# DARCY 23

# Vadose zone in a mountain hydrogeologic system: Serra da Estrela (Central Portugal) case studyVadose zone characterisation in a mountain hydrogeologic system: Serra da Estrela (Central Portugal) case study

ESPINHA MARQUES Jorge[1], DUARTE João M.[2], CONSTANTINO Alfredo T.[2], MARTINS Afonso [3],
AGUIAR Carlos4, ROCHA Fernando T.[5], INÁCIO M.[5], MARQUES José M.[6], CHAMINÉ Helder I.[7],[5],
TEIXEIRA José[5], SAMPER Javier[8], BORGES Frederico S.[1], CARVALHO José M.[7]

[1] Dep. Geologia (CGUP), Univ. Porto, R. Campo Alegre 687, 4169-007 Porto, Portugal,
jespinha@fc.up.pt
[2] Agroconsultores, Lda., R. Sampaio e Pina 7 1ºDto., 1070-248 Lisbon, Portugal,
jduarte@agroconsultores.pt
[3] Dep. Edafologia, UTAD, Apartado 1013, 5001-801 Vila Real, Portugal,
amartins@utad.pt
[4] Centro de Investigação da Montanha (CIMO), IPB, ESA, Bragança, Portugal,
cfaguiar@ipb.pt
[5] Centro de Minerais Industriais e Argilas (MIA), Univ. Aveiro, 3810-193 Aveiro, Portugal,
frocha@geo.ua.pt
[6] Dep. Engª Minas Georrecursos, IST, Av. Rovisco Pais, 1049-001 Lisbon, Portugal,
jmmarques@mail.ist.utl.pt
[7] Dep. Engª Geotécnica, ISEP, R. Dr. A. Bernardino Almeida 431, 4200-072 Porto, Portugal,
hic@isep.ipp.pt
[8] ETSI Caminos, Canales y Puertos, Univ. Coruña, Campus Elviña, 15192 A Coruña, Spain,
jsamper@udc.es

## Abstract

Understanding the role of the vadose zone is essential to accurately assess hydrogeological systems and the respective groundwater resources. The study area (Manteigas – Nave de Santo António – Torre sector, Serra da Estrela Mountain, Central Portugal), presents specific geological, morphotectonical and climatic characteristics which contribute to control the hydrogeologic regime. The regional vadose zone has particular features that contribute to control both the quantity and the quality of the groundwater resources. The characterisation of this zone was carried out in terms of structure, soil broad physical, chemical and mineralogical features and soil hydraulics. The study included fieldwork campaigns focused on geological and pedological features, soil permeability field tests, laboratory tests (including soil water retention at different pressure heads and clay mineralogy) and geomathematical modelling. Water retention data were used to derive the parameters of van-Genuchten water retention curve. The resulting characteristic curves allowed comparing the hydraulic features of Serra da Estrela soils with soils from other locations.

## Introduction

Mountain areas are usually the source of water resources of great quality and significant social and economic importance. The seasonality and spatial variability of groundwater signatures as well as the complex role of soils, geomorphology, geology, climate, land cover and human activities on the hydrology of mountain areas is rather difficult to model, even when relevant data are available. Understanding the role of the vadose zone is essential to accurately assess hydrogeological systems and the respective groundwater resources (e.g. Dingman 1994, NAP 2001). In particular, one should consider soil formation factors such as parent material, topography, climate, organisms and human action, which also control the volume of infiltration and groundwater recharge.

The study area corresponds to the Manteigas – Nave de Santo António – Torre sector, located in Serra da Estrela mountain (Central Portugal), that is, the river Zêzere drainage basin upstream of Manteigas village. The regional aquifer system presents specific geological, morphotectonical and climatic characteristics which contribute to control the local hydrogeological regime. Therefore, the corresponding vadose zone has particular features that control both the quantity and the quality of the groundwater resources.

The study was performed from 2003 to 2005 in the scope of a multidisciplinary hydrogeologic research named HIMOCATCH R&D Project (Espinha Marques et al. 2005). This regional scale vadose zone characterisation — supported by geological, pedological and hydrogeomorphological analysis — focused on the soil broad physical, chemical and mineralogical features, vadose zone structure, and soil hydraulics. Soil hydraulic and mineralogical features in this sector result from the particular way how the pedogenetic factors act in a mountain environment.

The tasks carried out included fieldwork campaigns focused on geological and pedological features, field and laboratory tests and geomathematical modelling. Soil samples were collected at selected sites. Field soil permeability tests were performed. Laboratory tests were conducted in order to determine, among other aspects, water retention at different pressure heads and clay mineralogy. Water retention data were used to derive the parameters of van-Genuchten water retention curve. The resulting characteristic curves allowed comparing Serra da Estrela soils with soils from other locations. Additionally, the effect of texture and organic matter on soil water retention was evaluated.

## Hydrogeologic framework

The Serra da Estrela region is part of the Central-Iberian Zone of the Iberian Massif (Ribeiro et al. 1990). The main lithotypes occurring in the region are (figure 1): i) Variscan granitic rocks; ii) Precambrian-Cambrian metasedimentary rocks; iii) alluvium and quaternary glacial deposits. The most important regional tectonic structure is the NNE-SSW Bragança-Vilariça-Manteigas fault zone (BVMFZ). According to Ribeiro et al. (1990), the origin of the Serra da Estrela Mountain is connected to an uplift process related to the reactivation of the BVMFZ megastructure during Cenozoic times, by the Alpine compressive tectonics, together with the reactivation of major ENE-WSW trending reverse faults (such as the Seia-Lousã fault).

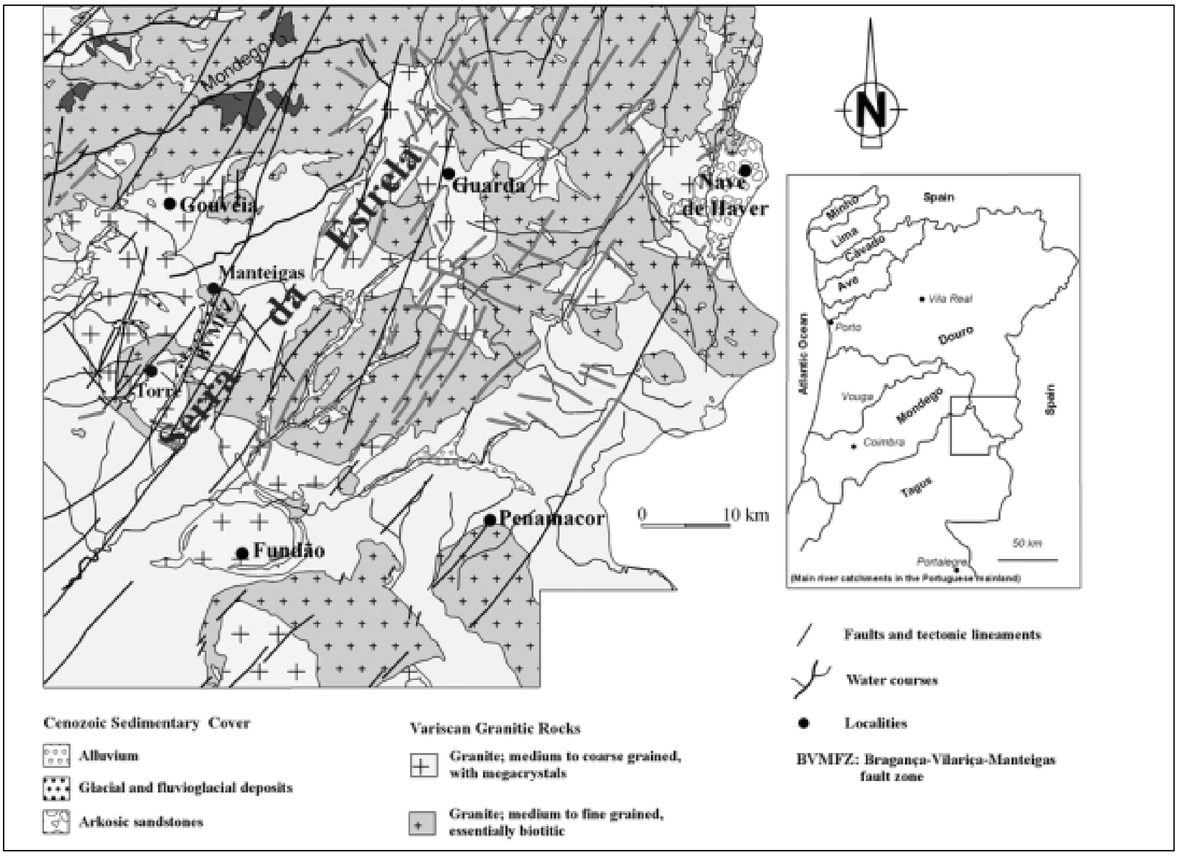

*Figure 1: Geological framework of Serra da Estrela region*
*(adapted from Geological Map of Portugal, 1/500.000, 5th Edition; Oliveira et al. 1992).*

An important issue related to the infiltration and aquifer recharge in the Serra da Estrela region consists on the identification of areas of prevailing fractured or porous circulation media (Espinha Marques et al. 2005). In particular, porous media are dominant in alluvium and quaternary glacial deposits as well as in the most weathered and brittled/sheared granites and metasedimentary rocks. Porous media usually occur at shallower depths (typically less than 50 m). On the other hand, fractured media occur in poorly weathered rocks. Such media may be present very close to the surface (especially on granitic outcrop dominated areas, with thin or absent sedimentary cover) or bellow the referred porous geologic materials. The regional hydrogeological units correspond closely to the major geological features (table 1): i) sedimentary cover, including alluvium and quaternary glacial deposits; ii) metasedimentary rocks, including schists and graywackes; and iii) granitic rocks.

Serra da Estrela is the highest mountain in the Portuguese mainland (with an altitude reaching 1993m a.s.l.) and is part of the Cordilheira Central, an ENE-WSW mountain range that crosses the Iberian Peninsula. This region shows distinctive climatic and geomorphologic characteristics that play an important role on the local water cycle. The river Zêzere drainage basin upstream of Manteigas, corresponds to an area of ca. 28 $km^2$ with an altitude ranging from 875 m a.s.l., at the streamflow gauge measurement weir of Manteigas, to 1993 m a.s.l., at the Torre summit (figure 2). The relief of the study area consists mainly of two major plateaus, separated by the NNE-SSW valley of the Zêzere river (Vieira 2004): the western Torre–Penhas Douradas plateau (1450-1993 m a.s.l.) and the eastern Alto da Pedrice–Curral do Vento plateau (1450-1760 m a.s.l.). Late Pleistocene glacial landforms and deposits are distinctive features of the upper Zêzere catchment, since the majority of the plateau area was glaciated during the Last Glacial Maximum (e.g. Daveau et al. 1997, Vieira 2004).

Espinha Marques et. al (2005) proposed 9 hydrogeomorphologic units, based on the spatial distribution of lithological, geomorphological and climatic features (figure 2): i) Eastern plateau; ii) Zêzere valley eastern slopes; iii) Lower Zêzere valley floor; iv) Nave de Santo António col; v) Upper Zêzere valley floor; vi) Zêzere valley western slopes; vii) Cântaros slopes; viii) Lower western plateau; ix) Upper western plateau.

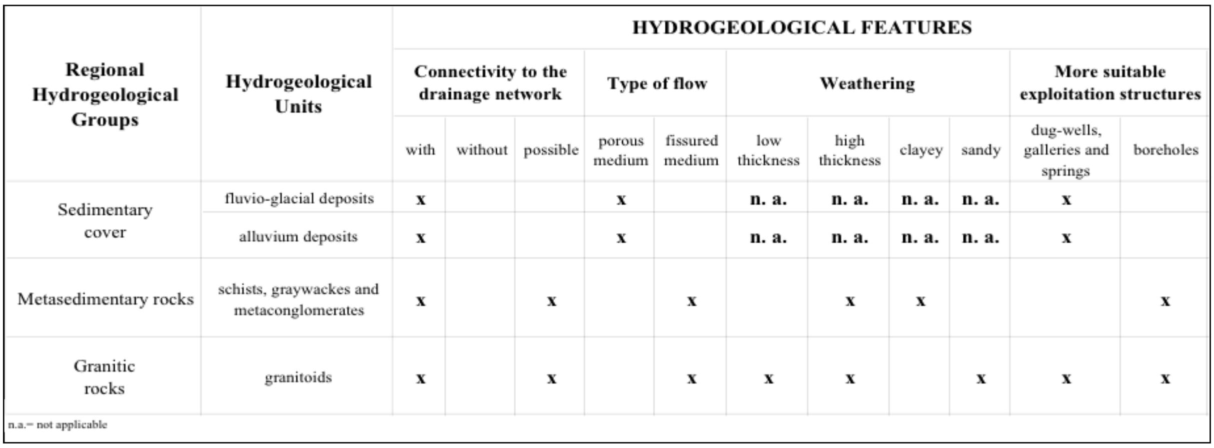

| Regional Hydrogeological Groups | Hydrogeological Units | HYDROGEOLOGICAL FEATURES | | | | | | | | | | |
|---|---|---|---|---|---|---|---|---|---|---|---|---|
| | | Connectivity to the drainage network | | | Type of flow | | Weathering | | | | More suitable exploitation structures | |
| | | with | without | possible | porous medium | fissured medium | low thickness | high thickness | clayey | sandy | dug-wells, galleries and springs | boreholes |
| Sedimentary cover | fluvio-glacial deposits | x | | | x | | n. a. | n. a. | n. a. | n. a. | x | |
| | alluvium deposits | x | | | x | | n. a. | n. a. | n. a. | n. a. | x | |
| Metasedimentary rocks | schists, graywackes and metaconglomerates | x | | x | | x | | x | x | | | x |
| Granitic rocks | granitoids | x | | x | | x | x | x | | x | x | x |

n.a.= not applicable

Table 1: Main hydrogeological features of Serra da Estrela mountain region

The Serra da Estrela climate has Mediterranean characteristics, such as dry and warm summers; the wet season extends from October to May, with a mean annual precipitation of ca. 2500 mm in the Torre summit and more than 2000 mm in the plateaus (Daveau et al. 1997; Vieira and Mora 1998). Precipitation seems to be mainly controlled by the slope orientation and the altitude. According to Vieira and Mora (1998), the warmest month is July and the coldest is January. Mean annual air temperatures are below 7ºC in most of the plateaus area and, in the Torre vicinity, they may be as low as 4ºC. The spatial and temporal irregularity of snow related phenomena has been analyzed in earlier studies (e.g. Mora and Vieira 2004).

## Vadose zone characterisation

Since soils contribute to control both the volume and the water chemistry in an aquifer system, they were the main target of the regional scale vadose zone study at Serra da Estrela. Soil features closely influence the volume of water that infiltrates as consequence of a precipitation event, contributing to control aquifer recharge as well as the short-term stream response.

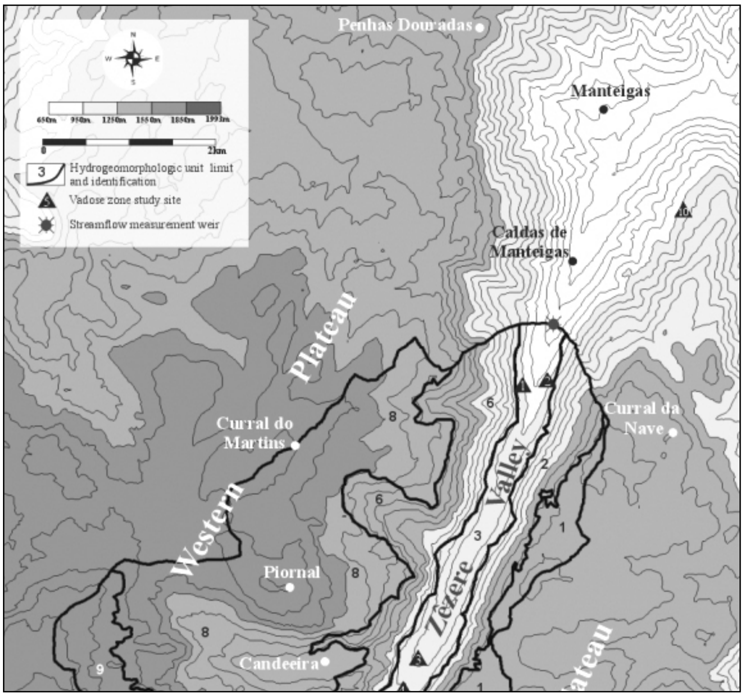

Figure 2: Hypsometric features of the river Zêzere drainage basin upstream Manteigas; vadose zone study sites; hydrogeomorphologic units: Eastern plateau (1); Zêzere valley eastern slopes (2); Lower Zêzere valley floor (3); Nave de Santo António col (4); Upper Zêzere valley floor (5); Zêzere valley western slopes(6); Cântaros slopes (7); Lower western plateau (8); Upper western plateau (9).

The most important factors usually pointed out as affecting the balance between infiltration and overland flow are the amount and characteristics of precipitation (or irrigation), the soil physical and chemical features (e.g. texture, organic matter content, saturated hydraulic conductivity at the surface, clay mineralogy, presence of water-repellent substances), previous soil water saturation, surface slope and roughness, land cover, land use and amount of evapotranspiration (e.g. Dingman 1994). The vadose zone study included several fieldwork campaigns carried out through 2004 and 2005. During these campaigns, soil samples were collected for physical, chemical and mineralogical characterisation (figure 2). Detailed vadose zone studies were carried out in specific sites; table 2 describes each study site in terms of parent material, relief, land cover and prevailing soil profile.

| Site | Parent material | Topography/Geoform | Land cover | Prevailing soil profile |
|---|---|---|---|---|
| 1 | Glacial deposit | Base of slope | Maritime pine woodland | A-C |
| 2 | Glacial deposit | Base of slope | Genista florida and Cytisus sp.pl. scrubland | A-C |
| 3 | Glacial deposit | Valley floor | Meso-hygrophilous grassland | A-C |
| 4 | Glacial deposit | Base of slope | Meso-xerophilous grassland | A-C |
| 5 | Glacial deposit | Col | Nardus stricta grassland | A-C |
| 6 | Granite | Base of slope | Heathland | A-C or A-C-R |

| Site | Parent material | Topography/Geoform | Land cover | Prevailing soil profile |
|---|---|---|---|---|
| 7 (I, II) | Glacial deposit | Base of slope | Heathland | A-C |
| 8 | Granite | Plateau | Nardus stricta grassland | A-R |
| 9 | Granite | Plateau | Common juniper shrubland | A-R |
| 10 | Granite | Slope | Quercus pyrenaica forest | A-B-C-R |

Table 2: Main features of the vadose zone study sites

The parent material of all studied soils is granite or granite derived glacial deposits. These soils are coarse-textured, as one can observe on the diagram of figure 3, obtained from analysis of A and C horizon samples. Other A horizon features (bulk density, total porosity, pH and organic matter) are presented in table 3, as well as the volumetric water content (θ) measured in A horizon undisturbed samples at different pressure heads (h): -50 cm, -100 cm, -500 cm and -15850 cm.

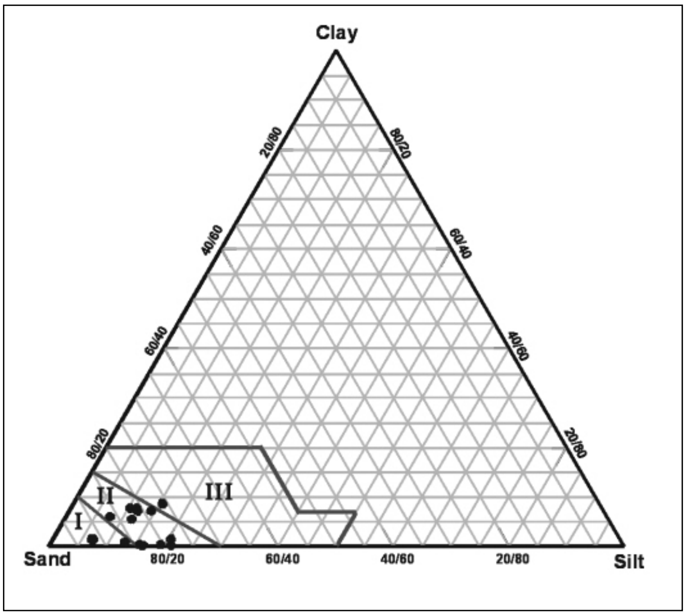

Figure 3: Soil textural classification; textural classes: sand (I), loamy sand (II) and sandy loam (III).

| Site | Bulk density (g.cm-3) | Total porosity (%) | pH | Organic matter (g. kg-1) | θ (% of volume) at different h values | | | |
|---|---|---|---|---|---|---|---|---|
| | | | | | -50 cm | -100 cm | -500 cm | -15850 cm |
| 1 | 1.25 | 44.7 | 4.6 | 71.7 | 23.3 | 19.9 | 14.3 | 12.3 |
| 2 | 1.26 | 49.6 | 4.6 | 57.4 | 29.3 | 23.8 | 15.7 | 12.2 |
| 3 | 1.16 | 52.7 | 4.8 | 71.6 | 34.4 | 30.8 | 22.4 | 18.6 |
| 4 | 1.21 | 42.7 | 4.4 | 48.8 | 23.5 | 19.5 | 14.3 | 11.5 |
| 5 | 0.94 | 49.7 | 4.1 | 133.1 | 42.0 | 33.7 | 25.5 | 22.2 |
| 6 | 1.07 | 45.2 | 4.7 | 103.8 | 29.3 | 23.8 | 17.8 | 16.4 |
| 7I | 0.88 | 51.9 | 4.1 | 187.5 | 44.7 | 37.2 | 26.8 | 25.2 |
| 7II | 1.09 | 53.4 | 4.3 | 71.1 | 35.7 | 28.5 | 21.5 | 19.1 |
| 8 | 0.68 | 62.2 | 4.3 | 240.5 | 57.3 | 50.9 | 40.8 | 38.1 |
| 9 | 0.88 | 55.6 | 4.3 | 188.4 | 46.1 | 37.7 | 28.7 | 26.9 |
| 10 | 0.96 | 48.4 | 4.8 | 84.1 | 31.2 | 26.0 | 18.8 | 15.8 |
| Average | 1.03 | 50.6 | 4.5 | 114.3 | 36.1 | 30.2 | 22.4 | 19.8 |

*Table 3: Main features of A horizon.*

Soil organic matter distribution in A horizon depends mainly on altitude (figure 4), due to a climatic effect. Higher soil organic matter contents usually correspond to the upper locations, where minimum mean yearly air temperature and maximum precipitation takes place. In fact, soils from Torre vicinity (figure 2) present the highest measured organic matter contents (240.5 $g.kg^{-1}$), whereas soils from lower areas present measured values ranging from 48.8 to 84.1 $g.kg^{-1}$. A significant effect of organic matter over bulk density and total porosity (with important implications on soil hydraulic properties) was observed: more organic soils tend to have lower bulk density and higher total porosity.

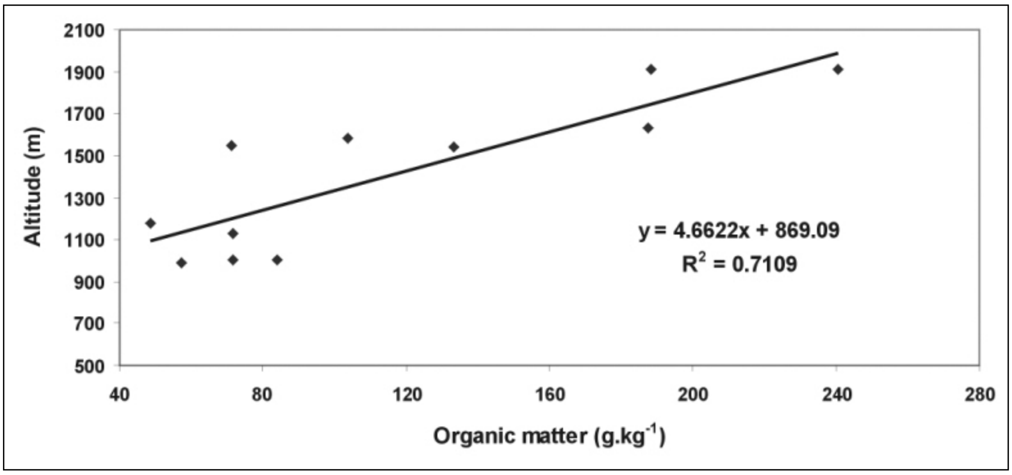

*Figure 4: Relation between soil organic matter and altitude.*

The mineralogical analyses of the soil fine fractions (silt and clay) reveals a mineralogy clearly detrital, rich in phyllosilicates (mainly micas), quartz, plagioclases and K-feldspars, having, as accessory minerals, siderite, opal C/CT, anhydrite, hematite, ilmenite, anatase, zeolites (mainly heulandite-clinoptilolite), gibbsite, rozenite and jarosites. Samples related to granites show higher amounts of phyllosilicates.

As a general rule, illite is the predominant clay mineral, but samples related to granites show a trend for a relative decrease of illite contents whereas kaolinite and, in some samples, vermiculite-Al and/or smectite, increase. Significant amounts of vermiculite-Al occur in sites 1, 3, 4 and 10 (the sampling sites corresponding to lower altitudes), particularly in their A horizons. On the other hand, the expansive clay minerals (smectite and irregular mixed-layers illite-smectite) show a relative increase in sites 2, 6, 8, 9 and 10 (essentially, soils developed on granites).

According to the soil map of Serra da Estrela region (Agroconsultores and Geometral 2004) the following pedologic units occur in this sector: (i) Humic, Leptic and Skeletic Umbrisols; (ii) Lithic and Umbric Leptosols; (iii) Umbric Fluvissols; (iv) Rock outcrops.

Field observations produced further information concerning the pedologic units occurrence, its spatial distribution according to the hydrogeomorphologic framework and its hydrologic classification by means of the Hydrologic Soil Groups system (from low runoff potential soils, group A, to high runoff potential soils, group D) — (e.g. USSCS 1964; Langan and Lammers 1991; Boulding 1993).

Some of the most distinctive features of the vadose zone in this sector of Serra da Estrela are the wide distribution of: i) granitic rock outcrops and ii) an umbric A horizon — and by consequence Umbrisols and Umbric Leptosols — thus reflecting the high organic matter content in the upper part of the soil profile. In the plateau and slopes of hydrogeomorphologic units 1 and 2 (see figure 2) similar sets of pedologic units occur: Leptic Umbrisols prevail (especially in unit 2); rock outcrops and Umbric Leptosols are secondary. Skeletic Umbrisols are dominant in units 3 (valley floor) and 4 (col); Humic Umbrisols and Umbric Fluvisols are subdominant. In unit 5, rock outcrops prevail, whereas Umbric Leptosols and Fluvisols are subdominant; minor occurrences of Leptic Umbrisols were registered. Rock outcrops are also dominant in the remaining units (6 to 9). Yet, in the upper part of unit 6 slopes, Lithic and Umbric Leptosols are subdominant, while in the lower part of the slopes these soils are replaced by Skeletic and Leptic Umbrisols. In the rocky slopes of unit 7, there are minor occurrences of Umbric and Lithic Leptosols. In the plateau area of units 8 and 9 Lithic and Umbric Leptosols are subdominant; less important areas of Leptic Umbrisols were recognized in unit 8.

Four types of vadose zone structures were identified in the region:

- Type i) Composed of a single granite layer with very thin or absent soil cover; present in granitic outcrop areas of plateaus and slopes. Water circulation in fractured medium. Included in soil hydrologic group D.
- Type ii) Composed of a soil layer typically less than 0.5 m thick overlying a continuous and hard granitic layer; described in sites 6, 8 and 9 (see table 2); present in plateaus, especially above 1600 m a.s.l., and slopes. Coexistence of porous and fractured media. Corresponding to Lithic and Umbric Leptosols (both integrating soil hydrologic group D).
- Type iii) Composed of a soil layer frequently between 0.5 and 1.0 m thick overlying a weathered granite layer and/or a slope deposit; described in sites 6 and 10; it is present in lower altitude slopes and plateaus (where chemical weathering processes are more active) or along tectonised zones. Both porous and fractured media. Corresponding essentially to Leptic Umbrisols with C horizon composed of weathered granite and/or a slope deposit. These soils are included in hydrologic group C.
- Type iv) composed of a soil layer frequently over 1.0 m thick overlying a glacial deposit; described in sites 1 to 5 and 7; present in base of slope, col and valley floor areas; porous

medium. Prevailing Skeletic and Humic Umbrisols (A, B or C hydrologic groups) and subdominant Umbric Fluvisols (C or D hydrologic groups).

The importance of *in situ* evaluations of saturated hydraulic conductivity ($K_s$) for accurate determination of water movement in the field related to infiltration and runoff is a well established fact (Reynolds 1993). Ks measured in the vadose zone is usually referred as *field-saturated hydraulic conductivity* ($K_{fs}$). As complete saturation is not achieved in such field tests, $K_{fs}$ can be a factor of 2 (or more) below $K_s$ (Bouwer 1978; Reynolds and Elrick 1987).

The soil permeability study consisted of a set of 40 field tests carried out in sites 1, 2, 3, 5, 6, 8, 9 and 10 by means of the constant head well permeameter also known as the *Guelph permeameter* method (e.g. Reynolds and Elrick 2002) — figure 5. In this study, a well hole 15 cm height and 6 cm of diameter (manually excavated with a soil auger) was used along with two successively ponded heads (5 and 10 cm); all tests refer to A horizon. The following expressions were then used to calculate $K_{fs}$:

$$K_{fs} = (G_2Q_2) - (G_1Q_1)$$

where

$$G_2 = \frac{H_1.C_2}{\pi\left[2H_1.H_2(H_2 - H_1) + a^2(H_1.C_2 - H_2.C_1)\right]}$$

and

$$G_1 = G_2\,(H_2C_1)/\,(H_1C_2)\ ;\ Q_1 = AR_1\ ;\ Q_2 = AR_2$$

$H_1$ and $H_2$ (L) are the two successively ponded heads ($H_1<H_2$); a is the well radius (L); $C_1$ and $C_2$ are shape factors corresponding to f($H_1$/a) and f($H_2$/a), respectively (see Reynolds and Elrick 2002); $R_1$ and $R_2$ are the steady rates of fall of the water in the permeameter reservoir ($LT^{-1}$) corresponding to $H_1$ and $H_2$ , respectively; A is the reservoir cross-sectional area ($L^2$).

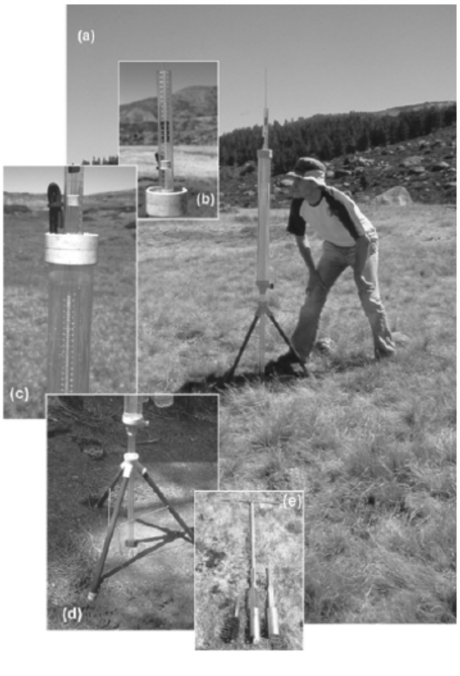

*Figure 5: The constant head well permeameter: general view (a), well head scale (b), water reservoir (c), tripod (d) and soil auger set (e).*

The measured $K_{fs}$ values are presented on table 4, each value representing the average of five field tests. In all cases the permeability (assuming estimated Ks) is high according to the SSDS (1993) classification.

The hydraulic description of the vadose zone also included the determination of soil characteristic curves. For this purpose, the analytical model proposed by van Genuchten (1980) was fitted to the measured water retention values (see table 3) by means of the RETC v6.0 code (van Genuchten et al. 1991; Yates et al. 1992) available at *http://www.ars.usda.gov/* internet site.

Van Genuchten defined the relationship between pressure head (h) and the soil volumetric water content (q) by the expression:

$$\theta(h) = \theta_r + \frac{\theta_s - \theta_r}{\left[1 + (\alpha h)^n\right]^m}$$

where

$$n = \frac{1}{1-m} \quad \text{and} \quad \alpha = \frac{1}{h_b}\left(2^{1/m} - 1\right)^{1-m}$$

θ and h are as defined earlier; $\theta_s$ is the water content at saturation; $\theta_r$ is the residual water content; $h_b$ is the bubbling pressure head; m is an empirical constant affecting the shape of the retention curve.

Table 5 presents the estimates of van Genuchten parameter values resulting from the application of RETC code to observed volumetric water contents; the best results were obtained considering $\theta_s$ values equal to the total porosity; $R^2$ values stand for the regression of observed versus fitted θ values. These results are compared to average values of coarse-textured soils obtained by experimental means by Carsel and Parrish (1988).

| **Site** | **Measured $K_{fs}$ (cm/h)** | **Estimated $K_s$ (cm/h)** |
|---|---|---|
| 1 | 7.7864 | 15.5729 |
| 2 | 4.7399 | 9.4798 |
| 3 | 4.1947 | 8.3894 |
| 5 | 3.3135 | 6.6270 |
| 6 | 12.7172 | 25.4345 |
| 8 | 4.6740 | 9.3481 |
| 9 | 12.8208 | 25.6416 |
| 10 | 12.5890 | 25.1781 |
| Average | 7.8544 | 15.7089 |

*Table 4: Measured values of field saturated hydraulic conductivity.*

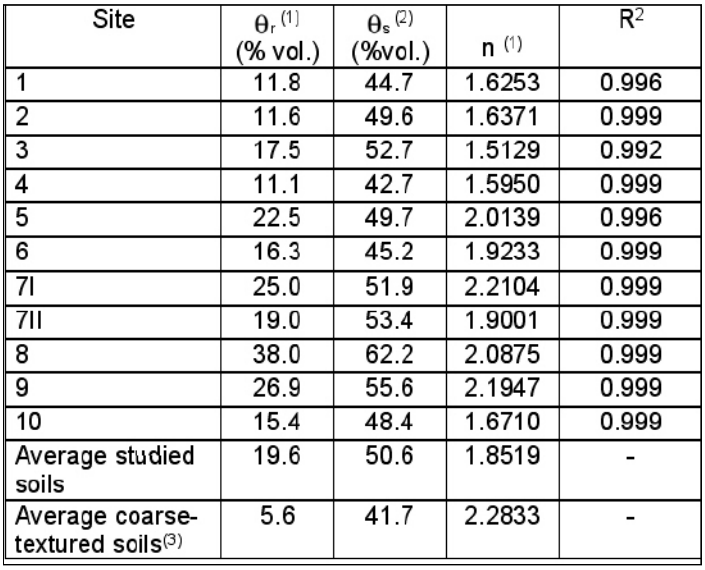

| Site | $\theta_r$ (1) (% vol.) | $\theta_s$ (2) (%vol.) | n (1) | $R^2$ |
|---|---|---|---|---|
| 1 | 11.8 | 44.7 | 1.6253 | 0.996 |
| 2 | 11.6 | 49.6 | 1.6371 | 0.999 |
| 3 | 17.5 | 52.7 | 1.5129 | 0.992 |
| 4 | 11.1 | 42.7 | 1.5950 | 0.999 |
| 5 | 22.5 | 49.7 | 2.0139 | 0.996 |
| 6 | 16.3 | 45.2 | 1.9233 | 0.999 |
| 7I | 25.0 | 51.9 | 2.2104 | 0.999 |
| 7II | 19.0 | 53.4 | 1.9001 | 0.999 |
| 8 | 38.0 | 62.2 | 2.0875 | 0.999 |
| 9 | 26.9 | 55.6 | 2.1947 | 0.999 |
| 10 | 15.4 | 48.4 | 1.6710 | 0.999 |
| Average studied soils | 19.6 | 50.6 | 1.8519 | - |
| Average coarse-textured soils(3) | 5.6 | 41.7 | 2.2833 | - |

*Table 5: Estimated values of the van Genuchten soil parameters.*

*(1) estimated; (2) assumed equal to total porosity; (3) after Carsel and Parrish (1988).*

Figure 6 illustrates the contrast between the hydraulic behaviour of Serra da Estrela soils and the reference soils of Carsel and Parrish (1988). It is noticeable that for analogous h values Serra da Estrela soils present higher θ values. This effect becomes more apparent in the curve region corresponding to greater suctions (more negative pressure heads), that is, where most water is retained in micropores. Since these soils present relatively high organic matter and low clay contents (see table 3 and figure 3) the observed trend should be explained by the former feature. The correlation coefficients (R) of organic matter versus water retention at -50 cm and -15850 cm (0.92 and 0.94) support this idea.

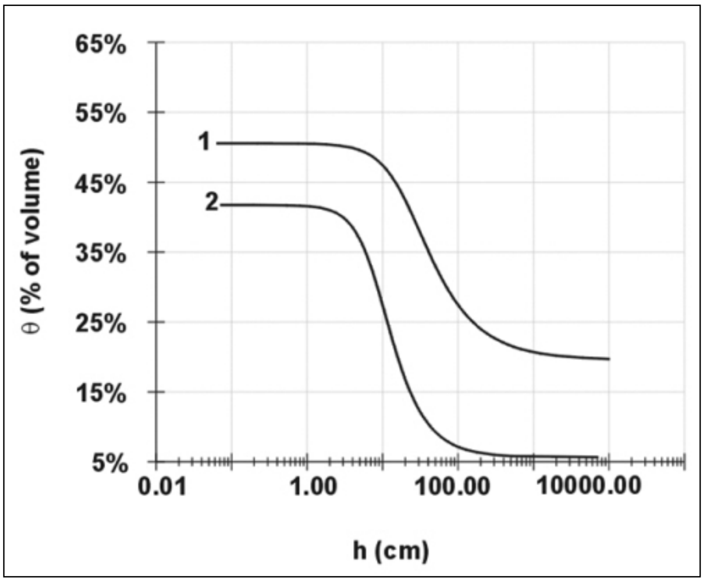

*Figure 6: Water-retention curves: Serra da Estrela soils (1) and average coarse-textured soils (2).*

## Concluding remarks

Given that the role of the vadose zone is essential to understand the genesis and evolution of groundwater resources, a multidisciplinary approach supported by geological, pedological and hydrogeomorphological analysis was carried out, providing important information to achieve a regional scale characterization of the vadose zone in the hydrogeological system of the Manteigas - Nave de Santo António-Torre sector. This description focused on the soil broad physical, chemical and mineralogical features, vadose zone structure, and soil hydraulics.

Even though coarse-textures and low pH tend to be generalized soil features in Serra da Estrela, organic matter content — and therefore bulk density and total porosity — is clearly related to altitude due to a climatic effect. Soil mineralogical study focused on clay mineralogy. In fact, soil fine fractions mineralogy is closely related to a detrital origin (with absolute predominance of quartz, mica/illite and feldspars). Nevertheless, some distinctive features are evident, particularly: samples related to granites show relatively higher amounts of phyllosilicates (but show a decrease in illite whereas kaolinite increases).

A distinctive trace of the vadose zone in this sector of Serra da Estrela is the wide distribution of granitic rock outcrops and an umbric A horizon — and by consequence Umbrisols and Umbric Leptosols — thus reflecting the high organic matter content in the upper part of the soil profile.

Four types of vadose zone structure were identified, with spatial distribution closely controlled by geology and hydrogeomofology. High runoff potential soil hydrologic groups (C and D) are dominant in spite of the high permeability of A horizon, measured by means of the constant head well permeameter.

The parameters of van-Genuchten water retention curve were derived from water retention data in A horizon samples. According to the resulting characteristic curves, it is noticeable that for analogous pressure head values Serra da Estrela soils present higher water retention values than the average coarse-textured soils, especially in the curve region corresponding to greater suctions (in which case water is mainly retained in micropores). This contrast should be explained by the high organic matter content of the studied soils.

## Acknowledgments

This study was performed under the scope of the HIMOCATCH R&D Project granted by the Portuguese Foundation for Science and Technology (FCT) and FEDER EU funds, contract POCTI/CTA/44235/02.

## References

- Agroconsultores, Geometral (2004). Elaboração da Carta de Solos e de Aptidão das Terras da Zona Interior Centro (Making of the Soil Map and Land Suitability of Zona Interior Centro). Instituto de Desenvolvimento Rural e Hidráulica, Lisbon.
- Boulding JR (1993) Subsurface characterization and monitoring techniques. In: The vadose zone, field screening and analytical methods. EPA/625/R-93/003.
- Bouwer H 1978 Groundwater Hydrology. McGraw-Hill, Inc. New York. 480 p.
- Carsel FF, Parrish RS (1988) Developing joint probability distributions of soil water retention characteristics. Water Resources Research 24 (5): 755-769.
- Daveau S, Ferreira AB, Ferreira N, Vieira G (1997) Novas observações sobre a glaciação da Serra da Estrela (New observations on the Serra da Estrela glaciation). Estudos do Quaternário 1:41-51.
- Dingman SL (1994). Physical hydrology. Prentice Hall. New Jersey. 575 p.
- Espinha Marques J, Marques JM, Chaminé HI, Afonso MJ, Carreira PM, Fonseca PE, Cabral J, Monteiro Santos FA, Vieira GT, Mora C, Gomes A, Teixeira J, Samper J, Pisani BJ, Aguiar C, Gonçalves JA, Almeida PG, Cavaleiro V, Carvalho JM, Sodré Borges F, Aires-Barros L, Rocha FT (2005) Hydrogeological study of a high mountain area (Serra da Estrela, Central Portugal): a multidisciplinary approach. Cadernos Lab. Xeol. Laxe 30: 145-166.
- Langan LN, Lammers DA (1991) Definitive criteria for hydrologic soil groups. Soil Survey Horizons 32 (3): 69-77.
- Mora C, Vieira GT (2004) Balance radiactivo de los altiplanos de la Sierra de Estrella (Portugal) en una mañana de invierno. Metodología y primeros resultados (Radiation balance of the plateaus of Sierra de Estrella (Portugal) in a winter morning. Methodology and first results). Bol. R. Soc. Esp. Hist. Nat. (Sec. Geol.) 99 (1-4): 37-45.
- NAP - National Academy Press (2001) Conceptual models of flow and transport in the fractured vadose zone. Washington, D.C., 374 pp.
- Oliveira JT, Pereira E, Ramalho M, Antunes MT, Monteiro JH ,Coords (1992) Carta Geológica de Portugal à escala 1/500 000 (Geological Map of Portugal, scale 1/500 000). 5th Edition. Portuguese Geological Survey, Lisbon.
- Reynolds WD, Elrick DE (2002) Constant head well permeameter (vadose zone). In: Dane JH, Clarke Topp G (ed) Methods of soil analysis, Soil Science Society of America, Inc., part 4, Physical methods: 844-858
- Reynolds WD (1993) Saturated hydraulic conductivity: field measurement. In: Carter MR (ed) Soil sampling and methods of analysis, Lewis Publ. 599-613.
- Reynolds WD, Elrick DE (1987). A laboratory and numerical assessment of the Guelph permeameter method. Soil Sci. 144:282-299.

- Ribeiro A, Kullberg MC, Kullberg JC, Manuppela G, Phipps S (1990) A review of Alpine tectonics in Portugal: Foreland detachment in basement and cover rocks, Tectonophisics, 184:357-366.
- SSDS, Soil Survey Division Staff (1993) Examination and description of soils. In: Soil Survey Manual. Agricultural Handbook 18: chapter 3.
- USSCS, U. S. Soil Conservation Service (1964) Hydrology. In: SCS National Engineering Handbook Section 4.
- Van Genuchten MT (1980) A closed-form equation for predicting the hydraulic conductivity of unsaturated soils. Soil Sci. Soc. Am. J. 44:892–898.
- Van Genuchten MT, Leij FJ, Yates SR (1991) The RETC code for quantifying the hydraulic functions of unsaturated soils. U. S. Environmental Protection Agency 85 p.
- Vieira GT (2004) Geomorfologia dos planaltos e altos vales da Serra da Estrela: ambientes frios do Plistocénico Superior e dinâmica actual (Geomorphology of the plateaus and high valleys of Serra da Estrela: cold environments from Late Pleistocene and present dynamics). Unpublished PhD Thesis, Department of Geography, University of Lisbon. 724p.
- Vieira GT, Mora C (1998) General characteristics of the climate of the Serra da Estrela. In Vieira GT (ed), Glacial and Periglacial Geomorphology of the Serra da Estrela. Guidebook for the field-trip. IGU Commission on Climate Change and Periglacial Environments, CEG and Department of Geography, University of Lisbon 26-36.
- Yates SR, van Genuchten MT, Warrick AW, Leij FJ (1992) Analysis of measured, predicted and estimated hydraulic conductivity using the RETC computer program. Soil Sci. Soc. Am. J. 56:347-354.

# DARCY 34

# Traçage de 66,7 km dans le karst de la Fontaine de Vaucluse

DUCLUZAUX Bruno

EKS Hydrogéologie, Le Morgon, Lacenas, France, info@hydrogeologie.com

## Abstract

The « Fontaine de Vaucluse » is the biggest spring in France. The average discharge is 18.5 m$^3$/s. Since October 2003, 8 tracer experiments have been carried out by EKS hydrogeology : 3 injections in the shaft of Fontaine de Vaucluse, 2 injections with no detection, 3 injections in the groundwater basin with a tracer-breakthrough curve at the spring. The tracer is ion iodide with continuous and on site measurements by chemical sensors, patented process TRACEAUTO®, Ducluzaux (2001).

The first two injections in the shaft of Fontaine de Vaucluse characterized the connection between sinkholes in the shaft and permanent springs. In February 2004, the tracer injected into sinkholes of Nesque stream spent 11.75 days to cover a distance of 21 km to the Fontaine de Vaucluse. Maximum velocity was 74.7 m/h. The Peclet number was 1500. The following injection took place at Notre-Dame-de-Lure in March 2004. For a distance of 56.6 km, maximum velocity was 74.6 m/h. In August 2005, a tracer test showed the connection between the shaft of Fontaine de Vaucluse and the municipal well.

March 31st, 2005 at 2:40 pm, an injection in sinkhole of Saint-Donat showed that the karst located at a few kilometers of river Durance belonged to the groundwater basin of Fontaine de Vaucluse. The time to first tracer arrival was 70 days after the injection. Maximum velocity was 40 m/h. Peak velocity was 32.9 m/h. Mean velocity was 31.9 m/h. The traced aquifer volume estimate was 100 106 m3, with a traced surface of 1500 m2, and a traced diameter of 43 m. All the tracer tests in Vaucluse karst showed a traced diameter around 40 m, thus it seems an intrinsic characteristic of the Vaucluse karst. The dispersivity was 260 m, the Peclet number was 255. The recovery of tracer injected was 10 %.

This tracer test of 66.7 km is the longest of Europe. With these new tracer tests, the groundwater basin of Fontaine de Vaucluse reaches 1210 km$^2$. The groundwater basin could extend to the east of Durance river, i.e. in the Alps. Important sinkholes of Durance could exist in Messinian period (-5.9 to -5.3 Ma). The main drain of Vaucluse karst could be a paleo Durance.

## 1. Introduction

La Fontaine de Vaucluse est la plus importante résurgence de France et l'une des premières au monde. Les traçages, techniquement difficiles sur cette source, sont donc rares. Les deux derniers datent de 15 et 30 ans. Depuis 2003, le bureau d'études EKS Hydrogéologie a réalisé 8 nouveaux traçages dans le karst de la Fontaine de Vaucluse. Les 3 traçages à partir du plateau de Vaucluse ont été entièrement financés et organisés par EKS.

Une synthèse sur la géologie et l'hydrogéologie du système karstique de la Fontaine de Vaucluse a été réalisée par Puig (1990). Le bassin d'alimentation proposé était de 1115 km$^2$. D'après la banque de données HYDRO, le débit moyen sur les 40 dernières années est de 18,5 m$^3$/s (d'après le Sorgomètre qui sous-estime les débits). Les débits sont mesurés par 2 stations, une visuelle datant de 1869 à relevé journalier manuel, le « Sorgomètre », une récente de 2004 avec un enregistreur automatique sur un vrai seuil, le « Moulin ». En basses eaux, le « Moulin » donne des débits 40 à 50 % plus élevés que le « Sorgomètre ». D'après l'organisme qui effectue des jaugeages sur la nouvelle station du « Moulin » (DIREN PACA), les débits du « moulin » sont plus fiables que ceux du « Sorgomètre ».

La méthodologie utilisée pour les traçages est décrite par Ducluzaux (2001). Le traceur employé est l'ion iodure, qui est mesuré en continu et in situ par des capteurs chimiques. Le seuil de détection d'une variation de la concentration en iodure est inférieur à 0,01 µg/l.

Pendant les 2 années de traçages, la concentration naturelle en iode a été mesurée par 23 analyses par ICP/MS. En excluant 4 résultats anormaux, la concentration en iode de la Fontaine de Vaucluse varie entre 1,7 µ/l et 3,4 µg/l. Elle est plus basse en hautes eaux qu'à l'étiage. La concentration naturelle moyenne en iode total est de 2,5 µg/l.

Cette communication présente les résultats des 3 traçages à partir du gouffre de la Fontaine de Vaucluse et des traçages des pertes de la Nesque et de Saint-Donat.

## 2. Trois traçages à partir du gouffre noyé de Fontaine de Vaucluse

Le premier traçage a débuté le 19 octobre 2003 à 11h45. Des plongeurs de la Société Spéléologique de Fontaine de Vaucluse ont injecté 838 g de traceur ion iodure dans la perte située à 50 m d'altitude dans le gouffre noyé de Fontaine de Vaucluse. Le débit (Sorgomètre) était de 11,1 $m^3/s$. Deux exutoires du système karstique de Vaucluse étaient surveillés, une source en amont du « restaurant Philip » et la source du Pagodon en aval du restaurant. La source du Pagodon est la plus basse du système karstique. Elle a un débit assez constant de 1 m3/s. Les pas de temps de mesures étaient de 5 et de 10 minutes.

Le traceur est arrivé à la source amont 1h15 après l'injection. Le maximum de concentration a eu lieu 1h35 après l'injection. La courbe de restitution montre deux pics bien nets, qui correspondent à deux cheminements différents entre le gouffre et la source. La source du Pagodon (source la plus en aval) a été atteinte 2h35 après l'injection. La courbe de restitution ne montre qu'un seul pic.

Une deuxième injection d'iode a eu lieu le 30 octobre 2003 à 14h00. Quelques dizaines de grammes d'iodure ont été injectées au milieu du gouffre noyé à 87 m d'altitude (niveau d'eau à 93 m ce jour là). Les deux sources pérennes surveillées ont détecté une courbe de restitution. Le résultat principal est la forte dispersion, avec un nombre de Péclet inférieur à 10, alors que le nombre de Péclet de la première injection était de 100.

Pour presque le même parcours souterrain, la dispersion est très différente selon le mode d'injection. L'injection directe dans le flux souterrain donne une dispersion faible de 3,8 m, alors qu'une injection diffuse dans le gouffre donne une dispersion forte de 37 m. Pour quasiment le même trajet, le nombre de Peclet est divisé par 10. La méthodologie d'injection est donc essentielle dans une opération de traçage, afin de ne pas attribuer à une caractéristique du milieu souterrain une valeur qui dépend de la technique employée.

Le 25 août 2005, un traçage pour le compte de la commune a caractérisé la relation entre le gouffre noyé de Fontaine de Vaucluse et le puits de captage communal. 8382 g d'ion iodure ont été injectés par les plongeurs à 44 m et 50 m d'altitude. Le traceur a d'abord été détecté à la source du Pagodon, puis dans la Sorgue, avant d'atteindre le puits situé à 20 m de la rivière. Le taux de restitution est bien sûr faible, 0,03 %, car la majorité du traceur est partie en aval dans la Sorgue. La preuve que l'eau du système karstique de Vaucluse est utilisée pour l'Alimentation en Eau Potable permettra d'améliorer la protection du karst de Vaucluse.

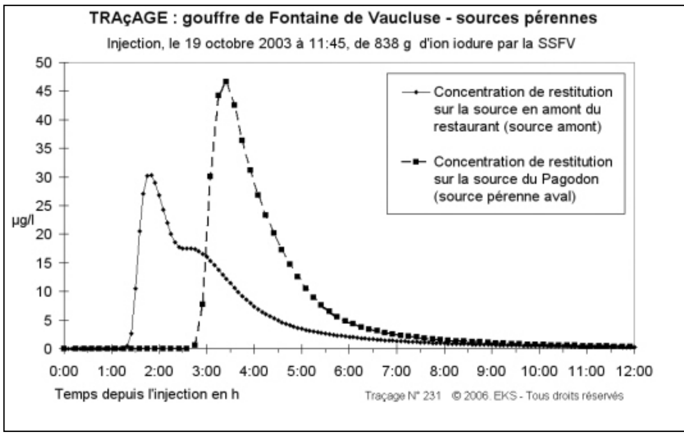

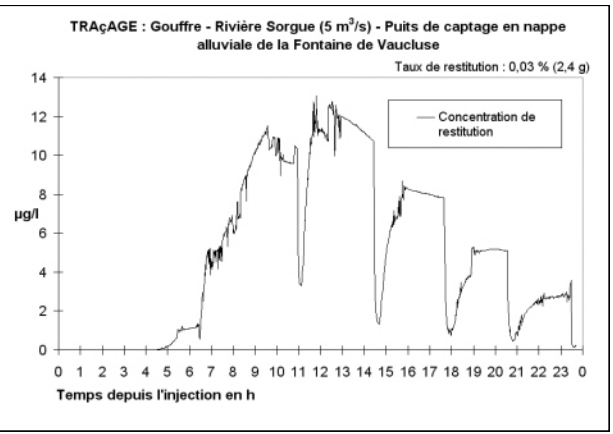

*Figure 1 : Courbes de restitution dans les deux sources pérennes du traceur injecté dans le gouffre noyé*
*Figure 2 : Courbe de restitution dans le puits de captage en nappe*

## Traçage des pertes de la Nesque

L'injection de 15 087 g d'ion iodure a eu lieu le 11 février 2004 à 14h00 dans les gorges de la Nesque au lieu-dit la Cathédrale (coordonnées L2E : x = 840225 m, y = 1898113 m, z = 540 m). Le lieu d'injection est à 21,07 km de la Fontaine. La dilution directe du traceur dans l'eau a duré 10 minutes. Le débit de la rivière Nesque au point d'injection était de 50 l/s, alors que le débit de la Nesque au barrage en amont des Gorges était de 120 l/s. Le débit de la Fontaine de Vaucluse était de 21,9 $m^3/s$ (Sorgomètre) ou de 24,3 $m^3/s$ (Moulin).
Quatre dispositifs indépendants (4 capteurs + 4 enregistreurs) étaient installés sur la source

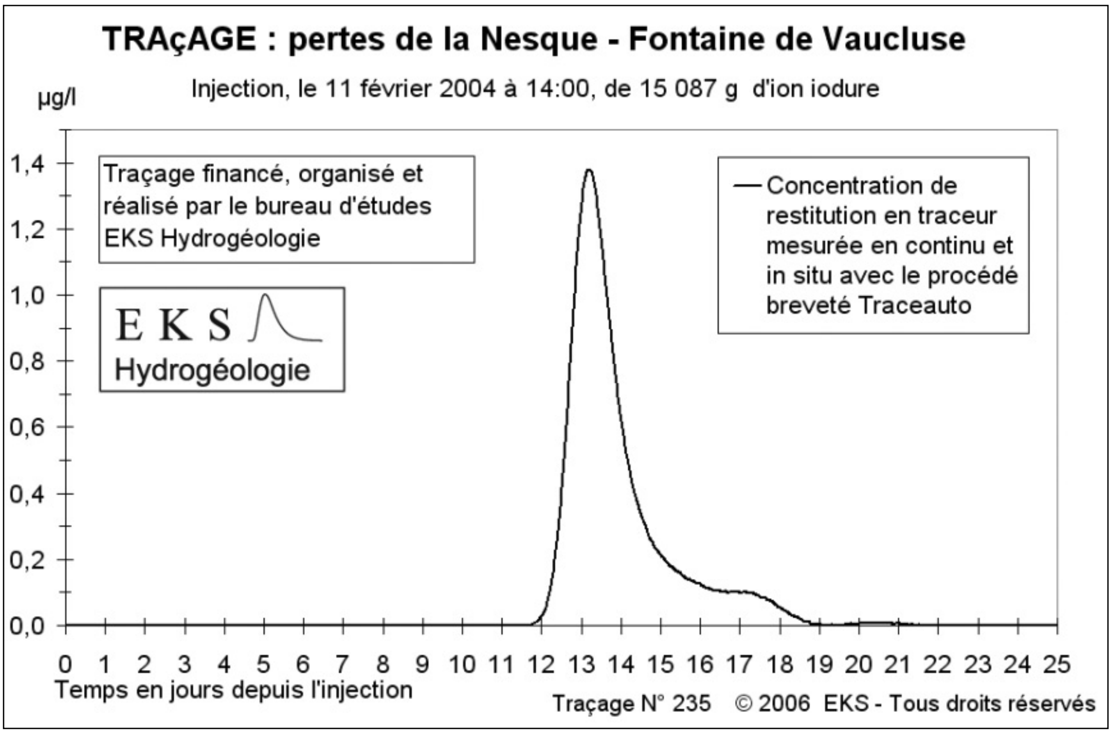

*Figure 3 : Courbe de restitution du traçage des pertes de la Nesque*

du Pagodon, exutoire le plus bas du système karstique de Vaucluse (coordonnées L2E : x = 824641 m, y = 1883936 m, z = 78,5 m). Le pas de temps était d'une mesure toutes les 20 minutes.

A partir du 23 février, un pic de restitution très net en traceur a été détecté sur les 4 dispositifs indépendants. La première détection du traceur a eu lieu le 23 février à 8h00, c'est à dire 11 jours et 18 heures après l'injection. La vitesse maximale du traceur est donc de 74,7 m/h. La vitesse modale est de 66,7 m/h et la vitesse minimale de 40,5 m/h.

Le taux de restitution calculé à partir des débits journaliers du « Moulin » est 63 %. La masse restituée est de 9,45 kg.

Le nombre de Peclet du premier pic est de 1500, et la dispersion de 14 m. Cette faible dispersion peut s'expliquer par l'injection du traceur directement dans le flux, sans stockage près de l'injection. De plus la crue du système a débuté avant le début de la restitution, et a poussé le traceur vers l'exutoire, Ducluzaux (1999).

La vitesse moyenne du traceur, en tenant compte des variations de débit, est de 63,08 m/h. Les vitesses moyennes des 3 pics visibles sont respectivement 66,0 m/h, 51,2 m/h et 42,8 m/h. Les dispersions sont les mêmes pour les 3 pics : 14 m. Le taux de restitution du dernier pic séparé est faible : 0,07 %.

Le volume écoulé à la Fontaine entre l'injection et le temps moyen est de $32\ 10^{6}$ $m^{3}$ à partir des débits du « Moulin » et $29\ 10_{6}$ $m^{3}$ à partir des débits du « Sorgomètre ». En divisant ce volume par la distance entre les points d'injection et de restitution, on calcule une surface tracée (1600 à 1400 $m^{2}$) et un diamètre tracé (environ 40 m). Ces définitions sont neutres sans aucune interprétation. Le diamètre donne une bonne idée de la dimension des conduits, bien qu'un drain karstique noyé ne soit pas forcément constitué d'un conduit unique mais souvent de plusieurs conduits parallèles. Pour les traçages sur la Fontaine de Vaucluse, l'interprétation physique exacte est plus délicate, mais nous verrons que le diamètre tracé caractérise bien le karst de la Fontaine de Vaucluse car le diamètre tracé est pratiquement constant quels que soient les débits et la distance.

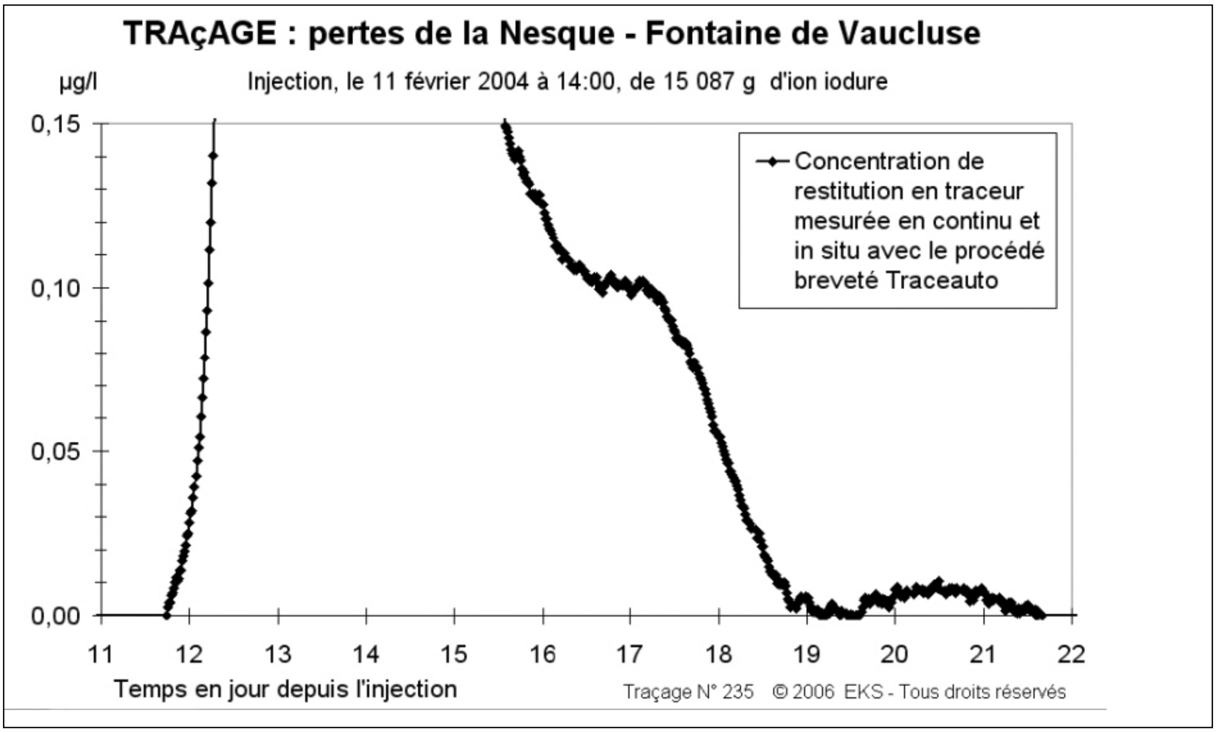

Figure 4 : Bas de la courbe de restitution du traçage des pertes de la Nesque

Interprétations :

La courbe de restitution est composée de 3 pics, entre 12 et 15 jours, entre 16 et 19 jours et entre 20 et 21 jours. Ces pics pourraient correspondre à des cheminements différents car les pertes de la Nesque sont graduelles. Le dernier pic bien séparé pourrait aussi avoir pour origine le fractionnement du nuage de traceur par le drain collecteur principal du système karstique. En effet, de fortes précipitations, 91 mm à Sault du 20 au 22 février, ont eu lieu sur le plateau pendant que le traceur avançait dans le karst. Le drain karstique principal provenant de la Montagne de Lure et le drain secondaire provenant des pertes de la Nesque pourraient se rejoindre à 12 km en amont de la Fontaine de Vaucluse, interprétation dans Ducluzaux (1999).

## 4. Traçage de Saint Donat

Le début de l'injection de 62 862 g d'ion iodure a eu lieu le 31 mars 2005 à 14h40 à 1 m en amont de la perte totale du ruisseau du ravin de la Combe d'Oursière. Les coordonnées Lambert 2 étendu de l'injection sont connues au mètre près par pointage sur les orthophotographies de l'IGN : x = 888901 m, y = 1901891 m, z = 451 m. Ce point est à 72 m de l'extrémité ouest de la chapelle Saint Donat. Le point d'injection est à 66 721 m du point de surveillance. Le débit du ruisseau 100 m en amont de l'injection était de 1 l/s et il était de 0,2 l/s au point d'injection. La dissolution totale de l'iode a duré une heure et 10 minutes. Le 31 mars 2005, le débit de la Fontaine de Vaucluse était de 7,65 $m^3/s$ (Sorgomètre) ou de 10,3 $m^3/s$ (Moulin).
Les conditions du traçage sont défavorables : basses eaux de la Fontaine, sécheresse depuis plusieurs mois, précipitations après l'injection qui ont pu entrainer une partie du traceur dans la Durance. Une perte importante de traceur près de l'injection et un faible taux de restitution sont prévisibles.
Cinq dispositifs indépendants (5 capteurs + 5 enregistreurs) étaient installés à la Fontaine de Vaucluse, 4 sur la source du Pagodon et 1 dans le captage de la source du restaurant Philip. Les pas de temps étaient d'une mesure toutes les 10 à 60 minutes selon la programmation des enregistreurs. Une sonde multiparamètre (température, conductivité, pH, oxygène dissous, potentiel d'oxydoréduction et profondeur) enregistrait les 6 paramètres physico-chimiques toutes les 20 minutes.
Les 5 capteurs ont enregistré le même pic de restitution en ion iodure centré fin juin 2005.
La première détection du traceur a eu lieu le 9 juin à 10h40, c'est à dire 69 jours et 20 heures après l'injection. La vitesse maximale du traceur est donc de 39,8 m/h. La vitesse modale est de 32,9 m/h et la vitesse minimale de 23,5 m/h. La vitesse moyenne, avec les débits du Sorgomètre, est de 31,9 m/h. Le volume écoulé à la Fontaine entre l'injection et le temps moyen est de 100 $10^6$ $m^3$, d'où une surface tracée de 1500 $m^2$, et un diamètre tracé de 43 m.
Par calage du premier pic sur le modèle advection-dispersion à une dimension, la dispersion calculée est de 261 m et le nombre de Peclet est de 255.

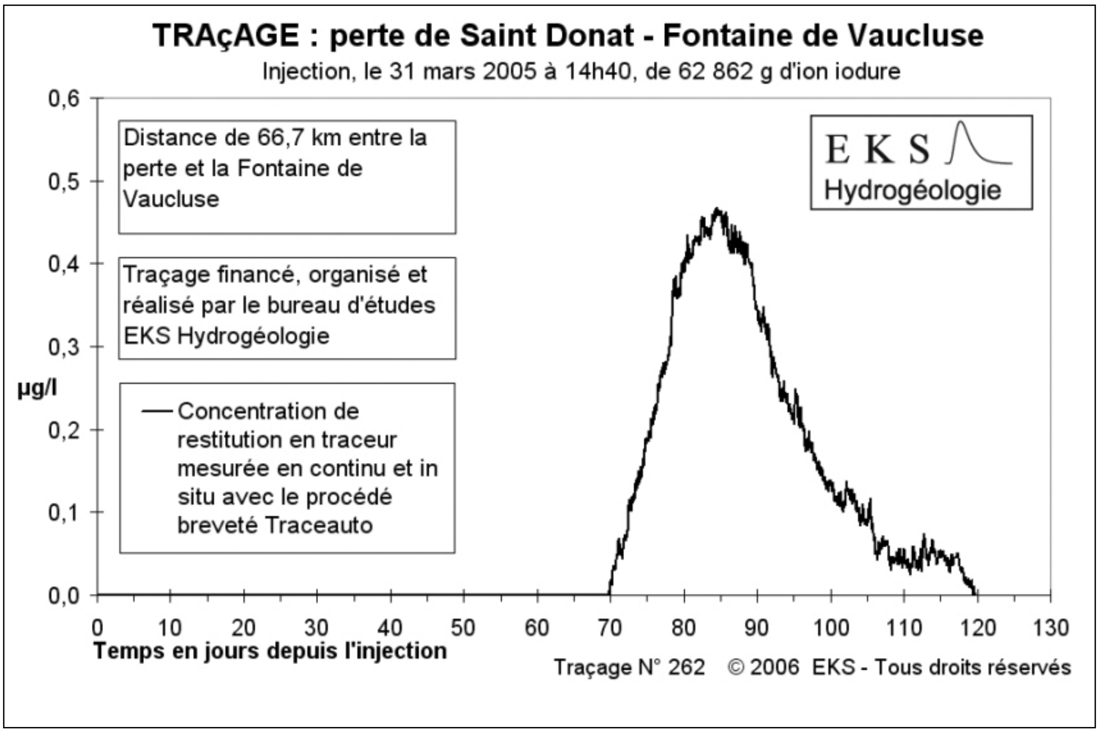

Figure 5 : Courbe de restitution du traçage de Saint Donat

Les enregistrements de tous les paramètres annexes montrent des évolutions régulières pendant toute la durée de la restitution du traceur : température et conductivité en augmentation, débit en diminution, pH, potentiel rédox et oxygène dissous stable. Aucun phénomène parasite de type physicochimique ne s’est produit pendant la restitution.

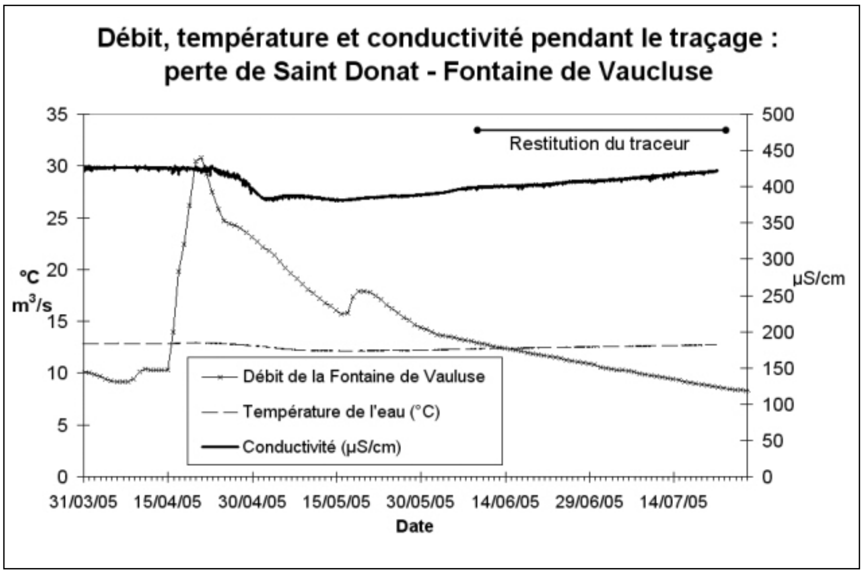

Figure 6 : Débit, température et conductivité pendant le traçage de Saint-Donat

A notre connaissance, ce traçage est le plus long d'Europe. Il est sans doute le plus long du monde avec des mesures en continu.

Interprétations :

Pour les traçages à partir du plateau de Vaucluse, la surface tracée est toujours de l'ordre de 1500 m$^2$ et le diamètre tracé de l'ordre de 40 m. Le diamètre tracé de 40 m semble donc une caractéristique intrinsèque du système karstique de Vaucluse.

Le taux de restitution calculé à partir des débits journaliers du Sorgomètre est 10 %, avec une masse restituée de 6,2 kg. La station du Moulin était en panne pendant la restitution, elle aurait donné un taux de restitution plus élevé. Ce taux de restitution faible vient des conditions défavorables de l'injection (sécheresse) et des caractéristiques de l'aquifère pendant le traçage. La forte crue après l'injection a pu pousser du traceur dans des systèmes annexes aux drains principaux. On ne peut donc pas déduire du faible taux de restitution qu'il existe d'autres exutoires du karst.

Le traçage de Saint-Donat permet d'étendre le bassin d'alimentation de la Fontaine de Vaucluse vers l'est, par rapport à celui proposé par Puig (1990). Les calcaires Barrémo-Bédoulien affleurant en bordure de la Durance, des pertes de la Durance alimentent probablement la Fontaine de Vaucluse. A l'affleurement, ces calcaires ne montrent aucune trace de karstification et toutes les fissures visibles sont colmatées par de l'argile. On peut donc estimer les pertes de la Durance à 50 l/s (perméabilité moyenne 10$^{-6}$ m/s et surface 500 x 100 m).

Les arguments isotopiques, et l'argument d'absence de variation de débit lié aux aménagements de la Durance, ne sont donc pas valables pour rejeter l'hypothèse de pertes de la Durance vers la Fontaine de Vaucluse.

Plus d'une centaine de forages ont été effectués par EDF dans les calcaires sous ou à proximité du lit de la Durance. Deux forages (AC 5 et AC 8) ne montrent aucune trace d'eau alors que leur fond est 20 m sous le niveau de la Durance.

Le niveau piézométrique à Saint-Donat est à 300 m d'altitude. Avec un gradient de 0,3 %, le niveau de l'eau du karst sous la Durance serait à 335 m, soit 110 m sous le cours d'eau actuel.

Le bassin d'alimentation de la Fontaine de Vaucluse pourrait donc s'étendre à l'est de la Durance, c'est-à-dire dans les Alpes, en suivant la structure anticlinale de Beaudouze.

Les forages EDF au niveau du barrage de Baumas ont montré une épaisseur maximum d'alluvions de 20 m (AUB 14) au-dessus des calcaires Barrémo-Bédoulien. Les essais de perméabilité et les coupes indiquent une probable karstification de ces calcaires. Des pertes importantes de la Durance ont pu avoir lieu au Messinien dans le défilé de Baumas. Le drain principal du karst géant de Vaucluse pourrait être une paléo Durance creusée pendant la période du Messinien (-5,9 à -5,3 Ma).

## 5. Synthèse des anciens traçages

L'évaluation de la fiabilité des traçages est basée uniquement sur des éléments techniques liés aux traçages. Pour éviter toute dérive, aucun argument de cohérence hydrogéologique ne doit être apporté pour valider un traçage.

L'eau de la Fontaine de Vaucluse est d'un beau vert fluorescent à l'étiage, en moyennes eaux et en hautes eaux. Il n'y a qu'après de très fortes crues que la couleur tourne au brun. Dans les eaux karstiques, ce vert est probablement dû à des matières organiques fluorescentes vertes. L'emploi de fluorescéine, colorant vert à fluorescence verte, est donc réservé à des opérateurs expérimentés, qui ont les moyens techniques de distinguer la fluorescence naturelle de celle de la fluorescéine.

Des associations de spéléologues, aidées du BRGM, ont réalisé 5 colorations à la fluorescéine à partir du plateau de Vaucluse de 1963 à 1970 : injection, fabrication, installation, relevés et interprétations des fluocapteurs aux charbons actifs. Aucune analyse d'eau n'a été réalisée. Ces bénévoles n'avaient aucune expérience préalable de la technique employée, car 30 jours avant l'injection de 1963 ils ne connaissaient pas l'existence des fluocapteurs, Jean (1982). Les fluocapteurs étaient remis tardivement au BRGM pour validation « officielle » des résultats. Pour la première coloration de 1963, les fluocapteurs ont été remis au BRGM 4 mois après l'injection, Jean (1982). Des fluocapteurs verts « à l'aide d'une simple lampe-torche » étaient montrés aux journalistes. Qu'un fluocapteur qui a passé 4 mois dans l'eau verte fluorescente de la Fontaine soit vert, et qu'ensuite les analyses officielles du BRGM au fluorimètre montre une fluorescence verte, est tout à fait normal, et cela ne prouve pas la réussite des colorations.

Les résultats scientifiques de la première coloration dite positive de 1963 sont donnés par Lallemand & Paloc (1964). Le premier fluocapteur « positif », immergé le 6 juillet, a été sorti de l'eau le 10 août 1963, soit 35 jours après l'injection. Ceux du 9 août sont négatifs. La vitesse maximale donnée est donc 26,2 m/h. Or en 1963, le débit moyen de la Fontaine avant le début de la restitution a été de 26 $m^3/s$ (Sorgomètre). Le débit moyen avant la restitution du traçage de 2004 a été de 20,3 $m^3/s$ (Sorgomètre) pour une vitesse 74,7 m/h. Le débit à l'entrée des Gorges était en 1963 de 400 l/s à 1000 l/s selon les auteurs. En 2004, il était de 120 l/s. Le résultat positif de 1963 est donc totalement impossible. En réalité la restitution aurait dû débuter le 16 juillet 1963, et être totalement terminée début août. Or tous les fluocapteurs journaliers jusqu'au 9 août étaient négatifs.

Cette technique, fluocapteur au charbon actif + fluorimètre, a été testée en 1989 par Couturaud & Puig (1992). En l'absence prouvée de restitution de fluorescéine, ils montrent que la fluorescence verte augmente avec la durée d'immersion du fluocapteur dans la Fontaine de Vaucluse. Les « courbes de restitution aux fluocapteurs » des premières colorations sont dues à un phénomène naturel et non à des restitutions de traceur. Couturaud & Puig (1992) ont également démontré l'absence de relation entre fluocapteurs et prélèvements d'eau. La relation est même inversée. Ils montrent également que les concentrations inférieures à 1 µg/l pour les fluocapteurs ne peuvent être significatives. Or lors des 5 colorations, les concentrations maximales en fluorescéine seraient restées inférieures à 1 µg/l (estimation à partir des conditions des colorations par rapport aux traçages valides). L'ensemble des résultats positifs annoncés des 5 colorations est donc à rejeter, car la technique de détection employée n'était pas assez sensible.

En employant la même technique des fluocapteurs, des dizaines d'autres relations avec des sources et des forages ont été « prouvées » lors des 5 colorations. Avec des arguments hydrogéologiques, toutes ces relations sont catégoriquement rejetées par Puig (1990), qui les qualifie de « fantaisistes » et de « trop contradictoire pour être acceptée ». La logique veut que l'on rejette également toutes les liaisons par fluocapteurs, y compris les « restitutions » à la Fontaine de Vaucluse, et pas seulement celles qui dérangent. La cohérence hydrogéologique ne peut être un argument pour valider un traçage.

En conclusion, le traçage des pertes de la Nesque de 2004 prouve qu'il faut rejeter le résultat positif de la coloration de 1963. La validation des 4 autres colorations (1966 à 1970) aux fluocapteurs doit également être rejetée à cause de la méthodologie de détection.

Les multitraçages de 1974 et 1989 posent des problèmes d'interprétation, à cause de l'emploi simultané de la fluorescéine et d'une rhodamine. Idstein & Ewers (2002) ont montré que les rhodamines étaient peu stables dans le milieu souterrain et que des produits de décomposition (DAR) très stables avaient la même fluorescence que la fluorescéine. Les deux courbes de restitution d'équivalent fluorescéine de 1974 et 1989 pourraient être dues soit à la fluorescéine, soit au produit de dégradation de la rhodamine, soit la somme des deux comme Idstein & Ewers (2002) l'ont souvent montré en réinterprétant d'anciens multitraçages.

En 1974, il n'y a eu aucune détection de rhodamine B. La liaison en 6 jours entre l'Aven du Château et la Fontaine de Vaucluse est valide, mais le fort taux de restitution pourrait être dû à la somme de la fluorescéine et du DAR B. La courbe de restitution de 1989 pourrait aussi être due à l'injection de sulforhodamine dans les pertes de Méthamis. La restitution tardive de 2 à 6 mois après l'injection rendent possible une dégradation totale de la sulforhodamine.

En 2003, il n'y avait qu'une (ou deux) relation certaine démontrée par traçage sur la Fontaine de Vaucluse, celle de l'Aven du Château en 1974, et éventuellement celle du Trou du Vent en 1989. Avant 2004, les connaissances des circulations alimentant l'une des plus grandes sources karstiques du monde étaient des plus rudimentaires. Il est anormal qu'une telle source karstique de renommée mondiale soit aussi mal connue. Pour comparaison, en 1988, sur la plus importance source karstique d'Amérique du Nord (débit maximum de 40 $m^3/s$), il y avait plus de 10 traçages fiables dont 4 avec des mesures en continu de traceur Smart (1988).

La présentation de résultats faussement positifs afin de satisfaire les organismes financeurs est un réel problème pour la gestion des grands aquifères. En effet les traçages sur les grands aquifères sont difficiles et nécessitent de véritables compétences. Sur la Fontaine de Vaucluse, les 5 liaisons soi-disant prouvées des traçages avant 1970 ont empêché la réalisation de traçages sérieux ensuite. Ce problème est malheureusement toujours d'actualité. En 1998, une étude sur le grand aquifère karstique du Vercors a montré que plus de 50 % des traçages validés par l'Agence de l'Eau et le Parc du Vercors avaient une restitution non démontrée. La méthode de validation était la cohérence hydrogéologique, alors que ce paramètre ne devrait normalement pas intervenir. Dans le Sud de la France, une grande partie des anciens traçages ont été réalisés avec des fluocapteurs, on peut donc douter de leur exactitude. Plus récemment, l'important traçage des pertes du Verdouble, Courtois et al. (2003), avec une durée de surveillance en continu d'une année et un temps de première arrivée donnée de 45 jours est en réalité un échec. La soi-disant « restitution en bouffée pendant les crues » est une simple interférence des matières organiques fluorescentes qui arrivent pendant les crues.

## 6. Conclusion

L'interrogation posée par le système karstique de Vaucluse est la multitude de failles d'orientation nord-sud ± 30°, alors que la Fontaine est à l'extrémité ouest de l'aquifère et que les circulations principales sont donc de l'est vers l'ouest. Ces failles subméridiennes avaient pendant un siècle limité le bassin d'alimentation vers l'est aux « champs de fracture de Banon ». Puig (1990) avait émis l'hypothèse avec des arguments géologiques et un bilan d'eau précis que la Montagne de Lure, à l'est des failles de Banon, appartenait au bassin d'alimentation. Les traçages de 2004 et 2005 ont prouvé l'extension du bassin d'alimentation jusqu'à la Durance.

En tant que bureau d'études, nous avons travaillé sur de nombreux forages situés dans les karsts profonds d'origine messinienne. Généralement les forages situés sur les axes des structures anticlinales est-ouest sont exploitables, et ils rencontrent des drains karstiques profonds situés sous le niveau actuel de la mer. Guerin (1973) a montré en Ardèche une phase de karstification d'axe préférentiellement est-ouest lors de la phase alpine de la fin du miocène (pontien).

Dans le karst de Vaucluse, une seule rivière souterraine est connue, celle du Trou Souffleur. Un collecteur de 100 l/s à l'étiage est suivi sur 1 km dans une galerie horizontale parfaitement est-ouest. De petits décrochements nord-sud à fort dénivelé montrent que le drain principal est au sud du Trou Souffleur. Nous supposons donc que le collecteur principal noyé passe sous l'axe de la structure anticlinale des Monts du Vaucluse.

Le drain est-ouest du système karstique de Vaucluse s'est donc formé à la fin du miocène

pendant la période messinienne (et probablement la phase alpine pontienne). Le drain principal provenant de la Montagne de Lure passe sous l'anticlinal des Monts du Vaucluse, et non dans les structures synclinales d'Apt ou de Saint Christol. Ce drain pourrait être une paléo-Durance creusée au Messinien.
La Figure 7 donne une carte de synthèse montrant le bassin d'alimentation avec le principal drain alimentant la Fontaine de Vaucluse et les 4 relations prouvées par traçage. Avec les nouvelles données de cet article, le bassin d'alimentation de la Fontaine de Vaucluse atteint 1210 $km^2$.

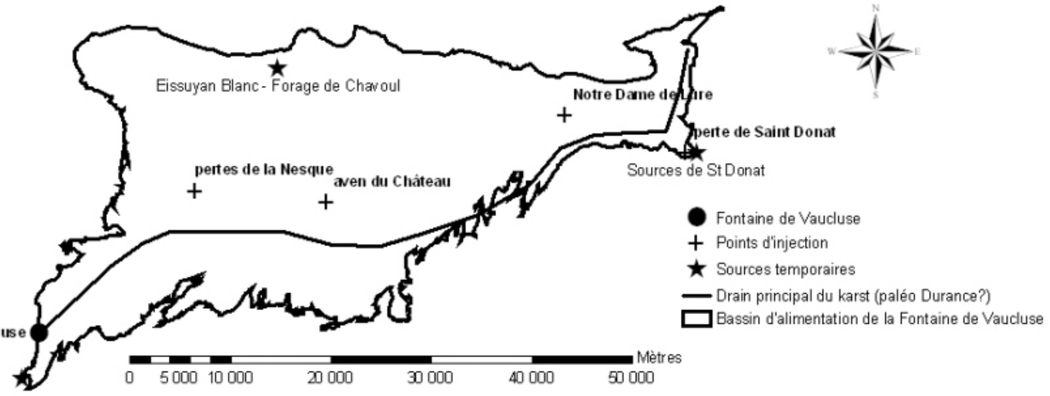

*Figure 7 : Carte du bassin d'alimentation de la Fontaine de Vaucluse*

## Références

- Courtois, N., Bakalowicz, M., Cubizolles, J., Dörfliger, N., Izac, JL. & Ladouche, B. (2003). Essai de traçage des pertes du Verdouble. Rapport BRGM/RP-52211-FR, 82p., 25fig.
- Couturaud, A. & Puig, J.M. (1992). Traçages en bordure du système karstique de Vaucluse - Karstologia , 20: 23-36, 6 fig.
- Ducluzaux, B. (1999). Mesure en continu et in situ des traceurs pour les traçages artificiels et naturels. Interprétation des courbes de restitution perturbées par des précipitations. Actes Neuvième Rencontre d'Octobre, Paris, France.
- Ducluzaux, B. (2001). Mesures en continu et in situ des traceurs par des capteurs chimiques. Application à l'ion iodure. 7th Conference on Limestone Hydrology and Fissured Media, Besançon, France, 20th-22th September, 2001. Sciences et Techniques de l'Environnement, Besançon, France, mém. H.S. 13: 129-132.
- Guerin, R. (1973). Un exemple du rôle de la tectonique et de microtectonique dans la géométrie des écoulements karstiques fossiles et actuels : le Bas-Vivarais calcaire. Thèse Montpellier, France. 120 p.
- Idstein, P. & Ewers, R. (2002). Unexpected characteristics of rhodamine WT as a groundwater tracer. – GSA Joint Annual Meeting (April 3–5, 2002) Lexington, Kentucky.
- Jean, R. (1982). A la recherche de la Sorgue et de la Nesque souterraine. Imp. des Tours, Châteaurenard, France. 108p.
- Lallemand, A. & Paloc, H. (1964). Possibilités offertes par la méthode de détection au charbon actif pour les expériences de coloration à la fluorescéine. – Spelunca, 4e série. 27-40.
- Puig, J.M. (1990), Le système karstique de la Fontaine de Vaucluse. Document du BRGM N° 180, Orléans, France. Thèse 208p.
- Smart, C.C. (1988). Quantitative tracing of the Maligne karst system, Alberta, Canada. Journal of Hydrology, 98 : 185-204.

## DARCY 35

# Hydrochemical relations between the percolation waters of the Trebiciano Abyssand the base-flow phreatic water of Trieste Karst aquifer

Enrico Merlak[1], Clarissa Brun[2], Fabio Gemiti[3], Rino Semeraro[2]

[1] Geologist. Author's Address: via Beda [3], 34139 Trieste, Italy
[2] Geokarst Engineering srl - AREA Science Park, Padriciano 99, 34012 Trieste, Italy,
geokarst@area.trieste.it
[3] Chemist. Author's Address: via Tedeschi [3], 34124 Trieste, Italy,
gemiti@tiscalinet.it

## Abstract

The percolation waters of the Trebiciano Abyss (the Karst of Trieste) have been studied for 20 months, in two points at 100 and 250 m depth, in order to detect the main physical-chemical parameters, according to the rainfalls, the outside temperature, the seasons and the hydrodynamic. Parallel to the physical-chemical research, a tracing test has been carried out, which has given the average of percolation rate. The tracing has shown that major flows of the percolating waters of the abyss are connected with the overlying dolines. The percolation has been studied by the relations between the physical-chemical characteristic of base-flow phreatic waters of karst aquifer.
It results that the percolating waters of the Trieste Karst are, on the average, different form the base-flow phreatic waters since: a) the percolating waters show high concentrations of $Ca^{2}$+ and $Ca(HCO_3)$ 2 and low concentrations of characteristic parameters: $K^{+}$, $Na^{+}$, $Cl^{-}$ and $NO_3$ ; b) base-flow phreatic waters show low concentrations of $Ca^{2+}$ and $Ca(HCO_3)_2$, and high concentrations of characteristic parameters: $K^{+}$; $Na^{+}$, $Cl^{-}$ and $NO_3$.

## 1. Introduction

The percolation waters of the Trebiciano Abyss (the Karst of Trieste, NE Italy), on whose bottom the underground Timavo river flows, have been studied for 20 months, in two points at 100 and 250 m depth, in order to detect the main physical-chemical parameters, according to the rainfalls, the outside temperature and the seasons. Beside studying the water dynamic and the chemistry of the abyss percolation system, the purpose was also to determine the main physical-chemical characteristics of the waters that flow in the vadose zone, since they considerably contribute to the feeding of the karst aquifer. Finally, to correlate the physical-chemical data of percolating waters with those of the base-flow phreatic waters of the Karst.

## 2. The karst aquifer

The Karst region, divided into Italy and Slovenia (Carso/Kras), is a structure made up of carbonate rocks, with an extension of about 1000 km$^2$ having more feeding ways (Fig.1) (Ballarin et al., 2000). In a saturated area the conduits develop both above and under the sea level and they are fed by a thick network of vertical cavities.

The springs are mainly placed in the north-west area of the Karst where: at about 2 m above the sea level the Timavo springs, the Sardos springs, and other minor ones are located, with an overall average flow of 15-20 m$^3$/s and a maximum flow over 100 m$^3$/s. The minimum flow, even after several dry months, is of about 7 m$^3$/s, which puts forward the hypothesis that the low Timavo springs might be mainly fed by waters external to the karst basin as well as by deep water systems communicating through big deposits of siliceous sands and clay that act as stores and slow down the flows. The maximum flows have been reckoned in about 150 m$^3$/s (Gemiti, 1984, 1996).

The above-mentioned springs were used for over 50 years for the water supply of Trieste and its province. In the 80s of the former century, after severe pollution, mainly due to wastewaters from the factories in Slovenia, of the Timavo/Reka River that feeds the Karst aquifer, the new waterworks, which capture the alluvial aquifer of Friuli were built. Therefore, at the moment, these springs are used exclusively as a reservoirs.

## 3. The vadose zone in the Trebiciano Abyss

The Trebiciano Abyss VG17 is located in the Karst on the side of a doline, at the height of 341 m above the sea level (Fig. 2) and it is 350 m deep. The abyss, conditioned by lithologies and by the structural asset, develops in a series of carbonate rocks of the upper Cretaceous: from the entrance to the depth of about 185 m in limestones, then to the maximum depth in dolomitic rocks (Forti et al., 1979). At the depth of about 270 metres the networks of shafts that characterise the abyss open in the enormous “Lindner Cavern”. On its bottom the under-

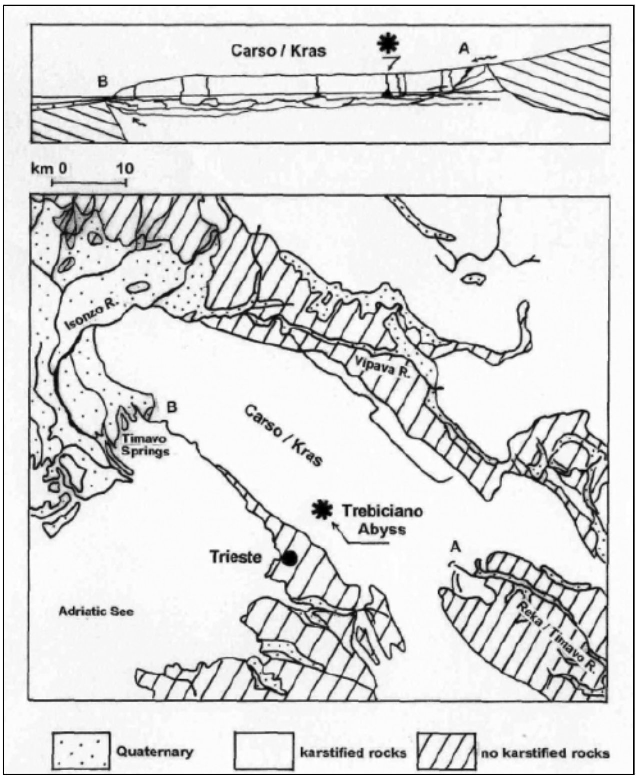

*Figure 1: The Karst area (Carso/Kras). The karstified rocks, in the vadose and phreatic zone, are made up of prevailing limestones, dolomitic limestones and dolostones; A: Timavo River in the sink hole San Canziano Caves / _kocjanske Jame; B: Timavo River springs.*

ground Timavo flows at an average height of 12-14 m a.s.l., in galleries under the sea level. The karstic hydrostructure of the vadose zone in this area is characterised by networks of shafts, which, sometimes, are supposed to be very near one another. These networks of shafts collect the waters that infiltrate through the surface, discharging them into the galleries and caverns placed in the epiphreatic area.

In the abyss two measurement stations have been placed. In the "Station A" at the depth of -100 m (points P1, P2, and P3) drip waters from stalactites have been measured and collected. In the "Station B" at the depth of -250 m (points 4 and 5) flowing waters have been measured and collected along the slopes and in fall. The monthly measurements refer to the period from December 1999 to June 2001.

Parallel to the physical-chemical research, a tracing test with Uranine and Tinopal CBS-X has been carried out, which has given the average percolation rate. The alkalinity ($HCO_3^-$), electrolytic conductivity and pH measurements have been carried out on the field together with those of temperature and percolation flow. The tracing has shown that major flows of the percolating waters of the abyss are connected with the overlying dolines.

## 4. Physical and chemical characteristics of vadose waters in the Trebiciano Abyss: the summary of results

The alkalinity ($HCO_3^-$), electrolytic conductivity and pH measurements have been carried out on the field together with those of temperature and percolation flow. The results are as follows:

- 94-97% of the ionic contents is composed of $Ca(HCO_3)_2$;
- the pH has always a seasonal variation with maximum values of 8.20 between December and February, and minimum values of 7.10 between July and October, following the trend of the ground temperature;

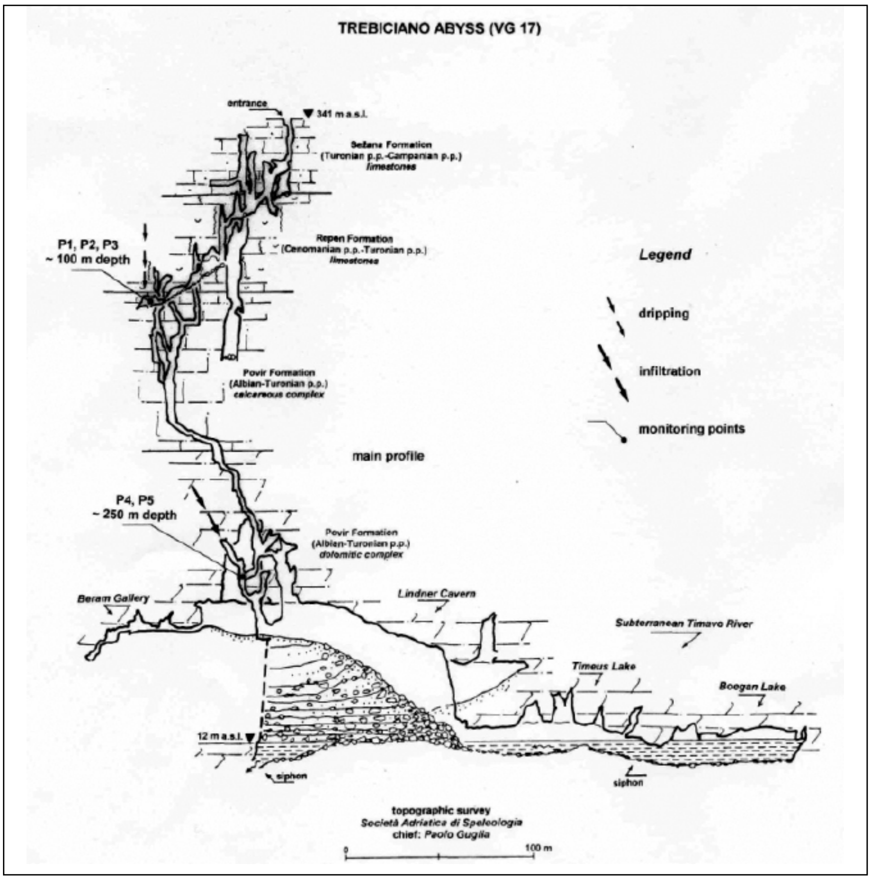

*Figure 2: Profile of Trebiciano Abyss.*
*The monitoring points: "Station A" at the depth of -100 m (points P1, P2, and P3), "Station B" at the depth of -250 m (points 4 and 5).*

- the water mineralization shows seasonal variations but is basically affected by the rainfalls, with minimum $Ca(HCO_3)_2$ values of about 180 mg/L in dry periods and maximum $Ca(HCO_3)_2$ values of about 510 mg/L in the following 2-5 days after heavy rainfalls;
- the typical ions of water ($Mg^{2+}$, $Na^+$, $K^+$, $NH_4^+$, $Cl^-$, $NO_3^-$, $SO_4^{2-}$, $PO_4^{3-}$,) are always present in small quantities, except for $SO_4^{2-}$ which ranges from 7 to 11 mg/L;
- the phosphates and the ammonium are present in traces;
- the concentrations of NaCl are low and very similar to those of the rainfalls, therefore the release of NaCl from the soil is excluded;
- the presence of nitrates and sulphates is exclusively due to the soil biological activity;
- the concentrations of $SiO_2$ are constant (about 1.5 mg/L) and come from the slow release of silica and from the phyllosilicates present in the soil;
- the water saturation index (calculated according to the AWWA principles) ranges from 0.4 to 1.2: the water is always supersaturated;
- the percolation water, beyond 100 m of depth, has a variable temperature from 10.2 to 11.2°C depending on seasons;
- the transfer time of the water infiltrating through the surface to the bottom (-300 m) is of a few hours, the flow and the reservoirs depend on the water storage in the epikarst.

## 5. Hydrodynamic and hydrochemistry of vadose and phreatic waters in the karst system

The results obtained are comparable to those detected in other cavities in the Karst basin, in different places, depths and times (Gemiti & Merlak, 1999). Thus, it has been ascertained that, within the bounds of single areas characterized by specific climates, the variations of the average characteristics of water are constant, therefore predictable. This should give the possibility to define in advance the base physical-chemical parameters of the Karst percolation waters, according to of the seasons, to the rainfalls and to the areas with similar climatic features. Another interesting result is that the measurement of the specific conductivity gives the exact situation of the water mineralization (it can be used also as a quality control of the analysis) since the composition is essentially $Ca(HCO_3)_2$ and the variations of the concentration of other ions are negligible.

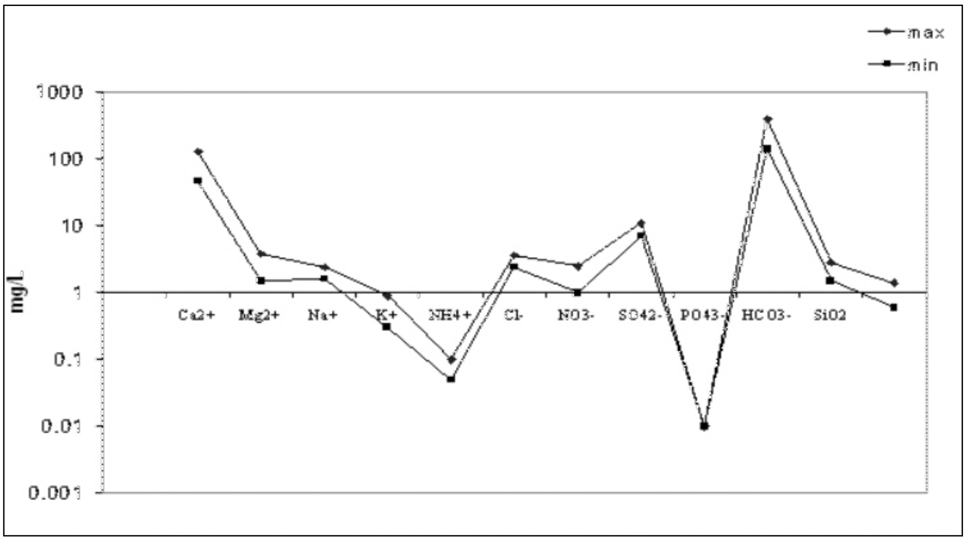

*Figure 3: Maximum and minimum concentrations of the solute (mg/L) $Ca^{2+}$, $Mg^{2+}$, $K^+$, $NH_4$, $Cl^-$, $NO_3$, $SO_4$, $PO_4$, $HCO_4^-$, $SiO_2$ and of the Saturation Index (Sat. Ind.) during the period of 20 months, in the percolating waters of the Trebiciano Abyss.*

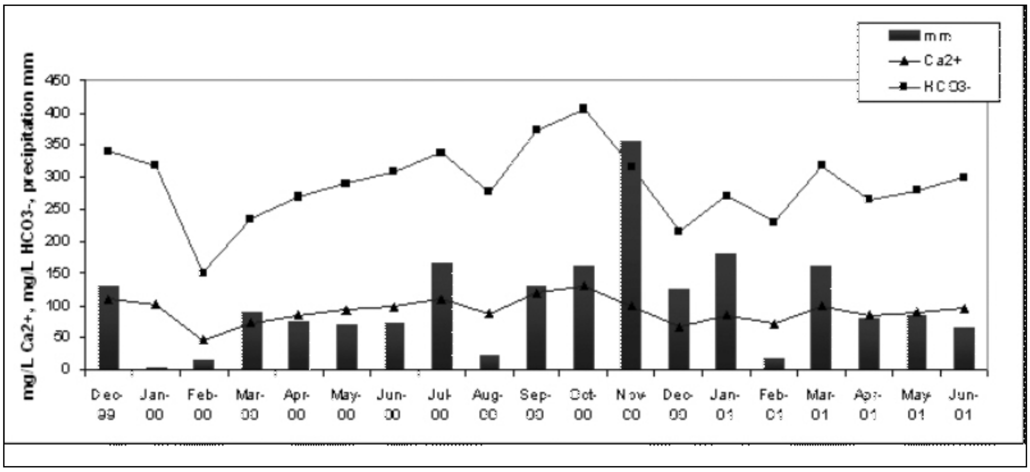

*Figure 4: (Average) variations of Ca$^{2+}$ and HCO$_3^-$ in the percolating waters of the Trebiciano Abyss in relation to the rainfalls.*

In Fig. 3 are the maximum and minimum ionic concentrations (mg/L) of the percolating waters in the Trebiciano Abyss at the depths of 100 and 250 metres (average of the values measured). The chemical picture is similar to those surveyed in other 6 karst cavities of the area. It shows that Ca(HCO$^3$) 2 represents about the 90-95% of the total composition. The major seasonal variations regard calcium and bicarbonate as shown in Fig. 4, they change depending on the season and depending on rainfalls.

The evaluation of the differences between the percolating waters of the Trieste Karst and other waters of the karstic system is interesting.

In Fig. 5 are the values of the average concentrations measured in the period November-December 1999 in the following waters:

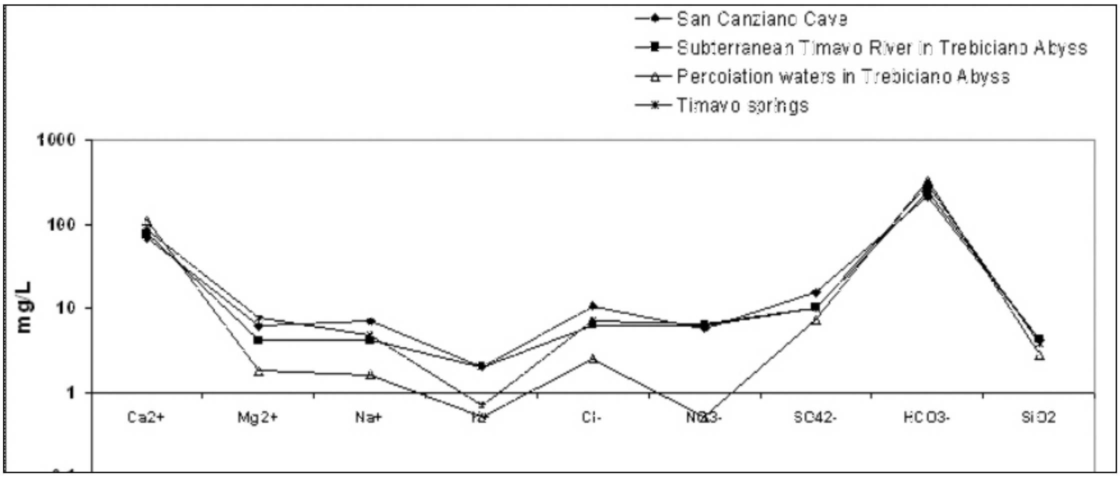

*Fig. 5: Variations of the average concentrations of the main chemical parameters of the waters of the karstic system i n the period November-December 1999.*

- the River Timavo /Reka, in the locality of Vreme, before entering San Canziano Cave/ kocjanske Jame;
- the underground Timavo on the bottom of the Trebiciano Abyss;
- the percolating waters in the Trebiciano Abyss;
- Timavo River springs.

It results that the percolating waters of the Trieste Karst are, on the average, different form the base-flow phreatic waters since:

a) the percolating waters show high concentrations of $Ca^{2+}$ and $Ca(HCO_3)_2$ and low concentrations of characteristic parameters: $K^+$, $Na^+$, $Cl^-$ and $NO_3$;

b) base-flow phreatic waters show low concentrations of $Ca^{2+}$ and $Ca(HCO_3)_2$, and high concentrations of characteristic parameters: $K^+$; $Na^+$, $Cl^-$ and $NO_3$.

The only exceptions to this framework concerns ascertained case of surface pollution concentrated in single areas. It is the case of the cave VG 6163, placed at about 200 metres from the Trebiciano Abyss and developed under the ex uncontrolled landfill of the Town hall of Trieste, closed in 1972. After more than thirty years, in this cave at -95 m, in the percolating waters the values of 170mg/L of $SO_4^{2}$- and of 25 mg/L of $K^+$ can be measured.

## References

- Ballarin L., D'Amelio L., Krokos A., Serra F., Semeraro R., 2000: Trieste Karst aquifer: review of hydrogeology and geochemistry. COST Action 621 "Groundwater management of coastal karstic aquifers", 7th Management Committee Meeting, Karst Research Institute, Postojna 23-25 March 2000, Guide-Booklet for the excursion: 20 pp.
- Forti F., Semeraro R., Ulcigrai F., 1979: Carsogenesi e geomorfologia dell'Abisso di Trebiciano. Atti Mem. Comm. Grotte "E. Boegan", 18: 51-99.
- Gemiti F., 1984: La portata del Timavo alle risorgive di S. Giovanni di Duino. Ann. Gr. Grotte Ass. XXX Ott., 7: 23-41.
- Gemiti F., 1996: Portata liquida e portata solida del Timavo alle risorgive di S. Giovanni di Duino. Hydrores, 13: 75-88.
- Gemiti F., Merlak E., 1999: Indagine sull'equilibrio carbonatico delle acque di percolazione di una cavità del Carso triestino (Pozzo 2° a NW di Gropada, ex VG 857). Atti 8° Conv. Reg. Spel. Friuli-Venezia Giulia, Località cave di Selz (Ronchi dei Legionari, Gorizia) 1999: 151-160.

# DARCY 40

# Hydrogeological caracterization of the Oxfordian limestones at the Bure URL

CRUCHAUDET M. , DELAY J.

ANDRA – Laboratoire de Recherche Souterrain de Meuse / Haute-Marne
Route Départementale 960 – 55290 BURE France
Martin.cruchaudet@andra.fr, Jacques.delay@andra.fr

Andra, The French National Radioactive Waste Management Agency, is constructing an Underground Research Laboratory for studying the feasibility of radioactive waste disposal in Jurassic-age Callovo-Oxfordian argillaceous rocks. One of the objectives of the investigations performed since 1994 was to caracterize the hydrogeological parameters of the rocks surrounding the argillaceous rocks, particularly the Oxfordian and Dogger limestone formations.

The Oxfordian limestones are a 280 m thick rock formation located on the top of the Callovo-Oxfordian argillaceous rocks. The hydrogeological studies performed by ANDRA are based on deep boreholes investigations.

At sector scale, ten boreholes were drilled between 1994 and 2004. The scientific programme in these boreholes included the following:

- Hydrogeological testing with and without packers to determine transmissivity,
- Long term piezometric head measurements,
- Geophysical logging to characterize the lithology and the porosity of the Oxfordian limestone formations,
- Fluid conductivity logging to identify inflow zones.

These hydrogeological measurements have allowed regional water flows to be outlined. These results also improved the knowledge of the spatial distribution of permeabilities.

At the URL site scale, the two access shafts of the underground laboratory were expected to drain all terrains, including the Oxfordian limestones.Thus, it was decided to monitor the influence of this drainage on the Oxfordian formation using a network of four monitoring boreholes. Two geological exploratory boreholes were also drilled in the main shaft axis and the auxilliary shaft axis. In these six boreholes, full hydrogeological tests were performed, with and without packers, and seven main inflow zones for the Oxfordian formation were identified with accuracy using the fluid conductivity logging method. Four monitoring boreholes, located between 70 m and 300 m from the shafts, were equipped with multipacker systems to monitor the hydraulic head of up to five groups of inflow zones, called porous levels. In the main shaft and the auxilliary shaft, a set of flowmeters was installed to monitor separately the water outflow of porous levels. For this purpose the shaft was equipped with water garlands every six meters.
Using the data from water inflows to the shaft, the transient responses of the piezometers provided hectometric scale measurements of transmissivities and storativities of the conducting layers. The variability of the responses indicated the limited heterogeneity of the porous levels. The similarity or difference of responses among intervals in different conducting zones enlightened the amount of vertical connectivity of the layers.

## References

- Delay J. , Rebours H. , Vinsot A. , Robin P. , 2005 – Scientific investigation in deep wells for nuclear waste disposal studies at the Meuse/Haute-Marne Underground Research Laboratory, Northeastern France. “Physics and chemistry of the Earth Special Issue” (Elsevier Ed.)
- Distinguin M. , Vinsot A. , Rebours H. , Delay J. , 2005 – Test hydrogéologique d’interférence à l’échelle du site – Expérimentation SPH – Laboratoire de recherche souterrain de Meuse / Haute-Marne – Rapport Andra n° D RP ADPE 05 0735/A

## DARCY 46

# News arguments for karst presence in Northern France chalk. Implication for Boulonnais area hydrogeology.

Aude A., Brunin A.S., Fayeulle M., Bracq P.
L.I.S.E
Université du Littoral Côte Opale, 32 Avenue Foch, 62930 Wimereux, France.
aude@opale.univ-littoral.fr

The presence of a karstic network can, locally and greatly, modify directions and velocities of groundwater flow with that implies for its vulnerability and on the protection of sources supply. In chalk, two large areas of the Paris Basin, Normandy and Gâtinais-Sénonais, are well know for the karstic network which have been observed and explored since the last century (Rodet, 1991). In Mons Basin (Belgium), alteration has given frequent morphologies and deposits (cryptokarstic forms), but endokarstik phenomena seem be non existent (Quinif Y and al, 1997). The chalk of Northern France and particularly in the Nord-pas-de-Calais region is compared for a long time with Mons Basin. Some arguments coming to contradict this assumption.(Bracq and al, 1994). New studies confirm presence of a karstic network in the Boulonnais area. 1) Several tracer tests conducted in the chalk show large velocities and vertical velocity between surface and water table (286mh$^{-1}$ to 1155mh$^{-1}$). 2) The test of active doline showed its capacity of more than 40m$^3$/h. 3) Field work show palaeokarst (metric pipes) and active pipes (dm). Presence of a karstic network in the Boulonnais area can explain river high-speed response to precipitations and significant risings. Indeed, presence of karst explain a fast answer, overflow of chalk aquifer and hydrogeological basin larger than drainage basin. Moreover, connection between chalk aquifer and jurassic aquifer by fault network is perhaps explanation for large jurassic groundwater recharge.

### Références

Bracq P., Crampon N., Colbeaux J.-P., 1994 – Karstic phenomena in the chalk of Northern France and particulary in the Nord-Pas-De-Calais Region. Consequence for groundwater quality and flow. Cost 65 Action, Hydrogeological aspect of Grounwater Protection in Karstic Area in French Karstic area, N. Crampon & M. Bakalowizc ed.
Quinif Y Y., Baele J.-M, Charlet J.-M., De Putter T., Dupuis C., Rorive A., Vandycke S., 1997 – A la recherche du karst perdu des craies du Bassin de Mons (Belgique). Ann. Soc. Géol. Du Nord, T5, p.361-371.
Rodet J., 1992 – La craie et ses karst. Thèse de Doc. Etat., Université de Rouen, 560 pp.

# DARCY 48

# Contribution of the structural geology to the knowing of water and gas transfers in the carbonate aquifer of Quézac (Lozère, France)

Durand V., Deffontaines B., Léonardi V. and Macquar J.-C.
UMR Sisyphe, UPMC, case 105, 4 place Jussieu, 75252 PARIS Cedex 05
veronique.durand@ccr.jussieu.fr

The aim of this study is to understand the fracturation and its relationship to the functioning of aquifers in a carbonate environment, with a specificity of gas intrusions in the groundwater. An example is taken on the Quézac site, in Lozère department (south Massif Central, France), where the Nestlé Waters company exploits the gaseous mineral water. We choose a multidisciplinary approach, in order to combine and complete the interpretations of each method. The morphostructural approach, combining aerial photographs and DEM analyses, helps to map the general fracturation of the area. The fracturation is thereafter related to the tectonic history, reconstructed by microtectonic measurements on the field. We give after some new perspectives of the local structure of the aquifer under the flat alluvial Tarn valley at Quézac by interpretations of well-logs, seismic profiles and Electrical Resistivity Tomography. At the end, the observations of the water and gas transfers inside the tectonic structures, as springs or karsts phenomena originating from the fracturation, are carefully discussed along the successive tectonic stresses on the rocks from the Jurassic to the Quaternary period. The tectonic-surrection history is related to the behaviour of the major structures. This leads to understand that the most important structures for the fluid transfers are the N-S and E-W faults, affecting the basement and the sedimentary cover. If the water acquires its geochemical properties in the carbonates rocks, the gas is of mantellic origin and flows towards the surface through the faults that affect the whole series of geological formations, from the basement to the sedimentary cover. The transfers of gas are favoured especially in this area, due to an assumed asthenospheric anomaly 25 km under the surface in this region, and the sedimentary cover being quite thin locally in the alluvial plain of Quézac, compared to the west side of the Causses. Furthermore, the presence of a major N-S fault intersecting E-W and NW-SE faults in this area presents a good advantage for the exploitation of gaseous water.

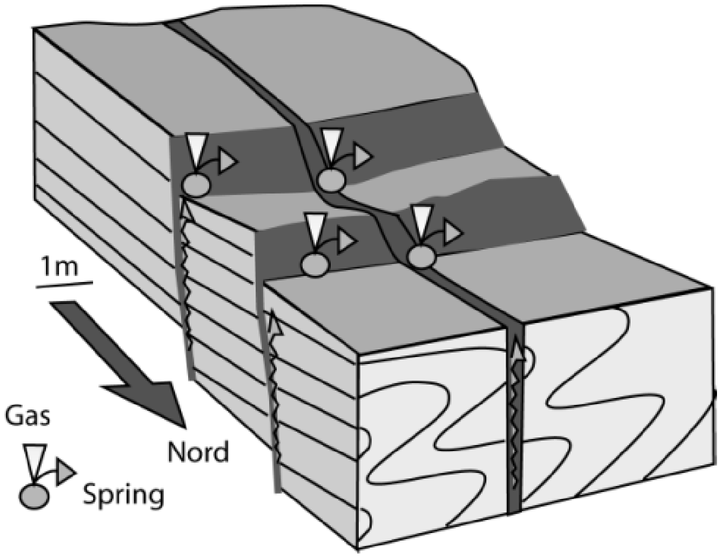

*Figure1. Schematic representation of the N-S and E-W faults conducting the water and gas transfers in the schist basement, from field observations*

# DARCY 49

# Experimental study of the accuracy of the specific yield estimation obtained from Magnetic Resonance Soundings

Boucher M.[1], [2], Baltassat J-M.[1], Girard J-F.[1], Lachassagne P.[3], Legchenko A.[4]

[1] BRGM ARN/RSC, BP 6009, 45060 Orléans, France, m.boucher@brgm.fr
[2] ISTO, UMR6113, r. de St Amand, BP 6759, 45067 Orléans, France
[3] BRGM, EAU/RMD, 1039 rue de Pinville, 34000 Montpellier, France
[4] IRD, LTHE, BP53, 38041 Grenoble Cedex 9, France

## Abstract

The Magnetic Resonance Sounding method (MRS) is a non-invasive geophysical tool that has the advantage to be sensitive exclusively to groundwater. This method is also appropriate for estimation of aquifer hydrodynamic parameters. MRS allows measurement of two parameters: the MRS water content and the relaxation time. The existing instrumental implementation does not allow detecting the part of water, which corresponds approximately to the specific retention capacity. Consequently, the MRS water content appears to be a good estimate of the specific yield of the aquifer. Number of MRS field studies and Nuclear Magnetic Resonance (NMR) measurements in laboratory were performed in the sandy-clayey formation of Sologne and in the chalk of the Hallue catchment (both in France). Our results show that the MRS method is an operational tool for groundwater investigations. However, field examples have shown that, depending on the geological context and more especially on magnetic susceptibility of the rocks, the MRS water content can over or under estimated the specific yield.

## Introduction

The proton Magnetic Resonance Soundings (MRS) is a non-invasive geophysical technique specially adapted to hydrogeological investigations. This method has the advantage of measuring signal with the amplitude directly related to mobile groundwater and the relaxation time correlating to the size of water filled pores.
However, the existing instrumental implementation does not allow measuring short signals (signal shorter than the instrumental dead time equal to 40 ms), and thus, some part of water in the aquifer characterized by a short relaxation time T2* cannot be detected. The relaxation time T2* depends on the distance existing between the water molecules and the pore walls but also on the magnetic properties of rocks. The aim of this work is to better understand the different factors influencing accuracy of magnetic resonance measurements.

## Method

The principle of Magnetic Resonance Sounding (MRS) technique consists of recording an oscillating with the Larmor frequency electromagnetic field after an excitation pulse. The MRS response decreases exponentially with the time constant T2* (Figure 1). The amplitude of MRS signal is directly linked with the quantity of water in the aquifer (Legchenko et al., 2004). The relaxation time is correlated to the distance between the water molecules and the pore walls (Kenyon, 1997): smaller is the distance, shorter is T2*.
The instrumental dead time of 40 ms between the end of excitation pulse and the beginning

of recording does not allow measuring the short time signal (i.e. signal shorter than 40 ms). Thus, the part of the water characterized by a short relaxation time T2* (bound and capillary water) cannot be detected (Figure 2). Consequently, it is generally assumed that the MRS water content appears to be close to the specific yield of the aquifer (Lubczynski et al., 2003; Lacchassagne et al. 2005). However, the relaxation time T2* depends also on the magnetic properties of the rock: more magnetic is the rock, shorter is the relaxation time T2* and more important is the part of invisible for MRS water. Consequently, depending on the geological context the specific yield can be over or under estimated.

In the lab, Nuclear Magnetic Resonance (NMR) measurements allow measuring the water content in samples using the same physical principle as MRS. Because, the condition in the lab are better defined, the recording signal is not affected by an instrumental dead time. It allows measuring the totality of water in the samples. The Figure 3 shows an example of comparison between the water content estimated with lab NMR and by weighing. Results provided by these two methods are similar.

## Field and lab measurements in sandy-clayey formation

Rock samples were extracted in the sandy-clayey formation of Sologne in the test site named Marcilly where many MR soundings were carried out. In order not to disturb the water content, a percussion core sampler was used. The samples were analyzed with the NMR spectrometer at 2 MHz in the department of applied geophysics of the Technical University of Berlin (TUB).

Results (Figure 4) show a good correlation between NMR parameters and geological log. The water content measured with MRS is lower than the water content measured with NMR. This result is in agreement with the fact that MRS water content, due to the instrumental dead time, is an estimation of the specific yield whereas, lab NMR spectrometer measures the total saturated porosity.

However, the difference between MRS water content (~10%) and lab NMR water content (~30%) is very important. Beside, the MRS relaxation time (200-400 ms) is more than ten times longer than the relaxation time from lab NMR measurements (<20 ms). The decrease of relaxation time when the static magnetic field increases (47 $\mu$T in the field vs. 47 mT in the lab) is due to paramagnetic properties of rocks. As a consequence of the presence of paramagnetic particles in this context, the specific yield measured with MRS is significantly underestimated.

## Chalk aquifer

In the investigated chalk aquifer a thick (tens meters) unsaturated zone was observed. Typically, in the chalk unsaturated zone, the fracture porosity (~2%) is empty of water and nearly all the matrix (with ~40% porosity) is saturated (Price et al. 2000). Another specificity of the chalk is its very low magnetic susceptibility. These two conditions (thick unsaturated zone and low magnetic susceptibility) allow detecting with MRS part of the capillary water above the water table. In this geological context, the specific yield is thus overestimated.

Field and laboratory experiments in the Hallue catchment show (Figure 5) that the MRS water content increase with depth whereas water content measured on samples was found not very variable and close to the full saturation of chalk (40%). Thus, less and less water is detectable with MRS from the water table up to the surface. Because of low magnetic susceptibility of chalk, the relaxation time T2* was found similar in the lab and in the field. In Figure 5, T2* increases with depth and MRS water content converges towards the water content measured in the laboratory, thus confirming that quantity of undetectable by MRS water is linked with the relaxation time T2*. Our experimental results (Figure 5) and numerical modeling results (Figure 6) are in a good agreement in-between.

## Conclusion

The MRS method is an operational tool to quantify the groundwater. However, interpretation of MRS results in term of specific yield must be carried out with a lot of care. Two field examples have shown that, depending on the geological context and more especially on magnetic susceptibility of the rocks, the MRS water content and hence the specific yield can be overestimated (in sand and clay formation) or underestimated (in chalk formation). The accuracy can be improved by considering the relaxation time T2* and simultaneous decrease of the dead time in the hardware. These ameliorations are actually under development.

## References

- Kenyon WE (1997) Petrophysical principles of applications of NMR logging. The Log Analist, March-April: .21-43.
- Lachassagne P, Baltassat JM, Legchenko A, de Gramont HM (2005) The links between MRS parameters and the hydrogeological parameters. Near Surface Geophysics 3: 259-265.
- Legchenko A, Baltassat JM, Bobachev A, Martin C, Robain H, Vouillamoz JM (2004) Magnetic resonance sounding applied to aquifer characterization. Ground Water 42, 3: 363-373.
- Lubczynsky M, Roy J (2003) Hydrogeological interpretation and potential of the new magnetic resonance sounding (MRS) method. Journal of Hydrology 283: 19-40.
- Price M, Low RG, McCann C (2000). Mechanisms of water storage and flow in unsaturated zone of Chalk aquifer. Journal of Hydrology 233: 47-71.

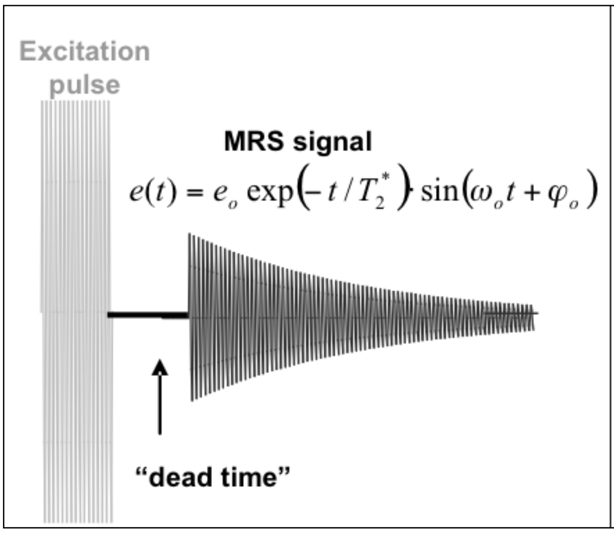

Figure 1: MRS signal recording

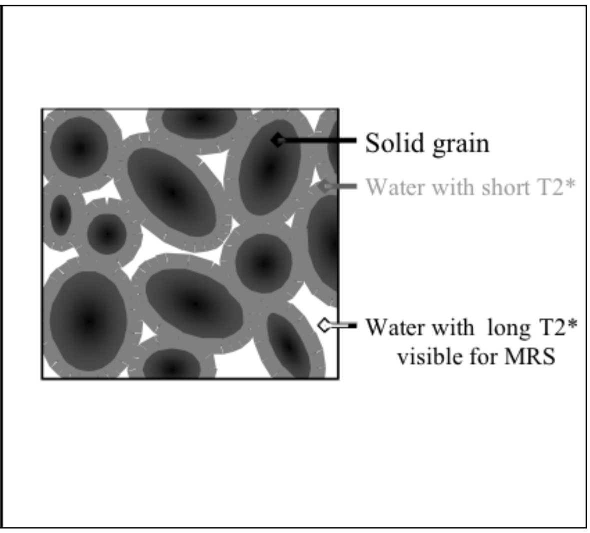

Figure 2: Detectable with MRS wate

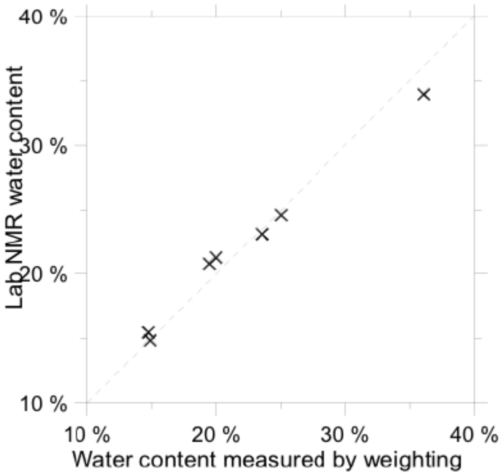

Figure 3: Comparison of water content measured with NMR and by weighting

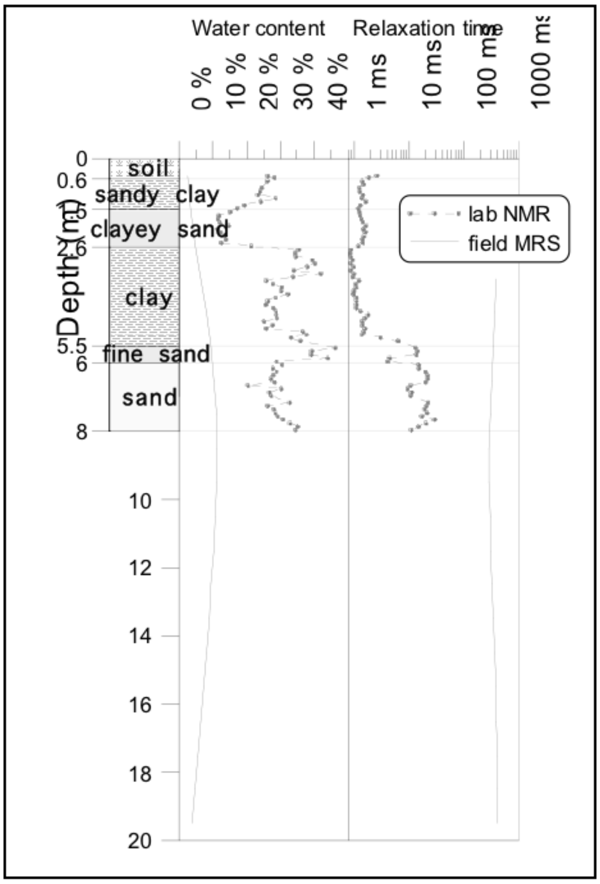

Figure 4: Comparison of lab NMR and field MRS results in Marcilly test site

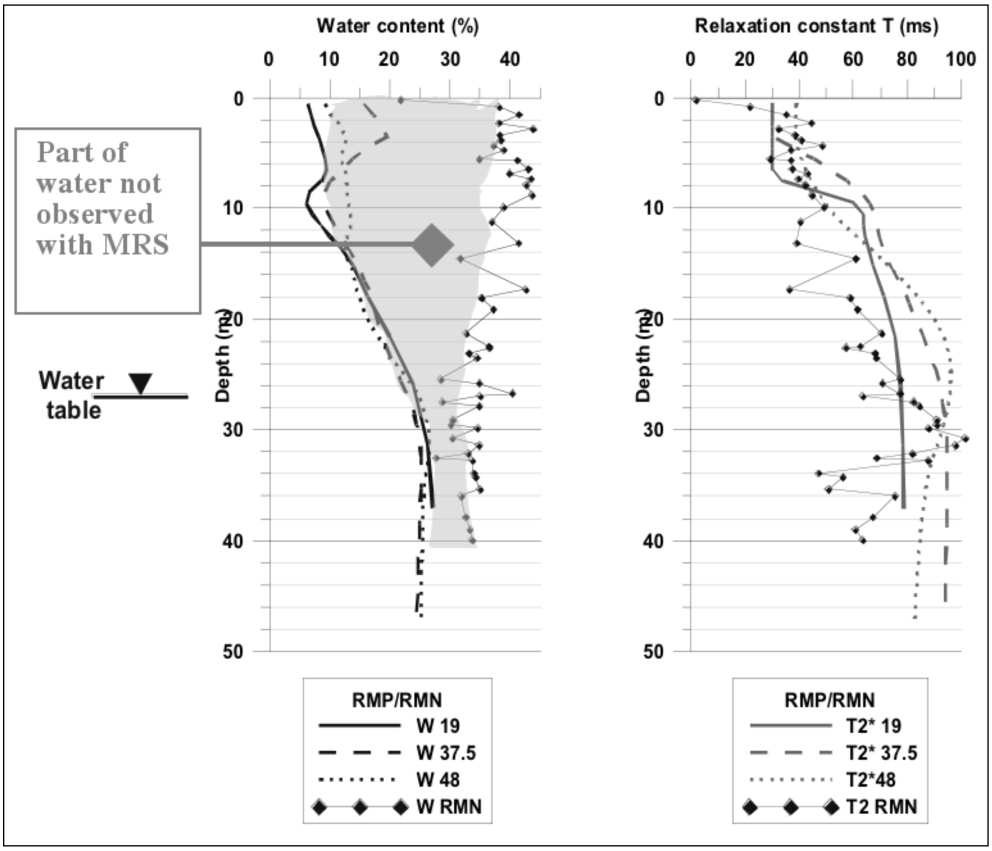

Figure 5: Comparison of lab NMR and field MRS results in Hallue catchment

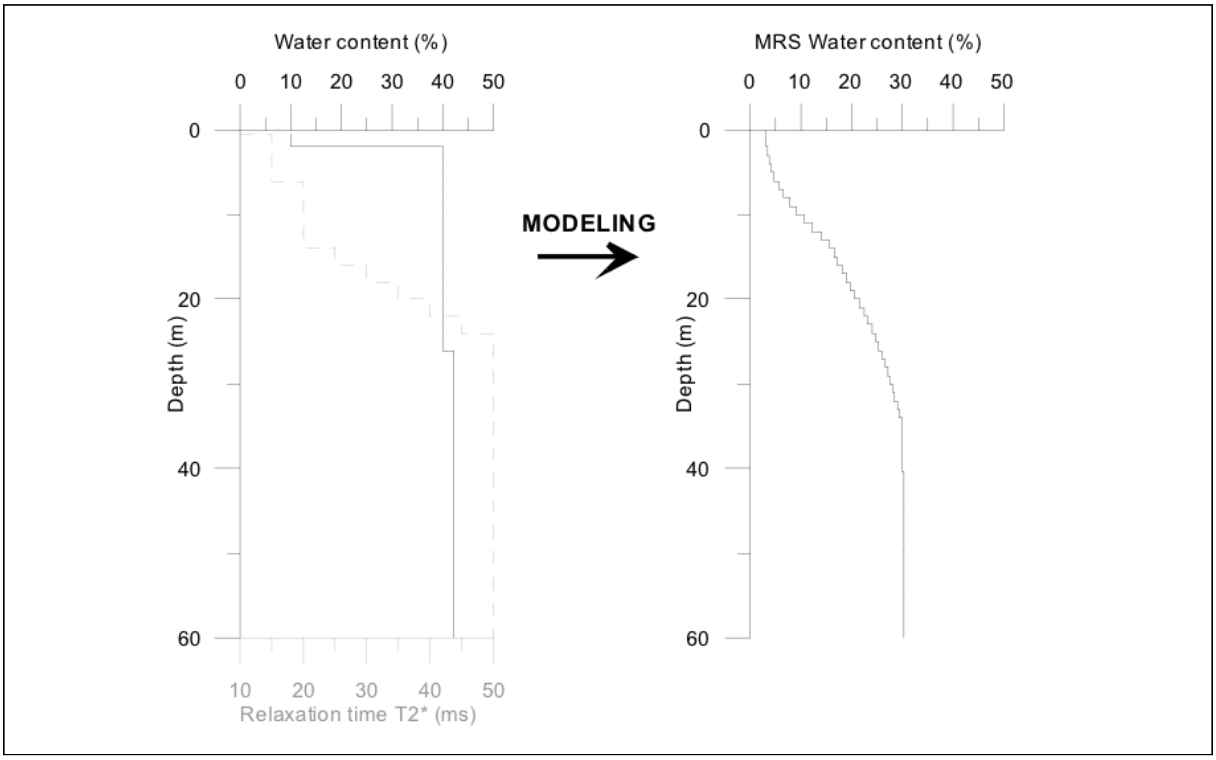

Figure 6: Modeling of a water content profile in chalk environment. On left: parameter of model; on right: result of modeling.

# DARCY 51

# Isotopic measurement of ng quantities of Th, in natural waters. Coupling $^{234}U/^{238}U$ and $^{230}Th/^{232}Th$ ratios to provide time-constraints on the evolution of aquifer groundwaters.

Innocent C(1)., Casanova J(1)., Buschaert S.(2)
(1) BRGM, 3 avenue Claude Guillemin BP 6009, 45060 Orléans cedex 2 – France
c.innocent@brgm.fr; j.casanova@brgm.fr
(2) ANDRA, 1/7, rue Jean Monnet, Parc de la Croix-Blanche, 92298 Châtenay-Malabry cedex – France
stephane.buschaert@andra.fr

During the past few years, the management of water resources has become an outstanding issue for Earth and Environmental Sciences. In this context, it is critical to put chronological constraints on the evolution of aquifer groundwaters. For this purpose, U-series do constitute appropriate systems to investigate the evolution of groundwaters in aquifers between 0 (present-day) and ca. 1 Ma in the past, owing to the disintegration constants of the different nuclides, namely $^{234}U$ and $^{230}Th$.

Coupling $^{234}U/^{238}U$ and $^{230}Th/^{232}Th$ ratios does provide quite important informations. In case of a closed-system evolution of a groundwater through time, neither with dissolution nor precipitation processes, additions of U and Th may only result from the input of incoming waters from the Earth's surface (as a matter of fact, it comes to a simple mixing between two water end-members, with varying proportions of each end-member through time). In such a case, the $^{234}U/^{238}U$ vs. $^{230}Th/^{232}Th$ diagram provides valuable informations on the average residence time of this groundwater in the aquifer. Now, considering an open-system evolution, featuring dissolution and/or precipitation processes for both U and Th, important constraints will be derived on the groundwater fluxes : the more it is sluggish, the more water-rock interactions will occur, resulting in an increasingly increasing $^{230}Th/^{232}Th$ ratio with time, as $^{230}Th$ will be provided from : i) the decay of $^{234}U$ present in the groundwater, and ii) $\alpha$-recoil from the rock, whereas $^{232}Th$ will not be dissolved.

An evolution model has been performed in order to constrain as precisely as possible these processes. Surprisingly, it is much easier in an open-system evolution, as it results in much higher $^{230}Th/^{232}Th$ ratios. As a consequence, the system is less sensitive (which does not mean non-sensitive, however!) to the assessment of the initial parameters.

The measurement of Th isotopic compositions on natural waters with a ppt-level Th content has been performed at BRGM. Liter volumes of water are necessary for the analysis to be safely carried out. The standard procedure for chemical extraction of U and Th has been improved, with handling and chemicals quantities reduced as possible, in order to lower blank levels. Isotopic measurements have been carried out on a MC-ICP-MS "Neptune", equipped with a ion counter coupled with a RPQ-filter, and an ApexR, Peltier-effect desolvator. The desolvatation improves the Th signal by a factor of 5 to 10, typically.

U and Th measurements were done on groundwaters from deep scientific boreholes from the Meuse/Haute-Marne site, provided by the ANDRA (Agence nationale de gestion des déchets radioactifs). Waters were recovered from two aquifers (Dogger and Oxfordian aquifers, respectively). These aquifers clearly define two distinct domains in the $^{234}U/^{238}U$ - $^{230}Th/^{232}Th$ diagram, with higher $^{230}Th/^{232}Th$ activity ratios for some Oxfordian groundwaters. $^{230}Th/^{234}U$ activity ratios, which provide additional informations on the state of the $^{238}U$ decay chain, are found to be lower than secular equilibrium in most of the groundwaters (whatever the aquifer). Implications on the residence time of these groundwaters in these two aquifers are discussed.

# DARCY 60

# Hydrogeological problems and groundwater modelling of the Gavorrano mine area (Italy)

BARSUGLIA Filippo[1], GARZONIO Carlo Alberto[2]

Università di Firenze – DIRES - Laboratorio Materiali Lapidei e Geologia dell'Ambiente e del
Paesaggio, Via Micheli 8-50121, Firenze, Italy, [1]
filippo.barsuglia@unifi.it; [2] carloalberto.garzonio@unifi.it;

## Abstract

The Gavorrano mining area is located in south-western Tuscany, within the Metalliferous Hills. Some of the drifts and lift systems are in perfect working order for the dewatering and safety operations. Groundwater rebound at the Gavorrano mine is regulated by submersible pumping systems. A surface circulation, due to the infiltration in fractured and karst carbonatic rocks, and a deep circulation of thermal water is present. Geological, geostructural, geomechanical and hydrogeological analyses as well as the measurement of the flow rate pumped by pumping systems and recent boreholes (geophysical tests, monitoring network, pumping tests, temperature analyses) have allowed us to draw up hydrogeological models, to formulate a hydrogeological balance and to try to predict the main water-flow directions. For this aim, pumping tests in the different points are being conducted out to evaluate the possibility of separating the different waters and to plan the re-utilization of the water resources.

## Introduction

During recent decades mining activities in Italy decreased progressively as they did in other countries. The decommissioning of a mine triggers a series of problems concerning social safety, health and economy. Furthermore the closure of mine activities is regarded as an environmental threat and an economic problem. The case history described in the paper is about the decommissioning of the Gavorrano mine located in the Colline Metallifere mining district (southern Tuscany). The Gavorrano mine was the largest pyrite mine in Europe throughout the 20th. Production ceased in 1981 and since then the mine has been under maintenance. A multipurpose study was begun in 1995 to evaluate the possibilities for the creation of a natural reserve and mining park by recovering the mining area with all its historical mining structures.

Figure 1: Valsecchi ventilation shaft

Figure 2: Geographical positioning of the Gavorrano mine area

The environmental rehabilitation will extend to the quarries, tailing ponds and spoil dump areas and will include reforestation, stabilisation, and restoration of significant old mining structures. Evaluations of the stability of slopes and underground openings, of the pollution caused by acid mine drainage due to the mining activity and of the recovery of water resources are major aspects o the rehabilitation project. In particular, the paper describes the hydrogeological programme for dewatering operations, the effects of the water level rebound and the evaluation of the hydrogeological conceptual model.

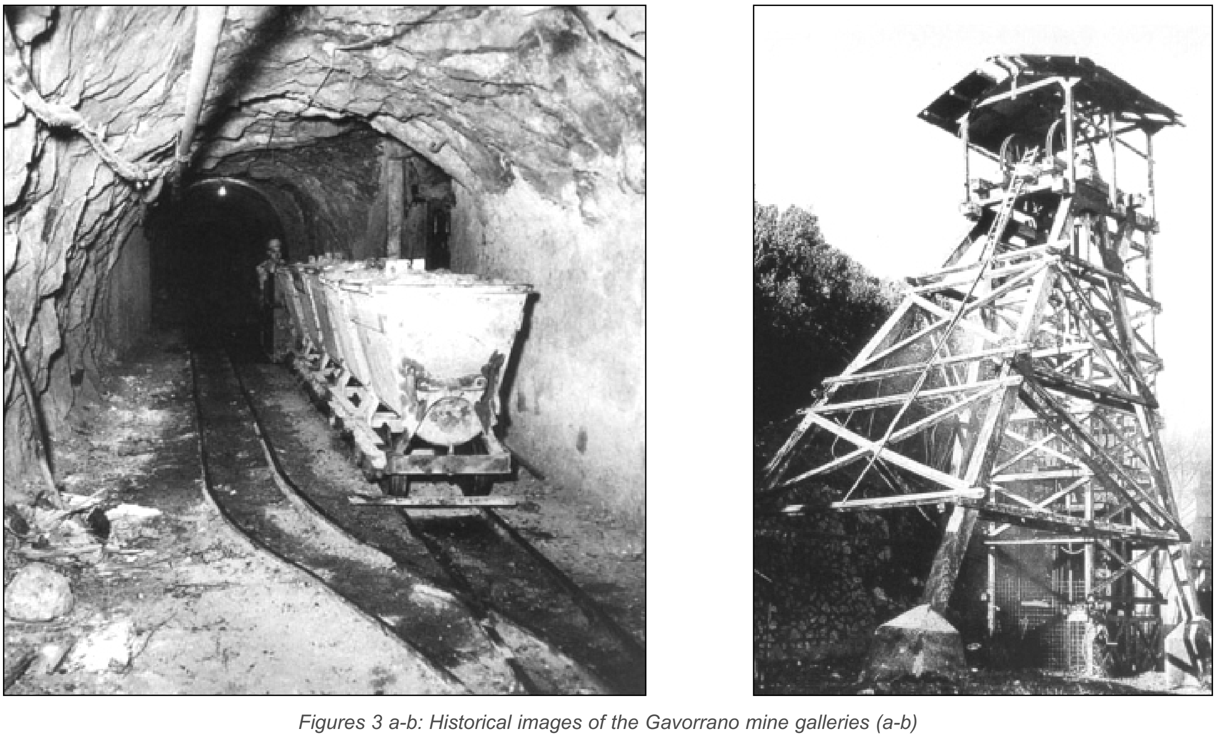

Figures 3 a-b: Historical images of the Gavorrano mine galleries (a-b)

The water drainage problem was analysed starting from the hydrogeological sketch of the area, through historical data concerning both water springs and water level recovery, to hydrochemical data. The analysis of this case history shows how important it is to monitor groundwater levels, both during and after mining activity, for formulating an hydrogeological conceptual model and the to keep records of water hydrochemistry throughout the maintenance phase in order to assess the potential for acid generation on closure.

## Geological and tectonic settings

Gavorrano is located in south-western Tuscany (Fig.2), within the Metalliferous Hills (Colline Metallifere), 10 kilometres from the sea (Follonica gulf).

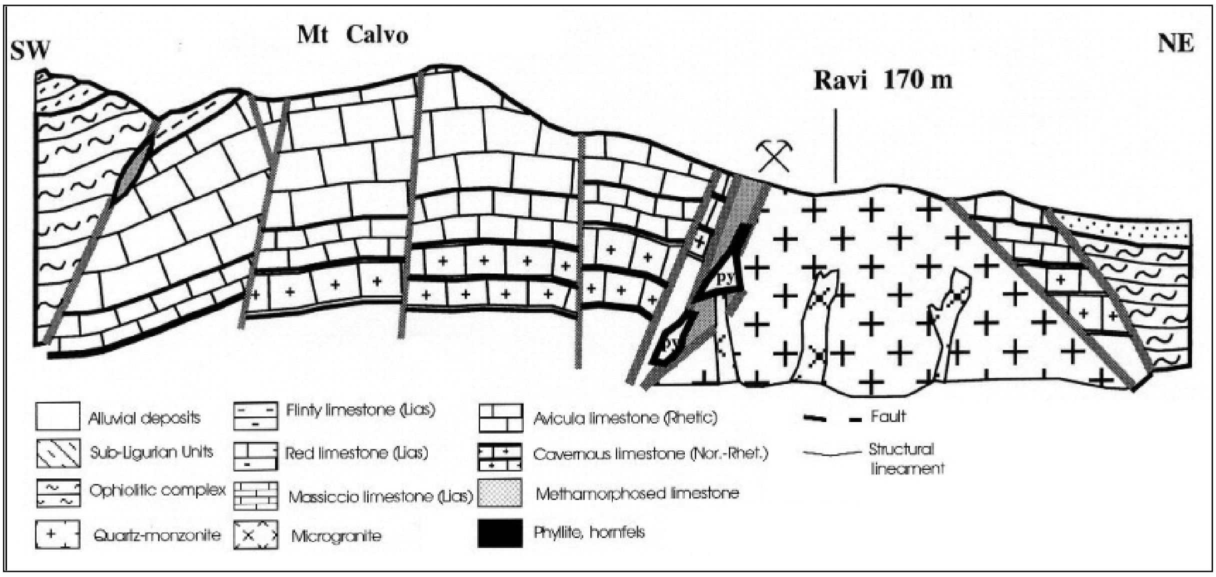

*Figure 4: Geological section of the Gavorrano area*

The area is characterized by rapid topographic changes passing from a very flat plain up to rocky hills with a maximum elevation of about 500m a.s.l. (Mt. Calvo). The Mt. Calvo ridge is just upward the Gavorrano village and it is linked to the lower relief of Finoria hill. New building have erected on the slopes of this hill.

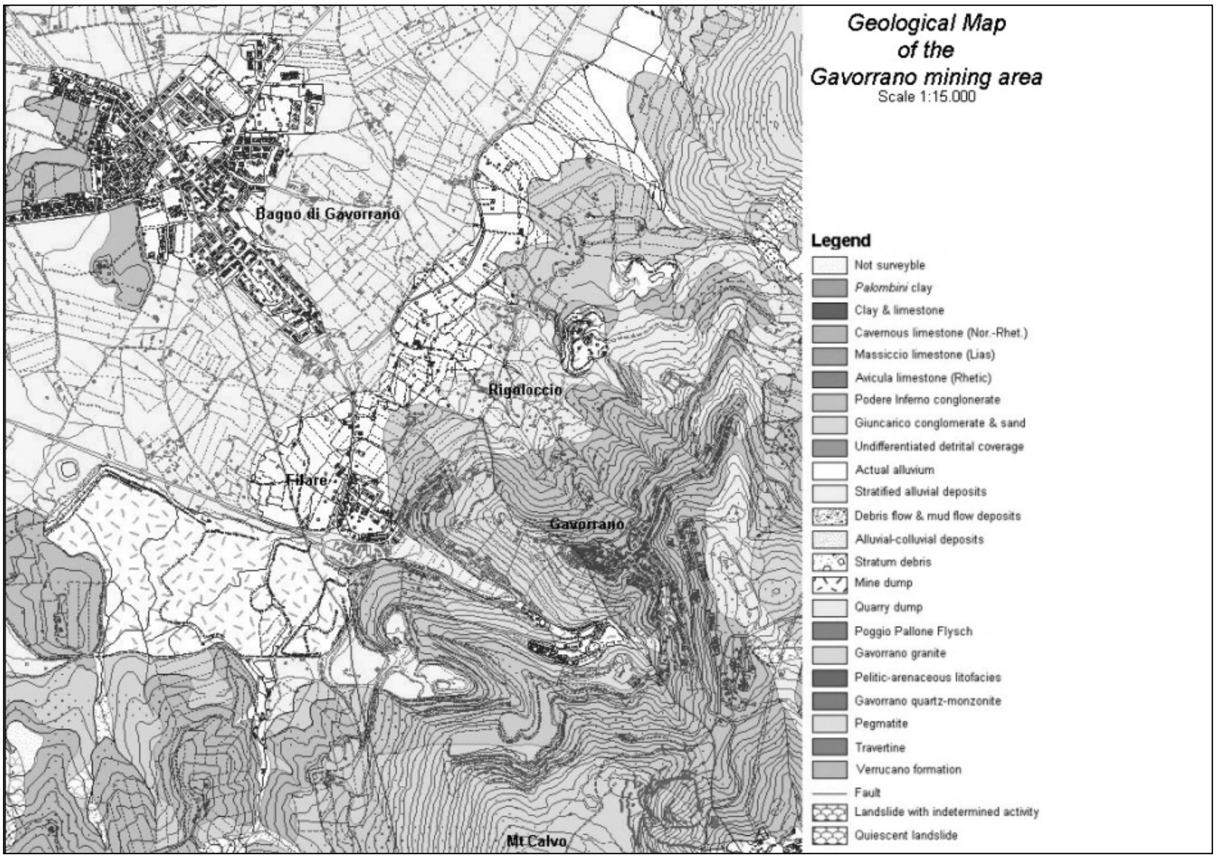

Figure 5: Geological map of the Gavorrano area

The area is characterized by NNW-SSE elongated post-orogenic basins developed over an antecedent extensional horst and graben structure consequent to opening of the Tyrrhenian sea. Tyrrhenian sea, with the development of the intrusive bodies, that decrease in age from west to east and are typical of this tectonic province. The activity of the province is attested by important geothermal fields (Larderello, Amiata) located within a major mining district (Campiglia, Elba island, Amiata). The quartz-monzonitic intrusion are shown on the geological map (fig.5). The intrusion, with successive micro-granitic dikes prevalently oriented N-S, NE-SW and NW-SE, is weathered at the surface and is frequently bounded by a thick zone of loose soil-like-material (Renone).

This weathering and alteration disappear along the mining drifts but the Renone has been often found along the tectonic contact. The intrusive body is limited by two normal faults (fig.5) on the eastern and western sides. Minor faults are located to the north of the intrusion (Rigoloccio), and to the west of Mt. Calvo, putting the stratigraphic series into contact. The geomechanical characterization of the area was performed mainly through a series of geomechanical field surveys. These field surveys were located within the main geological formations, both at the surface and in underground excavations (mine of Gavorrano). Their purpose was to characterize the rock masses for a general evaluation of their mechanical properties and to asses slope stability. The field work revealed the persistence and the frequency of two sub-vertical extensional discontinuity systems. The dominant sets were parallel and normal to the axis of the intrusive body and its main flow structures (lineations). Secondary sub-vertical faults with the same trend were observed at different sites, sub-parallel to the faults limiting the intrusive body. A NNW-SSE and ENE-WSW discontinuity direction characterize the rock mass. The former set is predominant except for the central part of the intrusive body where normal or cross joints are more frequent. These discontinuities, often accompanied by dike intrusions with pyrite mineralization, are characterized by changes in the dip angle due to their normal trend with respect to the flow lineations. This situation of highly jointed rock mass, along with superficial condition of poorly-crushed interlocked materials, lead to intensive and deep weathering processes. In particular at the faults, the de-cohesion phenomena of the quartz-monzonite due to fluid circulation, reach thickness of 50 meters.

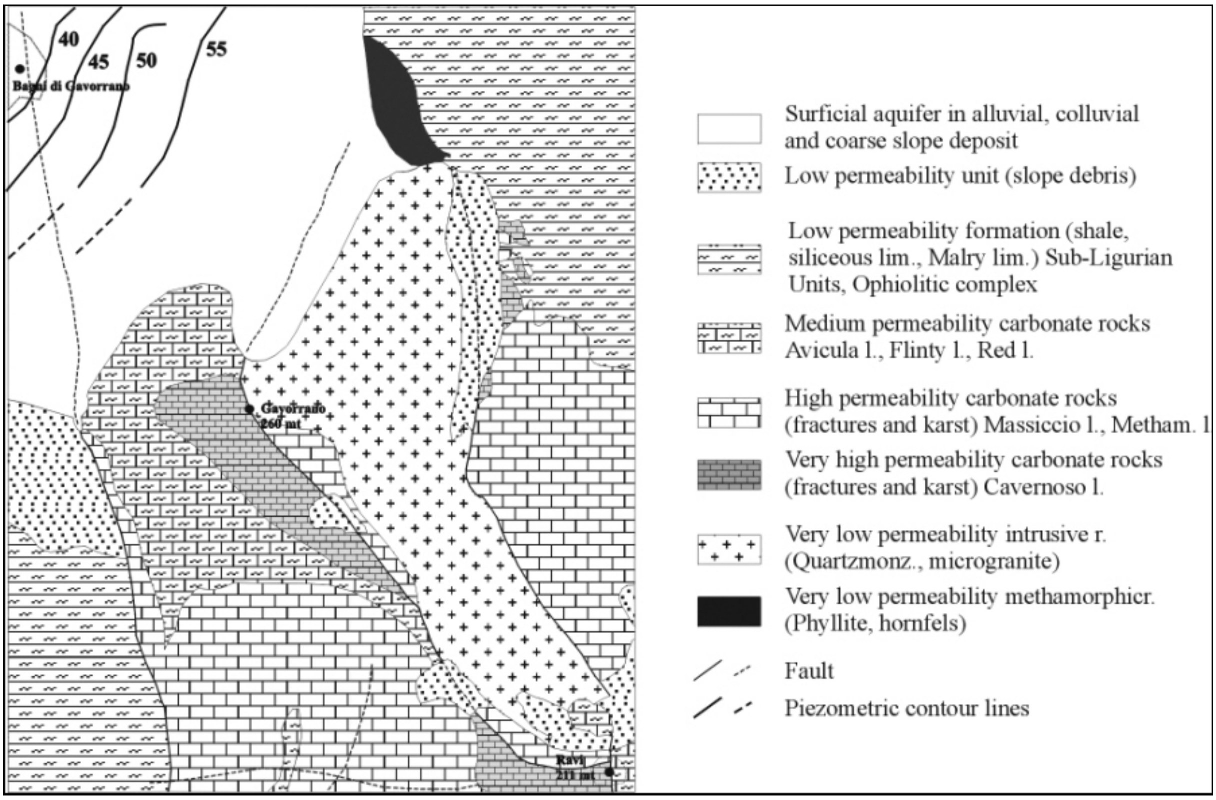

*Figures 6: Hydrogeological map of the gavorrano complex*

## Hydrogeological settings

The hydrogeological system in the Gavorrano area is complicated by the presence of three sub-systems: a superficial alluvial system, a Karstic system and a deep hydrothermal system. The first system consisted of a multiple aquifer in the area around the sub-inclined plane of the alluvial and debris planes of the village of Bagno di Gavorrano. Waters from the last two systems have been forcefully mixed by human action through mining. In fact, 500 m of production levels were excavated in more than a century of mining. The pre-existing groundwater circulation, with springs placed at the maximum height of 180m a.s.l., was depressed down to -250m a.s.l., when the old thermal springs (Bagno di Gavorrano) were drained through the underground drifts system. Hot springs (up to 47°C) were found during mining in specific ore bodies (Rigoloccio). Figure 6 shows an hydrogeological map representing lithotypes with different permeabilities. The permeability classes were attributed by considering: the lithology, the degree of fracturing, the degree of weathering and alteration, the presence of Karstic structures, as observable both at the surface and within mine drifts. Alluvial deposits have been separated from the other materials, because of their characteristics and their natural northward groundwater flow direction. Karstic features and degree of fracturing were determi-

ning factors in differentiating among carbonate rocks. Flysch and shales, due to their very low permeabilities, work as a permeability threshold controlling the location of main springs around the carbonate massif. Intrusive rocks are characterised by a relatively low permeability because of the superficial weathering and the low fracture density. A groundwater balance was calculated by attributing different coefficients of potential infiltration to the several liyhotyped and computing the contributing areas for each lithotype.
Average annual rainfall in the area ranges between 750 mm $y^{-1}$ and 800 mm $y^{-1}$ with an average evapo-transpiration of 430 mm $y^{-1}$ and a rainy season lasting from October to February with the maximum average monthly rainfall in November (120 mm) and very low precipitation in summer (20 mm in July). According to these data, the calculated evapo-transpiration and a series of infiltration coefficients, 1.1 $Mm^3$ of water form the annual groundwater recharge. It is important to note that rock mass properties, especially hydraulic conductivity, were strongly and permanently influenced by mining and subsequent induced processes (e.g.: tunnel presence, the increase of fracturing degree and the enlargement of existing fractures by acid water circulation and water level lowering which locally increased karst solution). In fact, tunnels and drifts form a drainage network characterised both by voids and refilled spaces.

## Hydrogeological, Geophysical and Chemical tests

A survey programme was drafted in the winter of 2003: "*Hydrogeological and geochemical monitoring survey for the utilization, conservation and development of the water resources for the safety of the Gavorrano mine*". This programme was developed before the second phase of the groundwater rebound in the mine. The programmed operations consisted of: drilling five boreholes down to -140 m a.s.l. (water table in the mine); permeability testing; installation of thermometers in the boreholes; seismic testing (down hole) and seismic surface profiling; electric testing (logs) and tomographies (hole surface), chemical and isotopic analyses and construction of hydrogeological model of the studied area.
During the drilling phase some permeability tests (Lefranc & Lugeon) were conducted in the new wells to find the hydrogeological coefficients of the geological formations. Before the installation of the parametric probes in the boreholes, a geophysical campaign was conducted in the mine area. The campaign consisted of seismic measurements with a "Down-hole" operating method.

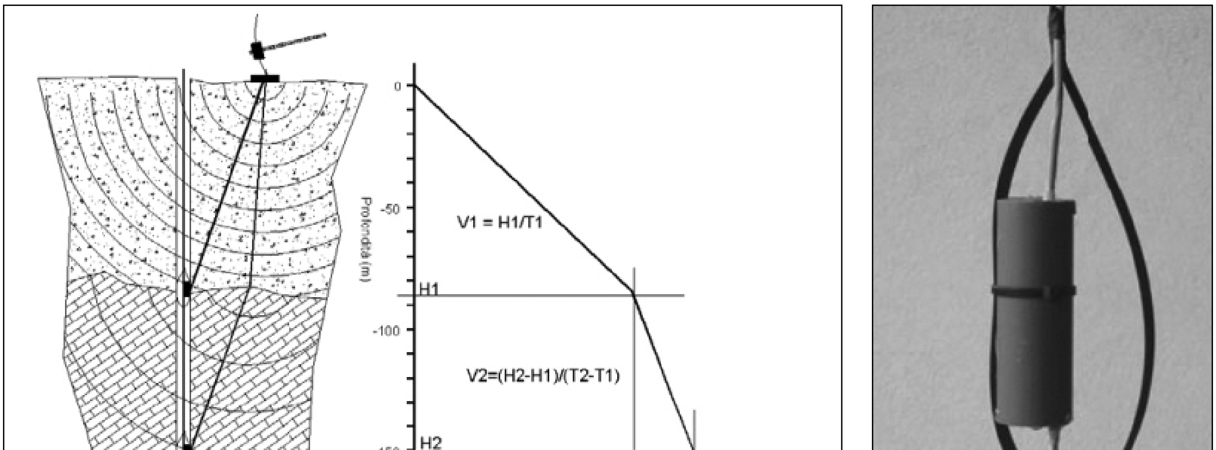

*Figure 7a-7b: Down-hole method(a) and hydrophone sketch image(b).*

Down-hole techniques consist of measuring the arrival times of seismic waves generated on the surface, by the inpact on an iron plate, to the geophones positioned in the borehole. In this particular case, the receiver system comprises three geophones one meter apart to that are connected to the acquisition data-logger (portable computer) on the surface. A steel spring holds geophones against the piezometric casing of the well; when the hammer strikes the iron plate it produces a seismic wave that is picked up by geophones. The waves reaches the data-logger that acquire and records the imcoming signal. After the first recording, the operator lowers the levels of the geophones inside the boreholes and continuos with additional strokes and recordings. At the end the data-logger has recorded all the signals coming from the iron plate picked by the geophones. All the recorded signals costructed data cone that was much bigger than cones created using classic geophysical methodes. So the geological information about the surroundings of the borehole is more detailed.

*Figures 8a-8b: Electrodes composed by iron small plate connected by cables to the surface(a-b).*

To monitor the water table, two of the five boreholes, we inserted 36 electrodes, 5 meters apart, starting from the bottom up to 25 meters from the topographic surface. The deeply placed electrodes made it possible to acquire resistivity measurements of the deeper geological formations for a larger area than classic resistivity measurements.

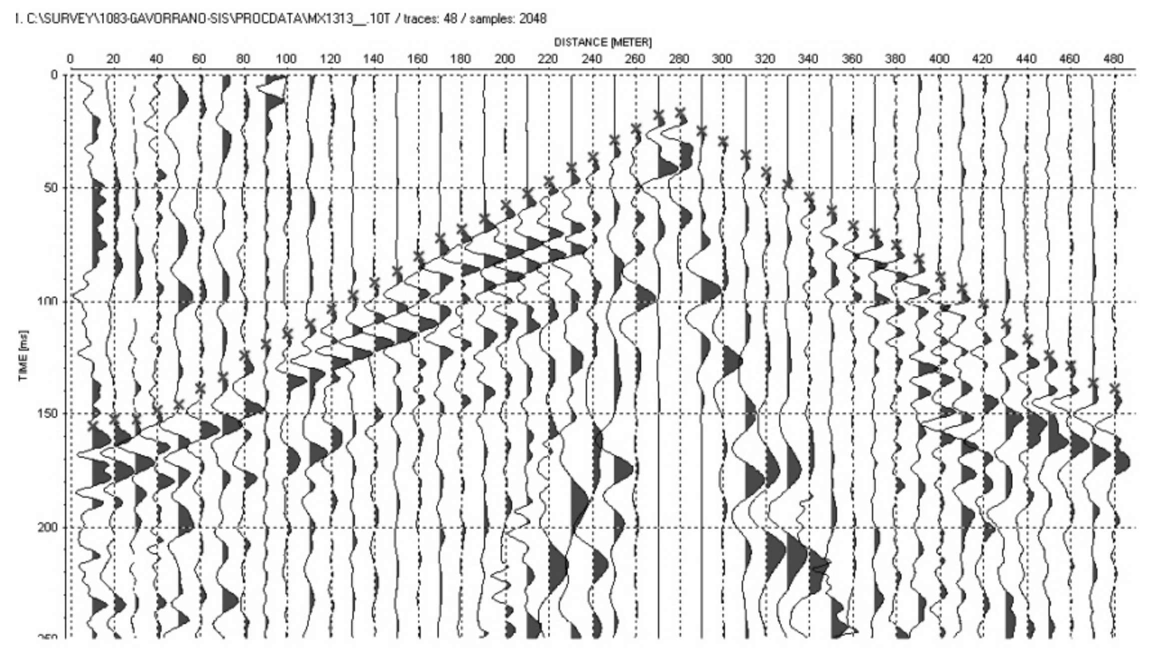

*Figure 9: Seismic refraction film*

Figures 9a-9b: OYO McSeis SX(a) and hydrophone(b).

The surface survey, using the seismic refraction profile method, recorded data over 3240 meters of terrain.
In this campaign we utilized a numerical seismogram (OYO McSeis SX) with 24 channels and vertical component geophones. Acquisitions were made with a receiver with 2048 samples/trace of each single channel distributed over 409.6 milliseconds with a sampling interval of 200 microseconds. The dinamic 18 bit digital sampling of the seismograph and the energy utilized for the source point permitted good recordings along the profiles.

The first step, in building model, was the substratum mapping, or rather, the map of the geological formation contacts. The contact surface was very important owing to the different permeability of the layers. Therefore, to build the hydrogeological model, it was necessary to know the stratigraphic surface. A manly detailed stratigraphic map was prepared with some cross sections showing the limestone basement and the most important geological formations involved in the three kinds of aquifers (Superficial alluvial, Karstic and Hydrothermal).

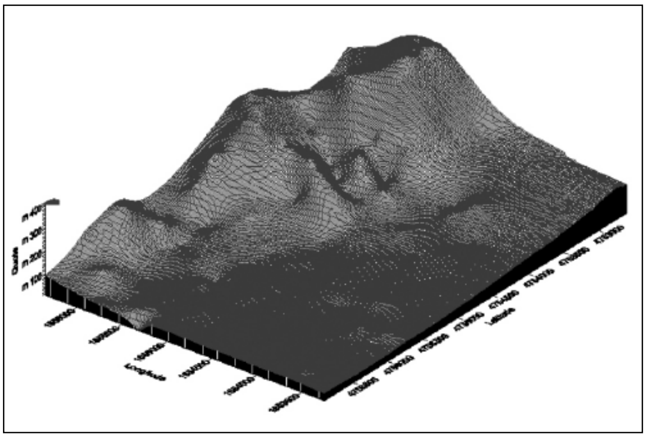

Figure 10: 3D plot of the calcareous substratum surface

After the seismic campaign a parametric probe was inserted in the boreholes at -130 meters a.s.l., with two acquisition channels, one for monitoring the water table the other one for measuring the temperature. Then, the operators were able to acquire data by connecting the PC-cable to the data-logger positioned in the surface box on the piezometric-pipe. Thus it was possible to acquire a large quantity of data, from the probes by setting the instruments with requested acquisition time and to closely monitor the water table in the Gavorrano area..
The chemical and isotopic analyses yielded very important. Some water samples were monitored during the drilling of the boreholes. The results of the analyses were compared with earlier tests on water samples acquired in the mine to check heavy-metal content and sulphate composition.

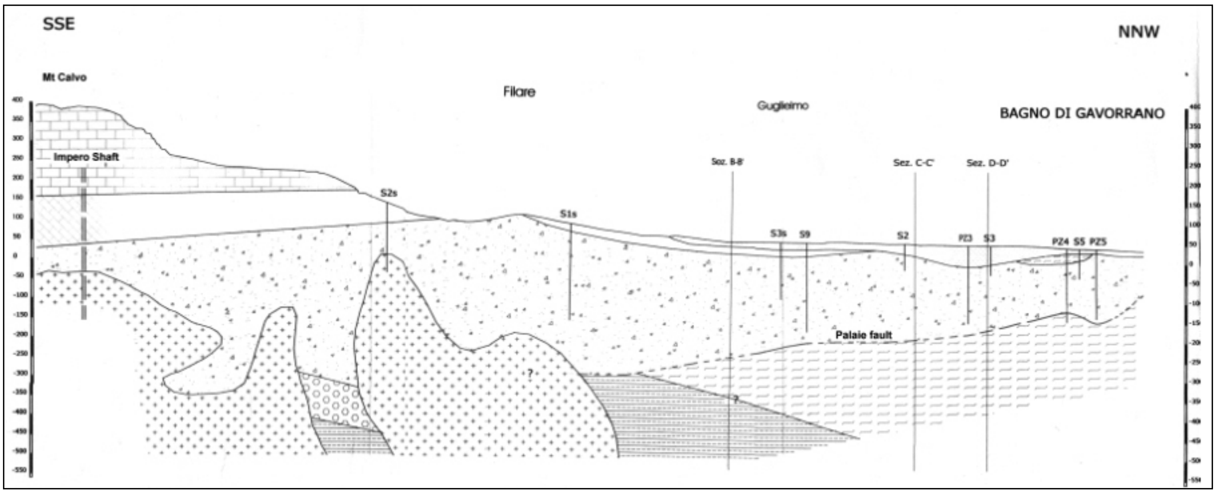

*Figure 11: Geological cross section from Mt Calvo to Bagno di Gavorrano village.*

The water composition proved identical to the previous test with only small differences in heavy metal and sulphate contents.

| | *PZ1* | *PZ2* | *PZ5* | | *PZ1* | *PZ2* | *PZ5* |
|---|---|---|---|---|---|---|---|
| *pH* | 7 | - | 6,6 | Cd (mg/l) | <0,001 | <0,001 | <0,001 |
| *SiO2 (mg/l)* | 9,1 | 30 | 24,1 | Co (mg/l) | 0,01 | <0,01 | <0,01 |
| *Al (mg/l)* | 0,25 | 1,22 | 0,42 | Cr (mg/l) | <0,01 | <0,01 | <0,01 |
| *Fe (mg/l)* | 42,8 | 3,06 | 1,75 | Cu (mg/l) | <0,01 | <0,01 | <0,01 |
| *Ca (mg/l)* | 296 | 91 | 310 | Hg (mg/l) | <0,005 | 0,0011 | <0,001 |
| *Mg (mg/l)* | 74 | 15 | 58 | Mo (mg/l) | 0,02 | <0,01 | <0,01 |
| *Ti (mg/l)* | <0,01 | 0,01 | <0,01 | Ni (mg/l) | 0,03 | <0,01 | <0,01 |
| *Mn (mg/l)* | 8,15 | 1,32 | 0,59 | Pb (mg/l) | <0,01 | <0,01 | 0,04 |
| *P (mg/l)* | <0,5 | 0,1 | <0,05 | Sb (mg/l) | <0,01 | <0,01 | <0,01 |
| *K (mg/l)* | 7 | 34,4 | 4,9 | Se (mg/l) | <0,03 | <0,03 | <0,03 |
| *SO4$^-$ (mg/l)* | 1045 | 16 | 712 | Sn (mg/l) | <0,01 | <0,01 | <0,01 |
| *Ag (mg/l)* | <0,005 | <0,005 | <0,005 | Sr (mg/l) | 3,14 | 0,63 | 5,08 |
| *As (mg/l)* | 0,02 | 0,051 | 0,029 | Tl (mg/l) | <0,03 | - | - |
| *B (mg/l)* | 0,05 | 0,03 | 0,41 | V (mg/l) | <0,01 | 0,01 | <0,01 |
| *Ba (mg/l)* | 0,1 | 0,44 | 0,07 | Zn (mg/l) | 0,49 | 0,05 | 0,03 |
| *Be (mg/l)* | <0,001 | 0,001 | <0,001 | | | | |

*Table 1: Chemical analysis table of the PZ1-PZ2-PZ5 borehole (2005)*

The flooding of mine levels is without doubt an important cause of instability for water properties. The reason lies in the fact that rock re-saturation and the filling of mining drifts are associated with the washing out of the sulphate-rich and heavy-metal-rich pyrite oxidation products. Up to now the analyses of the pumped waters have pointed out constant chemical properties. It will be necessary to verify the parameters when the old sectors of the mine are flooded. The new data and the discharge from the new pumping system of Rigoloccio shaft 3 highlighted the remarkable quantity of the water resources, in particular the volume of the thermal waters (with temperature of 38-40°). All the toxic elements (As, Hg, Pb, Cr, Zn, etc) were found in traces and the water was almost free of contamination of nutrient parameters (nitrate, phosphate, etc...). Sulphates are well beyond the allowable threshold value, while iron and manganese components change from sample to sample. The acidity was quite stable.

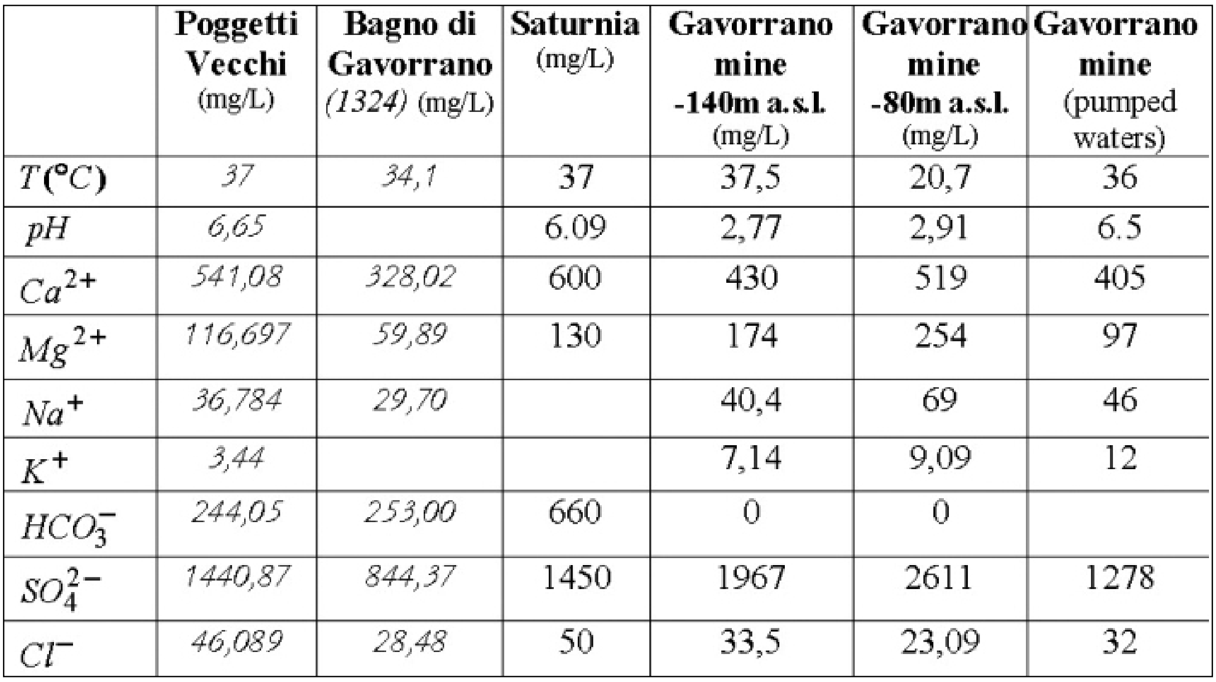

| | **Poggetti Vecchi** (mg/L) | **Bagno di Gavorrano** *(1324)* (mg/L) | **Saturnia** (mg/L) | **Gavorrano mine -140m a.s.l.** (mg/L) | **Gavorrano mine -80m a.s.l.** (mg/L) | **Gavorrano mine** (pumped waters) |
|---|---|---|---|---|---|---|
| $T$(°C) | 37 | 34,1 | 37 | 37,5 | 20,7 | 36 |
| $pH$ | 6,65 | | 6.09 | 2,77 | 2,91 | 6.5 |
| $Ca^{2+}$ | 541,08 | 328,02 | 600 | 430 | 519 | 405 |
| $Mg^{2+}$ | 116,697 | 59,89 | 130 | 174 | 254 | 97 |
| $Na^{+}$ | 36,784 | 29,70 | | 40,4 | 69 | 46 |
| $K^{+}$ | 3,44 | | | 7,14 | 9,09 | 12 |
| $HCO_3^-$ | 244,05 | 253,00 | 660 | 0 | 0 | |
| $SO_4^{2-}$ | 1440,87 | 844,37 | 1450 | 1967 | 2611 | 1278 |
| $Cl^-$ | 46,089 | 28,48 | 50 | 33,5 | 23,09 | 32 |

Table 2: Chemical analysis of some thermal springs in Tuscany (Italy)

Mine waters could become drinkable by removing, in order of importance, sulphates, magnesium, calcium, suspended material and small quantities of aluminium, iron, manganese and arsenic. From a cost/benefit analysis, the installation, continuous operation and maintenance of a water treatment plant proved unprofitable with the water's existing composition. Thus, it is preferable to find a different use, taking into account a possible future change in the water chemistry with the ongoing water rebound.

The hydrogeological model, after the acquisition of all data, make a large schema of the water situation of the Gavorrano mine area. The campaigns, served to formulate a diagram of the hypothetic flow directions to control the ancient spring (Bagno di Gavorrano), its re-activation and water table in the mining area . Data acquired during the second phase of the mine flooding (from -140m a.s.l. to -110m a.s.l.) the fives control points (boreholes) did differ considerably with the with respect to the previous results. Just one borehole showed important differences in the water table level. This one is located on the Palaie fault, in the centre of the village of Bagno di Gavorrano near the ancient Bagno spring, and it was supposed that the two aquifers (superficial and Karstic-hydrothermal) were connected by the same fault and the meteoric waters could recharge/discharge according to the amount of rainfall. So the level graph of this borehole shows the step trend due to the adjustment of the water table. On the whole, the level of the water table in this area has not changed from the last value recorded just before the second phase. The level of the water table in the mine was raised from -140m to -130m a.s.l., with the shutdown of the pumping system (Rigoloccio3 and Pozzo Roma).

There after, at one-month intervals the water level was raised to -110m a.s.l.. The reason for raising the water level only 30 meters can be sought in the geometry of the tunnels in the Gavorrano mine. The majority of the galleries is already flooded and located below -140m a.s.l.. However there is an another important chapter in the history of the mine and in the exploitation methods between -140m and -110m a.s.l.. . The deeper tunnels are the most recent; those closer to the surface are older and pose greater structural, chemical and hydrogeological risks therefore the flooding must go slowly. Now the water table is stable at -110m a.s.l., forced by the pumping system.

## Waters re-utilization

Thermal spa waters represent a good solution, and this is supported by a series of data available concerning some spa waters already exploited in Tuscany, that only differ in iron content. Irrigation is a possible use even if attention must be paid to the soil characteristics and the irrigation technique. Indeed, these waters have already been extensively used for this purpose in the area, but relatively high levels of heavy elements and metals have been found in natural soils, as well as in some irrigation ditches.

## References

- Arisi Rota F, Brondi A., Dessau G., Branzini M., Stea B., Vighi L., (1971) I Giacimenti minerari. In: La Toscana Meridionale., Rend. Soc. It. Min. Petr., 27, 357-559.
- Banks D., Younger P.L., & Dumpleton S. (1996) The historical use of mine-drainage and pyrite-oxidation waters in Central and Eastern England, United Kingdom. Hydrogeology Jour., 4 (4), 55-68
- Bell F.G., and Bullock S.E.T. (1996) The problems of acid mine drainage, with an illustrative case history. Environmental & Engineering Geosciences, II (3), Fall 1996, 369-392.
- Crosta G., Garzonio C. A. (1998a) Engineering geology problems in the closing down of mining areas I: relationships among mining, geology and subsidence problems. In Proceed. Environmental Management, Sivakumar M., Chowdhury R.N. eds., Pergamon, 2, 1141-1151.
- Crosta G., Garzonio C. A. (1998b) Engineering geology problems in the closing down of mining areas II: Hydrogeological problems of mining rehabilitation. In Proceed. Environmental Management, Sivakumar M., Chowdhury R.N. eds., Pergamon, 2,1153-1162.
- Crosta G. & Garzonio C. A. 2000 The underground water storage project in the Decommissioned Gavorrano mine (Tuscany, Italy) Proc. Eurock 2000, Aachen, 387-393.

# DARCY 62

# Groundwater system compartmentalized by a tectonic zone in the Kanto plain, central Japan

YASUHARA Masaya[1], INAMURA Akihiko[1], TAKAHASHI Masaaki[1], HAYASHI Takeshi[1], TAKAHASHI Hiroshi[1], MAKINO Masahiko[1], HANDA Hiroko[1], and NAKAMURA Toshio[2]

[1] Geological Survey of Japan, 1-1-1 Higashi, Tsukuba, Ibaraki 305-8567, Japan
masaya-yasuhara@aist.go.jp
[2] Center for Chronological Research, Nagoya University, Chikusa, Nagoya, Aichi 464-8601, Japan

## Abstract

In the Kanto plain, the largest Quaternary groundwater basin in Japan, water samples were obtained from 130 water supply boreholes with pumps installed to characterize the groundwater system. The spatial variation in chloride ($Cl^-$) concentration indicates that in its central part there exists groundwater with Cl- concentrations of more than 100 mg/l (up to 216 mg/l) between 200 m and 450 m depth below ground surface. This 8 km wide, 35 km long $Cl^-$-rich area, spreading from the northwest to the southeast, corresponds with the so-called Motoarakawa tectonic zone bounded by the faults on its long sides. We have found the $Cl^-$-rich groundwater also characterized by low $\delta D$, low $\delta^{18}O$, and high $\delta^{13}C$ values. Both the chemical and isotopic evidence strongly suggests the Motoarakawa tectonic zone divides the regional groundwater system in the Kanto plain into three distinct hydrologic subareas. Two faults which bound the Motoarakawa tectonic zone act as barriers to the southward and northeastward regional movements of groundwater. Apparent radiocarbon ages based on $d^{14}C$ show that the retention time of groundwater in the tectonic zone is far long in comparison with that outside the tectonic zone. In conclusion, the Motoarakawa tectonic zone groundwater was recharged by precipitation under cooler climate condition than the present. It was put under an isolated hydrologic environment for a long period of time with respect to the regional groundwater system, resulting in highly-evolved water chemistry with an elevated $Cl^-$ concentration. Contribution of pore water (formation water) squeezed out of the adjacent aquitards and/or deep-seated groundwater can not be ruled out as another possible source of water and $Cl^-$ for the tectonic zone groundwater.

## Introduction

The Kanto plain (about 8,000 $km^2$ in area), comprising the city of Tokyo in its southeastern part, is the largest Quaternary sedimentary basin in Japan (Fig. 1). In the central part of the Kanto plain, existence of groundwater with chloride concentrations as high as 100-150 mg/l was discussed by Ikeda (1984). In this study, the combination of major elements, and H, O and C isotopes determined on groundwater samples makes it possible to identify the spatial distribution and origin of the $Cl^-$-rich groundwater in more detail, and to characterize the geologically-controlled dynamic scheme of regional groundwater system in the Kanto plain.

## Study area

The study area (Fig. 1) lies on the central part of the Kanto plain, where geomorphology is characterized by a high ratio of pluvial upland to alluvial lowland area. The uplands are divided into several terraces of different ages and altitudes, generally a height difference between upland and lowland being 10-20 m. The bedrock is covered by a thick Neogene and Quaternary sediments up to 3500 m deep. Upper around 500-1000 m of these sediments are called Kazusa and Shimousa groups of late Pleiocene to Quaternary in age. Sand and gravel layers in Kazusa and Shimousa groups are interbedded with a lot of thick, extensive clay layers, forming excellent confined aquifers. Excessivepumping of the 100-400 m deep groundwater from these confined aquifers once caused serious land subsidence problems in and around the study area.

From northwest to southeast, there exists the 35 km long, 8 km wide Motoarakawa tectonic zone bounded by the Ayasegawa and Kuki faults on its long sides (Shimizu and Horiguchi, 1981). Recent geologic study on the Ayasegawa fault suggests a 9-11 m vertical displacement to the depth of around 30 m below the present ground surface (Katsumata et al., 2005). Further down, a vertical displacement is assumed to be 150-200m with an average slip rate of 0.1 m per 1,000 yrs. (Kiyohide Mizuno, personal communication), whereas details are not known about the Kuki fault 8 km northeast across the Motoarakawa tectonic zone. Characterizing hydrogeologic effects of the Motoarawaka tectonic zone on the regional groundwater system is of great importance for future appropriate management of groundwater resources in the Kanto plain from both quality and quantity points of view.

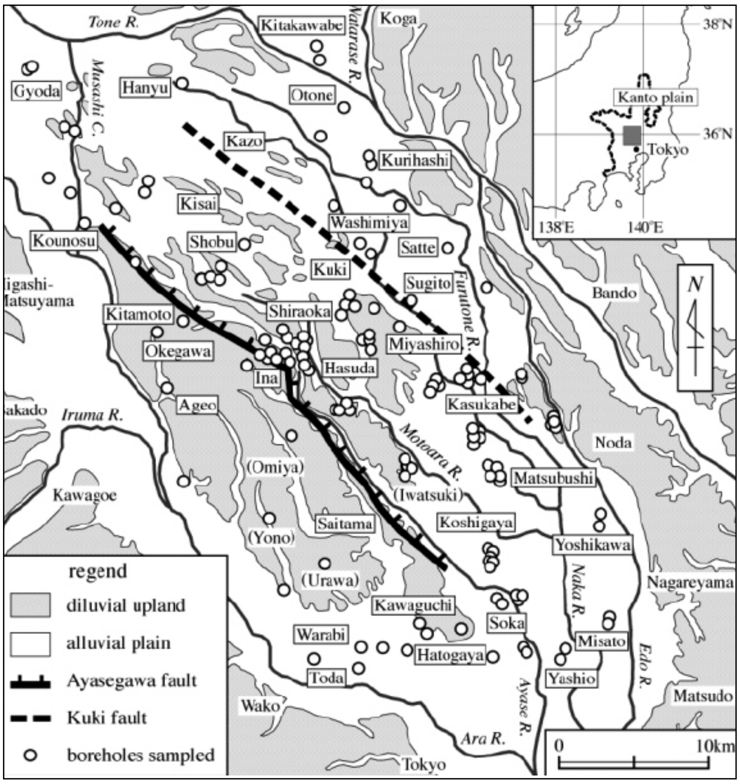

*Figure 1: The study area and location of sampled boreholes.*

## Water sampling and analyses

The diversity of hydrogeological setting of the area results in boreholes of widely different depths ranging from 20 to 450 m and screen settings. Among these, we selected 130 water supply boreholes typically with 200-400 m depths and nearly entire-screen set for the aquifers below 150 m (Fig. 1). These boreholes are screened extensively in the upper aquifers of the Kazusa groups. Groundwater sampling took place in 2003 and 2004 and water samples were analyzed for water chemistry and isotopes. At the Geological Survey of Japan, water chemistry was determined by ion chromatography and stable isotopes were analyzed by mass spectrometry following standard preparation methods ($CO_2$ equilibration for $\delta^{18}$O, reduction with zinc shot for dD, and acidification with phosphoric acid for $\delta^{13}$C$^{-}$DIC). For $\delta^{14}$C analysis, DIC was precipitated to $SrCO_3$ by adding carbon-free SrC$^{l2}$ solutions. $CO_2$ reacted from $SrCO_3$ precipitation was reduced to graphite using $H_2$. The $\delta^{14}$C was then measured by AMS system at the Nagoya University.

## Groundwater quality

The spatial variation in chloride (Cl$^{-}$) concentration (Fig. 2) clearly indicates that there exists groundwater with the elevated Cl- concentrations of more than 100 mg/l in Shobu, Shiraoka, Hasuda, Kasukabe, and Koshigata. Especially, groundwater with the very high Cl$^{-}$ contents is found in Shiraoka (216 mg/l and 184 mg/l for two different 310 m deep boreholes) and Kasukabe (163 mg/l, 160 mg/l, and 153 mg/l for 350 m, 270 m, and 350 m deep boreholes, respectively). Although extent of the $Cl^-$-rich groundwater is in good agreement with that of Ikeda (1984), Cl- concentration observed in this study is generally increased by 10-20% for the space of last 20 years.

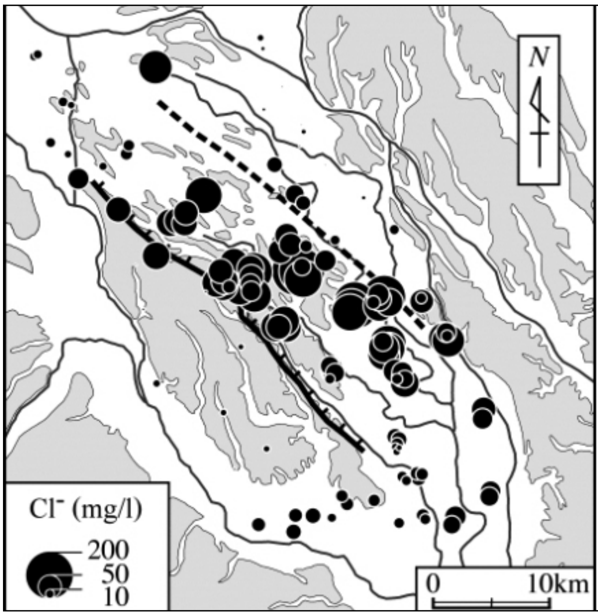

*Figure 2: Spatial variation of $Cl^-$ conc.*

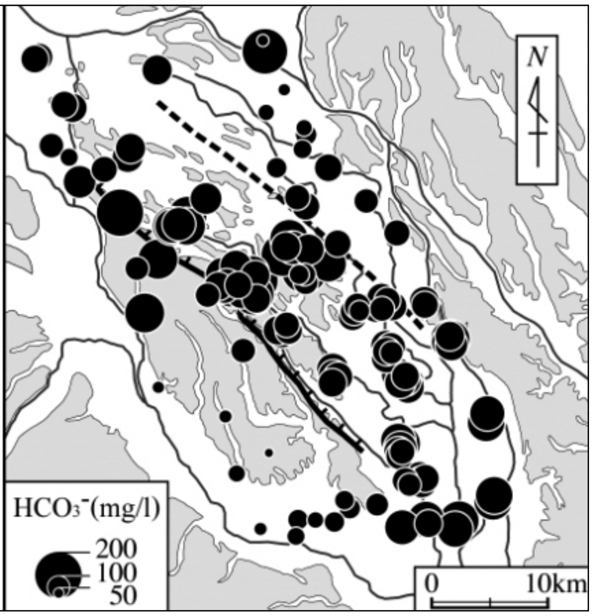

*Figure 3: Spatial variation of $HCO_3^-$ conc.*

Interestingly, this $Cl^-$-rich groundwater zone, spreading from northwest to southeast, nearly corresponds with the Motoarakawa tectonic zone outlined above. The $Cl^-$ contents of groundwater outside the Motoarakawa tectonic zone (such as in Washinomiya, Satte, Sugito, Noda, Kurihashi, Otone, and Kitakawabe to the north and Ageo, Saitama, Kawaguchi, Warabi, Toda, Hatogaya, Soka to the south) are in the range between 5 and 50 mg/l, being an order of magnitude lower than those inside the tectonic zone. The abrupt change in $Cl^-$ concentration on both sides of the Ayasegawa and Kuki faults indicates that the confined groundwater system in the Motoarakawa tectonic zone is not hydraulically interconnected with the aquifers outside the tectonic zone. Figure 3 shows the distribution of bicarbonate ($HCO_3^-$) concentration. The distinction is less clear for the $HCO_3^-$ distribution, the values possibly reflecting to some extent the amount of calcareous materials in the respective aquifers.

## Stable isotope composition

Figure 4 shows $\delta^{18}O$-$\delta D$ diagram of the groundwater samples in the study area. The groundwaters plot in the range –73 to –53‰ for $\delta D$ and –10.3 to –8.1‰ for $\delta^{18}O$. All points fall between the two local meteoric water lines with different d-parameters ($=\delta D\text{-}^{8}x\delta^{18}{}_{0}$) of 10‰ and 15d. Toward the depleted end of the range, there is a tendency for groundwater to show a smaller d-parameter value.

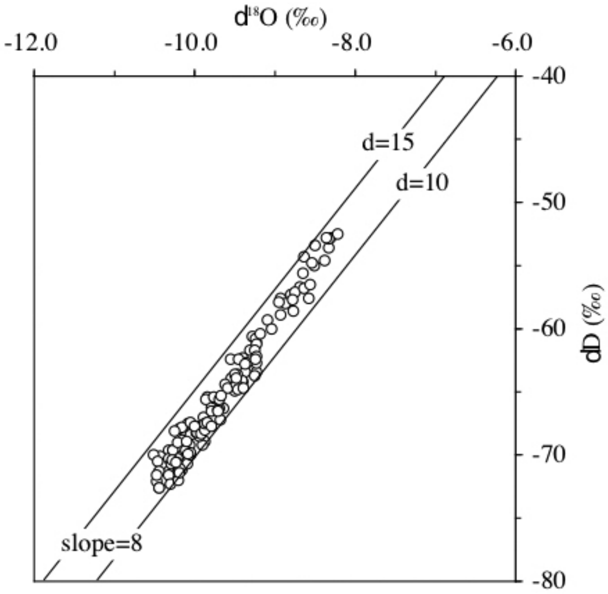

Figure 4: δ18O-δD diagram.

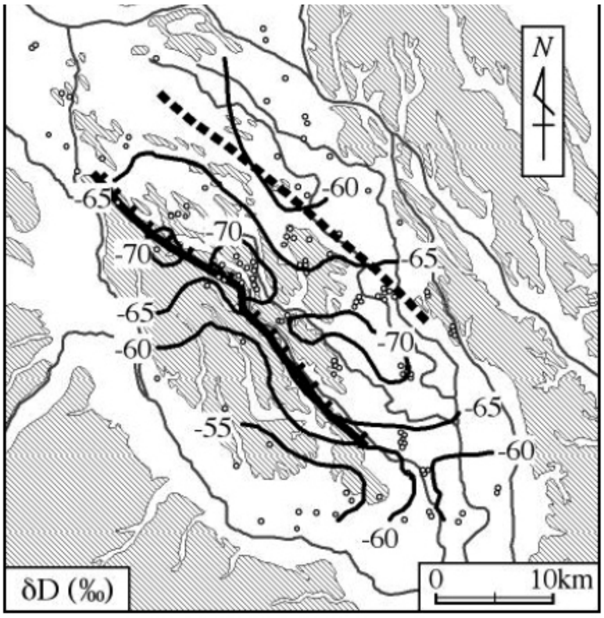

Figure 5: Contour of δD values.

The δD values indicate significant variations across the study area (Fig. 5). In the Motoarakawa tectonic zone, groundwater is generally characterized by the depleted δD values of –70 to –65‰. The most depleted groundwater with the δD values of less than –70‰ were found in Shiraoka, Hasuda, and Kasukabe in the middle and lower parts of the tectonic zone. Outside the tectonic zone, in contrast, groundwater to the south has the more enriched δD values by 5-10‰ as in Ina and Saitama, and the distribution shows an increase in δD from –65‰ in the immediate area of the Ayasegawa fault to -55‰ in Yono, Urawa, Kawaguchi, Warabi, and Toda around 5 km away from the fault. This is also the case for the Kuki fault. Groundwater in Washimiya, Kazo, Kurihashi, and Otone outside the tectonic zone shows the enriched δD values of more than –60‰. As is mentioned in Fig. 4, isotopically-depleted groundwater has a smaller d-parameter value in the study area. Therefore, groundwater in the Motoarakawa tectonic zone reluts in showing the smaller δ-parameter values in comparison with those outside the tectonic zone. These distinct differences in dD and d-parameter values on both sides of the Ayasegawa and Kuki faults strongly suggest that the groundwater system in the Motoarakawa tectonic zone does not communicate with that in the aquifers outside the tectonic zone.

As for $\delta^{13}C$, groundwater in the Motoarakawa tectonic zone generally has the enriched $\delta^{13}C$ values in the range –14 to –10‰ (Fig. 6). And the $\delta^{13}C$ distribution in Fig. 6 displays a general pattern of decreasing $\delta^{13}C$ value with distance from the tectonic zone. This also suggests the discontinuity between the groundwater system in the tectonic zone and the outside.

## Tectonic zone and groundwater system

We have found the $Cl^-$-rich groundwater in the Motoarakawa tectonic zone also characterized by low δD, low $\delta^{18}O$, small d-parameter, and high $\delta^{13}C$ values. In addition, a marked difference in piezometric level on both sides of the Ayasegawa and Kuki faults is reported by Hayashi *et al*. (2003). These evidences strongly support the hypothesis that the Motoarakawa tectonic zone divides the regional groundwater system in the Kanto plain into three distinct hydrologic subareas. The Ayasegawa and Kuki faults, which bound the Motoarakawa tectonic zone on

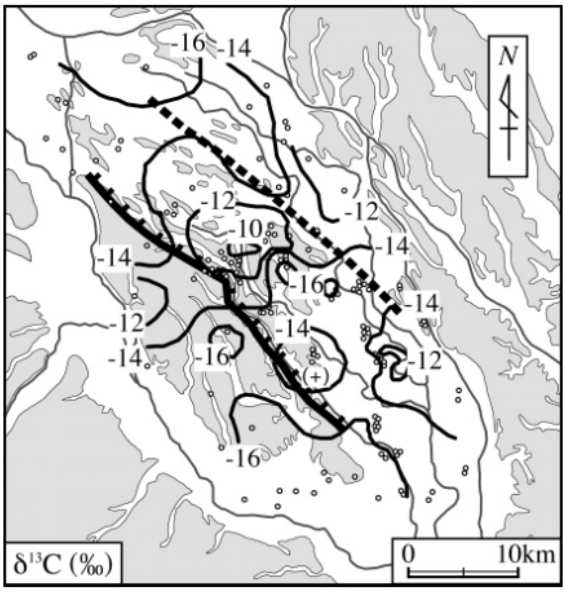

*Figure 6 Contour of δ13C values.*

the southern and northern sides respectively, act as barriers to southward and northeastward regional movements of groundwater in the Kanto plain. On the other hand, groundwater in the Motoarawaka tectonic zone, separated from these regional groundwater systems, is thought to flow southeastward in the narrow area between the faults. Apparent radiocarbon ages of 24,000-30,000 yrs, obtained on the basis of $\delta^{14}$C for the Motoarakawa tectonic zone groundwater, are almost two times those outside the tectonic zone. The increasing age and $\delta^{13}$C value toward the center of the tectonic zone may agree with the hypothesis that the tectonic zone groundwater was isolated with respect to the actively-circulating regional groundwater system of the Kanto plain and was under an isolated hydrologic environment for a long period of time. With regard to the origin of the isotopically-depleted tectonic zone groundwater with very higher apparent ages, the major potential source is assumed to be the “fossil” water recharged under cooler climate condition than the present. In the tectonic zone, groundwater had been put under a relatively stagnant hydrologic condition for a long period of time, resulting in highly-evolved water chemistry with an elevated Cl- concentration. Contribution of pore water squeezed out of the adjacent aquitards due to the excessive pumping and/or upward movement of the $Cl^-$–rich deep-seated groundwater is likely to be another possible sources of water and $Cl^-$ for the tectonic zone groundwater. The more detailed elucidation of the origins of water and $Cl^-$ in the Motoarakawa tectonic zone groundwater is the subject of our future study.

## References

- Hayashi T, Uchida Y, Yasuhara M, Marui A, Sakura Y, Miyakoshi A (2003) Groundwater flow system of the Kanto Plain estimated from the chemical composition and stable isotopes. Journal of Japanese Association of Hydrological Sciences 33: 125-136. (in Japanese with English abstract)
- Ikeda K (1984) Chemical characteristics of groundwater in the central part of the Kanto Plain Hydrology 14: 36-49. (in Japanese with English abstract)
- Katsumata N, Sugai T, Hachinohe S, Mizuno K (2005) Geomorphological development of the Omiya upland. Proc. General Meeting of the Association of Japanese Geographers 67: 259. (in Japanese)
- Shimizu Y, Horiguch, M (1981) Motoarakawa tectonic belt in northeastern part of Omiya upland, Kantyo plain, central Japan. The Memoirs of Geological Society of Japan 20: 95-102. (in Japanese with English abstract)

# DARCY 73

# Measurements of the chemico-osmotic efficiency coefficient in the Callovo-Oxfordian shale of the Paris Basin.

Gueutin, P. (1), de Greef, V. (2), Cruchaudet, M. (3), Gonçalvès, J. (1), Cosenza, P. (1) et Violette, S. (1)

(1) UMR SISYPHE, Université Pierre et Marie Curie, Boite 125, 4 Place Jussieu, 75252 PARIS Cedex 5
(2) LMS, Laboratoire de Mécanique des Solides, Ecole Polytechnique, 91128 PALAISEAU cedex
(3) ANDRA, Laboratoire de recherche souterrain de Meuse/Haute-Marne, RD 960, 55290 BURE
gueutin@ccr.jussieu.fr

The Callovo-Oxfordian is the shale layer studied by ANDRA as a potential nuclear waste repository. Overpressures are measured in this layer. These overpressures can have different origins, one of these could be an osmotic process. If it is effective, this process would have a great influence on the transport of radionuclides by restricting this transport to the surroundings aquifers, which are the Dogger and the Oxfodian, two regional aquifers in the Paris Basin.

The osmostic process is the movement of water, across a semi-permeable membrane, driven by a chemical potential gradient. The chemico-osmotic efficiency coefficient represents the capacity of the membrane to restrict the ionic transport without restricting the transport of the water. The chemico-osmotic efficiency coefficient ranges between 1 and 0. The value of 1 represents a perfect membrane, which completly restricts the ionic transport, while, the value of 0 represents the absence of membrane effect, thus the absence of ionic restriction.

In this study, our goal is to measure the chemico-osmotic efficiency coefficient of the Callovo-Oxfordian shale. Two methods are used, one at the sample scale and one at the field scale, in the ANDRA's underground laboratory. The purpose, of these two methods, is to follow the pressure evolution after a perturbation of the solute concentration.

At the sample scale (fig 1), a central borehole is drilled in the cylinder-shape sample. The pressure difference is measured between the solution in the borehole and the solution which surrounds the sample. When a pressure equilibrium is attained with the initial reference ionic solution (supposed to be that of the pore water of the Callovo-Oxfordian shale), the solute concentration within the borehole is modified and the evolution of the pressure is measured.

For the underground laboratory experiment (fig 2), processed by ANDRA, a new borehole in the Callovo-Oxfordian shale has been drilled. This borehole is divided into four rooms, where the pressure can be measured. When the pressure equilibrium is reached, a less salty solution than the reference solution is injected in one room and a more salty solution is injected in another room. Similarly to the experiment at the sample scale, the pressure evolution is followed.

The osmotic efficiency coefficient is deduced by an inverse approachfrom these experiments using the theorical model of Revil et al. (2004).

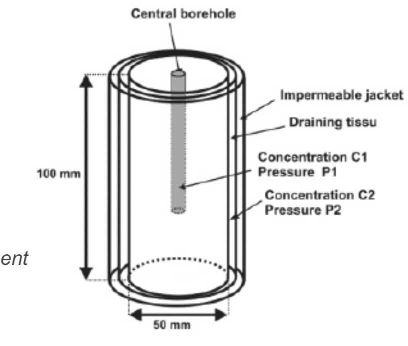

*Figure 1 : Diagram of the experiment at the sample scale*

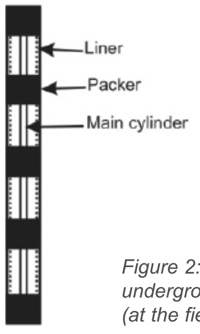

*Figure 2: Diagram of the underground laboratory experiment (at the field scale)*

## References

Revil, A., Leroy, P. and Titov, K., (2005), Characterization of the transport properties of the argillaceous sediments : Application to the Callovo-Oxfordian argillite, Journal of Geophysical Research, 110: B06202, doi:10.1029/2004JB003441.

## DARCY 75

# Input of chemical and isotopic studies in the elaboration of the new conceptual flow model of the Maastrichtien aquifer system in Senegal

Aranyossy J.F.[1], Faye A.[2], Møller K.N.[3], Sarr M.[4], Emsellem Y.[5]
[1] ANDRA, France. jean-francois.aranyossy@andra.fr
[2] University Cheich Antia Diop, Dakar, Senegal. abfaye@sentoo.sn
[3] COWI A/S, Parallelvej 2, DK-2800 Lyngby, Denmark. klm@cowi.dk
[4] SGPRE / MHHE, Senegal. mamadusaar@sentoo.sn
[5] ItalPros, yvesemsellem@watermodel.com

### General Context

The Maastrichtien aquifer, which underlies more than two third of Senegal, represents the most important groundwater reservoir in the region. However, its present exploitation only corresponds to a small fraction of its total estimated reserve (> 20 $MMm^3$). This presentation summarises how the chemical and isotopic data were integrated into the global aquifer system study[1] and how they contributed to the overall understanding the hydraulic functioning of the aquifer and to the subsequent elaboration of the new conceptual flow model. The general approach was based on a comprehensive integration of all the different components on the system at different level of space and time: geology, intrinsic hydraulic properties; piezometry; hydrochemistry.

### Chemical and isotopic data

Statistical treatment of about 800 representative points has led to consider three distinct geographical zone in the Maastrichtien aquifer (fig.1): the **Eastern Zone**, of low mineralization ($<600 mgl^{-1}$), gradually evolving from $Ca\text{-}Mg\text{-}HCO_3$ water in the South East, towards $Na\text{-}K\text{-}HCO_3$ water in the occidental part; the **Central Zone**, with high salinity Na-Cl water (750 to 3500 $mg.l^{-1}$), often associated with high fluoride contents; the **Western Zone** (Horst Ndiass area), with generally low mineralized $Ca\text{-}Mg\text{-}HCO_3$ water, with some local Na-K $HCO_3$ and Na-Cl water buckets of marine origin, related to localized intensive pumping. Numerous isotopic data ($^{18}O$, $^{2}H$, $^{3}H$, $^{13}C$, $^{14}C$, $^{36}Cl$, $^{11}B$, $^{234}U/^{238}U$, $^{230}Th$, $^{3}He$, $^{4}He$) confirmed this geographical repartition and contributed to define the new conceptual groundwater flow model.

### The new conceptual model

Contrary to the previous conceptual flow model (which assumed a continuous flow towards the Atlantic Ocean), the new conceptual model considers three independent zones, with three different hydraulic regimes (figure1):

- In the Eastern Zone, the groundwater flow has a general centripetal direction. The present recharge mainly occurs from the South and South-eastern edges of the basin, and in a minor importance along the upper course of the Senegal River.
- Being "hydraulically blocked" by the geological structure of the Central Zone and its steady saline waters, the main outlet of the groundwater circulation in the Eastern Zone occurs by vertical ascending drainage area through the upper formation of Upper Continental (Continental Terminal). Quantitative estimation of the actual recharge of the aquifer, together with the estimate of possible evaporation rate through the deep unsaturated zone in the Ferlo sustain this hypothesis.
- In the Western Zone, structurally isolated from the rest of the of the Maastrichtien aquifer, a "more usual vertical recharge", directly generated by the infiltration of the precipitation on the Horst Ndiass, is compensated by the present exploitation (actually superior to the present recharge) and by the natural (or locally artificial) equilibrium with the see level.

---

[1] the "Water Sector Project", Coordinated by the World Bank and financed by the Nordic Development Fund. (1998-2001)

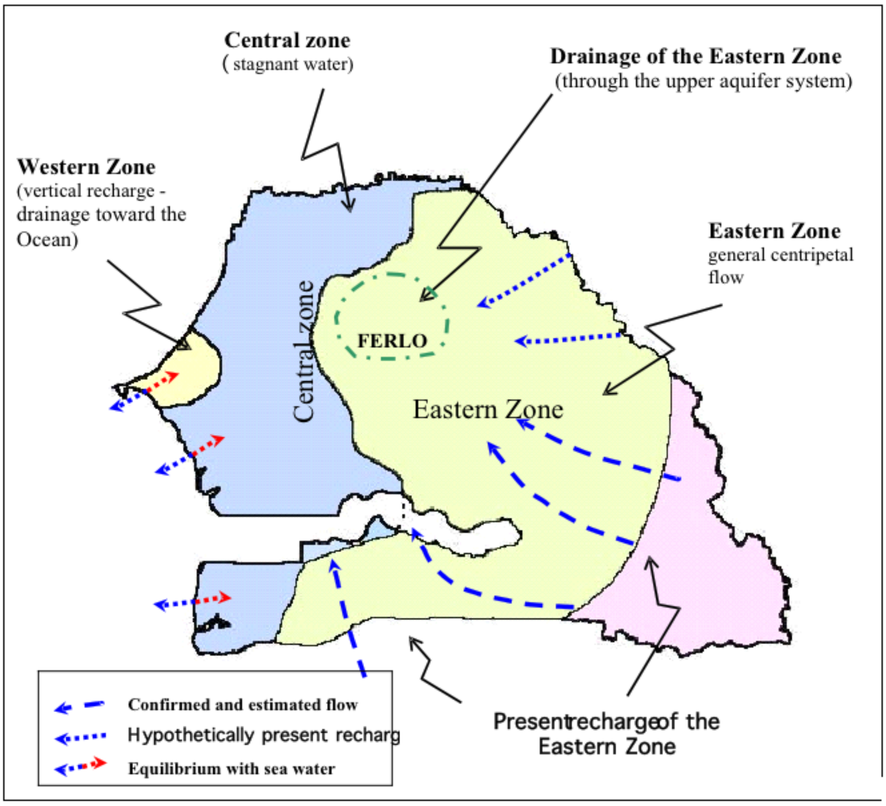

Fig 1 : New Conceptual flow model of the Maastrichtien aquifer system in Senegal

## References

- Cowi/Polyconsult/SGPRE (2001)- Caractéristiques hydrogéologiques du système aquifère maastrichtien au Sénégal. Rapport de synthèse
- Faye, A. (1994) - Recharge et paléorecharge des aquifères profonds du bassin du Sénégal. Apport des isotopes stables et radioactifs de l'environnement, et implications paléohydrologique et paléoclimatique. Thèse es Sciences Département de Géologie FST/UCAD - Dakar - 87 pages
- Travi, Y. (1988)- Hydrogéochimie et hydrogéologie des aquifères fluorés du bassin du Sénégal. Origine et condition de transport du fluor dans les eaux souterraines. Thèse es Sciences Université Paris.

# DARCY 82

# Les grands transferts hydrodynamiques dans le bassin sédimentaire du Nord Ouest Saharien de l'Algérie (Monts des Ksour - Plate forme Saharienne)

MANSOUR. H*, MERZOUGUI. T**, NADJI. A*, FOUKRACHE. M*, ZEROUAL. I*
* FSTGAT, Département des Sciences de la Terre – Université d'Oran – BP 1524 es sénia
l_mansou@yahoo.fr
**GTZ/AHT, groupe : projet gestion intégrée de l'eau. Béni Abbes, Béchar, Algérie

Il s'agit d'un système hydrogéologique d'échelle régionale où la chaîne des Monts des Ksour n'en constitue qu'un maillon de cet l'immense appareil hydraulique, englobant les piémonts Nord des Monts des Ksour (bordure Sud du Chott Gharbi), les piémonts Sud des Monts des Ksour (les inféro flux et le Complexe Terminal de la Hamadet Bent Touadjine), la plate forme Saharienne (Hamadas et grand Erg occidental) et la vallée de la Saoura.

Au sein des piémonts Nord des Monts des Ksour, les formations gréseuses Jurassico-Crétacées disposent de grandes possibilités aquifères, alimentées d'une part latéralement par les calcaires dolomitiques de l'Aaléno-Bajocien et d'autre part par écoulement hypodermique, particulièrement au droit des Theniet qui constituent des couloirs privilégiés d'alimentation.

Les piémonts Sud des Monts des Ksour, parcourus par le réseau aérien des oueds Zousfana, Namous, Gharbi, et Segguer constituent un vaste système hydrogéologique jouant le rôle de carrefour entre le domaine Atlasique au nord et les terrains de couches rouges du Complexe Terminal, sous jacents à la dalle Hamadienne au Sud.

La Hamada Sud Oranaise, par l'intermédiaire de l'entablement des calcaires Miocènes joue un rôle de relais, permettant de drainer les eaux souterraines, issues des piémonts de l'Atlas et de la nappe sous l'Erg vers la vallée de la Saoura. La grande source de Béni Abbès constitue l'exutoire par excellence de la nappe de l'Erg au droit de cette localité.
La limite occidentale du système est intimement liée à la présence des formations Carbonifères du bassin de Taghit – Béchar, qui à leur tour interviennent pour suralimenter l'aquifère de la Hamada Sud Oranaise.

La Hamada du Guir peut constituer un Karst parsemé de Dayas qui joueraient le rôle de dolines. Nous aurions donc une ensemble de drains partant des différentes dayas et pouvant donner un conduit principal au droit des paléo-oueds. Nous n'aurons donc pas un ensemble continu mais un système de réseaux karstiques pouvant évoluer séparément.
L'apport de l'hydrologie isotopique confirme que les réserves héritées des pluviaux Quaternaires se trouvent mêlées à un apport sporadique actuel, particulièrement au niveau du Grand Erg Occidental.

En climat hyper aride, la répartition des pluies ainsi que la faiblesse de leur volume global nous a conduit à s'interroger sur l'origine de la ressource : faut-il faire intervenir la superficie et admettre l'existence de bassin d'alimentation particulièrement étendu ou supposer un apport d'eaux anciennes emmagasinées lors de pluviaux Quaternaires avec un renouvellement actuel très faible. Nous serons donc amené à prendre en compte de très grandes superficies, telles que les piémonts de la plate forme Saharienne (O. Namous, Zoubia, Rharbi et

Sougguer), le bassin de la Saoura dans ses aspects généraux, le grand erg occidental et l'Atlas Saharien occidental (monts des Ksour). Les principales ressources en eaux souterraines sont localisées dans deux systèmes aquifères importants (fig. 01):

- *Le Continental Intercalaire* dans les Monts des Ksour, représenté par des dépôts sablo-gréseux et sablo-argileux avec une puissance pouvant atteindre 1200 m à Labiod Sidi Cheikh.
- *Le complexe terminal* au niveau des piémonts et de la plate forme Saharienne, défini par un empilement d'aquifères superposés attribués au Mio-Plio-Quaternaire.

Une réflexion et une optique régionale ont été tentées pour appréhender des questions pertinentes telles que le rôle hydrodynamique de la flexure Sud Atlasique le long du versant Sud des monts des Ksour, l'impact de l'hydrologie superficielle dans la réalimentation de la plate forme Saharienne ou encore le degré de liaison relatif aux échanges verticaux (phénomène de drainance) entre les différents aquifères superposés, particulièrement entre le *Continental Intercalaire* et le *Complexe Terminal.*

## II – CONSIDERATIONS GENERALES

### 1 - Les Monts des Ksour dans leur cadre régional

*L'Atlas Saharien, chaîne montagneuse d'une longueur d'environ 1000 Km, orientée SW-NE, forme la troisième unité par référence à l'Atlas Tellien et les hauts plateaux. Intercalé entre le domaine Saharien au Sud, demeuré relativement stable au cours de l'orogénèse Alpine et le domaine Tellien au Nord à terrains plus allochtones (fig. 01).*

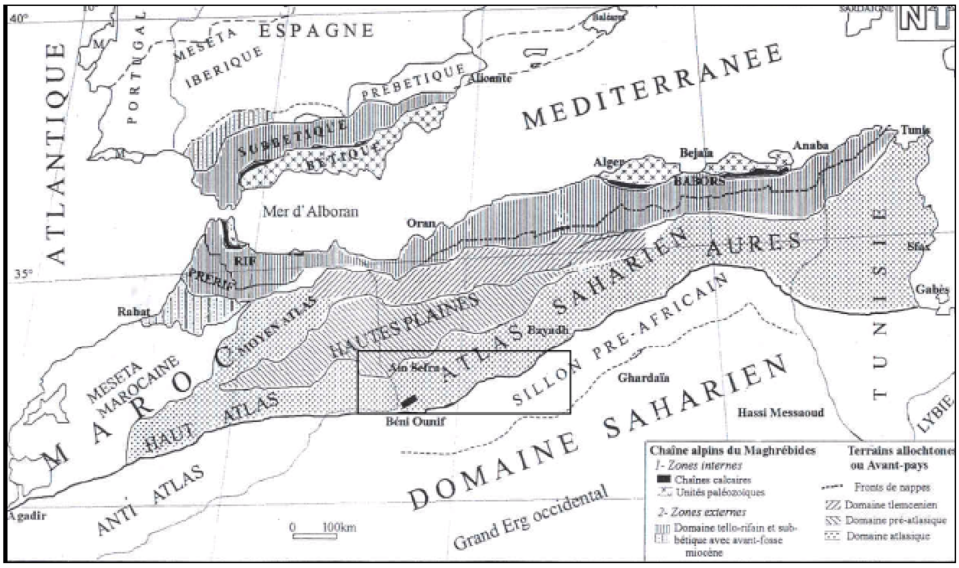

Figure 1 : Les Monts des Ksour dans leur cadre régional (Benest, 1985)

### 2 - Cadre géologique

#### *2.1. Cadre géologique général*

L'Atlas Saharien occidental, faisant partie d'une chaîne montagneuse plissée a subi au cours des périodes géologiques une tectonique intense, matérialisée par des plis anticlinaux, généralement coiffés, pincés, faillés, souvent déversés et parallèles à la direction générale Nord Est – Sud Ouest de cette chaîne. Ces anticlinaux d'âge Jurassique sont séparés par des zones déprimées, parfois perchées, formant de vastes plaines, comblées par des formations continentales gréso-argileuse d'âge Crétacé inférieur. Caractérisées par une double perméabilité (fissures et interstices), ces formations continentales, attribuées au Barrémo-Albo-Aptien, communément désignées sous le vocable Continental Intercalaire sont le siège des grands écoulements d'eaux souterraines de cette partie de l'Atlas Saharien.

### *2.2. l'accident Sud Atlasique*

La limite séparant l'Atlas Saharien de la plate forme est marquée avec beaucoup plus de précision par une série d'accidents en coulisse qui se présentent en forme de flexure, de plis failles ou de failles dont l'ensemble constitue la flexure Saharienne. Une meilleure compréhension de cette limite tectonique est obtenue grâce à la sismique par l'imagerie des failles réactivées. L'architecture des structures compressives dépend du pendage des failles préexistantes et sur leur azimut en relation avec les paléocontraintes durant la compression (fig. 2).

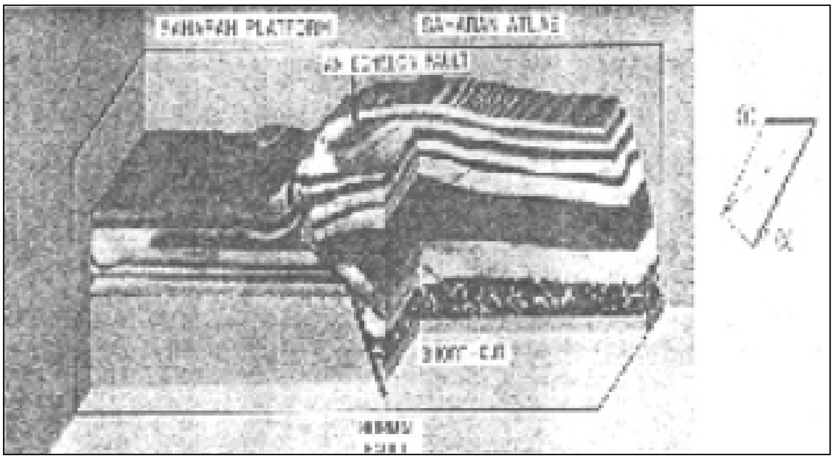

*Figure 2 : Diagramme représentant un modèle expérimental d'une faille de chevauchement décrochante Sud Atlasique (Letouzey, 1992)*

A l'échelle locale (Djebel Kerdacha), les terrains Crétacés dessinent une structure synclinale à flancs renversés (fig. 3). On y repère la barre Cénomano-Turonienne qui affleure d'une façon ininterrompue parallèlement au Djebel Kerdacha. Les affleurements des argiles rougeâtres microconglomératiques gypsifères et de grés blanchâtres du Crétacé inférieur et du Cénomanien sont limités surtout sur le flanc NE de Kerdacha où le cœur Liasique plus ancien affleure.

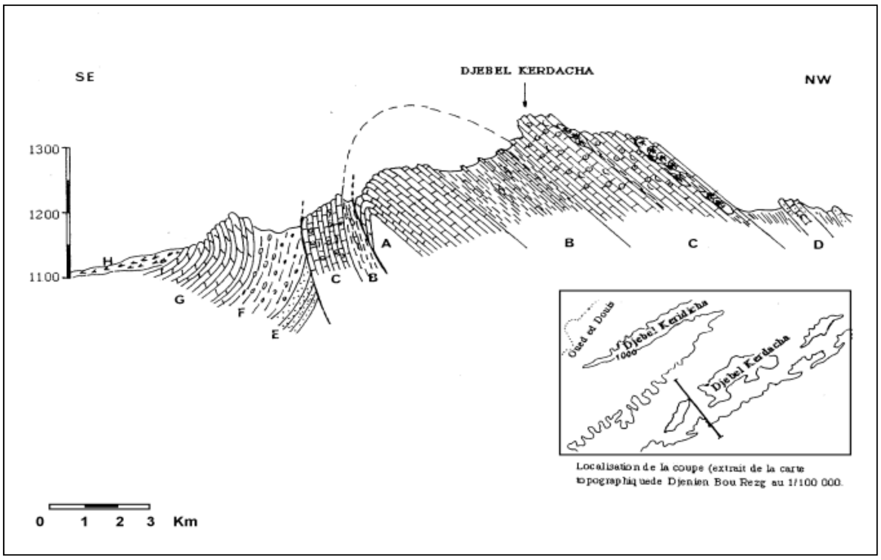

Localisation de la coupe (extrait de la carte topographique de Djenien Bou Rezg au 1/100 000.

*Figure 3 : La flexure Sud Atlasique affectant le chaînon de Kerdacha.*
*A : Calcaires lités noirs (Lias moyen),*
*B : Marno-calcaires (Lias supérieur),*
*C : Calcaire de la formation de Kerdacha (Bojocien),*
*D : ensemble argilo-gréseux de la formation de Tifkirt (Bajo-Bathonien),*
*E : Grés de la formation de Tiout (Crétacé inférieur),*
*F : Argiles gypsifères (Cénomanien inférieur),*
*G : Calcaires dolomitiques de la formation de Khoundjaïa (Cénomano-Tutonien),*
*H : Eboulis récents.*

# DARCY 82

### 3 - Hydrologie Saharienne

L'étude hydrologique a porté sur les différents sous bassins versants, constituant le flanc sud de l'Atlas saharien occidental. Du point de vue climatologique, une synthèse des principaux paramètres, régissant le climat des Monts des Ksour et de la plate forme a été proposée. On citera particulièrement l'apport par les précipitations, représentant une lame d'eau moyenne de 160 mm relative à l'ensemble de la zone cartographiée. L'étude hydrologique a pris en compte les grands émissaires descendant de l'Atlas Saharien occidental. Elle a permis ainsi de faire ressortir les apports alimentant d'une part la plate forme à partir des :

- Oued Namous (Aïn séfra au droit de Aïn Hadjadj): 23 millions de m$^3$
- Oued Gharbi (Mellah, Rechag et Tafarhit) : 34 millions de m$^3$
- Oued Segguer (Brizina au droit Larouia): 30 millions de m$^3$

et d'autre part les apports alimentant en partie la vallée de la Saoura, à partir de l'oued Zousfana et son affluent principal l'oued Zoubia : soit un apport de 40 millions de m3 .Les crues exceptionnelles ayant un débit notable, permettant de régénérer les eaux souterraines du Continental Intercalaire, du Complexe Terminal et les terrasses des grands inféro flux peuvent atteindre des débits instantanés compris entre 600 et 1000 m$^3$/s :

## III – HYDROGEOLOGIQUE REGIONALE

Le Barrémo-Albo-Aptien, représenté par le Continental Intercalaire s'étend largement vers le Sud. Le Mio-Pliocène, représenté par le Complexe Terminal, caractérisé par les formations rougeâtres continentales, repose en discordance vers le Sud de la plate forme sur le Continental Intercalaire où il constitue un système hydrogéologique complexe

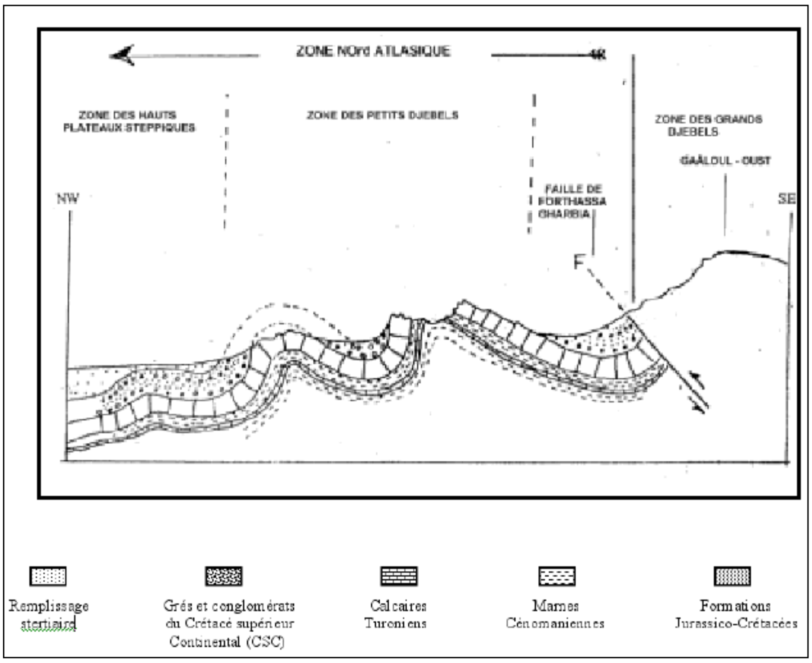

*Figure 4 : Coupe schématique de la structure Jurassico-Crétacée des piémonts Nord des Monts des Ksour (in ALGEO, 1977)*

### 1 - Piémonts Nord des Monts des Ksour

Le raccordement des hautes plaines Oranaises dans sa partie Sud avec les Monts des Ksour se fait par l'intermédiaire de l'accident Nord Atlasique. Au pied des Djebels Oust et Gaâloul, on note des terrains appartenant au Crétacé supérieur continental, au Turonien et Cénomanien. Au Sud des Djebels, s'étale une vaste étendue de grés Jurassique supérieur, surmontés plus au Sud à Sfissifa par les grés Crétacé inférieur du Continental Intercalaire. La coupe schématique (fig. 04) établie par ALGEO (1977) montre un plissement assez important de synclinaux et d'anticlinaux séparés des hauts djebels par une faille majeure alignée Sud Ouest - Nord Est (faille de Forthassa), faisant partie des satellites de l'accident Nord Atlasique.

L'alimentation se fait à partir des piémonts Nord des Monts des Ksour par voie hydrodynamique entre les formations gréseuses Jurassico-Crétacées et les calcaires dolomitique de l'Aaleno-Bajocien ainsi que écoulement hypodermique, particulièrement au droit des Teniet qui constituent des couloirs privilégiés d'alimentation.

## 2 - Piémonts Sud des Monts des Ksour (Planche I).

La région Oued Namous – Oued Gharbi constitue un vaste système hydrogéologique jouant le rôle de carrefour entre la chaîne Atlasique au Nord et les terrains de couches rouges du Complexe terminal, sous jacents à la dalle Hamadienne au Sud. Il y a lieu de distinguer 02 grands ensembles morphologiques différents : les nappes des terrasse (nappes des inféro-flux) et la nappe du Complexe Terminal (Hamada Bent Touadgine).

### *2.1. Nappes des terrasses des grands oueds*

Les eaux sont contenues dans les terrasses des grands oueds, constituant des ressources, généralement exploitées pat les nomades. Malgré la très forte évapotranspiration, les niveaux piézométriques sont maintenus grâce aux crues, génératrices de débits importants, issues de l'Atlas Saharien, dévalant des Inféro flux des bassins des oueds Namous, Gharbi et Segguer.

### *2.2. Nappe du Complexe Terminal (Hamada Bent Touadjine)*

Il s'agit de formations sablo-argileuses de couleur rouge avec quelques passages de calcaires lacustres et de grés. L'épaisseur recoupée par les forages varie entre 150 et 350 mètres. Les formations sous jacentes sont constituées par le complexe Cénomano-Turonien, épais de 150 mètres. Selon les sondages pétroliers, la limite méridionale d'extension du Cénomanien le long de l'oued Namous se situe approximativement entre Garet Es Slougui et Djorf El Atfa (planche I). Au Sud de cette zone, le Complexe Terminal repose directement sur le *Continental intercalaire.*

<u>Les données de forages</u>
* *Forages hydrauliques :* les forages recoupent la totalité du Complexe Terminal ; certains pénètrent en partie dans le Continental Intercalaire. Les épaisseurs du Complexe Terminal et du Continental Intercalaire diminuent vers l'Ouest (Hamada comprise entre Oued Namous et Oued Zoubia) où le Jurassique est moins profond.
Cependant, on peut remarquer que les niveaux statiques varient entre 19 m (forage n°44, Guern-Zaïa) et 206 m (forage n°56, Ni-1), signe évident de la présence d'un système aquifère multicouches, conditionné particulièrement par des échanges hydrodynamiques verticaux. Nous assistons ainsi à un phénomène de drainance ascendante, impliquant l'alimentation du Complexe Terminal par le Continental Intercalaire.
* *Forages pétroliers :* dans la Hamada comprise entre l'oued Namous et l'oued Gharbi (Hamada Bent Touadjine), des sondages profonds réalisés par des firmes pétrolières (SN Répal, Sonatrach) ont permis de mettre en évidence un certains nombre d'informations, relatives à la limite d'extension du Cénomanien ainsi que de l'épaisseur du Complexe Terminal et du Continental Intercalaire(fig. 10). Epais de 140 m, Le Cénomanien disparaît entre les forages Taj.1 et Btji.1 laissant reposer directement le Complexe Terminal sur le Continental

Intercalaire. Ces deux unités hydrogéologiques diminuent d'épaisseur du Nord vers le Sud. Le Trias profond de 1940 m au forage taj.1 remonte à 500 m au niveau du forage Nm.1, caractérisant un bassin subsident au niveau de Hamadet Bent Touadjine.

## 3 - Plate forme Saharienne

### *3.1. Hamada Sud Oranaise*

La base de la série est représentée par des formations grossières, fortement redressées au pied des monts des Ksour. Au delà, viennent des sables et argiles rouges qui atteignent de grandes épaisseurs au Nord, en raison du fléchissement de la plate forme Saharienne au contact de l'accident Sud Atlasique.
L'ensemble Hamadien à été largement disséqué par les oueds Quaternaires (Zousfana, Namous, Gharbi et Seggueur) qui dévalent à partir des piémonts Atlasiques . Par la suite, l'instauration du climat désertique en permettant la mobilisation par les vents de sables entraînés au Sud lors des phases pluviales, va permettre la formation du Grand Erg Occidental qui fossilisera par la suite les lits des paléo oueds. La Hamada elle même disparaissant sous l'épais manteau sableux.
La coupe schématique établie entre l'Atlas des Monts des Ksour et la vallée de la Saoura (fig. 05) permet de faire ressortir la complexité du système hydrogéologique du Nord Ouest Saharien. En effet, l'entablement des calcaires Pliocènes joue un rôle de relais, permettant de drainer les eaux souterraines, issues de la Hamada et la nappe sous l'Erg vers la vallée de la Saoura.
Au Nord, la limite de l'aquifère est indissociable des contreforts de l'Atlas et des apports du Continental Intercalaire (liaison hydrodynamique). Les inféro flux (Zousfana et Namous) quant à eux qui drainent le versant méridional de l'Atlas, interviennent principalement par voie aérienne (crues de printemps) et écoulement hypodermique. La limite occidentale du système est intimement liée à la présence des formations Carbonifères du bassin Taghit – Béchar, qui à leur tour peuvent intervenir pour suralimenter l'aquifère de la hamada Sud Oranaise.

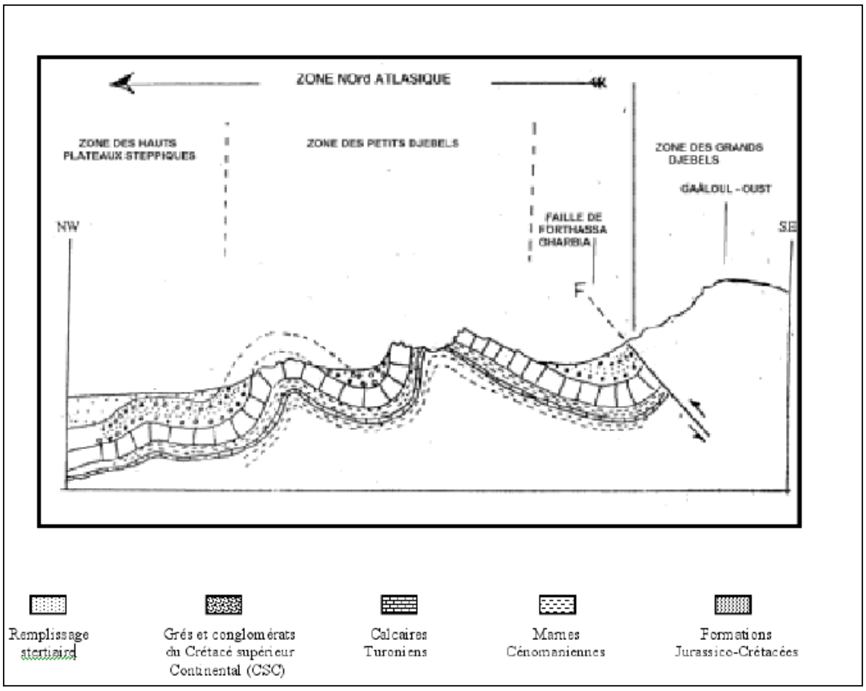

*Figure 5. Coupe géologique schématique Atlas Saharien – Hamada – Grand Erg – Saoura*
*T : Barre de calcaires Turonien de la bordure Atlasique,*
*C : Cénomanien,*
*Ci : Continental Intercalaire*
*1 : Formations détritiques grossières à la base e la série,*
*2 : Sables et argiles rouges,*
*3 : Poudingues de carapace calcaire, 4 : Entablement calcaire,*
*5 : Grand Erg*

### *3.2. Hammada du Guir)*

Il s'agit d'un plateau faiblement incliné depuis Boudenib (1150m) jusqu'aux chaînes d'Ougarta (650m). Long de 200 km et large de 110 km, le plateau est orienté du NW au SE. La butte témoin de Gara Diba (Béni Abbes) permet de faire le passage à la Hamada Sud Oranaise dont elle est séparée par l'oued Saoura.

Au Sud Est, la nappe aurait comme exutoires naturels les 'puits sources' de Zguilma ; le sondage d'Igli n° 01 montrera qu'il y a également des apports depuis les calcaires gris bleus à entroques du Viséen. Les eaux qui émergent à la base de la Hamada sont en partie drainées par la Saoura. Au Sud, l'écoulement des eaux de la Hamada se trouverait bloqué par la présence de formations Primaires. Au Sud Ouest, la présence de l'oued Berraber dont les eaux de crue s'infiltrent sous les sables de l'erg Er Raoui, justifient les ressources disponibles plus au Sud dans la région de Tabelbala qui serait alimentée à la fois par la chaîne de l'Ougarta et les formations Hamadiennes.

En tout état de cause, nous admettons que la dalle Hamadienne peut constituer un karst parsemé de dayas qui joueraient le rôle de dolines. Les eaux de pluie ruissellent sur la Hamada et viennent s'accumuler dans les dayas où une grande partie s'évaporera, le reste s'infiltrera. Par référence au karst, nous aurions un ensemble de drains partant des différentes dayas et pouvant donner un conduit principal au droit des paléo oueds. Nous n'aurons donc pas une nappe continue mais un ensemble de réseaux karstiques pouvant évoluer séparément.

### *3.3. Le Grand Erg Occidental*

La distribution des courbes isopièzes autour du massif d'El Khella, établie par Roche (1973) confirme son rôle dans l'alimentation de la nappe de l'Erg. Les pertes observées sur l'oued Zousfana en amont de Taghit, traduisent l'existence de réseaux karstiques dans les calcaires Carbonifères. Etant donné l'importance des pluviaux Quaternaires, il est évident que ces réseaux karstiques peuvent être très développés. L'esquisse hydrogéologique réalisée par Schoeller (1945) montre que la nappe de l'Erg suralimente la haute Saoura entre Igli et Béni Abbes (fig. 6a). La grande source de Béni Abbès (30 l/s) constitue l'exutoire par excellence de la nappe de l'Erg au droit de cette localité. A la lisière septentrionale du grand Erg, trois dômes piézométriques qui correspondent exactement aux secteurs où les oueds Namous, Gharbi et Seggueur perdent leur tracé linéaire pour s'épandre à la surface de la Hamada (fig. 6b)). La recharge de la nappe sur ces trois points nous paraît tout à fait évidente.Les gradients élevés de la bordure Atlasique décroissent rapidement pour n'être plus que de 0.8 à 0.5 ‰ à une centaine de kilomètres, à l'emplacement des dômes piézométriques. C'est également là que le *Continental Intercalaire* passe au contact direct du *Tertiaire Continental*, l'un réalimentant l'autre.

L'hypothèse de l'alimentation de la nappe de l'Erg par celle du *Continental Intercalaire* reste très hypothétique ; par contre des pertes de la 1ère au profit de la 2ème pourrait se produire. Les résidus secs très faibles pour des régions aussi arides (340 à 600 mg/l) nous amènent à penser que les pertes par évaporation sont pratiquement nulles. La profondeur assez élevée des eaux et la relative épaisseur de la nappe sous l'Erg contribuent à une protection efficace contre l'évaporation.

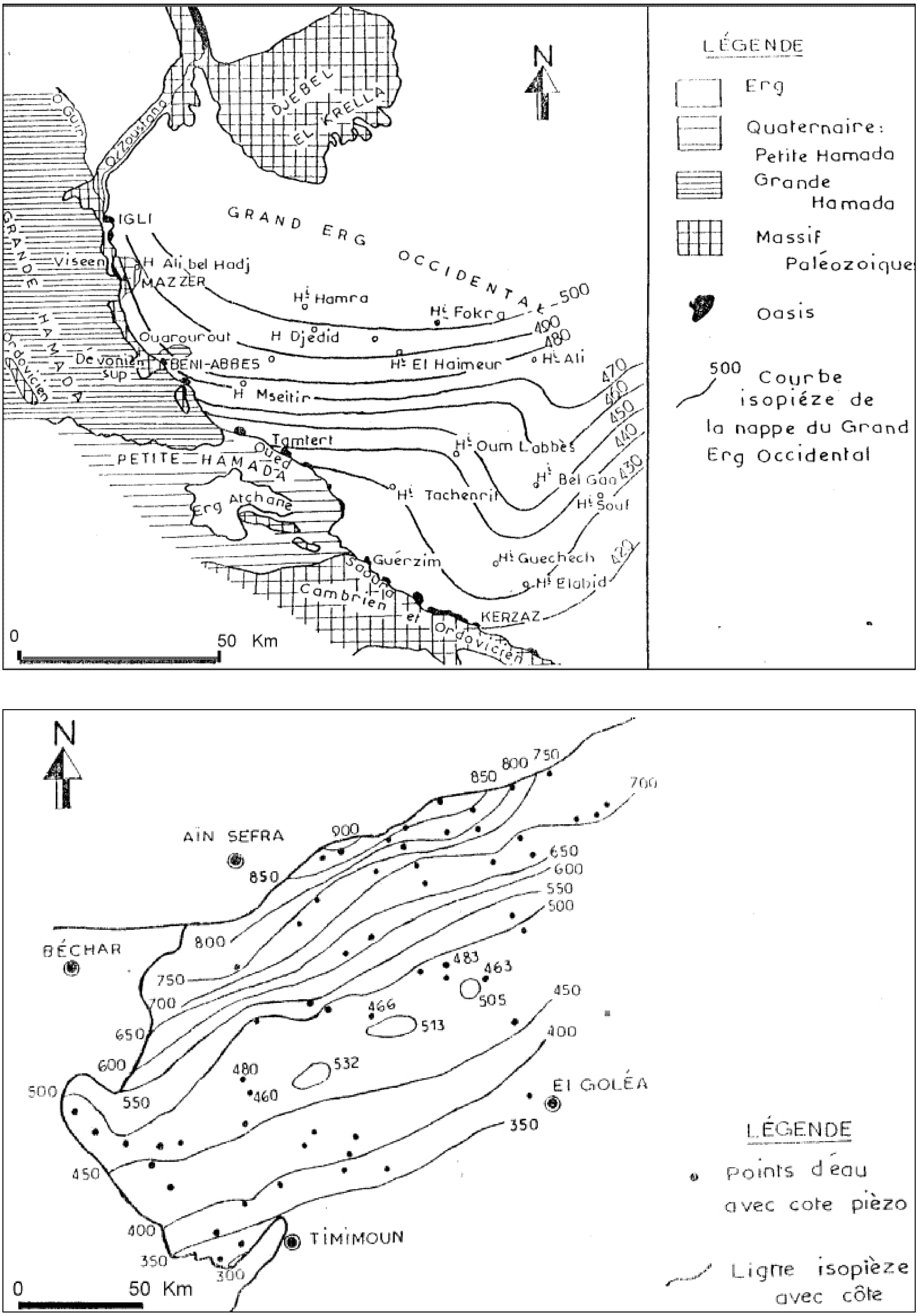

Figure 6 : Esquisse piézométrique du Grand Erg Occidental d'après Schoeller (1945) rnet (1964)

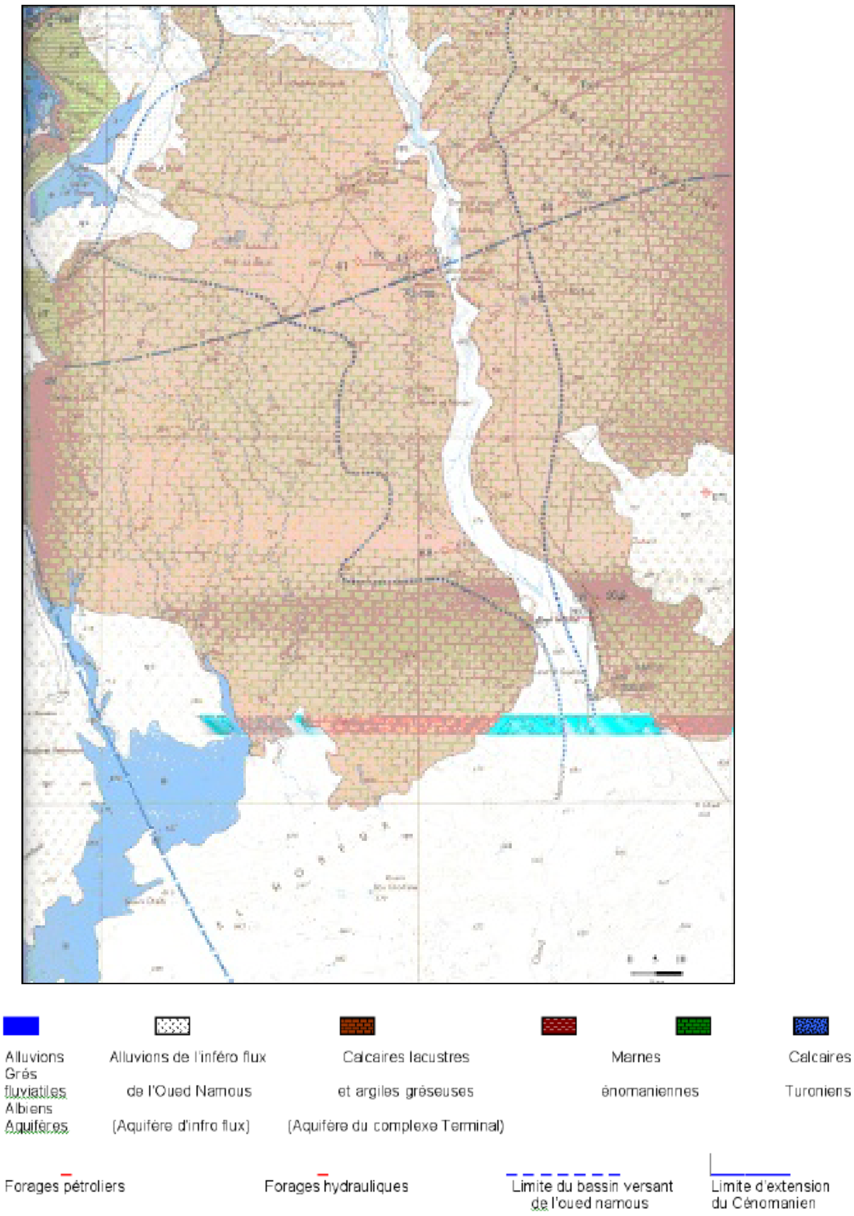

*Planche 1 : Carte géologique de la Hamadet Bent Touadgine : région Oued Namous – Oued Gharbi*
*Extrait de la carte hydrogéologique de Béchar*

## IV. CONCLUSION

Après les interprétations et conclusions tirées de l'étude hydrogéologique, reposant sur l'analyse du bilan de l'eau (quantification des apports), les caractéristiques lithologiques (conditions aux limites) et structurales (Flexure Sud Atlasique) des formations pouvant constituer des aquiductes ou des écrans, il s'est avéré qu'on est en présence de deux phénomènes majeurs marquant l'hydrogéologie régionale du Nord Ouest du Sahara Algérien :

- Immense appareil hydraulique, régit par un hydrodynamisme complexe, commandé par la présence de l'accident Sud Atlasique, qui selon la région jouera le rôle de flux à potentiel imposé (partie occidentale au droit Béni Ounif), de flux nul (partie orientale à El Abiodh Sidi Cheikh) ou flux mixte (partie centrale au droit de Moghrar).
- Symbiose hydraulique, à l'échelle régionale entre les Monts des Ksour, les piémonts de la plate forme Saharienne, le Grand Erg Occidental et la vallée de la Saoura.

L'hydrologie de surface, basée en grande partie sur l'analyse des débits fréquentiels a pris en compte les grands émissaires descendant de l'Atlas Saharien Occidental. Elle nous a permis de dresser un constat, illustrant des apports capables d'alimenter 02 entités hydrogéologiques distinctes :

- Domaine oriental, parcouru par les Oued Namous, Gharbi et Segguer, alimentant les piémonts de la plate forme saharienne avec un apport total de 84 Millions de mètres cubes.
- Domaine occidental, drainé par la Zousfana et son affluent principal, alimentant la grande vallée de la Saoura avec un apport moyen de 40 Millions de mètres cubes.

Les crues exceptionnelles, d'un débit notable permettent de régénérer les eaux souterraines du **Continental Intercalaire**, du *Complexe Terminal* et des terrasses des grands inféro flux. Les débits instantanés calculés à partir des données hydrométriques sont compris entre 600 $m^3$ /s et 1000 $m^3$ /s.

Les piémonts Sud des Monts des Ksour, parcourus par le réseau aérien des oueds Zousfana, Namous, Gharbi, et Segguer constituent un vaste système hydrogéologique jouant le rôle de carrefour entre le domaine Atlasique au nord et les terrains de couches rouges du Complexe Terminal, sous jacents à la dalle Hamadienne au Sud.

Les caractéristiques des différents forages hydrauliques nous indiquent qu'on est en présence d'une nappe très complexe, contenue à la fois dans le Mio-Pliocène (Complexe Terminal) et dans le Barremo-Albo-Aptien (**Continental Intercalaire**). C'est donc un système aquifère multicouche, conditionné particulièrement par des échanges hydrodynamiques verticaux. Nous assistons à un phénomène de drainance ascendante, impliquant l'alimentation du Complexe Terminal par le **Continental Intercalaire**.

La Hamada Sud Oranaise, par l'intermédiaire de l'entablement des calcaires Miocènes joue un rôle de relais, permettant de drainer les eaux souterraines, issues des piémonts de l'Atlas et de la nappe sous l'Erg vers la vallée de la Saoura.

## Références

- ALGEO., 1977 – Etude géophysique de la région de Djenane El Adham et Forthassa Nord (Mecheria – Aïn Séfra). Rapport ANRH, 52 p, 11Fig, 13 Pl.
- BEKHEDDA B., 1992 – Contribution à l'étude hydrogéologique du synclinal de Béni Ounif (Monts des Ksour, Atlas Saharien). Mém. Ing, Univ-Oran, 162 p, 77 Fig.
- CONRAD G., MARCE A. et OLIVE P. 1975 – Mise en évidence par le tritium de la recharge actuelle des nappes libres de la zone aride Saharienne (Algérie). Journal of Hydrology. n° 27, Amsterdam, pp. 207 – 224.
- CORNET A. et GOUSKOV N., 1952 – Les eaux du Crétacé inférieur continental dans le Sahara Algérien. (nappe Albienne). Travaux de l'institut des recherches Sahariennes (Tome III), 4ème partie, pp. 144 – 169.
- DOUIHASNI M., 1976 – Etude géologique de Aïn Ouarka – Boussemghoun. Analyse structurale (Partie centrale des Monts des Ksour, Atlas Saharien, Algérie). Thèse 3ème cycle, Univ – Oran, 272 p, 52 fig, 4 pl.
- GALMIER D., 1970 – Photogéologie de la région de Aïn Séfra (Atlas Saharien, Algérie). Thèse doctorat d'état. Fasc. Sc. De Paris. 320 p, 9 cartes.
- KRADCHI B. et MESBAHI K., 2001 - Essai de synthèse cartographique des écoulements souterrains des synclinaux des Monts des ksour (Atlas Saharien occidental). Mém. Ing, Univ – Oran, 81 p, 57 fig.
- MANSOUR H., SAFA A et BEKHEDDA B., 1998 - La flexure Sud Atlasique et son rôle hydrodynamique dans la réalimentation de la plateforme Saharienne (cas du synclinal de Béni-Ounif). Journées d'études sur les zônes arides, retroperspectives, enjeux et réalités ; Adrar.
- MANSOUR H. et VERDEIL P., 1992 - Hydrogéologie de la source de Béni-Abbes : son alimentation et son captage (Sahara Nord occidental). Fenêtre ouverte sur la Science au désert. Adrar

- MANSOUR H., 1993 – Les isotopes dans l'eau du Sahara Nord Occidental Algérien (Grand Erg Occidental – Hamada du Guir). 2ème journées Tunisiennes de géologie appliquées, Sfax, pp. 88 – 111.
- MEKIDECHE D., MANSOUR H., SAI W., TOUT S. et YOUNSI N., 1995 – Notice explicative de la carte hydrogéologique de la région de Béchar au 1/500.000e . ANRH. Projet PNUD/ALG/88/021. 73 p, 33 fig, 6 tabl, 1 carte.
- RAHMANI A., 1993 – Contribution à l'étude hydrogéologique du synclinal El Hendjir – Aïn Séfra - Tiout (partie centrale des Monts des Ksour, Atlas Saharien). Mém. Ing. Univ – Oran, 100 p, 55 fig.
- ROCHE M.A., 1973 – Hydrogéologie de la haute Saoura (Sahara Nord Occidental). Nouvelle série, n°43, Pub. Serv. Géol. Algérie.
- SALHI A., 2002 – Evolution paléogéographique et dynamique de la bordure méridionale du sillon Atlasique au cours du Lias et du Dogger (région de Béni ounif, Atlas Saharien Occidental, Algérie). Thèse magister, Univ – Oran, 138 p, 66 fig.
- VIALLY et Al., 1994 – Basin inversion alongthe North African Margin The Atlas Saharan (Algéria). Ed. Technip. Paris, 1994, pp. 79 – 118.
- YELLES CHAOUCHE A.K., AïT OUALI R., BRACENE R., DEDER M.E.M et DJELLIT H., 2001 – Chronologie de l'ouverture des Monts du bassin des Ksour au début du Mésozoïque. Bull. Soc. Géol. France, t. 172, n° 3, pp. 283 – 293.
- YOUSFI M., 1984 – Etude géochimique et isotopique de l'évaporation et de l'infiltration en zone non saturée sous climat aride. Béni Abbes, Algérie. Thèse 3ème cycle. Paris. 274 p.
- YOUSFI N. et Aït AHMED C., 1992 – Contribution à l'étude hydrogéologique de la grande source de Béni Abbes (Sahara Nord Occidental). Mém. Ing. Univ – Oran, 396 p, 126 fig.
- ZIANE F., 2004 – Le volcanisme Triasique de Djenien Bou- Rezk. Cartographie, pétrographie et mise en place. (Monts des Ksour, Atlas Saharien Occidental). Mém. Ing. Univ – Oran, 46 p, 7 fig, 17 pl.

## DARCY 83

# Multi isotopic and geochemical characterisation of water bodies in the Adour-Garonne district: clues for interconnection et heterogeneities – The CARISMEAU research project

Négrel Ph.[1], Petelet-Giraud E.[1], Roy S.[1], Dutartre Ph.[1], Fournier I.[2]

[1] BRGM, 3 av. C. Guillemin BP 6009 Orléans Cedex 2, France
p.negrel@brgm.fr; e.petelet@brgm.fr; s.roy@brgm.fr; p.dutartre@brgm.fr

[2] Agence de l'Eau Adour-Garonne, 90, rue du Férétra, 31078 Toulouse cedex, France
isabelle.fournier@eau-adour-garonne.fr

The main objective of the Water Framework Directive (WFD, 2000/60/EC) is to prevent further deterioration and protect and enhance the status of aquatic ecosystems, and with regard to their water needs, terrestrial ecosystems and wetlands directly depending on the aquatic ecosystems. The success of the Directive, in achieving this purpose and its related objectives, will be mainly measured by the status of water bodies. Water bodies are therefore the units that will be used for reporting and assessing compliance with the Directive's principal environmental objectives.

Within the framework of the directive, a research project of multi isotopic and geochemical characterisation of water bodies in the Adour-Garonne district (SW France) is starting jointly between the French Water Agency Adour-Garonne and BRGM. The CARISMEAU research project is focused on the Adour-Garonne district, which covers 116 000 km$^2$ represents 1/5 of the territory. It is limited by the Massif Central to the east, by the Armorican Massif to the north, by the Pyrénées to the south and by the Atlantic Ocean to the west. Considering the WFD concept, the Adour-Garonne district encompasses the Adour, Garonne, Dordogne and Charente river basins. The district fully covers the Aquitaine and Midi-Pyrénées regions and partly the Auvergne, Languedoc-Roussillon, Limousin and Poitou-Charente regions. It represents 6900 councils for a total of around 6.7 millions inhabitants.

Aims of CARISMEAU are to provide further characterization of those groundwater bodies or groups of bodies which have been identified as being of primary importance and/or at risk in the district. This approach is based on the WFD / Annex II which stated that this characterization shall include (1) relevant information on the impact of human activity and, where relevant, (2) information on the stratification characteristics of the groundwater within the groundwater body, (3) on the estimates of the directions and rates of exchange of water between the groundwater body and associated surface systems, (4) provide sufficient data to calculate the long term annual average rate of overall recharge, and (5) provide further characterization of the chemical composition of the groundwater, including specification of the contributions from human activity.

For that purpose, combined geochemical analysis (major and trace elements) and multi-parameters logging, common isotopic methods with $\sigma^{18}O$ and $\sigma^{2}H$ of the water molecule and $\sigma^{34}S_{SO4}$ and $\sigma^{18}O_{SO4}$; innovative isotopic method with strontium isotopes and potential isotopic methods with boron and lithium isotopes will be applied on one demonstrative water body named the Eocene sands aquifer. This water body constitutes a major aquifer used for drinking water, agriculture irrigation, gas storage and thermo-mineral water resource. This aquifer extends over the Adour-Garonne district, being an artesian system to the west of the district and confined with piezometric levels around 250m to the east of the district. Investigations will be carried out on the two extreme hydrological states of the aquifer (high and low water stages) using the multi-parameters logging in order to rapidly define the heterogeneity of the water body and help for the sampling strategy.

# DARCY 88

## An assessment of the groundwater resources in the western margin of the Taoudenni basin, Mauritania

Bertone[1] F., Renard[2] P., Kerrou[2] J., Moix[2] P. and Perrochet[2] P.
[1]BCEOM, Montpellier, France
[2]Centre d'Hydrogéologie, Université de Neuchâtel, Suisse
f.bertone@bceom.fr, philippe.renard@unine.ch

Because of its large amount of mineral resources the region around Zouerate in the north-western part of Mauritania is of high interest for investors. Furthermore, as in any arid region, the water resources are scarce in this part of the Sahara desert and may constitute the limiting factor for the economical development of the region. Assessing the groundwater resources is therefore a very important issue for the Mauritanian government.

In this framework, an extensive study of the hydrogeology of the region has been carried out. The region has approximately the size of Austria. From a geological point of view, it is divided in two main zones: the Archean basement (Dorsale Réguibat) on the western side, which is mainly constituted of fractured magmatic and metamorphic rocks, and the margin of the Taoudenni sedimentary basin on the eastern side which is constituted by a complex series of aquifers (fractured siltstones and carbonates) and aquitard (essentially siltites).

The geometry of the main aquifers has been deduced from a combination of different techniques including: the analysis of new geological maps made by the BGS and the BRGM, the construction of a digital elevation model from remote sensing data, the refinement of the geological map from satellite images treatment, the identification of fracturation patterns on satellite images, the interpretation of aerial magnetometric data, and a hydrogeological interpretation to obtain a hydrostratigraphic log and a series of geological sections through the domain.

A survey of about 600 groundwater observation points, including differential GPS leveling, allowed for the first time to describe the regional flow in this region. It appeared clearly that a few sebkhas (Bou Talha for example) are the main regional discharge zones. The piezometric map also suggests that recharge is potentially occurring in several areas of the domain.

To estimate the fluxes, a 2D regional finite element model has been constructed, calibrated in steady state and transient modes, based on historical records since 1957. The main constraint of the model is to honor the orders of magnitude of the transmissivity data acquired by pumping tests. Three different conceptual models of recharge have been tested: regional recharge including dune fields, intermediate, and localized recharge. Order of magnitude of the discharge rates in the sebkhas were estimated with the empirical formulas of Coundrain-Ribstein and further calibrated with PEST. The calculated results show that it seems possible to increase significantly the water abstraction for the next 40 years. The consequences would be a lowering of the fluxes to the sebkhas and an important lowering of the groundwater levels in the desert. This increased exploitation may obviously have a long time impact if the climate of the region is not changing.

However, many uncertainty remains in this model. One important issue is the distribution of the recharge areas and the potential role of the dunes in the system. The deep structure of the basin remains as well essentially unknown. Further exploration work is required to answer these questions.

# DARCY 89

## Fissured hydrogeosystems of the basement : state of knowledge and consequence on their management

Faillat J.P.
Centre Universitaire de Nîmes, Espace GIS, 120 rue Georges Besse, 30035 Nîmes
jean-pierre.faillat@unimes.fr

In spite of a generally low hydraulic continuity, the fissured aquifers of the basement made up of metamorphic or magmatic rocks, frequent in the part of the earth's crust economically accessible to the hydrogeologic means of investigation, can be regarded as pertaining to the whole of large aquifers. The rational management of the water resources which they contain, because of their strong heterogeneity, supposes a knowledge and a conceptual modelling of the reservoir as exact as possible. The complexity of these hydrogeosystems implies a plurimethodologic approach carrying on the observation and of measurements on the outcrops, in the careers, the springs, wells and drillings, the use of maps and various types of aerial photographies, geophysics, the hydrochimies, etc....
Information obtained afterwards of the work carried out on metric scales with kilometric in many areas, often using experimental sites, results in proposing a diagram of the fissured hydrogeosystems. In this diagram, various surface formations, mainly of the alterites, with particularly varied characteristics, top on hard rocks basement comprising of the networks of fissures hydraulically active, more or less regularly distributed, mainly of origins tectonics (fractures), result of the superposition of the effects of generating phenomena of discontinuities. Alterites and hard rocks constitute a unit compared to a double-layered aquifer of the model drain (the fissured hard rock) - capacity (surface incemented rock). The drain allows relatively significant but located flows and transmits quickly and far the influence from pumpings, following certain preferential directions, in the case of a proven anisotropy. The capacity provides the main part of exploitable volumes of water, coming from pores of interstices, but slowly. This organization and the availability of the equipment of suitable drilling logically involved, since the middle of the Seventies, the exploitation of the water resources of the basement by the intermediary of the networks of fissures hydraulically active.
The hydraulic characteristics of the fissured medium conditioning the possibilities of management are strongly forced by the interactions between the alterites and fissured hard rocks, the space of the fissures, in particular in-depth distribution or following certain privileged directions, and that of the pockets or the corridors of tweathering, like by the partitioning of the aquifers. In addition to hydraulic fonctioning, the geochemical nature of the aquifer will strongly contribute to the quality of water resulting from the basement, with sometimes the awkward presence of heavy metals in excess, or, a contrario, of reducing minerals supporting denitrification, etc...
If an overall diagram of the organization and functioning of the fissured aquifers are currently accessible, differing points however remain to specify, in particular with regard to the distribution of the fissures and that of the alterites.

### References

- Faillat J.P. , 1986 - Aquifères fissurés en zone tropicale humide : structure, hydrodynamique et hydrochimie (Afrique de l'Ouest) - Thèse de Doctorat ès Sciences, U.S.T.L., Montpellier, 536 p., 169 fig., 60 tab., biblio.
- Faillat J.P. et C. Drogue C. , 1987 - Influence de l'effet d'échelle, de l'hétérogénéité et de la connexité des aquifères fissurés sur la réaction des forages en zone de socle (Afrique de l'Ouest). Journal of Hydrology, 90, p. 159-182.
- Faillat J.P., Somlette L. et Sicard T. , 1999 - Contrôles redox et hydrodynamique des nitrates et zonation hydrochimique verticale des nappes de fissures du socle. Possibilité de généralisation. Bull. Soc. géol. Fr., t. 170, n° 2, 229-240.

# DARCY 90

## Interaction between different groundwaters: characterizing multiple sources through strontium isotope tracing, sedimentary versus fractured bedrock aquifers

Négrel Ph., Petelet-Giraud E. , Pauwels H.

BRGM, 3 av. C. Guillemin BP 6009 Orléans Cedex 2, France
p.negrel@brgm.fr; e.petelet@brgm.fr; h.pauwels@brgm.fr

Water resources in hard-rocks (such as granite, gneiss…) commonly involve different hydrogeological compartments such as overlying sediments, weathered rock, the weathered-fissured zone, and the fractured bedrock. Water resources in sedimentary aquifers (carbonate, chalk…) should reflect the recharge, water-rock interactions within the aquifers and possibly the matrix heterogeneity. Strontium-isotope ratios vary in nature because one of the strontium isotopes ($^{87}$Sr) is formed by the radioactive decay of the naturally occurring element rubidium ($^{87}$Rb). The $^{87}$Sr/$^{86}$Sr ratios are mainly used as tracers of water-rock interaction. The primary sources of Sr in groundwater are atmospheric input, dissolution of Sr-bearing minerals, and anthropogenic input.

The first example includes major and trace elements, as well as strontium isotopes study of ground- and surface waters in small catchments of the Armorican Massif, Brittany) to define the main constraints on runoff, and respective contributions of the different natural and man-made end-members on the chemical composition of water resources. Aquifers of these study sites are all hardrock aquifers, the groundwater of which are threatened by intensive agricultural activities. The range in Sr contents in groundwater agrees with other groundwater sampled from granite aquifer in France such as the Margeride Mountains and the Cantal (Massif Central), the Hérault watershed (southern France), the Morvan (southeastern Paris Basin) and the Vosges (northeastern France). The Sr content is well correlated with Mg, both being related to agricultural practises. $^{87}$Sr/$^{86}$Sr ratios range from 0.71265 to 0.72009, in, agreement with values found in other hard rock aquifers from France.The combined used of $^{87}$Sr/$^{86}$Sr and Mg/Sr ratios to all these groundwater allow to define the different end-members (rain, agricultural practise, water-rock interaction) both in the three Brittany catchments and elsewhere in France Particularly, in hard-rock aquifer, besides identification of anthropogenic impact on groundwater; Sr-isotope tracing defines and identifies the relative signature of groundwater circulation in alterite and underlying weathered-fissured and fractured bedrock.

In the second example (Somme catchment, sedimentary aquifer), strontium-isotope ratios measured in groundwater range from 0.70769 to 0.70808, clearly higher than that of Chalk matrix (0.707337). Variations of Sr-isotope signatures and Mg/Sr ratios in groundwater may help identifying different groundwater bodies. The variations of Sr-isotope signatures in groundwater from the Chalk aquifer are really significant (about $4.10^{-4}$), suggesting either a heterogeneity of the Chalk matrix or complex water-rock interactions and/or anthropogenic input. The lack of relationship between Cl contents and $^{87}$Sr/$^{86}$Sr ratio precludes major anthropogenic disturbance on Sr. The different signatures in groundwater are better explained by matrix heterogeneity, which can present lateral facies variations, than by a strong anthropogenic influence. All the above support the hypothesis of another Sr source in the groundwater with a more radiogenic $^{87}$Sr/$^{86}$Sr ratio. Radiogenic Sr could in part be provided by thin marly-clayey beds in the Chalk aquifer through ion exchange or desorption of Sr from clays with a more radiogenic signature. Another hypothesis concerns dolomitisation of the Chalk that could induce a coupled increase of the Mg/Sr and $^{87}$Sr/$^{86}$Sr ratios.

These studies from contrasted geological environments support the use of Sr isotopes as a powerful tool in characterising the heterogeneities, the water rock interactions in different water bodies, as well as in constraining the anthropogenic input versus natural Sr occurrence.

# DARCY 100

## Acquisition of isotopic composition in carbon of groundwater in the recharge area

Gillon M., Barbecot F., Marlin C., Gibert E.
Laboratoire IDES UMR 8148, CNRS-Université Paris Sud-11, bâtiment 504, 91 405 Orsay cedex.
gillon@geol.u-psud.fr, barbecot@geol.u-psud.fr, marlin@geol.u-psud.fr, egibert@geol.u-psud.fr

This study aims to reconstruct the different mechanisms responsible for the geochemical and isotopic composition of the $^{14}$C time tracer, in the unsaturated zone (UZ) of the recharge area of aquifers. The water dissolved inorganic carbon (TDIC) mineralization occurs mainly within the UZ through the dissolution of $CO_2$ or carbonates. In order to estimate the role of each phase, the distribution and evolution of $CO_2$ pressure as well as the $^{13}$C and $^{14}$C composition of $CO_2$, water and carbonates are followed on two specific sites: (1) the homogeneous and free-carbonate Fontainebleau sands (Yvelines, France), allowing for the study of $CO_2$-water impact single process; (2) The homogeneous and carbonated Astian sands (Herault, France), gathering all the exchanges between gas, water and the carbonated matrix.

In both these two sites, the $^{13}$C contents of $CO_2$ are representative of a soil covered by C3-plants (Fontainebleau sands: below a forest: -25,5 to -23,0 ‰ and below a grassland: -27,0 to -23,0 ‰, Astian sands in agricultural area: -24,0 to -22,0 ‰) (Bender, 1971; Deines, 1980).

On the Fontainebleau sands site, the σ$^{13}$C of $CO_2$ is rather constant in depth, although it seems vary seasonally near the sub-surface (Bacon et al., 1998; Hass et al., 1983; Palta and Gregory, 1997). First experimental results show a dependence of $^{13}$C contents of $CO_2$ originating from bacterial degradation of organic matter with temperature, σ$^{13}$C equals –28,5 ‰ at 30°C and varies between –31,0 and –27,0 ‰ at 3°C. However, a further detailed study is required to define the specific role of temperature. On an other hand, the $CO_2$ is transported by diffusion downward to the water table. The diffusion coefficient is found experimentally equal to 1,5.10-6 (± 0,5.10$^{-6}$) m$^2$.s$^{-1}$ (Ogata et al., 1961).

In the Astian sands, $CO_2$ is enriched in $^{13}$C with depth, from -24,0 to -22,0 ‰. This enrichment is due to exchanges between the gas and carbonated matrix via the water TDIC. Exchanges between the three phases lead, upward to surface, to respectively (1) a $^{13}$C depletion of carbonate from -4,0 to -10,0 ‰ and (2) an increase in $^{14}$C activity, between 0 and 40 pMC due to precipitation of secondary calcite. The carbonate composition is thus the result of a mixing between two calcites, the calcitic matrix and the secondary calcite. The isotopic composition of carbonates in the Astian sands allows to estimate the precipitation-dissolution flux of this secondary calcite (9.10$^{-9}$ to 2.10$^{-7}$ molC.g $^{-1}$ rock.y$^{-1}$).

### References

- Bacon D.H. and Keller C.K., 1998 - Carbon dioxide respiration in the deep vadose zone: Implications for groundwater age dating. Water Resources Research, 34(11), pp. 3069-3077
- Bender M.M., 1971 - Variations in the $^{13}$C/$^{12}$C ratios of plants in relation to the pathway of photosynthetic carbon dioxide fixation. Phytochemistry, 10(6), pp. 1239-1244
- Deines P., 1980 - The isotopic composition of reduced organic carbon. In: Fritz P. and Fontes J.Ch. (Eds), Hanbook of Environmental, Isotopes Geochemistry, vol.1, The Terrestrial Environment, A, Elsevier, Amsterdam, pp. 331-405
- Haas H., Fisher D.W., Thorstenson D.C and Weeks E.P., 1983 - $^{13}CO_2$ and $^{14}CO_2$ measurements on soil atmosphere sampled in the sub-surface unsaturated zone in the western great plains of the US. Radiocarbon, 25(2), pp. 301-314
- Ogata A. and Banks R.B., 1961 - A solution of the differential equation of longitudinal dispersion in porous media. USGC Professional Paper 411-A. Reston, Virginia: U.S. Geological Survey
- Palta J.A. and Gregory P.J., 1997 - Drought affects the fluxes of carbon to roots and soil in 13C pulse-labelled plants of wheat, Soil Biology and Biochemistry, 29(9/10), pp.1395-1403

# DARCY 118

# Hydrogeologic investigation and water supply systems in hard rocks of North Alentejo region (Portugal)

CHAMBEL António [1], DUQUE Jorge [2], BENEDOVA Katerina [3]

[1] University of Évora, Department of Geosciences, Apart. 94, 7002-554 Évora, Portugal, achambel@uevora.pt
[2] Politechn. Inst. of Beja, Agriculture High School, Apart. 158, 7801-902 Beja, Portugal, jduque01@gmail.com
[3] Charles University, Faculty of Science, Albertov 6, 128 43 Prague 2, Czech Republic, benedova.k@seznam.cz

## Abstract

Some new water companies are beginning to take care of water supply systems in Portugal, taking the place of municipalities, that were mainly the previous responsible for it. Great part of water supply in South Portugal was based on groundwater. The initial idea of these new companies was to implement new distribution systems based on surface origins, but, in less populated areas, pipe extension to little villages is very expensive and difficult. So, the decision was to scientifically study the old supply systems, determine where there were or not problems, and, in the last cases, go on with investigation in order to create new wells. Field work, flow tests, aerial photography analysis, geophysics (VLF-EM method) and water prospection drillings were used, in order to better understand the hydrogeological features and to create guaranty conditions for the future on groundwater based supply systems. The work proved successful, with new 4 productive wells supplying 4 different supply systems.

## 1. Introduction

The region of North of Alentejo, on the central part of Portugal, has been supplied by groundwater since ever. But, on the last years, there is a change on the supply systems, with tendency to increase the superficial origins for human uses. This change is the result of new politics concerning water management in Portugal, with the tendency to the privatization of many supply systems. This was the case of Nisa and Gavião municipalities, where this work took place.

But Alentejo is a semi-arid region of South Portugal with desertification problems and aged people. Corresponding to one third of the Portuguese territory and with only about 5% of the total population, this means that only few urban areas are really interesting in face of the private financial investment. To extend the pipes from distant lakes to many places with less then some few hundreds inhabitants are expensive. To increase the problem, great part of Alentejo territory is based on hard rocks, which means low productive hydogeological areas. But, with some investigation, the results may be positive.

## 2. Supply systems of North Alentejo

The area of interest is situated in the Alto Alentejo region, in central-east Portugal (fig.1). The municipalities where the investigation took place are localized in Portalegre district, in Nisa and Gavião counties. In Nisa county, the exploration was carried out in the little villages of: Amieira do Tejo, Vila Flor, Albarrol, Falagueira, Monte Claro, Monte Matos, Velada, Chão da Velha and Cacheiro. In the municipality of Gavião, only the supply system of Outeiro village was searched.

## 3. Geomorphological and climatic conditions

From the morphological point of view this part of North Alentejo is a plateau, whit altitudes ranging between 200 and 330 m above sea level. Only in the zones near river Tejo, north of the study area (figure 1), the altitudes go below 100 m, forming a deep valley, where the surface is more disrupted. The rivers have formed high amount of meanders, which is typical of schist topography. On the contrary, the rivers passing through granite formations show more straight morphologic directions and the presence of meanders is less visible. The levelling is well protected in the granite zone, but in the schist metamorphic area the landscape is modified, with small hills and deep valleys in the vicinity of the main rivers. Fragments of regular hills are kept only on the highest points (Ribeiro et al. 1965). Quartzite rocks dominate the landscape on the municipality of Nisa, forming a NNW-SSE direction ridge 463 m above sea level.

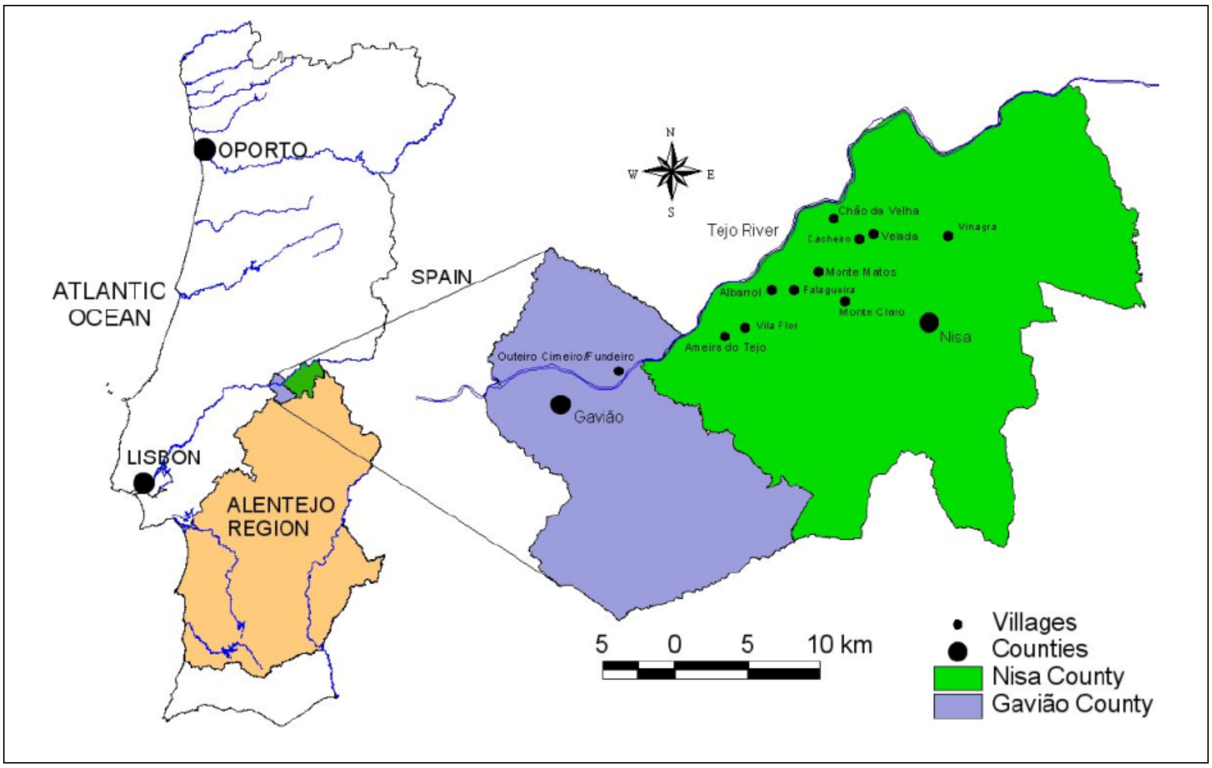

Figure 1: Location map of the study area.

Climate of this part of Alentejo is Mediterranean, with dry and warm summers and mild, rainy winters (Daveau 1985). In general the mean annual precipitation ranges between 700 and 800 mm (http://snirh.inag.pt/). In the eastern part of the area the mean annual precipitation approaches to lower values and in the western part exceed 800 mm. The precipitation is not uniformly distributed throughout the year. The highest values are reached from October to April, whereas the precipitation in July and August is not significant. The worst drought in decades afflicted Portugal in year 2005, as can be seen in figure 2.

## 4. Geological characteristics of the area

The studied area is part of the Hesperian Massif, the Paleozoic Shield of the Iberian Peninsula. It is inserted on the Central Iberian Zone, one of the geostructural divisions of the

Hesperian Massif defined by Julivert et al. (1974).

The area (figure 3) is basically composed by a metamorphic schist and greywacke complex occupying a considerable extension. The complex is constituted by black or grey argillaceous schists, quartz-mica schists and quartz-calcosilicate schists. The schists alternate with layers of sandstone, greywackes or quartz greywackes. The rocks are highly folded and the main schistosity direction is WNW-ESE.

Some Ordovician formations are represented by quartzite rocks and by clay schists with fossils. The quartzite rocks form a synclinal structure with two parallel ridges in the northern part of the area. The south top of the quartzite crest is elevated approximately 200 m above the schist-greywacke terrain. The quartzite is represented by both wide layers and thin layers with intercalations of quartzite schists.

In the south, the boundary of the complex is the contact with the granite of Nisa. Along the contact the metasediments are transformed into schists with cordierite and hornfels. The width of the cordierite schist band is less than 1 km. The hornfels are dark, compact, pelitic or quartz-pelitic type.

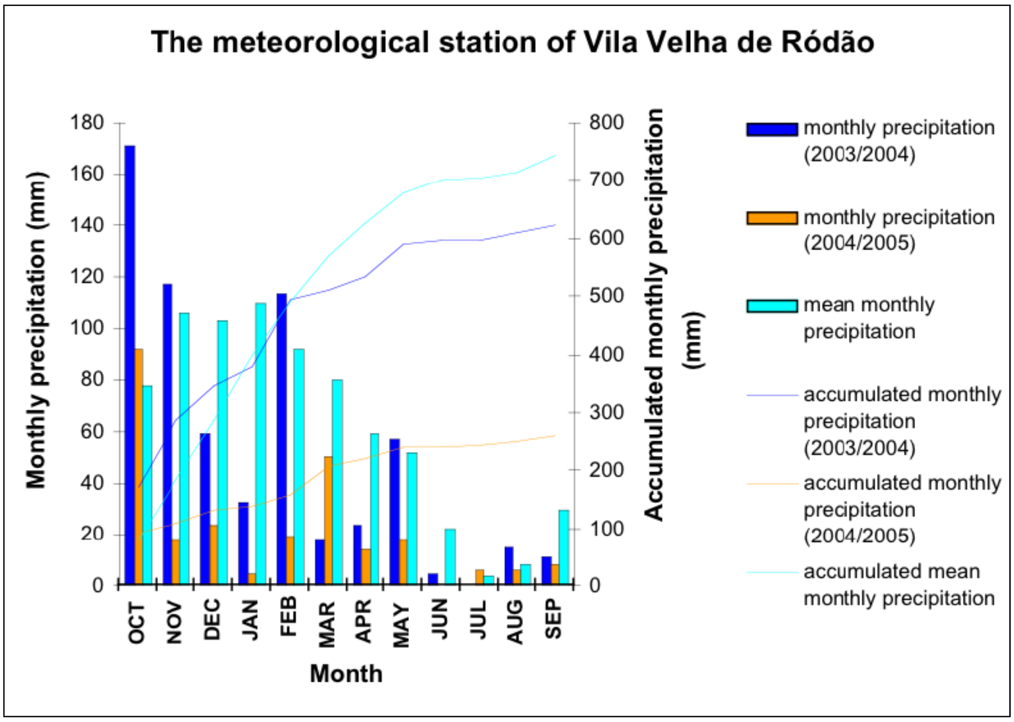

*Figure 2: Distribution of precipitation in hydrological years 2003/2004 and 2004/2005 (modified from http://snirh.inag.pt/).*

An important uranium area occurs in metamorphic aureole between Nisa and Monte Claro. The area is approximately 5 km length and 50-400 m width (ERHSA 2001). Mineralization of disseminated type is formed, between others, by autunite, torbernite and pecheblenda. Pyrite minerals are also observed. The secondary uranium minerals appear especially on the surface of cleavage, in the narrow fractures and in the crushing zones. The mineralization occurs also in adjacent granites.

The slate and greywacke complex is in some areas cut by pre-variscan porphyries, generally with N-S, NNW-SSE or WNW-ESE directions and also accompanied by microgranite, dolerite, aplite, pegmatite, rhyolite and quartz veins. The quartz veins in schists are generally parallel with schist cleavage, direction WNW-ESE or E-W. The quartz veins are frequently brecciate type. The milky quartz has undergone an intense fracture, and these fractures were subsequently filled in by secondary quartz with zonal structure of milky and smoky quartz. These veins are generally mineralized by uranium. The quartz veins are here essential to the success of water drillings.

The granite massif of Nisa, south of the area, is formed by coarse-grained two mica granites. Fine and intermediate grained granites are observed close to the contact zone with the schists. Granites and schists are sometimes covered by tertiary sediments. Layers of arkoses (Beira Baixa arkoses), on major part overlaid by more recent conglomerate layers, are present in the area. The conglomerates are constituted especially by badly rounded siliceous fragments – quartzite, quartz, lydite, varying in size.

Finally some Quaternary fluvial deposits of gravels, sands and clays are accumulated especially along the main river and affluents. Deluvial deposits also occur in the proximity of the quartzite rocks and have been formed by fragments of these rocks, sometimes angular or rounded, of big dimension, and sometimes mixed up with fine clay material.

## 4. Hydrogeology of the area

The investigation took place in an area that have only a few villages, each one with few tens or hundreds inhabitants, generally old people. These places have been since ever supplied by groundwater, but many times with problems that result from a deficient management of water resources and bad conditions of the technical supports (pumps, distribution, etc.).

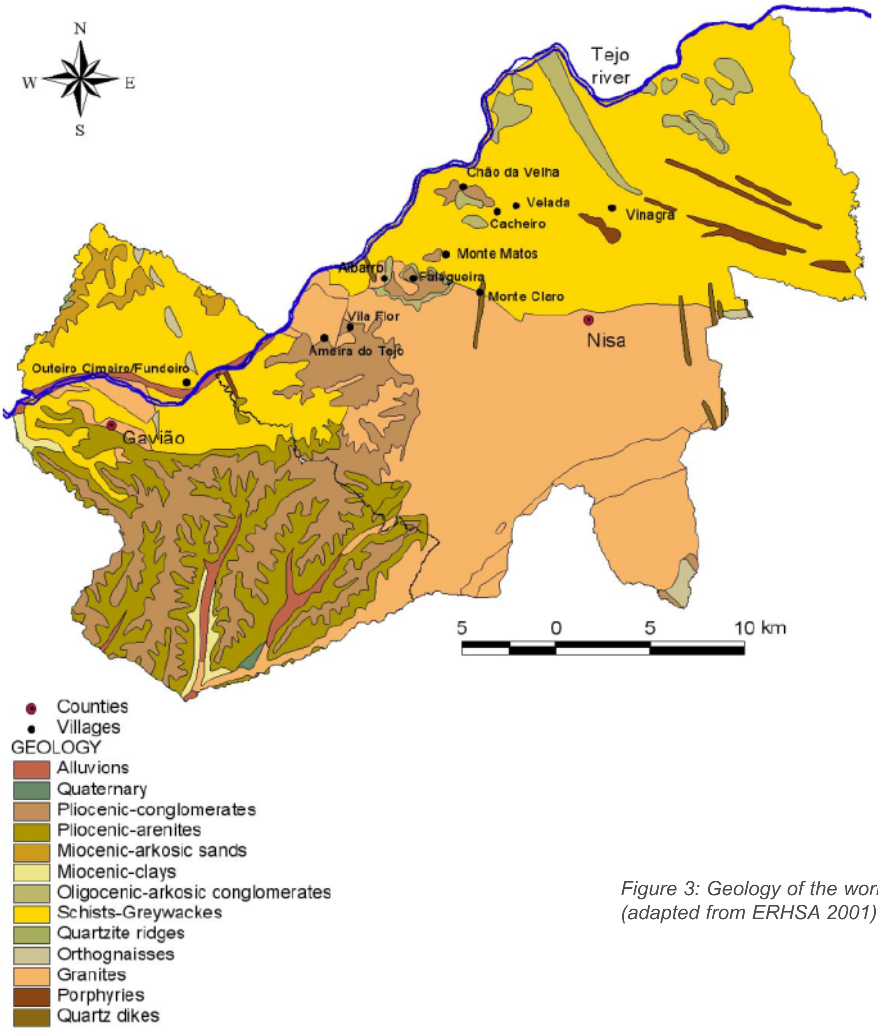

*Figure 3: Geology of the working area (adapted from ERHSA 2001).*

Hydrogeological research has not been a priority in the past and the wells have been constructed without any technical support. The supply systems were responsibility of the municipalities. But now new private companies are responsible by the systems. These factors led some companies to try to understand how they can maintain their groundwater supply systems without problems in the next decades, which gave the opportunity to study for the first time the conditions of the actual wells, to drill new ones and to establish the global management of these little systems. In the past, when a well failed, a new drill was done, and so on. The global study and analysis of the supply systems were never done in the study area, and all the management was based on the moment, on the day to day problems, which caused many interruptions on the supplies, sometimes with the firemans distributing potable water on tanks to the population during dry periods that could last for weeks.

On these new conditions, 8 systems were investigated to detect the problems and solve the water shortness for future. Two municipalities were involved (Nisa and Gavião), on places where it will be to expensive to bring the pipes from the lakes on the future.

Basically the aquifers are on hard rocks, with one exception on one partial system, based on some sand and clay covering layers of the Tejo river sediments.

The hydrogeological units involved in the prospection area are (figure 4):

- Sector of Amieira-Montalvão
- Sector of the igneous rocks of Nisa, Portalegre and Santa Eulália
- Aquifer System of Tejo-Sado Basin (left margin of Tejo Basin in Alentejo region)

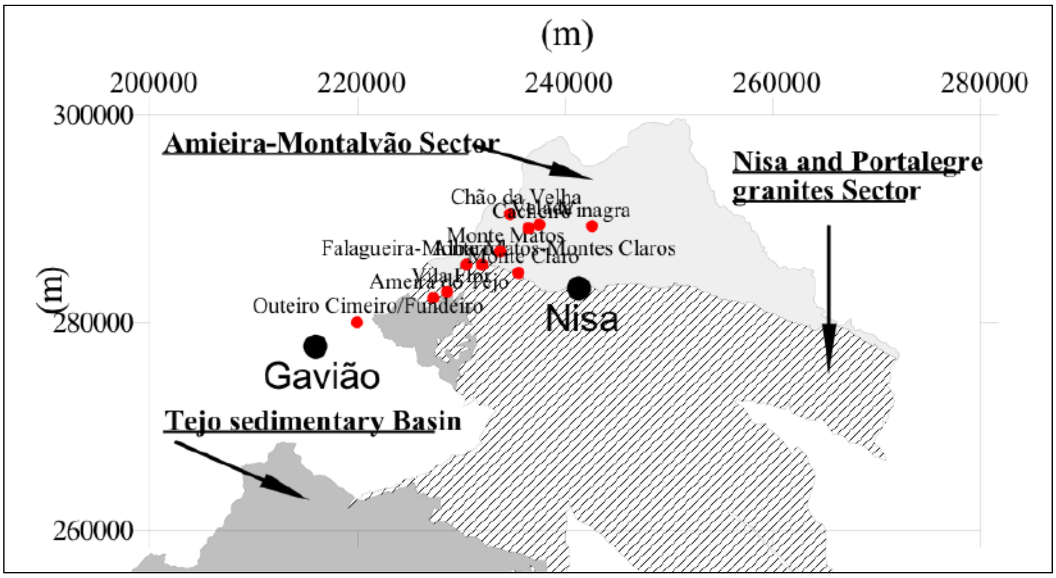

Figure 4: Water supply systems on the three hydrogeologic sectors present on the studied area.

The hydrogeological sector of Amieira-Montalvão is related with the schist-greywacke complex. The sector is characterized as a heterogeneous and anisotropic hard rock aquifer. The groundwater occurs mainly in relation with quartz fractured veins.

The Amieira-Montalvão sector is one of the less explored and less productive areas in Alentejo, but, due to the little dimension of the villages, still guaranty sufficient water yields to satisfy the population needs. Special hydrogeological importance must be given to Ordovician quartzite ridges, despite its little use till now. The hydrogeological potential of the quartzite area is higher than the average of the complex (ERHSA, 2001). Also hornfels are distinguished by higher yields from the schist-greywacke complex. Main drainage direction in surveyed area is from SE to NW to the Tejo river valley (ERHSA 2001).

The hydrogeological sector of the igneous rocks of Nisa, Portalegre and Santa Eulália corresponds to granite massifs with a weathered superficial zone of less than 2 meters and an incipient fracture net. It is the less productive area of Alentejo (Chambel et al. 2002).
Three zones can be distinguished in both this hard rock sectors:

- superficial weathered zone
- intermediate zone (coexistence between weathered and fractured rock)
- zone of compact and fractured rock

The aquifer system of Tejo-Sado Basin is here represented by an area with conglomerate and arkoses formations south and southeast of Amieira do Tejo. It has only few meters of thickness (maximum 20-30 m) in the studied area and the waters have a very low level of mineralization. All these villages have some water supply problems, generally questions related with the shortness of water during summer or shortness during special events, like festivity days, when the normal population more than double and the water consumption increases.

## 5. Hydrogeologic investigation

The intention of this study was to investigate if there were or not supply water problems on the moment with the actual installed structures in the two counties, Nisa and Gavião.
In the places of Vinagra and Albarrol there was no need to investigate, once in the first one it was decided that it will be supplied by superficial waters of an artificial lake and in the second one, with only 7 inhabitants, a new drilling was executed and it has positive artisianism.
On the other areas, the hydrogeological survey began with field work, in order to evaluate the well construction conditions, the water distribution patterns and the geological and hydrogeological environment. The villages that have water supply problems were mainly inserted on the schists and greywacke complex, more precisely on the Amieira-Montalvão Sector (see figure 4), and the presence of water is clearly linked to the existence of quartz fractured veins on these lithologies. On the igneous rocks the open fractures are essential, and the possibility to get water from wells is much low than on the previous lithologies, as can also be seen in table 1 (Nisa, Portalegre and S. Eulália Sector, see figure 4).

| Sectors | Media (L/s) | Median (L/s) | Minimum (L/s) | Maximum (L/s) | Standard deviation | Number of wells with instant yield values | Total number of deep wells | Total number of wells |
|---|---|---|---|---|---|---|---|---|
| Amieira-Montalvão (schists and greywackes) | 1.86 | 1.34 | 0.47 | 6.94 | 2.11 | 8 | 12 | 46 |
| Nisa, Portalegre and S. Eulália Granites | 0.65 | 0.38 | 0 | 5.56 | 0.94 | 44 | 125 | 431 |

*Table 1: Statistical results of instant yields of the two hydrogeologic low productive sectors of North Alentejo present on the region and identified during the Project "Study of Groundwater Resources of Alentejo Region" (ERHSA 2001, Chambel et al. 2002).*

Nine pumping tests were organised on eight wells in October and November 2004 in localities (see figures 3 and 4): Chão da Velha, Cacheiro, Herdade Demansas and Cabeço Vermelho (Falagueira-Monte Claro-Monte Matos System), Vila Flor, Taipas and Amieira crossroad (Amieira do Tejo System) and Outeiro Fundeiro.
The geological background of the wells is the following:

- The well GGT-10 of Chão da Velha is situated in schists formation.
- The well GGT-14 and the emergency large well GGT-15 of Herdade Demansas are localized on the margin of the metamorphysed band contact between the schist and greywacke formation and the granites. From the lithological point of view the bedrock is formed by schists.

- The well GGT-13 of Cabeço Vermelho is in the hornfels zone. The well is crossed by a fractured quartz vein visible at surface.
- The wells of Amieira do Tejo and Vila Flor systems are situated in granites. The well GGT-5 is on coarse-grained granite. The well GGT-2, in the locality of Taipas, is on the fine and intermediate-grained granites. The well GGT-1, in the east part of Amieira, near a crossroad, is localized also in fine and intermediate-grained granite covered by a very small layer of gravels originated from adjacent conglomerate formation.
- Geological background on the well GGT-16, in Outeiro, is formed by schists of the schist and greywacke complex.
- The well GGT-9, in Cacheiro, is situated in Beira Baixa arkoses formation, on transition with conglomerates. The arkoses overlay the schist and greywacke bedrock.

The geologic profiles of all these wells are not known, once in the past the companies haven't make reports or, when they exist, they are not serious.
From the 9 pumping and recovery tests, 8 pumping were step tests and 1 was a pumping test at constant discharge rate. The duration of the pumping tests range between 17 and 29 hours and the recovery test lasted between 2 and 3 hours (table 2). Water levels were recorded mainly in the pumping wells, once there were not piezometric wells on the area.

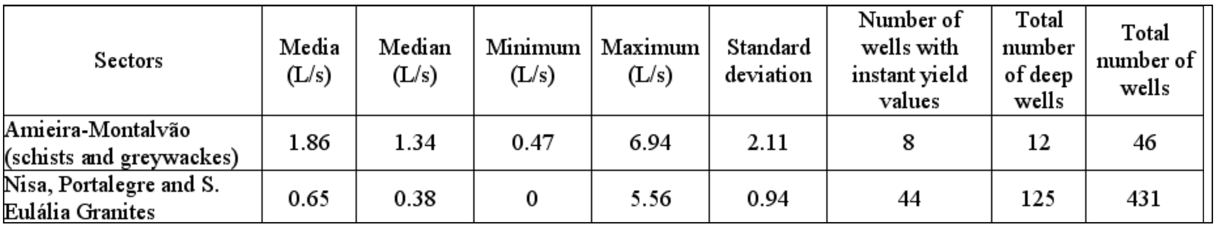

| Sectors | Media (L/s) | Median (L/s) | Minimum (L/s) | Maximum (L/s) | Standard deviation | Number of wells with instant yield values | Total number of deep wells | Total number of wells |
|---|---|---|---|---|---|---|---|---|
| Amieira-Montalvão (schists and greywackes) | 1.86 | 1.34 | 0.47 | 6.94 | 2.11 | 8 | 12 | 46 |
| Nisa, Portalegre and S. Eulália Granites | 0.65 | 0.38 | 0 | 5.56 | 0.94 | 44 | 125 | 431 |

*Table 2: Summary of aquifer test features in Nisa and Gavião counties (SGC – Schists and Greywackes Complex).*

The Aqfis (Oliveira 1990, Almeida & Oliveira 1990) and AquiferTest codes were used for analysis of the step tests and recovery tests.
Aquifer test data was analyzed by methods based on well-flow equation using the conceptual double porosity model (Moench 1984, Streltsova 1976). The concept of double porosity considers two coexisting media: porous blocks and fractures that separate the blocks. In reality, the double porosity aquifer are formed either by blocks with dense net of fine fissures separated by sparse net of wider fractures or formed by blocks with pore porosity separated by fractures. The aquifer permeability is determined especially by the fractures hydraulic conductivity. The storage capacity is related with the pore water volume in blocks. The Aqfis programme is based on the flow equation in double porosity media established by Barenblatt et al. (1960), Warren & Root (1963), Kazemi et al. (1969), Streltsova (1976), Boulton & Streltsova (1977), Moench, (1984), among others.
Conventional Theis-Jacob recovery method was used to compare the results. Conventional well-flow equations used to analyze aquifer test data are thought to be inadequate to describe groundwater flow through fractured rocks (Gringarten 1982). However, in case that the specific features of fracture aquifer (considerable filtering anisotropy and heterogeneity, existence of sparse wide fractures disturbing radial flow to well and effect of double porosity in double porosity aquifer) are not significant, the flow will approach the flow in an unconsolidated homogenous aquifer (Jetel 1982). This occurs for example in very low-permeability rocks where the fractures are numerous enough and evenly distributed throughout the aquifer. Since the discharge before recovery was variable, the correction of time (Jetel 1982) was done.

Figure 5 shows an example of the flow tests, for the GGT-14 well of Falagueira system. In this case, drawdown measurements were also done in a 3.5 m diameter hand dug well 17.5 m apart (GGT-15). Both drawdowns are represented in relation with discharge in this figure. Figures 6 and 7 show examples of flow and recovery flow interpretation tests on several of the studied areas. The final transmissivity calculated values are presented in table 3.

The results had permitted to show that, considering the village's population, no water supply problems exist on Outeiros (only an inappropriate pump), Cacheiro and Vila Flor (on both the water is sufficient). On the other systems (Chão da Velha, Falagueira, Amieira do Tejo) it was necessary to act, in order to detect potential places for new drillings and reinforce the actual water supply systems.

The survey proceeds with the stereoscopic analysis of black and white 1:25,000 aerial photos, in order to detect the main structural alignments than can represent fracture directions.

To confirm the first approach, geophysics VLF-EM method was used. The VLF-EM method is established on principles of inducing of a secondary electromagnetic field in the bodies with different resistivities. A transmitter and a receiver are used as in any other electromagnetic methods. In case of the VLF method used on this work, the transmitter is a military radio using frequencies between 15 and 30 kHz that emits a very powerful signal (300-1000 kW) (ABEM 1990) and generates an horizontal circular electromagnetic field. This field is called primary. The generation of a secondary field is related with the conductivity of geological formations. The conductivity is inversely related to the resistivity of the geological body.

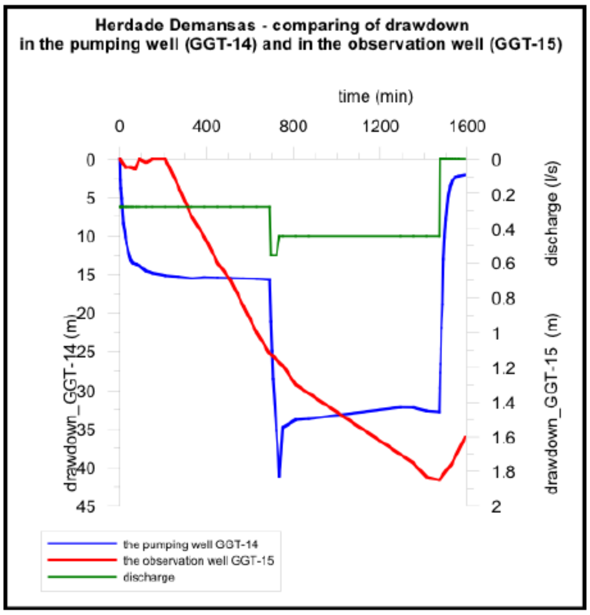

Figure 5: Comparing drawdown in the pumping well GGT-14 and observation well GGT-15, at distance 17.5 m, in Falagueira system.

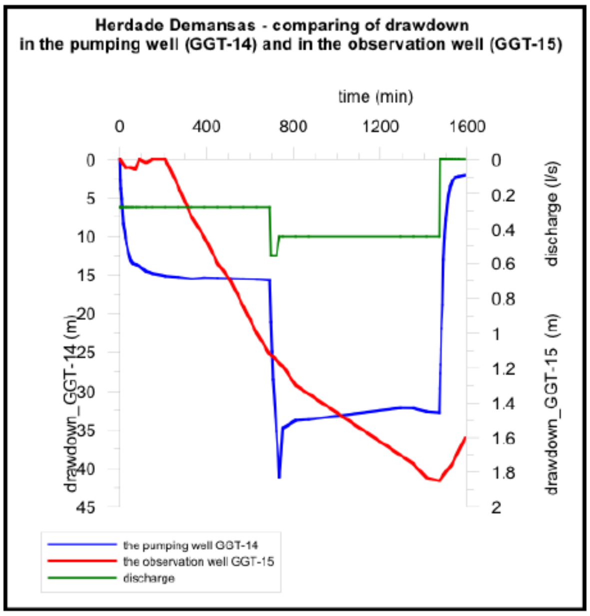

Figure 6: The analysis of the pumping test for the well GGT-13, in Falagueira system.

These techniques are mostly applicable for detecting steeply dipping structures like fractures and faults zones behaving as conductors, which are located in geological formations with high resistivity (for example in hard rock geological environments).

There receiver was a WADI instrument (ABEM 1990, ABEM 1991), developed by ABEM Corporation. This receiver records horizontal and vertical magnetic components (Hz, Hx) of electromagnetic field and display it by percentage ratio (Hz/Hx). The equipment measures the real and also imaginary part. The prospection by VLF-EM method is done along measuring lines, the profiles. Several of parallel profiles can (and must) be done at the same place, to a better interpretation.

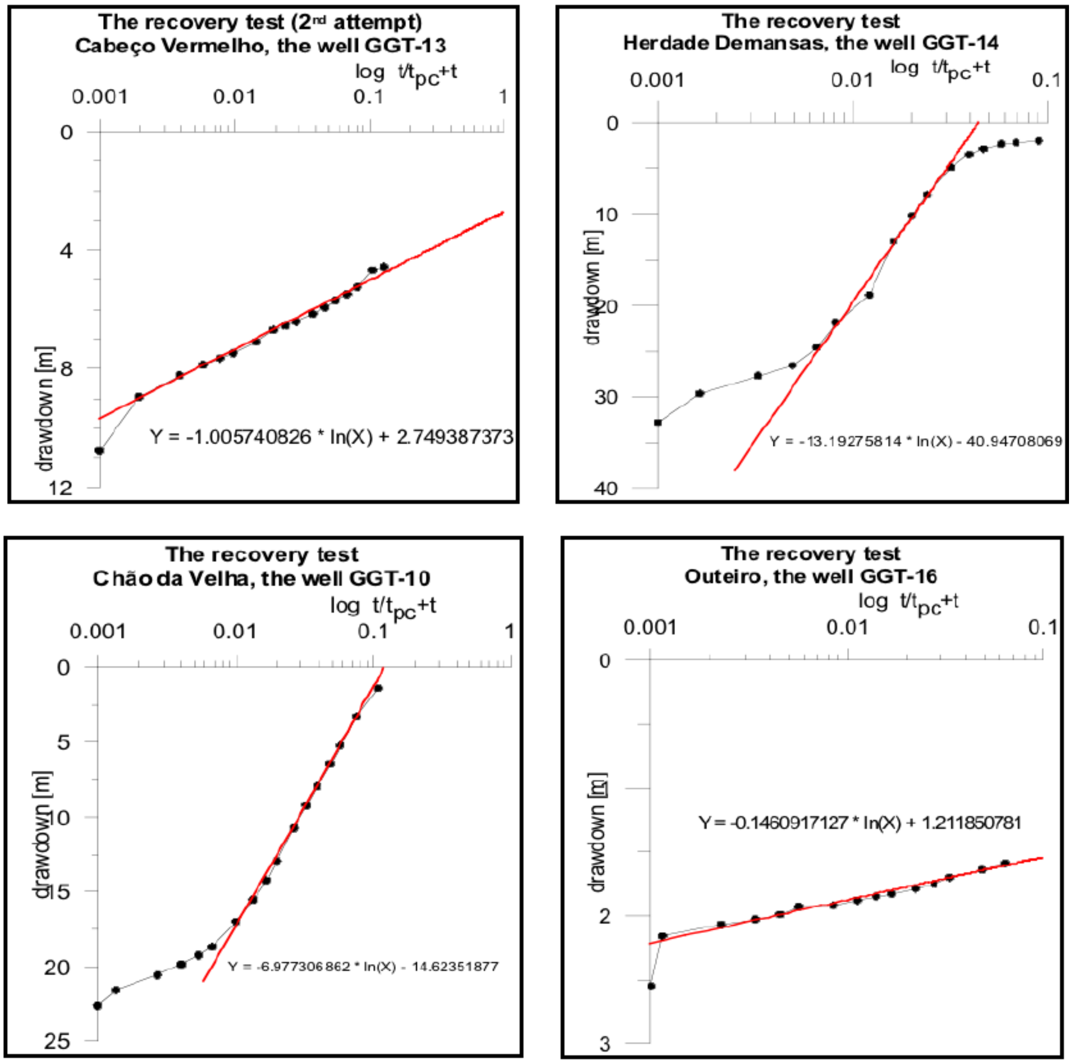

*Figure 7: Examples of recovery tests interpretation for several wells (GGT-13 and GGT-14: Falagueira system; GGT-10: Chão da Velha system; GGT-16: Outeiro system). Results on table 3.*

| Water supply system | Locality | Well ID | Transmissivity ($m^2$/day) Aqfis | Transmissivity ($m^2$/day) Theis and Jacob recovery test |
|---|---|---|---|---|
| Chão da Velha | Chão da Velha | GGT-10 | 0.77 | 0.16 |
| Outeiros | Outeiro Fundeiro | GGT-16 | 24.8 | 36.5 |
| Amieira do Tejo | Taipas | GGT-2 | 5.3 | 2.15 |
|  | Amieira crossroad | GGT-1 | 0.22 | - |
| Vila Flor | Vila Flor | GGT-5 | 4.2 | 0.97 |
| Falagueira/Monte Claro/Monte Matos | Cabeço Vermelho 1st attempt | GGT-13 | 12.1 | 4.1 |
|  | Cabeço Vermelho 2nd attempt | GGT-13 | 2.6 | 3.8 |
|  | Herdade Demansas | GGT-14 | 1.1 | 0.23 |
| Cacheiro | Cacheiro | GGT-9 | 1.8 | 0.9 |

*Table 3: Transmissivity values obtained from the flow tets.*

Four kinds of graphic images result from the interpretation: 1) Multi profile plot; 2) Real data; 3) Filtered data; 4) Vertical cross-sections. Areas for VLF-EM survey were chosen between Falagueira-Monte Claro villages and in surroundings of Chão da Velha and Amieira do Tejo villages. The potential places for exploration were chosen in points where faults intersect and outside the villages, in order to avoid water contamination by the sewage systems. The most important anomalies were again investigated on the field, in order to detect directly the potential fractures. Some examples of the results are presented in figures 8 and 9 (multiprofiles in Falagueira and Chão da Velha systems) and figure 10 (vertical cross section on Chão da Velha system).

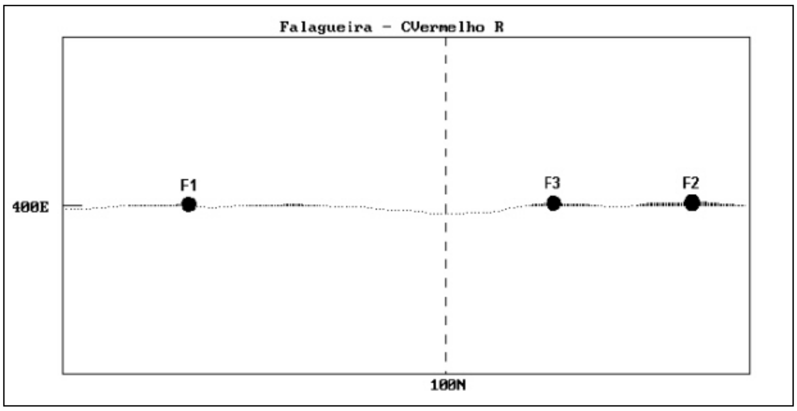

*Figure 8: Location of the recommended wells in the area of Cabeço Vermelho, Falagueira system (multi profile plot of WADI).*

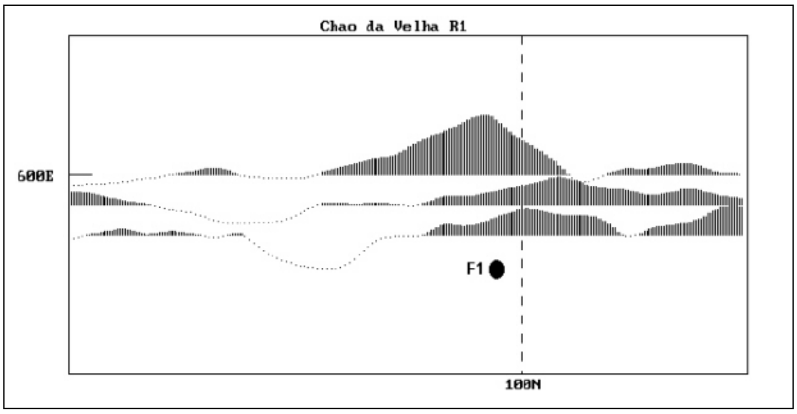

*Figure 9: Location of the recommended wells in the place of Chão da Velha (multi profile plot of WADI). F1 was transformed in a weel.*

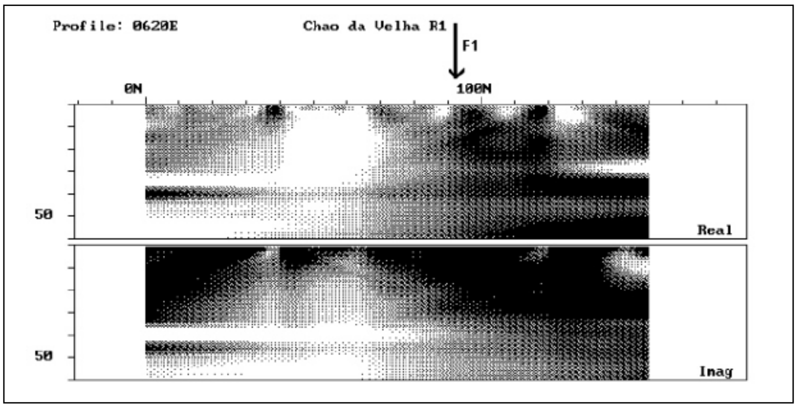

*Figure 10: Location of the recommended wells in the place of Chão da Velha (vertical cross section of WADI). F1 was transformed in a well.*

On Falagueira and Amieira do Tejo sytems it was not possible to drill on the detected VLF-EM points, once there were problems on the negotiation with the land's owners.
On Chão da Velha the new well has an instant yield of 36,000 L/h. The flow test showed that after 8 h of pumping at 18,000 L/h the water level drawdown was 9.37 m for a 100 m deep well and a pump position at 75 m (the hydrostatic level was 19.05 m).
On Velada system the new drill was defined by the geological conditions of the area. A big 3-4 m large quartz filled fault was visible on a road cutting and the well was done on the top of it. Also electric wires above the place haven't permitted the use of VLF instrument. The instant yield was 60,000 L/h and it has a drawdown of 7.93 m for a 121 m well, after 8 h pumping at a rate of 18,000 L/h. The initial level was 39.80 m and the pump is at 75 m.
On Amieira do Tejo system the drillings were done on municipal land inside the village, fact that hasn't permitted to use VLF prospection. Two drillings were considered unproductive (with instant yields of 2,400 L/h and 1,800 L/h, respectively). The third one was productive and was transformed in a well. It has an instant yield of 45,000 L/h. The flow test showed that after 24 h of pumping at 18,000 L/h the water level drawdown was 6.32 m for a 79 m deep well. The pump position is at 67 m and the hydrostatic level was at 20.30 m
On Falagueira system the drilling was located on the centre of a valley, inside a little property with a nearby electric wire, what doesn't also permit the VLF use. An alignment was detected on the aerial photos, coinciding with the valley. The well produced an instant yield of 12,000 L/h. The flow test showed that after 24 h of pumping at 6,000 L/h the water level drawdown was 8.07 m for a 121 m deep well. The pump position is at 70 m and the hydrostatic level was at 6.5 m.
All the transmissivity values are represented in table 4,

| Water supply system | Locality | Well ID | Transmissivity ($m^2$/day) Aqfis |
|---|---|---|---|
| Falagueira/Monte Claro/Monte Matos | Falagueira | RA1 | 15.1 |
| Chão da Velha | Chão da Velha | RA2 | 36.7 |
| Velada | Velada | RA3 | 60.7 |
| Amieira do Tejo | Amieira do Tejo | RA4 | 8.4 |

*Table 4. Transmissivity values for the new wells on North Alentejo region.*

Radiological groundwater analysis concerning the Total Indicative Doses (TID) in the last 4 new wells was also performed. It was verified that RA3 was the only one which TID is below the permitted law value (DIT<0.1). The radiological concern is related to uranium mineralizations that occur in the hornfels belt produced between the granites, on south, and schists, on the north (see figure 3).

## 6. Conclusions

In the last years, tendency to privatization of water supply systems led to the conversion of some old groundwater systems on surface water demands. But some little systems are difficult to avoid, once Alentejo is a semi-arid region with sparse villages, to much expensive to be linked by water pipes to the main superficial water reservoirs.
Based on hard rocks, the low productive hydrogeological sectors are mainly formed by the schist and greywacke complex on the north part and by granites on south. Between them, an

hornfels belt with uranium-bearing minerals. Eight supply systems in two municipalities (Nisa and Gavião) were investigated to detect the problems and solve the supply water shortness for future.

The investigation was based on the inventory of the public wells, flow tests on all of them, chemical analysis and the verification of the well conditions, some with tens of years without any maintenance. The real needs of the population on the moment and on the future and the real productive capacity of the wells were evaluated.

Some of the places have real problems, others not so. On the first case, hydrogeological investigation took place at local scale. Aerial photographs were used to detect the fracture pattern, field work were carried on to observe the possible productive fractures and geophysical electromagnetic method (VLF-EM) was used to define some fracture network. The next step was to drill new wells. The flow detected during the drillings show productivities between 1,600 L/h and 60,000 L/h in 6 wells. Only 2 of the drillings were not transformed in wells. The flow tests show transmissivities between 8 and 60 $m^2$/day, against values between 0.16 and 36.6 $m^2$/day of previous 7 wells.

The water has some problems with excess of iron and high component of radiation. The $\alpha$-total, $\beta$-total and the Total Indicative Dose were analysed. The results show that these waters present high content of radioactive elements, which was somehow expected, once they occur on the area of a metamorphic belt with high concentration of uranium minerals that were explored in the past.

## Acknowledges

Special thanks to the company Águas do Norte Alentejo, SA, for the permission to use the data, and to Paulo Furtado by his initial field work.

## References

- ABEM (1990) ABEM instruction manual, CM-Tryck AB, Bromma.
- ABEM (1991) ABEM interpretation guide, CM-Tryck AB, Bromma.
- Almeida C & Oliveira MM (1990) Caracterização hidráulica de aquíferos fracturados. In: Livro de Homenagem a Carlos Romariz, Secção de Geologia Económica e Aplicada, Dep. Geologia, Universidade de Lisboa, Lisboa, 30-64.
- Barenblatt G, Zheltov I & Kochina I (1960) Basic concepts in the theory of seepage of homogeneous liquids in fissured rocks (strata). Journ. Appl. Math. Mech. Engl. Transl., 24, 1286-1303.
- Boulton N & Streltsova T (1977) Unsteady flow to a pumped well in a fissured water bearing formation. Journ. Hydrology, 35, 257-270.
- Chambel A, Duque J & Nascimento J (2002) Hidrogeologia das Rochas Cristalinas do Alentejo: Nova Cartografia Proposta com Base nos Resultados do Projecto “ERHSA”. In: Proceedings do 6º Congresso da Água – A Água é d’Ouro, Porto, CD-88.
- Daveau S (Edt.) (1985). Mapas climáticos de Portugal. Nevoeiro e nebulosidade. Contrastes térmicos. Centro de Estudos Geográficos, Memória nº 7, Lisboa, 84.
- ERHSA (2001) Project “Estudo dos Recursos Hídricos Subterrâneos do Alentejo”. Comissão de Coordenação da Região Alentejo, Évora.
- Gringarten A (1982) Flow test evaluation of fractured reservoirs. Recent Trends in Hydrogeology, Spec. Pap. Geol. Soc. Am., 189, T. N. Narasimhan Ed., Boulder, Colo., EUA, 237-263.
- http://snirh.inag.pt/ National System of Water Resources Information, Portuguese Water Institute.
- Jetel J (1982) Ur_ování hydraulick_ch parametr_ hornin hydrodynamick_mi zkou_kami ve vrtech, Academia Praha.
- Julivert M, Fontboté J, Ribeiro A & Conde L (1974) Memória Explicativa del Mapa Tectonico de la Peninsula Iberica y Baleares. Inst. Geol. Min., España.

- Kazemi H, Seth M & Thomas G (1969) The interpretation of interference tests in naturally fractured reservoirs with uniform fracture distribution. Journ. Petrol. Technology, 246, 463-472.
- Moench A (1984) Double-porosity models for a fissured groundwater reservoir with fracture skin. Water Resources Research, 20 (7), 831-846.
- Oliveira MM (1990) AQFIS – Um programa para gerar curvas rebaixamento/tempo para aquíferos fracturados. VII Simpósio de Geologia Aplicada e do Ambiente, GEOLIS, IV, 97-107.
- Ribeiro O, Teixeira C, Carvalho H, Peres A & Fernandes AP (1965) Carta geológica de Portugal na escala de 1/50000 – Notícia explicativa da folha 28-B Nisa, Servicos Geológicos de Portugal, Lisboa.
- Streltsova T (1976) Hydrodynamics of groundwater flow in a fractured formation. Water Resources Research, 12 (3), 405-414.
- Warren J & Root P (1963) The behaviour of naturally fractured reservoirs. Journ. Petrol. Technology, 228, 3 (3), 245-255.